Catalytic Oxidation Reactions Using Hydrogen Peroxide

Thesis submitted in accordance with the requirements of Cardiff University for the degree of Doctor of Philosophy

Greg Sharp

School of Chemistry

Cardiff University

2023

Abstract

The research within this thesis has focussed principally on two reactions: the selective oxidation of benzyl alcohol via in-situ hydrogen peroxide (H_2O_2) synthesis, and the catalytic wet peroxide oxidation of phenol. Additionally, investigations involving the direct synthesis of H_2O_2 from H_2 and O_2 were conducted in relation to the selective oxidation of benzyl alcohol in order to gain better insight into the individual reaction pathways.

The selective oxidation of benzyl alcohol via in-situ H_2O_2 synthesis has been investigated previously in the literature and provides a lower temperature alternative to aerobic oxidation methodologies, which typically require reaction temperatures in the range of 80-120 ^oC, whilst oxidation via in-situ generated H_2O_2 allows for operation at temperatures approaching 50 ^oC. Furthermore, by generating H_2O_2 in-situ, the limitations of using commercial H_2O_2 produced through the anthraquinone auto-oxidation process can be mitigated.

In this work, investigations have focussed on optimising the support material for a Pd-based heterogeneous catalyst, incorporating secondary and tertiary metals alongside Pd and synthesising catalysts through different preparation methodologies with the objective of increasing benzyl alcohol conversion and limiting catalyst deactivation. Particular attention has been given to Pd, FePd and AuPd supported catalyst, with FePd and AuPd catalysts representing the most promising candidates for future development. Pd-based heterogeneous catalysts represent a ubiquitous and well-studied class of catalysts for the direct synthesis of H_2O_2, with factors including nanoparticle size, the influence of support material, the oxidation state of Pd and the effects of secondary metal alloying having received previous research attention. It should be noted that the direct synthesis of H_2O_2 utilises lower reaction temperatures (20 ^oC in this Thesis) compared to the selective oxidation of benzyl alcohol (50 ^oC) and that the degradation of H_2O_2 is promoted at higher temperatures.

In collaboration with Selden Research Ltd. the development of novel disinfectants using catalysis was undertaken, with the intention of developing chemical disinfectants that incorporate benign and non-toxic components that naturally degrade after use. The catalytic wet peroxide oxidation of phenol has been used in this work as a model reaction system to develop and maximise the oxidative ability of a mixture containing ascorbic acid and sodium percarbonate, which operates as a source of H_2O_2. This was used in conjunction with a heterogeneous source of a Fenton-type metal catalyst. This work was conducted under the assumption that reaction systems that delivered higher levels of conversion of phenol may also offer high efficacy when used as a disinfectant. Investigations have focussed on selecting the optimal Fenton-type catalyst, optimising the concentrations of each component of the reaction mixture, and examining the effects of pH on both the extent of catalytic metal leaching and towards the overall conversion of phenol.

Acknowledgements

Firstly, I would like to thank my supervisor Professor Graham Hutchings for supporting me throughout the entire PhD programme, and without whom this thesis would not have been possible. I would also like to thank Dr Richard Lewis for going above and beyond to tirelessly assist me over the past 4 years, for fixing endless broken pieces of equipment and for reading over so many thesis drafts without a word of complaint.

I would like to give thanks to the other members of staff at Cardiff University. Thank you to Mark and Sam for your training on numerous pieces of equipment. Thank you to Greg and Chris for keeping several labs operational and responding quickly to calls for assistance when something breaks. Thank you to Dr David Morgan for all of your support with conducting and analysing XPS data over the years. Thank you to Dr Tom Davies for your training and constant support at operating electron microscopes. I would also like to thank Dr Emma Campbell for her assistance in the running of CO-DRIFTS measurements. Thanks to Junhong Liu at Shanghai Jiao Tong University for performing STEM and EDX analysis. Many thanks to Professor Duncan Wass and Professor Stuart Taylor for their efforts to periodically review my progress, and for their insightful comments and suggestions.

Special thanks to all the students of 'Team H_2O_2' who worked in the windowless basement lab of 0.90 and put up with the endless whirring of the autoclaves. A special thanks as well to all the students of the CCI who worked in the labs and offices in Main Building and the TRH, the support of many of whom has been invaluable.

Finally, I would like to thank my family, who have supported me constantly throughout my life, for which I am immensely grateful.

Table of Contents

1 Introduction

1.1 Introduction to Catalysis

The term catalysis was first coined in 1836 by the Swedish chemist Jöns Jacob Berzelius, when he described 'catalytic power' as the action of one chemical body causing decomposition or forming new compounds from another body, which itself does not become a part of.[1]
The scientific canon has progressed greatly since then, and catalysis is now better described as an increase in the rate of a chemical reaction, without affecting the overall change in standard Gibbs energy of the reaction, using a catalyst.
The phenomenon of catalysis can be described with the Arrhenius equation. (Equation 1.1)

Eq. 1.1

$$k = Ae^{\frac{-E_a}{RT}}$$

k = rate constant
A = pre-exponential factor
E_a = activation energy (J mol^{-1})
R = universal gas constant (8.314 J K^{-1} mol^{-1})
T = temperature (K)

In a chemical reaction, a catalyst acts by decreasing the activation energy of a given reaction pathway, often by providing an alternative and lower energy mechanism for the transformation to occur. This alternative pathway may result in a greater number of reaction intermediates or transition states than the original uncatalysed pathway. Consequently, a chemical reaction through this new pathway happens more readily, at an increased rate of reaction. This is shown in Figure 1.1.

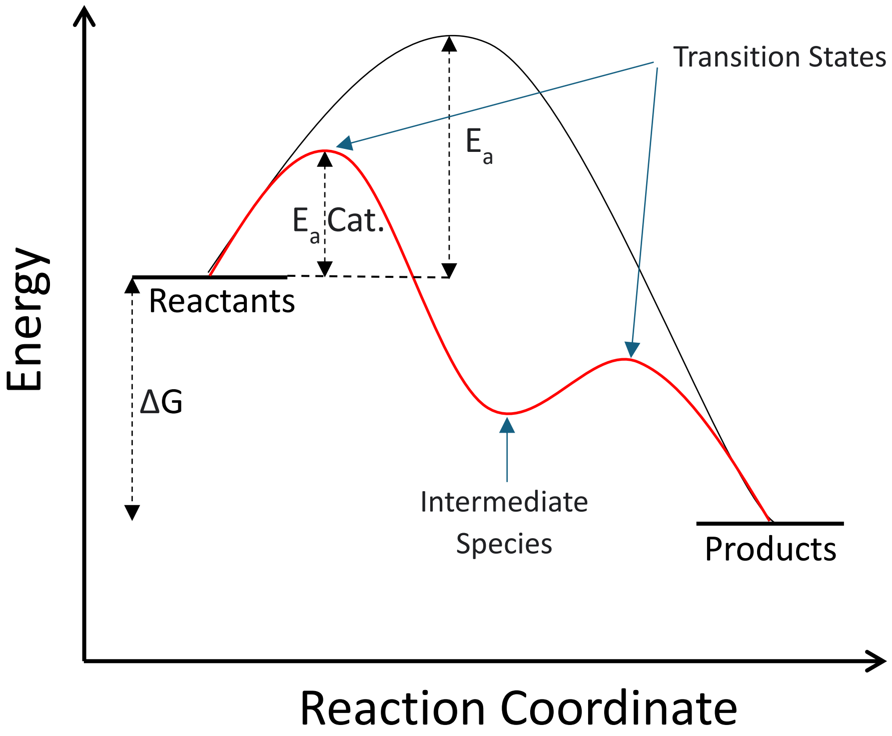

Figure 1.1. Schematic energy diagram for a catalysed versus uncatalysed reaction of A + B → C.
E_a = activation energy of uncatalysed reaction
E_a Cat. = activation energy of catalysed reaction
ΔG = change in Gibbs free energy of the reaction

As shown in Figure 1.1, in an uncatalyzed chemical reaction, a large activation energy (E_a) might limit the rate of reaction even if the change in Gibbs free energy of the reaction is highly favourable. The addition of a catalyst may enhance this rate of reaction by providing an alternative reaction pathway with a lower activation energy, which is therefore more kinetically favourable. It is this decrease in the activation energy for the catalysed reaction relative to that of the uncatalyzed reaction by which a catalyst increases the rate of a chemical reaction. The overall Gibbs free energy of the reaction is unchanged by the action of the catalyst, and catalysis does not influence the thermodynamics of the reaction but is instead a kinetic phenomenon.
The change in Gibbs free energy associated with a given chemical reaction is defined in Equation 1.2.

Eq. 1.2 $$\Delta G = \Delta H - T\Delta S$$

ΔG = change in Gibbs free energy
ΔH = change in enthalpy
T = temperature
ΔS = change in entropy

The change in Gibbs free energy associated with a chemical reaction describes the susceptibility of that reaction to occur spontaneously, with negative values of ΔG indicating a thermodynamically favourable reaction. Additionally, if a given chemical reaction has a negative ΔG value, it may still proceed slowly due to a high activation energy, and is thus kinetically slow, despite being thermodynamically favourable.

It is difficult to understate the significance of catalysis on modern society, with catalytic processes responsible for significant advances in a diverse array of fields, including materials manufacturing, agriculture, technology, automotives, etc. Moreover, of the $4trillion collected in global revenue by the chemical industry in 2019, approximately 85% involved catalysis at some level.[2] Consequently, researchers have conducted significant amounts of research into developing new catalysts and improving existing catalytic processes.

1.1.1 Green Chemistry

The development and utilisation of catalysis in industry represents one of the core pillars of 'Green Chemistry', which is defined as the 'design of chemical products and processes to reduce or eliminate the use and generation of hazardous substances'.[3]

The concept of Green Chemistry was first envisioned by Paul Anastas and Nicolas Eghbali in 1998 as a framework for scientists to use when approaching the design of chemical reactions in order to deliver more environmentally benign and sustainable processes.[4] Moreover, with a rapidly growing global population and the effects of anthropogenic climate change becoming increasingly apparent, the advancement and development of sustainable and environmentally benign chemical processes through catalysis is of paramount importance. Green Chemistry is divided into 12 principles which were described by Anastas and Eghbali and are outlined as follows:[3]

1. **Prevention.** Preventing the formation of waste is easier than cleaning up waste that has already been produced.
2. **Atom Economy.** Chemical synthesis should aim to incorporate all materials utilised into the final product.
3. **Less Hazardous Chemical Synthesis.** Chemical synthesis should be designed to utilise and produce substances that pose minimal or no toxicity to human health or the environment.
4. **Designing Safer Chemicals.** New chemical products should be designed, whilst both maintaining their efficacy and reducing toxicity.
5. **Safer Solvents and Auxiliaries.** Auxiliary substances in chemical processes, such as solvents and separating agents, should be made unnecessary when possible and should be benign.
6. **Design for Energy Efficiency.** Energy requirements for chemical processes should be minimized, and wherever possible chemical synthesis should be conducted under ambient conditions.

7. **Use of Renewable Feedstocks.** Chemical feedstocks should be supplied by renewable sources and no deplete finite stocks wherever possible.
8. **Reduce Derivatives.** Derivatization, which requires additional reagents and waste production should be avoided wherever possible.
9. **Catalysis.** The use of catalytic reagents is superior to stoichiometric reagents.
10. **Design for Degradation.** Chemical products should be designed to degrade after use into benign compounds, rather than remain in the environment.
11. **Real-Time Analysis for Pollution Prevention.** Development of analytical methods to monitor and control the real-time formation of hazardous substances during chemical processes.
12. **Inherently Safer Chemistry for Accident Prevention.** During chemical processes, substances and the form of substances should be selected in order to prevent or minimize the potential for chemical accidents.

Uniting and quantifying many of these principles in a manner that allows for the environmental costs of individual chemical reactions to be described and compared remains a non-trivial task. To this end, numerous metrics have been employed that attempt to quantify factors such as the overall atom economy or energy intensity associated with a given chemical process.[5] One such metric is the 'environmental factor' (E factor), which expresses the masses of all waste products divided by the masses of the desired products, and thus pertains to the efficiency with which products are produced.[5, 6] This is shown in Equation 1.3.

Eq 1.3
$$E\,factor = \frac{mass\ of\ total\ waste}{mass\ of\ desired\ product}$$

An E factor value of 0 represents a perfectly efficient reaction from the perspective of atom economy, wherein no waste is produced, whilst increasingly greater values indicate greater fractions of waste produced relative to the mass of the desired product. Whilst the E factor does not necessarily encapsulate other aspects of the environmental impacts of a chemical reaction, such as CO_2 production or energy consumption, it is nonetheless an important and widely used method for assessing chemical processes.[6]

Alternative metrics have also been proposed to encapsulate other areas of a reactions 'greenness', such as the 'C factor', which relates the mass of CO_2 produced compared to the mass of products. Additionally, the energy intensity of a process can be defined using an energy intensity quotient (EI), which relates the total energy required for a chemical process to the total mass of desired products that may be generated.[5]

1.1.2 Homogeneous Catalysis

Catalysis can be broadly separated into three distinct categories, homogeneous catalysis, heterogeneous catalysis and bio-catalysis.

Homogeneous catalysts are a class of catalysts in which the catalyst is in the same phase as the reagents, such as a solvated organometallic metal complex in a liquid phase.[7]

Some examples of reactions involving homogeneous catalysts are shown in Table 1.1.

Table 1.1. Examples of chemical reactions utilising homogeneous catalysts.

Reaction	Function	Example Catalyst	Reference
Sonogashira Coupling	Formation of C-C bond	$Pd(PPh_3)_4$ + CuI	[8]
Fenton's Reaction	Formation of oxygen-based radicals from H_2O_2	$FeSO_4$, $CuSO_4$	[9]
Sharpless Epoxidation	Chiral epoxidation of allylic alcohols	$Ti(OCH(CH_3)_2)_4$	[10]

The major strength and diversity in the use of homogeneous catalysts, specifically organometallic complexes, comes from the use of ligands to modulate the catalytic activity of the metal centre. In addition to the electronics of the metal centre itself, the choice of ligands used will have an additional electronic effect, further altering the electronic structure of the metal centre.[7] The steric effect, which arises from the geometric structure of the ligand, will also have a significant effect on the overall reaction and can profoundly influence selectivity.[7]

One major limitation of homogeneous catalysis is the need for the separation of the metal catalyst from final product streams, which incurs additional costs and failure to do so results in metal contamination of products and loss of catalytic material.

1.1.3 Bio-Catalysis

Bio-catalysis is the use of an enzyme as a catalyst in a chemical reaction. Unlike metal-based catalysis, enzymes are often active only for very specific reactions or classes of reactions, examples of which are shown in Table 1.2.

Table 1.2. Examples of enzyme catalysed reactions.[11]

Enzyme Class	Reaction
Alcohol Dehydrogenase	Conversion of alcohol to aldehyde/ketone
Ene Reductase	Reduction of C=C
Peroxide Reductase	Destruction of H_2O_2
Lipase	Hydrolysis of fats

The development and use of biocatalytic reaction pathways have several major advantages over equivalent conventional synthetic chemical reactions. For example, biocatalysts often function under mild conditions and in aqueous media. Moreover, enzymes are often highly stereospecific, which eliminates the need for additional functionalisation or protecting groups to improve product selectivity.[11] This in turn reduces the use of potentially toxic reagents like protecting groups, as well as the costs for their separation from product streams and eventual disposal. Consequently, biocatalysis represents a promising method to deliver highly efficient and sustainable catalytic reactions, however a number of limitations are associated with their use. For example, enzymes typically only function within narrow temperature and pH ranges, with denaturing and deactivation of the enzyme occurring outside of these conditions.[12] Additionally, the production and purification of enzymes is often costly and presents a barrier to their adoption at an industrial scale.[13] Finally, similarly to homogeneous catalysts, enzymes can often require separation from final product steams, adding additional cost to any chemical processes involving the use of enzymes.

1.1.4 Heterogeneous Catalysis

Heterogeneous catalysis is a class of catalysis where the catalyst is in a different phase than the reaction mixture, such as a solid catalyst in a liquid reaction, or a solid catalyst in a gas phase reaction.
Some examples of common processes involving heterogeneous catalysis are shown in Table 1.3.

Table 1.3. Examples of reactions utilising heterogeneous catalysts.

Reaction	Function	Example Catalyst	Reference
Steam Reforming	Synthesis of syngas (H_2 and CO)	Ni/α-Al_2O_3	14
Haber-Bosch Process	Synthesis of NH_3	Fe_3O_4 (magnetite)	15
Hydrocarbon Cracking	Cleavage of C-C bonds in hydrocarbons	ZSM-5	16

Heterogeneous catalysis is reported to proceed through several general possible mechanisms. The Langmuir-Hinshelwood mechanism describes the reaction of two adjacent adsorbed atoms or molecules on the surface of a catalyst.[17, 18] In this mechanism, reactant molecules adsorb onto the surface of the catalyst and dissociate. The dissociated atoms can then react to form a new molecule that can then desorb from the surface of the catalyst.[18] A schematic illustration of this is shown in Figure 1.2, wherein A_2 and B_2 represent generic reactants and AB represents a reaction product.

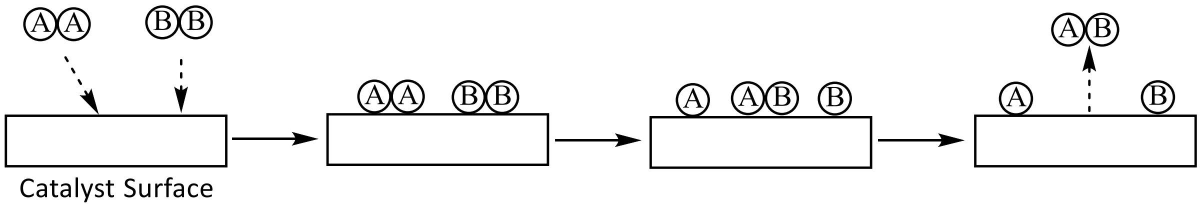

Figure 1.2. Schematic diagram of a bimolecular reaction through the Langmuir-Hinshelwood mechanism.[18]

Secondly, the Eley-Rideal mechanism describes an adsorbed atom or molecule on the surface of a catalyst reacting with another molecule that is in the liquid or gas phase, and not adsorbed in the catalyst surface.[17] This is illustrated in Figure 1.3, wherein A_2 and B_2 represent generic reactants and AB represents a reaction product.

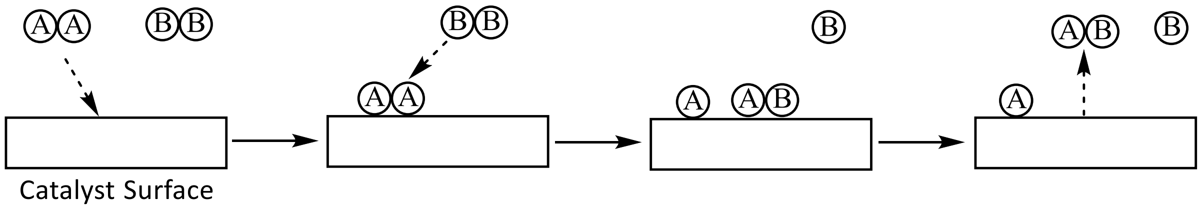

Figure 1.3. Schematic diagram of a bimolecular reaction through the Eley-Rideal mechanism.

Finally, through the Mars-van Krevelen mechanism, an adsorbed species may react with another atom that is incorporated within the lattice structure of the catalyst, which can then be subsequently regenerated by the adsorption of a successive reactant.[17] This is illustrated in Figure 1.4, wherein A_2 represents a generic reactant, B represents an atom incorporated into the lattice structure of the catalyst, and AB represents a reaction product.

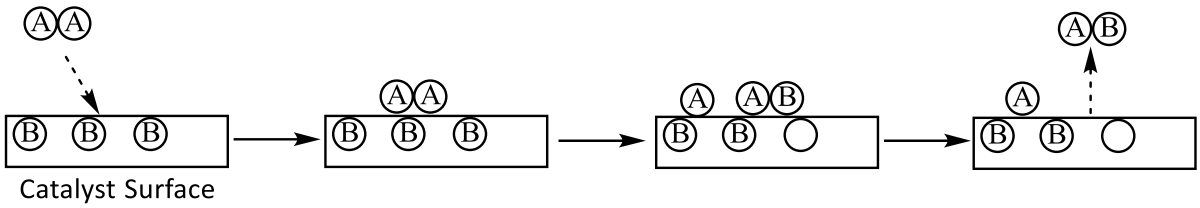

Figure 1.4. Schematic diagram of a bimolecular reaction through the Mars-van Krevelen mechanism.

Unlike homogeneous catalysts, heterogeneous catalysts are in principle easy to remove from final product stream and re-use, although in practice, some limitations are associated with their development and use. For example, the deactivation of a catalyst during its use in a chemical reaction represents a significant challenge for researchers to overcome when designing viable catalysts. Catalysts may undergo deactivation in-situ through numerous mechanisms, such as the poisoning of active sites, coking of the catalytic surface, the aggregation or sintering or nanoparticles, the loss of catalytic metal through leaching, and changes in the oxidation state of catalytic metals.[19] Clearly, losses in catalytic activity as a consequence of their use need to be prevented or limited for a catalyst to truly be reusable. Additionally, achieving high product selectivity can be challenging, and requires careful control to develop efficient reactions. Therefore, the development of heterogeneous catalysts that are not only active, but feature both high selectivity and resistance to deactivation and dissolution remains a key objective for researchers.

1.2 Hydrogen Peroxide

Chlorine containing compounds such as molecular chlorine and sodium hypochlorite are commonly used chemical oxidants in industry due to their high availability, selectivity, and comparatively low cost.[20] However, concerns associated with the release of chlorine containing compounds into the environment and the subsequent formation of carcinogenic compounds has led to efforts to seek alternative chemical oxidants for industrial applications.[20]

For this purpose, hydrogen peroxide (H_2O_2) is an attractive chemical oxidant that offers potential environmental benefits over the use of other stoichiometric oxidants such as chlorine, sodium hypochlorite, permanganate or t-BuOOH. This is because the only side product associated with oxidation by H_2O_2 is H_2O, whereas other agents can often generate potentially toxic by-products that require separation from final product streams, and appropriate storage and disposal. Additionally, H_2O_2 has a very high active oxygen content (% w/w) when compared to many other commonly used chemical oxidants, as shown in Table 1.4.[21]

Table 1.4. Comparison of the active oxygen content and by-products associated with several common oxidants. (Adapted from Campos-Martin *et al.*)[21]

Oxidant	Active Oxygen Content (% w/w)	By-product
H_2O_2	47.1	H_2O
t-BuOOH	17.8	tBuOH
N_2O	36.4	N_2
NaClO	21.6	NaCl
NaBrO	13.4	NaBr

Presently, the vast majority of H_2O_2 consumption arises from the paper bleaching industry, and from chemical synthesis, with some more limited applications found in the textiles industry, as well as wastewater treatment.[22] Currently, the most prominent use of H_2O_2 in chemical synthesis is in the Hydrogen Peroxide Propylene Oxide (HPPO) process, in which propylene is converted into propylene oxide, using H_2O_2 and a TS-1 catalyst,[23] although many other reactions utilising H_2O_2 have been reported in the literature.[22, 24] Some examples of this include cyclohexanone ammoximation,[25] phenol hydroxylation,[26] cyclohexane oxidation,[27] benzyl alcohol oxidation[28] and the oxidation of methane.[29]

1.2.1 Hydrogen Peroxide Production

The isolation of hydrogen peroxide (H_2O_2) was first reported in 1818 by Jacques Louis Thenard,[30] when he reacted barium peroxide with nitric acid to generate H_2O_2.[31] This was subsequently improved by using HCl and H_2SO_4 to give the overall reaction shown in Equations 1.4 – 1.6.[31]

Eq. 1.4 $$BaO_2 + 2HCl \rightarrow BaCl_2 + H_2O_2$$

Eq. 1.5 $$BaCl_2 + H_2SO_4 \rightarrow BaSO_4 + 2HCl$$

Eq. 1.6 $$BaO_2 + H_2SO_4 \rightarrow BaSO_4 + H_2O_2$$

Significant limitations are associated with the reaction created by Thenard, such as high costs, low yields of H_2O_2 and high levels of impurity in product streams.[31]

Since then, many alternative methods to generate H_2O_2 have been investigated by the scientific community, with the anthraquinone autoxidation process representing the most industrially relevant and ubiquitous method.

1.2.2 The Anthraquinone Autoxidation Process

The anthraquinone autoxidation (AO) reaction was first patented in 1939 by IG Farbenindustrie AG.[32] Today, the AO process represents the primary method of H_2O_2 generation and is responsible for over 95% of global production of H_2O_2. [22]

A general schematic for the synthesis of H_2O_2 via the anthraquinone process can be seen in Figure 1.5. Firstly, 2-alkylanthraquinone is hydrogenated, most commonly using an Al_2O_3 or SiO_2 supported Pd catalyst, to form 2-alkylanthrahydroquinone.[21] Following this, the anthrahydroquinone is oxidised in air, through a radical mechanism, to regenerate the anthraquinone and produce a stoichiometric amount of H_2O_2.[21] This process facilitates the production of a solution of H_2O_2 of around 0.8-1.9 wt.%,[21] which is then concentrated through a liquid-liquid extraction to form an aqueous solution of H_2O_2 with a concentration of 15-40 wt.%.[20] Finally, a final concentration of 50-70 wt.% of H_2O_2 is attained through a distillation process, whilst the anthraquinone and supported catalyst can be recycled and used again.[20]

Undesired unselective hydrogenation can also occur, reducing the carbon ring of the anthrahydroquinone. This is shown in Figure 1.6. Because of this over hydrogenation, the anthraquinone carrier molecule must be continually replenished, adding additional cost to the process.

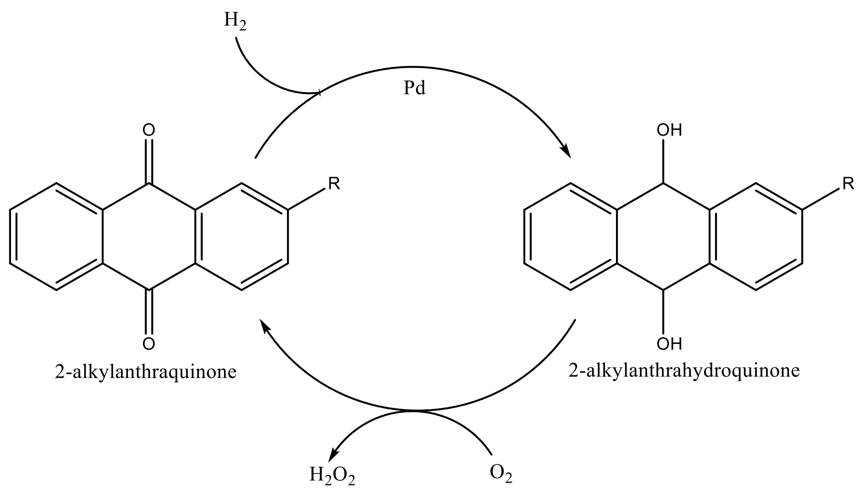

Figure 1.5. Formation of H_2O_2 using the AO method.[21]

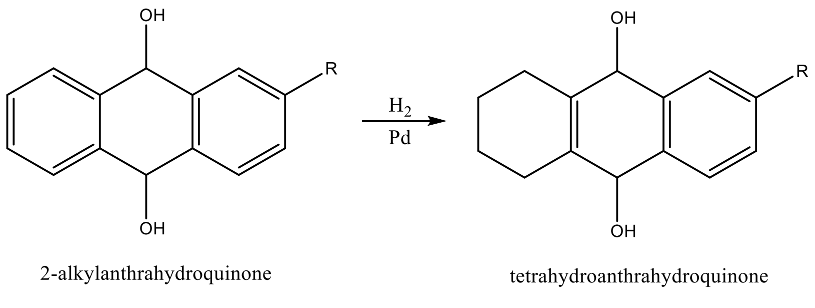

Figure 1.6. Over-hydrogenation of anthrahydroquinone.[21]

Due to decades of use and improvement, the AO process represents a highly efficient and high yield system, capable of generating solutions of H_2O_2 in concentrations of up to 70%, with a selectivity of >99% towards H_2O_2 formation,[20] although some significant limitations are associated with its use. Firstly, the non-selective hydrogenation of anthraquinone and deactivation of the catalyst necessitate their continued and costly replacement, as well as the removal of organic impurities from final product streams.[33] Additionally, high costs associated with the manufacture of H_2O_2 require its production on a large scale at a centralised plant, at concentrations often significantly higher than those required at point of use. The subsequent storage and transportation of highly concentrated H_2O_2 (up to 70 %) poses further safety concerns due to the possibility of explosive decomposition products. To limit the degradation of H_2O_2, stabilising agents such as acetic and phosphoric acid are added to solutions of H_2O_2, which may require removal from final product streams.[34, 35] Additionally, due to the low solubility of the anthraquinone carrier molecule in H_2O, toxic solvents such as benzene or xylene[20] are required, the use of which imparts additional hazards and does not conform with the goals of green chemistry as described in Section 1.1.1. A summary of the advantages and drawbacks associated with the AO process are shown in Table 1.5.

Table 1.5. List of advantages and disadvantages associated with H_2O_2 via the AO process.

Advantage	Disadvantage
Most cost-efficient method of H_2O_2 synthesis (at a large scale)	High plant setup costs require large scale production at localised facilities
Highly selective formation of H_2O_2 (>99 %)[20]	Generates H_2O_2 at higher concentrations than required at point of use
-	Storage and transportation of concentrated H_2O_2 (up to 70 %) carries hazard
-	Additional stabilising agents may require removal from product streams
-	Requires hazardous organic solvents (e.g. benzene, xylene)[20]
-	Deactivation of catalyst and non-selective hydrogenation of the anthraquinone carrier molecule require their costly replenishment

The drawbacks associated with the AO process have led researchers to investigate alternative methods for H_2O_2 production. Examples of this include an H_2/O_2 fuel cell method, an H_2/O_2 plasma method and the direct synthesis from H_2/O_2 using precious metal catalysts.

1.2.3 H_2/O_2 Fuel Cell Method

An alternative method utilises a fuel cell reactor to directly synthesise H_2O_2 from H_2 and O_2 without the two gasses meeting. This method functions by separating an anode and cathode with an electrolyte membrane. H_2 can then be introduced to the anode, and subsequently dissociate to form H^+.

Molecular O_2 is introduced into an electrolyte solution, such as HCl, which the cathode is submerged in. Newly generated H^+ crosses the electrolyte membrane to the cathode and reacts with adsorbed O_2 to form either H_2O_2 or H_2O.[35, 36] This is exemplified in Equations 1.7 – 1.8.

Eq. 1.7 $$O_2 + 2H^+ + 2e^- \rightarrow H_2O_2$$

Eq. 1.8 $$O_2 + 4H^+ + 4e^- \rightarrow 2H_2O$$

Because H_2 and O_2 never physically come into contact, the fuel cell methodology prevents the formation of explosive mixtures of H_2 and O_2 and thus, provides an important safety element when compared to other methods that combine the gasses directly. Additionally, electrical energy can be generated from the reaction system in tandem with the synthesis of H_2O_2.

1.2.4 H_2/O_2 Plasma Method

The H_2/O_2 plasma method often utilises a high-voltage electrode and grounding electrode, separated by a dielectric barrier.[35] The reaction operates by employing a dielectric barrier discharge methodology, wherein a high intensity electric field is generated between the two electrodes, that transforms the reactant H_2 and O_2 gases into a plasma. Collisions with high energy electrons convert H_2 and O_2 into radical species which are reported to directly react form H_2O_2 and H_2O.[35]

It has been proposed that the activation of H_2 into 2 $H^\bullet$ facilitates the formation of H_2O_2 through an $HOO^\bullet$ intermediate, by equations 1.9 – 1.10.[35, 37]

Eq. 1.9 $$H^\bullet + O_2 \rightarrow HO_2^\bullet$$

Eq. 1.10 $$2\ HO_2^\bullet \rightarrow H_2O_2 + O_2$$

However, the activation of O_2 into $O^\bullet$ or O_2^* may results in the formation of H_2O through the formation of $HO^\bullet$ intermediates.[35, 37]

One advantage of the H_2/O_2 plasma method is that H_2O_2 can by synthesised without the need for an expensive precious metal catalyst, or solvent system. However, unlike the fuel cell method, mixtures of H_2 and O_2 gases are highly explosive under typical reaction conditions, for example if H_2 content is between 4-94 % by volume, and O_2 content is between 6-96 %.[35] Therefore, reaction conditions must be carefully controlled and optimised to maximise reaction efficiency whilst working outside the explosive concentration range for H_2 and O_2 mixtures .

1.2.5 Noble Metal Direct Synthesis of H_2O_2

The direct synthesis of H_2O_2 (DSHP) from H_2 and O_2 was originally patented in 1914 by Henkel and Weber, who demonstrated that H_2O_2 could be produced through the reaction of pressurised H_2 and O_2 in water, over a 'suitable catalytic agent', such as palladium or platinum. [38] In more recent years, it has received significant research attention as a possible industrially viable means to generate H_2O_2 at the point of use, and in the required concentrations, circumventing many of the drawbacks associated with the AO process.

The general DSHP reaction can be described through Equations 1.11 – 1.14. [22]

Eq. 1.11	Synthesis: $H_2 (g) + O_2 (g) \rightarrow H_2O_2 (l)$	$\Delta G^o_{298K} = -120.5\ kJ\ mol^{-1}$
Eq. 1.12	Combustion: $H_2 (g) + ½\ O_2 (g) \rightarrow H_2O (l)$	$\Delta G^o_{298K} = -237.2\ kJ\ mol^{-1}$
Eq. 1.13	Decomposition: $H_2O_2(l) \rightarrow H_2O(l) + ½\ O_2 (g)$	$\Delta G^o_{298K} = -116.7\ kJ\ mol^{-1}$
Eq. 1.14	Hydrogenation: $H_2O_2(l) + H_2(g) \rightarrow 2H_2O (l)$	$\Delta G^o_{298K} = -354.0\ kJ\ mol^{-1}$

Fundamental challenges to the reaction are evident from Equations 1.11 – 1.14. Namely, the direct formation of H_2O (via combustion (Eq. 1.12)) is thermodynamically favourable compared to the formation of H_2O_2. In addition to this, further hydrogenation (Eq. 1.14) or decomposition (Eq. 1.13) of H_2O_2 is also thermodynamically favoured, with these competitive pathways further limiting yields of the desired product. As such, high catalyst selectivity towards H_2O_2 formation, with limited activity towards reaction pathways that result in the formation of H_2O are essential for an efficient reaction system. In addition, the direct synthesis of H_2O_2 necessitates the mixing of H_2 and O_2 gas , which are explosive at concentrations between 5-95 % of H_2 in O_2. To mitigate the risk of explosion, dilution of the reactants in an inert gas such as N_2 or CO_2 is necessary, though this is detrimental to the rate of reaction.

It has been proposed that the mechanism of H_2O_2 formation over a heterogeneous catalyst follows a Langmuir-Hinshelwood type mechanism.[35] The first step in this proposed mechanism is the dissociative adsorption of H_2, followed by the sequential addition of surface hydrogen atoms to adsorbed molecular O_2, which has not undergone bond cleavage. A general schematic for this is shown in Figure 1.7.

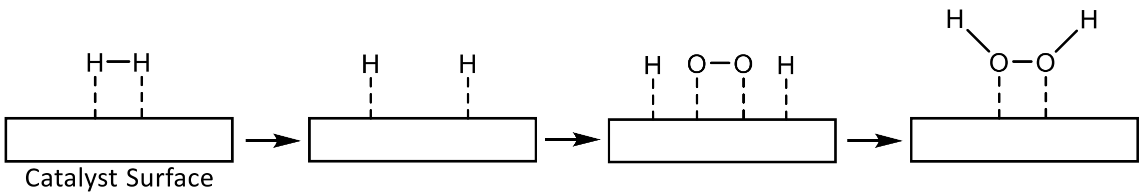

Figure 1.7. General schematic for the proposed Langmuir-Hinshelwood type mechanism for the precious metal catalysed direct synthesis of H_2O_2.[22, 35]

In essence, this mechanism proposes that the formation of H_2O_2 occurs through a two-step hydrogenation of diatomic O_2 by surface H* species, wherein the oxygen-oxygen bond is maintained. Dissociation of the oxygen-oxygen bond results in the formation of H_2O. This absence of an O_2 bond cleavage step for the formation of H_2O_2 has been supported by isotope labelling experiments, wherein a mix of $^{18}O_2$ and $^{16}O_2$ oxygen were used as the oxygen feedstock component for the direct synthesis reaction. No synthesised H_2O_2 species featured both ^{18}O and ^{16}O atoms, which would have required O_2 cleavage to occur.[39] Furthermore, if cleavage of the O_2 bond does occur, it is regarded as irreversible and leads to the formation of the unwanted by-product H_2O.[39-41] Therefore, for a catalyst to be highly selective towards H_2O_2 synthesis, it must have a limited capacity to cleave the O_2 bond, whilst readily dissociating H_2 into 2H*, where * denotes a species adsorbed at a surface.

An alternative mechanism was proposed by Wilson and Flaherty, wherein H_2O_2 is instead formed through a pathway similar to the oxygen reduction reaction.[41] In this mechanism, H_2 undergoes dissociative adsorption, followed the by the loss of an electron by the surface H* species to release H^+. O_2 then adsorbs onto the surface whilst maintaining the O-O bond and is subsequently the target of two sequential proton-electron transfers to form H_2O_2.[41] These elementary steps are shown in Equations 1.15 – 1.18.[41]

Eq. 1.15 $$H_2 + 2^* \rightleftharpoons 2H^*$$
Eq. 1.16 $$H^* \rightleftharpoons H^+ + e^- + {}^*$$

Eq. 1.17 $$O_2 + {}^{**} \rightleftharpoons O_2^{**}$$
Eq. 1.18 $$O_2^{**} + H^+ + e^- \rightleftharpoons OOH^{**}$$
Eq. 1.19 $$OOH^{**} + H^+ + e^- \rightleftharpoons H_2O_2^{**}$$

The occurrence of this mechanism over a Langmurian type pathway is supported by several reaction features. Firstly, the authors cited that the rate of H_2O_2 formation was observed to be dependent on H_2 pressure, but independent of O_2 pressure. Conversely, the Langmurian type model predicts H_2O_2 formation to be independent of H_2 pressure but to be dependent on O_2 pressures.[41] In further support of this mechanism, the authors also investigated the rate of H_2O_2 formation using both protic and aprotic solvents, as shown in Table 1.6.

Table 1.6. Initial rate of H_2O_2 formation using a 3.8%Pd/SiO_2 catalyst and protic or aprotic solvents in a semi-batch reactor. (Adapted from Wilson and Flaherty).[41]

Solvent	Protic/aprotic	Initial Rate of H_2O_2 Formation ($mol_{H2O2}\ mol_{Pd}^{-1}\ s^{-1}$)
MeOH	Protic	1.5×10^{-3}
H_2O	Protic	1.3×10^{-3}
$(CH_3)_2SO$	Aprotic	$<1.7 \times 10^{-6}$
CH_3CN	Aprotic	$<1.7 \times 10^{-6}$

Reaction Conditions: Catalyst (20 mg), solvent (40 mL), reactant gasses (H_2 (4.2 kPa), O_2 (4.2 kPa), and balance N_2) with a flow rate of 60 mL min^{-1}, 295 K, 0 - 0.17 hr

It was reported that the presence of a protic solvent such as H_2O or MeOH was essential for the formation of H_2O_2, whilst the use of an aprotic solvent such as $(CH_3)_2SO$ or CH_3CN resulted in extremely low initial rates of H_2O_2 formation.[41] For example, when MeOH was used as a solvent, the initial rate of H_2O_2 formation was 1.5×10^{-3} $mol_{H2O2}\ mol_{Pd}^{-1}\ s^{-1}$ but when Ch_3CN was instead utilised, the initial rate of H_2O_2 formation was $<1.7\times10^{-6}$ $mol_{H2O2}\ mol_{Pd}^{-1}\ s^{-1}$.
This observation was used to rationalise a proton-electron transfer step as described in Eq 1.15 – 1.19. as opposed to the sequential hydrogenation of O_2 described in the Langmurian

type reaction pathway (Figure), wherein hydrogenation of O_2 would be considered to occur without the involvement of solvated H^+ ions, but by surface H* species. [41, 42]

1.2.5.1Pd Based Catalysts in the Direct Synthesis of H_2O_2

Pd based catalysts have been the subject of considerable research efforts, due to their high catalytic activity towards the synthesis of H_2O_2, and many factors in their design have been suggested to be consequential towards the activity and selectivity of the catalyst towards the direct synthesis of H_2O_2. Examples of such factors include the speciation of surface Pd as either Pd^0 or Pd^{2+},[43, 44] the size and dispersion of nanoparticles,[45, 46] and the nature of the support material.[47]

The speciation of surface Pd, as either Pd^{2+} or Pd^0 has received much attention in the literature, and it is still debated as to which is the most active species in the DSHP reaction. Moreover, the oxidation state of Pd is liable to change over the course of a reaction, given the high pressure H_2/O_2 environment, meaning that analysis of pre, in-situ and post-reaction catalysts are required for a more complete picture of the effects of Pd speciation. It has been reported that PdO has a lower ability to degrade H_2O_2 compared to metallic Pd^0, and thus PdO catalysts exhibit higher H_2O_2 productivities and H_2 selectivities relative to Pd^0.[44, 48, 49]
For example, Choudhary *et al.*[48] compared the catalytic activity of different 5 wt.% Pd/carbon catalyst towards the direct synthesis and degradation of H_2O_2, wherein the Pd/carbon catalysts had either only Pd^0 present, or a mixture of Pd^0 and Pd^{2+}. The Pd^{2+} had been generated on a given catalyst through pretreatment with an oxidizing agent, such as $HClO_4$ or H_2O_2, and the catalytic activity of the resultant catalysts as reported by the authors are shown in Table 1.7.

Table 1.7. Comparison of the Phases of Pd Present (Pd^0/PdO) with the resultant catalytic activity of 5 wt.% Pd/carbon catalysts towards the direct synthesis and degradation of H_2O_2. (Adapted from Choudhary *et al.)*[48]

Oxidizing Agent	**Phases of Pd Present**	**H_2O_2 Yield (%)**	**H_2 Conversion (%)**	**Rate Constant for H_2O_2 Decomposition (min^{-1}) x10^3**
None	Pd^0	0.0	37.8	84.2
$HClO_4$ (1.0 M)	Pd^0,PdO	7.9	53.4	9.4
H_2O_2 (30 wt.%)	Pd^0,PdO	4.6	70.9	2.1

Direct synthesis reaction conditions: Catalyst (500 mg), acidified H_2O (150 mL, 0.02 M H_2SO_4), H_2 in O_2 (2.8 vol%, 11.5 mL min^{-1}, 1 atm), 22 °C, 3 hr.
Decomposition reaction conditions: Catalyst (200 mg), acidified H_2O (150 mL, 0.02 M H_2SO_4), H_2O_2 (6 mL, 5 wt/V%), 22 °C

The authors reported that when only Pd^0 was present, the Pd/carbon catalyst was unable to synthesise H_2O_2, and the decomposition of H_2O_2 was greatly favoured. However, when a mixture of Pd^0 and PdO were present, through oxidation of the catalyst by either $HClO_4$ or H_2O_2, the rate of H_2O_2 decomposition was greatly reduced, and H_2O_2 was generated in-situ.

For example, the Pd/carbon catalyst that was oxidised by $HClO_4$ offered an H_2O_2 yield of 7.9%, and a rate constant towards the decomposition of H_2O_2 or $9.4x10^3$ min^{-1}, compared to the $84.2x10^3$ min^{-1} offered by the Pd catalyst that had not been oxidised and had no PdO initially present.
This finding is in agreement with DFT calculations which have determined that reactions on the Pd^0 (111) surface favour formation of H_2O, whereas the PdO (101) surface has a much lower ability to undertake the relevant side reactions that lead to H_2O formation, such as O_2 and H_2O_2 bond scission.[50]

Conversely, Ouyang *et al.* reported that reduced Pd^0 sites can be oxidised in-situ to PdO, forming mixed interfaces of Pd and PdO.[43] In this study, a range of 1-5 wt.% Pd/TiO_2 catalysts were compared for H_2O_2 synthesis, with nanoparticle size kept constant (ca. 2.4 nm). Catalytic data as reported by the authors is shown in Table 1.8.

Table 1.8. Comparison of the catalytic activity towards the direct synthesis of H_2O_2, and the ratios of surface Pd^0: Pd^{2+} present on a series of 1-5 wt.% Pd/TiO_2 catalysts. (Adapted from Ouyang *et al.*)[43]

Catalyst	Mean Pd Nanoparticle Diameter (nm)	Dispersion (%)	Surface Concentration of Pd^0 (%)	Surface Concentration of Pd^{2+} (%)	H_2O_2 Productivity (mol_{H2O2} g_{Pd}^{-1} h^{-1})	H_2O_2 Selectivity (%)
1%Pd/TiO_2	2.2	51	52.4	47.6	2.99	61
3%Pd/TiO_2	2.2	48	57.7	42.3	1.92	45
5%Pd/TiO_2	2.5	45	64.8	35.2	1.24	41

Reaction Conditions: Catalyst (50 mg), acidified EtOH (60 mL, conc. H_2SO_4 0.38 mL), O_2:H_2:N_2 (36:9:15, 60 mL min^{-1}, 1 atm), 10 °C, 0.5 hr

From the findings presented in Table, it was determined that both H_2O_2 selectivity and activity were significantly enhanced at lower Pd loadings, where the ratio of Pd^0: Pd^{2+} was closer to 1 (i.e., an equal ratio of both oxidation states). At higher metal loadings, where the ratio of Pd^0: Pd^{2+} was increasingly greater than 1, H_2O_2 synthesis was more limited.[43] For example, the 1%Pd/TiO_2 catalyst offered a productivity of 2.99 mol_{H2O2} g_{Pd}^{-1} hr^{-1} and had a surface concentration of Pd^0 or 52.4 %, whilst the 5%Pd/TiO_2 catalyst offered a productivity of 1.24 mol_{H2O2} g_{Pd}^{-1} hr^{-1} and had a surface concentration of Pd^0 or 64.8 %. Additionally, Pd nanoparticles were approximately equivalent sizes regardless of metal loading, confirming that nanoparticle size effects were not influencing catalytic activity, whilst only a modest decrease in Pd dispersion of 6% was observed when the metal loading was increased from 1 – 5%. Regardless, the authors did not attribute the observed changes in catalytic activity to an effect of Pd dispersion, but instead that altering Pd loading directly modulated the speciation of Pd and that H_2O_2 formation may occur most preferentially at the interfaces between Pd^0 and PdO.[43]

Additionally, Liu *et al.* showed that PdO/SiO_2 was almost entirely inactive in the synthesis of H_2O_2, and required an in-situ pre-reduction step that resulted in a reduction of 30% of surface PdO to Pd^0, in order for activity towards the synthesis of H_2O_2 to occur.[51] Moreover, Flaherty and co-workers reported that PdO nanoparticles exhibited an induction period of approximately 30 minutes before H_2O_2 synthesis occurred, whereas Pd^0 nanoparticles could catalyse H_2O_2 formation immediately.[52]

There can also be a contribution from homogeneous and colloidal Pd that has been removed from the surface of its supporting material, due to reaction conditions that promote Pd dissolution. For example, Chinta *et al.* investigated a 5 wt.% Pd supported on microspheroidal silica in an aqueous solution of HCl and NaBr, for catalytic activity towards the direct synthesis of H_2O_2.[40] The authors reported that leached Pd species were present as $PdCl_4^{2-}$ and colloidal Pd in the working solution, due to dissolution of Pd from the silica support, and further investigation revealed that colloidal Pd was the active species in the reaction. Based on previous literature,[53] the authors proposed that this reaction pathway operated through the cycling of colloidal Pd to $PdCl_4^{2-}$, wherein O_2 and $2Cl^-$ coordinate to Pd, before the peroxy species is protonated by HCl to generate H_2O_2. Subsequent reduction of $PdCl_4^{2-}$ regenerates the original colloidal Pd.[40] This is shown in figure.

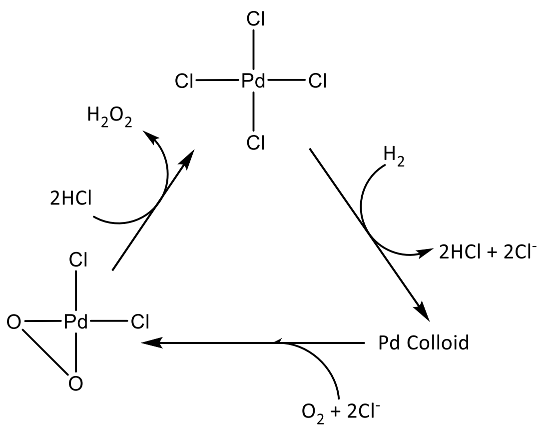

Figure 1.8. Proposed mechanism for the synthesis of H_2O_2 via colloidal palladium.[40]

The size and dispersion of Pd nanoparticles has also been demonstrated to be a significant factor towards the selectivity of the catalyst towards the synthesis of H_2O_2. Tian *et al.*[54] examined a series of 0.5-5 wt.% Pd/hydroxyapatite (Hap) catalysts for a correlations between the mean nanoparticle size and selectivity towards H_2O_2 synthesis, the results of which are shown in Table 1.9.

Table 1.9. Comparison of the mean nanoparticle size and H_2O_2 selectivity of 0.5-5 wt.% Pd/HAp catalysts in the direct synthesis of H_2O_2 reaction. (Adapted from Tian *et al.*)[54]

Catalyst	Mean Nanoparticle Size (nm)	H_2 Conversion (%)	H_2O_2 Selectivity (%)	H_2O_2 Productivity ($mol_{H2O2}\ g_{Pd}^{-1}\ hr^{-1}$) x$10^{-3}$
0.5%Pd/HAp	1.6	2.1	94	1857
1.0%Pd/HAp	1.9	5.8	67	1873
3.0%Pd/HAp	2.5	15.5	45	1126
5.0%Pd/HAp	2.6	17.8	43	741

Reaction Conditions: Catalyst (50 mg), acidified EtOH (60 mL, 0.36 mL H_2SO_4), H_2:O_2:N_2 (9:36:15, 60 mL min^{-1}, 1 atm), 10 °C, 1000 rpm, 0.5 hr.

The authors suggested that the mean Pd nanoparticle size was a significant factor in dictating the selectivity of the catalyst towards H_2O_2 synthesis. For example, the 0.5%Pd/HAp catalyst, which had a mean nanoparticle size of 1.6 nm offered an H_2O_2 selectivity of 94 %, whereas the 5.0%Pd/HAp catalysts which had mean nanoparticle size of 2.6 nm, offered an H_2O_2 selectivity of 43 %. The apparently high selectivity associated with smaller Pd nanoparticles was attributed to an observed positive charge ($Pd^{\delta+}$) that accompanied smaller nanoparticles, which was suggested to suppress the dissociative adsorption of O_2, which leads to H_2O formation.[54]

More recently, Yu *et al.*[45] reported the synthesis of highly active and selective single-atom palladium catalysts for use in the direct synthesis of H_2O_2. The authors compared the catalytic activity of a 0.05wt.% PdO/TiO_2 catalyst (containing single-atom Pd sites) and a range of 0.5-3.0 wt.% Pd/TiO_2 catalyst (containing Pd nanoparticles) and found that the single-atom Pd catalyst was able to generate significantly higher yields of H_2O_2 at >99 % selectivity. For example, the 0.05%Pd/TiO_2 catalyst offered an H_2O_2 yield of 108 $mol_{H2O2}\ g_{Pd}^{-1}\ hr^{-1}$ at >99 % selectivity towards H_2O_2, whereas a 1 wt.% and 2 wt.% Pd/TiO_2 only offered H_2O_2 yields of 7.9 and 5.3 $mol_{H2O2}\ g_{Pd}^{-1}\ hr^{-1}$ respectively, at an H_2O_2 selectivity of 58 and 50 %. To rationalise these observations, the authors used DFT calculations and reported that on single-atom Pd sites (relative to Pd ensembles), the cleavage of the O_2 bond is greatly inhibited, whilst the activation of O_2 to form OOH* and H_2O_2 is promoted.[45]

1.2.5.2 Bi- and Tri-metallic Pd Based Catalysts in the Direct Synthesis of H_2O_2

Whilst supported Pd nanoparticle catalysts have received much attention in the literature, in order to generate H_2O_2 at high selectivity, acidic conditions and the presence of halide counterions (Cl^-, Br^-) are typically required.[55] This limits the potential for the industrial use of Pd catalysts because acidic reaction conditions may promote the leaching of catalytic metal, necessitating the costly replacement of catalysts, whilst additional halide counterions would likely require removal from any product streams, incurring additional costs. As a consequence, researchers have focussed on incorporating secondary and tertiary metals into Pd based catalysts in order to improve catalytic yields and selectivity towards H_2O_2 formation, with many bi- and tri-metallic analogues being reported in the literature, such as AuPd,[56] RuPd,[57] NiPd[58] and AuPdPt.[59]

Early works by Landon *et al.* compared the catalytic activity of (5 wt.%) Au, Pd and AuPd/Al_2O_3 catalysts towards the direct synthesis of H_2O_2, the results of which are shown in Table 1.10.[60]

Table 1.10. Comparison of Pd, Au and AuPd/Al_2O_3 catalysts towards the direct synthesis of H_2O_2. (Adapted from Landon *et al.*)[60]

Catalyst	H_2 Conversion (%)	H_2O_2 Selectivity (%)	Rate of H_2O_2 Formation (mol_{H2O2} kg_{cat}^{-1} hr^{-1}) $x10^{-3}$
5%Pd/Al_2O_3	80	1	1530
5%Au/Al_2O_3	6	53	370
2.5%Au-2.5%Pd/Al_2O_3	63	14	4460

Reaction Conditions: Catalyst (5 mg), MeOH (5.6 g), H_2O (2.9 g), 5%H_2/CO_2 (382 psi), 25%O_2/CO_2 (153 psi), 2 °C, 0.5 hr

From this work, the authors demonstrated that whilst a Pd/Al_2O_3 catalyst offered a greater rate of H_2O_2 formation than the analogous Au/Al_2O_3 catalyst, at $1530x10^{-3}$ and $370x10^{-3}$ mol_{H2O2} kg_{cat}^{-1} hr^{-1} respectively, the AuPd/Al_2O_3 catalyst offered the highest rate of H_2O_2 formation, of $4460x10^{-3}$ mol_{H2O2} kg_{cat}^{-1} hr^{-1}.[60] Also of significance was the enhanced H_2O_2 selectivity of the AuPd catalyst (14 %) compared to the Pd/Al_2O_3 catalyst (1 %), which demonstrated that incorporating secondary metals alongside Pd may be capable of enhancing the selectivity of the catalyst towards H_2O_2 formation.[60]

The works of Edwards *et al.* investigated the incorporation of Au into Pd catalysts further, wherein the authors demonstrated that a (5 wt.%) AuPd/TiO_2 catalyst could achieve over double the H_2O_2 productivity (64 mol_{H2O2} kg^{-1}_{cat} hr^{-1}) value that could be achieved by a 5% Pd/TiO_2 catalyst (31 mol_{H2O2} kg^{-1}_{cat} hr^{-1}), and that the equivalent 5% Au/TiO_2 catalyst was almost entirely inactive.[56, 61] This trend was replicated on Al_2O_3, carbon, SiO_2 and α-Fe_2O_3 supports, demonstrating the applicability of utilising Au and Pd catalysts across a range of support materials.[56, 62] Comparisons of each Pd and AuPd catalyst from these earlier works of Edwards *et al.* towards the direct synthesis of H_2O_2 are shown in Table 1.11. In their work, the authors reported that AuPd nanoparticles supported on carbon offered the greatest catalytic activity of any supported catalyst, with a productivity of 110 mol_{H2O2} kg^{-1}_{cat} hr^{-1}. The authors attributed the enhanced catalytic activity of the carbon supported catalyst to a more favourable surface composition and size distribution of nanoparticles. Namely, AuPd nanoparticles were larger and present as random alloys, compared to the TiO_2 and Al_2O_3 supported catalysts, which featured smaller nanoparticles that were present as core-shell structures.[56]

Table 1.11. Comparison of AuPd catalysts using different support materials towards the direct synthesis of H_2O_2. (Adapted from Edwards *et al.*)[56]

Catalyst	Productivity ($mol_{H2O2}\ kg^{-1}_{cat}\ hr^{-1}$)
5%Pd/Al_2O_3	12
2.5%Au-2.5%Pd/Al_2O_3	18
5%Pd/TiO_2	21
2.5%Au-2.5%Pd/TiO_2	64
5%Pd/Carbon	42
2.5%Au-2.5%Pd/Carbon	110
2.5%Au-2.5%Pd/SiO_2	48
5%Pd/α-Fe_2O_3	4
2.5%Au-2.5%Pd/α-Fe_2O_3	16

Reaction Conditions: Catalyst (5 mg), MeOH (5.6 g), H_2O (2.9 g), 5%H_2/CO_2 (382 psi), 25%O_2/CO_2 (153 psi), 2 °C, 0.5 hr.

The origin of this synergistic effect remains the subject of considerable debate, with factors such as electronic effects and nanoparticle morphology receiving particular attention. In one study, Han *et al.* investigated the effects of the addition of Au to Pd nanoparticles towards the direct synthesis of H_2O_2 using a series of AuPd/SiO_2 catalysts with varying molar ratios of Au and Pd.[63] Several of the molar ratios of Au: Pd and the corresponding rate and selectivity of H_2O_2 formation as reported by the authors are shown in Table 1.12.[63]

Table 1.12. The effects of Pd: Au ratio of a AuPd/SiO_2 catalyst ([Pd]: 3.3 wt.%, [Au]: 0.37 – 19.2 wt.%) on the rate and selectivity of H_2O_2 formation in the direct synthesis of H_2O_2. (Adapted from Han *et al.*)[63]

Surface ratio of Pd: Au (molar ratio Pd/Au)	Rate of H_2O_2 Formation ($mol_{H2O2}\ g_{Pd}^{-1}\ hr^{-1}$)	H_2O_2 Selectivity (%)
Only Pd	0.99	12
3.6/1	1.70	52
2.4/1	1.82	51
1/1.2	1.89	59
1/1.5	0.87	62

Reaction Conditions: Catalyst (50 mg), acidified EtOH (100 mL, HCl 0.12 M), O_2/H_2 mixture (4:1, flow rate 50 mL/min, 1 atm), 10 °C, 5 hr.

The authors reported that an optimal ratio of Au: Pd existed that offered the greatest rate of reaction towards the formation of H_2O_2. From the catalysts examined by the authors, the optimal surface ratio of Pd: Au was determined to be 1/1.2, which resulted in a rate of H_2O_2 formation of 1.89 $mol_{H2O2}\ g_{Pd}^{-1}\ hr^{-1}$. Increasing or decreasing the molar ratio of Pd away from this value resulted in a decrease in the rate of H_2O_2 synthesis. Additionally, the authors observed an increase in H_2O_2 selectivity as the ratio of Au increased, from 51% to 62% when the surface ratio of Pd/Au changed from 2.4/1 to 1/1.5. To rationalise these observations, the authors suggested that two factors were likely contributing to the observed trends in catalytic activity for the AuPd catalysts. Firstly, the transfer of electron density from Au sites to adjacent Pd sites was observed through CO-DRIFTS and XPS analysis, confirming the electronic modulation of Pd sites and likely leading to a suppression in the cleavage of the O_2 bond known to lead to H_2O formation.[63] Secondly, a change to the surface composition of the catalyst through the incorporation of increasing levels of Au resulted in a loss of Pd sites which are responsible for the cleavage of the O_2 bond and subsequent formation of H_2O.[63]

In addition to this, DFT calculations have supported the suggestion that surface morphological features likely play a role in the enhanced activity and selectivity associated with AuPd nanoparticles, when compared to Pd nanoparticles.[64, 65]
When compared to a mono-Pd surface, computational modelling has shown adjacent Pd and Au sites to inhibit the crucial O_2 bond scission step, which leads to H_2O formation. This was explained by the weakness of the Au-O bond relative to the O-O bond, and the comparatively stronger Pd-O bond, which overall causes oxygen desorption to be favoured over oxygen dissociation at mixed Au-Pd sites.[65] Therefore, mixed Pd and Au sites were proposed to be an origin of the enhanced observed selectivity towards H_2O_2, through the inhibition of the formation of H_2O.[64]

In addition to the attention given to the alloying of Au and Pd nanoparticles, numerous other bimetallic catalysts have been synthesised and tested for catalytic activity towards the direct synthesis of H_2O_2. For example, Choudhary *et al.*[66] and Ntainjua *et al.*[57] have previously investigated the effects of Ru incorporation into Pd catalysts towards the direct synthesis of H_2O_2. Firstly, Choudhary *et al.*[66] determined that the incorporation of Ru into a 2.5%Pd/ZrO_2 catalyst resulted in a decrease in H_2 yield, accompanied by an appreciable increase in both H_2 conversion and decomposition. Conversely, Ntainjua *et al.*[57] observed a promotional effect upon the incorporation of Ru into a Pd/TiO_2 catalyst, as shown in Table 1.13.

Table 1.13. Comparison of the catalytic activity of 5 wt.% Pd, Ru and RuPd/TiO_2 catalysts towards the direct synthesis of H_2O_2. (Adapted from Ntainjua *et al.*)[57]

Catalyst	H_2O_2 Productivity ($mol_{H2O2}\ kg_{cat}^{-1}\ hr^{-1}$)
5%Pd/TiO_2	30
5%Ru/TiO_2	14
2.5%Ru-2.5%Pd/TiO_2	51
0.5%Ru-4.5%Pd/TiO_2	143

Reaction Conditions: Catalyst (10 mg), MeOH (5.6 g), H_2O (2.9 g), 5%H_2/CO_2 (420 psi), 25%O_2/CO_2 (160 psi), 2 °C, 1200 rpm, 0.5 hr.

As shown in Table, both Pd and Ru/TiO_2 catalysts offered low H_2O_2 productivities, of 30 and 14 $mol_{H2O2}\ kg_{cat}^{-1}\ hr^{-1}$ respectively. However, incorporation of both metals on a single support greatly enhanced the level of H_2O_2 synthesis. For example, the 2.5%Ru-2.5%Pd/TiO_2 catalyst offered an H_2O_2 productivity of 51 $mol_{H2O2}\ kg_{cat}^{-1}\ hr^{-1}$, but the 0.5%Ru-4.5%Pd/$TiO_2$ catalyst offered an H_2O_2 productivity of 143 $mol_{H2O2}\ kg_{cat}^{-1}\ hr^{-1}$, demonstrating the ability of small quantities of Ru in conjunction with Pd to greatly promote H_2O_2 synthesis.[57]
Further examples of secondary metals when used in conjunction with Pd reported to have promoting effects towards the direct synthesis of H_2O_2 include Zn,[67] Ni,[68] Ag[69] and Sb.[70]

Similarly to Au, the enhancements towards H_2O_2 synthesis upon incorporation of secondary metals into Pd based catalysts has been suggested to often result from the disruption of contiguous Pd ensembles through the addition of secondary metals to the Pd surface.[22] The presence of contiguous Pd ensembles has been reported to facilitate O_2 bond cleavage, thus leading to the undesired formation of H_2O.[64, 65, 71]

Whilst bimetallic catalysts have received much attention in the literature, a promising method to further enhance catalytic performance has been to dope small quantities of tertiary metals into AuPd catalysts. For example, Edwards *et al.*[72] investigated the effects of the incorporation of Pt at a tertiary metal in a (5 wt.%) AuPd/CeO_2 towards the direct synthesis of H_2O_2. The results of several key catalysts from their investigation are shown in Table 1.14.

Table 1.14. The effects of Pt incorporation in a 5 wt.% AuPd/CeO_2 catalyst towards the direct synthesis and degradation of H_2O_2.(Adapted from Edwards *et al.*)[72]

Concentration of Metal in Catalyst (wt. %)				
Au	**Pd**	**Pt**	**H_2O_2 Prouctivity (mol_{H2O2} kg_{cat}^{-1} hr^{-1})**	**H_2O_2 Degradation (mol_{H2O2} kg_{cat}^{-1} hr^{-1})**
2.50	2.50	0.00	68	145
2.45	2.45	0.10	109	46
2.40	2.40	0.20	170	145
2.28	2.28	0.45	100	459

Reaction Conditions: Catalyst (10 mg), MeOH (5.6 g), H_2O (2.9 g), 5%H_2/CO_2 (420 psi), 25%O_2/CO_2 (160 psi), 2 °C, 1200 rpm, 0.5 hr.

As shown in Table 1.14, when small quantities of Pt were incorporated into the AuPd catalyst, significant enhancements in the H_2O_2 productivity offered by that catalyst were achieved. For example, the AuPd/CeO_2 bimetallic catalyst offered an H_2O_2 productivity of 68 mol_{H2O2} kg_{cat}^{-1} hr^{-1}, but when 0.2 wt.% of Pt was doped into the catalyst, the H_2O_2 productivity was enhanced to 170 mol_{H2O2} kg_{cat}^{-1} hr^{-1}, with no increase in the level of H_2O_2 degradation. Additionally, the authors noted that only specific loadings of Pt (0.2 wt.%) offered optimal levels of H_2O_2 synthesis, and that catalysts containing higher or lower loading were less active towards the synthesis of H_2O_2. This enhanced catalytic activity was attributed to changes in the surface composition of the catalyst, wherein the incorporation of Pt either promoted the formation of Au(core)/Pd(shell) structures, which were suggested to be favourable for the synthesis of H_2O_2, or through a redispersion of surface Pd, caused by the addition of Pt.[72]

1.2.5.3 The Influence of Support Material of Pd Based Catalysts on the Direct Synthesis of H_2O_2

The support material for immobilised nanoparticles may play a significant role in whether the catalyst has a high or low activity. Consequently, many different support materials have been investigated in the direct synthesis of H_2O_2, including many metal oxides,[47, 73] carbons,[47, 74] zeolites[34, 75] and heteropolyacids.[76, 77] Indeed, the support used may have a significant impact on the size and morphology of the supported nanoparticles, which may then influence the overall catalytic activity of the catalyst.[78]

Comparisons of the catalytic activity as reported in the literature of (5 wt.%) AuPd catalysts using a variety of support materials towards the direct synthesis of H_2O_2 are shown in Table 1.15.

Table 1.15. Comparison of the catalytic activity of a number of 5 wt.% AuPd catalyst using different support materials towards the direct synthesis of H_2O_2.

Catalyst	Temp. (°C)	Pressure (psi)	Time (hr)	Solvent	H_2O_2 Productivity (mol_{H2O2} kg_{cat}^{-1} hr^{-1})	Reference
2.5%Au-2.5%Pd/Al_2O_3	2	537	0.5	MeOH/H_2O	15	47
2.5%Au-2.5%Pd/MgO	2	537	0.5	MeOH/H_2O	29	47
2.5%Au-1.8%Pd/ZSM-5	2	537	0.5	MeOH/H_2O	102	74
2.5%Au-1.8%Pd/Y	2	537	0.5	MeOH/H_2O	78	74
2.5%Au-2.5%Pd/TS-1	2	580	0.5	MeOH/H_2O	114	34
2.5%Au-2.5%Pd/TiO_2	2	580	0.5	MeOH/H_2O	64	34
2.5%Au-2.5%Pd/SiO_2	2	580	0.5	MeOH/H_2O	74	34
2.5%Au-2.5%Pd/C	2	580	0.5	MeOH/H_2O	110	76
2.5%Au-2.5%Pd/ $Cs_{2.5}H_{0.5}PW_{12}O_{40}$	2	580	0.5	MeOH/H_2O	236	76

The Hutchings group have previously investigated the effects of support material on the catalytic activity of AuPd nanoparticles.[47, 79] For example, Ntainjua *et al.* prepared a series of 5 wt.% supported AuPd catalysts by a wet co-impregnation methodology and found that there was a strong correlation between the isoelectric point of a given support material and the activity of the catalyst.[47] For example, the authors reported that 2.5%Au-2.5%Pd/carbon and 2.5%Au-2.5%Pd/ TiO_2 catalysts offered H_2O_2 productivity values of 110 and 64 mol_{H2O2} kg_{cat}^{-1} hr^{-1} respectively.[47] Conversely, the 2.5%Au-2.5%Pd/Al_2O_3 and 2.5%Au-2.5%Pd/MgO catalysts investigated offered H_2O_2 productivity values of 15 and 29 mol_{H2O2} kg_{cat}^{-1} hr^{-1} respectively. The authors correlated H_2O_2 productivity of each catalyst with the iso-electric point of the support, namely, catalysts with a low iso-electric point such as SiO_2 and carbon had higher levels of H_2O_2 productivity. This contrasts with catalysts with higher iso-electronic points, such as MgO and Al_2O_3 which both exhibited relatively low levels of H_2O_2 productivity.[47] From this, the authors cited the iso-electric point of the support material as a significant parameter when selecting support materials. However, the authors did not identify a specific mechanism through which this promotion occurs. Instead, they observed that catalyst supports with higher isoelectric values such as Al_2O_3 and MgO also offered significantly greater levels of H_2O_2 hydrogenation compared to the more acidic supported catalysts, including TiO_2 and SiO_2.[47]

In a similar study, Richards *et al.*[79] prepared a series of 1 wt.% supported AuPd catalysts using an excess chloride co-impregnation methodology on a range of metal oxide supports, including TiO_2, SiO_2 and Al_2O_3. When these catalysts were utilised in the direct synthesis of H_2O_2, the authors observed that within their series, in disagreement with the work of Ntainjua *et al.*,[47] there was no correlation between the iso-electronic point of the support and the H_2O_2 productivity offered of a given catalyst. For example, a 0.5%Au-0.5%Pd/TiO_2 catalyst offered a productivity 85 mol_{H2O2} kg_{cat}^{-1} hr^{-1}, whilst the analogous 0.5%Au-0.5%Pd/Al_2O_3 catalyst offered a productivity of 75 mol_{H2O2} kg_{cat}^{-1} hr^{-1}. This observation demonstrates that a wide variety of interlinking factors play a role in determining the activity of a given catalyst, and the authors reported that the choice of support played a key role in controlling Pd nanoparticle size and oxidation state.[79] Overall, given the competing conclusions of the above authors, it is unclear to what extent the iso-electric point of the support material is a significant factor in determining catalytic activity towards the synthesis of H_2O_2.

Beyond metal oxides, zeolites and carbon supports have also been investigated, with TS-1 and ZSM-5 representing common choices for catalyst development.[34, 80-82] Lewis, *et al.*[34] compared the activity of a 5 wt. % AuPd catalyst supported on TS-1 with that of analogous TiO_2 and SiO_2 supported catalysts. When comparing the catalytic activity of each catalyst towards the direct synthesis of H_2O_2, the authors reported that the TS-1 supported AuPd catalyst offered the greatest H_2O_2 productivity (100 mol_{H2O2} kg_{cat}^{-1} hr^{-1}), compared to either the TiO_2 (64 mol_{H2O2} kg_{cat}^{-1} hr^{-1}) or SiO_2 (74 mol_{H2O2} kg_{cat}^{-1} hr^{-1}) supported catalysts. The authors reported that again, the iso-electric point of the support couldn't be cited as the sole factor influencing the catalytic activity, given the almost identical isoelectric points for the SiO_2 and TS-1 supports.[34] Therefore, other factors including the dispersion of Pd, the oxidation state of Pd, and the morphology of nanoparticles must also be considered when selecting support materials for nanoparticle catalysts.

Regarding carbon, whilst it has been reported to be a highly effective support in the direct synthesis reaction,[47, 83, 84] a variety of tuneable factors intrinsic to the carbon material itself can influence the overall activity of the catalyst. For example, Yook *et al.*[74] undertook a systematic investigation into the effects of both the pore structure and surface functionalisation towards catalyst activity and selectivity, using supported AuPd catalysts. The authors found that mesoporous carbons were generally superior to microporous carbons due to diffusion limitations of H_2 entering the micropores, and the increased difficulty for H_2O_2 to leave the micropores, resulting in higher levels of H_2O_2 degradation.[74] Additionally, a high density of oxygen functionalisation on the surface of the carbon was also shown to enhance H_2O_2 synthesis, by promoting the alloying and dispersion of AuPd nanoparticles.[74]

1.2.5.4 The Effects of Halides and Acids Towards the Direct Synthesis of H_2O_2

In order to improve H_2O_2 selectivity above that achievable with a catalyst alone, acids and halides can be added to reaction mixtures, such as Cl^-, Br^-, HNO_3, H_2SO_4, H_3PO_4 and solid heteropolyacids.[85-88] The use of these strong acid promoters is often associated with the

inhibition of H_2O_2 degradation pathways, wherein the excess of H^+ limits the deprotonation of H_2O_2 to the more reactive ^-OOH species, that favour degradation.[52]
In addition to this, halides such as Cl^- or Br^- have been suggested to compete with oxygen for active sites that favour O-O bond scission, thus acting as inhibitors of H_2O formation reaction pathways. [52, 89] Alternatively, it has also been suggested that the electronegative character of halides, such as Cl^-, may allow it to reduce electron back donation from a metal catalyst surface to the oxygen π^* orbitals, thus stabilising the O-O bond and inhibiting bond scission.[90] Other works have suggested that Br^- in particular may have a more complex role in modulating catalytic activity. For example, Centomo *et al.*[91] and Biasi *et al.*[92] have both reported that the presence of Br^- may actively cause the restructuring of catalytic Pd, with the change in Pd morphology often leading to enhancements towards. the synthesis of H_2O_2.
Moreover, it has been reported that in the case of HCl and HBr, the presence of H^+ was required in addition to the halide counterion for any improvements in H_2O_2 selectivity or productivity to occur, alluding to the significance of protons in the direct synthesis reaction.[93]

The concentration of an additive plays a significant role in its effectiveness. At sufficiently high concentrations of inorganic acids, metal leaching can become excessive and limit the selectivity towards H_2O_2 as well as reducing catalyst lifetime.[94] For example, Gallina *et al.*[95] found that by doping in a mixture of H_3PO_4 and NaBr at an optimal concentration into a reaction, synthesis of H_2O_2 could be enhanced, but excessive concentrations of either H_3PO_4 or NaBr would lead to Pd dissolution from the solid catalyst.

In addition to using additives in reaction mixtures, they have been utilised in catalyst pre-treatments to improve reaction selectivity. For example, Edwards *et al*.[96] demonstrated that when TiO_2 was pre-treated with 2 wt.% HNO_3 prior to the immobilisation of AuPd, the catalyst was able to achieve greater selectivity and productivity towards the synthesis of H_2O_2 than the analogous catalyst that had not undergone any pre-treatment. This enhancement was attributed to an observed decrease in mean particle size of AuPd nanoparticles for the pre-treated catalyst, a reduction in large Au rich nanoparticles, and a general improvement in the dispersion of Au within the catalyst, although the author noted that a change in surface acidity of the catalyst could also play a role.[96]

Lewis *et al.*[88] reported a similar observation, wherein improvements in H_2O_2 selectivity and productivity were observed when 5% Pd supported on either carbon, TiO_2 or ZrO_2 was prepared through a wet-impregnation methodology that incorporated dilute HNO_3 in the metal deposition step. When prepared through this methodology, incorporation of HNO_3 during catalyst synthesis greatly improved the distribution of nanoparticle sizes, as well as limiting the reduction of Pd^{2+} species to Pd^0 over the course of a reaction.[88]

1.3 Benzyl Alcohol Oxidation

1.3.1 The Aerobic Oxidation of Benzyl Alcohol

Benzyl alcohol oxidation represents a well-studied model reaction system for the oxidation of alcohols and its reaction products are industrially useful chemicals, such as benzaldehyde, which can be used in pharmaceutical production, plastics and flavourings.[97]
Reagents with high active oxygen content, such as O_2 and H_2O_2 have been an attractive choice of reagent for this reaction, due to a high atom economy and the generation of non-toxic biproducts, compared to conventional stoichiometric oxidants such as dichromate and permanganate, which are both expensive and toxic.[98, 99]

A general scheme of the catalytic oxidation of benzyl alcohol by O_2 is shown in Figure 1.9.

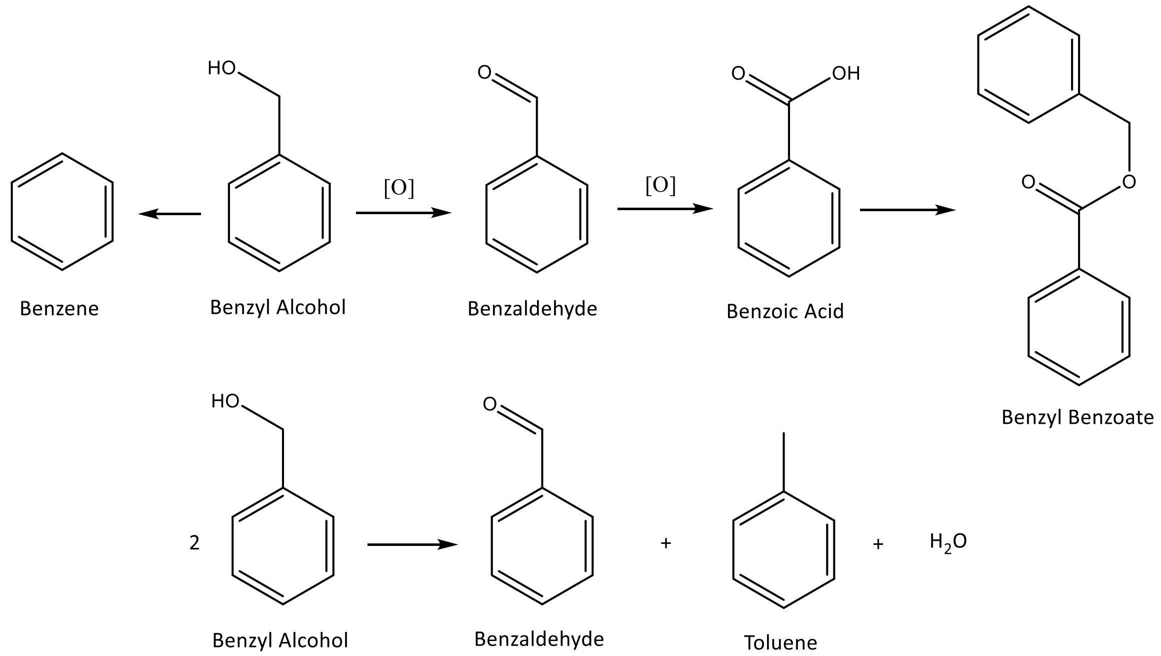

Figure 1.9. General reaction scheme for benzyl alcohol oxidation.[100]

Firstly, benzyl alcohol is catalytically oxidised to benzaldehyde. Subsequent oxidations can also lead to the formation of benzoic acid and benzyl benzoate though it should be noted that the auto-oxidation of benzaldehyde to benzoic acid has been reported to occur at room temperature.[101] Toluene may also be formed, with Sankar *et al.* suggesting that this occurs through a disproportionation reaction that takes place between two molecules of benzyl alcohol.[102] Benzene and dibenzyl ether are also reported products.[103]

The aerobic oxidation of benzyl alcohol has been studied extensively using Pd based heterogeneous catalysts, due to their reported high catalytic activity.[97, 104] Typically, reactions are carried out at temperatures in excess of 100 °C,[97, 105, 106] whilst a variety of solvents have been utilised, including H_2O, cyclohexane and xylene,[97, 107] in addition to solvent free conditions.[101]

1.3.1.1 Proposed Reaction Mechanism

A comprehensive surface-based reaction mechanism for the Pd catalysed aerobic oxidation of benzyl alcohol was proposed by Savara *et al.*[103, 108, 109] The most relevant elementary steps for benzaldehyde, benzoic acid and toluene formation are as follows. (Figures 1.10 – 1.12)

Firstly, the dissociative adsorption of benzyl alcohol adjacent to an adsorbed oxygen atom generates a surface alkoxy intermediate, and subsequent hydrogen abstraction by Pd generates benzaldehyde.

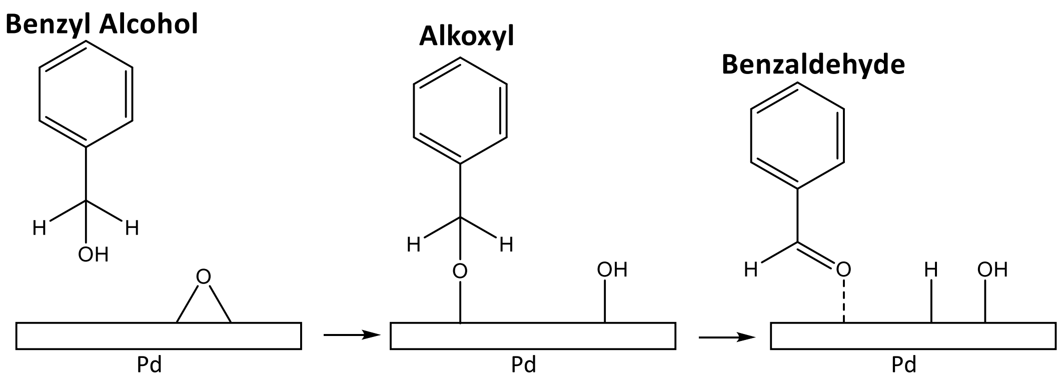

Figure 1.10. Proposed aerobic formation of benzaldehyde from benzyl alcohol.[103]

Conversely, cleavage of the carbon-oxygen bond in the alkoxyl intermediate can occur, creating a surface alkyl intermediate. Combination of a surface hydrogen atom and the alkyl intermediate results in the formation of toluene.

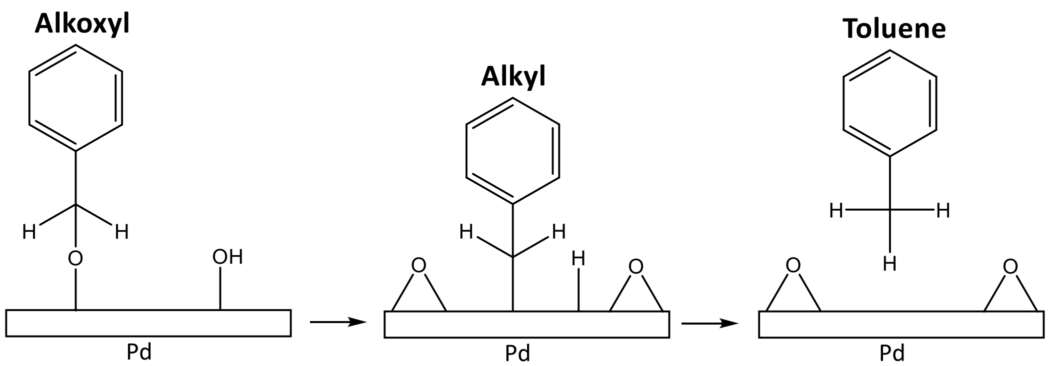

Figure 1.11. Proposed aerobic formation of toluene from benzyl alcohol.[103]

Finally, the postulation of a carbonyloxyl species is invoked to describe the formation of benzoic acid, benzene and benzyl benzoate. This carbonyloxyl intermediate is proposed to form through oxidation of the alkoxyl species, and is ultimately reduced by surface hydrogen to produce benzoic acid.[103] Alternatively, the elimination of CO_2 facilitates the formation of benzene.

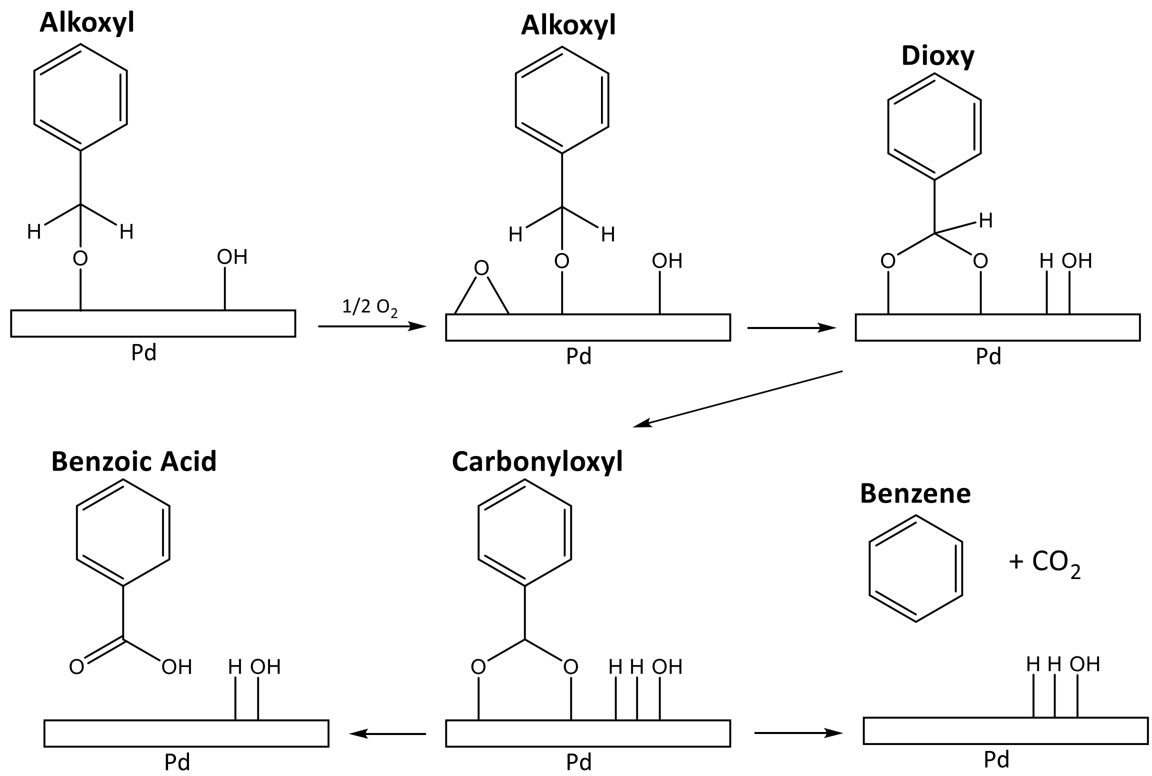

Figure 1.12. Proposed oxidative formation of benzoic acid and benzene from benzyl alcohol.[103]

Interestingly, whilst benzaldehyde readily autooxidises to benzoic acid at room temperature,[101] benzyl alcohol oxidation reactions are often reported to proceed with high selectivity towards benzaldehyde, implying that under the reaction conditions typically employed, this facile autooxidation of benzaldehyde does not readily occur.[101, 110, 111] To investigate this, Sankar *et al.*[101] utilised electron paramagnetic resonance (EPR) spectroscopy to characterise the radical species present during the autooxidation of benzaldehyde. In their work, the authors reported that the addition of small quantities of benzyl alcohol (2 wt.%) to the reaction mixture was able to effectively inhibit the formation of benzoic acid, which they attributed to the interception of intermediate radical species towards benzoic acid formation by benzyl alcohol. Crucially, this radical interception could be performed by alternative chemical species, such as 3-methyl-2butenol and triphenylmethane, which suggested that the chemical moiety responsible for this radical interception was a benzylic or allylic α-hydrogen, acting as an H donor.

1.3.1.2 The Effects of Particle Size of Pd-Based Catalysts

Pd based heterogeneous catalysts have received much attention in the aerobic oxidation of benzyl alcohol, due to their reported high activity and selectivity.[97, 104] Consequently, several properties of supported Pd based catalysts have been a common subject of investigation, namely, nanoparticle size, morphology, secondary metal modifiers and supporting materials.

Li *et al.*[112] have previously investigated the effects of the size of Pd nanoparticles on the aerobic oxidation of benzyl alcohol. The authors prepared a range of size tuned Pd nanoparticle catalysts, supported on an NaX zeolite, with the mean nanoparticle size of each catalyst varied between 2 - 10.5 nm. These catalysts were tested for their activity towards the solvent-free aerobic oxidation of benzyl alcohol, and results from their study are shown in Table 1.16.

Table 1.16. The effects of mean nanoparticle size towards the solvent-free aerobic oxidation of benzyl alcohol using a 1.35 wt.% Pd/NaX catalyst. (Adapted from Li *et al*.)[112]

Mean Nanoparticle Size (nm)	Benzyl Alcohol Conversion (%)	Benzaldehyde Selectivity (%)	Intrinsic TOF (hr^{-1})
2.0	36	95	630
2.8	66	97	2970
5.4	25	94	1550
10.5	8	97	1590

Reaction Conditions: Catalyst (100 mg), benzyl alcohol (48.5 mmol), O_2 (3 mL min^{-1}), 100 °C, 4 hr.

The authors observed that a catalyst with a mean Pd nanoparticle size of 2.8 nm offered the optimal conversion of benzyl alcohol, of 66 %. Larger and smaller nanoparticles offered decreased conversions of benzyl alcohol, such as the catalysts with mean nanoparticle sizes of 2.0 and 5.4 nm, which offered benzyl alcohol conversion of 36 % and 25 % respectively.[112] It was speculated that this apparent size dependence related to the ratios of exposed Pd terraces relative to edge or corner sites. Specifically, the authors speculated that benzyl alcohol may adsorb at Pd terrace sites via an interaction with the π-bonds of the phenyl ring, promoting the formation of a Pd alcoholate species, whereas adjacent edge or corner sites may promote an H-abstraction step to form the carbonyl. Given that an intermediate size of nanoparticle (2.8 nm) was reported to offer the greatest turnover frequency, with a TOF of 2970 hr^{-1}, and that both smaller and larger nanoparticles offered lower TOF values of 630 and 1550 hr^{-1} respectively, the specific morphology of nanoparticles as a result of their size is likely a significant factor in determining overall catalytic activity. This also suggests that the improved Pd dispersion as a result of decreasing Pd nanoparticle sizes does not necessarily lead to enhanced catalytic activity, when compared to nanoparticle size effects.

Chen *et al.*[113] reported similar findings, wherein a range of supported Pd/ SiO_2-Al_2O_3 were prepared with mean nanoparticle sizes between 2.2 and 10 nm. These catalysts were again tested in the solvent-free aerobic oxidation of benzyl alcohol, with nanoparticles in the range of 3.6 - 4.3 nm achieving the highest turnover frequencies of the series. Nanoparticles that exceeded or fell below this range were reported to be far less active in the benzyl alcohol oxidation reaction.[113] Similarly to Li *et al.*,[112] Chen *et al.* also proposed that this size effect may originate from the ratio of Pd terrace and corner or edge sites, with terrace sites responsible for the adsorption of benzyl alcohol via interactions between the phenyl ring and Pd, followed by the formation of a Pd-alcoholate. Corner or edge sites are then suggested to be responsible for an H-abstraction step to form the carbonyl.

Finally, Zhou *et al.*[114] prepared two samples of 5 wt.% Pd supported on organic covalent polymer (COP) and compared their catalytic activity towards the solvent free aerobic oxidation of benzyl alcohol, the results of which are shown in Table 1.17.[114]

Table 1.17. Comparison of mean nanoparticle size towards the solvent free aerobic oxidation of benzyl alcohol using a 5 wt.% Pd/COP catalyst. (Adapted from Zhou *et al*.)[114]

Mean Nanoparticle Size (nm)	Benzyl Alcohol Conversion (%)	Benzaldehyde Selectivity (%)
7.7	32.0	57.1
9.9	21.1	89.8

Reaction conditions: Catalyst (4 mg), benzyl alcohol (100 mmol), O_2 (30 mL min^{-1}), 160 °C, 1 hr

The Pd/COP catalyst with a mean Pd nanoparticle size of 7.7 nm, offered a benzyl alcohol conversion of 32.0 %, with a benzaldehyde selectivity of 57.1 %. Conversely, the Pd/COP catalyst with the larger mean nanoparticle size of 9.9 nm offered a lower benzyl alcohol conversion of 20.1 % with a superior benzaldehyde selectivity of 99.4 %. From these data, the authors noted that the smaller mean Pd nanoparticles could deliver a higher benzyl alcohol conversion, but a reduced selectivity towards benzaldehyde, with toluene constituting the major secondary product.[114] It was suggested that this may have occurred because a greater number of the sites present on the catalyst with smaller nanoparticles favoured a disproportionation reaction between two benzyl alcohol molecules, to form equimolar toluene and benzaldehyde.[114] Conversely, the larger mean Pd nanoparticles had a lower overall conversion but any benzyl alcohol that was converted did so with higher selectivity towards benzaldehyde. The authors concluded that nanoparticle size may have a significant effect on product selectivity, as well as overall catalytic activity.[114]

1.3.1.3 The Effects of Secondary Metals in Pd-Based Catalysts

The incorporation of a secondary metal alongside Pd has been shown to have promoting effects towards the overall catalytic activity in the aerobic oxidation of benzyl alcohol. In particular, supported AuPd bimetallic catalysts represent a well-studied example of this, receiving significant attention in the literature.[111, 115-120]

Dimitratos *et al.*[119] observed significant enhancements towards the oxidation of benzyl alcohol upon the incorporation of both Au and Pd into a bimetallic catalyst. To do this, the authors compared the catalytic activity of 1 wt.% Au, Pd and AuPd catalysts, supported on activated carbon towards the aerobic oxidation of benzyl alcohol. The results of several key catalysts are shown in Table 1.18.

Table 1.18. Comparison of the catalyric activity of 1 wt.% Au, Pd and AuPd/carbon catalysts towards the aerobic oxidation of benzyl alcohol. (Adapted from Dimitratos *et al.*)[119]

Catalyst	Benzyl Alcohol Conversion (%)	Benzaldehyde Selectivity (%)
1%Au/carbon	0	-
1%Pd/carbon	18	91
0.3%Pd/carbon	20	93
0.73%Au-0.27%Pd/carbon	96	94

Reaction conditions: Catalyst (metal/benzyl alcohol = 1/500 mol/mol), benzyl alcohol (0.3 mmol, 0.3 M), H_2O (10 mL), O_2 (1.5 atm), 60 °C, 3 hr, 1250 rpm.

Whilst the Au/carbon catalysts was inactive towards the oxidation of benzyl alcohol under the conditions used in the study, the 1%Pd and 0.3%Pd/carbon catalysts offered benzyl alcohol conversions of 18 % and 20 % respectively. When both metals were used in combination, as in the 0.73%Au-0.27%Pd/carbon catalyst, a benzyl alcohol conversion of 96 % was observed, representing a significant enhancement in catalytic activity over the monometallic analogues. Additionally, the authors reported that the AuPd nanoparticles were random alloys. The origin of this enhancement in catalytic activity was proposed to be related to both geometric and electronic effects associated with the alloying of Au and Pd, such as the occurrence of Au-Pd bifunctional sites, and a change in the inter-atomic distances in AuPd catalysts, compared to monometallic Au or Pd catalysts.

Wu *et al.*[120] also reported a strong synergistic effect when Au and Pd bimetallic nanoalloys are formed. The authors compared a range of mesoporous silica supported AuPd catalysts, with varying ratios of Au and Pd to their monometallic Pd or Au-only analogues. It was reported that the Pd-only catalyst offered a benzyl alcohol conversion of 16 % and a benzaldehyde selectivity of 66.4 %, while the Au-only catalyst converted 4.9 % of benzyl alcohol with a 42.2 % selectivity to benzaldehyde. However, when incorporated together as a bimetallic alloy, catalytic activity could be greatly enhanced, with an $Au_{18}Pd_{82}$ catalyst achieving 96 % conversion of benzyl alcohol at 50.9 % selectivity.[120] It was also observed that an optimal ratio of Au and Pd existed, and deviations from this value reduced overall substrate conversion. To explain this phenomenon, the authors correlated the ratio of Au/Pd in the catalyst with the ratio of PdO/Pd that was present initially in each catalyst and concluded that high catalytic activity could be explained through low levels of surface PdO and conversely high levels of Pd^0 present.[120] Moreover, DFT calculations and XPS data showed that the addition of Au to Pd could stabilise the oxidation state of Pd^0 and prevent the formation of less active PdO sites, which were reported to decrease catalytic activity.[120]

Nanoparticle morphology is also reported to be a factor in catalytic activity, with increases in catalytic activity associated with catalysts featuring core-shell type morphologies.[110, 121] For example, Au(core)/Pd(shell) supported on either TiO_2 or carbon have been reported to have superior turnover frequencies to both a random alloy AuPd and an Au(shell)/Pd(core) type catalyst.[121] Additionally, selectivity towards benzaldehyde was slightly improved for Au(core)/Pd(shell) catalysts compared to the equivalent random alloy analogue, but significant quantities of toluene were still formed for both TiO_2 and carbon supported catalysts.[121] Further to this, Silva *et al.*[122] investigated the effects of AuPd ratio for Au(core)/Pd(shell) nanoparticles in the aerobic oxidation of benzyl alcohol. This was done by synthesising Au nanoparticles, supported on SiO_2 coated Fe_2O_3 cores, and depositing 0-40 mol% of Pd onto the surface of the Au particles, to create a varied level of Pd enrichment whilst maintaining the Au(core) Pd(shell) structure. From this, a maximum conversion of benzyl alcohol (87.7 %) was observed at 10 mol% of Pd, with dramatic decreases in activity at both higher and lower loadings of Pd.[122] For example, when 13 mol% of Pd was incorporated into the catalyst, a benzyl alcohol conversion of 64.6 % was achieved, whilst catalyst incorporating only 7 mol% of Pd offered a benzyl alcohol conversion of 67 %. Notably, the 10 mol% loading of Pd corresponded to the mass of Pd needed to theoretically cover all Au nanoparticles in a Pd monolayer. DFT calculations were used to rationalise this observation, which suggested that a Pd monolayer was favourable because it balanced the adsorption of benzyl alcohol, which was favourable on Pd surfaces, with the desorption of benzaldehyde, which was disfavoured.[122] As increasing layers of Pd were added, then the adsorption of benzyl alcohol became increasingly favoured, but the desorption of products becomes increasingly difficult.[122] Conversely, decreasing Pd loading to a level below 10 mol% disrupted the Pd monolayer, and limited the number of active Pd sites available for catalysis whilst exposing a growing number of much less active Au sites.[122]

1.3.1.4 The Effects of Support Materials Using Pd-Based Catalysts

Many different classes of supports have been investigated for the aerobic oxidation of benzyl alcohol, including metal oxides, zeolites and carbons.[97, 121, 123-126] Indeed, the choice of support material has been shown to have a large influence on the activity of Pd-based nanoparticles in the aerobic oxidation of benzyl alcohol.[97] For example, basic supports have previously been reported to promote hydrogen abstraction, potentially increasing the rate of oxidative hydrogenation of alcohols.[107] One example of this is in the use of basic titanite nanobelts, wherein Lu *et al.*[127] synthesised a series of Pd based catalysts supported on TiO_2 nanobelts and titanite ($CaTiSiO_5$) nanobelts. They found that titanite nanobelts had an almost identical conversion of benzyl alcohol to catalysts supported on TiO_2 nanobelts, but exhibited an almost 100 % selectivity to benzaldehyde, compared to 71.7 % selectivity for TiO_2 nanobelt catalysts. To explain this effect, the author cited the greater basicity of the titanite nanobelt structure as a key factor in suppressing the formation of toluene, whilst promoting the H-abstraction step during the oxidation of the alcohol.[127]

The incorporation of heteroatoms can have a profound effect on the activity of otherwise identical supporting materials, through mechanisms such as enhancements to the metal-support interactions, or by promoting metal nanoparticle dispersion.[97]
In one study Chen *et al*.[128] incorporated N atoms into an SBA-15 mesoporous support, through heat treatment with NH_3. They prepared a series of catalysts in this manner, by altering the heat treatment temperature between 750 and 950 ^{o}C, and observed that the higher temperature treatments caused a greater extent of N incorporation into the support.[128]

Moreover, when Pd was subsequently immobilised through a sol process, supports with a greater N content had correspondingly greater amounts of Pd deposited during the catalyst preparation process. Key catalysts from this investigation are shown in Table 1.19.

Table 1.19. Comparison of the effects of N and Pd content of a Pd/SBA catalyst towards the aerobic oxidation of benzyl alcohol. (Adapted from Chen *et al.*)[128]

Measured N Content of Catalyst (wt.%)	Measured Pd Content of Catalyst (wt.%)	Benzyl Alcohol Conversion (%)	Benzaldehyde Selectivity (%)
0.0	0.60	42.0	85.0
3.6	1.33	55.0	90.2
4.9	1.52	58.9	91.5
13.5	1.88	63.5	93.7

Reaction conditions: Catalyst (40 mg), benzyl alcohol (4 g), O_2 (20 mL min^{-1}), 180 ^{o}C, 3 hr.

As is shown in Table, the conversion of benzyl alcohol and selectivity towards benzaldehyde both increased in correlation with higher Pd and N content. For example, the Pd/SBA catalyst with no N content in the catalyst also had the lowest amount of catalytic Pd present on the catalyst (0.6 wt.%), and the correspondingly lowest conversion of benzyl alcohol (42.0 %). As N content increased, so too did Pd content, leading to a maximum Pd content of 1.88 wt.% and a corresponding benzyl alcohol conversion of 63.5 % associated with that catalyst. This led the authors to conclude that terminal -NH_x functionalities enhanced the levels of Pd loading that could be achieved during the catalyst preparation procedure through the promoting the deposition of Pd, which caused the enhancement in activity.[128] However, TOF values were not reported by the authors and given the differing Pd content of each catalyst, and the previously discussed effects of Pd nanoparticle size and dispersion on catalytic activity, it is difficult to directly compare the catalytic activity of each catalyst.
However,Ji *et al.*[129] compared a Pd/SBA-15 with a Pd/ZrSBA-15 catalyst,wherein Zr atoms had been incorporated into the structure of the SBA-15 support during synthesis. They found that both catalysts had approximately equivalent Pd content, but the ZrSBA-15 supported catalyst has a more favourable dispersion of Pd atoms, loaded into pore channels. Indeed, whilst both catalysts had almost 100 % selectivity to benzaldehyde, the Pd/ZrSBA-15 had an enhanced conversion of benzyl alcohol (95.2 %) compared to the Pd/SBA catalyst (86.3 %), showing that the incorporation of Zr atoms into the support structure had a promoting effect on the dispersion of Pd nanoparticles, which resulted in an enhancement towards catalytic activity.[129]

1.3.2 The Oxidation of Benzyl Alcohol via in-situ H_2O_2 Synthesis

Whilst O_2 represents a promising choice of oxidant, its use typically requires high temperatures for high conversions of benzyl alcohol to be achieved, with reaction temperatures in excess of 100 ^{o}C typical.[105, 109, 118, 120, 130]
An alternative method that has been investigated more recently in the literature involves the use of H_2 in tandem with O_2, using either methanol or water as a solvent, with reactions typically conducted between 30 – 60 ^{o}C.[100, 131] This method generates H_2O_2 in-situ and though

research on this reaction methodology is more limited, it represents a potential method to reduce energy costs associated with running high temperature aerobic oxidation reactions.

Moreno *et al.*[115] compared the conversion of benzyl alcohol offered when using a series of 2.5 wt.% AuPd/TS-1 catalysts with varying Ti/Si ratios present in the support, under both aerobic conditions and using H_2 and O_2 in tandem. When these catalysts were utilised at 30 ^oC, the authors reported moderate enhancements towards the conversion of benzyl alcohol when H_2 and O_2 were used in tandem than compared to the aerobic conditions. Examples of this are shown in Table 1.20.

Table 1.20. Comparison of the catalytic activity of 2.5%AuPd/TS-1 catalysts towards the oxidation of benzyl alcohol, using O_2 or $H_2 + O_2$ gasses. (Adapted from Moreno *et al.*)[115]

Catalyst	Reaction Conditions	Benzyl Alcohol Conversion (%)	Benzaldehyde Selectivity (%)
2.5%AuPd/TS-1 (APX)	O_2	4.7	61.2
2.5%AuPd/TS-1 (APX)	$H_2 + O_2$	6.6	92.8
2.5%AuPd/TS-1 (AP12)	O_2	1.8	69.1
2.5%AuPd/TS-1 (AP12)	$H_2 + O_2$	7.0	92.6

Reaction Conditions: Catalyst (10 mg), benzyl alcohol (0.25 g, 2.3 mmol), MeOH (5.6 g), H_2O (2.9 g), where applicable (5% H_2/CO_2 (420 psi), 25% O_2/CO_2 (150 psi)), 30 °C, 0.5 hr, 1200 rpm.

When the 2.5%AuPd/TS-1 (APX) catalyst was used under aerobic conditions, a benzyl alcohol conversion of 4.7 % was offered, at a 61.2 % selectivity towards benzaldehyde. However, when the same catalyst was used alongside H_2 and O_2 in tandem, the conversion of benzyl alcohol was enhanced to 6.6 %, whilst a far greater selectivity of 92.8 % was reported. The authors concluded that the formation of peroxide species by the catalyst under the $H_2 + O_2$ environment was potentially highly beneficial towards the oxidation of benzyl alcohol at milder temperatures, and that the incorporation of H_2 into the reaction mixture enhanced catalytic activity. Whilst utilising mixtures of H_2 and O_2, H_2O_2 was generated in-situ, however it should be noted that H_2O_2 is not necessarily the primary oxidant species. This will be discussed further below, but several publications have suggested that radical oxygen species, such as hydroxyl or hydroperoxyl radicals may be key to the reaction mechanism.[28, 100] Alternatively, when using a Pd/TS-1 supported catalyst, Lyu *et al.*[132] have suggested that H_2O_2 generated at the surface of Pd nanoparticles may react with adjacent Ti^{4+} sites of the TS-1 support, generating a Ti-OOH species, which the authors have suggested may be an active species in the oxidation of benzyl alcohol. However, this proposal is specific to the use of a TS-1 support, and alternative metal oxides support materials are discussed below.

Santonastaso *et al*.[28] demonstrated that benzyl alcohol can be oxidised at 50 ^oC by utilising mixtures of H_2 and O_2 over precious metal catalysts. For example, using a 5 wt.% AuPd/TiO_2 catalyst, a 5.9 % conversion of benzyl alcohol was offered at a selectivity of 90 % to benzaldehyde, with toluene and benzoic acid as minor side products. The authors also investigated the effects of the support material on the oxidation of benzyl alcohol, comparing the catalytic activity of 5 wt.% AuPd supported on MgO, TiO_2 and CeO_2. When the MgO support was used, a benzyl alcohol conversion of 1.8 % was observed, whilst the TiO_2 and CeO_2 supported catalysts offered benzyl alcohol conversions of 5.9 % and 8.6 % respectively. From these observations, the authors suggested that the acidity or basicity or the catalyst may be a significant factor in the overall activity of the catalyst. Significantly, in agreement with the work of *Moreno et al.*,[115] the reaction proceeded at temperatures where limited oxidation occurred using O_2 alone. The authors also reported that catalytic activity could be inhibited by introducing radical quenching agents to the reaction mixture, such as $NaNO_2$ and Na_2SO_3, suggesting that a radical oxidation mechanism might be taking place.[28]

Crombie *et al.*[100] developed this further and investigated a series of Pd-based bimetallic catalysts supported on TiO_2. In addition to the already established AuPd/TiO_2 catalyst, other catalyst formulations, including CoPd, MnPd and FePd yielded a significant increase over the activity of the mono Pd/TiO_2 analogue, particularly FePd. This indicated the potential for a variety of secondary metals to be utilised in catalyst design for this reaction. Using electron paramagnetic resonance (EPR) spectroscopy, the authors then investigated the nature of the radical oxidants that had previously been inferred and found that either hydroxyl (·OH) or hydroperoxyl (·OOH) radicals were produced by the catalyst from H_2 and O_2, in agreement with previous findings, and suggesting an alternate reaction mechanism to the aerobic oxidation mechanism.[133] Additionally, methoxy (·OMe) radicals were also reported, originating from a reaction between the methanol solvent and hydroxyl or hydroperoxyl radicals generated by the catalyst. From this observation, it was suggested that the methanol solvent may act as a radical propagating agent, which was cited as the reason for previously reported enhanced activity when using a methanol only solvent, compared to an H_2O solvent.[28, 100] However, the authors noted that the enhanced solubility of H_2 in methanol relative to H_2O may also be a factor in the greater conversion offered when methanol was used as a solvent compared to H_2O.[100]

1.4 Advanced Oxidation Processes

Advanced oxidation processes (AOPs) are chemical processes in which highly reactive hydroxyl radicals are generated, primarily for the treatment and degradation of organic pollutants in wastewater.[134]

Such processes first received attention in the 1980s as a method for the purification of drinking water, but have since been studied for their capacity to treat wastewater streams, particularly those containing unwanted organic pollutants such as phenols, organic solvents and pharmaceuticals.[134, 135] At their core, AOPs are two step processes wherein the first step involves the generation of the radical oxidant, and the second step is the reaction of the radical species with the target compound(s) being degraded.[136] To this end, numerous AOPs have been developed, a few of which are shown in Table 1.21.

Table 1.21. Examples of AOPs [134, 136-142]

Type of AOP	Specific Reaction Components
Wet Air Oxidation	O_2 Environment, high temperature & pressure
Catalytic Wet Air Oxidation	Metal catalyst, O_2 Environment, high temperature & pressure
UV-Based Oxidation	UV/O_3
UV-Based Oxidation	UV/H_2O_2
Photocatalytic Oxidation	$TiO_2/UV/H_2O_2$
Catalytic Wet Peroxide Oxidation	Fenton's reagent (Fe^{2+}/H_2O_2)
Catalytic Wet Peroxide Oxidation	Supported Metal Catalyst, H_2O_2

As the current work is primarily focussed on the oxidation of phenol, the AOPs herein will be discussed in the context of the oxidation of phenol.

Phenol is an aromatic 6-membered carbon ring, with a hydroxyl substituent. The structure of phenol is shown in Figure 1.13.

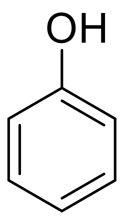

Figure 1.13. Structure of phenol

An important criterion for AOPs is to degrade phenol and phenolic derivatives such as benzoquinones, hydroxyphenols, chlorophenols and nitrophenols, which are commonly found in industrial waste streams.[143] Due to their high toxicity to human and aquatic life, satisfactory purification methods are required to prevent damage to both the environment and human health.[144, 145]

Many of the cyclic intermediates of the phenol oxidation reaction are more toxic than phenol itself and it's not until many of the phenolic derivatives have been oxidised to the low weight organic acids or mineralized entirely that the toxicity of the mixture is greatly reduced. Such intermediates are shown in Figure 1.14.

1.4.1 Radical Oxidants

As previously discussed, a feature of AOPs is the generation of hydroxyl radicals as the main oxidising species to degrade organic pollutants. Hydroxyl radicals are highly oxidising species, with an oxidation-reduction potential of 2.85 eV, and typically with lifetimes on the scale of nanoseconds.[138] For example, hydroxyl radicals have a half-life of approximately 1 nanosecond in biological systems.[146] Hydroxyl radicals can react very rapidly with organic molecules, including phenols, ketones, ethers etc. and significantly degrade such compounds, making them a highly attractive oxidant. As such, suitable precursors are required to generate hydroxyl radicals, and many AOPs have focussed on utilising H_2O_2, O_3, O_2 or a combination of the three. Due to the incredibly short lifetime of the hydroxyl radical, on the nanosecond scale, it must be generated in-situ and immediately consumed in the desired reaction. As previously mentioned, there are numerous ways to generate hydroxyl radicals.

Equation 1.20 describes the photochemical decomposition of H_2O_2. Homolytic cleavage of the oxygen bond generates two hydroxyl radicals.[147]

Eq 1.20 $$H_2O_2 + h\nu \rightarrow 2\ HO^\bullet$$

Following the generation of hydroxyl radicals by any means, several propagation reactions may take place as shown in Equations 1.21 – 1.22.[147]

Eq 1.21 $$H_2O_2 + HO^\bullet \rightarrow H_2O + HO_2^\bullet$$
Eq 1.22 $$HO_2^\bullet + H_2O_2 \rightarrow H_2O + O_2 + HO^\bullet$$

Finally, a series of termination steps are possible, exemplified in Equations 1.23 – 1.25.[147] These can lead to annihilation of hydroxyl and hydroperoxyl radicals to reform hydrogen peroxide.

Eq 1.23 $$2\ HO^\bullet \rightarrow H_2O_2$$
Eq 1.24 $$HO^\bullet + HO_2^\bullet \rightarrow H_2O + O_2$$
Eq 1.25 $$2\ HO_2^\bullet \rightarrow H_2O_2 + O_2$$

Hydroperoxyl radicals ($HO_2^\bullet$) are much less significant in the degradation of organic compounds as hydroxyl radicals are, due to their lower reactivity. Moreover, hydroperoxyl radicals act as scavengers towards hydroxyl radicals, generating water and molecular oxygen.[148]
Additional methods to generate hydroxyl radicals in-situ are discussed in the following sections.

1.4.2 Catalytic Wet Air Oxidation

Wet Air Oxidation (WAO) is the use of an oxidant, such as molecular oxygen, to generate active oxygen radicals in the liquid phase, namely hydroxyl radicals, under high temperature and pressure. This type of process has been investigated in the treatment of pollutants in wastewater streams, such as phenol, chlorophenols or methoxyphenols.
The requirement for high temperature and high-pressure reactions, typically from 150 – 400 ^{O}C and 2 to 40 MPa, has prompted investigation into alternative catalytic process in order to reduce the overall energy costs.[137, 139]

In Catalytic Wet Air Oxidation (CWAO), catalysts are incorporated into the process and catalyse the generation of hydroxyl radicals. Due to the presence of the catalyst, reaction times are shorter and reaction conditions can be milder (though still far from ambient conditions), with temperatures from 125 – 250 ^{O}C and pressures of 1 – 5 MPa.[145, 149]
Two forms of catalyst are prevalent in CWAO processes, the first being supported noble metals, such as Pt, Au, Ag, Ru and Rh.[149] The second class of catalysts are transition metal

oxides, including Cu, Co, Ni and Mn.[149] Examples of catalytic metals utilised in CWAO reactions are shown in Table 1.22.

Table 1.22. Examples of catalytic species used in the CWAO of phenol.[145, 150-152]

Metal(s)	Support Material
Cu, Ni, Mn, Pt, Pd	Al_2O_3
Ru, Pt, Pd	TiO_2
Pd	ZSM-5
Cu, Ni, Ru, Pt, Pd	CeO_2
Cu, Fe, Ru Pt, Pd, Rn	Activated Carbon (AC)
CuO	Unsupported

Supported noble metal catalysts have been shown to be very active in the CWAO of phenol. In an investigation into Ru-containing supported catalysts at 413 K and an O_2 partial pressure of 20 bar, Ru/AC was capable of 100% conversion of phenol and 70% mineralization of organics after 3 hours.[152] Conversely, AC alone could only achieve a phenol conversion of 10% and 4% mineralization.
Additionally, under the same conditions, Ru/graphite showed similar activity, with a phenol conversion of 97% and 64% mineralization. ZrO_2 supported Ru was also shown to exhibit 71% phenol conversion and 17% mineralization of organics, compared to unloaded ZrO_2, which exhibited 1% conversion and 0% mineralization respectively.[152]

As for the exact reaction mechanism of phenol oxidation under catalytic wet air conditions, numerous suggestions have appeared in the literature.[153-156] It is well understood that heterogenous catalysts, containing metals such as Cu, Fe, Mn etc. are able to generate free radical species, such as hydroxyl radicals, and thus degrade phenolic compounds through free radical chain reactions.[157] However, it has been suggested that there can also be a redox component to the reaction in which the catalyst serves to activate oxygen and phenol, the contribution of which is dependent on the activity of the catalyst, and selectivity to each reaction pathway.[157]

Additionally, the reaction pathway and formation of observable intermediates are highly dependent on pH, temperature and concentration of oxidant.
For example, as shown in Figure 1.14, under acidic conditions hydroxylation can take place at the *ortho*, *meta* or *para* positions of phenol. Further oxidation of a given hydroxyquinone leads to the corresponding benzoquinone and yet further oxidation yields a mixture of organic acids, including muconic, maleic, fumaric, oxalic and acetic acid. Finally, the reaction ends in formation of the mineralization products CO_2 and H_2O.[158]

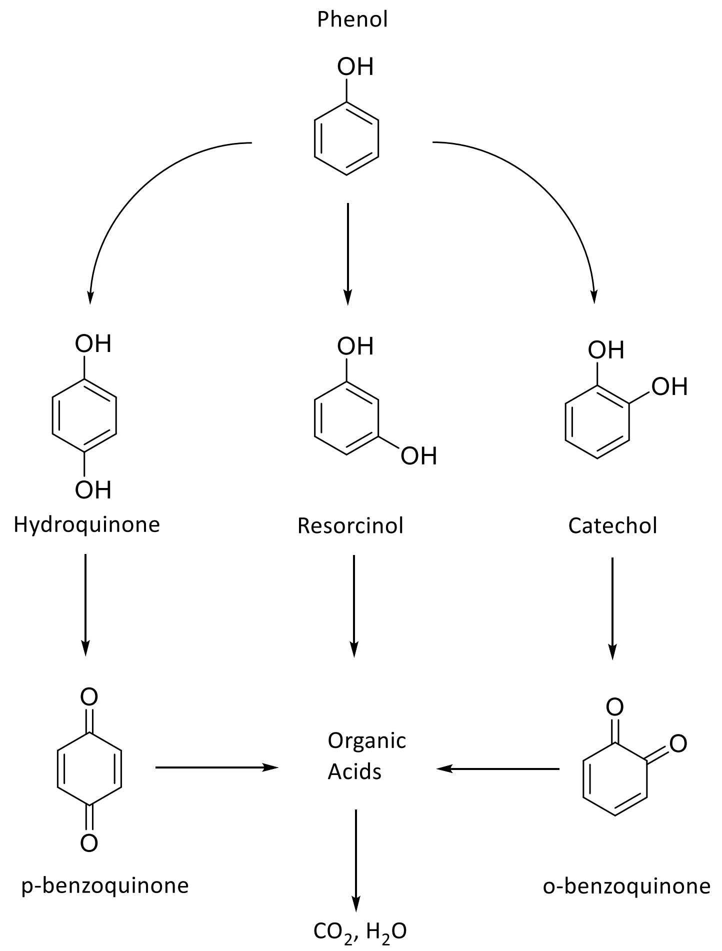

Figure 1.14. General reaction pathway for the oxidation of phenol with hydroxyl radicals under acidic conditions. [140, 158]

Under basic conditions (pH = 8), a very different reaction sequence may take place. Using a commercially available catalyst (Cu-0203) from Engelhard, consisting of CuO (67-66%), $CuO \cdot Cr_2O_3$ (20-30%) and a synthetic graphite (1-3%), it was demonstrated that in an aqueous bicarbonate media and maintaining the pH of the reaction mixture at 8, a different set of intermediates could be observed over the course of the reaction. This is shown in Figure 1.15.[159]

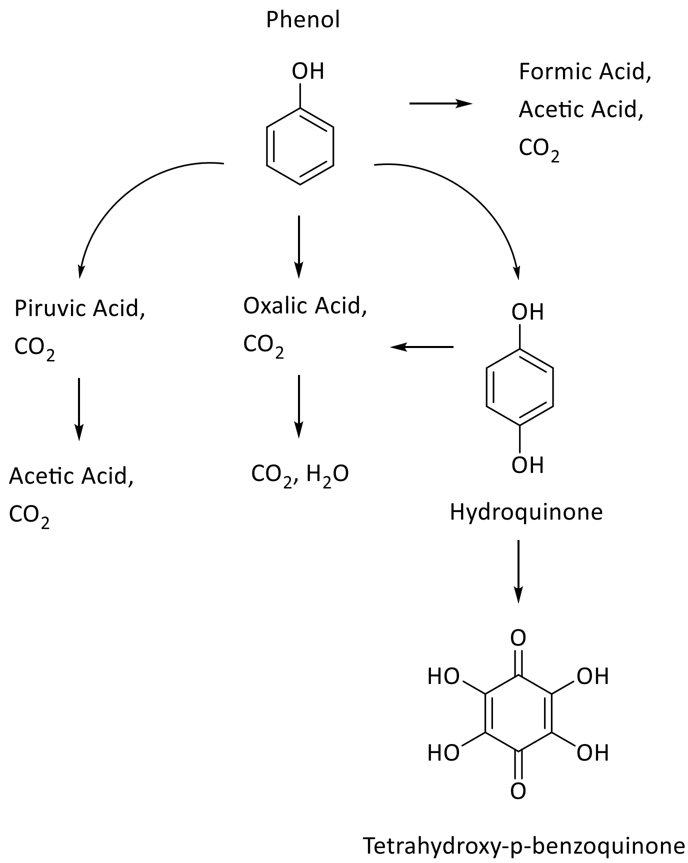

Figure 1.15. Proposed reaction pathway for CWAO of phenol at pH = 8 (bicarbonate media)[159]

Under these conditions, the only observed hydroxyquinone intermediate was hydroquinone. Whereas no catechol or resorcinol was detectable in the reaction mixture. Instead, it appeared that phenol was either hydroxylated to hydroquinone, or degraded directly to a number of organic acids, such as pyruvic, acetic, formic and oxalic acid, and then mineralized to CO_2 and H_2O.[159]

Despite the activity of many catalysts in CWAO processes, limitations exist in its application. Metal oxides and to a lesser extent, noble metal catalysts undergo deactivation in the hot and often acidic reaction media due to metal leaching and poisoning. Indeed, the production of low weight organic acids over the course of the oxidation reaction only further decreases pH and contributes to catalyst leaching.[157]
Additionally, deposits of carbon-based compounds can significantly decrease the activity of a catalyst, by blocking reactants from accessing active sites on the catalyst itself.[157] Consequently, stability and long-term activity of catalysts are a key consideration in the development of CWAO processes.

1.4.3 Catalytic Wet Peroxide Oxidation

Catalytic wet peroxide oxidation (CWPO) is an AOP in which hydrogen peroxide is utilised as a precursor in the catalytic generation of reactive radicals, such as the hydroxyl radical, to degrade organic molecules in water. CWPO is an attractive alternative to other AOPs, including CWAO and photocatalytic oxidation because it can operate at far milder conditions and without the need for a UV source.[160] For example, where CWAO processes might operate between 1 – 5 MPa, many CWPO reactions are carried out under atmospheric pressure.[142, 145, 149, 161]

As with other AOPs, a primary objective of the CWPO of phenol is to achieve mineralisation of organic pollutants in wastewater streams, such as phenol and its intermediate oxidation products (e.g. shown in Figure) into CO_2 and H_2O. The overall reaction for the mineralization of phenol by H_2O_2 is shown in Equation 1.26.[162]

Eq. 1.26 $$C_6H_5OH + 14H_2O_2 \rightarrow 6CO_2 + 17H_2O$$

Much attention has been given to developing optimal catalysts for use in CWPO processes, and many candidates have been synthesised and tested, some examples of which are shown in Table 1.23.

Table 1.23. Examples of catalysts used in the CWPO of phenol.[141, 142, 161, 163-169]

Metal(s)	**Support Material**
Ce, Fe, Zr	Pillared Clay
CuO	γ-Al_2O_3
Cu, Fe	Zeolites (ZSM-5, Y5)
Au, CuO, Fe	Activated Carbon
Cu	Poly(4-vinylpyridine)
$CuSO_4 \cdot 5H_2O$, $FeSO_4$	Unsupported

Two prominent methods of CWPO will be discussed in the following sections, namely classical Fenton reactions, and non-ferrous Fenton-like reactions.

1.4.3.1 Fenton's Reaction

One method of phenol oxidation that has received much attention is the use of 'Fenton's reagent' in aqueous solution. Fenton's reagent is a mixture of Fe^{2+} and H_2O_2 in solution, typically using homogenous $FeSO_4$ as a source of Fe^{2+}.

This system functions optimally at pH values of 2.5 – 4.0, through the catalytic decomposition of H_2O_2 by Fe^{2+} to generate hydroxyl radicals, as shown in Equation 1.27.[140, 170] At pH values exceeding 4, homogenous Fe species can form insoluble Fe hydroxides which precipitate out of solution and no longer take part in Fenton chemistry. At exceeding low pH values below 2.5, abundant H^+ can act as a radical scavenger and limit the available hydroxyl radicals available for reaction with target compounds. Thus, the chemistry of Fenton's reagent is highly dependent on pH.[170]

Eq. 1.27 $$Fe^{2+} + H_2O_2 \rightarrow Fe^{3+} + HO^{\bullet} + HO^-$$

As previously discussed, hydroxyl radicals have very short lifetimes and need continual catalytic regeneration for effective oxidation to take place. It has been reported in the literature that Fenton's reagent takes part in a series of elementary reactions in solution, which are exemplified Equations 1.28 - 1.30, where RH represents a generic oxidisable species.[171, 172]

Eq. 1.28 $HO^{\bullet} + RH \rightarrow H_2O + R^{\bullet}$

Eq. 1.29 $R^{\bullet} + Fe^{3+} \rightarrow R^{+} + Fe^{2+}$

Eq. 1.30 $R^{+} + H_2O \rightarrow ROH + H^{+}$

After the initial formation of the hydroxyl radical, hydrogen abstraction may take place, resulting in a radical $R^{\bullet}$ species which may reduce Fe^{3+}, with the resulting cationic R^{+} undergoing hydroxylation by H_2O.[171]

Eq. 1.31 $HO^{\bullet} + H_2O_2 \rightarrow H_2O + HO_2^{\bullet}$

Eq. 1.32 $HO_2^{\bullet} + Fe^{3+} \rightarrow Fe^{2+} + O_2 + H^{+}$

Eq. 1.33 $HO^{\bullet} + Fe^{2+} \rightarrow Fe^{3+} + HO^{-}$

Eq. 1.34 $HO^{\bullet} + HO^{\bullet} \rightarrow H_2O_2$

Alternative reactions are shown in Equations 1.31 – 1.34. For example, the hydroxyl radical may react with hydrogen peroxide, forming water and a hydroperoxyl radical, or it may oxidise Fe^{2+} in solution and generate hydroxide. Additionally, two hydroxide radicals may eliminate each other to reform hydrogen peroxide.[171]

For the oxidation of phenol itself, a general reaction pathway is shown in figure.[140, 158] Under the acidic conditions needed for the use of Fenton's reagent, the reaction follows a pathway synonymous with that observed in CWAO reactions. Namely, hydroxylation of phenol at the *ortho, meta* or *para* position, followed by oxidation to the corresponding *ortho* or *para* benzoquinones, degradation to organic acids and finally, mineralization to CO_2 and H_2O.
However, it is noteworthy that many carboxylic acids produced during the oxidation process, such as oxalic and acetic acid are considerable more resistant to mineralization than their precursor phenolic compounds, and thus often make up a considerable amount of leftover refractory organic compounds after a given reaction.[173] A number of practical aspects limit the usefulness of homogenous Fe^{2+} in an industrial context. Firstly, due to the homogenous nature of the catalyst, subsequent separation of dissolved iron is necessary to purify waste streams after treatment, incurring additional cost and complexity to the process. Additionally, the narrow pH range of 2.5 – 4.0 in which the catalyst functions requires initial acidification of reaction systems and in the context of wastewater treatment, subsequent neutralisation.[170]

Such barriers to its use have led to the development of alternative heterogenous Fenton catalysts, in an attempt to limit the need for precise operating pH conditions and removal of homogenous iron from waste streams. Heterogenous ferrous Fenton catalysts are primarily composed of Fe^{3+} immobilised in a support material.[135] A considerable number of heterogenous ferrous catalysts have been reported in the literature, utilising supports such as activated and aerogel carbons, Alumina, zeolites, mesoporous silicas, pillared clays and polymeric supports.[170, 174-176] Some examples of heterogenous ferrous catalysts involved in phenol oxidation reactions are shown in Table 1.24, wherein TS-1 (a commercial titanium silicate), ZSM-5 (an aluminosilicate zeolite) and a silicate were utilised as frameworks and tested for both activity and Fe leaching.

Total organic carbon (TOC) removal is a measure of the mass of carbon removed from solution through mineralization.

Table 1.24. Examples of different heterogenous Fe catalysts in the CWPO of phenolic solutions[a]. (Adapted from Ovejero *et al.*)[173]

Catalyst	TOC Removal (%)	Fe Leaching (%)
Fe-TS-1 (1) (0.6 wt%)	64.1	15.7
Fe-TS-1 (2) (1.2 wt%)	66.0	18.3
Fe-TS-1 (3) (4.4 wt.%)	70.7	42.4
Fe-ZSM-5 (2.5 wt.%)	68.2	95.3
Fe-silicate (3.6 wt.%)	79.1	43.1

Reaction conditions: Phenolic solution (140 mL, 1000 ppm), H_2O_2 (5000 ppm), catalyst (84 mg, 600 mg/L), pH 5.6, 373 K, 1 MPa, 120 minutes.

The increasing Fe leaching observed across the series of Fe-TS-1 materials can be explained through the increasing prevalence of extraframework Fe as metal loading increases. Additionally, almost complete leaching of Fe content in Fe-ZSM-5 was accounted to the ubiquitous presence of extraframework Fe, which the authors observed through UV-Vis spectroscopy. Indeed, for the Fe-ZSM-5, the presence of Al in the zeolitic framework greatly decreased the incorporation of Fe, whilst no extraframework Al was observed spectroscopically.[173]
The examples shown in Table 4 demonstrate the ability of ferrous catalysts to not only oxidize phenolic compounds, but also to mineralize organic material. However, Fe leaching is significant under such hot and acidic reaction conditions, which exemplifies a recurring challenge in the development of heterogenous Fenton catalysts, namely, metal leaching and catalyst deactivation.[160, 170]

In recent years, much work has been carried out to develop heterogenous ferrous catalysts that are highly active and stable in Fenton type reactions for the oxidation of phenol, and attention has been paid to the different factors that can influence catalyst activity and stability. These factors include catalyst support material, phenol concentration, temperature and reaction time. For example, an iron oxychloride (FeOCl) catalyst has been developed and shown to be highly efficient in the generation of hydroxyl radicals and in the degradation of organic compounds, including phenol, bisphenol A and ethylbenzene. Indeed, utilising FeOCl as a catalyst allowed for 100% degradation of phenol contained within a phenolic solution, after 30 minutes (phenol (100 ppm), H_2O_2 (530 ppm), FeOCl (200 mg L^{-1}), 313 K, pH = 4).[177]
Perhaps most significantly, under the testing conditions given, Fe leaching was reported at values between 0.57-1.25 ppm, suggesting that even at low pH, the catalytic species is highly resistant to dissolution and deactivation.[177]

However, making a comparison between catalytic species presented in the literature is often not straightforward as vastly different conditions may be used across different studies, including H_2O_2 and phenol concentrations, catalyst loading and temperature. Additionally, some studies may discuss catalytic activity in terms of phenol conversion, whilst others focus on TOC removal or chemical oxygen demand (COD), which is a measure of the mass of oxygen that can be consumed in a reaction with a volume of solution containing oxidizable materials. With this being said, the FeOCl catalyst exemplifies the possibility to overcome the extreme extent of Fe leaching detailed in Table, through tuning the catalyst itself, and the reaction conditions.

Another example of this is in an (3.9% w/w) Fe/γ-Al_2O_3 species used in the CWPO of phenol. This catalyst exhibited a phenol conversion of 98% after 125 minutes, and total degradation of phenol after 240 minutes, with a TOC removal of 44% (phenol (100 ppm), H_2O_2 (500 ppm), catalyst (125 mg), 323 K, initial pH 3).[178] Additionally, under such conditions, metal leaching was reported as 0.7 mg L^{-1} after 240 minutes, which accounts for a loss of 0.6% of initial Fe by weight. Interestingly, Bautista *et al.* examined the effect of initial phenol concentration on Fe leaching over the course of an 8-hour reaction, the results of which are summarised in Table 1.25.[178] It was observed that increasing the initial phenol concentration had little impact on the conversion of phenol itself, whilst TOC removal values steadily decreased with increasing initial phenol concentration. Consequently, the concentration of oxalic acid detectable at the end of the reaction greatly increased with increasing initial concentration of phenol.

Perhaps most significantly, the concentration of Fe leachate detected in the final reaction mixture was greatly increased with increasing phenol concentration, which was attributed to the higher concentration of oxalic acid and other low weight organic acids that are products of the degradation reaction.[178]

Table 1.25. Effect of initial phenol concentration on activity and Fe leaching of (3.9% w/w) Fe-γ-Al_2O_3. (Adapted from Bautista *et al.*)[178]

Initial Phenol Concentration (ppm)	Initial H_2O_2 Concentration (ppm)	Phenol Conversion (%)	TOC Removal (%)	Organic Acid Concentration (ppm)	Fe Leaching (ppm)
100	100	100	59.8	18.1	0.9
500	500	100	54.3	130.0	3.9
1000	1000	99.7	45.6	208.8	5.3
1500	1500	99.4	42.7	312.7	7.4

Reaction Conditions: Catalyst (125 mg), 323 K, initial pH 3, 8 hours.[178]

The final example to be discussed is an (4% w/w) Fe/Activated Carbon catalyst. The activity and stability of the species was investigated in the CWPO of phenol at temperatures from 298-348 K, the results of which are in Table 1.26.[168] Whilst phenol conversion reaches 93% at 298 K, total phenol removal is achieved at higher temperatures. Additionally, TOC removal increases with temperature, whilst interestingly, organic acid concentration also increases concurrently. This suggests that the aromatic intermediates of phenol oxidation are more quickly degraded at higher temperatures, but low weight organic acids remain prevalent products.[168] As such, greater levels of Fe leaching are also observed as temperature increases, which was correlated to the concentration of organic acids, particularly oxalic acid, present in the final reaction mixture.[168]

Table 1.26. Effect of temperature on activity and Fe leaching of (4% w/w) Fe/Activated Carbon. (Adapted from Zazo *et al.*)[168]

Temperature (K)	Phenol Conversion (%)	TOC Removal (%)	Organic Acid Concentration (ppm)	Fe Leaching (ppm)
298	93	75	11.2	0.3
323	100	84	21.8	2.4
348	100	88	31.2	7.8

Reaction Conditions: Catalyst (25 mg), phenol (100 mg L^{-1}), H_2O_2 (500 mg L^{-1}), initial pH 3, 4 hours.[168]

1.4.3.2 Non-Ferrous Fenton Catalysts

Non-ferrous Fenton-like catalysts are a broad group of metal catalysts that are capable of generating hydroxyl radicals from H_2O_2 by CWPO reactions, and thus have potential for AOPs.

1.4.3.3 Fenton's Reaction Using Copper

A popular alternative to iron is copper, which reacts readily with H_2O_2 by Equations 1.35 – 1.36.[135]

Eq. 1.35 $$Cu^{2+} + H_2O_2 \rightarrow Cu^{+} + HO^{\bullet} + HO^{-}$$

Eq. 1.36 $$Cu^{+} + H_2O_2 \rightarrow Cu^{2+} + HO^{\bullet} + HO^{-}$$

This redox cycle leads to the in-situ generation of both hydroxyl radicals and peroxyl radicals, as well as the continual cycling between Cu^{2+} and Cu^{+}.[135]

This reactive property has been exploited in the development of catalytic species, both heterogenous and homogenous in nature, examples of which are shown in Table 1.27.

Table 1.27. Examples of Cu based Fenton catalysts used in the CWPO of phenol.[142, 165, 166]

Catalyst	Phenol Conversion (%)	TOC Removal (%)	Cu Leaching (%)
Cu-ZSM-5 (3.52 wt.%)	[a]95	33.9	3.9
Cu-Y5 (3.54 wt.%)	[a]100	62.1	7.1
$CuSO_4 \cdot 5H_2O$	[b]95	40	n/a
Cu-γAl_2O_3	[b]85	20	7.5
Cu-poly(4-vinylpyridine)	[b]80	5	10
Cu-Activated Carbon (4.6 wt.%)	[c]100	70	n/a

Reaction conditions: [a] Phenol solution (200 mL, 188 ppm), H_2O_2 (680 ppm), catalyst (20 mg, 100 ppm), 353 K, 180 minutes.[165]

[b] Phenol solution (1000 ppm), H_2O_2 (14 equivalents), Cu(II) concentration (200 ppm), 303 K, 120 minutes.[142]

[c] Phenol solution (500 mL, 1000 ppm), H_2O_2 (1700 ppm), catalyst (1 g), 353 K, 180 minutes.[166]

The data presented in Table 1.27 demonstrates the ability of Cu based catalysts to effectively catalyse the oxidation of aqueous phenol, and in many cases mineralise large percentages of organic material. Many more catalytic species have been developed to these ends. One example is a CuO nanosheet, which was synthesised by addition of NaOH and H_2O_2 to wastewater that had been artificially polluted with $CuSO_4$.[179] It was found that CuO nanosheets had a much greater activity when compared to commercial CuO. For example, in dark conditions, CuO nanosheets could reach a phenol conversion of 80% compared to the 25% converted by commercial CuO after 60 minutes (phenol (50 ppm), H_2O_2 (100 mmol L^{-1}), initial pH = 6, catalyst (150 mg L^{-1})).[179]

Table 1.28. Properties of Cu loaded activated carbon catalysts. (Adapted from Liou and Chen)[166]

Copper Loading (wt%)	Micropore Volume (cm^3 g^{-1})	Surface Area (m^2 g^{-1})	Phenol Conversion (%)	TOC Removal (%)
4.6	0.219	670	100	70
9.8	0.150	437	100	75
38.9	0.148	436	100	80

Reaction conditions: Phenol solution (500 mL, 1000 ppm), H_2O_2 (0.1 M), catalyst (1 g), 353 K, 180 minutes

Under the reaction conditions shown in Table 1.28, total conversion of phenol was reached after approximately 15 minutes, for each Cu loading investigated (4.6 - 38.9 wt.%), though the reaction was allowed to proceed for a total of 180 minutes.[166] TOC removal values also increased slightly as Cu loading was increased, which might suggest that increasing the number of active sites accordingly increases the catalytic activity. However, no leaching analysis was carried out, nor was the possibility of leached Cu acting as a homogenous catalyst investigated, which could also be a contributing factor to the differing TOC values.

The effect of H_2O_2 concentration was investigated, and it was observed that increasing the H_2O_2 concentration from 0.1 M to 0.2 M allowed the (4.6 wt%) Cu/activated carbon to facilitate the removal of 85% of TOC, instead of the 70% observed when 0.1 M H_2O_2 was used.[166] This outlines the significant role that H_2O_2 concentration plays in the overall reaction, such that when all H_2O_2 is decomposed, no further oxidation can take place.

A novel example in the literature of an active Cu catalyst is a Cu-ZSM-5 catalyst supported on paper-like sintered stainless-steel fibres (PSSF). Cu was incorporated by either ion-exchange (IE) or impregnation (IM) into a ZSM-5 zeolite that was supported on paper-like sintered stainless-steel fibres, with the effect of preparation being an object of investigation.[180] Each catalyst had a Cu loading of 2.4 wt.% and was labelled as either Cu-ZSM-5/PSSF (IM) or Cu-ZSM-5/PSSF (IE) and subsequently tested for its activity and stability.

Unlike the previous examples discussed which were utilised in batch reactors, Cu-ZSM-5/PSSF was tested in a fixed bed reactor (2 cm i.d.m 10 cm length) under continuous flow (phenol (1000 ppm), H_2O_2 (5100 ppm), 353 K, flow rate (2 mL min^{-1}), catalyst bed height (2 cm), 11

hours).[180] Under these conditions, Cu-ZSM-5/PSSF (IE) was able to achieve 100% phenol conversion over the first hour, which was maintained over the entire 11-hour experiment.
Concurrently, Cu-ZSM-5/PSSF (IM) achieved 99% phenol conversion over the first hour, but that value had decreased to 70% by the 11th hour.
Cu leaching was also examined, and it was reported that Cu leaching reached values of 180 ppm for Cu-ZSM-5/PSSF (IM) after the first hour, whereas Cu-ZSM-5/PSSF (IE) experienced a dissolution of approximately 40 ppm after the same amount of time.[180]

The different activities as a function of time observed for the IE and IM Cu-ZSM-5/PSSF catalysts can be explained in terms of metal leaching. Where Cu immobilised on the surface of ZSM-5 through impregnation appeared more able to be leached into the reaction medium, Cu incorporated into zeolite channels through ion-exchange was regarded as considerably more stable, due to the lower observed leaching in the ion-exchange catalyst.[180]

1.4.3.4 Fenton's Reaction Using Cerium

Cerium is another element capable of degrading H_2O_2 to generate hydroxyl radicals. In a process analogous to the Fe^{2+}/Fe^{3+} and Cu^{+}/Cu^{2+} discussed previously, cerium may also cycle between Ce^{3+} and Ce^{4+} in the presence of H_2O_2 to generate hydroxyl and hydroperoxyl radicals, as shown in Equations 1.37 – 1.38.[135]

Eq. 1.37 $$Ce^{3+} + H_2O_2 \rightarrow Ce^{4+} + HO^{\bullet} + HO^{-}$$

Eq. 1.38 $$Ce^{4+} + H_2O_2 \rightarrow Ce^{3+} + HO_2^{\bullet} + H^{+}$$

This property has resulted in the investigation and utilisation of cerium containing compounds, most notably ceria (CeO_2) in Fenton-like reactions.
However, it has been demonstrated that without surface functionalisation, CeO_2 is incapable of generating hydroxyl radicals from hydrogen peroxide, which It instead forms a stable ($\equiv Ce^{3+}\text{-}OOH^{-}$) complex at the catalyst surface.[135, 181]
Instead, incorporating sulphate groups at the surface of ceria by sulphonation creates an acidic environment that is capable of protonating the aforementioned peroxide species at the surface of the catalyst. This facilitates an electron transfer from the 4f orbital of Ce^{3+} and the protonated peroxide may undergo homolytic cleavage of the oxygen bond, as shown in equation.[181] A barrier to the use of cerium in CWPO processes is the toxicity of the element, which is known to be cytotoxic to human and aquatic life in its metal oxide form.[182]

1.4.3.5 Fenton's Reaction Using Bimetallic Catalysts

An alternative line of investigation has been directed towards bimetallic supported catalysts. Much attention has been given to improving on Fe or Cu based catalysts by incorporating a secondary metal, into the catalyst to alter the physicochemical properties of the primary metal, and by extension the catalytic activity.[162, 183-188]

In one example of this, a $CuO\text{-}Co_3O_4/\gamma\text{-}Al_2O_3$ catalyst was investigated in the degradation of phenol using an H_2O_2/HCO_3^{-} oxidant system.[189]

$CuO-Co_3O_4/\gamma-Al_2O_3$ was compared to the activity of $CuO/\gamma-Al_2O_3$ and $Co_3O_4/\gamma-Al_2O_3$ respectively, the results of which are shown in Table 1.29.

Table 1.29. Comparison of $\gamma-Al_2O_3$ supported CuO and Co_3O_4 catalysts on phenol oxidation. (Adapted form Yibing *et al.*)[189]

Catalyst	Phenol Conversion (%)	TOC Removal (%)	Cu Leaching (ppm)	Co Leaching (ppm)
$CuO/\gamma-Al_2O_3$	39.0	37.0	0.75	-
$Co_3O_4/\gamma-Al_2O_3$	14.2	9.8	-	0.08
$CuO-Co_3O_4/\gamma-Al_2O_3$	90.0	51.0	0.6	-

Reaction conditions: Phenol (0.5 mmol/L), $NaHCO_3$ (15 mmol/L), H_2O_2 (50 mmol/L), catalyst (10 mg), 318 K, 1 hour.

As shown in Table 1.29, the bimetallic Cu-Co species presents a far higher level of phenol degradation and TOC removal than either monometallic catalyst, which was accounted to a synergistic effect between Cu and Co. Additionally, reduced levels of Cu and Co leaching were observed in the bimetallic species, relative to the respective monometallic catalysts, suggesting the incorporation of Co into the material enhances stability.[189]

The utilisation of $NaHCO_3$ has a number of effects on the reaction as a whole. Firstly, it makes the reaction mixture weakly basic, compared to the slightly acidic conditions that would otherwise be present in a solution of aqueous phenol. This may be responsible for the relatively low levels of metal leaching observed (<1 ppm) compared to Cu catalysts discussed previously.[189] Secondly, the bicarbonate (HCO_3^-) or carbonate (CO_3^{2-}) in solution are both capable of reacting with hydroxyl radicals, to generate radical carbonate anions. This is shown in Equations 1.39 – 1.40.[190]

Eq. 1.39 $$HO^\bullet + HCO_3^- \rightarrow H_2O + CO_3^{-\bullet}$$
Eq. 1.40 $$HO^\bullet + CO_3^{2-} \rightarrow HO^- + CO_3^{-\bullet}$$

It has been suggested that radical carbonate anions may be potent radical oxygen species in such oxidation reactions.[190]

In another example, hollow shell Fe-Cu bimetallic silicate-1 supported catalysts were prepared and compared to Fe silicate-1 catalysts for their ability to degrade phenol through a CWPO reaction, the results of which are shown in Table 1.30. They were also compared to the activity of conventional (non-hollow shell) silicate-1 zeolites.[184] The purpose of incorporating Cu into the catalyst was to alter the physicochemical properties of the catalyst in an attempt to improve activity, whilst the use of hollow shell silicate-1 zeolites was intended to overcome some of the limitations associated with use conventional zeolites in heterogenous liquid phase catalysis. For example, diffusion of reactants to active sites, and of products away from active sites can be limited by narrow and lengthy pore channels in the structure of the zeolite.[184]

Table 1.30. Comparison of Silicate-1 supported Fe and Cu containing catalysts. (Adapted from Dai *et al.*)[184]

Catalyst	Phenol Conversion (%)	Cu Leaching (ppm)	Fe Leaching (ppm)
Fe_2O_3/S-1	25	-	1.86
Fe_2O_3-CuO/S-1	70	0.93	1.67
Fe_2O_3/S-1 (hollow shell)	85	-	0.44
Fe_2O_3-CuO/S-1 (hollow shell)	100	0.35	0.28

Reaction conditions: Phenol (50 mL, 1000 ppm), H_2O_2 (14 equivalents), catalyst (100 mg), 323 K, 100 minutes, initial pH 6.2

It is clear that in terms of catalytic activity and stability, hollow shell Fe_2O_3-CuO/S-1 is superior to conventional Fe_2O_3-CuO/S-1, whilst the incorporation of CuO into the catalytic structure served to improve the rate of phenol conversion when compared to the corresponding Fe catalyst.

The cause of this effect is attributed to a decrease in the redox potential for the reaction in Equation 1.41 when compared to Equation 1.42.[184]

Eq. 1.41 $$Fe^{3+} + Cu^{+} \rightarrow Fe^{2+} + Cu^{2+} \qquad 0.60\ eV$$

Eq. 1.42 $$Fe^{3+} + e^{-} \rightarrow Fe^{2+} \qquad 0.77\ eV$$

Additionally, it was found that the Fe_2O_3-CuO nanoparticles were larger than the pores in the hollow-shell zeolite structure, which was suggested to be a decisive factor in the increased stability observed for the hollow shell catalysts.[184]

Further to this, the reusability of hollow shell and conventional Fe_2O_3-CuO/S-1 catalysts were tested over the course of five successive reactions under the conditions described in Table 10. It was found that the phenol degradation promoted by the hollow shell Fe_2O_3-CuO/S-1 decreased from 100% to 80%, whereas the conventional Fe_2O_3-CuO/S-1 saw phenol conversion values decrease from, 70% to 20% after the 5 runs, further supporting the enhanced stability of the hollow shell species.[184]

Despite the advances in the recent literature towards limiting the extent of metal leaching in-situ, total prevention of dissolution is likely not feasible for applications in catalytic wet peroxide oxidation reactions.

Metal leaching occurs in liquid phase reactions, primarily either as a result of the dissolution of an already soluble catalytic species, or through a chemical reaction between metal nanoparticles and the reaction medium itself.[191] In the latter case, the cleavage of the metal-oxygen bonds that anchor the nanoparticle to the support material may occur, due to the action of species such as acids within the reaction mixture. Alternatively, chelating agents may form complexes with catalytic metal species which subsequently causes a loss of catalytic metal from the support.[191] Overall, the process of metal dissolution is one driven by thermodynamics, wherein a negative value of Gibbs free energy (Equation 1.2) provides a driving force for the reaction of the catalytic metal with components within the reaction mixture, and the eventual removal of catalytic metal from the support material. Correspondingly, the rate at which metal leaching occurs is driven by kinetics, and thermodynamically favourable processes may still be kinetically slow.

Numerous parameters may determine the extent and rate of metal dissolution, including the nature of the reaction solvent, temperature, the choice of catalytic metal, the choice of support material and the presence of acidic and basic agents.[191] For example, catalytic metals may be more or less soluble depending on the solvent present, whilst high temperatures and increasingly acidic conditions promote the dissolution of metals. Consequently, researchers have focussed on optimising catalysts and reaction conditions to minimise the extent of metal dissolution. This has been done through numerous ways, for example catalytic metals and support materials can be selected to maximise stability under reaction conditions, whilst catalyst preparation methods and heat treatments may also play a significant role in subsequent extent of metal dissolution.[192] For example, the rate of metal leaching may be decreased through mechanisms such as the immobilisation of catalytic metals in zeolite pores as described above. Alternatively, more mild reaction conditions such as lower temperatures, neutral pH or benign solvents can be employed.[191] Additionally, if possible, liquid phase reactions can be redesigned into gas phase processes to prevent metal dissolution into a liquid phase.

1.5 Ascorbic Acid: Chemistry and Prooxidant Activity

Ascorbic acid (AH_2), also referred to as vitamin C, is an organic reducing agent with the structure shown in Figure 1.16. It is generally utilised as an antioxidant, due to its ability to scavenge oxygen-based radicals, such as hydroxyl, hydroperoxyl and superoxide. This radical scavenging occurs because ascorbic acid acts as a single hydrogen atom reducing agent, converting itself into monodehydroascorbate, a resonance stabilised radical that preferentially reacts with other radicals to terminate propagating chain reactions.[193] Monodehydroascorbate may also disproportionate with another molecule of monodehydroascorbate, forming equimolar ascorbate and dehydroascorbate.[193]

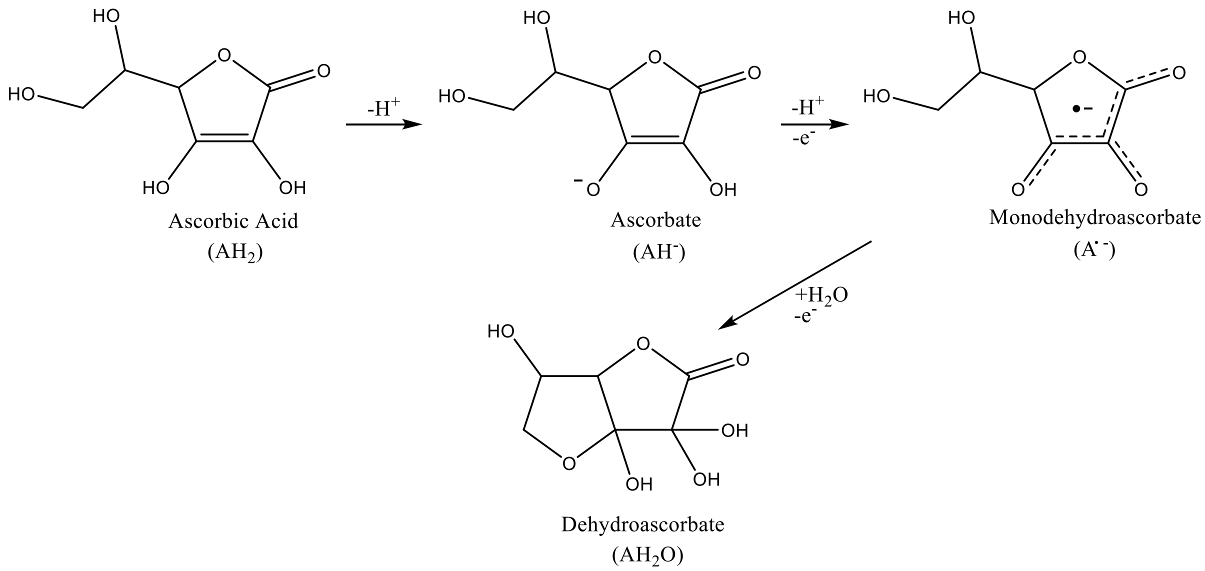

Figure 1.16. Proposed generalised pathway for the oxidation of ascorbic acid.[193, 194]

Paradoxically, in the presence of metals such as Cu and Fe, under aerobic conditions, ascorbic acid has been shown to enhance the extent of oxidation towards a target molecule that may be otherwise achieved.[193] One proposed mechanism this observation is shown in Equations 1.43 – 1.46.[193, 195]

Eq. 1.43 $$Fe^{3+} + AH^- \rightarrow Fe^{2+} + A^{\bullet -} + H^+$$

Eq. 1.44 $$Fe^{2+} + O_2 \rightarrow O_2^{\bullet -} + Fe^{3+}$$

Eq. 1.45 $$2\ O_2^{\bullet -} + 2\ H^+ \rightarrow H_2O_2 + O_2$$

Eq. 1.46 $$Fe^{2+} + H_2O_2 \rightarrow Fe^{3+} + HO^{\bullet} + HO^-$$

Firstly, ascorbate (AH^-), the deprotonated form of AH_2, reduces Fe^{3+} to from monodehydroascorbate ($A^{\bullet -}$). Oxygen can then be converted to a superoxide radical $O_2^{\bullet -}$, which subsequently forms H_2O_2. Fe^{2+} can then initiate Fenton's chemistry and generate the highly reactive hydroxyl radical. However, there is some uncertainty within the literature as to the precise mechanism by which catalytic activity is enhanced. An alternative proposal is shown in Equations 1.47 – 1.48.[196, 197]

Eq. 1.47 $$HA^{\bullet -} + O_2 \rightarrow HO_2^{\bullet} + A$$

Eq. 1.48 $$HO_2^{\bullet} + AH_2 \rightarrow HA^{\bullet -} + H_2O_2$$

This proposal requires for O_2 to instead react with the monodehydroascorbate radical to generate hydroperoxyl, instead of superoxide, and then subsequently forming H_2O_2.[196, 197] Regardless of the specific mechanism, ascorbic acid has been shown to reduce Fenton-type metals in-situ and also facilitate the formation of H_2O_2 from O_2.

It has been shown that Fe^{3+}/H_2O_2 systems are much less efficient oxidation systems than Fe^{2+}/H_2O_2, due to the increased formation of $HOO^{\bullet}$ by Fe^{3+} rather than the more reactive $HO^{\bullet}$ species, which is generated through the catalytic degradation of H_2O_2 by Fe^{2+}.[198] By

incorporating reducing agents such as ascorbic acid into the reaction system, in-situ reduction of Fe^{3+} to the more active Fe^{2+} can be achieved, promoting the rate of oxidation of a target molecule.[198] For example, Bolobajev *et al*. examined the comparative extent of degradation of alachlor (Figure 1.17) between an Fe^{3+}/H_2O_2 and Fe^{2+}/H_2O_2 system, with and without ascorbic acid (AA), wherein catalytic Fe was present as homogeneous species.[198]
The authors reported that alachlor degradation and $HO^{\bullet}$ production was much lower for the Fe^{3+} system, but the addition of ascorbic acid caused Fe^{3+} to be reduced to Fe^{2+} in-situ. For example, both the Fe^{2+}/H_2O_2 and the $Fe^{3+}/H_2O_2/AA$ systems were able to degrade all alachlor present in the reaction mixture after 60 minutes, whereas a mixture of Fe^{3+}/H_2O_2 with no ascorbic acid present only degraded approximately 20 % of the alachlor present after 120 minutes. This led the authors to conclude that the primary mechanism for ascorbic acid promotion of Fenton's chemistry is through the in-situ reduction of Fe^{3+} to Fe^{2+}.[198] Although, regardless of the exact mechanism, it is widely reported that H_2O_2 is generated in-situ from oxygen and ascorbic acid, and that Fenton's metals facilitate the generation of highly reactive hydroxyl radicals.[193, 196, 197, 199] This property has led to research into the utilisation of ascorbic acid for applications such as cancer treatment [195, 200] and in the enhancement of oxidation reactions.[198, 201-203]

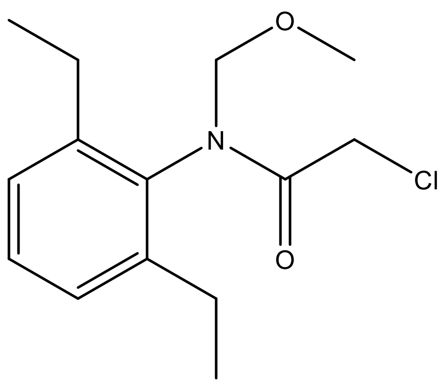

Figure 1.17. Chemical structure of alachlor.

1.6 Research Aims

Two primary reactions were investigated in this thesis, the selective oxidation of benzyl alcohol via the in-situ synthesis of H_2O_2, and the ascorbic acid promoted catalytic wet peroxide oxidation of phenol. Firstly, the objective of investigations into the selective oxidation of benzyl alcohol was to improve upon catalytic yields of benzaldehyde already reported in the literature, in order to further develop the feasibility of such an in-situ methodology towards benzyl alcohol valorisation. A particular focus was directed towards catalyst design and optimisation, with factors such as the choice support material, the alloying of Pd with a secondary metal and the inclusion of tertiary metals into a supported AuPd catalyst receiving particular attention. Additional factors under investigation included the method of catalyst preparation and heat treatment protocols in addition to the ratios of catalytic metals present in bimetallic Pd-based catalysts.

Secondly, the ascorbic acid promoted catalytic wet peroxide oxidation of phenol was investigated, using phenol oxidation as a model reaction system. The objective of this study was to investigate the efficacy of utilising ascorbic acid as an oxidation promoter alongside hydrogen peroxide using a supported transition metal catalyst. This research was conducted in collaboration with Selden Research Ltd. with the objective of using research findings for applications to inform research towards anti-microbial applications. Key areas that were investigated include the choice of catalytic metal, the concentration of the reactants used, the effects of additional additives to the reaction mixture and the choice of H_2O_2 source, in addition to the effects of homogeneous contributions from catalytic leachate.

1.7 References

1. Berzelius, J., *Edinburgh New Philosophical Journal* **1836,** *21*, 223.
2. Vogt, C., Weckuysen, B., The concept of active site in heterogeneous catalysis. *Nat. Rev.* **2022,** *6*, 89-111.
3. Anastas, P., Eghbali, N., Green Chemistry: Principles and Practice. *Chem. Soc. Rev.* **2010,** *39*, 301-312.
4. Anastas, P., Warner, J., *Green chemistry theory and practice*. Oxford University Press: New York, 1998.
5. Calvo-Flores, F., Sustainable Chemistry Metrics. *ChemSusChem* **2009,** *2*, 905-919.
6. Sheldon, R., Bode, M., Akakios, S., Metrics of green chemistry: waste minimization. *Curr. Opin. Green Sustain. Chem.* **2022,** *33*, 100569.
7. Leeuwen, P., *Homogeneous catalysis: Understanding the art*. Springer Science & Business Media: 2006.
8. Wang, D., Shuanhu, G., Sonogashira coupling in natural product synthesis. *Org. Chem. Front.* **2014,** *1*, 556-566.
9. Bokare, A., Choi, W.,, Review of iron-free Fenton-like systems for activating H2O2 in advanced oxidation processes. *J. Hazard Mater.* **2014,** *275*, 121-135.
10. Sharpless, B., Katsuki, T., The First Practical Method for Asymmetric Epoxidation. *J. Am. Chem. Soc.* **1980,** *102*, 5974-5976.
11. Bell, E., Finnigan, W., et al., Biocatalysis. *Nat. Rev. Methods Primers* **2021,** *1*, 46.
12. Blanco, G., *Medical Biochemistry*. 2017.
13. Saravanan, A., Kumar, P., et al., A review on catalytic-enzyme degradation of toxic environmental pollutants: Microbial enzymes. *J. Hazard Mater.* **2021,** *419*, 126451.
14. Zhang, H., Sun, Z., Hu, Y., Steam reforming of methane: Current states of catalyst design and process upgrading. *Renewable Sustainable Energy Rev.* **2021,** *149*, 111330.
15. Humphreys, J., Lan, R., Tao, S., Development and Recent Progress on Ammonia Synthesis Catalysts for Haber–Bosch Process. *Adv. Energy Sustainability Res.* **2021,** *2*, 2000043.
16. Ji, Y., Yang, H., Yan, W., Strategies to Enhance the Catalytic Performance of ZSM-5 Zeolite in Hydrocarbon Cracking: A Review. *Catalysts* **2017,** *7*, 367.
17. Prins, R., Eley-Rideal, the other mechanism. *Top. Catal.* **2018,** *61*, 714-721.
18. Hagemeyer, A., Colpe, A.,, *Encyclopedia of condensed matter physics*. Academic: 2005.
19. Martín, A., Mitchell, S., et al., Unifying views on catalyst deactivation. *Nat. Catal.* **2022,** *5*, 854-866.

20. Wilson, N., Bregante, D., et al., Production and use of H_2O_2 for atom-efficient functionalization of hydrocarbons and small molecules. *Catalysts* **2017,** *29*, 122-212.
21. Campos-Martin, J., Blanco-Brieva, G., Fierro, J., Hydrogen peroxide synthesis: An outlook beyond the anthraquinone process. *Angew. Chem. Int. Ed.* **2006,** *45*, 6962 - 6984.
22. Lewis, R., Hutchings, G., Recent Advances in the Direct Synthesis of H_2O_2. *Chem. Cat. Chem* **2019,** *11*, 298 - 308.
23. Russo, V., Tesser, R., et al., Chemical and technical aspects of propene oxide production via hydrogen peroxide (HPPO Process). *Ind. Eng. Chem. Red.* **2013,** *52*, 1168-1178.
24. Targhan, H., Evans, P., Bahrami, K., A review of the role of hydrogen peroxide in organic transformations. *J. Ind. Eng. Chem.* **2021,** *104*, 295-332.
25. Hu, Y., Dong, C., et al., Cyclohexanone ammoximation over TS-1 catalyst without organic solvent in a microreaction system. *Chem. Eng. Sci.* **2018,** *187*, 60-66.
26. Thangaraj, A., Kumar, R., Ratnasamy, P., Catalytic properties of crystalline titanium silicalites II. Hydroxylation of phenol with hydrogen peroxide over TS-1 zeolites. *J. Catal.* **1991,** *131*, 294-297.
27. Crombie, C., Lewis, R., et al., The influence of reaction conditions on the oxidation of cyclohexane via the in-situ production of H_2O_2. *Catal. Letters* **2020,** *151*, 164-171.
28. Santonastaso, M., Freakley, S., et al, Oxidation of benzyl alcohol using in situ generated hydrogen peroxide. *Org. Process Res. Dev.* **2014,** *18*, 1455-1460.
29. Kang, J., Park, E., Selective Oxidation of Methane over Fe-Zeolites by In Situ Generated H_2O_2. *Catalysts* **2020,** *10*, 299.
30. Thenard, L., Observations sur des nouvelles combinaisons entre l'oxigène et divers acides. *Ann. Chim. Phys.* **1818,** *8*, 306-312.
31. Jones, C., *Applications of hydrogen peroxide and derivatives*. Royal Society of Chemistry: 2007.
32. Riedl, H., Pfleiferer, G. 1939.
33. Samanta, C., Direct synthesis of hydrogen peroxide from hydrogen and oxygen: An overview of recent developments in the process. *Appl. Catal. A-Gen.* **2008,** *350*, 133 - 149.
34. Lewis, R., Ueura, K., et al., The direct synthesis of H_2O_2 using TS-1 supported catalysts. *Chem. Cat. Chem* **2019,** *11*, 1673-1680.
35. Yi, Y., Wang, L., et al., A review on research progress in the direct synthesis of hydrogen peroxide from hydrogen and oxygen: noble-metal catalytic method, fuel-cell method and plasma method. *Catal. Sci. Technol* **2016,** *6*, 1593.
36. Otsuka, K., Yamanaka, I., One step synthesis of hydrogen peroxide through fuel cell reaction. *Electrochimica Acta.* **1990,** *35*, 319-322.
37. Yi, Y., Zhou, J., et al., Continuous and Scale-Up Synthesis of High Purity H_2O_2 by Safe Gas-Phase H_2/O_2 Plasma Reaction. *AIChE J.* **2014,** *60*, 415-419.
38. Henkel, H., Weber, W. 1914.
39. Dissanayake, D., Lunsford, J., The direct formation of H_2O_2 from H_2 and O_2 over colloidal palladium. *J. Catal.* **2003,** *214*, 113 - 120.
40. Chinta, S., Lunsford, J., A mechanistic study of H_2O_2 and H_2O formation from H_2 and O_2 catalysed by palladium in an aqueous medium. *J. Catal.* **2004,** *225*, 249 - 255.
41. Wilson, N., Flaherty, D., Mechanism for the direct synthesis of H_2O_2 on Pd clusters: heterolytic reaction pathways at the liquid-solid interface. *J. Am. Chem. Soc.* **2016,** *138*, 574 - 586.
42. Wilson, N., Priyadarshini, P., et al., Direct synthesis of H_2O_2 on Pd and Au_xPd_1 clusters: Understanding the effect of alloying Pd with Au. *J. Catal.* **2018,** *357*, 163 - 175.
43. Ouyang, L., Tian, P., et al, The origin of active sites for direct synthesis of H_2O_2 on Pd/TiO_2 catalysts: Interfaces of Pd and PdO domains. *J. Catal.* **2015,** *321*, 70-80.
44. Gaikwad, A., Sansare S., Choudhary, V., Direct oxidation of hydrogen to hydrogen peroxide over Pd-containing fluorinated or sulfated Al_2O_3, ZrO_2, CeO_2, ThO_2, Y_2O_3 and Ga_2O_3 catalysts in stirred slurry reactor at ambient conditions. *J. Mol. Catal. A Chem.* **2002,** *181*, 143-149.
45. Yu, S., Cheng, X., et al., High activity and selectivity of single palladium atom for oxygen hydrogenation to H_2O_2. *Nat. Commun.* **2022,** *13*, 4737.

46. Menegazzo, F., Signoretto, M., et al., When high metal dispersion has a detrimental effect: Hydrogen peroxide direct synthesis under very mild and nonexplosive conditions catalyzed by Pd supported on silica. *J. Catal.* **2012,** *290*, 143-150.
47. Ntainjua, E., Edwards, J., et al, The role of the support in achieving high selectivity in the direct formation of hydrogen peroxide. *Green Chem.* **2008,** *10*, 1162-1169.
48. Choudhary, V., Gaikwad, A., Sansare, S.,, Activation of supported Pd metal catalysts for selective oxidation of hydrogen to hydrogen peroxide. *Catal. Letters* **2002,** *83*, 235-239.
49. Blanco-Brieva, G., Cano-Serrano, E., et al., Direct synthesis of hydrogen peroxide solution with palladium-loaded sulfonic acid polystyrene resins. *Chem. Commun.* **2004,** *0*, 1184-1185.
50. Wang, F., Xia, C., et al., How does the oxidation state of palladium surface affect the reactivity and selectivity of direct synthesis of hydrogen peroxide from hydrogen and oxygen gases? A density functional study. *J. Am. Chem. Soc.* **2019,** *141*, 901-910.
51. Liu, Q., Gath, K., et al., The active phase in the direct synthesis of H_2O_2 from H2 and O_2 over Pd/SiO_2 catalyst in a H_2SO_4/ethanol system. *Catal. Letters* **2009,** *132*, 342-348.
52. Flaherty, D., Direct synthesis of H_2O_2 from H_2 and O_2 on Pd catalysts: Current understanding, outstanding questions and research needs. *ACS Catal.* **2018,** *8*, 1520-1527.
53. Stahl, S., Thormann, J., et al., Oxygenation of Nitrogen-Coordinated Palladium(0): Synthetic, Structural, and Mechanistic Studies and Implications for Aerobic Oxidation Catalysis. *J. Am. Chem. Soc.* **2001,** *123*, 7188-7189.
54. Tian, P., Ouyang, L., et al, The origin of palladium particle size effects in the direct synthesis of H_2O_2: Is smaller better? *J. Catal.* **2017,** *349*, 30-40.
55. Wilson, N., Flaherty, D., Mechanism for the Direct Synthesis of H_2O_2 on Pd Clusters: Heterolytic Reaction Pathways at the Liquid−Solid Interface. *J. Am. Chem. Soc.* **2015,** *138*, 574-586.
56. Edwards, J., Carley, A., et al., Direct synthesis of hydrogen peroxiede from H_2 and O_2 using supported Au-Pd catalysts. *Faraday Discuss.* **2008,** *138*, 225 - 239.
57. Ntainjua, E., Freakley, S., Hutchings, G., Direct synthesis of hydrogen peroxide using ruthenium catalysts. *Top. Catal.* **2012,** *55*, 718 - 722.
58. Crole, D., Underhill, R., et al., The direct synthesis of hydrogen peroxide from H_2 and O_2 using Pd-Ni/TiO_2 catalysts. *Phil. Trans. R. Soc.* **2020,** *378*.
59. Gong, X., Lewis, R., et al., Enhanced catalyst selectivity in the direct synthesis of H_2O_2 through Pt incorporation into TiO_2 supported AuPd catalysts. *Catal. Sci. Technol.* **2020,** *10*, 4635.
60. Landon, P., Collier, P., et al., Direct synthesis of hydrogen peroxide from H_2 and O_2 using Pd and Au catalysts. *Phys. Chem. Chem. Phys* **2003,** *5*, 1917-1923.
61. Edwards, J., Solsona, B., et al., Direct synthesis of hydrogen peroxide from H_2 and O_2 using TiO_2-supported Au–Pd catalysts. *J. Catal.* **2005,** *236*, 69-79.
62. Edwards, J., Solsona, B., Direct synthesis of hydrogen peroxide from H_2 and O_2 using Au-Pd/Fe_2O_3 catalysts. *J. Mater. Chem.* **2005,** *15*, 4595-4600.
63. Han, Y., Zhong, Z., et al, Au promotional effects on the synthesis of H_2O_2 directly from H_2 and O_2 on supported Pd-Au alloy catalysts. *J. Phys. Chem. C* **2007,** *111*, 8410 - 8413.
64. Li, J., Ishihara, T., Yoshizawa, K., Theoretical revisit of the direct synthesis of H_2O_2 on Pd and Au@Pd surfaces: A comprehensive mechanistic study. *J. Phys. Chem. C* **2011,** *115*, 25359 - 25367.
65. Ham, H., Hwang, G., et al., On the role of Pd ensembles in selective H_2O_2 formation on PdAu alloys. *J. Phys. Chem. C* **2009,** *113*, 12943 - 12945.
66. Choudhary, V., Samanta, C., Choudhary, T., Direct oxidation of H_2 to H_2O_2 over Pd-based catalysts: Influence of oxidation state, support and metal additives. *Appl. Catal. A-Gen.* **2006,** *308*, 128-133.
67. Wang, S., Gao, K., et al., Effect of Zn addition on the direct synthesis of hydrogen peroxide over supported palladium catalysts. *Appl. Catal. A-Gen.* **2017,** *531*, 89-95.
68. Maity, S., Eswaramoorthy, M., Ni–Pd bimetallic catalysts for the direct synthesis of H_2O_2 – unusual enhancement of Pd activity in the presence of Ni. *J. Mater. Chem.* **2016,** *4*, 3233-3237.

69. Gu, J., Wang, Z., et al., Direct synthesis of hydrogen peroxide from hydrogen and oxygen over activated-carbon-supported Au-Ag alloy catlysts. *Catal. Sci. Technol.* **2016,** *6*, 809-817.
70. Ding, D., Xu, X.,, Promotional effects of Sb on Pd-based catalysts for the direct synthesis of hydrogen peroxide at ambient pressure. *Chin. J. Catal.* **2018,** *39*, 673-681.
71. Stakyov, A., Kamachi, T., et al., Theoretical Study of the Direct Synthesis of H_2O_2 on Pd and Pd/Au Surfaces. *J. Phys. Chem. C.* **2008,** *112*, 19501-19505.
72. Edwards, J., Pritchard, J., et al, The Direct Synthesis of Hydrogen Peroxide Using Platinum-Promoted Gold–Palladium Catalysts. *Angew. Chem. Int. Ed.* **2014,** *53*, 2381-2384.
73. Edwards, J., Parker, S., et al., Effect of acid pre-treatment on AuPd/SiO_2 catalysts for the direct synthesis of hydrogen peroxide. *Catal. Sci. Technol.* **2013,** *3*, 812.
74. Yook, S., Kwon, H., et al., Significant Roles of Carbon Pore and Surface Structure in AuPd/C Catalyst for Achieving High Chemoselectivity in Direct Hydrogen Peroxide Synthesis. *ACS Sustainable Chem. Eng.* **2017,** *5*, 1208-1216.
75. Li, G., Edwards, J., et al., Direct synthesis of hydrogen peroxide from H_2 and O_2 using zeolite-supported Au-Pd catalysts. *Catal. Today* **2007,** *122*, 361-364.
76. Freakley, S., Lewis, R., et al., Direct synthesis of hydrogen peroxide using Au-Pd supported and ion-exchanged heteropolyacids precipitated with various metal ions. *Catal. Today* **2015,** *248*, 10-17.
77. Park, S., Choi, J., et al., Direct synthesis of H_2O_2 from H_2 and O_2 over Pd catalyst supported on $Cs_{2.5}H_{0.5}PW_{12}O_{40}$-MCF silica. *Catal. Today* **2012,** *185*, 162-167.
78. Cuenya, B., Synthesis and catalytic properties of metal nanoparticles: Size, shape, support, composition, and oxidation state effects. *Thin Solid Films* **2010,** *518*, 3127-3150.
79. Thomas Richards, R. L., David Morgan and Graham Hutchings, The direct synthesis of hydrogen peroxide over supported Pd-based catalysts: An investigation into the role of the support and secondary metal modifiers. *Catal. Letters* **2022**.
80. Barnes, A., Lewis, R., et al., Improving catalytic activity towards the direct synthesis of H_2O_2 through Cu incorporation into AuPd catalysts. *Catalysts* **2022,** *12*, 1396.
81. Jin, Z., Liu, Y., et al., Direct Synthesis of Pure Aqueous H_2O_2 Solution within Aluminosilicate Zeolite Crystals. *ACS Catal.* **2021,** *11*, 1946-1951.
82. Ji, X., Chen, D., et al., Sustainable direct H2O2 synthesis over Pd catalyst supported on mesoporous carbon: The effect of surface nitrogen functionality. *Catal. Today* **2021,** *376*, 1-8.
83. Edwards, J., Thomas, A., et al., Comparison of supports for the direct synthesis of hydrogen peroxide from H_2 and O_2 using Au–Pd catalysts. *Catal. Today* **2007,** *122*, 397-402.
84. Edwards, J., Solsona, B., et al., Switching Off Hydrogen Peroxide Hydrogenation in the Direct Synthesis Process. *Science* **2009,** *323*, 1037-1041.
85. Ntainjua, E., Piccinini, M., et al., Effect of halide and acid additives on the direct synthesis of hydrogen peroixde using supported gold-palladium catalysts. *ChemSusChem* **2009,** *2*, 575-580.
86. Lewis, R., Edwards, J., et al., Solid acid additives as recoverable promoters for the direct synthesis of hydrogen peroxide. *Ind. Eng. Chem. Red.* **2017,** *56*, 13287-13293.
87. Alotaibi, F., Al-Mayman, S., et al., Direct synthesis of hydrogen peroxide using Cs-containing heteropolyacid-supported palladium-copper catalysts. *Catal. Letters* **2019,** *149*, 998-1006.
88. Lewis, R., Ntainjua, E., et al., Improving the performance of Pd based catalysts for the direct synthesis of hydrogen peroxide via acid incorporation during catalyst synthesis. *Catal. Commun.* **2021,** *161*, 106358.
89. Qingsheng Liu, J. L., The roles of chloride ions in the direct formation of H_2O_2 from H_2 and O_2 over Pd/SiO_2 catalyst in a H_2SO_4/ethanol system. *J. Catal.* **2006,** *239*, 237-243.
90. Marshall, S., Medlin, W., Surface-level mechanistic studies of adsorbate-adsorbate interactions in heterogeneous catalysis by metals. *Surf. Sci. Rep.* **2011,** *66*, 173-184.
91. Centomo, P., Meneghini, C., et al., EXAFS in situ: The effect of bromide on Pd during the catalytic direct synthesis of hydrogen peroxide. *Catal. Today* **2015,** *248*, 138-141.
92. Biasi, P., Sterchele, S., et al., Application of the Catalyst Wet Pretreatment Method (CWPM) for catalytic direct synthesis of H_2O_2. *Catal. Today* **2015,** *246*, 207-215.

93. Choudhary, V., Samanta, C., Role of chloride or bromide anions and protons for promoting the selctive oxidation of H_2 by O_2 to H_2O_2 over supported Pd catalysts in an aqueous medium. *J. Catal.* **2006,** *238*, 28-38.
94. Dissanayake, D., Lunsford, J., Evidence for the role of colloidal palladium in the catalytic formation of H_2O_2 from H_2 and O_2. *J. Catal.* **2002,** *206*, 173-176.
95. Gallina, G., Garcia-Serna, J., et al., Bromide and acids: A comprehensive study on their role on the hydrogen peroxide direct synthesis. *Ind. Eng. Chem. Red.* **2017,** *56*, 13367-13378.
96. Edwards, J., Ntainjua, E., et al., Direct synthesis of H_2O_2 from H_2 and O_2 over gold, palladium, and gold-palladium catalysts supported on acid-pretreated TiO_2. *Angew. Chem. Int. Ed.* **2009,** *48*, 8512-8515.
97. Chan-Thaw, C., Sacara, A., Villa, A., Selective benzyl alcohol oxidation over Pd catalysts. *Catalysts* **2018,** *8*, 431.
98. Ryland, B., Stahl, S., Practical aerobic oxidations of alcohols and amines with homogeneous copper/TEMPO and related catalyst systems. *Angew. Chem. Int. Ed.* **2014,** *53*, 8824-8838.
99. Sheldon, R., Recent advances in green catalytic oxidations of alcohols in aqueous media. *Catal. Today* **2015,** *247*, 4-13.
100. Crombie, C., Lewis, R., et al., Enhanced selective oxidation of benzyl alcohol via in sity H_2O_2 production over supported Pd-based catalysts. *ACS Catal.* **2021,** *11*, 2701-2714.
101. Sankar, M., Nowicka, E., et al, The benzaldehyde oxidation paradox explained by the interception of peroxy radical by benzyl alcohol. *Nat. Commun.* **2014,** *5*, 3332.
102. Sankar, M., Nowicka, M., et al., Controlling the Duality of the Mechanism in Liquid-Phase Oxidation ofBenzyl Alcohol Catalysed by Supported Au–Pd Nanoparticles. *Chem. Eur. J.* **2011,** *17*, 6524-6532.
103. Savara, A., Chan-Thaw, C., et al., Benzyl Alcohol Oxidation on Carbon-Supported Pd Nanoparticles: Elucidating the Reaction Mechanism. *ChemCatChem* **2014,** *6*, 3464-3473.
104. Vinod, C., Wilson, K., Lee, A., Recent advances in the heterogeneously catalysed aerobic selective oxidation of alcohols. *J. Chem. Technol. Biotechnol.* **2011,** *86*, 161-171.
105. He, Q., Miedziak, P., et al., Switching-off toluene formation in the solvent-free oxidation of benzyl alcohol using supported trimetallic Au-Pd-Pt nanoparticles. *Faraday Discuss.* **2013,** *162*, 365-378.
106. Nowicka, E., Althahban, S., et al., Benzyl alcohol oxidation with Pd-Zn/TiO2: computational and experimentalstudies. *Sci. Technol. Adv. Mater.* **2019,** *20*, 367-378.
107. Mallat, T., Baiker, A., Oxidation of Alcohols with Molecular Oxygen on Solid Catalysts. *Chem. Rev.* **2004,** *104*, 3037-3058.
108. Savara, A., Chan-Thaw, C., et al., Molecular Origin of the Selectivity Differences between Palladium and Gold–Palladiumin Benzyl Alcohol Oxidation: Different Oxygen Adsorption Properties. *Chem. Cat. Chem* **2017,** *9*, 253-257.
109. Savara, A., Rossetti, I., et al., Microkinetic modelling of benzyl alcohol oxidation on carbon-supported palladium nanoparticles. *Chem. Cat. Chem* **2016,** *8*, 2482-2491.
110. Enache, D., Edwards, J., et al., Solvent-free oxidation of primary alcohols to aldehydes using Au-Pd/TiO_2 catalysts. *Science* **2006,** *311*, 362-365.
111. Li, G., Enache, D., et al., Solvent-free oxidation of benzyl alcohol with oxygen using zeolite-supported Au and Au-Pd catalysts. *Catal. Letters* **2006,** *110*, 7-13.
112. Li, F., Zhang, Q., Wang, W., Size dependence in solvent-free aerobic oxidation of alcohols catalyzed by zeolite-supported palladium nanoparticles. *Appl. Catal. A-Gen.* **2008,** *334*, 217-226.
113. Chen, J., Zhang, Q., et al., Size-dependent catalytic activity of supported palladium nanoparticles for aerobic oxidation of alcohols. *Adv. Synth. Catal.* **2008,** *350*, 453-464.
114. Zhou, Y., Xiang, Z., et al., Preparation and characterization of covalent organic polymer supported palladium catalysts for oxidation of CO and benzyl alcohol. *Ind. Eng. Chem. Red.* **2014,** *53*, 1359-1367.

115. Moreno, I., Dummer, M., et al., Selective oxidation of benzyl alcohol using in situ generated H_2O_2 over hierarchical Au-Pd titanium silicate catalysts. *Catal. Sci. Technol.* **2013,** *3*, 2425.
116. Peneau, C., He, Q., et al., Selective catalytic oxidation using supported gold-palatinum and palladium-platinum nanoalloys prepared by sol-immobilisation. *Phys. Chem. Chem. Phys.* **2013,** *15*, 10636.
117. Morad, M., Sankar, M., et al., Solvent-free aerobic oxidation of alcohols using supported gold palladium nanoalloys prepared by a modified impregnation method. *Catal. Sci. Technol.* **2014,** *4*, 3120.
118. Enache, D., Barker, D., et al., Solvent-free oxidation of benzyl alcohol using titania-supported gold-palladium catalysts: Effect of Au-Pd ratio on catalytic performance. *Catal. Today* **2007,** *122*, 407-411.
119. Dimitratos, N., Villa, A., et al., Pd and Pt catalysts modified by alloying with Au in the selective oxidation of alcohols. *J. Catal.* **2006,** *244*, 113-121.
120. Wu, P., Cao, Y., et al., Formation of PdO on Au-Pd bimetallic catalysts and the effect on benzyl alcohol oxidation. *J. Catal.* **2019,** *375*, 32-43.
121. Tiruvalam, R., Pritchard, J., et al., Aberration corrected analytical electron microscopy studies of sol-immobilized Au + Pd, Au{Pd} and Pd{Au} catalysts used for benzyl alcohol oxidation and hydrogen peroxide production. *Faraday Discuss.* **2011,** *152*, 63-86.
122. Silva, T., Teixeira-Neto, E., et al., Volcano-like behaviour of Au-Pd core-shell nanoparticles in the selective oxidation of alcohols. *Sci. Rep.* **2014,** *4*, 5766.
123. Nagy, G., Gál, T., et al., Selective aerobic oxidation of benzyl alcohol on alumina supported Au-Ru and Au-Ir catalysts. *Mol. Catal.* **2020,** *492*, 110917.
124. Adam, F., Ooi, W., Selective oxidation of benzyl alcohol to benzaldehyde over Co-metalloporphyrin supported on silica nanoparticles. *Appl. Catal. A-Gen.* **2012,** *445-446*, 252-260.
125. Choudhary, V., Dumbre, D., Magnesium oxide supported nano-gold: A highly active catalyst for solvent-free oxidation of benzyl alcohol to benzaldehyde by TBHP. *Catal. Commun.* **2009,** *10*, 1738-1742.
126. Nakashima, D., Ichihashi, Y., Promoted partial oxidation activity of alkali metal added-Co catalysts supported on NaY and NaUSY zeolites in the gas-phase catalytic oxidation of benzyl alcohol. *J. Mol. Catal. A Chem.* **2006,** *259*, 108-115.
127. Lu, Y., Zhu, H., et al., Palladium Nanoparticles Supported on Titanate Nanobelts for Solvent-Free Aerobic Oxidation of Alcohols. *ChemcatChem* **2015,** *7*, 4131-4136.
128. Chen, Z., Zou, P., et al., Nitrogen-Incorporated SBA-15 Mesoporous Molecular Sieve Supported Palladium for Solvent-Free Aerobic Oxidation of Benzyl Alcohol. *Catal. Letters* **2015,** *145*, 2029-2036.
129. Ji, R., Zhai, S., et al., Enhanced metal–support interactions between Pd NPs and ZrSBA-15 for efficient aerobic benzyl alcohol oxidation. *RSC Adv.* **2016,** *6*, 70424.
130. Goksu, H., Burhan, H., et al., Oxidation of benzyl alcohol compunds in the presence of carbon hybrid supported platinum nanoparticles (Pt@CHs) in oxygen atmosphere. *Sci. Rep.* **2020,** *10*, 5439.
131. Martinez, J., Mazarío, J., et al., A tandem process for in situ H_2O_2 formation coupled with benzyl alcohol oxidation using Pd–Au bimetallic catalysts. *Dalton Trans.* **2022,** *51*, 17567-17578.
132. Lyu, J., Niu, J., et al., In Situ Hydrogen Peroxide Production for Selective Oxidation of Benzyl Alcohol over a Pd@Hierarchical Titanium Silicalite Catalyst. *ACS Omega* **2020,** *5*, 16865-16874.
133. Richards, T., Harrhy, J., et al., A residue-free approach to water disinfection using catalytic in situ generation of reactive oxygen species. *Nat. Catal.* **2021,** *4*, 575-585.
134. Deng, Y., Zhao, R.,, Advanced oxidation processes (AOPs) in wastewater treatment. *Curr. Pollution. Rep.* **2015,** *1*, 167-176.
135. Bokare, A., Choi, W., review of iron-free Fenton-like systems for activating H_2O_2 in advanced oxidation processes. *J. Hazard. Mater.* **2014,** *275*, 121-135.
136. Milkos, D., Remy, C., et al., Evaluation of advanced oxidation processes for water and wastewater treatment - a critical review. *Water Res.* **2018,** *139*, 118-131.
137. Levec, J., Pintar, A., Catalytic wet-air oxidation processes: a review. *Catal.* **2007,** *124*, 172-184.

138. Suzuki, H., Araki, S., Yamamoto, H., Evaluation of advanced oxidation precesses (AOP) using O_3, UV, and TiO_2 for the degradation of phenol in water. *Water Process Eng.* **2015,** *7*, 54-60.
139. Villegas, L., Mashhadi, N., et al., A short review of techniques for phenol removal from wastewater. *Curr. Pollution. Rep.* **2016,** *2*, 157-167.
140. Zazo, J., Casas, J., Chemical pathway and kinetics of phenol oxidation by Fenton's reagent. *Environ. Sci. Technol.* **2005,** *39*, 9295.
141. Maduna, K., Katovic, A., Zrnčević, S., Investigation of the catalytic wet peroxide oxidation of phenol over different types of Cu/ZSM-5 catalyst. *J. Hazard. Mater.* **2007,** *144*, 663-667.
142. Castro, I., Stüber, F., et al., Supported Cu(II) polymer catalysts for aqueous phenol oxidation. *J. Hazard. Mater.* **2009,** *163*, 809-815.
143. Raza, W., Lee, J., et al, Removal of phenolic compounds from industrial waste water based on membrane-based technologies. *Ind. Eng. Chem. Res.* **2019,** *71*, 1-18.
144. Saha, N., Bhunia, F., Kaviraj, A., Toxicity of Phenol to Fish and Aquatic Ecosystems. *Environ. Contam. Toxicol.* **1999,** *63*, 195-202.
145. Guerra-Que, Z., Pérez-Vidal, H., et al., Treatment of phenol by catalytic wet air oxidation: a comparative study of copper and nickel supported on γ-alumina, ceria and γ-alumina–ceria. *RSC Adv.* **2019,** *9*, 8463-8479.
146. *Comprehensive Toxicology (Second Edition)*. Elsevier: Oxford, 2010.
147. *Advanced Oxidation Processes for Wastewater Treatment: Emerging Green Chemical Technology*. Academic Press: London, 2018.
148. Inchaurrondo, N., Cechini, J., et al., Strategies for enhanced CWPO of phenol solutions. *Appl. Catal. B.* **2012,** *111-112*, 641-648.
149. Jing, G., Luan, M., Chen, T., Progress of catalytic wet air oxidation technology. *Arab. J. Chem.* **2016,** *9*, 1208-1213.
150. Stüber, F., Font, J., et al., Carbon materials and catalytic wet air oxidation of organic pollutants in wastewater. *Top. Catal.* **2005,** *33*, 3-50.
151. Cybulski, A., Catalytic Wet Air Oxidation: Are Monolithic Catalysts and Reactors Feasible? *Ind. Eng. Chem. Res.* **2007,** *46*, 4007-4033.
152. Castillejos-López, E., Maroto-Valiente, A., et al., Comparative study of support effects in ruthenium catalysts applied for wet air oxidation of aromatic compounds. *Catal. Today* **2009,** *143*, 355-363.
153. Santos, A., Yustos, P., et al., Route of the catalytic oxidation of phenol in aqueous phase. *Appl. Catal. B.* **2002,** *39*, 97-113.
154. Pintar, A., Levac, J., Catalytic oxidation of organics in aqueous solutions: I. Kinetics of phenol oxidation. *J. Catal.* **1992,** *135*, 345-357.
155. Bhargava, S., Tardio, J., et al., Wet Oxidation and Catalytic Wet Oxidation. *Ind. Eng. Chem. Res.* **2006,** *45*, 1221-1258.
156. Liotta, L., Gruttadauria, M., et al., Heterogeneous catalytic degradation of phenolic substrates: Catalysts activity. *J. Hazard. Mater.* **2009,** *162*, 588-606.
157. Kim, K., Ihm, S., Heterogeneous catalytic wet air oxidation of refractory organic pollutants in industrial wastewaters: A review. *J. Hazard. Mater.* **2011,** *15*, 16-34.
158. Mijangos, F., Varona, F., Villota, N., Changes in Solution Color During Phenol Oxidation by Fenton Reagent. *Environ. Sci. Technol.* **2006,** *40*, 5538-5543.
159. Santos, A., Yustos, P., et al., Lower toxicity route in catalytic wet oxidation of phenol at basic pH by using bicarbonate media. *Appl. Catal. B.* **2004,** *53*, 181-194.
160. Márquez, J., Levachuk, I., Sillanpää, M., Application of Catalytic Wet Peroxide Oxidation for Industrial and Urban Wastewater Treatment: A Review. *Catalysts* **2018,** *8*, 673.
161. Mnasri-Ghnimi, S., Frini-Srasra, N., Catalytic wet peroxide oxidation of phenol over Ce-Zr-modified clays: Effect of the pillaring method. *Korean. J. Chem. Eng.* **2015,** *32*, 68-73.

162. Jiang, S., Zhang, H., et al., Preparation and characterization of porous Fe-Cu mixed oxides modified ZSM-5 coating/PSSF for continuous degradation of phenol wastewater. *Microporous Mesoporous Mater.* **2017,** *240*, 108-116.
163. Baloyi, J., Ntho, T., Moma, J., Synthesis and application of pillared clay heterogeneous catalysts for wastewater treatment: a review. *RSC Adv.* **2018,** *8*, 5197-5211.
164. Guo, J., Al-Dahhan, M., Catalytic Wet Oxidation of Phenol by Hydrogen Peroxide over Pillared Clay Catalyst. *Ind. Eng. Chem. Res.* **2003,** *42*, 2450-2460.
165. Valkaj, K., Wittine, O., et al., Phenol oxidation with hydrogen peroxide using Cu/ZSM5 and Cu/Y5 catalysts. *Pol. J. Chem. Tehchnol.* **2011,** *13*, 28-36.
166. Liou, R., Chen, S., CuO impregnated activated carbon for catalytic wet peroxide oxidation of phenol. *J. Hazard. Mater.* **2009,** *172*, 498-506.
167. Domínguez, C., Quintanilla, A., et al., Kinetics of wet peroxide oxidation of phenol with a gold/activated carbon catalyst. *Chem. Eng. J.* **2014,** *253*, 486-492.
168. Zazo, J., Casas, J., et al., Catalytic wet peroxide oxidation of phenol with a Fe/active carbon catalyst. *Appl. Catal. B.* **2006,** *65*, 261-268.
169. Rey, A., Faraldos, M., et al., Catalytic wet peroxide oxidation of phenol over Fe/AC catalysts: Influence of iron precursor and activated carbon surface. *Appl. Catal. B.* **2009,** *86*, 69-77.
170. Navalon, S., Alvaro M., Garcia, H., Heterogeneous Fenton catalysts based on clays, silicas and zeolites. *Appl. Catal. B.* **2010,** *99*, 1-26.
171. Szpyrkowicz, L., Juzzolino, C., Kaul, S., A Comparative study on oxidation of disperse dyes by electrochemical process, ozone, hypochlorite and fenton reagent. *Wat. Res.* **2001,** *35*, 2129-2136.
172. Yavuz, Y., Koparal, A., Ögütveren, Ü., Phenol Removal through Chemical Oxidation using Fenton Reagent. *Chem. Eng. Technol.* **2007,** *30*, 583-586.
173. Ovejero, G., Sotelo, J., et al., Wet Peroxide Oxidation of Phenolic Solutions over Different Iron-Containing Zeolitic Materials. *Ind. Eng. Chem. Res.* **2001,** *40*, 3921-3928.
174. Liou, R., Chen, S., et al., Fe (III) supported on resin as effective catalyst for the heterogeneous oxidation of phenol in aqueous solution. *Chemosphere* **2005,** *59*, 117-125.
175. Ramirez, J., Maldonado-Hódar, F., et al., Azo-dye Orange II degradation by heterogeneous Fenton-like reaction using carbon-Fe catalysts. *Appl. Catal. B.* **2007,** *75*, 312-323.
176. Muthuvel, I., Swaminathan, M., Highly solar active Fe(III) immobilised alumina for the degradation of Acid Violet 7. *Sol. Energy Mater. Sol. Cells* **2008,** *92*, 857-863.
177. Yang, X., Xu, X., et al., Iron Oxychloride (FeOCl): An Efficient Fenton-Like Catalyst for Producing Hydroxyl Radicals in Degradation of Organic Contaminants. *J. Am. Chem. Soc.* **2013,** *135*, 16058-16061.
178. Bautista, P., Mohedano, A., et al., Highly stable Fe/γ-Al2O3 catalyst for catalytic wet peroxide oxidation. *J. Chem. Technol. Biotechnol.* **2011,** *86*, 497-504.
179. Fang, M., Zheng, R., et. al., CuO nanosheet as a recyclable Fenton-like catalyst prepared from simulated Cu(II) waste effluents by alkaline H2O2 reaction. *Environ. Sci.: Nano.* **2019,** *6*, 105-114.
180. Wu, Y., Zhang, H., Yan, Y., High efficiency of phenol oxidation in a structured fixed bed over Cu-ZSM-5/PSSF prepared by ion-exchanged method. *Chem. Eng. J.* **2020,** *380*, 122466.
181. Wang, Y., Shen X., Chen, F., Improving the catalytic activity of CeO2/H2O2 system by sulfation pretreatment of CeO2. *J. Mol. Catal. A Chem.* **2014,** *381*, 38-45.
182. Asati, A., Santra, S., et al., Surface-Charge-Dependent Cell Localization and Cytotoxicity of Cerium Oxide Nanoparticles. *ACS nano* **2010,** *4*, 5321-5331.
183. Sun, Q., Liu, M., et al., Synthesis of Fe/M (M = Mn, Co, Ni) bimetallic metal organic frameworks and their catalytic activity for phenol degradation under mild conditions. *Inorg. Chem. Front.* **2017,** *4*, 144-153.
184. Dai, C., Zhang, A., et al., Hollow zeolite-encapsulated Fe-Cu bimetallic catalysts for phenol degradation. *Catal. Today* **2017,** *297*, 335-343.
185. Xia, M., Long, M., et al., A highly active bimetallic oxides catalyst supported on Al-containing MCM-41 for Fenton oxidation of phenol solution. *Appl. Catal. B.* **2011,** *110*, 118-125.

186. Wang, Y., Zhao, H., Zhao, G., Iron-copper bimetallic nanoparticles embedded within ordered mesoporous carbon as effective and stable heterogeneous Fenton catalyst for the degradation of organic contaminants. *Appl. Catal. B.* **2015,** *164*, 396-406.
187. Dükkancı, M., Gündüz, G., et al., Characterization and catalytic activity of CuFeZSM-5 catalysts for oxidative degradation of Rhodamine 6G in aqueous solutions. *Appl. Catal. B.* **2010,** *95*, 270-278.
188. Zarin, S., Aslam, Z., et al., Synthesis of bimetallic/carbon nanocomposite and its application for phenol removal. *J. Iran Chem. Soc.* **2018,** *15*, 2689-2701.
189. Li, Y., Jawad, A., et al., Synergistic degradation of phenols by bimetallic CuO–Co3O4@γ-Al2O3 catalyst in H2O2/HCO3− system. *Chinese J. Catal.* **2016,** *37*, 963-970.
190. Jawad, A., Ly, X., et al., Degradation of Chlorophenols by Supported Co–Mg–Al Layered Double Hydrotalcite with Bicarbonate Activated Hydrogen Peroxide. *J. Phys. Chem. A* **2014,** *118*, 10028-10035.
191. Sádaba, I., Granados, M., Riisager, A., Taarning, E., Deactivation of solid catalysts in liquid media: the case of leaching of active sites in biomass conversion reactions. *Green Chem.* **2015,** *17*, 4133.
192. Sankar, M., Qian, H., et al., Synthesis of Stable Ligand-free Gold-Palladium Nanoparticles Using a Simple Excess Anion Method. *ACS Nano* **2012,** *6*, 6600-6613.
193. Njus, D., Kelley, P., et al., Ascorbic acid: The chemistry underlying its antioxidant properties. *Free Radic. Biol. Med.* **2020,** *159*, 37-43.
194. Tu, J., Njus, D., Schelgel, H., A theoretical study of ascorbic acid oxidation and HOO/O_2^- radical scavenging. *Org. Biomol. Chem.* **2017,** *15*, 4417.
195. Du, J., Cullen, J., Buettner, H., Ascorbic acid: Chemistry, biology and the treatment of cancer. *BBA* **2012,** *1826*, 443-457.
196. Boatright, W., Oxygen dependency of one-electron reactions generating ascorbate radicals and hydrogen peroxide from ascorbic acid. *Food Chem.* **2016,** *196*, 1361-1367.
197. Strizhak, P., Basylchuk, A., et al., Oxidation of ascorbic acid by air oxygen catalysed by copper (II) ions in batch and continuous flow stirred tank reactors: bistability, oscillations and stochastic resonance. *Phys. Chem. Chem. Phys.* **2000,** *2*, 4721-4727.
198. Bolobajev, J., Trapido, M., Goi, A., Improvement in iron activation ability of alachlor Fenton-like oxidation by ascorbic acid. *Chem. Eng. J.* **2015,** *281*, 566-574.
199. Zhou, P., Zhang, J., et al., Generation of hydrogen peroxide and hydroxyl radical resulting from oxygen-dependent oxidation of L-ascorbic acid via copper redox-catalyzed reactions. *RSC Adv.* **2016,** *6*, 38541.
200. Putchala, M., Ramani, P., et al., Ascrobic acid and its pro-oxidant activity as a therapy for tumours of oral cavity - A systematic review. *Arch. Oral Biol.* **2013,** *58*, 563-574.
201. Sun, H., Xie, G., et al., Ascorbic acid promoted magnetite Fenton degradation of alachlor: Mechanistic insights and kinetic modeling *Appl. Catal. B* **2020,** *267*, 118383.
202. Hou, X., Huang, X., et al., Fenton oxidation of organic contaminants with aquifer sediment activated by ascorbic acid. *Chem. Eng. J.* **2018,** *348*, 255-262.
203. Zhou, H., Zhang, H., et al., Critical review of reductant-enhanced peroxide activation processes: Trade-off between accelerated Fe3+/Fe2+ cycle and quenching reactions. *Appl. Catal. B* **2021,** *286*, 119900.

2 Experimental

2.1 Introduction

This Chapter describes the catalyst preparation techniques that were used in Chapters 3-5. Additionally, the experimental procedures and analytical techniques used to analyse reaction mixtures and catalysts are discussed.

2.2 Catalyst Preparation

n.b. reported concentrations of metal salt precursors are based on the concentration of metal in solution, not of the metal salt.

2.2.1 Excess Chloride Co-Impregnation of Pd-Based Catalysts

An excess chloride co-impregnation methodology was utilised for the synthesis of all Pd based catalysts tested in Chapter 3. A generic procedure for the synthesis of a 0.5%Au-0.5%Pd/Al_2O_3 catalyst is described below, based on a previously reported methodology.[200]

1 g of a 0.5%Au-0.5%Pd/Al_2O_3 catalyst was made by the following procedure. An acidified solution of $PdCl_2$ (0.833 ml, [Pd] = 6 mg mL^{-1}, 0.58 M HCl) and a solution of $HAuCl_4{\cdot}3H_2O$ (0.417 mL, [Au] = 12 mg mL^{-1}) were added to a 50 mL round-bottom flask. The total volume of the mixture was adjusted to 16 mL using HPLC grade deionised water and heated under (65 ^{o}C) under stirring. The support (0.99 g) was added slowly, and the solution was stirred (95 ^{o}C, 16 hr). The dried catalyst was finely ground, and heat treated under reductive conditions (flowing 5% H_2/Ar, 500 ^{o}C, 4 hr, 10 ^{o}C min^{-1}).

2.2.2 Wet Co-Impregnation of Pd-Based Catalysts

A wet co-impregnation methodology was utilised for the synthesis of catalysts tested in Chapter 4. A generic procedure for the synthesis of a 0.5%Au-0.5%Pd/Al_2O_3 catalyst is described below, based on a previously reported methodology.[201]

1 g of a 0.5%Au-0.5%Pd/Al_2O_3 catalyst was made by the following procedure. A solution of $PdCl_2$ (0.833 mL, [Pd] = 6 mg mL^{-1}, 0.12 M HCl) and a solution of $HAuCl_4$ (0.417 mL, [Au] = 12 mg mL^{-1}) was added to a 50 mL round-bottom flask. The total volume of the mixture was adjusted to 16 mL using HPLC grade deionised water and heated (65 ^{o}C). The support (0.99 g) was added slowly, and the solution was stirred (95 ^{o}C, 16 hr). The dried catalyst was finely ground, and heat treated under either reductive (flowing 5% H_2/Ar, 500 ^{o}C, 4 hr, 10 ^{o}C min^{-1}), or oxidative conditions (flowing compressed air, 500 ^{o}C, 4 hr, 10 ^{o}C min^{-1}).

2.2.3 Sol-Immobilisation of Pd-Based Catalysts

A sol-immobilisation methodology was also utilised for the synthesis of some catalysts tested in Chapter 4. A generic procedure for the synthesis of a 0.5%Au-0.5%Pd/Al_2O_3 catalyst is described below, based on previously reported methodology.[202]

1 g of a 0.5%Au-0.5%Pd supported catalyst was made by the following procedure. A solution of $PdCl_2$ (0.833 mL, [Pd] = 6 mg mL^{-1}) and a solution of $HAuCl_4 \cdot 3H_2O$ (0.417 mL, [Au] = 12 mg mL^{-1}) was added to HPLC grade deionised water (400 mL). A solution of PVA (1.3 mL, 1 wt.%, MW 10000, 80% hydrolysed) was added to give a metal/PVA ratio of 1/1.3 w/w. A solution of $NaBH_4$ (3.618 mL, 0.1 M) so that the ratio of metal/$NaBH_4$ was 1/5 mol/mol was then added. After 30 minutes of stirring, the support was added (0.99 g). The mixture was acidified with H_2SO_4 (75 wt.%) to a pH of 1. After 2 hours of stirring, the mixture was filtered under vacuum and the solid catalyst was washed with distilled water (2 L). The solid catalyst was dried under vacuum (25 ^oC, 16 hr) before being finely ground and calcined under flowing compressed air (500 ^oC, 4 hr, 10 ^oC min^{-1}).

2.2.4 Wet Co-Impregnation of Fenton-Type Catalysts

A wet co-impregnation methodology was employed for the synthesis of all catalysts tested in Chapter 5. A generic procedure, using a 2%Cu/Al_2O_3 catalyst as an example is described:

5 g of 2%Cu/Al_2O_3 was made by the following procedure. A solution of $Cu(NO_3)_2 \cdot 2.5H_2O$ ([Cu] = 2.466 mg mL^{-1}, 16 mL) was added to H_2O (24 mL) and heated (65 ^oC) under stirring. The Al_2O_3 support (4.9 g) was added slowly, and the mixture was stirred (95 ^oC, 16 hr). The resultant powder was finely ground, 1 g of which was then calcined in static air (750 ^oC, 3 hr, 5 ^oC min^{-1}).

2.3 Catalyst Testing

2.3.1 The Direct Synthesis of H_2O_2

Investigations of the direct synthesis of H_2O_2 were conduction in a 50 mL Parr stainless steel autoclave, equipped with a PTFE liner. The catalyst (10 mg) was added to a solvent mixture of water (2.9 g) and methanol (5.6 g) and sealed in the reactor. The reactor was purged three times with 100 psi of 5% H_2/CO_2 and then charged with 5% H_2/CO_2 (420 psi, 2.76 mmol) and 25% O_2/CO_2 (160 psi, 5.26 mmol). The reaction mixture was then stirred (1200 rpm) for 30 minutes at 20 ^oC. After completion, the catalyst was removed from the mixture by filtration and H_2O_2 concentrations were determined by titration of aliquots of reaction mixture, using acidified $Ce(SO_4)_2$ (8 x 10^{-3} mol L^{-1}) and a phenanthroline iron(II) sulfate indicator. A change in colour from red to blue indicated the end point of the titration, and the reaction between H_2O_2 and $Ce(SO_4)_2$ is shown in Equation 2.1.

Eq. 2.1 $$H_2O_2 + 2\ Ce(SO_3)_2 \rightarrow Ce_2(SO_4)_3 + H_2SO_4 + O_2$$

Analysis of reactant gasses was done using a Varian CP-3380 with a Porapak Q column.

Catalytic activity was presented in terms of 'productivity', which is described by Equation 2.2.

Eq. 2.2 $$\text{Productivity}\left(\text{mol}_{\text{H2O2}}\ \text{kg}^{-1}{}_{\text{cat}}\ \text{hr}^{-1}\right) = \frac{\text{mol H}_2\text{O}_2\ \text{produced}}{\text{mass of catalyst (kg)}\times\text{time (hr)}}$$

H_2 conversion was determined using GC, by comparing post-reaction gas samples with 'blank reactions' wherein no catalyst was present, but all other conditions were kept identical to a standard synthesis reaction. The area of H_2 for this blank reaction represented the concentration of H_2 when no conversion occurred. CO_2 operated as an internal standard, and the area of the H_2 peak was divided by the area of CO_2 to give H_2/CO_2. Post reaction gas samples were taken, and the H_2/CO_2 was compared to the blank reaction to determine H_2 conversion by the Equation 2.3.

Eq. 2.3 $$H_2\ conversion\ (\%) = \frac{{}^{area\ H_2}\!/_{area\ CO_{2_{blank}}} - {}^{area\ H_2}\!/_{area\ CO_{2_{reaction}}}}{{}^{area\ H_2}\!/_{area\ CO_{2_{blank}}}} \times 100$$

The initial number of moles of H_2 was determined using the ideal gas equation, shown in Equation 2.4. Following this, the number of moles of H_2 converted during the reaction was calculated and the selectivity for the formation of H_2O_2 in terms of H_2 was calculated using Equation 2.5.

Eq. 2.4 $$n = \frac{pV}{RT}$$

N= Moles of gas (mol)
P= Pressure of gas (Pa)
V= Volume of gas (m^3)
R= Universal gas constant (8.314 J K^{-1} mol^{-1})
T= Temperature (K)

Eq. 2.5 $$H_2O_2\ Selectivity = \frac{moles\ H_2O_2\ formed}{moles\ H_2\ converted} \times 100$$

2.3.2 Degradation of H_2O_2

Investigations into the degradation of H_2O_2 were conducted in a 50 mL Parr stainless steel autoclave, equipped with a PTFE liner. The catalyst (10 mg) was added to a mixture of H_2O_2 (0.68 g, 50 wt.% H_2O_2), H_2O (2.22 g) and methanol (5.6 g) and sealed in the reactor (giving an approximately 4% solution of H_2O_2). The initial concentration of H_2O_2 was determined by titrating aliquots of the initial reaction mixture, using acidified $Ce(SO_4)_2$ (8×10^{-3} mol L^{-1}) and a phenanthroline iron(II) sulfate indicator. The reactor was purged three times with 100 psi of 5% H_2/CO_2 and then charged with 5% H_2/CO_2 (420 psi, 2.76 mmol). The reaction mixture was then stirred (1200 rpm) for 30 minutes at 20 ^oC. After completion, the catalyst was removed from the mixture by filtration and H_2O_2 concentrations were determined by titration of aliquots of reaction mixture with acidified $Ce(SO_4)_2$ (8 x 10^{-3} mol L^{-1}) and a phenanthroline iron(II) sulfate indicator. Comparison of the initial and finals concentrations of H_2O_2 were used to determine the degradation of H_2O_2. The activity of the catalysts studied in this thesis towards the degradation of H_2O_2 was expressed as a productivity (mol_{H2O2} kg^{-1}_{cat} hr^{-1}), in order to standardise both mass of catalyst and time.

2.3.3 Oxidation of benzyl alcohol via the in-situ synthesis of H_2O_2

Investigations into the oxidation of benzyl alcohol were conducted in a 50 mL Parr stainless steel autoclave, equipped with a PTFE liner. The catalyst (10 mg) was added to a mixture of methanol (7.13 g), benzyl alcohol (1.04 g, 9.6 mmol) and the internal standard mesitylene (0.43 g, 3.58 mmol). This was sealed in the reactor and purged three times with 100 psi of 5% H_2/CO_2 and then charged with 5% H_2/CO_2 (420 psi, 2.76 mmol) and 25% O_2/CO_2 (160 psi, 5.26 mmol). The reaction mixture was then heated to 50 ^oC whilst being stirred at 100 rpm. Once 50 ^oC was reached, the reaction temperature was maintained and the reaction mixture was stirred (1200 rpm) for 30 minutes. Once complete, the reactor was cooled to 15 ^oC using ice water. The catalyst was removed by filtration and product analysis was conducted using gas chromatography, using a Varian 3200 GC with a CP Wax 42 column and flame ionization detector. Analysis of reactant gasses was conducted using a Varian CP-3380 with a Porapak Q column, with H_2 conversion values determined using the methodology described in Section 2.3.1. H_2 selectivity was calculated using Equation 2.6, wherein it was assumed that one mole of H_2 oxidised one mole of benzyl alcohol in a ratio of 1: 1.

Eq. 2.6
$$H_2\ Selectivity = \frac{moles\ product\ formed}{moles\ H_2\ converted} \times 100$$

When a catalyst was used in sequential benzyl alcohol oxidation reactions, the above process was followed with the following exception. After 30 minutes, the reactor was cooled to 15 ^oC using ice water and a gas sample was taken for analysis. The remaining gas was removed from the reactor, which was then purged three times with 100 psi of 5% H_2/CO_2 and then charged with 5% H_2/CO_2 (420 psi, 2.76 mmol) and 25% O_2/CO_2 (160 psi, 5.26 mmol). The reactor was heated to 50 ^oC and then stirred (1200 rpm) for 30 minutes. This was repeated as many times as necessary, and once the reaction reached completion, the catalyst and reaction mixture were separated and analysed as described above.

For catalyst re-use experiments, 0.4 g of the catalyst was used under the reaction conditions detailed above. After completion of the first reaction, the recovered catalyst was washed with methanol (5 times, 2 mL) and dried under vacuum (25 ^oC, 18 hr) before being used again under the reaction conditions described above.

To quantify reaction products, standard solutions of observed reaction products including benzaldehyde, benzoic acid and toluene were calibrated over a range of concentrations. To do this, standard solutions of benzyl alcohol, internal standard (mesitylene) and reaction products were created. The area of the signal offered by GC analysis of each compound and of mesitylene was compared with the signal areas of a range of known concentrations (mol L^{-1}) of each compound, and calibration curves were constructed. By taking the ratio of the signals from a reaction product and the internal standard, the ratio of concentrations of the reaction product and the internal standard was determined, using the calibration curves shown in Figure 2.1, and by Equation 2.7:

Eq. 2.7 $$\frac{\left(Product_{Signal\ Area}/Mesitylene_{Signal\ Area}\right)}{m} = \left(Product_{mol/L}/Mesitylene_{mol/L}\right)$$

Where m is the slope of the straight line. From this, the concentration of a given reaction product can be determined, given that the initial concentration of mesitylene is known.

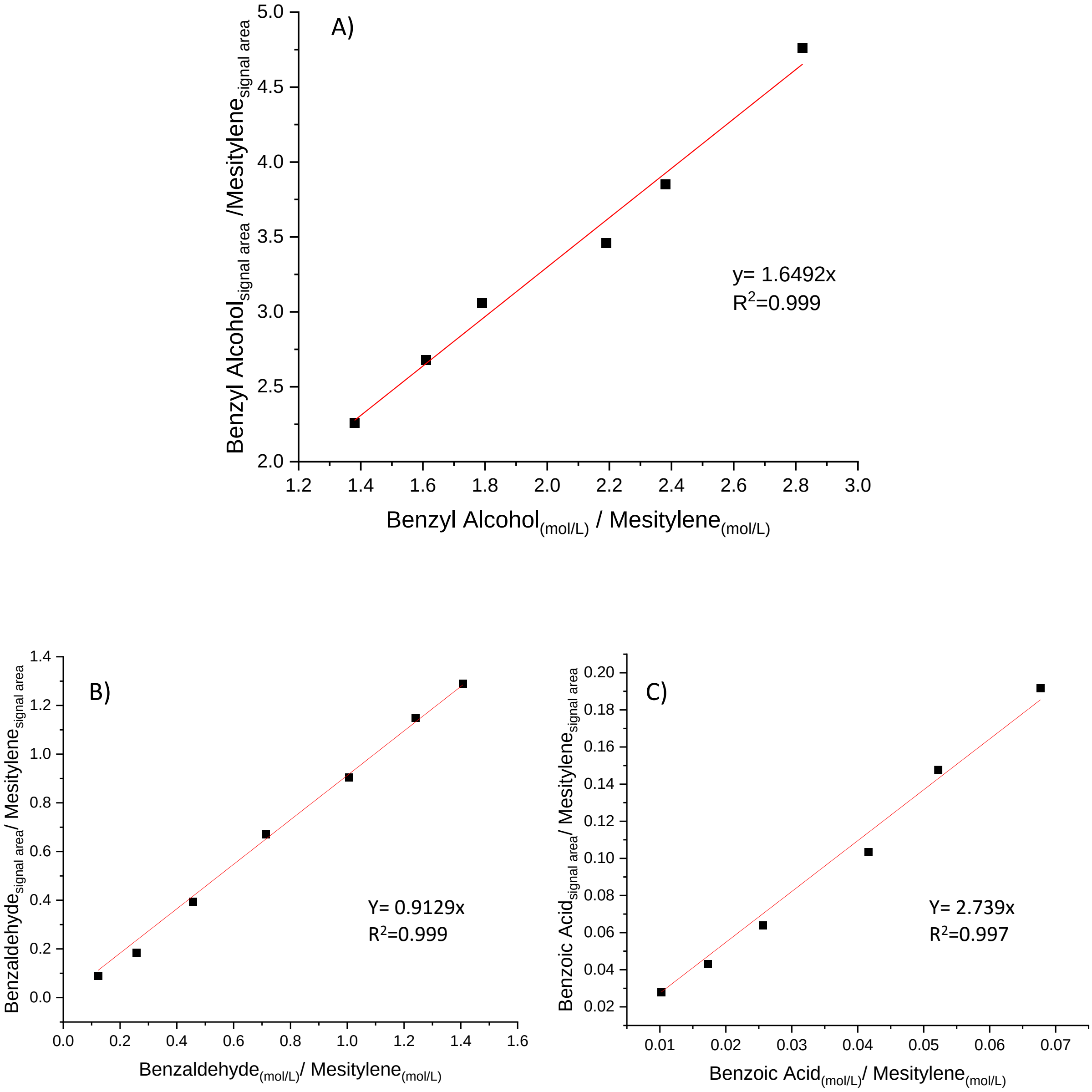

Figure 2.1. Calibration curve to determine A) the conversion of benzyl alcohol and yields of B) benzaldehyde and C) benzoic acid from the selective oxidation of benzyl alcohol via in-situ H_2O_2 synthesis.

2.3.4 Catalytic Wet Peroxide Oxidation of Phenol

Investigations into the catalytic wet peroxide oxidation of phenol were conducted in a 25 mL round bottom flask with magnetic stirring. The catalyst (100 mg) was loaded into a catalyst bed. Freshly prepared 'oxidant solution' (10 mL) containing ascorbic acid (0.04 g, 0.4 wt.%) and sodium percarbonate (0.03 g, 0.3 wt.%) equivalent to 975 ppm H_2O_2 in H_2O, was passed manually through the catalyst bed with a pipette. 5 mL of the resulting solution was added to a solution of phenol (5 mL, 1000 ppm) in a round-bottom flask, and stirred for 60 minutes (1000 rpm, 20 ^{o}C). A schematic diagram of this is shown in Figure 2.2. Periodically throughout the reaction, aliquots of reaction mixture (1 mL) were removed and added to methanol (1 mL) to quench any radical species, and subsequently analysed by HPLC using a reverse phase column at 30^{o}C, with a mobile phase of H_2O and acetonitrile. A gradient elution method was used, changing the solvent ratio of H_2O:acetonitrile from 100:0 to 20:80 over 25 minutes, at a flow rate of 0.25 mL min^{-1}.

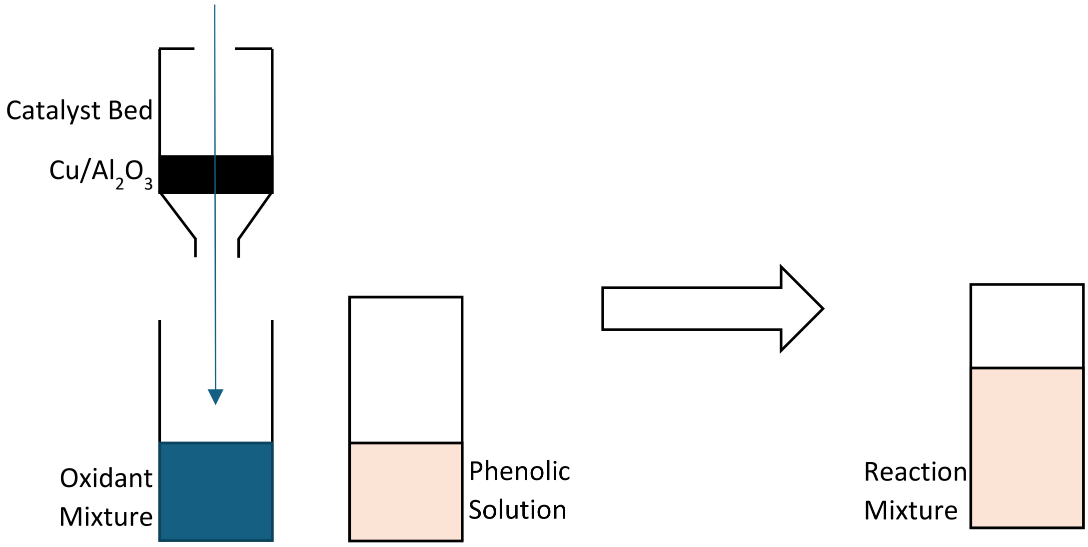

10 mL of oxidant Solution passed through loaded catalyst bed.

5 mL of oxidant solution added to 5 mL of 1000 ppm phenol, stirring at 1000 rpm, 20 ^{o}C.

Figure 2.2. Schematic diagram showing the configuration of the catalyst bed and reactor.

The conversion of phenol and quantification of reaction products was determined via high performance liquid chromatography (HPLC) using an Agilent 1260 Infinity HPLC, equipped with an Agilent Poroshell 120 SB-C18 reverse phase column, and analysed by a DAD detector.

To calculate the conversion of phenol and yields of reaction products, calibration curves (Figure 2.3.) were generated by comparing known concentrations of a given reactant or product with the corresponding signal area offered by that compound via HPLC.

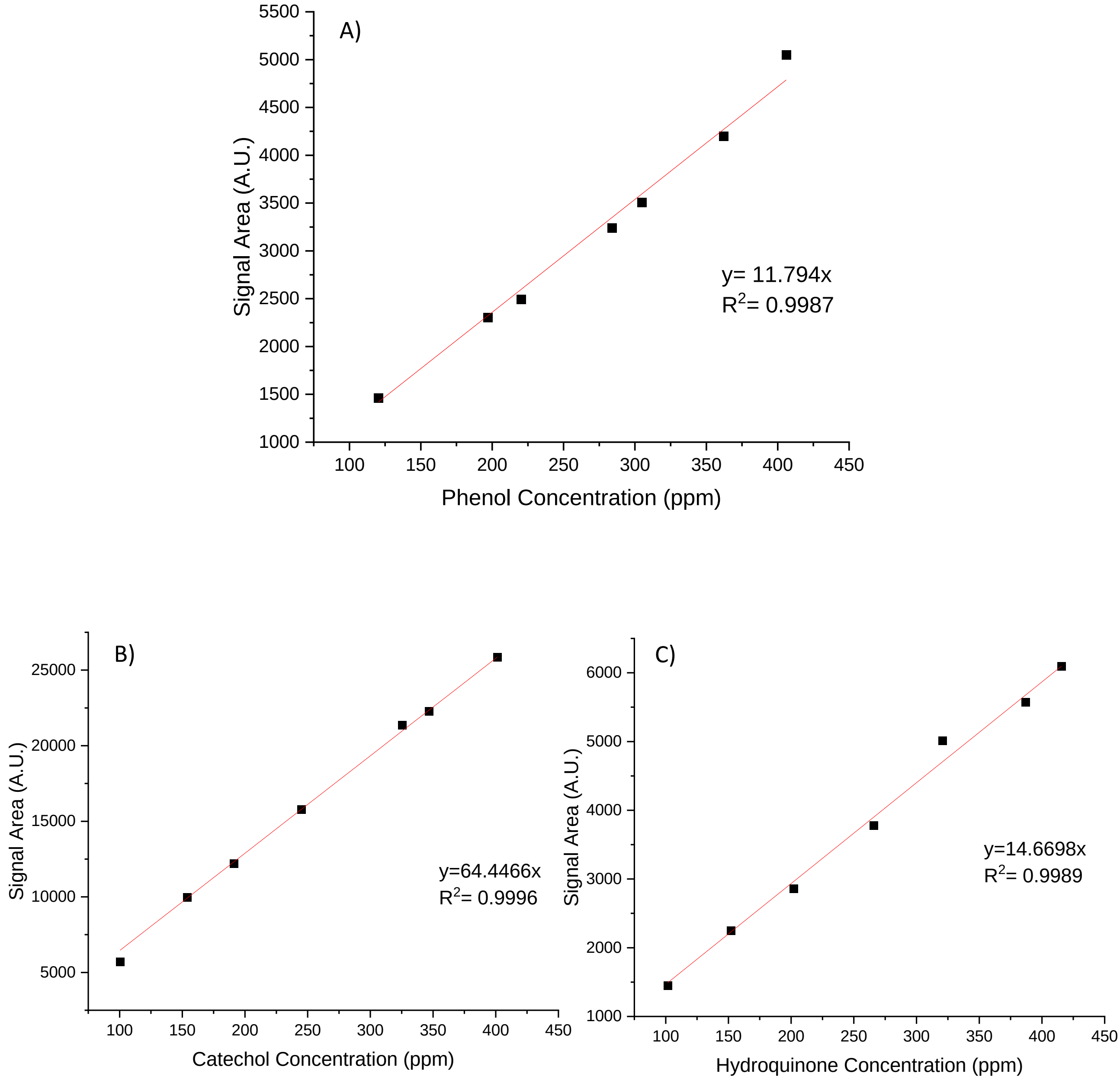

Figure 2.3. Calibration curve to determine A) the conversion of phenol and yields of B) catechol and C) hydroquinone, during the catalytic wet peroxide oxidation of phenol.

Conversion between a signal area and concentration was done using Equation 2.8:

Eq. 2.8 $$Concentration\ (ppm) = Signal\ Area/m$$

Where m is the slope of the calibration curve.
The conversion of phenol was calculated using Equation 2.9.

Eq. 2.9 $$Phenol\ conversion\ (\%) = \frac{initial\ moles\ of\ phenol - final\ moles\ of\ phenol}{initial\ moles\ of\ phenol} \times 100$$

Yields of reaction products were calculated using Equation 2.10.

Eq. 2.10 $$Yield\ (\%) = \frac{moles\ of\ a\ product\ formed}{moles\ of\ phenol\ converted} \times 100$$

2.4 Analytical Techniques

2.4.1 Gas Chromatography

Gas chromatography (GC) is an analytical technique used to separate the substituent components of a chemical mixture. This allows for the independent analysis of each component within the mixture. A generic diagram of a gas chromatograph is shown in Figure 2.4.

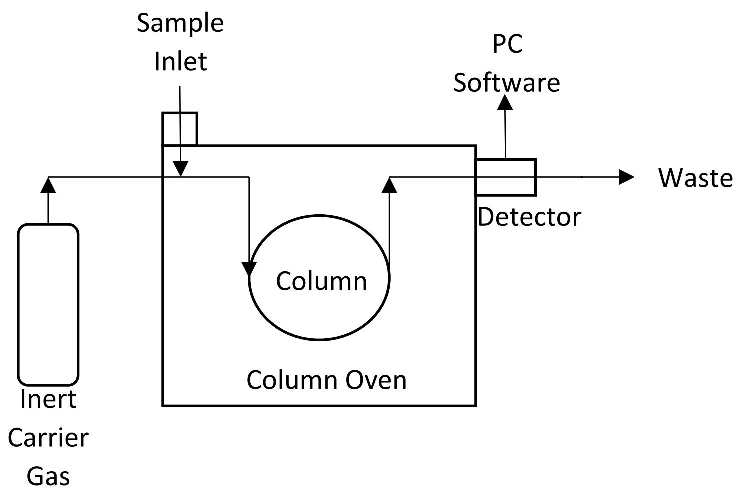

Figure 2.4. Generic construction of a gas chromatograph.

GC operates as follows. A liquid sample is vapourised and introduced at the sample inlet, wherein an inert gaseous mobile phase such as N_2 or Ar carries the vapourised sample down the column. The sample will encounter a 'stationary phase' contained within the column, which can be either a lining or packed component within the column. An appropriately selected stationary phase will allow the constituent parts of a sample to be separated because the differing polarities of each component within the sample will interact to a different magnitude with the stationary phase. The degree of this interaction will slow the transit of different compounds through the column, with stronger interactions between an analyte and the stationary phase resulting in greater retention times. Eventually all compounds will leave the column and be detected, usually by either a flame ionisation detector or thermal conductivity detector, though other methods of detection exist.

Each component in a gas chromatograph serves a specific function, and each is highly tuneable to improve analytical methods. For example, the flow rate of the carrier gas can be increased to improve analysis efficiency or decreased to improve compound separation. The temperature can be modulated to alter retention times, with high operating temperatures typically yielding lower retention times.
Two types of column construction are generally utilised, with either packed columns or capillary columns representing the most ubiquitous forms used. Packed columns contain a solid support, coated in a stationary phase, with which the column is packed. These columns are generally several millimetres in diameter. Alternatively, capillary columns are often as narrow as 0.1 mm and the stationary phase is coated instead onto the walls of the column.

Two commonly used detector types are flame ionisation detectors and thermal conductivity detectors. With flame ionisation detectors, an H_2 flame pyrolyzes samples leaving the column. The pyrolysis of these compounds forms cations and electrons which produce a measurable current between two adjacent electrodes, which is converted into a chromatogram. It should be noted that this type of detector only works for hydrocarbons, due to the ability of hydrocarbons to form carbocations and electrons on pyrolysis. Small molecules such as H_2O, H_2 and N_2 are not observable using this type of detector.

Alternatively, thermal conductivity detectors can be used, and can measure both hydrocarbons and small molecules such as H_2, N_2, etc. However, response factors are significantly lower when using this detector type than the flame ionisation detector. Thermal conductivity detectors work by comparing the thermal conductivity of the carrier gas, relative to a mixture of the carrier gas and a given sample, the presence of which usually deviates from the thermal conductivity of the carrier gas and produces a measurable signal on a chromatogram.

2.4.2 High Performance Liquid Chromatography

Whilst many forms of high-performance liquid chromatography (HPLC) exist, in this work, reversed-phase chromatography was used and will be discussed herein.

Reversed phase HPLC operates under similar principles to gas chromatography, namely, an analyte is introduced into a mobile phase, which passes through a column containing a stationary phase. Differing levels of interaction between the analyte and the mobile and stationary phases results in differing retention times for each component of the analyte and thus, facilitates the separation of compounds. These can again be measured using a detector and a chromatogram recorded. A generic diagram of an HPLC is shown in Figure 2.5.

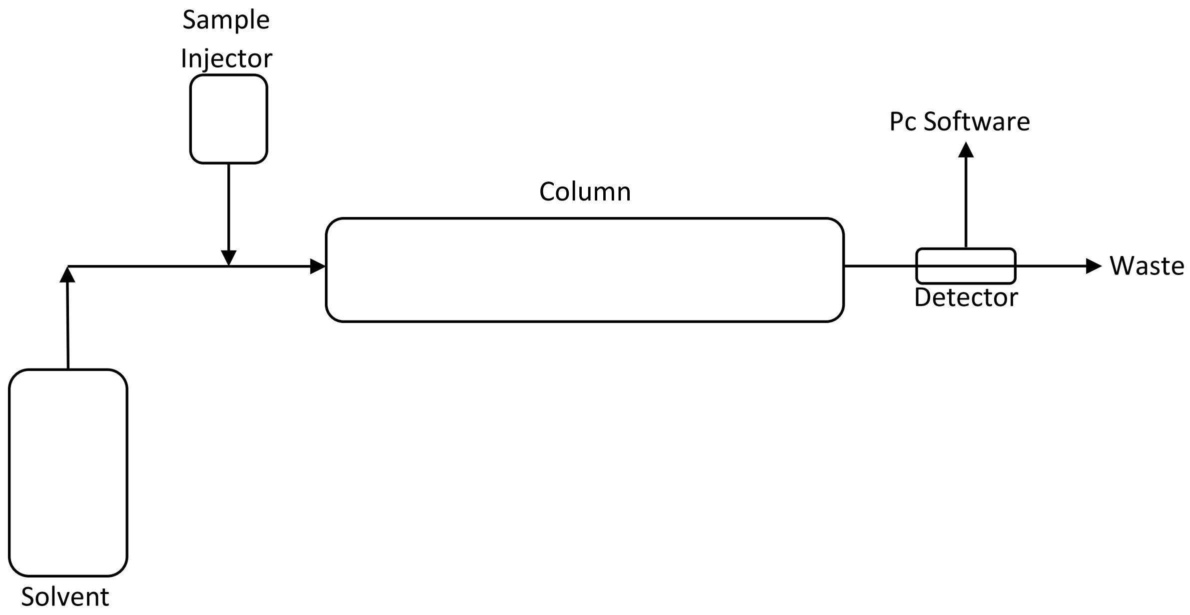

Figure 2.5. Generic construction of an HPLC.

One key feature of reversed phase HPLC lies in the mobile phase, which can be a mixture of two or more solvents with differing and tuneable polarities. Generally, water is used in conjunction with an organic solvent, such as acetonitrile or methanol, and the relative composition of the two allows for the polarity of the mobile phase to be modulated to aid in compound separation.
Indeed, the relative composition of the mobile phase can be altered throughout a separation procedure. This is called gradient elution. Alternatively, an isocratic elution method can be used, wherein the composition of a mobile phase is kept constant throughout the entire process.

The choice of stationary phase also plays a significant role in the separation of components in an analyte. In reversed phase HPLC, the stationary phase is generally hydrophobic and is often composed of functionalised silica with groups including phenyl, cyano and octadecyl moieties. Due to the hydrophobic nature of the stationary phase, hydrophobic compounds typically interact more strongly with it and can have longer retention times, whereas hydrophilic compounds may favour the water based mobile phase and elute sooner.

For the detection of compounds, a variety of detectors can be used, such as a diode array detector (DAD), a charged aerosol detector (CAD) or a refractive index detector (RID), though many others exist.
A DAD uses UV-vis spectroscopy to identify compounds. Light shines through a sample and is refracted into different wavelengths by a prism and collected by an array of diodes. This method allows for analysis of a range of wavelengths depending on what wavelengths the target molecules absorb in, however, the compound under observation must have a chromophore.

A CAD nebulizes the eluent of a column, which agglomerates into particles, the size of which is dependent on the quantity of analyte present. Ionized N_2 gas is passed over the agglomerated particles, which transfers charge from the gas into the agglomerates, and imparts charge onto them, with larger particles receiving greater charge. Finally, the net charge of the agglomerated particles is measured by an electrometer and produces a signal proportional to the overall charge recorded.

An RID compares the refractive indexes of the HPLC solvent with that of the solvent containing the analyte. The presence of the analyte alters the refractive index of the solvent system in which it is solvated and thus, a signal can be produced based on the difference in refractive index between the solvent and the analyte containing solvent system.

2.4.3 Microwave Plasma Atomic Emission Spectroscopy

Microwave plasma atomic emission spectroscopy (MP-AES) is a technique used to investigate the elemental composition of a liquid mixture. This enables the quantification of metal leachate present in a reaction mixture, or of the metal content of a catalyst that has been digested in an acidic medium. MP-AES functions as follows. Microwave radiation is used to heat a source of N_2 into a plasma, and the sample is introduced to the plasma where it is atomised. Respective elements present undergo atomic excitation and emission, emitting photons of characteristic wavelengths that are unique to a given element. Comparison of the intensities of these emitted photons with a calibration curve of known concentrations of an element allows for the accurate quantification of elements .

In Chapter 5, for the quantification of metal leachate in post reaction solutions, an Agilent 4100 MP-AES was used. Metal concentrations for Cu were determined using newly prepared calibration solutions of 5, 10, 15 and 20 mg mL^{-1}, recording the intensities of atomic emissions of Cu at a wavelength of 327.4 nm.

2.4.4 Inductively Coupled Plasma Mass Spectroscopy

Inductively coupled plasma mass spectroscopy (ICP-MS) can also be used to determine the elemental composition of a liquid mixture. In this technique, a liquid sample is atomised by a plasma torch, which has been generated by inductively heating an inert gas such as argon. Mass spectrometry is used to analyse the atomised sample, which is separated based on the mass to charge ratio of its components.[203] The intensity of each signal can be calibrated to known standard concentrations and accurate quantification of elements present within the sample can be performed. One advantage of ICP-MS over MP-AES is the significantly lower detection limit of the former, which can often detect elements in concentrations as low as 0.001 µmol L^{-1}, compared to typical detection limits as low as 0.1 µmol L^{-1} when using MP-AES.[203]

ICP-MS was used in Chapters 3 and 4 for the quantification of metal leachate in reaction solutions. ICP-MS experiments were conducted by Simon Waller at Cardiff University, using an Agilent 7900 ICP-MS with an I-AS auto sampler.

2.5 Catalyst Characterisation

2.5.1 X-Ray Photoelectron Spectroscopy

X-ray photoelectron spectroscopy (XPS) is an analytical technique in which information about the chemical and electronic environment of elements at the surface of a material can be investigated and quantified. This works through exploiting the photoelectric effect, wherein irradiation of an atom with electromagnetic radiation can cause the emission of an electron. The electron that is ejected from the material has a discrete and measurable kinetic energy, related to both the energy of incident radiation and the energy of binding. This is described in Equation 2.11.

Eq. 2.11 $$E_{hv} = E_k + E_B + \Phi$$

E_{hv} is the energy of the incident x-ray, E_k is the kinetic energy of the emitted photon, E_B is the binding energy of the emitted photon and Φ is the 'work function' of the spectrometer. [204]

If the energy of incident x-rays is kept constant and the kinetic energy of liberated electrons is measured, the binding energy of given electrons can be inferred. Indeed, the binding energy of a given electron is dependent on the chemical environment of the atom, and by comparing both the kinetic energy and quantity of electrons being emitted by a sample, both the total coverage and chemical environment of surface atoms can be measured.[204]
XPS is considered a surface analysis technique, and information about electrons from deeper within a sample is not generally obtained. This is because the inelastic mean free path, which is the average distance that an electron can travel through a solid material before it loses energy, is very small, and thus inelastic scattering of photoelectrons generated within a sample alters the kinetic energy of the electron and thus no longer provides useful information.[205]

All XPS data presented in Chapters 3-5 was carried out by Dr David Morgan at Cardiff University, using a Thermo Scientific K-Alpha+ photoelectron spectrometer, with a monochromatic Al kα X-ray source at 72 W. Pass energies of 40 eV were used for high-resolution spectra, and 150 eV for survey scans. All spectra were analysed using CasaXPS Version 2.3.26rev1.1k, and calibrated to a C1s line at 284.8 eV.

2.5.2 X-Ray Diffraction Spectroscopy

X-rays can be diffracted by elastic scattering upon incidence with atoms. When atoms are arranged in an ordered lattice, these diffraction waves interfere both constructively and destructively with the x-rays diffracted from adjacent atoms. The diffraction of x-rays by two ordered lattice planes is shown in Figure 2.6.

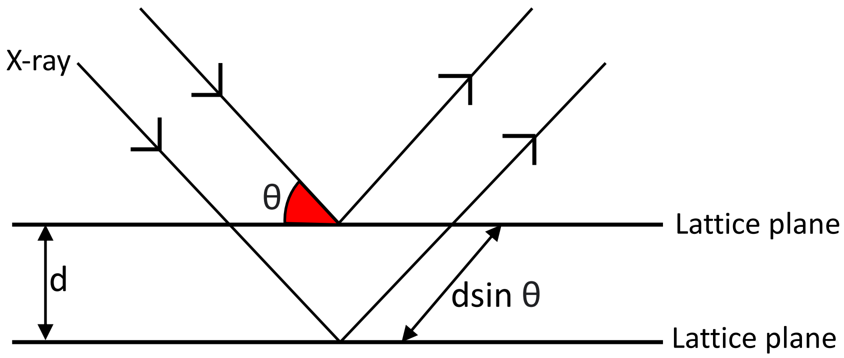

Figure 2.6. General schematic of the diffraction of incident X-rays by two lattice planes.

The directions in which diffracted waves interfere constructively or destructively is described by the Braggs equation, where diffraction at any integer value of the wavelength results in constructive interference. This is shown in Equation 2.12.

Eq. 2.12 $$n\lambda = 2d\ sin\Theta$$

n is an integer value, λ is the wavelength of incident x-rays, d is the spacing distance between diffraction planes, and Θ is the angle of incident x-rays.
By keeping the wavelength of light constant, and rotating the material through a continuum of angles, the intensity of diffracted x-rays can be measured as a function of the incident angle of x-rays. This information can be then used to determine the spacing between diffraction planes (d), which is unique for a given material, and can be used to identify the crystal structures of unknown samples.[206]

XRD spectra were collected using a (θ-θ) PANalytical X'pert Pro powder diffractometer, using a Cu kα radiation source, operating at 40 KeV and 40 mA. All samples were analysed on an amorphous silicon wafer, using a 40-minute scan and 2θ values of 10-80^{o}. The International Centre for Diffraction Data (ICDD) data base was used to identify diffraction patterns.

2.5.3 Diffuse Reflectance Infrared Fourier Transform Spectroscopy (DRIFTS)

Infrared (IR) spectroscopy operates on the principle that molecules absorb infra-red radiation at discrete frequencies related to the vibrational modes of a given molecule. Different functional groups (O-H, C=C, C-H, etc.) absorb different wavelengths of light that are characteristic of a given vibrational mode of that functional group, and thus IR spectroscopy is a useful tool for identifying chemical groups within compounds or mixtures.[207] Crucially, a given vibrational mode must cause a change in dipole for it to be visible via IR spectroscopy. Therefore, simple diatomic molecules such as O_2 and H_2 are not visible via IR spectroscopy as there is no change in dipole across any vibrational mode.

Historically, IR spectroscopy has involved scanning a sample over a series of individual wavelengths sequentially and measuring either the absorbance or reflectance of IR light from the sample. However, Infrared Fourier transform (FTIR) spectroscopy operates by splitting a beam of IR light that contains many wavelengths into two separate beams. One beam reflects off of a flat mirror, whilst the other beam reflects off a second mirror that can move very accurately over small distances, allowing for small changes in the pathlength of this beam. The interference of these two beams allows for the sequential transmission of specific wavelengths of light and the resulting spectrum is recorded as an interferogram.[208, 209] DRIFTS is a technique that exploits this phenomenon by measuring the light reflected from a sample to generate a spectrum, as shown in Figure 2.7.

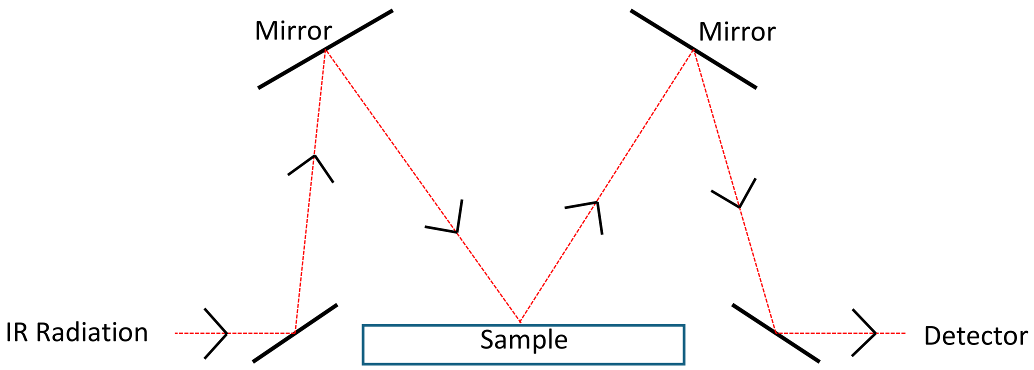

Figure 2.7. Schematic diagram for the configuration of a DRIFTS spectrometer.[207]

DRIFTS data presented in Chapters 3 and 4 used CO as a probe molecule to investigate the electronic and structural properties of Pd based catalysts.

All CO-DRIFTS measurements were taken on a Bruker Tensor 27 spectrometer, with a mercury cadmium telluride detector. Samples were loaded into a Praying Mantis high temperature cell before being purged by N_2 for 30 minutes at a flow rate of 75 mL min^{-1}. Samples were exposed to 10% CO/Ar for 15 minutes at room temperature and a flow rate of 50 mL min^{-1}, after which time the signals associated with CO had reached their maximum intensity. Samples were purged again with N_2 for 15 minutes at room temperature and a flow rate of 75 mL min^{-1}, after this time, CO peaks had ceased to shrink, confirming that all CO vibrational signals corresponded to adsorbed CO. A spectrum was recorded every 1 minute, for each stage of the procedure.

2.5.4 Electron Microscopy

Electron microscopy is a technique that utilises electrons instead of light to image materials at the nanometre scale. The two methodologies used herein were transmission electron microscopy (TEM) and scanning transmission electron microscopy (STEM).

In essence, a beam of electrons is focussed onto a thin layer of a sample, wherein a given electron may either transmit through the sample, or it may interact with the sample in such a way that results in either elastic or inelastic scattering, or through a number of 'secondary effects', resulting in backscattered electrons, secondary electrons Auger emissions or X-ray emissions.[210, 211] This is shown in Figure 2.8.[210, 211]

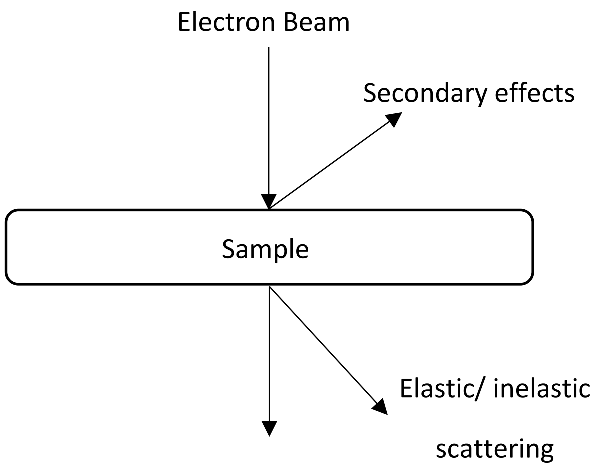

Figure 2.8. Interactions of an electron beam with a sample in TEM. Secondary effects include secondary electrons, backscattered electrons, Auger emissions or X-ray emissions.[211]

In TEM, it is the electrons that penetrate the sample without scattering that are collected to form an image, known as a bright field image. It should be noted that scattered electrons can also be detected and analysed to form a dark field image,[211] or electrons scattered at greater angles can be collected and form high angle annular dark field (HAADF) images.[212] This is shown in Figure 2.9. Contrast in an image is a result of varying levels of electron scattering as a function of the thickness or density of the region of a sample that the beam is travelling through, with thicker or denser areas of a sample resulting in darker contrasts as greater numbers of electrons are scattered.

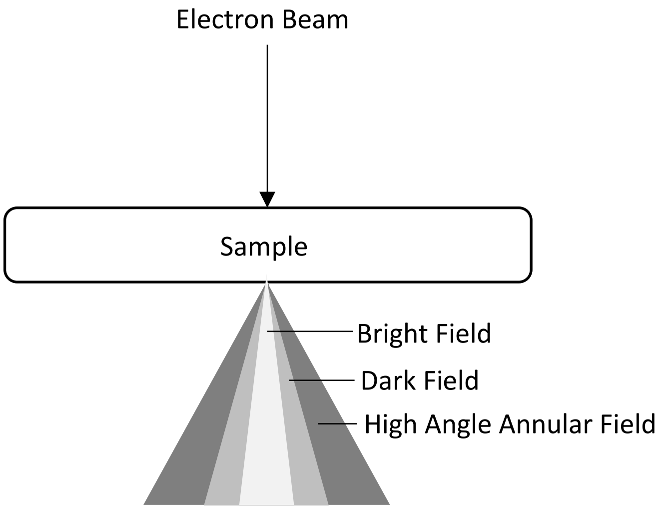

Figure 2.9. Diagram of imaging regions associated with electron scattering.

X-rays that are generated as a result of the incident electron beam transiting the sample can also be detected and analysed. This involves a technique called energy disperse X-ray (EDX) analysis, which correlates the specific energy of the emitted X-ray to the discrete electronic energy levels unique to each element, and thus allows for elemental identification.

TEM images were collected using a JEOL JEM-2100 operating at 200 kV. Material samples were immobilised on 300 mesh Cu grids coated with holey carbon film.
STEM images were collected by Junhong Liu at Shanghai Tong University, using a probe corrected Hitachi HF5000 STEM, operating at 200 kV. The microscope was equipped with both high angle annular dark field (HAADF) and bright field (BF) detectors, in addition to a secondary electron detector and Oxford Instruments XEDS detector.

2.5.5 BET Isotherm

Determination of the surface area of materials can be performed using the BET isotherm, as shown in Equation 2.13.[213]

Eq. 2.13 $$\frac{P/P_0}{n(1-P/P_0)} = \frac{1}{n_m C} + \frac{C-1}{n_m C}(P/P_0)$$

Where P is the pressure, P_0 is the saturation pressure of an adsorbate at a given temperature, n is the amount of adsorbed gas at P/P_0, n_m is the monolayer capacity of the adsorbate and C is the BET constant.

Plotting $(P/P_0)/n(1-P/P_0)$ against P/P_0 provides a graph with the slope of $(C-1)/n_mC$, which allows for the extraction of the term n_m.
The surface area can then be determined by Equation 2.14.[213]

Eq. 2.14 $$S_a = \frac{n_m L \sigma_m}{m}$$

Where Sa is the specific surface area, L is the Avagadro constant, σ_m is the cross sectional area of the adsorbate and m is the mass of the adsorbate.[213]

Surface areas presented in Chapters 3-5 were determined using a Quantachrome Quadrasorb-Evo. Samples (approximately 0.05 g) were degassed at 250 ^oC for 4 hours prior to analysis. 5-point BET analysis was conducted through the physisorption of N_2 at -77 Kelvin, which was cooled by a liquid N_2 dewar.

2.6 References

1. Richards, T., Lewis, R., et al, The direct synthesis of hydrogen peroxide over supported Pd-based catalysts: An investigation into the role of the support and secondary metal modifiers. *Catal. Letters* **2022**.
2. Pritchard, J., He, Q., et al, The effect of catalyst preparation method on the performance of supported Au–Pd catalysts for the direct synthesis of hydrogen peroxide. *Green Chem.* **2010,** *12*, 915-921.
3. Pritchard, J., Kesavan, L., et al, Direct Synthesis of Hydrogen Peroxide and Benzyl Alcohol Oxidation Using Au−Pd Catalysts Prepared by Sol Immobilization. *Langmuir* **2010,** *26*, 16568-16577.
4. Wilschefski, S., Baxter, M., Inductively Coupled Plasma Mass Spectrometry: Introduction to Analytical Aspects. *Clin. Biochem. Rev.* **2019,** *40*, 115-133.
5. Hollander, J., Jolly, W., X-Ray Photoelectron Spectroscopy. *Accounts Chem. Res.* **1970,** *3*, 193-200.
6. Bradley, C., X-ray photoelectron spectroscopy: Progress and perspectives. *J. Electron Spectros. Relat. Phenomena* **2010,** *178-179*, 2-32.
7. Leofanti, G., Tozzola, G., et al, Catalyst characterization: characterization techniques. *Catal. Today* **1997,** *34*, 307-327.
8. Guerrero-Perez, M., Patience, G. , Experimental methods in chemical engineering: Fourier transform infrared spectroscopy—FTIR. *Can. J. Chem. Eng.* **2019,** *98*, 25-33.
9. Dutta, A., *Spectroscopic Methods for Nanomaterials Characterization*. 2017.
10. Tibiletti, D., Amieiro-Fonseca, R., et al., DFT and In Situ EXAFS Investigation of Gold/Ceria−Zirconia Low-Temperature Water Gas Shift Catalysts: Identification of the Nature of the Active Form of Gold. *J. Phys. Chem. B.* **2005,** *109*, 22553-22559.
11. Goodhew, P., Beanland, R., Humphreys, J., *Electron Microscopy and Analysis*. CRC Press: 2014.
12. Zhou, X., Thompson, G., *Electron and Photon Based Spatially Resolved Techniques*. 2017.
13. Otten, M., Hihg-Angle annular dark-field imaging on a tem/stem system. *J. Microsc.* **1992,** *17*, 221-230.
14. Ambroz, F., Macdonald, T., Evaluation of the BET Theory for the Characterization of Meso and Microporous MOFs. *Small Methods* **2018,** *2*, 1800173.

3 The Selective Oxidation of Benzyl Alcohol via the in-situ Production of H_2O_2 Using Supported Pd Based Catalysts

3.1 Introduction

The in-situ direct synthesis of hydrogen peroxide (H_2O_2) from molecular H_2 and O_2 over a heterogenous catalyst, followed by the oxidation of a target molecule as a one-pot methodology has promising applications in the fields of chemical synthesis and water remediation. Examples in the recent literature of this include the oxidation of benzyl alcohol, cyclohexane, propylene epoxidation, the total oxidation of phenol and the disinfection of greywater.[22, 27, 130, 132, 214-216]

Historically, the synthesis of aldehydes and ketones from alcohols has been achieved through the use of stoichiometric oxidants, such as permanganate or dichromate.[217, 218] However, the use of such reagents presents issues with downstream purification, atom economy, toxicity, and cost. Conversely, using oxygen-based oxidants, such as O_2 and H_2O_2 has the potential to overcome many of these issues. For example, the only by-product generated in-situ and associated with the use of H_2O_2 as an oxidant is H_2O, eliminating the need for extensive downstream purification. However, as discussed in Chapter 1, using preformed commercial H_2O_2 has significant drawbacks including high upfront production costs, a centralised point of manufacture necessitating the transportation and storage of highly concentrated H_2O_2, the production of contaminated wastewater, and the use of H_2O_2 stabilisers such as acetic and phosphoric acid which need to be subsequently removed from product streams.[21, 34] Using molecular O_2 in the synthesis of benzaldehyde from benzyl alcohol circumnavigates these issues, but requires high reaction temperatures, often in excess of 100 ^{o}C, whereas oxidation with H_2O_2 facilitates high conversions under more mild conditions, with temperatures in the range of 30 - 50 ^{o}C typical.[27, 130, 131, 218-223] Moreno *et al.* compared the activity of a range of supported catalysts and demonstrated that generating H_2O_2 in-situ, as opposed to using O_2 as an oxidant, allowed for higher conversions of benzyl alcohol at 30 ^{o}C, with a far greater selectivity to benzaldehyde.[114] For example, when using a 1.25%Au-1.25%Pd/TS-1 catalyst for the oxidation of benzyl alcohol at 30 ^{o}C, when O_2 was used as the oxidant a benzyl alcohol conversion of 1.8 % was offered. However, when H_2 was used in tandem with O_2, the same catalyst offered a benzyl alcohol conversion of 7 %.[114]

Indeed, Pd is known to be active in the direct synthesis of H_2O_2 and has been shown to catalyse the oxidation of benzyl alcohol to benzaldehyde under both aerobic conditions and with H_2O_2.[127, 218, 224] Through the incorporation of secondary and even tertiary metals into the catalyst, such as Au and Pt, the net production of H_2O_2 can be significantly enhanced compared to a Pd-only analogue under conditions optimised for H_2O_2 synthesis.[61, 225, 226] These Pd based bimetallic catalysts have also been demonstrated to be active for the oxidation of benzyl alcohol via in-situ H_2O_2 synthesis.[27, 218] Although the current research on this tandem reaction is limited, examples of Pd based catalysts are shown in Table A3.1. Indeed, prominent examples in the literature include the work of Crombie *et al.* who reported a 0.5%Fe-0.5%Pd/TiO_2 catalyst, which offered a turnover towards benzaldehyde formation of 783 $mol_{Benzaldehyde}$ kg_{cat}^{-1} hr^{-1} after 30 minutes, at a selectivity of 96 %.[218] Alternatively, Martinez *et al.* employed a 0.8%Pd-0.2%Au-H catalyst, which offered a turnover of 124 $mol_{Benzaldehyde}$ kg_{cat}^{-1} hr^{-1}, with a selectivity of 58 % over 8 hours.[130]

A general scheme for the oxidation of benzyl alcohol via in-situ H_2O_2 synthesis is shown in Figure 3.1. The reaction has been reported to proceed via a radical pathway, where either hydroxyl or hydroperoxyl radicals are generated from H_2 and O_2 at the surface of the catalyst, which may be subsequently released into the reaction solution.[132, 218] Additionally, electron paramagnetic resonance analysis has revealed that the solvent may play a role in the propagation of radical oxidants, with Crombie *et al.* reporting the presence of methoxyl radicals, arising from a reaction between the alcohol solvent and hydroxyl or hydroperoxyl radicals generated by the catalyst.[218] Interestingly, a benzyl alcohol radical has also been shown to be generated in the absence of either H_2 or O_2, and arising as a result of a hydrogen abstraction of the benzylic α-hydrogen taking place at the surface of the catalyst.[218]

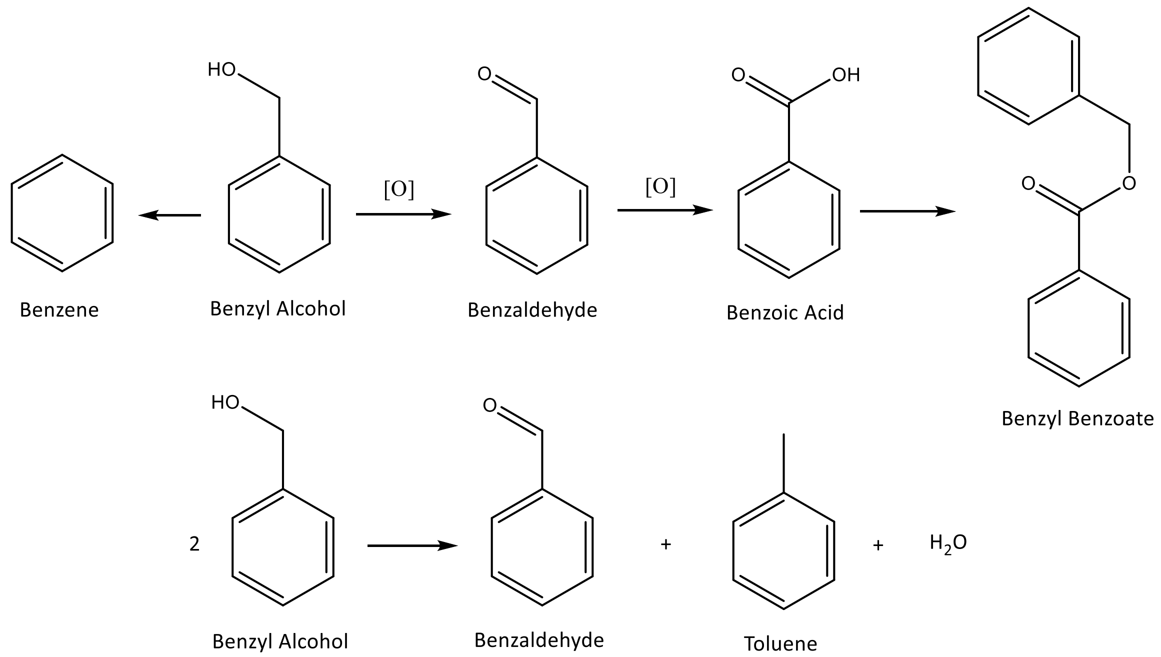

Figure 3.1. General scheme for the oxidation of benzyl alcohol.[218]

The objective of this work was to improve catalytic performance in the selective oxidation of benzyl alcohol to benzaldehyde via in-situ H_2O_2 synthesis, with previous studies demonstrating the potential for such an in-situ approach to benzyl alcohol valourisation.[27, 114, 218] The main focus of this work was catalyst design and optimisation, with a focus on the choice of support, the alloying of Pd with a range of secondary metals and the inclusion of tertiary metals into a supported AuPd catalyst, given these factors have previously been demonstrated to promote catalytic performance towards the direct synthesis of H_2O_2.[46, 225]

3.2 The Effect of Support Material for AuPd Nanoparticles in the Selective Oxidation of Benzyl Alcohol via in-situ H_2O_2 Synthesis

Crombie *et al.* have previously shown that Pd-based catalysts prepared through an excess chloride co-impregnation methodology offer promising activity and high selectivity towards the selective oxidation of benzyl alcohol, with the alloying of Pd with Au or Fe in particular offering significant improvements in catalytic activity compared to monometallic Pd analogues.[218] Based on this previous work, initial studies were conducted using supported AuPd nanoparticles, due to their reported high activity for the direct synthesis of H_2O_2, as well as in the oxidation of benzyl alcohol.[218, 224]

It has previously been reported that the choice of catalyst support plays a significant role in the quantity of H_2O_2 that can be produced by the direct synthesis reaction, with the catalyst preparation method also known to alter the catalytic activity.[46, 227] For example, Ntainjua *et al.* reported that the iso-electric point of the support material was a key factor in the overall performance of AuPd catalysts when prepared by a wet co-impregnation method.[46] From this study, it was reported that supports with low iso-electric values such as carbon and TiO_2 generated the highest concentrations of H_2O_2, whilst high iso-electric point supports favoured H_2O_2 degradation.[46] Conversely, Richards *et al.* prepared an analogous series of catalysts on a variety of supports through an excess chloride co-impregnation methodology and did not observe any correlation between the iso-electric point of the support used and its resultant catalytic activity, highlighting the key role of catalyst synthesis procedure in influencing the activity of the resultant catalyst.[227]

Whilst no explicit correlation between the H_2O_2 productivity of a catalyst and its capacity to oxidise benzyl alcohol has thus far been reported in the literature, it is likely that a successful oxidation catalyst must at least be capable of the generating surface hydroxyl and hydroperoxyl intermediates that subsequently form either H_2O_2 or H_2O, or degrading H_2O_2 via a radical pathway.[218] The catalytic activities of a series of Pd based catalysts as reported by Crombie *et al.* are shown in Figure 3.2, comparing the turnover numbers for both the direct synthesis of H_2O_2, and benzyl alcohol conversion in the selective oxidation of benzyl alcohol via in-situ H_2O_2 synthesis.[218] It should be noted that different reaction conditions were used for the direct synthesis of H_2O_2 and for the selective oxidation of benzyl alcohol via in-situ H_2O_2 synthesis, as detailed in Figure 3.2. From this data, catalysts that produced higher concentrations of H_2O_2 did not appear to universally facilitate greater conversions of benzyl alcohol, but in general, catalysts that produced more H_2O_2 often also converted more benzyl alcohol than their less active analogues. However, there are clearly other factors influencing the quantity of benzyl alcohol converted by a given catalyst as it can be seen in Figure 3.2 that FePd and AuPd catalysts are by far the most active, offering turnover numbers of 789 and 744 mol_{BA} mol_{metal}^{-1} hr^{-1} respectively. The FePd catalyst however exhibits a more moderate turnover number towards H_2O_2 synthesis, of 293 mol_{H2O2} mol_{metal} hr^{-1} [1] when compared to the AuPd catalyst, which offered 939 mol_{H2O2} mol_{metal}^{-1} hr^{-1} The authors cited the enhanced generation of hydroxyl and hydroperoxyl radicals via a Fentons-type pathway as the likely cause of the enhanced benzyl alcohol oxidation achieved by the FePd catalyst.[218] Indeed, the CoPd catalyst may also have enhanced yields of benzaldehyde through the same mechanism, given the reported ability for heterogeneous Co to undertake Fentons reaction,[8, 228-230] although the authors did not explore this.

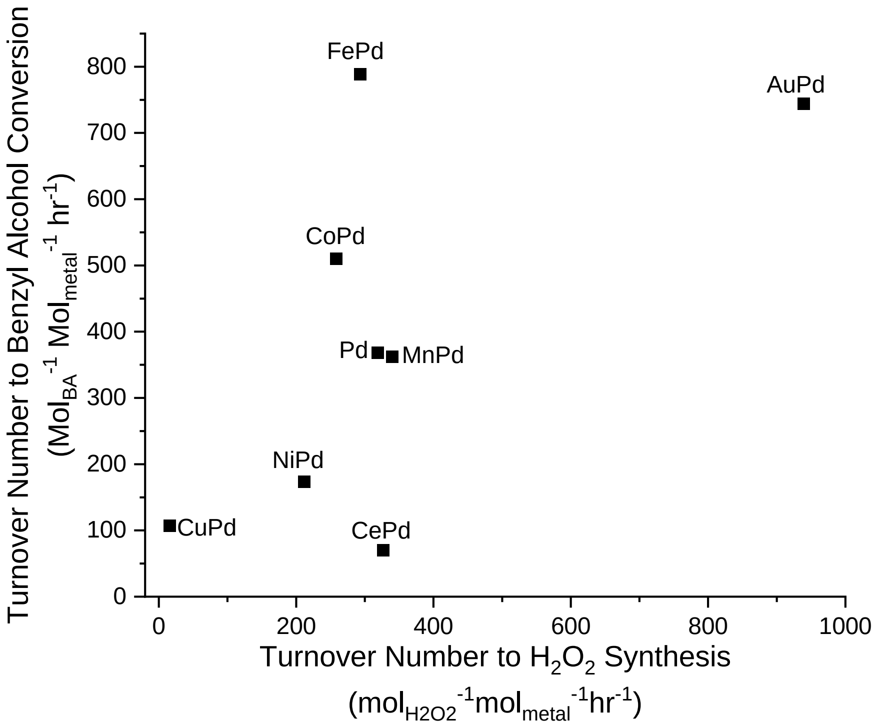

Figure 3.2. Comparison of turnover numbers towards H_2O_2 synthesis and benzyl alcohol oxidation, as reported by Crombie *et al.* for a series of 0.5%X-0.5%Pd/TiO_2 catalysts.[218]

H_2O_2 direct synthesis conditions: Catalyst (0.01 g), H_2O (2.9 g), MeOH (5.6 g), 5% H_2/CO_2 (420 psi mmol), 25% O_2/CO_2 (160 psi), 0.5 hr, 25 °C, 1200 rpm.

Benzyl alcohol oxidation reaction conditions: Catalyst (0.01 g), MeOH (7.13 g), benzyl alcohol (1.04 g, 9.62 mmol), mesitylene (0.42 g), 5% H_2/CO_2 (420 psi, 2.76 mmol), 25% O_2/CO_2 (160 psi, 5.24 mmol), 0.5 hr, 50 °C, 1200 rpm.

In order to determine an optimal support for both in-situ H_2O_2 synthesis and selective oxidation of benzyl alcohol, a series of 0.5%Au-0.5%Pd supported catalysts were synthesised by an excess chloride co-impregnation methodology and evaluated for their activity towards H_2O_2 synthesis, H_2O_2 degradation and the selective oxidation of benzyl alcohol. The range of supports were selected based on those previously reported in the literature for the direct synthesis of H_2O_2 or in the selective oxidation of benzyl alcohol via in-situ H_2O_2 synthesis.[27, 46, 218, 227] The purpose of studying the H_2O_2 synthesis reaction in conjunction with the selective oxidation of benzyl alcohol was to better understand any relationships between the two intimately linked reactions.

Firstly, the direct synthesis of H_2O_2 was investigated, as shown in Table 3.1.

Table 3.1. Comparison of the catalytic activities of supported 0.5%Au-0.5%Pd/X catalysts on the direct synthesis and degradation of H_2O_2 using different support materials.

Catalyst	Productivity (mol_{H2O2} kg_{cat}^{-1} hr^{-1})	Turnover Number (mol_{H2O2} mol_{metal}^{-1} hr^{-1})	H_2 Conversion (%)	H_2O_2 Selectivity (%)	H_2O_2 Concentration (wt. %)	Degradation (mol H_2O_2 kg_{cat}^{-1} hr^{-1})
AuPd/Al_2O_3	61	837	54	19	0.12	416
AuPd/CeO_2	20	279	18	2	0.04	284
AuPd/TiO_2 (P25)	80	1105	41	35	0.16	503
AuPd/Nb_2O_5	19	265	4	86	0.03	40
AuPd/ZrO_2	9	122	11	13	0.02	268
AuPd/Carbon (G60)	13	182	58	4	0.03	425

H_2O_2 direct synthesis reaction conditions: Catalyst (0.01 g), H_2O (2.9 g), MeOH (5.6 g), 5% H_2/CO_2 (420 psi, 2.76 mmol), 25% O_2/CO_2 (160 psi, 5.24 mmol), 0.5 hr, 20 °C, 1200 rpm.
H_2O_2 degradation reaction conditions: Catalyst (0.01 g), H_2O_2 (50 wt.%, 0.69 g), H_2O (2.21 g), MeOH (5.6 g), 5% H_2/CO_2 (420 psi, 2.76 mmol), 0.5 hr, 20 °C, 1200 rpm

From these data, it was observed that using a TiO_2 support facilitated the greatest extent of H_2O_2 synthesis, followed by Al_2O_3 which offered H_2O_2 productivity values of 80 and 61 mol_{H2O2} kg_{cat}^{-1} hr^{-1} respectively. The remaining supported catalysts, CeO_2, Nb_2O_5, ZrO_2 and carbon (G60) all exhibited comparatively lower levels of productivity, such as the AuPd/ZrO_2 and AuPd/Nb_2O_5 catalysts, which achieved H_2O_2 productivities of 9 and 19 mol_{H2O2} kg_{cat}^{-1} hr^{-1} respectively. The activity of the AuPd/TiO_2 catalyst, which offered an H_2O_2 productivity of 80 mol_{H2O2} kg_{cat}^{-1} hr^{-1}, agreed well with similar experiments in the literature, with reported productivity values of both 75 and 68 mol_{H2O2} kg_{cat}^{-1} hr^{-1} at a reaction temperature of 25 °C, as opposed to the 20 °C used in this work.[218, 231]
Additionally, when this data is compared to equivalent catalysts tested under the commonly used 2 °C operating temperatures, the same general trends in catalytic activity are observed.[227] For example, at 2 °C, as reported by Richards et al. AuPd/TiO_2, AuPd/Al_2O_3 and AuPd/ZrO_2 catalysts exhibited H_2O_2 productivities of 85, 75 and 10 mol_{H2O2} kg_{cat}^{-1} hr^{-1} respectively, compared to the values of 80, 61 and 9 mol_{H2O2} kg_{cat}^{-1} hr^{-1} observed at 20 °C in this work.[227] It should be noted that whilst the reported productivity values across the two reaction temperatures are largely comparable, the conversion of H_2 was greatly enhanced at 20 °C compared to 2°C. For example, in this work the AuPd/TiO_2 catalyst offered an H_2 conversion of 41 % at 20 °C, but in the work of Richards et al. , an H_2 conversion of 19 % was offered at 2 °C.[227]

The ability of each catalyst to degrade H_2O_2 was then investigated and is shown in Table 3.1. Degradation is defined as the sum of the hydrogenation and decomposition pathways of H_2O_2 as described in Chapter 1. The greatest extent of H_2O_2 degradation was again achieved by the AuPd/TiO_2 catalyst, offering a degradation of 503 mol_{H2O2} kg_{cat}^{-1} hr^{-1}, with the AuPd/Al_2O_3 and AuPd/carbon catalysts also delivering similarly high levels of degradation of 416 and 425

mol_{H2O2} kg $_{cat}$ $^{-1}$ hr^{-1} respectively. The AuPd/Nb_2O_5 catalyst offered very low levels of degradation, and a hydrogen selectivity of 86 % towards the H_2O_2 synthesis route, due to its very low levels of H_2 conversion, suggesting that this Nb_2O_5 supported catalyst had a very low overall activity towards any reaction pathway associated with the direct synthesis of H_2O_2. This data is generally in good agreement with previous literature, although a large disparity appears between the degradation values reported herein and that of the literature.[227] This is possibly due to the different operating conditions employed in this study, where the higher temperature (20 ^{o}C) used in this work, greatly promoted H_2O_2 degradation relative to the low temperature conditions (2 ^{o}C) often employed in the literature.[46, 79, 227, 232] Indeed, it has been demonstrated that elevated reaction temperatures can significantly promote the degradation of H_2O_2.[231, 233]

The same series of catalysts was then investigated in the selective oxidation of benzyl alcohol via in-situ H_2O_2 synthesis, with this data shown in Figure 3.3 and Table 3.2.

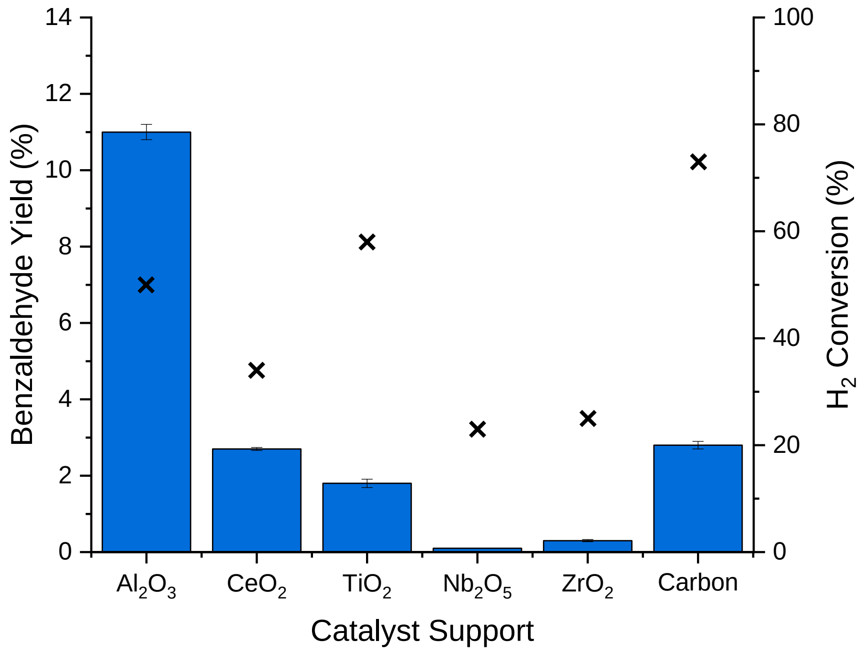

Figure 3.3. Comparison of the catalytic activities of supported 0.5%Au-0.5%Pd/X on the oxidation of benzyl alcohol using different support materials. **Key;** Benzaldehyde (*blue bars*), H_2 conversion (*crosses*).

Benzyl alcohol oxidation reaction conditions: Catalyst (0.01 g), MeOH (7.13 g), benzyl alcohol (1.04 g, 9.62 mmol), mesitylene (0.42 g), 5% H_2/CO_2 (420 psi, 2.76 mmol), 25% O_2/CO_2 (160 psi, 5.24 mmol), 0.5 hr, 50 ^{O}C, 1200 rpm.

Table 3.2. Comparison of the catalytic activities of supported 0.5%Au-0.5%Pd on the oxidation of benzyl alcohol using different support materials.

Catalyst	Benzyl Alcohol Conversion (%)	Benzaldehyde Yield (%)	Selectivity to Benzaldehyde (%)	Turnover Number (mol_{BA} mol_{metal}^{-1} hr^{-1})	H_2 Conversion (%)	H_2 Selectivity (%)	Residual H_2O_2 (mmol)
AuPd/Al_2O_3	11.0	11.0	100	2919	50	77	0.161
AuPd/CeO_2	2.7	2.7	100	716	34	28	0.048
AuPd/TiO_2	1.8	1.8	100	478	58	11	0.182
AuPd/Nb_2O_5	0.1	0.1	100	27	23	2	0.042
AuPd/ZrO_2	0.3	0.3	100	80	24	4	0.029
AuPd/Carbon (G60)	2.8	2.8	100	743	73	13	0.034

Benzyl alcohol oxidation reaction conditions: Catalyst (0.01 g), MeOH (7.13 g), benzyl alcohol (1.04 g, 9.62 mmol), mesitylene (0.42 g), 5% H_2/CO_2 (420 psi, 2.76 mmol), 25% O_2/CO_2 (160 psi, 5.24 mmol), 0.5 hr, 50 ^{O}C, 1200 rpm.

All supported 0.5%Au-0.5%Pd catalysts offered 100 % selectivity towards benzaldehyde formation, with no overoxidation to benzoic acid and no formation of toluene or any other side reaction product as shown in Figure 3.1. As previously discussed, one possible origin for this high selectivity is due to the radical scavenging ability of benzyl alcohol.[100] Sankar *et al.* reported that the low bond-dissociation energy of the benzylic α-hydrogen present in benzyl alcohol facilitates the abstraction of this hydrogen atom, which is able to subsequently quench radical intermediate species that lead to the overoxidation of benzaldehyde to benzoic acid.[100] Indeed, high selectivity for this reaction has been reported previously in the literature, with Crombie *et al.* reporting >99 % selectivity to benzaldehyde at a benzyl alcohol conversion of 2.8 %.[218] In instances where this high selectivity was not observed, such as in the work of Santonastaso *et al.* which reported a benzaldehyde selectivity of 90 % at a benzyl alcohol conversion of 5.9 %, a metal loading of 5 wt.% was used for the AuPd/TiO_2 catalysts,[27] compared to the 1 wt.% used in this and in the work of Crombie at al.[26] Additionally, the catalyst used in the work of Santonastaso *et al.* was prepared through a conventional impregnation methodology,[27] whereas Crombie *et al.* used an excess chloride co-impregnation methodology.[218] It is possible that total metal loading or preparation method are ultimately responsible for this observed difference in product selectivity, though no systematic study into the effects of either factor has thus far been conducted for this tandem reaction. It is not likely that benzyl alcohol conversion was a significant factor in the observed differences in benzaldehyde selectivity. This is because the AuPd/Al_2O_3 catalyst used in this work offered a benzyl alcohol conversion of 11.0 %, with 100 % selectivity towards the formation of benzaldehyde, whereas the 2.5%Au-2.5%Pd/TiO_2 catalyst used in the work of Santonastaso offered a lower benzyl alcohol conversion of 5.9 % at a selectivity towards benzaldehyde of 90 %.[27]

Despite exhibiting the highest activity towards the direct synthesis of H_2O_2, the 0.5%Au-0.5Pd%/TiO_2 catalyst had only a moderate yield of benzaldehyde, at 1.8 %. This value is somewhat lower than previously reported in the literature for an identical catalyst, with Crombie *et al.* reporting a benzaldehyde yield of 2.8 % and an H_2 conversion of 72 %, compared to the 58 % reported in this work.[218] This difference in activity may be a result of differences in the TiO_2 support material, which was a commercial P25 TiO_2 in both the work of Crombie *et al.* and in this work. P25 TiO_2 is a mixture of the anatase and rutile forms of TiO_2 and any discrepancies in the ratios of these two forms between commercial lots may lead to changes in the activity of resultant catalysts.

Catalysts supported on CeO_2 and carbon (G60) both outperformed the TiO_2 analogue, with 2.7 and 2.8 % benzaldehyde yields respectively, compared to the TiO_2 which offered a benzaldehyde yield of 1.8 %. Additionally, both offered significantly lower H_2O_2 productivity levels than the TiO_2 analogue, under H_2O_2 direct synthesis conditions (Table 3.1), with H_2O_2 productivity values of 20 and 13 $mol_{H2O2}\ kg_{cat}^{-1}\ hr^{-1}$ offered by the CeO_2 and carbon supported catalysts respectively, compared to the productivity of 80 $mol_{H2O2}\ kg_{cat}^{-1}\ hr^{-1}$ offered by the TiO_2 supported catalyst. Notably, the Al_2O_3 supported catalyst delivered the greatest yield of benzaldehyde from the series, with 11.0 %. Additionally, both Nb_2O_5 and ZrO_2 supported AuPd catalysts, whilst having some limited capacity to synthesise hydrogen peroxide, had almost no activity in the selective oxidation of benzyl alcohol. A comparison of the H_2O_2 productivity and benzyl alcohol conversion of each AuPd/X catalyst is shown in Figure 3.4.

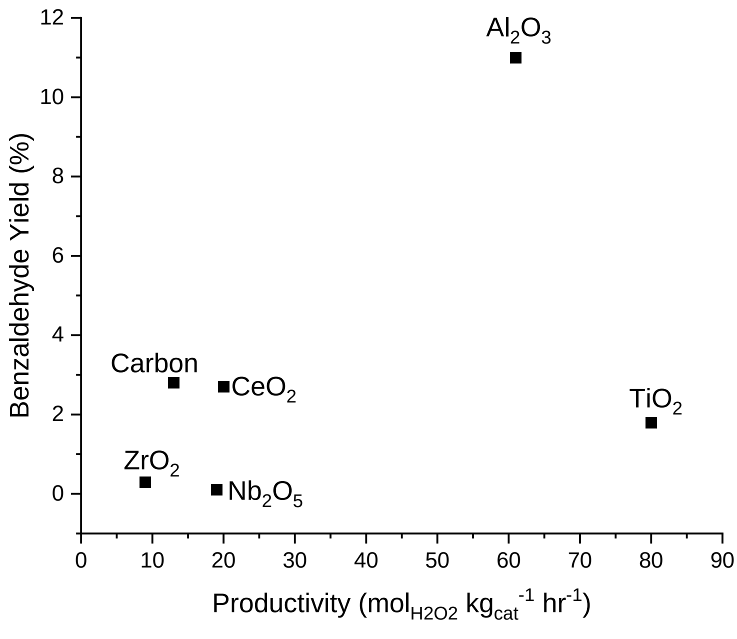

Figure 3.4. Comparison of H_2O_2 productivity benzaldehyde yield for a series of AuPd/X catalysts.
H_2O_2 direct synthesis conditions: Catalyst (0.01 g), H_2O (2.9 g), MeOH (5.6 g), 5% H_2/CO_2 (420 psi mmol), 25% O_2/CO_2 (160 psi), 0.5 hr, 20 °C, 1200 rpm.
Benzyl alcohol oxidation reaction conditions: Catalyst (0.01 g), MeOH (7.13 g), benzyl alcohol (1.04 g, 9.62 mmol), mesitylene (0.42 g), 5% H_2/CO_2 (420 psi, 2.76 mmol), 25% O_2/CO_2 (160 psi, 5.24 mmol), 0.5 hr, 50 °C, 1200 rpm.

Indeed, there appeared to be no obvious correlation in this series, between the ability of a catalyst to oxidise benzyl alcohol in-situ and its ability to either produce or degrade H_2O_2. A direct comparison between both reactions may not necessarily valid, due to the different operating temperatures and solvent systems, however the reported values for H_2O_2 productivity over the direct synthesis of H_2O_2 reaction (Table 3.1) and the residual H_2O_2 after the oxidation of benzyl alcohol reaction (Table 3.2) appear to correlate well. For example, the AuPd/TiO_2 catalyst offered both the highest productivity and residual H_2O_2 of 80 mol_{H2O2} kg_{cat}^{-1} hr^{-1} and 0.182 mmol respectively, whereas the AuPd/Al_2O_3 catalyst offered the second highest in both metrics, of 61 mol_{H2O2} kg_{cat}^{-1} hr^{-1} and 0.161 mmol. Conversely, the AuPd/ZrO_2 was the least active across both metrics, offering a productivity of 9 mol_{H2O2} kg_{cat}^{-1} hr^{-1} and 0.029 mmol of residual H_2O_2 following the oxidation of benzyl alcohol. Therefore, comparisons between the two reactions might be reasonable, using the H_2O_2 direct synthesis reaction as a more optimal set of reaction conditions to better outline the different activities of each catalyst.

There was no correlation between the H_2 conversion of a catalyst and the yield of benzaldehyde that it produced. Additionally, if we consider the H_2 selectivity for the oxidation of benzyl alcohol as a reaction with a stoichiometry of 1:1 with respect to H_2 and benzyl alcohol, then the AuPd/Al_2O_3 catalyst appears to be highly selective in the utilisation of H_2. Indeed, the AuPd/Al_2O_3 catalyst offered an H_2 selectivity of 77 %, compared to the AuPd/TiO_2 catalyst, which had a similar H_2 conversion, but an H_2 selectivity of only 11.0 %. However, it should be noted that this H_2 selectivity value is a metric that indicates how efficiently a catalyst may be utilising H_2 in the reaction system but cannot be considered a complete stoichiometric description of the synthesis of benzaldehyde. This is because there exists the possibility for a limited contribution from O_2, acting independently as the primary oxidising agent, without any contribution from H_2.[214] This will be investigated in Section 3.4.
Additionally, there exists the possibility of some contribution from the activation of benzyl alcohol by the catalyst itself, resulting in the abstraction of the benzylic α-hydrogen without any involvement of radical oxygen species, H_2 or O_2. Indeed, using electron paramagnetic resonance (EPR) spectroscopy, Crombie *et al.* observed the generation of a benzyl alcohol radical, PHCH$^\bullet$(OH), when benzyl alcohol was exposed to an AuPd/TiO_2 catalyst in the absence of H_2 and O_2.[218]

Due to its high activity in the oxidation of benzyl alcohol, Al_2O_3 was selected as a support for further catalyst development.

3.3 The Effect of Secondary Metal Incorporation in an X-Pd/Al_2O_3 Catalyst Towards the Selective Oxidation of Benzyl Alcohol via in-situ H_2O_2 Synthesis

The alloying of Pd with a range of secondary metals has shown great promise for the direct synthesis of H_2O_2 and the selective oxidation of benzyl alcohol. Crombie et al. demonstrated that the alloying of Fenton active metals such as Fe, Co and Mn with Pd have been shown to enhance the yield of benzaldehyde compared to monometallic Pd or in some instances AuPd based catalysts when using a TiO_2 support.[218] Therefore, given the enhanced catalytic activity reported in Section 3.2 associated with the use of an Al_2O_3 supported AuPd catalyst, a range of secondary metals (Fe, Cu, Ru, Zn, Pt, Mn and Co) were selected for alloying with Pd in Al_2O_3 supported catalysts, based on their previously reported use in either the in-situ oxidation of benzyl alcohol, or for the direct synthesis of H_2O_2.[56, 218, 234] Al_2O_3 was selected as a support due to its high activity in the previous Section. The range of catalysts studied, and their activities in the direct synthesis of H_2O_2 are shown in Table 3.3.

Table 3.3. Comparison of the catalytic activity of supported 0.5%X-0.5%Pd/Al_2O_3 toward the direct synthesis of hydrogen peroxide.

Catalyst	Productivity (mol_{H2O2} kg_{cat}^{-1} hr^{-1})	Turnover Number (mol_{H2O2} mol_{metal}^{-1} hr^{-1})	Hydrogen Conversion (%)	H_2O_2 Selectivity (%)	H_2O_2 Concentration (wt. %)
0.5Pd	33	702	17	33	0.07
1.0Pd	29	309	19	28	0.06
0.5Au-0.5Pd	61	837	54	19	0.12
0.5Fe-0.5Pd	29	214	19	28	0.06
0.5Cu-0.5Pd	0	0	-	-	0.00
0.5Ru-0.5Pd	23	236	12	36	0.05
0.5Zn-0.5Pd	38	306	17	40	0.08
0.5Pt-0.5Pd	34	463	38	16	0.07
0.5Mn-0.5Pd	29	213	7	74	0.06
0.5Co-0.5Pd	34	255	17	34	0.07

H_2O_2 direct synthesis reaction conditions: Catalyst (0.01 g), H_2O (2.9 g), MeOH (5.6 g), 5% H_2/CO_2 (420 psi, 2.76 mmol), 25% O_2/CO_2 (160 psi, 5.24 mmol), 0.5 hr, 20 °C, 1200 rpm.

For the direct synthesis of H_2O_2, there was a clear synergistic effect when Au and Pd were alloyed, resulting in greatly enhanced levels of productivity. For example, the 0.5%Au-0.5%Pd/Al_2O_3 catalyst offered a productivity of 61 mol_{H2O2} kg_{cat}^{-1} hr^{-1}, compared to the 0.5%Pd and 1.0%Pd/Al_2O_3 catalysts, which offered productivity values of 33 and 29 mol_{H2O2} kg_{cat}^{-1} hr^{-1} respectively. This synergistic effect of Au and Pd has previously been reported for a variety of catalyst supports, including TiO_2, SiO_2, Al_2O_3 and carbon.[226, 235]

It has been suggested in the literature that this enhancement in catalytic activity associated with the alloying of Au and Pd may be a result of an electronic modification of Pd sites by Au centres.[62] For example, adjacent Au sites have been shown to weaken the Pd-O bond between O_2 and Pd, stabilising the O-O bond of O_2 through an electronic effect.[236]

Alternatively, as previously discussed, it has also been proposed that isolation effects can inhibit the dissociation of the O_2 over contiguous Pd ensembles bond that leads to H_2O formation, and thus increased H_2O_2 productivity may be achieved by inhibiting degradation pathways.[63, 64] This was proposed to occur where Au and Pd sites are adjacent at the surface of AuPd nanoalloys. Due to the weakness of the Au-O bond relative to the Pd-O bond, molecular O_2 binds preferentially at the Pd site and much less favourably to the adjacent Au site.[64] Disrupting this multi-site adsorption of O_2 has been reported to stabilise the O_2 bond and inhibit the subsequent formation of H_2O.[63]

In this work, the enhanced levels of H_2O_2 productivity for the 0.5%Au-0.5%Pd catalyst compared to both 0.5%Pd and 1.0%Pd catalysts are also accompanied by a profound increase in H_2 conversion, from 17 % and 19 % for the Pd catalysts, to 54 % for the AuPd. Consequently, the increased production of H_2O_2 may not be the exclusive result of an inhibition in H_2O_2 degradation, but also of an enhancement to the overall ability of the catalyst to utilise H_2 and O_2.

A very limited enhancement was observed upon the incorporation of Zn or Pt into Pd/Al_2O_3 catalysts, wherein the resulting ZnPd or PtPd/Al_2O_3 catalysts offered productivity values of 38 and 34 mol_{H2O2} kg_{cat}^{-1} hr^{-1} respectively, but otherwise there was no clear significant benefit on H_2O_2 productivity associated with the incorporation of any other metal. The incorporation of Cu appeared to entirely inhibit the H_2O_2 synthesis reaction, at the metal loading used, which is in agreement with previous literature.[200] DFT calculations have suggested that the formation of H_2O_2 is thermodynamically unfavourable on Cu clusters and alloys of precious metals with Cu.[237] However, it has also been reported that very low loadings of Cu can enhance the synthesis of H_2O_2, when incorporated into zeolite or TiO_2 supported AuPd catalysts.[79, 238] Therefore, enhanced H_2O_2 synthesis may be possible, given appropriate support materials and metal loadings. It should be noted that metal loadings of Cu reported to promote the synthesis of H_2O_2 are as low as 0.025 %, whereas in this work, a loading of 0.5 % was used.

Whilst generally incapable of enhancing H_2O_2 productivity, the incorporation of secondary metals did appear to sometimes enhance the reaction selectivity towards H_2O_2 formation. For example, when comparing catalysts with an equivalent conversion of H_2 of 17 %, 0.5%Pd/Al_2O_3 had an H_2O_2 selectivity of 33 % and CoPd had an H_2O_2 selectivity of 34 % whereas the H_2O_2 selectivity for ZnPd was enhanced to 40 %.

The same catalysts were then tested in the selective oxidation of benzyl alcohol via in-situ H_2O_2 synthesis, as shown in Figure 3.5 and Table 3.4.

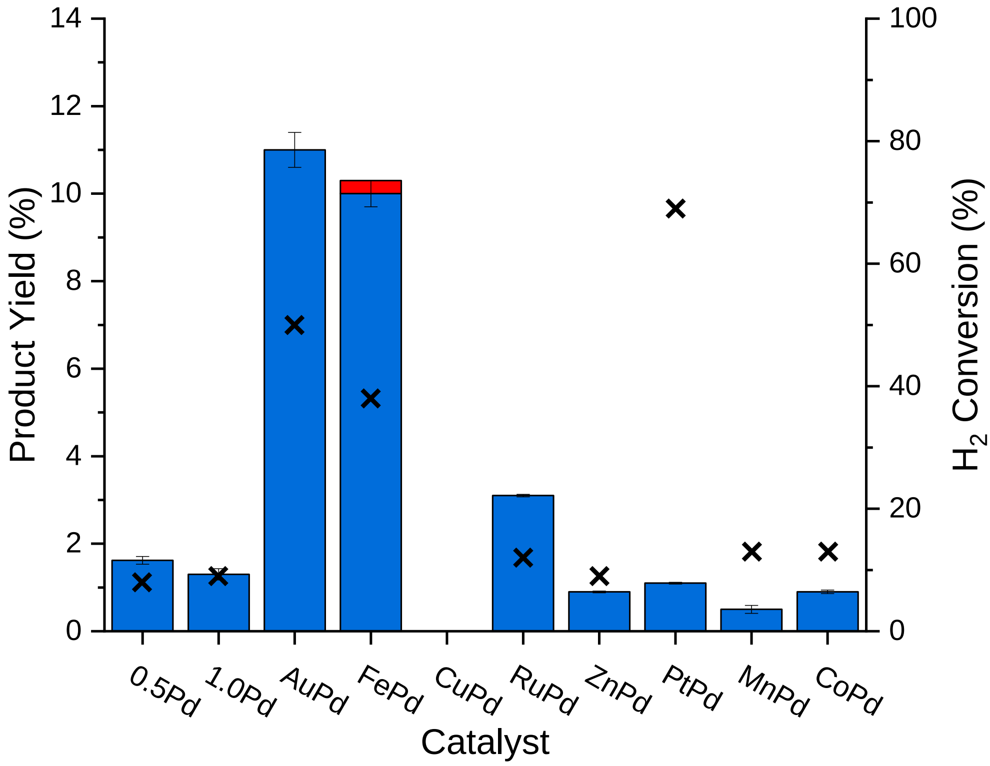

Figure 3.5. Comparison of the catalytic activities of supported 0.5%X-0.5%Pd/Al_2O_3 on the selective oxidation of benzyl alcohol via in-situ H_2O_2 synthesis.
Key; Benzaldehyde (*blue bars*), benzoic acid (*red bars*), H_2 conversion (*crosses*).
Benzyl alcohol oxidation reaction conditions: Catalyst (0.01 g), MeOH (7.13 g), benzyl alcohol (1.04 g, 9.62 mmol), mesitylene (0.42 g), 5% H_2/CO_2 (420 psi, 2.76 mmol), 25% O_2/CO_2 (160 psi, 5.24 mmol), 0.5 hr, 50 ^{O}C, 1200 rpm.

Table 3.4. Comparison of the catalytic activities of supported 0.5%X-0.5%Pd/Al_2O_3 on the selective oxidation of benzyl alcohol via in-situ H_2O_2 synthesis.

Catalyst	Benzaldehyde Yield (%)	Benzoic Acid Yield (%)	Benzaldehyde Selectivity (%)	Turnover Number (mol_{BA} mol_{metal}^{-1} hr^{-1})	H_2 Conversion (%)	H_2 Selectivity (%)	Residual H_2O_2 (mmol)
0.5Pd	1.6	0	100	654	8	70	0.063
1.0Pd	1.3	0	100	266	9	50	0.057
0.5Au-0.5Pd	11.0	0	100	2919	50	77	0.161
0.5Fe-0.5Pd	10.0	0.3	97	1406	38	95	0.075
0.5Cu-0.5Pd	0	0	100	0	0	0	0.000
0.5Ru-0.5Pd	3.1	0	100	617	12	90	0.065
0.5Zn-0.5Pd	0.9	0	100	140	9	35	0.076
0.5Pt-0.5Pd	1.1	0	100	291	69	6	0.053
0.5Mn-0.5Pd	0.5	0	100	70	13	12	0.056
0.5Co-0.5Pd	0.9	0	100	131	13	22	0.065

Benzyl alcohol oxidation reaction conditions: Catalyst (0.01 g), MeOH (7.13 g), benzyl alcohol (1.04 g, 9.62 mmol), mesitylene (0.42 g), 5% H_2/CO_2 (420 psi, 2.76 mmol), 25% O_2/CO_2 (160 psi, 5.24 mmol), 0.5 hr, 50 ^{O}C, 1200 rpm.

In the oxidation of benzyl alcohol, the 0.5%Pd/Al_2O_3 catalyst performed marginally better than the 1% Pd/Al_2O_3 analogue, with benzaldehyde yields of 1.6 % and 1.3 % respectively. This may suggest that lower metal loadings might lead to a more optimal nanoparticle size. However, these values are close and may fall within the range of experimental error.

Additionally, a strong synergistic effect becomes apparent when the activities of these Pd-monometallic catalysts are compared to the 0.5%Au-0.5%Pd/Al_2O_3 catalyst, which achieved a benzaldehyde yield of 11.0 % and an H_2 conversion of 50 %, compared to the limited H_2 conversions of the 1%Pd and 0.5%Pd/Al_2O_3 catalysts, which offered H_2 conversions of 9 % and 8 % respectively.

Previous work has demonstrated an enhanced activity for benzyl alcohol oxidation using bimetallic catalysts when Au was replaced with a Fenton's capable metal, such as Fe, Co or Mn, using a TiO_2 support.[218]

In this work, when an Al_2O_3 support was used, no catalyst formulation investigated was able to exceed the activity of the AuPd catalyst, with the FePd and RuPd analogues representing the only other bimetallic catalysts capable of significant enhancements over the monometallic Pd catalyst, which offered benzaldehyde yields of 10.0 % and 3.1 % respectively. Though it is worth noting that AuPd and FePd catalysts when supported on Al_2O_3 delivered significantly higher yields of benzaldehyde than when supported on TiO_2, under identical reaction conditions.[218] Incorporating Cu appeared to entirely inhibit the ability of Pd to participate in the oxidation of benzyl alcohol, likely as a result of the inability of CuPd to catalyse the direct synthesis of H_2O_2 at the metal loadings used in this work, as discussed above.[237]

All catalysts tested exhibited 100 % selectivity to benzaldehyde, with the exception of the FePd catalyst, which had a selectivity of 97.2 %, due to a small quantity of overoxidation to benzoic acid. This small loss of selectivity associated with FePd/Al_2O_3 is in agreement with the work of Crombie *et al.* who, under identical reaction conditions, observed a similar selectivity to benzaldehyde of 96 %, when using the analogous FePd/TiO_2 catalyst.[218] This loss in selectivity to benzaldehyde may be a feature of the incorporation of Fe into the catalyst, and associated with the proposed Fentons chemistry undertaken at Fe sites.[218] If the small loss of selectivity when using the FePd/Al_2O_3 catalyst were exclusively a result of increasing levels of benzyl alcohol conversion, then the same loss of product selectivity should have also be observed when using the AuPd/Al_2O_3 catalyst, which was not the case. Overall, the FePd/Al_2O_3 catalyst offered an approximately equivalent benzaldehyde yield to the AuPd/Al_2O_3, at 10.0 % and 11.0 % respectively, but only consumed 38 % of the available H_2, compared to the 50 % consumed by the AuPd/Al_2O_3. As a result, the FePd/Al_2O_3 catalyst exhibited an H_2 selectivity of 95 %, indicating that it is likely highly efficient at utilising H_2 in the oxidation of benzyl alcohol. Additionally, RuPd/Al_2O_3 offered an H_2 selectivity of 90 %, but only had a very limited H_2 conversion of 12 % and benzaldehyde yield of 3.1 %. Therefore, whilst only having limited catalytic activity, RuPd was also highly efficient with its conversion of H_2, although this may not remain true at longer reaction times when greater amounts of H_2 are converted.

XPS analysis performed by Dr David Morgan (Cardiff Catalysis Institute) revealed the oxidation states of Pd present at the surface of each catalyst, as shown in Table 3.5. For all catalysts, regardless of secondary metal, a mixture of Pd^0 and Pd^{2+} was obtained after heat treatment with 5% H_2 (500 °C, 4hr, 10 °C/min). Whilst much debate has taken place in the literature over whether Pd^0 or Pd^{2+} represents the active site for the H_2O_2 synthesis or degradation reactions, Ouyang *et al.* have suggested that the interface between Pd^0 and Pd^{2+} may be the site where H_2O_2 synthesis occurs, suggesting that a mixture of Pd oxidation states is required for efficient H_2O_2 synthesis.[42, 239] However, all catalysts presented in Table 3.5 feature broadly similar or identical ratios of Pd^0 and Pd^{2+}. As a result, it cannot be suggested that the different levels of H_2O_2 productivity or benzyl alcohol oxidation offered by each catalyst are a result of more optimal Pd oxidation state ratios that were initially present at the surface of each catalyst before use in the reaction. However, the oxidation state of Pd has been demonstrated to change in-situ as a result of the reactant gases, with Crombie *et al.* reporting the in-situ reduction of Pd under reaction conditions identical to those used herein for the oxidation of benzyl alcohol.[218] The change in Pd oxidation state as a result of the H_2/O_2 rich environment of the reaction mixture will be investigated in Section.

Other factors such as electronic effects, particle size distribution and specific reaction mechanisms also likely play a significant role in the overall activity of each given catalyst.

Table 3.5. Effects of secondary metal in supported 0.5X-0.5Pd/Al_2O_3 on the oxidation state of Pd as determined by XPS analysis.[a]

Catalyst	Pd^0:Pd^{2+}
0.5Pd/Al_2O_3	0.51 : 0.49
1.0Pd/Al_2O_3	0.39 : 0.61
0.5Au-0.5Pd/Al_2O_3	0.45 : 0.55
0.5Fe-0.5Pd/Al_2O_3	0.55 : 0.45
0.5Cu-0.5Pd/Al_2O_3	0.61 : 0.39
0.5Ru-0.5Pd/Al_2O_3	0.54 : 0.46
0.5Zn-0.5Pd/Al_2O_3	0.54 : 0.46
0.5Pt-0.5Pd/Al_2O_3	0.48 : 0.52
0.5Mn-0.5Pd/Al_2O_3	0.45 : 0.55
0.5Co-0.5Pd/Al_2O_3	0.50 : 0.50

[a]Catalysts were exposed to a reductive heat treatment (5% H_2/Ar, 500 °C, 4 hr, 10°C min^{-1}) before XPS analysis.

To investigate possible electronic effects associated with the alloying of Au or Fe with Pd, diffuse reflectance infrared Fourier transform spectroscopy was performed for 0.5%Au-0.5%Pd/Al_2O_3, 0.5%Fe-0.5%Pd/Al_2O_3 and 1.0% and 0.5%Pd/Al_2O_3, using CO as a probe molecule, as shown in Figure 3.6.

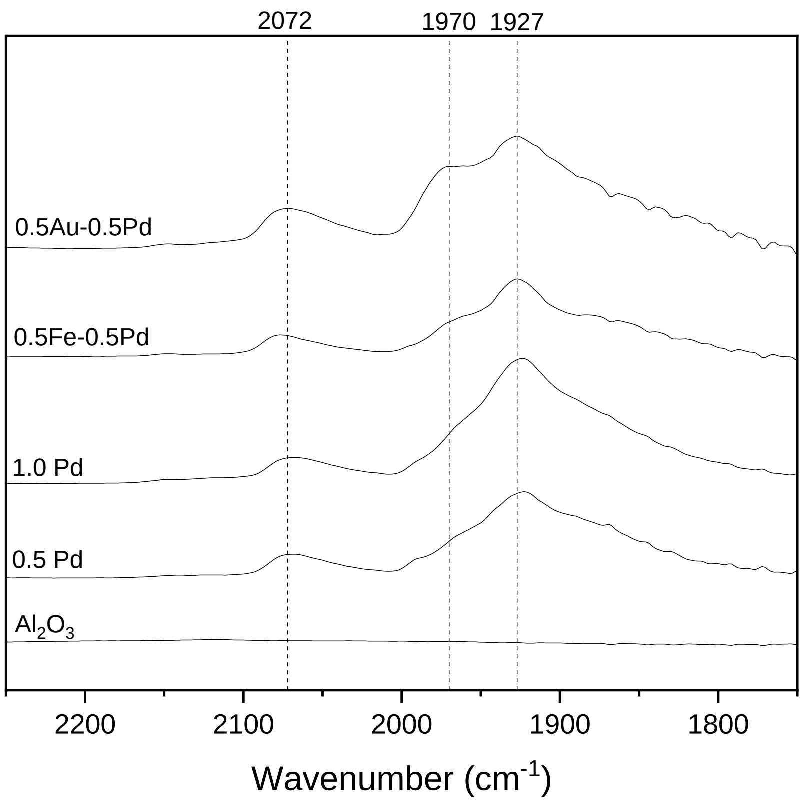

Figure 3.6. CO-DRIFTS spectra for X-Pd/Al_2O_3 catalysts.

Three general signals were observable in the region of 2200-1800 cm^{-1}, associated with the vibrational frequencies of adsorbed CO. Additionally, no signals were associated with the Al_2O_3 support in the region of 2200-1800 cm^{-1}, confirming that all observed signals were the result of CO adsorption on metal nanoparticles. The signal centred on 2072 cm^{-1} corresponds to linearly adsorbed CO at Pd sites, whilst the broader envelope with maxima centred on 1970 and 1927 cm^{-1} are the result of two-fold bridged and three-fold bridging adsorption of CO respectively.[240-245]

The incorporation of Au into Pd nanoparticles caused a significant increase in the intensity of the signal associated with two-fold bridging of CO, suggesting that Au present at the surface of nanoparticles may be disrupting large ensembles of Pd that favour three-fold bridging adsorption of CO, in favour of two-fold bridging configurations. Alternatively, this may be a result of the better dispersion of nanoparticles and smaller mean particle size. A similar but less intense effect was also observed for the FePd catalyst, which also exhibited a greater intensity signal associated with two-fold bridging of CO compared to the Pd/Al_2O_3 analogues. Additionally, the position of the signal associated with linear CO adsorption shifted to higher wavenumbers upon the incorporation of secondary metals. For example, both the 1.0%Pd and 0.5%Pd exhibited a linear CO adsorption signal centred on 2069 cm^{-1}, whereas for the AuPd, this feature was slightly blue-shifted and appears at 2072 cm^{-1}. For the FePd, this signal is blue shifted further and has a value of 2076 cm^{-1}.

In the literature, the shifting of wavenumbers associated with linear CO adsorption to lower values (red-shift) is often associated with a charge-transfer of electron density from Au sites to adjacent Pd sites, resulting in a greater degree of back-bonding from Pd d-orbitals to CO π^* anti-bonding orbitals.[62, 239] Therefore, the apparent blue shift associated with AuPd, relative to either Pd analogue may suggest that Au is exerting an electron withdrawing effect on adjacent Pd sites, and reducing the degree of back-bonding to CO π^* anti-bonding orbitals. The even greater degree of blue shifting associated with the FePd catalyst may also suggest that Fe had a greater electron-withdrawing effect on adjacent Pd sites. This observation was unexpected because Au is often reported to have an electron-donating effect on adjacent Pd sites, for example when AuPd nanoparticles have been supported on TiO_2, SiO_2 or $CeZrO_4$,[239, 246-248] and a corresponding red-shift has often been reported for the signal associated with linearly adsorbed CO. However, Brehm *et al.* has previously reported a similar blue shift to that seen herein, upon the alloying of Au and Pd using a AuPd/TiO_2 catalyst.[249]

Alternatively, it has been suggested that the overall dispersion of nanoparticles can have a significant effect on the wavenumber associated with linearly adsorbed CO. For example, Zhang *et al.* observed a blue shift from 2090 cm^{-1} to 2103 cm^{-1} when the mean nanoparticle size of Pd/Al_2O_3 was decreased from 13.1 nm to 7.7 nm.[250]

STEM and EDX analysis of the 1%Pd/Al_2O_3, 0.5%Au-0.5%Pd/Al_2O_3 and 0.5%Fe-0.5%Pd/Al_2O_3 catalysts was performed by Junhong Liu (Shanghai Jiao Tong University), as shown in Figures 3.7 – 3.9. Analysis of the 1%Pd/Al_2O_3 catalyst, as shown in Figure 3.7, confirmed the presence of Pd nanoparticles, which displayed a significant range of sizes, from many tens on nanometres to sub-ten nanometres. However, the incorporation of either Fe or Au appeared to assist in the dispersion of Pd, preventing the agglomeration of large Pd nanoparticles. For example, many small nanoparticles consisting of Au and Pd are shown in Figure 3.8. Additionally, energy dispersive X-ray (EDX) mapping and linescanning revealed the occurrence of interaction between Au and Pd within nanoparticle structures, suggesting that alloying of the two metals had occurred. Analysis of the 0.5%Fe-0.5%Pd/Al_2O_3 catlayst, as shown in Figure 3.9, again revealed the proximity of Fe and Pd within nanoparticle structures, suggesting that alloying also occurred between these two metals. Interestingly, EDX linescanning demonstrated the presence of smaller nanoparticles with significant quantities of Fe incorporated into the nanoparticles, whereas larger nanoparticles exhibited significantly higher levels of Pd.

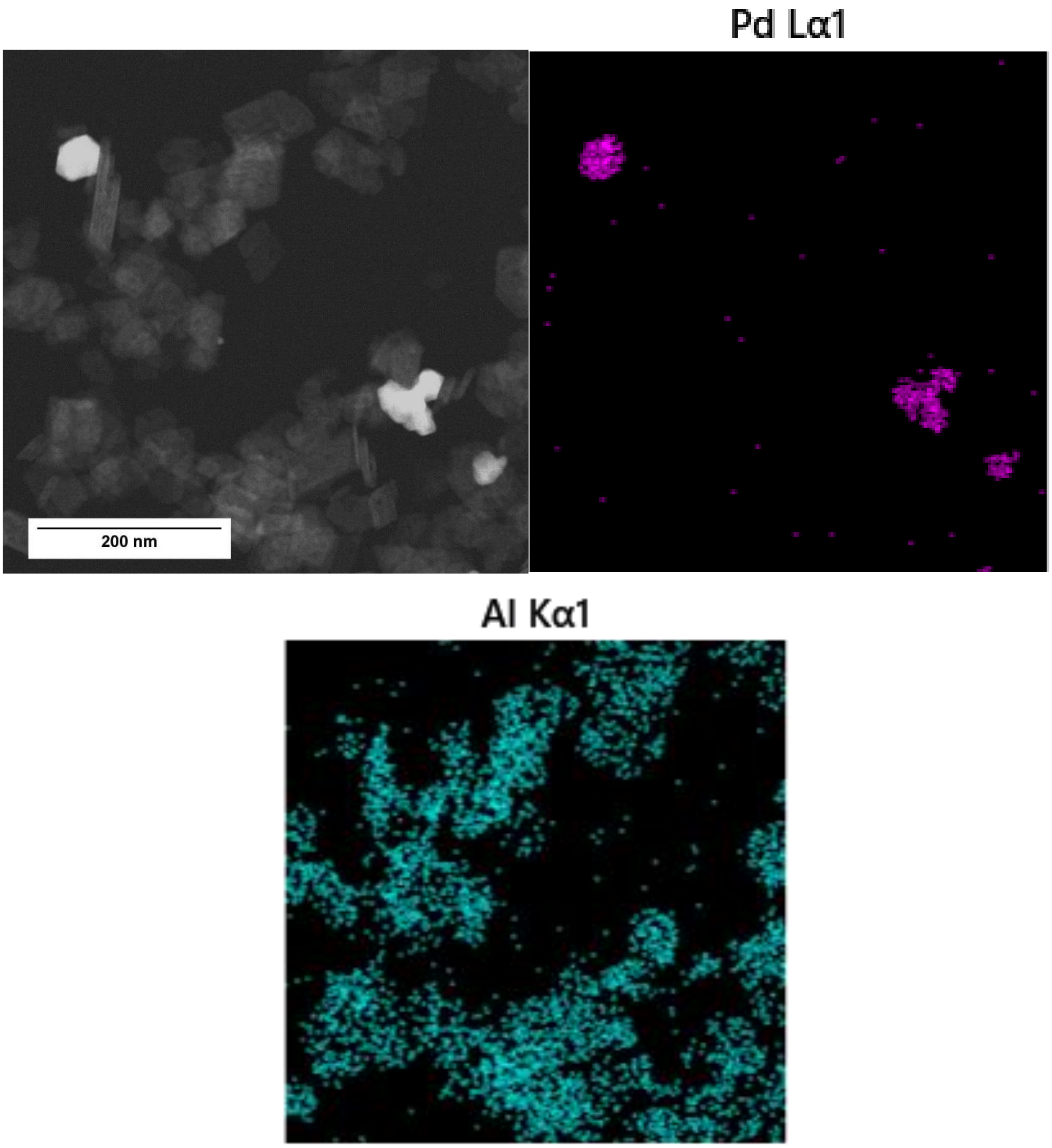

Figure 3.7. STEM micrograph and EDX mapping of the 1%Pd/Al_2O_3 catalyst.

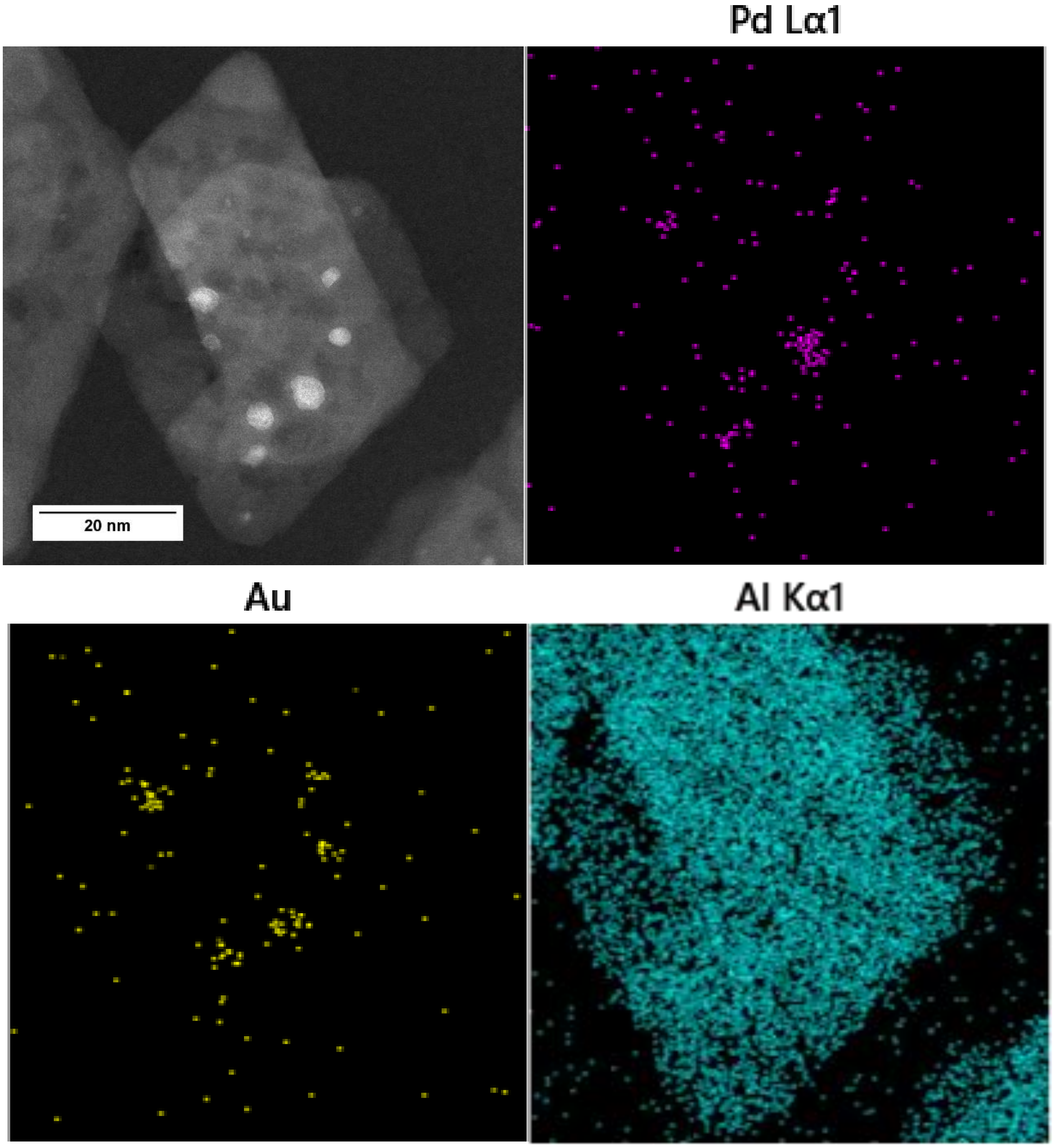

Figure 3.8. STEM micrograph and EDX mapping of the 0.5%Au-0.5%Pd/Al_2O_3 catalyst.

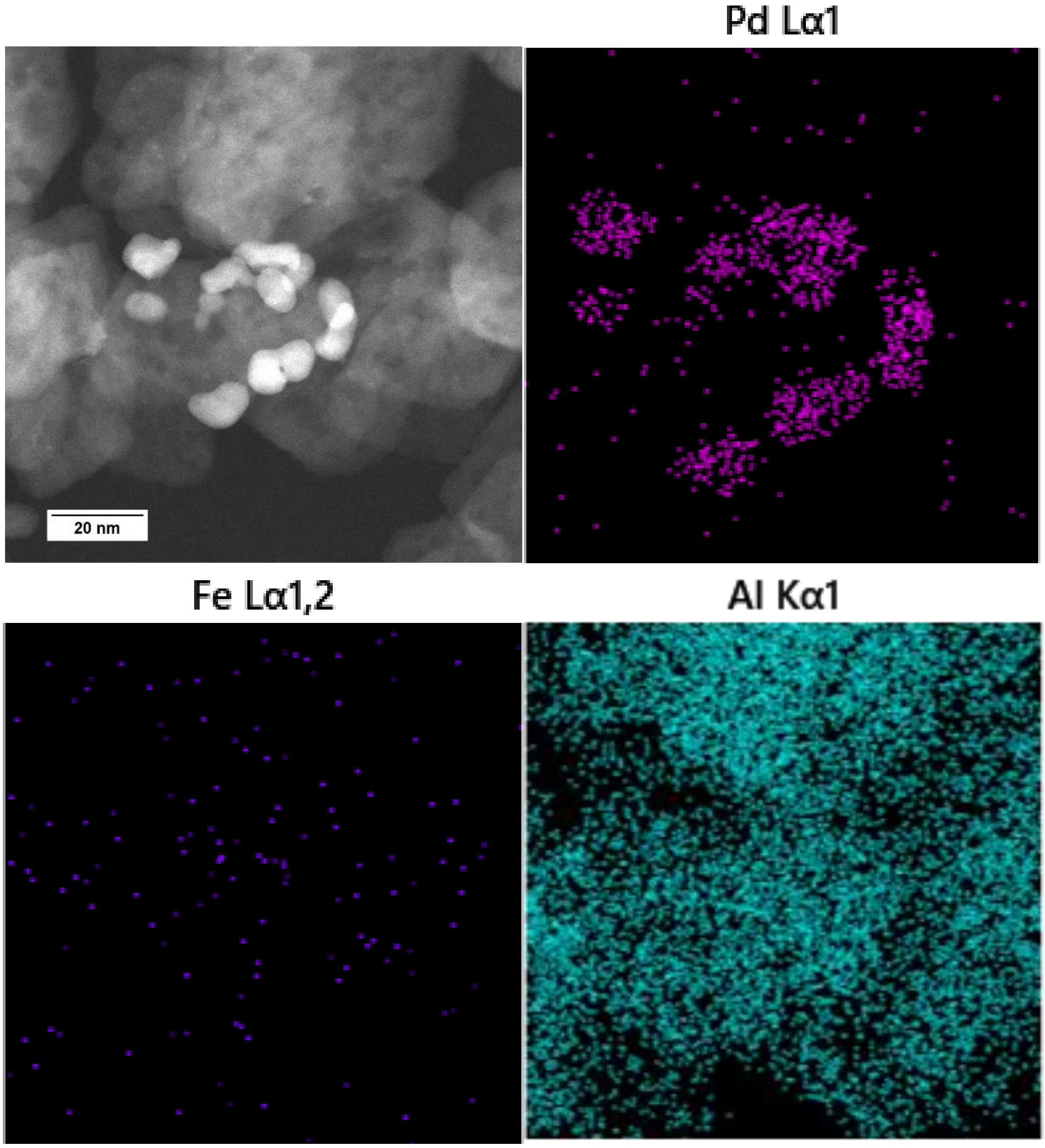

Figure 3.9. STEM micrograph and EDX mapping of the 0.5%Fe-0.5%Pd/Al_2O_3 catalyst.

3.4 The Oxidation of Benzyl Alcohol Under Aerobic and Reductive Conditions, Using 0.5%Au-0.5%Pd, 0.5%Fe-0.5%Pd and 1%Pd/Al_2O_3 Catalysts

In order to determine the increased efficacy that using both H_2 and O_2 in tandem to generate H_2O_2 in-situ could offer over that which could be achieved by using aerobic conditions or preformed H_2O_2 as oxidants, a series of supplementary reactions were performed. Analogous conditions were used, wherein instead of employing the previously used H_2/O_2 mixture diluted in CO_2, an equivalent partial pressure of O_2/CO_2 and the corresponding H_2/CO_2 mixtures were used separately, to provide either purely aerobic or purely reducing reaction conditions in which the benzyl alcohol reaction could take place. Additionally, a third set of conditions were used, in which 2.76 mmol of preformed commercial H_2O_2, equivalent to the number of mmol of H_2 utilised under the standard H_2/O_2 conditions were used to determine the efficacy of generating H_2O_2 in-situ. n.b. for all reactions, total pressure was fixed at 580 psi using CO_2. The results of this investigation are shown in Figure 3.10 and Table 3.6.

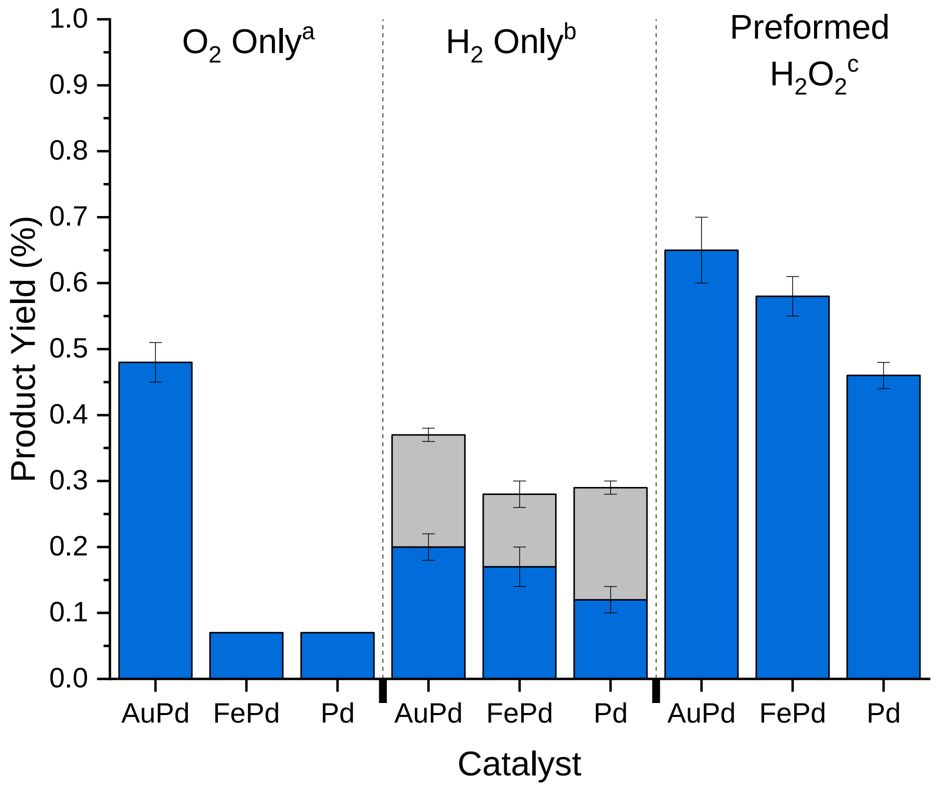

Figure 3.10. Catalytic activity of the 0.5%Au-0.5%Pd, 0.5%Fe-0.5%Pd and 1.0%Pd/Al_2O_3 catalysts when using O_2, H_2 or H_2O_2 as reactants in the selective oxidation of benzyl alcohol.

Key; benzaldehyde yield (*blue bars*), toluene yield (*grey bars)*.

Aerobic oxidation of benzyl alcohol reaction conditions: [a]Catalyst (0.01 g), MeOH (7.13 g), benzyl alcohol (1.04 g, 9.62 mmol), mesitylene (0.42 g), CO_2 (420 psi), 25% O_2/CO_2 (160 psi, 5.24 mmol), 0.5 hr, 50 °C, 1200 rpm.

H_2 oxidation of benzyl alcohol reaction conditions: [b]catalyst (0.01 g), MeOH (7.13 g), benzyl alcohol (1.04 g, 9.62 mmol), mesitylene (0.42 g), H_2/CO_2 (420 psi, 2.76 mmol), CO_2 (160 psi), 0.5 hr, 50 °C, 1200 rpm.

Oxidation of benzyl alcohol using ex-situ H_2O_2 reaction conditions: c catalyst (0.01 g), MeOH (7.00 g), benzyl alcohol (1.04 g, 9.62 mmol), mesitylene (0.42 g), H_2O_2 (50 wt.%, 0.13 mL, 2.76 mmol), CO_2 (580 psi), 0.5 hr, 50 °C, 1200 rpm.

Table 3.6. Catalytic activity of the 0.5%Au-0.5%Pd, 0.5%Fe-0.5%Pd and 1.0%Pd/Al_2O_3 catalysts when using O_2, H_2 or H_2O_2 as reactants in the selective oxidation of benzyl alcohol.

Catalyst	Reaction Conditions	Benzyl Alcohol Conversion (%)	Benzaldehyde Yield (%)	Toluene Yield (%)	Benzaldehyde Selectivity (%)
0.5%Au-0.5%Pd/Al_2O_3	O_2 [a]	0.5	0.5	0.0	100
0.5%Fe-0.5%Pd/Al_2O_3	O_2 [a]	0.1	0.1	0.0	100
1.0%Pd/Al_2O_3	O_2 [a]	0.1	0.1	0.0	100
0.5%Au-0.5%Pd/Al_2O_3	H_2 [b]	0.4	0.2	0.2	55
0.5%Fe-0.5%Pd/Al_2O_3	H_2 [b]	0.3	0.2	0.1	61
1.0%Pd/Al_2O_3	H_2 [b]	0.3	0.1	0.1	42
0.5%Au-0.5%Pd/Al_2O_3	H_2O_2 [c]	0.7	0.7	0.0	100
0.5%Fe-0.5%Pd/Al_2O_3	H_2O_2 [c]	0.6	0.6	0.0	100
1.0%Pd/Al_2O_3	H_2O_2 [c]	0.5	0.5	0.0	100
0.5%Au-0.5%Pd/Al_2O_3	In-situ H_2O_2 [d]	11.0	11.0	0.0	100
0.5%Fe-0.5%Pd/Al_2O_3	In- situ H_2O_2 [d]	10.3	10.0	0.0	97
1.0%Pd/Al_2O_3	In-situ H_2O_2 [d]	1.3	1.3	0.0	100

Aerobic oxidation of benzyl alcohol reaction conditions: [a]Catalyst (0.01 g), MeOH (7.13 g), benzyl alcohol (1.04 g, 9.62 mmol), mesitylene (0.42 g), CO_2 (420 psi), 25% O_2/CO_2 (160 psi, 5.24 mmol), 0.5 hr, 50 ^oC, 1200 rpm.

H_2 oxidation of benzyl alcohol reaction conditions: [b]Catalyst (0.01 g), MeOH (7.13 g), benzyl alcohol (1.04 g, 9.62 mmol), mesitylene (0.42 g), H_2/CO_2 (420 psi, 2.76 mmol), CO_2 (160 psi), 0.5 hr, 50 ^oC, 1200 rpm.

Oxidation of benzyl alcohol using ex-situ H_2O_2 reaction conditions: [c]Catalyst (0.01 g), MeOH (7.00 g), benzyl alcohol (1.04 g, 9.62 mmol), mesitylene (0.42 g), H_2O_2 (50 wt.%, 0.13 mL, 2.76 mmol), CO_2 (580 psi), 0.5 hr, 50 ^oC, 1200 rpm.

Oxidation of benzyl alcohol via in-situ H_2O_2 synthesis reaction conditions: [d]Catalyst (0.01 g), MeOH (7.13 g), benzyl alcohol (1.04 g, 9.62 mmol), mesitylene (0.42 g), 5% H_2/CO_2 (420 psi, 2.76 mmol), 25% O_2/CO_2 (160 psi, 5.24 mmol), 0.5 hr, 50 ^OC, 1200 rpm.

Firstly, the oxidation of benzyl alcohol using O_2 was investigated using the 0.5%Au-0.5%Pd, 0.5%Fe-0.5%Pd and 1%Pd/Al_2O_3 catalysts. Under these aerobic conditions, conversions of benzyl alcohol were low, with the AuPd catalyst offering a benzyl alcohol conversion of 0.5 %, whilst for both FePd and Pd, only a 0.1 % conversion was achieved. When compared to the in-situ H_2O_2 conditions, using both H_2 and O_2 in tandem, significant enhancements were clearly achieved in terms of overall benzyl alcohol conversion. For example, the AuPd catalyst offered a benzyl alcohol conversion of 11.0 % when using H_2 and O_2 in tandem, compared to the 0.5 % conversion of benzyl alcohol under aerobic conditions. This is in agreement with the work of Crombie *et al.*[218] and Santonastaso *et al.*[27] who have both previously reported increased conversions of benzyl alcohol when H_2 is incorporated alongside O_2, at 50 ^oC, whereas the aerobic oxidation of benzyl alcohol is often performed at higher temperatures, with 100 ^oC typical.[27, 220-223] This again demonstrates the efficacy of incorporating both H_2 and O_2 at more mild temperatures, where aerobic activity is limited.

The complementary H_2 conditions were then utilised, which again offered only low conversions of benzyl alcohol. For example, when the AuPd catalyst was used under these reductive conditions, a benzyl alcohol conversion of 0.4 % was offered, at a product selectivity for benzaldehyde of 54.7 %. Instead, significant proportions of toluene were formed, which was not observed under either the O_2 or the H_2/O_2 conditions, suggesting that toluene formation was suppressed by the presence of O_2 in the H_2/O_2 mixture. Similarly low conversions of benzyl alcohol were also observed for both the FePd and Pd catalysts, again demonstrating the high efficacy of utilising both H_2 and O_2 in the reaction mixture. Finally, when preformed H_2O_2 was utilised in the place of H_2 or O_2, similarly low levels of conversion were observed. For example, the AuPd catalyst offered a benzyl alcohol conversion of 0.7 %, whilst the FePd and Pd catalysts offered benzyl alcohol conversion of 0.6 % and 0.5 % respectively. Again, the very low benzyl alcohol conversions offered when using preformed H_2O_2 compared to generating H_2O_2 in-situ from H_2 and O_2 further demonstrate the efficacy of this methodology when operated at 50 ^oC.

A significant limitation of these type of blank reactions is related to the oxidation state of Pd. It was reported by Crombie *et al.* and will be investigated in this work in Section 3.7, that Pd^{2+} sites undergoes an in-situ reduction to Pd^0 during the selective oxidation of benzyl alcohol via in-situ H_2O_2 synthesis.[218] This occurs in the presence of both H_2 and O_2 as reactant gasses, and in the work of Crombie *et al.* resulted in the total reduction of all surface Pd of the Pd/TiO_2 and $AuPd/TiO_2$ catalysts used in their work after 30 minutes.[218] In this work, when 'O_2 only' reactions were performed, no in-situ reduction of Pd will likely occur due to the lack of H_2 and consequently, the actual proportion of oxidation states of Pd will be different under the 'O_2 only' conditions compared to when both H_2 and O_2 are present. Wu *et al.* have previously reported that for the aerobic oxidation of benzyl alcohol, by increasing the proportions of surface PdO relative to Pd^0 for AuPd/silica catalysts, decreasing levels of benzyl alcohol conversion were offered by the catalyst.[223]

In this work, when evaluating the oxidative contributions from O_2 during the oxidation of benzyl alcohol via in-situ H_2O_2 synthesis, it may be possible that the increasing proportion of Pd^0 present on a catalyst when both H_2 and O_2 gasses are present could enhance the level of aerobic oxidation, given the findings of Wu *et al.* described above.[223]

Conversely, future work should investigate the possibility for the in-situ oxidation of Pd sites during the aerobic 'O_2 only' reaction conditions via XPS, to determine if a link can be made between an increasing concentration of PdO and benzyl alcohol conversion.

Further investigations into the oxidative contributions of O_2 using the 'benzyl alcohol oxidation via in-situ H_2O_2 synthesis' reaction conditions , when both H_2 and O_2 are present, will be conducted in Chapter 4, Section 4.4.

3.5 The Effect of Au:Pd Ratio of The AuPd/Al_2O_3 Catalyst Towards the Selective Oxidation of Benzyl Alcohol via in-situ H_2O_2 Synthesis

The activity of bimetallic AuPd catalysts in the direct synthesis of H_2O_2 has been shown to be highly dependent on the ratio of Au and Pd.[232] It is therefore likely that the oxidative activity of the catalyst towards the selective oxidation of benzyl alcohol can also be modulated in the same manner. As such, a range of AuPd/Al_2O_3 catalysts were prepared with varying Au and Pd content, between a purely Au and a purely Pd monometallic catalyst. The total metal loading of each catalyst was fixed at 1% by mass. The activity of these catalysts towards the direct synthesis of H_2O_2 is shown in Table 3.7.

Table 3.7. Effects of metal loading ratio in a AuPd/Al_2O_3 catalyst in the direct synthesis of hydrogen peroxide.

Catalyst	Productivity (mol H_2O_2 kg_{cat}^{-1} hr^{-1})	Turnover Number (mol_{H2O2} mol_{metal}^{-1} hr^{-1})	H_2 Conversion (%)	H_2O_2 Selectivity (%)	H_2O_2 Concentration (wt. %)
1.0Au	0	0	-	-	0
0.75Au-0.25Pd	83	1342	21	63	0.17
0.625Au-0.375Pd	82	1221	37	41	0.16
0.5Au-0.5Pd	61	837	54	19	0.12
0.375Au-0.625Pd	63	869	33	37	0.13
0.25Au-0.75Pd	53	642	32	31	0.11
0.125Au-0.875Pd	40	454	25	29	0.08
1.0Pd	29	309	19	28	0.06

H_2O_2 direct synthesis Reaction conditions: Catalyst (0.01 g), H_2O (2.9 g), MeOH (5.6 g), 5% H_2/CO_2 (420 psi, 2.76 mmol), 25% O_2/CO_2 (160 psi, 5.24 mmol), 0.5 hr, 20 °C, 1200 rpm.

In the direct synthesis of H_2O_2, the 1%Au/Al_2O_3 catalyst was unable to convert H_2 and thus, resulted in an H_2O_2 productivity of 0. As was observed previously, the 1%Pd catalyst offered a moderate productivity of 29 mol_{H2O2} kg_{cat}^{-1} hr^{-1}, but strong synergistic effects were observed upon the utilisation of Au and Pd in tandem, with the 0.5Au-0.5Pd/Al_2O_3 offering a productivity of 61 mol_{H2O2} kg_{cat}^{-1} hr^{-1}.

Interestingly, the Au enriched catalysts clearly favoured H_2O_2 synthesis and exhibited higher selectivity to H_2O_2 than their Pd enriched analogues. For example, the 0.75Au-0.25Pd/Al_2O_3 catalyst reached a productivity of 83 mol_{H2O2} kg_{cat}^{-1} hr^{-1}, whereas the 0.25Au-0.75Pd/Al_2O_3 catalyst had a productivity of only 53 mol_{H2O2} kg_{cat}^{-1} hr^{-1}.

When investigating the effects of AuPd ratio on H_2O_2 productivity using a AuPd/TiO_2 catalyst under ambient conditions, Santos *et al.* observed a similar trend, where 0.5Au-0.5Pd/TiO_2 and 0.75Au-0.25Pd/TiO_2 catalysts offered higher levels of H_2O_2 productivity than 0.25Au-0.75Pd/TiO_2 and 1.0Pd/TiO_2 analogues.[231] It has been reported previously in the literature that increasing the Au content relative to Pd increases the activation enthalpy of the formation of both H_2O_2 and H_2O, but that the activation enthalpy of H_2O formation increases by a greater amount, thereby leading to a net enhancement in selectivity towards H_2O_2 synthesis.[41] Therefore, it is possible that this electronic effect is the origin of the observed enhancement in H_2O_2 synthesis. Alternatively, as previously discussed, isolation effects arising from Au sites at the surface of AuPd nanoparticles may be enhanced by the increasing concentration of Au relative to Pd in each catalyst. It should however be noted that the general trend in enhanced H_2O_2 synthesis observed in this work is not universally applicable to all cases, and contrary to these findings, catalysts with equal metal loadings of Pd and Au, or greater levels of Pd than Au have been reported in other studies to yield enhanced H_2O_2 productivities, for example when a TiO_2 support is used.[232] However the testing of these AuPd/TiO_2 catalysts was conducted at 2 °C and may not be directly comparable to the ambient conditions used herein.[232] This series of catalysts were then used in the selective oxidation of benzyl alcohol via in-situ H_2O_2 synthesis, as shown in Figure 3.11 and Table 3.8.

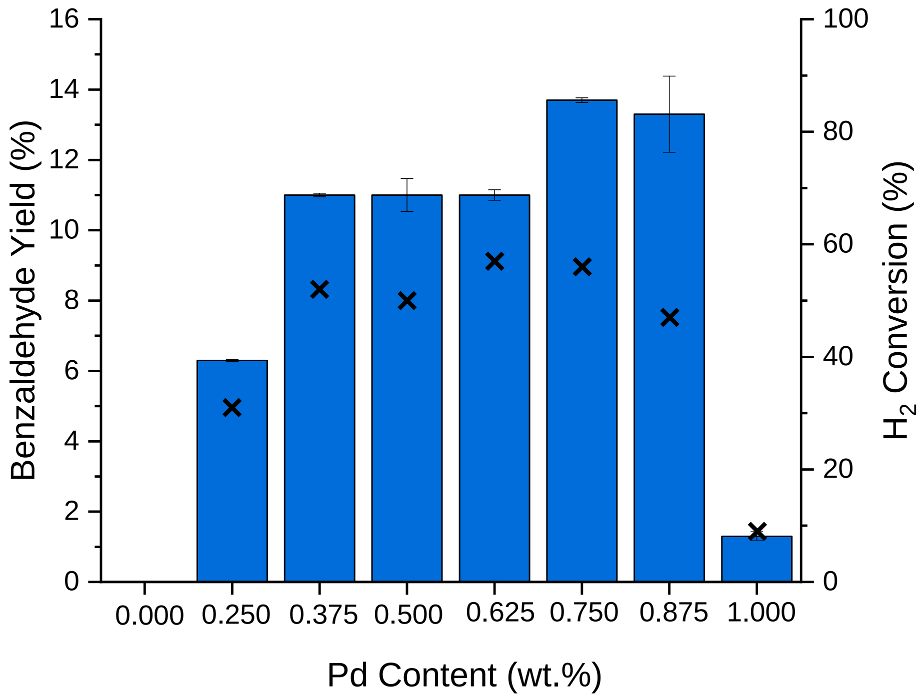

Figure 3.11. The effect of Au/Pd ratio on the in-situ oxidation of benzyl alcohol using AuPd/Al_2O_3 catalysts. Total metal loading fixed at 1 wt.%. **Key;** Benzaldehyde yield (*bars*), H_2 conversion (*crosses*). **Benzyl alcohol oxidation reaction conditions:** Catalyst (0.01 g), MeOH (7.13 g), benzyl alcohol (1.04 g, 9.62 mmol), mesitylene (0.42 g), 5% H_2/CO_2 (420 psi, 2.76 mmol), 25% O_2/CO_2 (160 psi, 5.24 mmol), 0.5 hr, 50 ^{o}C, 1200 rpm.

Table 3.8. The effects of Au:Pd ratio of supported AuPd/Al_2O_3 on the in-situ oxidation of benzyl alcohol.

Catalyst	Benzaldehyde Yield (%)	Benzoic Acid Yield (%)	Benzaldehyde Selectivity (%)	Turnover Number (mol_{BA} mol_{metal}^{-1} hr^{-1})	H_2 Conversion (%)	H_2 Selectivity (%)	Residual H2O2 (mmol)
1.0Au	0.0	0.0	100	0	-	0	0.000
0.75Au-0.25Pd	6.3	0.0	100	1965	31	71	0.219
0.625Au-0.375Pd	11.0	0.0	100	3154	52	74	0.230
0.5Au-0.5Pd	11.0	0.0	100	2919	50	77	0.161
0.375Au-0.625Pd	11.0	0.0	100	2716	57	67	0.159
0.25Au-0.75Pd	13.7	0.0	100	3163	56	85	0.128
0.125Au-0.875Pd	13.3	0.0	100	2883	47	99	0.084
1.0Pd	1.3	0.0	100	266	9	50	0.058
0.5Pd	1.6	0	100	654	8	70	0.063

Benzyl alcohol oxidation reaction conditions: Catalyst (0.01 g), MeOH (7.13 g), benzyl alcohol (1.04 g, 9.62 mmol), mesitylene (0.42 g), 5% H_2/CO_2 (420 psi, 2.76 mmol), 25% O_2/CO_2 (160 psi, 5.24 mmol), 0.5 hr, 50 ^{O}C, 1200 rpm.
n.b. Total metal loading fixed at 1 wt.%.

As was seen for the 0.5%Au-0.5%Pd/Al_2O_3 catalyst in the previous Section, all AuPd formulations offered 100 % selectivity to benzaldehyde, with no observable toluene, benzene, benzoic acid or other products.
The 1%Au/Al_2O_3 catalyst was entirely inactive in the oxidation of benzyl alcohol, which is likely due to its corresponding total inactivity in the direct synthesis of H_2O_2, meaning no radical oxidants species can be formed. The 1%Pd/Al_2O_3 catalyst was able to facilitate only a limited conversion of benzyl alcohol, with a benzaldehyde yield of 1.3 %.
The incorporation of Au into the catalyst caused a pronounced increase in hydrogen conversion and benzaldehyde yield, compared to yields offered by either the 1%Pd or 0.5%Pd/Al_2O_3 catalysts. Additionally, a clear correlation was established, wherein catalysts with higher relative metal loadings of Pd, with correspondingly lower levels of Au resulted in enhanced levels of benzaldehyde yield.
For example, the 0.75Au-0.25Pd/Al_2O_3 catalyst offered a benzaldehyde yield of 6.3 %, compared to the 0.25Au-0.75Pd/Al_2O_3 catalyst, which offered a benzaldehyde yield of 13.7 %.
These Pd-rich bimetallic catalysts also had comparatively lower levels of residual H_2O_2 in the post reaction solution than their Au rich counterparts. Indeed, the 0.75Au-0.25Pd/Al_2O_3 catalyst had 0.219 mmol of residual H_2O_2 present in solution after a 30-minute reaction, whereas the 0.125Au-0.875Pd/Al_2O_3 catalyst had only 0.084 mmol of residual peroxide. This

may indicate that this H_2O_2, or its radical precursors, are being increasingly utilised in the oxidation of benzyl alcohol, as Pd ratio increases, or that less H_2O_2 or more H_2O is synthesised as Pd ratio increases. An investigation into the catalytic activity of each catalyst towards the degradation of H_2O_2 may provide information towards this hypothesis and should be considered for future work.

The most active catalysts from the series were the 0.25Au-0.75Pd/Al_2O_3 catalyst, which offered a benzaldehyde yield of 13.7 %, and the 0.125Au-0.875Pd/Al_2O_3 catalyst, which had within error an equivalent yield of benzaldehyde, accompanied by an appreciable decrease in H_2 conversion of 9 %. This suggests that at longer reaction times where iso-conversion of H_2 is achieved, the more Pd enriched catalyst may deliver higher product yields without compromising on the rate enhancing effects of the incorporation of Au.

Indeed, when the H_2 selectivity with respect to benzaldehyde yield was examined, the 0.125Au-0.875Pd/Al_2O_3 catalyst appeared to be a highly efficient and selective catalyst, with an H_2 selectivity of 99 %, compared to the 85 % H_2 selectivity observed for the 0.25Au-0.75Pd/Al_2O_3 catalyst and the 77 % H_2 selectivity observed for the 0.5Au-0.5Pd/Al_2O_3 catalyst. Increasing Pd content within this series of catalysts therefore appeared to increase the efficiency and selectivity with which H_2 was consumed, whilst promoting the oxidation of benzyl alcohol. However, the extremely high selectivity of 99 %, offered by the 0.125Au-0.875Pd/Al_2O_3 catalyst indicates that under the reaction conditions utilised, some oxidative activity from O_2, or activation of benzyl alcohol by the catalyst itself may be contributing to the overall yields of benzaldehyde.

Although the reaction conditions utilised in the direct synthesis of H_2O_2 and the in-situ oxidation of benzyl alcohol via in-situ H_2O_2 synthesis reactions feature different solvent systems and reaction temperatures, the catalytic trends observed under both sets of conditions appear to complement each other well. Considering both data sets of data for the direct synthesis of H_2O_2 and the selective oxidation of benzyl alcohol via in-situ H_2O_2 synthesis (Table 3.7 and 3.8), it appears that Pd enriched catalysts favour the benzyl alcohol oxidation process, whereas Au enriched catalysts promote the synthesis of H_2O_2.

To illustrate this, a comparison of the turnover numbers towards the direct synthesis of H_2O_2 and conversion of benzyl alcohol of each catalyst is shown in Figure 3.12.

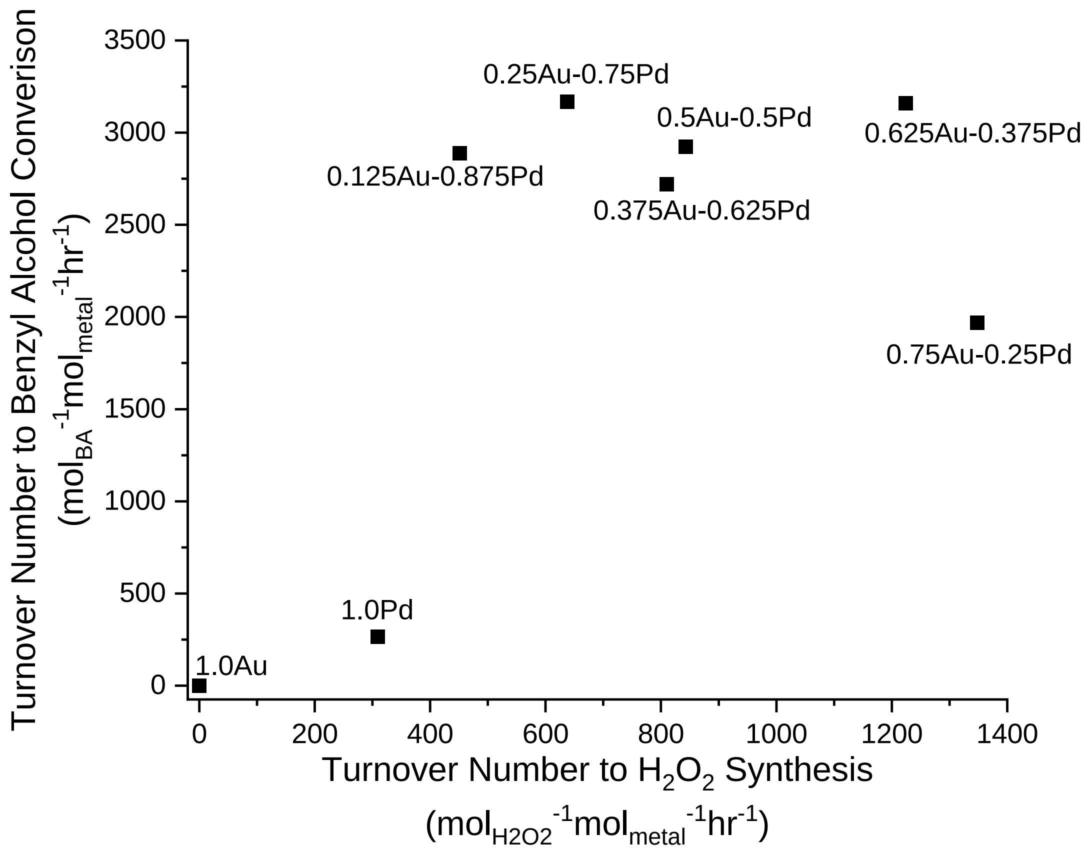

Figure 3.12. Comparison of turnover numbers towards the synthesis of H_2O_2 and oxidation of benzyl alcohol for a series of $AuPd/Al_2O_3$ catalysts.

H_2O_2 direct synthesis conditions: Catalyst (0.01 g), H_2O (2.9 g), MeOH (5.6 g), 5% H_2/CO_2 (420 psi mmol), 25% O_2/CO_2 (160 psi), 0.5 hr, 20 °C, 1200 rpm.

Benzyl alcohol oxidation reaction conditions: Catalyst (0.01 g), MeOH (7.13 g), benzyl alcohol (1.04 g, 9.62 mmol), mesitylene (0.42 g), 5% H_2/CO_2 (420 psi, 2.76 mmol), 25% O_2/CO_2 (160 psi, 5.24 mmol), 0.5 hr, 50 °C, 1200 rpm.

A correlation between the direct synthesis of H_2O_2 and conversion of benzyl alcohol offered by different catalysts was not observed previously in this work when AuPd nanoparticles were supported on a range of support materials and may indicate an antagonistic relationship between the two concurrent reactions.

The mechanism for benzyl alcohol oxidation via in-situ H_2O_2 synthesis has been suggested to proceed via a series of radical intermediates, namely hydroxyl or hydroperoxyl radicals, with a methoxyl radical also reported, arising from the methanol solvent.[218] As previously discussed, the incorporation of Au into Pd nanoparticles can inhibit the dissociation of the oxygen-oxygen bond in molecular O_2, which would otherwise lead to the formation of radical oxygen based surface species.[63] The greater ratios of Pd relative to Au may enhance the generation of these radical oxygen species, and consequently enhance the rate of benzyl alcohol oxidation, whilst diminishing the total concentration of H_2O_2 generated. Additionally, it has also been shown that incorporation of Au into Pd nanoparticles promotes the release of H_2O_2 from the metal surface, due to the relative weakness of the Au-O bond compared to the Pd-O bond.[63] However, Au incorporation may also promote the release of intermediate radical oxygen species from the metal surface for the same reason. Indeed, Richards e*t al.* demonstrated through EPR spectroscopy that Au can promote the release of radical oxygen species, such as hydroxyl and hydroperoxyl radicals from Pd nanoparticle catalysts, and that optimisation of the relative ratios of Au and Pd can enhance or inhibit the overall quantity of radical oxygen species observable in the reaction mixture.[132]

Overall, a clear synergistic effect was observed when Au and Pd were alloyed, enhancing both the concentrations of H_2O_2 synthesised and the quantity of benzyl alcohol that was oxidised, compared to the equivalent 1%Pd or 0.5%Pd/Al_2O_3 catalyst. Modulation of the relative concentrations of Au and Pd incorporated in the catalyst resulted in enhancements in the activity of either the direct synthesis of H_2O_2 or of the oxidation of benzyl alcohol. The origin of this enhancement to oxidative activity may derive from a balance in the ratio Au and Pd, where Pd sites catalyse the synthesis of H_2O_2 and its radical oxygen-based precursors, whilst adjacent Au sites promote the release of H_2O_2 or radical oxygen species from the surface of the metal. No XPS data was collected for this series of catalysts, and future work should determine the ratios of surface Pd^0: Pd^{2+} present for each catalyst to determine whether a correlation can be made between the oxidation state of Pd and catalytic activity. It should be noted however that a significant decrease in the oxidation of benzyl alcohol was not observed until the relative loading of Pd reached 0.75%, whilst a consistent increase in the synthesis of H_2O_2 was observed as relative Au loading increased.

To further investigate the effects of Au in AuPd nanoparticles, diffuse reflectance infrared Fourier transform spectroscopy was performed for this series of catalysts, using CO as a probe molecule, the results of which are shown in Figure 3.13.

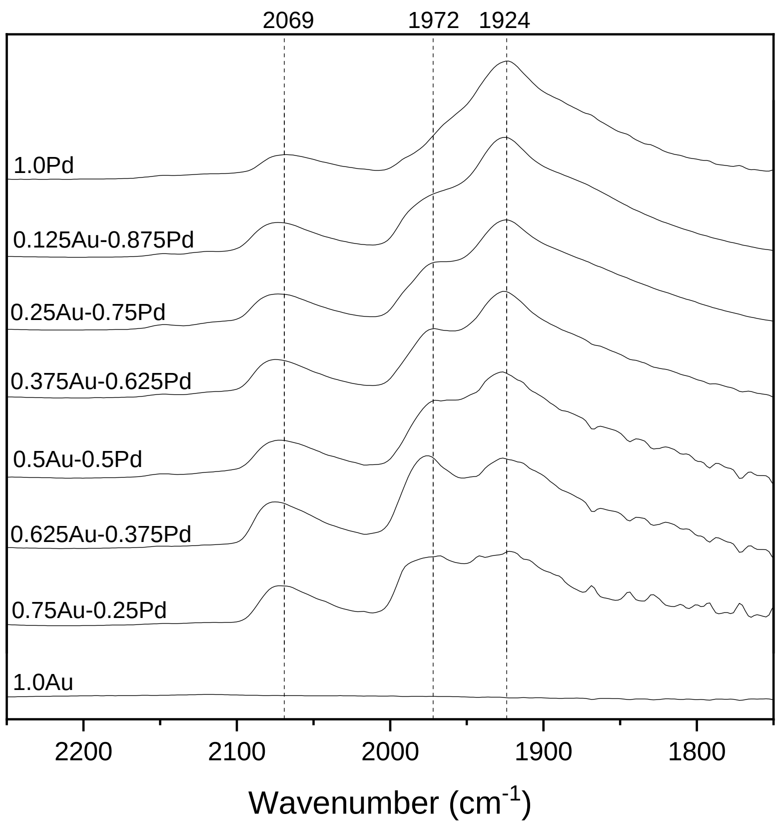

Figure 3.13. CO-DRIFTS spectra comparing a range of Au:Pd ratios of AuPd/Al_2O_3 catalysts.

As previously discussed, the signal centred on 2069 cm^{-1} corresponds to linearly adsorbed CO at Pd sites, whilst the broad envelope centred on 1972 and 1924 cm^{-1} are the result of bridged and three-fold bridging adsorption of CO respectively.[240-245] No CO adsorption signals were observed in the region of 2200-1800 cm^{-1} for the 1%Au catalyst, confirming that adsorption bands are a result of CO adsorption at Pd sites. For all AuPd catalysts, the linear CO adsorption band at 2069 cm^{-1} is shifted to a higher wavenumber relative to the 1%Pd catalyst, which as previously discussed, may suggest an electron withdrawing effect of adjacent Au sites, or may be a result of changes in the mean nanoparticle size. Additionally, as the relative Au content of the AuPd catalyst increases, the intensity of the two-fold CO adsorption signal centred on 1972 cm^{-1} increases relative to the three-fold CO adsorption signal at 1924 cm^{-1}. This may suggest an increasing preference for two-fold bridging adsorption of CO compared to three-fold bridging, resulting from the increasing surface content of Au disrupting larger ensembles of Pd that favour three-fold bridging. The signal associated with linearly adsorbed CO also increases in intensity, relative to the signals associated with bridging configurations, as total Au content increases and Pd content decreases. This indicates an increasing tendency for CO to adsorb linearly, rather than in a bridging configuration, which may suggest that greater levels of Au in the catalyst are disrupting larger ensembles of surface Pd. Overall, the general observation that increasing Au content in a catalyst increases the resultant H_2O_2 productivity, whilst increasing Pd content enhances benzyl alcohol oxidation, appears to correlate well with

the observed changes in CO-adsorption modes. Namely, the increasing tendency for CO to adsorb in a linear or two-fold bridging configuration, with increasing Au content, as opposed to three-fold bridging which was more favourable at greater Pd concentrations. Au sites adjacent to Pd sites have been shown to promote H_2O_2 synthesis through a number of previously discussed mechanisms,[41, 62-64, 236] and the increasing tendency for linear CO and two-fold CO bridging adsorption modes may suggest an increasing prevalence of Au Pd interface sites.
Indeed, this change in adsorption configuration likely arises as a result of either nanoparticle size distribution, or isolation effects arising from increasing surface concentrations of Au in AuPd nanoparticles. The distributions of nanoparticle sizes were not investigated for this series of catalysts, and future work should focus on determining mean nanoparticle sizes for comparison with the above CO-DRIFTS data, to support or refute whether changes in nanoparticle sizes across the series may be causing the changes in CO-DRIFTS data reported.

3.6 Effect of Fe:Pd Metal Loading Ratio of The FePd/Al_2O_3 Catalyst Towards the Selective Oxidation of Benzyl Alcohol via in-situ H_2O_2 Synthesis

From the investigation into the effect of secondary metal, the second most active bimetallic catalyst was FePd/Al_2O_3, which had very similar yields of benzaldehyde to the equivalent AuPd analogue, with 10.0 % and 11.0 % respectively. Additionally, the FePd/Al_2O_3 catalyst offered lower levels of hydrogen conversion, at 38 %, compared to the 50 % offered by the AuPd/Al_2O_3 catalyst.
Previous work in the literature has suggested that the enhanced oxidative activity associated with FePd catalysts is a result of the bifunctionality of the catalyst, wherein Pd sites catalyse the synthesis of H_2O_2 and Fe sites subsequently undertake Fentons chemistry to generate a greater flux of radical oxidants than can be achieved by Pd alone.[218] Therefore, optimisation of the ratios of Pd and Fe, in order to balance and maximise the synthesis of H_2O_2 and subsequent Fentons reactions, was a key motivation of this study.
Therefore, whilst maintaining a total metal loading of 1%, further optimisation studies were conducted using the FePd/Al_2O_3 catalyst, with metal loading ratios varied between a monometallic Pd and monometallic Fe catalyst. Firstly, the direct synthesis of H_2O_2 was investigated, which is shown in Figure 3.14 and Table 3.9.

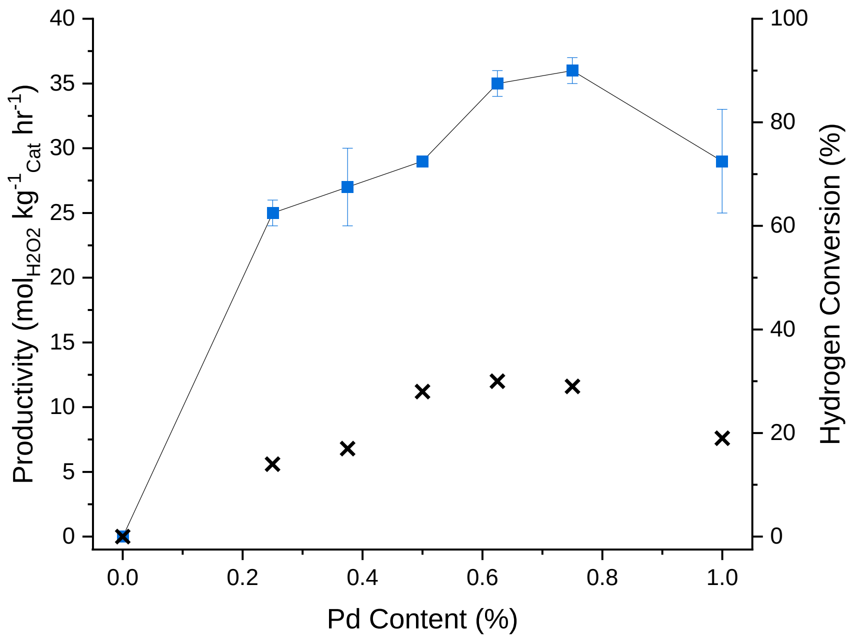

Figure 3.14. The effect of Fe/Pd ratio on the direct synthesis of H_2O_2 using $FePd/Al_2O_3$ catalysts. Total metal loading fixed at 1 wt.%. **Key;** H_2O_2 productivity (*squares*), H_2 conversion (*crosses*).
H_2O_2 direct synthesis reaction conditions: Catalyst (0.01 g), H_2O (2.9 g), MeOH (5.6 g), 5% H_2/CO_2 (420 psi, 2.76 mmol), 25% O_2/CO_2 (160 psi, 5.24 mmol), 0.5 hr, 20 °C, 1200 rpm.

Table 3.9. Effect of Fe:Pd ratio on the direct synthesis of H_2O_2 using $FePd/Al_2O_3$.

Metal	Productivity (mol H_2O_2 kg_{cat}^{-1} hr^{-1})	Turnover Number (mol_{H2O2} mol_{metal}^{-1} hr^{-1})	H_2 Conversion (%)	H_2O_2 Selectivity (%)	H_2O_2 Concentration (wt. %)
0.5Pd	33	702	17	33	0.07
1.0Pd	29	309	19	28	0.06
0.25Fe-0.75Pd	36	316	29	22	0.07
0.375Fe-0.625Pd	35	326	30	22	0.07
0.5Fe-0.5Pd	29	214	19	29	0.06
0.625Fe-0.375Pd	27	183	17	30	0.06
0.75Fe-0.25Pd	25	190	14	32	0.05
1.0Fe	0	0	-	-	0.00

H_2O_2 direct synthesis reaction conditions: Catalyst (0.01 g), H_2O (2.9 g), MeOH (5.6 g), 5% H_2/CO_2 (420 psi, 2.76 mmol), 25% O_2/CO_2 (160 psi, 5.24 mmol), 0.5 hr, 20 °C, 1200 rpm.

When the FePd catalyst series was tested for the direct synthesis of H_2O_2, as shown in Figure 3.14 and Table 3.9, increasing the concentration of Fe relative to Pd caused a small decrease to both the productivity and hydrogen conversion of a given catalyst. For example, the

0.5%Fe-0.5%Pd catalyst offered a productivity of 29 mol_{H2O2} kg_{cat}^{-1} hr^{-1} and an H_2 conversion of 19 %, whereas the 0.75Fe-0.25Pd catalyst offered a productivity of 25 mol_{H2O2} kg_{cat}^{-1} hr^{-1} and an H_2 conversion of 14 %.

Conversely, when the proportion of Pd exceeded that of Fe, a limited increase in activity for H_2O_2 synthesis was observed, with increased Pd content correlating with enhanced H_2O_2 productivity and H_2 conversion, when compared to the 0.5%Fe-0.5%Pd catalyst. For example, the 0.25Fe-0.75Pd catalyst offered a productivity of 36 mol_{H2O2} kg_{cat}^{-1} hr^{-1} and an H_2 conversion of 29 %.

The FePd/Al_2O_3 catalyst series was then investigated in the selective oxidation of benzyl alcohol via in-situ H_2O_2 synthesis, which is shown in Figure 3.15 and Table 3.10.

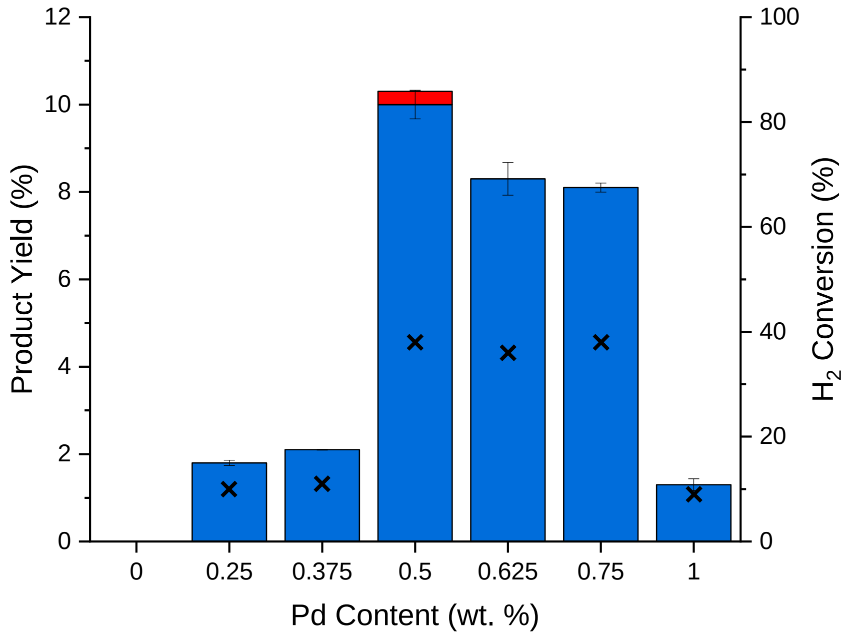

Figure 3.15. The effects of Fe/Pd ratio of supported FePd/Al_2O_3 on the in-situ oxidation of benzyl alcohol. Total metal loading fixed at 1 wt.%. **Key;** Benzaldehyde yield (*blue bars*), benzoic acid yield (*red bars*), H_2 conversion (*crosses*).

Benzyl alcohol oxidation reaction conditions: Catalyst (0.01 g), MeOH (7.13 g), benzyl alcohol (1.04 g, 9.62 mmol), mesitylene (0.42 g), 5% H_2/CO_2 (420 psi, 2.76 mmol), 25% O_2/CO_2 (160 psi, 5.24 mmol), 0.5 hr, 50 ^{O}C, 1200 rpm.

Table 3.10. The effects of Fe/Pd ratio of supported $FePd/Al_2O_3$ on the in-situ oxidation of benzyl alcohol. Total metal loading fixed at 1 wt.%.

Catalyst	Benzyl Alcohol Conversion (%)	Benzaldehyde Yield (%)	Benzoic Acid Yield (%)	Benzaldehyde Selectivity (%)	Turnover Number (mol_{BA} mol_{metal}^{-1} hr^{-1})	H_2 Conversion (%)	H_2 Selectivity (%)	Residual H2O2 (mmol)
1.0Fe	0	0	0.0	0	0	0	-	0.000
0.75Fe-0.25Pd	1.8	1.8	0.0	100	219	10	63	0.059
0.625Fe-0.375Pd	2.0	2.0	0.0	100	261	11	63	0.048
0.5Fe-0.5Pd	10.3	10	0.3	97	1406	38	92	0.075
0.375Fe-0.625Pd	8.3	8.3	0.0	100	1476	36	80	0.071
0.25Fe-0.75Pd	8.1	8.1	0.0	100	1350	38	74	0.074
1.0Pd	1.3	1.3	0.0	100	266	9	50	0.058

Benzyl alcohol oxidation reaction conditions: Catalyst (0.01 g), MeOH (7.13 g), benzyl alcohol (1.04 g, 9.62 mmol), mesitylene (0.42 g), 5% H_2/CO_2 (420 psi, 2.76 mmol), 25% O_2/CO_2 (160 psi, 5.24 mmol), 0.5 hr, 50 ^{O}C, 1200 rpm.

The 0.5%Fe-0.5%Pd/Al_2O_3 catalyst offered the highest conversion of benzyl alcohol of the series, at 10.3 %, with 97 % selectivity to benzaldehyde, with 3 % selectivity to benzoic acid. Unlike the AuPd analogue, altering the Pd: Fe ratio from 1: 1 (wt/wt) resulted in a decrease in the yield of benzaldehyde. Indeed, increasing the concentration of Pd in the catalyst caused a gradual decrease in product yield, but increasing the relative concentration of Fe greatly inhibited both the conversion of H_2 and the yield of benzaldehyde. For example, the 0.25%Fe-0.75%Pd/Al_2O_3 catalyst offered a benzyl alcohol conversion of 8.1 % and an H_2 conversion of 38 %, whereas the 0.75%Fe-0.25%Pd/Al_2O_3 catalyst offered a benzyl alcohol conversion of only 1.8 % and an H_2 conversion of 10 %. Again, the 1%Pd/Al_2O_3 catalyst showed only limited activity, with a benzyl alcohol conversion of 1.3 %, whilst the 1%Fe/Al_2O_3 catalyst converted no benzyl alcohol, due to its inability to undertake the direct synthesis of H_2O_2.

As discussed above, it has previously been reported that the enhancement in activity for FePd catalysts in the oxidation of benzyl alcohol, relative to the monometallic Pd analogue is a result of the occurrence of Fentons processes.[218] In essence, H_2O_2 generated by Pd centres, directly from H_2 and O_2, undergoes disproportionation via Fentons pathways at Fe sites, generating radical oxygen species, such as hydroxyl and hydroperoxyl radicals.[218] This additional pathway for the generation of radical oxygen species was cited as the primary reason for enhanced activity of FePd relative to a Pd monometallic catalyst,[218] and may be the reason for the enhanced levels of benzyl alcohol conversion observed in this work.

3.7 Extended Reaction Times of 0.5%X-0.5%Pd/Al_2O_2 Versus 1%Pd/Al_2O_3 Catalysts in the Selective Oxidation of Benzyl Alcohol via in-situ H_2O_2 Synthesis

Large differences were observed between the extent of H_2 conversion between the 0.5%Fe-0.5%Pd/Al_2O_3 (38 %), 0.5%Au-0.5%Pd/Al_2O_3 (50 %) and 1.0%Pd/Al_2O_3 (9 %) catalysts after a

30-minute reaction time. In order to compare the catalytic activity of each catalyst at extended reaction times, given the differing rates of H_2 conversion for each catalyst, and to begin to investigate whether any deactivation of a given catalyst is occurring, increased reaction times of up to 90 minutes were investigated for the selective oxidation of benzyl alcohol via in-situ H_2O_2 synthesis. This is shown in Figure 3.16 and Tables A3.3 – A3.5.

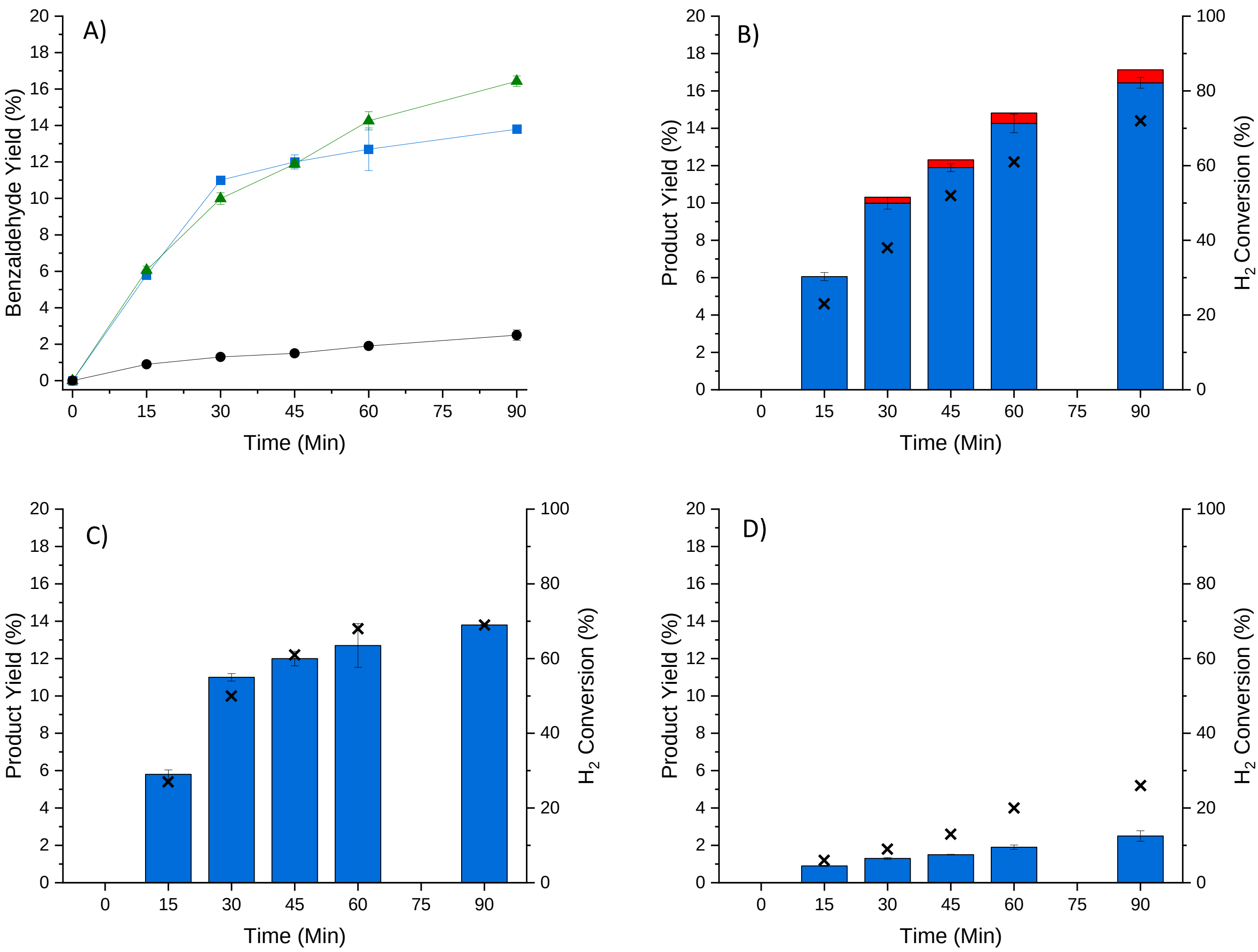

Figure 3.16. The in-situ oxidation of benzyl alcohol as a function of time using; A) 0.5%Fe-0.5%Pd/Al_2O_3, 0.5%Au-0.5%Pd/Al_2O_3 and 1%Pd/Al_2O_3. B) 0.5%Fe-0.5%Pd/Al_2O_3, C) 0.5%Au-0.5%Pd/Al_2O_3 and D) 1%Pd/Al_2O_3.
Key; A) 0.5%Fe-0.5%Pd/Al_2O_3 (green *triangles*), 0.5%Au-0.5%Pd/Al_2O_3 (blue *squares*) and 1%Pd/Al_2O_3 (*black circles*), B-D) benzaldehyde yield (*blue bars*), benzoic acid yield (*red bars*), H_2 conversion (*crosses*).
Benzyl alcohol oxidation reaction conditions: Catalyst (0.01 g), MeOH (7.13 g), benzyl alcohol (1.04 g, 9.62 mmol), mesitylene (0.42 g), 5% H_2/CO_2 (420 psi, 2.76 mmol), 25% O_2/CO_2 (160 psi, 5.24 mmol), 0.5 hr, 50 ^{o}C, 1200 rpm.

Firstly, the 0.5%Fe-0.5%Pd/Al_2O_3 catalyst was investigated, with its activity measured at time points between 15 and 90 minutes. In this reaction, the only products observed were benzaldehyde and benzoic acid, with a 96.1 % selectivity to benzaldehyde after 90 minutes. Conversion of benzyl alcohol and H_2 occurred continuously over the entire time period investigated, though the rate of product formation slowed significantly beyond 30 minutes. This could be a result of either diminishing H_2 availability or deactivation of the catalyst itself. Under the reaction conditions used in this study, H_2 and O_2 were present at an initial ratio of 1:1.9, wherein 2.76 mmol of H_2 was initially available in the reaction mixture, compared to 5.24 mmol of O_2. Therefore, H_2 was the limiting reagent with respect to O_2.

As such, the decrease in the rate of benzaldehyde formation over the course of the reaction, may be the result of diminishing availability of H_2. Indeed, the overall product yields of oxidation reactions via in-situ H_2O_2 synthesis have been shown to be highly dependent on the relative pressures of H_2 and O_2, with conversion greatly inhibited at lower concentrations of H_2 relative to O_2.[214] Indeed, for the AuPd/Al_2O_3 and FePd/Al_2O_3 catalysts, H_2 conversion appeared to increase linearly up to 50 %, after which further conversion of H_2 plateaued significantly, suggesting that the diminishing availability of H_2 may have been a factor in the decreasing rate of benzyl alcohol conversion at later points of the extended reaction time.

The concentration of residual H_2O_2 remained almost constant throughout the entire reaction, with 0.051 mmol present after 15 minutes, and a slight decrease observed from 0.075 mmol at 30 minutes to 0.068 mmol present at 90 minutes.

In this work, it is possible that the elevated temperatures utilised increased the rates of reaction and caused an equilibrium between the H_2O_2 synthesis and degradation pathways to be reached significantly faster, and thus, maintained a constant concentration of H_2O_2 in solution. A similar observation was made by Crombie *et al.* using a 0.5%Fe-0.5%Pd/TiO_2 catalyst, where at extended reaction times under identical conditions to this work, the concentration of H_2O_2 in solution remained approximately constant for the duration of the reaction.[218]

The same analysis was performed on 0.5%Au-0.5%Pd/Al_2O_3, which also showed continual oxidation of benzyl alcohol over a 90-minute period, although a significant plateauing of catalytic activity occurred after 30 minutes, to an even greater extent than when FePd/Al_2O_3 was used. This plateau in activity for AuPd supported catalysts has previously been observed in the literature when a TiO_2 support was used, for both 5% and 1% AuPd catalysts.[27, 218] Here, the more severe initial loss in activity may be a result of the high levels of H_2 conversion exhibited by the AuPd catalyst over the initial 30 minutes of the reaction, by which time 50 % of H_2 had already been consumed, compared to the 38 % consumed when FePd was used. Interestingly, despite the greater initial conversion of H_2 by AuPd, both catalysts consumed approximately 70 % of the available H_2 after 90 minutes.

Key differences are apparent between the FePd/Al_2O_3 and the AuPd/Al_2O_3 catalysts when compared at iso-conversion of H_2. For example, when 70 % of H_2 was converted, the AuPd/Al_2O_3 catalyst offered a yield of benzaldehyde of 13.8 %, at 100 % product selectivity, and an H_2 selectivity of 69 %. Conversely, FePd/Al_2O_3 offered a yield of benzaldehyde of 16.4 %, at 96.1 % selectivity, with an H_2 selectivity of 83 %. Therefore, at iso-conversion of H_2,

$FePd/Al_2O_3$ produced greater quantities of benzaldehyde, at a higher H_2 selectivity. This finding agrees with the work of Crombie *et al.* who found that 0.5%Fe-0.5%Pd/TiO_2 also offered a greater level of benzaldehyde yield and H_2 selectivity compared to an equivalent 0.5%Au-0.5%Pd/TiO_2.[218]

Unlike the $FePd/Al_2O_3$ catalyst, the $AuPd/Al_2O_3$ catalyst facilitated an initial generation of a relatively high concentration of H_2O_2 in solution, at 0.161 mmol after 30 minutes. This was accompanied by a general subsequent decrease in H_2O_2 and by the end of the reaction, the concentration of H_2O_2 had decreased to a minimum level of 0.086 mmol. Similar observations were also reported by Crombie *et al.* using an analogous 0.5%Au-0.5%Pd/TiO_2 catalyst.[218] This earlier work correlated the loss of H_2O_2 with a possible deactivation of the catalyst.[218] It should be noted that the authors also observed changes in the oxidation state of catalytic Pd as a result of in-situ reduction over the course of the reaction, leading to increased prevalence of Pd^0 sites which, as discussed previously, have been reported to be highly active in the degradation of H_2O_2.[218] Therefore, a change in catalytic selectivity from H_2O_2 synthesis to H_2O_2 degradation may be occurring as a result of these in-situ changes to the Pd oxidation state.
To investigate this further, XPS analysis of the 3d region for Pd in the 0.5%Au-0.5%Pd/Al_2O_3 catalyst as a function of time was conducted. This is shown in Figure A3.4.
Before use, 0.5%Au-0.5%Pd/Al_2O_3 had approximately equivalent levels Pd^0 and Pd^{2+} present at the surface of the catalyst, but reduction of Pd^{2+} to Pd^0 occurred rapidly over the course of the reaction. Indeed, a shift in binding energy from 336.6 to 335.0 eV occurred for the 3d5/2 transition for Pd after only a 15-minute reaction time, which qualitatively indicates a change in oxidation state towards Pd^0 and a corresponding decrease in the concentration of Pd^{2+} present on the surface of the catalyst.
A similar analysis was conducted on the 0.5%Fe-0.5%Pd/Al_2O_3 and 1%Pd/Al_2O_3 catalysts and is shown in Figure 3.17. For this analysis, the binding energy associated with the Pd 3d5/2 region was compared using a fresh catalyst and a catalyst that had been used for 30 minutes in the selective oxidation of benzyl alcohol via in-situ H_2O_2 synthesis.
Indeed, as was observed using the 0.5%Au-0.5%Pd/Al_2O_3 catalyst, the in-situ reduction of Pd occurred for both catalysts. For example, a shift in binding energy from 336.5 to 335.5 eV and from 336.9 to 336.5 eV occurred for the 1%Pd and 0.5%Fe-0.5%Pd/Al_2O_3 catalysts respectively, confirming a qualitative reduction of Pd^{2+} to Pd^0. As suggested by Crombie *et al.* this in-situ reduction of Pd may represent one contributing factor to an overall possible loss in catalytic activity.

Additionally, as shown in Figure A3.5, whilst surface chloride was present on the unused catalyst, a total loss of surface chloride was observed as the reaction proceeded. Indeed, most or all the intensity of the signal associated with the Cl had diminished within the first 15 minutes of the reaction, suggesting that the loss of surface chloride was very fast under the reaction conditions used. Whilst there has been no study on the effects of surface or solvated chloride on the selective oxidation of benzyl alcohol via in-situ H_2O_2 synthesis, strong promotional effects have been associated with their use in the direct synthesis of H_2O_2, for both surface chloride and solvated ions.[92, 232, 251]

For example, Brehm *et al.* investigated the effects of the loss of surface chloride towards the direct synthesis of H_2O_2 using a 0.5%Au-0.5%Pd/TiO_2 catalyst and demonstrated that upon re-use, the H_2O_2 productivity of the catalyst decreased from 96 to 38 mol_{H2O2} kg^{-1}_{cat} hr^{-1}.[232] This decrease in catalytic activity was correlated with a loss of surface chloride from the catalyst.[232] Therefore, it is possible that the loss of chloride from the surface of the catalyst may have contributed to the overall deactivation of the catalyst towards the oxidation of benzyl alcohol.

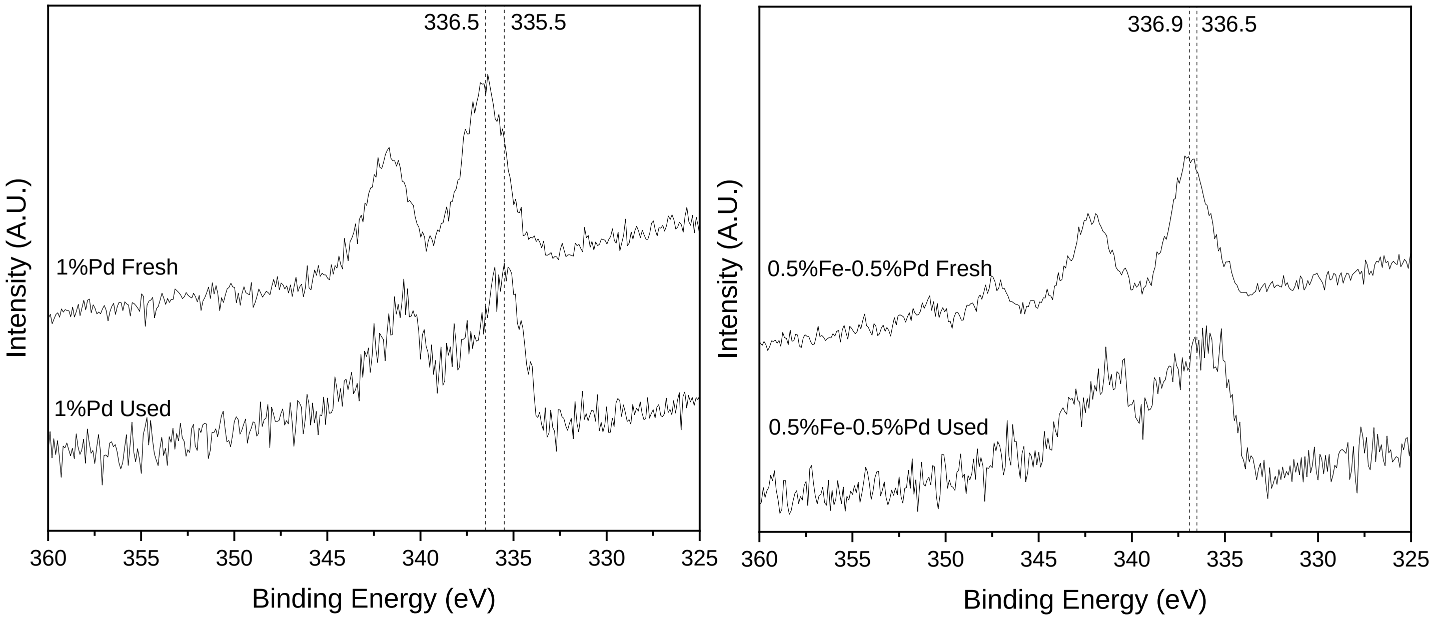

Figure 3.17. XPS spectra of the Pd3d regions of fresh and used 1%Pd/Al_2O_3 and 0.5%Fe-0.5%Pd/Al_2O_3 catalysts.

Benzyl alcohol oxidation reaction Conditions: Catalyst (0.01 g), MeOH (7.13 g), benzyl alcohol (1.04 g, 9.62 mmol), mesitylene (0.42 g), 5% H_2/CO_2 (420 psi, 2.76 mmol), 25% O_2/CO_2 (160 psi, 5.24 mmol), 0.5 hr, 50 ^{O}C, 1200 rpm.

Finally, the 1% Pd/Al_2O_3 catalyst was examined over a 90 minute reaction. This monometallic catalyst also had 100 % selectivity to benzaldehyde, but only 2.5 % conversion to benzaldehyde after 90 minutes. This again demonstrates the strong synergistic effect exhibited by both AuPd and FePd catalysts. Indeed, incorporating either Fe or Au into the supported Pd nanoparticles increased the rate of H_2 conversion significantly, above that which was obtained with Pd alone. For example, either FePd or AuPd catalysts facilitated H_2 conversions of approximately 70 % after 90 minutes, compared to an H_2 conversion of 34 % for Pd.

3.8 Sequential Reactions of 0.5%X-0.5%Pd/Al_2O_2 Versus 1%Pd/Al_2O_3 Catalysts in the Selective Oxidation of Benzyl Alcohol Via in-situ H_2O_2 Synthesis

From the investigation into extended reaction times (Figure 3.18), it may be suggested that the plateau in activity at longer reaction times exhibited by the 0.5%Au-0.5%Pd/Al_2O_3 and 0.5%Fe-0.5%Pd/Al_2O_3 catalysts could be a result of either the diminishing pressure of H_2, which was the limiting reagent, or the result of catalyst deactivation. To investigate this further, a series of sequential reactions were conducted, wherein the same reaction mixture and catalyst were used in sequential 30-minute reactions, but reactant gasses were replaced every 30 minutes, restoring the initial pressures of H_2 and O_2. This is shown in Figure 3.18 and Table A3.6 – A3.8.

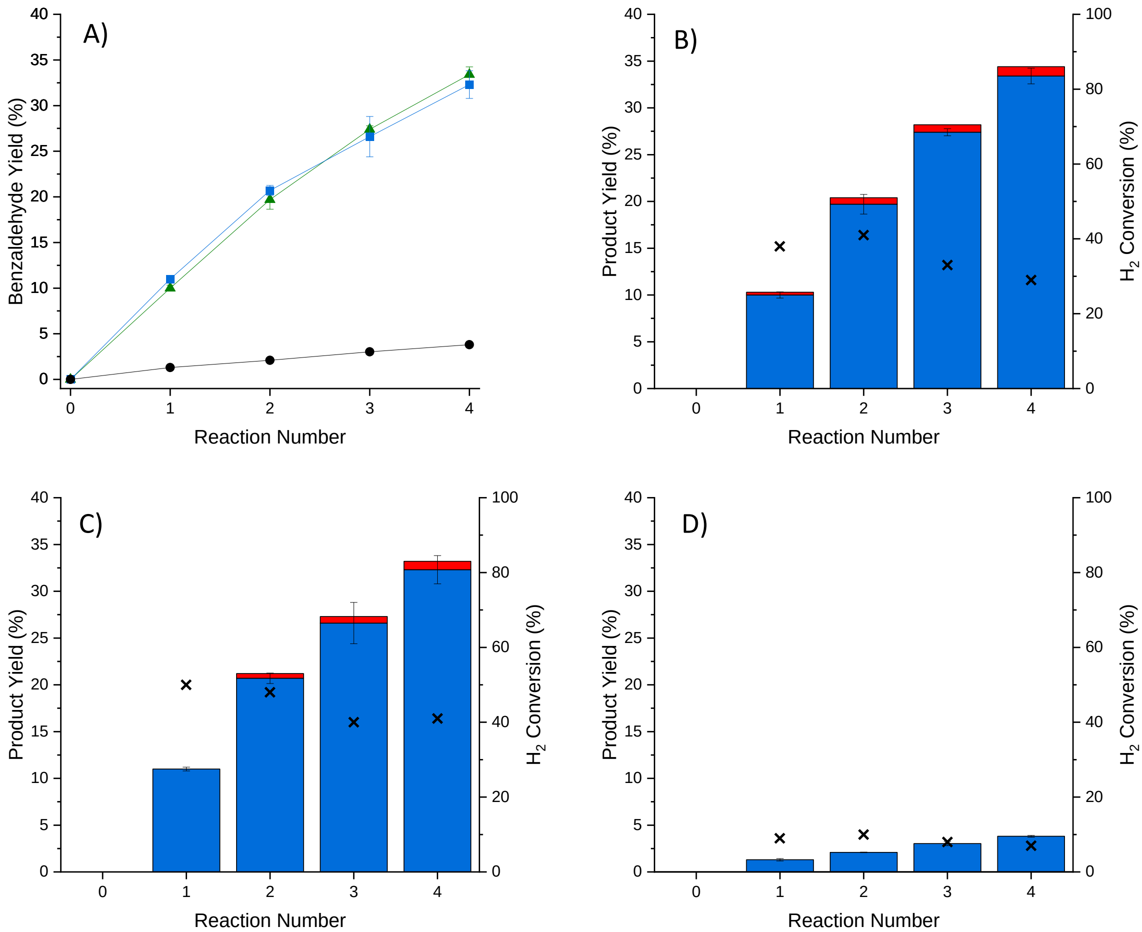

Figure 3.18. The effects of sequential reactions in the selective oxidation of benzyl alcohol via in-situ H_2O_2 synthesis, using; A) 0.5%Fe-0.5%Pd/Al_2O_3, 0.5%Au-0.5%Pd/Al_2O_3 and 1%Pd/Al_2O_3. B) 0.5%Fe-0.5%Pd/Al_2O_3, C) 0.5%Au-0.5%Pd/Al_2O_3 and D) 1%Pd/Al_2O_3.

Key; A) 0.5%Fe-0.5%Pd/Al_2O_3 (green *triangles*), 0.5%Au-0.5%Pd/Al_2O_3 (blue *squares*) and 1%Pd/Al_2O_3 (*black circles*), B-D) Benzaldehyde yield (*blue bars*), benzoic acid yield (*red bars*), H_2 conversion (*crosses*).

Benzyl alcohol oxidation reaction conditions: Catalyst (0.01 g), MeOH (7.13 g), benzyl alcohol (1.04 g, 9.62 mmol), mesitylene (0.42 g), 5% H_2/CO_2 (420 psi, 2.76 mmol), 25% O_2/CO_2 (160 psi, 5.24 mmol), 0.5 hr, 50 ^{O}C, 1200 rpm.

Firstly, the 0.5%Fe-0.5%Pd/Al_2O_3 catalyst was investigated in this manner. Over the course of all sequential reactions, a selectivity towards benzaldehyde of approximately 97 % was maintained, with benzoic acid constituting the only other observable product.
When compared to the extended reaction times experiment for the same catalyst (Figure 3.16), yields of benzaldehyde were significantly enhanced when reactant gases were replaced, at identical reaction times. For example, after a 60-minute reaction when reactant gases weren't replaced, the yield of benzaldehyde offered by the 0.5%Fe-0.5%Pd/Al_2O_3 catalyst was 14.3 %, compared to 19.7 % when the gases were replaced. This strongly suggests that consumption of H_2 gas played a significant role in the decreased rate of reaction and was not exclusively due to catalyst deactivation.
However, it should be noted that the catalysts' ability to convert H_2 decreased over the sequential reactions, from 38 % in the first reaction to 29 % in the fourth. Moreover, the additional yield of benzaldehyde with each successive reaction also gradually decreased over the four reactions, from a 10.0 % yield of benzaldehyde from the first reaction to an additional 6.0 % yield of benzaldehyde generated after the fourth reaction.
The decrease in H_2 conversion suggests that some level of catalyst deactivation occurred over the course of the reactions, and this may be a key reason for the progressively decreasing benzaldehyde yield per reaction.
The reactor was purged three times with 100 psi of 5% H_2/N_2 between each sequential reaction before gasses were replaced, so residual gasses from the previous reaction are not likely to significantly influence the subsequent reaction.

The same analysis was performed for the 0.5%Au-0.5%Pd/Al_2O_3 catalyst. Similarly, to the FePd catalyst, benzaldehyde yields were again significantly enhanced when reactant gases were recharged to their initial pressures every 30 minutes. For example, after 60 minutes with no recharging of gases, the 0.5%Au-0.5%Pd/Al_2O_3 catalyst offered a benzaldehyde yield of 12.7 %, compared to a 20.7 % yield when the gases were recharged. However, a similar reduction in H_2 conversion was again observed across sequential reactions, decreasing from 50 % conversion in reaction one to 41 % conversion in reaction four.
In addition to this, the reduction in additional benzaldehyde yield from each successive reaction, from 11.0 % after reaction one to 5.7 % after reaction four also suggests that deactivation of the catalyst may be occurring. This reduction in activity is not likely a result of diminishing availability of benzyl alcohol, which remains in vast excess. For example, after reaction number 3 using the 0.5%Au-0.5%Pd/Al_2O_3 catalyst, a total benzyl alcohol conversion of 27.3 % had taken place, with 72.7 % (6.98 mmol) of the initial benzyl alcohol still present compared to the initial 2.76 mmol of H_2 present at the start of each reaction. Future work could investigate this further by utilising a flow reactor setup, wherein the concentration of benzyl alcohol and H_2 are maintained at a constant level. This would allow this disambiguation of the effects of both catalyst deactivation and substrate consumption towards the loss of 'additional benzaldehyde yield' over successive reactions observed in this work.

A selectivity to benzaldehyde of 100 % was observed for reaction one, but the formation of benzoic acid was observed from reaction two onwards, resulting in a similar overall benzaldehyde selectivity to the 0.5%Fe-0.5%Pd/Al_2O_3 catalyst, of 97.3 %. This finding was unexpected because it represents the first observation of the formation of benzoic acid by an

$AuPd/Al_2O_3$ catalyst in this work. As previously discussed, Sankar *et al*. demonstrated the ability of benzyl alcohol to prevent overoxidation of benzaldehyde to benzoic acid by acting as a radical scavenger to quench radical intermediate species.[100] Additionally, the authors observed that concentrations of benzyl alcohol as low as 2 wt.% were sufficient to prevent the overoxidation of benzaldehyde to benzoic acid.[100] However, it should be noted that their study was conducted under aerobic conditions at 120 ^oC, in the absence of a catalyst. Indeed, where H_2 and O_2 are used in tandem and in the presence of a catalyst, small quantities of secondary products such as benzoic acid and toluene are often reported, even when benzyl alcohol conversion is low.[27, 114, 130, 131] Examples of this are shown in Table A3.1.
It is clear that the catalyst itself plays a highly significant role in determining product selectivity, and that competitive scavenging of intermediate radicals by benzyl alcohol is in many cases insufficient to prevent overoxidation to benzoic acid, in the presence of a catalyst. For example, Lyu e*t al.* compared a Pd@HTS-1-OR catalyst, which offered a benzyl alcohol conversion of 46.4 % at 100 % selectivity to benzaldehyde, to a commercial Pd/C which offered a conversion of only 6.9 % at a selectivity of 90.4 %.[131]
In the present work, given that formation of benzoic acid occurs only from reaction number 2 onwards, it may ultimately be a consequence of the quantity of benzyl alcohol converted and the increasing statistical likelihood of a reaction involving benzaldehyde to take place as its concentration increases. Alternatively, in-situ structural changes to the catalyst, such as metal reduction or oxidation, nanoparticle agglomeration and metal leaching could be a contributing factor, although these processes would have occurred in the extended reaction time reactions and if true, may have led to the formation of benzoic acid under those reaction conditions, which was not observed.

Finally, the 1%Pd/Al_2O_3 catalyst was compared to the more active bimetallic analogues. For this catalyst, both H_2 conversions and benzaldehyde yields were significantly lower than those observed for either AuPd or FePd catalysts across all sequential reaction numbers. For example, after reaction one, the 1%Pd/Al_2O_3 catalyst offered a benzaldehyde yield of 1.3 %, and an H_2 conversion of 9 %. After reaction four, the total yield of benzaldehyde offered was 3.8 %, with a further conversion of H_2 of 7 %, compared to the $AuPd/Al_2O_3$ and $FePd/Al_2O_3$ catalysts, which offered total benzaldehyde yields of 32.3 % and 33.4 % respectively after reaction four.
Similarly, to the bimetallic analogues, the 1%Pd/Al_2O_3 catalyst also appeared to return diminishing yields of additional benzaldehyde after reaction one, decreasing from 1.3 % in reaction one to 0.8 % in reaction four.

Overall, all three catalysts appeared to exhibit deactivation over sequential reactions. Indeed, catalysts prepared through the excess chloride co-impregnation methodology have previously been shown to undergo deactivation over sequential reactions in the in-situ oxidation of benzyl alcohol.[218] As discussed previously, the in-situ reduction of Pd^{2+} to Pd^0 was observed over a 30-minute reaction (Figures 3.17 and A3.4) for the three catalysts and may be a contributing factor to the loss of catalytic activity.[218] Other mechanism of catalyst deactivation, such as nanoparticle agglomeration, and metal leaching will be investigated in section 3.10.

3.9 'Hot Filtration' Reactions of 0.5%X-0.5%Pd Catalysts in the Selective Oxidation of Benzyl Alcohol via In-Situ H_2O_2 Synthesis

It has been previously reported that metal leachate can exhibit homogeneous activity, both in the direct synthesis of H_2O_2 [252] and in analogous in-situ oxidation reactions, such as in the oxidation of phenol, or of benzyl alcohol.[218, 253]

Therefore, an investigation into the activity of homogeneous metal leachate was conducted for 0.5%Au-0.5%Pd/Al_2O_3, 0.5%Fe-0.5%Pd/Al_2O_3 and 1.0%Pd/Al_2O_3 catalysts, in which the heterogeneous catalyst was reacted for 30 minutes under standard testing conditions for benzyl alcohol oxidation, before being removed by filtration. The reaction mixture was then returned to the autoclave, reactant gases refreshed to their initial pressures and the reaction resumed for 30 minutes. Consequently, the only catalytic metal present would be from metal leachate. The results of this are shown in Figure 3.19 and Table 3.11.

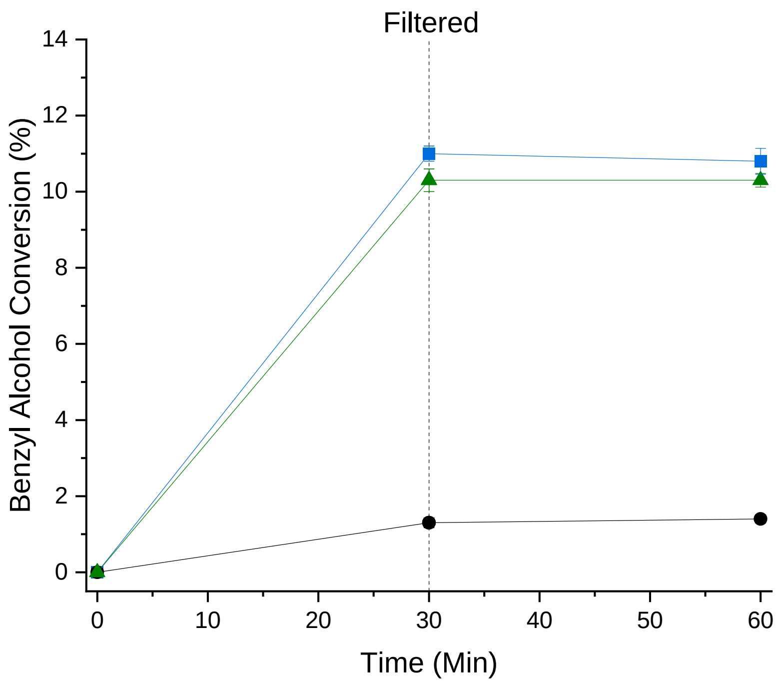

Figure 3.19. Hot filtration reactions of Al_2O_3 supported Pd based catalysts in the selective oxidation of benzyl alcohol via In-Situ H_2O_2 synthesis. **Key;** 1%Pd/Al_2O_3 (*circles*), 0.5%Fe-0.5%Pd/Al_2O_3 (*triangles*), 0.5%Au-0.5%Pd/Al_2O_3 (*squares*).

Benzyl alcohol oxidation reaction conditions: Catalyst (0.01 g), MeOH (7.13 g), benzyl alcohol (1.04 g, 9.62 mmol), mesitylene (0.42 g), 5% H_2/CO_2 (420 psi, 2.76 mmol), 25% O_2/CO_2 (160 psi, 5.24 mmol), 0.5 hr, 50 ^{O}C, 1200 rpm.

Table 3.11. Hot filtration reactions of Al_2O_3 supported Pd based catalysts in the selective oxidation of benzyl alcohol via In-Situ H_2O_2 synthesis.

Catalyst	Benzyl Alcohol Conversion (%)	Benzaldehyde Yield (%)	Benzoic Acid Yield (%)	Turnover Number (mol_{BA} mol_{metal}^{-1} hr^{-1})	H_2 Conversion (%)	H_2 Selectivity (%)	Residual H_2O_2 (mmol
Pd/Al_2O_3	1.3	1.3	0.0	266	9	50	0.057
Pd/Al_2O_3 Filtrate	1.4	1.4	0.0	-	-	-	0.054
$AuPd/Al_2O_3$	11.0	11.0	0.0	2919	50	77	0.161
$AuPd/Al_2O_3$ Filtrate	10.8	10.8	0.0	-	-	-	0.122
$FePd/Al_2O_3$	10.3	10.0	0.3	1406	38	95	0.075
$FePd/Al_2O_3$ Filtrate	10.3	10.0	0.3	-	-	-	0.058

Benzyl alcohol oxidation reaction conditions: Catalyst (0.01 g), MeOH (7.13 g), benzyl alcohol (1.04 g, 9.62 mmol), mesitylene (0.42 g), 5% H_2/CO_2 (420 psi, 2.76 mmol), 25% O_2/CO_2 (160 psi, 5.24 mmol), 0.5 hr, 50 ^{O}C, 1200 rpm.

For all catalysts, the associated filtrate reaction had no additional observable yield of benzaldehyde outside of the range of experimental error. Additionally, the H_2 conversions offered by the AuPd, FePd and Pd catalysts were approximately zero. Therefore, it is likely that the metal leachate generated over the course of a 30-minute reaction is not contributing to overall catalytic activity in the oxidation of benzyl alcohol, and that all catalytic action originates from the heterogeneous material. The quantity of leached metal observable in the reaction mixture after a 30-minute reaction is discussed in Section 3.10.

3.10 Evaluation of Re-Usability of 0.5%X-0.5%Pd and 1.0%Pd/Al_2O_3 Catalysts in the Selective Oxidation of Benzyl Alcohol via in-situ H_2O_2 Synthesis

Due to observed deactivation of catalysts in the sequential reactions section, additional re-use experiments were conducted in order to investigate this further. For these experiments, a given catalyst that had been used in the benzyl alcohol oxidation reaction was collected by filtration and washed with methanol. It was then dried under vacuum at room temperature before being used again in a subsequent benzyl alcohol oxidation reaction. This was done to prevent any change in Pd oxidation states that may occur under an aerobic environment, in addition to limiting nanoparticle agglomeration processes associated with higher temperatures. The results of this are shown in Figure 3.20 and Table 3.12.

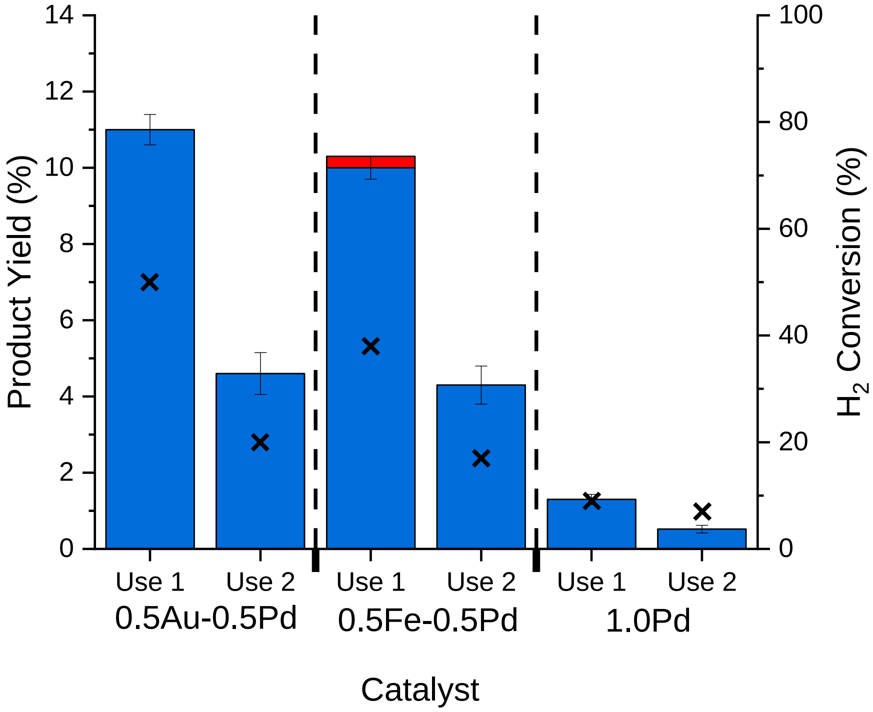

Figure 3.20. Effects of re-using 0.5%X-0.5%Pd/Al_2O_3 and 1%Pd/Al_2O_3 catalysts in the selective oxidation of benzyl alcohol via In-Situ H_2O_2 synthesis.

Key; benzaldehyde yield (*blue bars*), H_2 conversion (*crosses*).

Benzyl alcohol oxidation reaction conditions: Catalyst (0.01 g), MeOH (7.13 g), benzyl alcohol (1.04 g, 9.62 mmol), mesitylene (0.42 g), 5% H_2/CO_2 (420 psi, 2.76 mmol), 25% O_2/CO_2 (160 psi, 5.24 mmol), 0.5 hr, 50 ^{O}C, 1200 rpm.

Table 3.12. Effects of re-using 0.5%X-0.5%Pd/Al_2O_3 and 1%Pd/Al_2O_3 catalysts in the selective oxidation of benzyl alcohol via In-Situ H_2O_2 synthesis.

Catalyst	Reaction Number	Benzaldehyde Yield (%)	Benzoic Acid Yield (%)	Turnover Number (mol_{BA} mol_{metal}^{-1} hr^{-1})	H_2 Conversion (%)	H_2 Selectivity (%)	Residual H_2O_2 (mmol)
AuPd	Use 1	11.0	0.0	2919	50	77	0.161
AuPd	Use 2	4.6	0.0	1220	20	80	0.091
FePd	Use 1	10.0	0.3	1406	38	95	0.075
FePd	Use 2	4.3	0.0	604	17	87	0.046
Pd	Use 1	1.3	0.0	266	9	50	0.057
Pd	Use 2	0.5	0.0	117	7	27	0.039

Benzyl alcohol oxidation reaction conditions: Catalyst (0.01 g), MeOH (7.13 g), benzyl alcohol (1.04 g, 9.62 mmol), mesitylene (0.42 g), 5% H_2/CO_2 (420 psi, 2.76 mmol), 25% O_2/CO_2 (160 psi, 5.24 mmol), 0.5 hr, 50 ^{O}C, 1200 rpm.

When used in this way, the 0.5%Au-0.5%Pd/Al_2O_3 catalyst underwent a significant level of deactivation after its first use, with benzaldehyde yield decreasing from 11.0 % to 4.6 % and H_2 conversion decreasing from 50 % to 20 %.
This loss in activity is significantly greater than the deactivation observed in the equivalent 'sequential reaction' using the AuPd catalyst, where the additional yield of benzaldehyde decreased to only 9.7 %, with an H_2 conversion of 48 %. (Figure 3.18)
Similar levels of deactivation also occurred with both the FePd and Pd catalysts. For example, the FePd catalyst offered a benzaldehyde yield of 10.0 % after use one, but only a benzaldehyde yield of 4.3 % after use two. Additionally, the H_2 conversion facilitated by this catalyst decreased from 38 % to 17 %.
Indeed, when prepared through the excess chloride co-impregnation methodology, analogous AuPd cataysts have been reported to undergo deactivation upon re-use.[79, 232] For example, as previously discussed, in the direct synthesis of H_2O_2, Brehm *et al.* demonstrated that upon re-use, 0.5%Au-0.5%Pd/TiO_2 experienced a decrease in H_2O_2 productivity from 96 to 38 $mol_{H2O2}\ kg^{-1}_{cat}\ hr^{-1}$. The authors attributed this decreased activity to a loss of chloride ions from the surface of the catalyst to the reaction mixture, as observed using XPS. Subsequent re-addition of chloride to the reaction mixture in the form of $CaCl_2$ and $MgCl_2$ salts greatly promoted H_2O_2 synthesis, further supporting the role of chloride in this class of catalysts in the direct synthesis of H_2O_2.[232]
It is possible that a loss of chloride contributed to the apparent loss of catalytic activity upon reuse of a catalyst. As shown in in Figure A3.5. a total loss of surface chloride from the AuPd/Al_2O_3 catalyst was observed after a 30-minute reaction. Additionally, the experimental procedure for the reuse reactions requires the replacement of the reaction mixture in which the chloride ions are solvated, with a fresh reaction mixture containing no additional chloride, removing them from the reaction mixture.
However, the role of chloride ions has not been explicitly determined in the oxidation of benzyl alcohol via in-situ H_2O_2 synthesis and given the differing reaction conditions between the direct synthesis of H_2O_2 and the oxidation of benzyl alcohol, other mechanisms of deactivation cannot be discarded without further investigation, such as nanoparticle agglomeration and metal leaching.
Therefore, to investigate the extent of metal dissolution that may be taking place over the course of a reaction using the Pd, AuPd and FePd catalysts, ICP-MS was conducted Simon Waller (Cardiff University Analytical Services), the results of which are shown in Table 3.13.

Table 3.13. Metal dissolution of the Pd, AuPd and FePd/Al_2O_3 catalysts over the course of 30 minutes in the selective oxidation of benzyl alcohol via in-situ H_2O_2 synthesis, using ICP-MS

Catalyst	Concentration of Pd in Reaction Solution (μg/L)	Total Loss of Pd (%)	Concentration of Au in Reaction Solution (μg/L)	Total loss of Au (%)	Concentration of Fe in Reaction Solution (μg/L)	Total Loss of Fe (%)
0.5%Au-0.5%Pd	3.56	0.071	1.08	0.022	-	-
0.5%Fe-0.5%Pd	2.16	0.043	-	-	5.06	0.101
1%Pd	2.00	0.02	-	-	-	-

Benzyl alcohol oxidation reaction conditions: Catalyst (0.01 g), MeOH (7.13 g), benzyl alcohol (1.04 g, 9.62 mmol), mesitylene (0.42 g), 5% H_2/CO_2 (420 psi, 2.76 mmol), 25% O_2/CO_2 (160 psi, 5.24 mmol), 0.5 hr, 50 ^{O}C, 1200 rpm.

The observed metal leaching was low across all catalysts, with Fe representing the greatest loss in catalytic metal from any catalyst, wherein 0.1 % of the total Fe content of the 0.5%Fe-0.5%Pd catalyst was detectable in the post-reaction mixture. When the 0.5%Au-0.5%Pd catalyst was used, Pd and Au leaching was again very low, with a loss of catalytic metal of 0.071 % for Pd and 0.022 % for Au respectively. For the 1%Pd catalyst, only 0.02 % of Pd was lost from the catalyst after one use. This observation suggests that a loss in catalytic metal was not responsible for the decrease in activity of a catalyst after re-use and rationalises the lack of a catalytic contribution from homogeneous Pd and Fe observed during the hot-filtration reactions (Section 3.9).

Following this, the extent of nanoparticle agglomeration that may have taken place over the course of the reaction was investigated using TEM, the results of which are shown in Table 3.14.

Table 3.14. Particle size observed via TEM, of the 0.5%Au-0.5%Pd/Al_2O_3 catalyst before and after use in the selective oxidation of benzyl alcohol via In-Situ H_2O_2 synthesis.

Catalyst	Use	Mean Nanoparticle Size (nm)	Standard Deviation (nm)
AuPd	Fresh	3.01	1.75
AuPd	Used	3.65	3.12

Benzyl alcohol oxidation reaction conditions: Catalyst (0.01 g), MeOH (7.13 g), benzyl alcohol (1.04 g, 9.62 mmol), mesitylene (0.42 g), 5% H_2/CO_2 (420 psi, 2.76 mmol), 25% O_2/CO_2 (160 psi, 5.24 mmol), 0.5 hr, 50 ^{O}C, 1200 rpm.

Whilst the particle size distributions were not determined for the 1%Pd and 0.5%Fe-0.5%Pd/Al_2O_3 catalysts, due to either large particle sizes in the many tens on nm, or due to insufficient observable nanoparticles, a limited increase in the average nanoparticle size was observed for the 0.5%Au-0.5%Pd/Al_2O_3 catalyst. For example, before use in the benzyl alcohol oxidation reaction, the mean size of nanoparticles in the 0.5%Au-0.5%Pd/Al_2O_3 catalyst was 3.01 nm, which increased to 3.65 nm after use. Additionally, the standard deviation in the size of nanoparticles increased from 1.75 to 3.12 nm. Therefore, both the mean size of nanoparticles and their size distribution increased as a result of their use in the benzyl alcohol oxidation reaction. Whilst there has been no investigation in the literature into the size dependency of Pd based nanoparticles on the oxidation of benzyl alcohol via in-situ H_2O_2 synthesis, such investigations have been undertaken for Pd catalysts used in both the direct synthesis of H_2O_2 and for the aerobic oxidation of benzyl alcohol, which represent the two most relevant analogous reactions.[53, 254, 255] In the case of the direct synthesis of H_2O_2, Tian *et al.* observed that a mean nanoparticle size of 1.5 nm for a series of Pd/hydroxyapatite supported catalysts offered the greatest selectivity towards H_2O_2 synthesis.[53] Similarly, Youngjin *et al.* observed that from a range of Pd/carbon supported catalysts, when Pd nanoparticles had a mean nanoparticle size of 3 nm, superior H_2O_2 selectivity could be achieved compared to catalysts with a greater mean nanoparticle size.[254] Zhang *et al.* investigated the size dependency of Pd nanoparticles in a series of Pd/Al_2O_3 supported catalysts for the aerobic oxidation of benzyl alcohol and determined that a mean nanoparticle size of 3.6-4.3 nm offered the greatest catalytic turnover.[255] Therefore, it may be possible that a size dependency may exist for the oxidation of benzyl alcohol via in-situ H_2O_2 synthesis exists. Moreover, the limited increase in mean nanoparticle size and large increase in the range of nanoparticle sizes associated with the catalysts use in the reaction may have a contributing effect on the observed loss in catalytic activity.

3.11 The Effects of Using 0.5%Au-0.5%Pd/Al_2O_3 with 1%Fe/Al_2O_3 Catalysts as a Physical Mixture in the Selective Oxidation of Benzyl Alcohol via in-situ H_2O_2 Synthesis

Previous literature has found that using Fe in place of Au in AuPd/TiO_2 based catalysts could deliver enhanced yields of benzaldehyde.[218] As previously discussed, to describe this effect the authors suggested that a tandem process could be occurring, in which Pd sites primarily synthesise H_2O_2 and Fe sites convert the H_2O_2 into oxygen based radicals via Fenton's chemistry that ultimately leads to benzyl alcohol oxidation.[218] Whilst no enhancement in yield was observed in this work from using FePd/Al_2O_3 versus AuPd/Al_2O_3 catalysts, the relatively high product yield and concentration of residual H_2O_2 associated with AuPd catalysts leads to the possibility of incorporating a Fenton's active component into this system.

One method of utilising Fe to enhance the activity of AuPd supported catalysts was to employ a physical mixture of the two, where the Fe catalyst could undertake Fenton's chemistry to utilise the residual H_2O_2 present in the reaction mixture. To do this, a 1%Fe/Al_2O_3 catalyst was used in conjunction with the AuPd/Al_2O_3 catalyst as a physical mixture. This 1%Fe/Al_2O_3 catalyst was prepared using a wet co-impregnation methodology, using $FeCl_3$ as a precursor, and was heat treated under flowing H_2 (500 ^oC, 4hr, 10 ^oC/min). A wet impregnation methodology was used for the preparation of this catalyst in order to not incorporate any additional chloride ions into the reaction mixture that might be present on the catalyst surface if it were prepared by an excess-chloride impregnation method.

The results of this are shown in Figure 3.21 and Table 3.15.

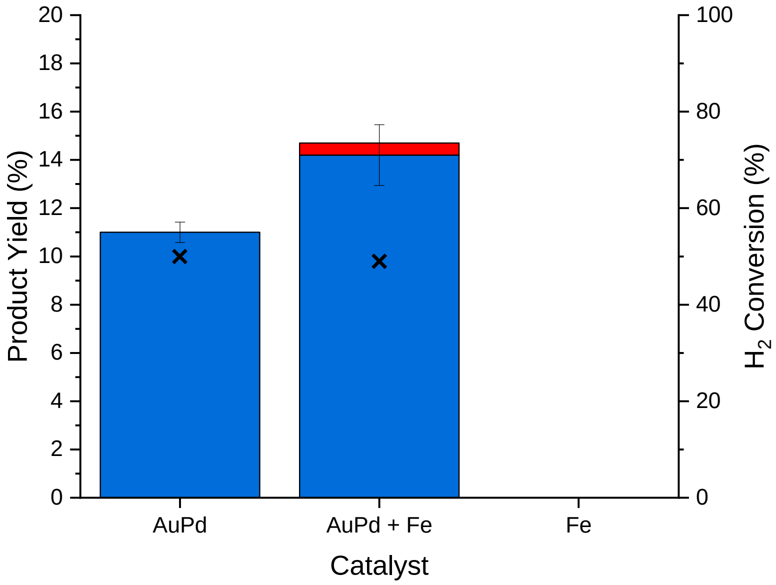

Figure 3.21. 0.5%Au-0.5%Pd/Al_2O_3 versus physical mixture of 1%Fe/Al_2O_3 + 0.5%Au-0.5%Pd/Al_2O_3 in the selective oxidation of benzyl alcohol via In-Situ H_2O_2 synthesis. **Key;** benzaldehyde yield (*blue bars*), benzoic acid yield (*red bars*), H_2 conversion (*crosses*).
Benzyl alcohol oxidation reaction conditions: Catalyst (0.01 g), MeOH (7.13 g), benzyl alcohol (1.04 g, 9.62 mmol), mesitylene (0.42 g), 5% H_2/CO_2 (420 psi, 2.76 mmol), 25% O_2/CO_2 (160 psi, 5.24 mmol), 0.5 hr, 50 ^{O}C, 1200 rpm.

Table 3.15. Effects of the addition of 1%Fe/Al_2O_3 as a physical mixture with 0.5%Au-0.5%Pd/Al_2O_3 in the selective oxidation of benzyl alcohol via in-situ H_2O_2 synthesis.

Catalyst	Benzaldehyde Yield (%)	Benzoic Acid Yield (%)	Benzaldehyde Selectivity (%)	Turnover Number (mol_{BA} mol_{metal}^{-1} hr^{-1})	H_2 Conversion (%)	H_2 Selectivity (%)	Residual H_2O_2 (mmol)
0.5%Au-0.5%Pd	11.0	0.0	100	2919	50	77	0.161
0.5%Au-0.5%Pd + 1.0%Fe	14.2	0.5	97	1084	49	99	0.136
1.0%Fe	0.0	0.0	-	0	0	-	0.000

Benzyl alcohol oxidation reaction conditions: Catalyst (0.01 g), MeOH (7.13 g), benzyl alcohol (1.04 g, 9.62 mmol), mesitylene (0.42 g), 5% H_2/CO_2 (420 psi, 2.76 mmol), 25% O_2/CO_2 (160 psi, 5.24 mmol), 0.5 hr, 50 ^{O}C, 1200 rpm.

When the 1%Fe/Al_2O_3 catalyst was used in conjunction with the 0.5%Au-0.5%Pd/Al_2O_3 catalyst, a clear enhancement in benzaldehyde yield was observed compared to using the

AuPd catalyst in isolation. Indeed, the yield of benzaldehyde was increased from 11.0 % to 14.2 % by the addition of this Fe/Al_2O_3 co-catalyst. A small quantity of benzaldehyde was over-oxidised to benzoic acid, which is consistent with the use of Fe in this reaction and may represent a generic feature of utilising Fenton type chemistry and its associated flux of oxygen-based radicals.

When Fe/Al_2O_3 was used in isolation, no yield of benzaldehyde was observed, and no residual H_2O_2 was detectable in the reaction mixture. This demonstrated that the Fe/Al_2O_3 catalyst was not taking part in the H_2O_2 synthesis reaction, and any enhancement associated with its use was related to H_2O_2 that had already been generated by the AuPd catalyst.

Additionally, when the 0.5%Au-0.5%Pd/Al_2O_3 and 1%Fe/Al_2O_3 catalysts were employed as a physical mixture, the concentration of residual H_2O_2 was reduced to 0.136 mmol, compared to when the AuPd was used alone, which resulted in 0.161 mmol of residual H_2O_2. Therefore, it is likely that the additional Fe based catalyst operates via Fenton's chemistry as an additional route to generate oxygen-based radicals, consuming H_2O_2 that was synthesised in-situ by the AuPd catalyst. These findings support the work of Crombie *et al.* who proposed that the enhancement associated with the use of an FePd/TiO_2 catalyst, compared to a Pd/TiO_2 analogue was due to Fentons reactions taking place at Fe sites.[218] Here, the physical separation between Fe sites and Pd sites demonstrates that the enhanced activity that arose from the FePd catalyst was not likely exclusively a result of electronic or geometric changes to Pd nanoparticles that arose upon the incorporation of Fe. However, electronic or geometric changes to Pd nanoparticles arising from Fe incorporation in Pd nanoparticles could also have been a contributing factor.

The majority of residual H_2O_2 remains is solution and was not utilised by either Fe or AuPd catalysts to generate radical oxygen species. Therefore, the potential remains to tune this secondary Fentons active catalyst to increase the consumption of H_2O_2 and increase the amount of benzyl alcohol converted, although an increase in oxidation by this pathway may result in a further loss of selectivity to benzaldehyde.

3.12 Effects of the Addition of Pt into a 0.5%Au-0.5%Pd/Al_2O_3 Catalyst in the Selective Oxidation of Benzyl Alcohol via in-situ H_2O_2 Synthesis

The incorporation of Pt into AuPd based catalysts has been shown to have promotional effects in the direct synthesis of H_2O_2. This has been shown to occur using a variety of supports, including TiO_2, CeO_2 and TS-1.[71, 226, 256] Significantly, these enhancements in activity often occur when the concentration of Pt is very low, relative to the overall metal loading. For example, Lewis e*t al.* reported a 2.4%Au-2.4%Pd-0.2%Pt/TS-1 supported catalyst that had a productivity value of 167 mol_{H2O2} $kg^{-1}{}_{cat}$ hr^{-1}, compared to a 2.5%Au-2.5%Pd/TS-1 catalyst which achieved an H_2O_2 productivity of 100.[256] Additionally, Gong *et al.* demonstrated a strong relationship between the metal loading of Pt in a PtAuPd/TiO_2 trimetallic catalyst and the associated enhancement in catalytic activity. The authors determined that Pt loadings of 1 mol% delivering the greatest levels of H_2O_2 productivity, and Pt loadings in excess of 10 mol% reduced H_2O_2 productivity relative to an AuPd bimetallic.[226]

In this work it was investigated whether this same promotional effect towards the direct synthesis of H_2O_2 could occur using an Al_2O_3 supported catalysts. Additionally, whilst no direct correlation between the concentration of H_2O_2 synthesised and the quantity of benzyl alcohol converted has been observed in this work, a key motivation of this investigation was to determine whether the incorporation of small quantities of Pt into an AuPd supported catalyst could promote the in-situ oxidation of benzyl alcohol. A series of 1%AuPdPt/Al_2O_3 catalysts were synthesised, with Pt loadings between 0.005 % and 0.04 %, whilst the Au:Pd ratio was fixed at 1:1 (wt/wt). These catalysts were examined for their activity towards both the synthesis and degradation of H_2O_2, and the selective oxidation of benzyl alcohol. The effects of Pt doping into a AuPd/Al_2O_3 catalyst on the direct synthesis of H_2O_2 is shown in Figure 3.22 and Table 3.16.

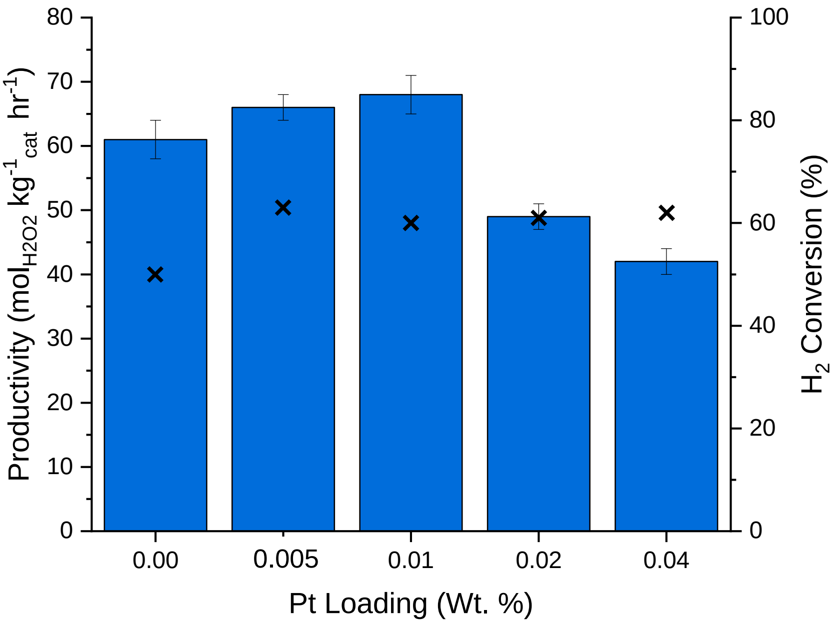

Figure 3.22. Effects of the addition of Pt into 0.5%Au-0.5%Pd/Al_2O_3 in the direct synthesis of H_2O_2. Total metal loading fixed at 1% and ratio of Au:Pd set to 1:1. **Key;** H_2O_2 productivity (*squares*), H_2 conversion (*crosses)*.

H_2O_2 direct synthesis reaction conditions: Catalyst (0.01 g), H_2O (2.9 g), MeOH (5.6 g), 5% H_2/CO_2 (420 psi, 2.76 mmol), 25% O_2/CO_2 (160 psi, 5.24 mmol), 0.5 hr, 20 °C, 1200 rpm.

Table 3.16. Effects of the addition of Pt into 0.5%Au-0.5%Pd/Al_2O_3 in the direct synthesis of H_2O_2.

Catalyst	Pt Loading (wt.%)	Productivity (mol_{H2O2} kg_{cat}^{-1} hr^{-1})	Turnover Number (mol_{H2O2} mol_{metal}^{-1} hr^{-1})	H_2 Conversion (%)	H_2O_2 Selectivity (%)	H_2O_2 Concentration (wt. %)	Degradation (mol_{H2O2} kg_{cat}^{-1} hr^{-1})
1.0Pt	1.0	0	0	64	0	0.00	569
0.5Pt-0.5Pd	0.5	34	463	38	16	0.07	372
0.5Au-0.5Pd	0.0	61	837	54	19	0.12	416
0.005Pt-AuPd	0.005	66	916	63	18	0.14	602
0.01Pt-AuPd	0.01	68	862	60	20	0.14	640
0.02Pt-AuPd	0.02	49	681	61	15	0.10	524
0.04Pt-AuPd	0.04	42	649	59	10	0.08	654

H_2O_2 direct synthesis reaction conditions: Catalyst (0.01 g), H_2O (2.9 g), MeOH (5.6 g), 5% H_2/CO_2 (420 psi, 2.76 mmol), 25% O_2/CO_2 (160 psi, 5.24 mmol), 0.5 hr, 20 °C, 1200 rpm.
H_2O_2 degradation reaction conditions: Catalyst (0.01 g), H_2O_2 (50 wt.%, 0.69 g), H_2O (2.21 g), MeOH (5.6 g), 5% H_2/CO_2 (420 psi), 0.5 hr, 20 °C, 1200 rpm.
n.b. Total metal loading fixed at 1 wt.% and ratio of Au:Pd set to 1:1.

It was observed that doping 0.01 % Pt into an AuPd catalyst was able to deliver a small enhancement in H_2O_2 synthesis, over the bimetallic AuPd analogue, with productivity increasing from 61 to 68 mol_{H2O2} kg_{cat}^{-1} hr^{-1} . Other Pt loadings, between 0.005 % and 0.04 % did not achieve any greater levels of H_2O_2 synthesis over that which was offered by the AuPd catalyst. Additionally, H_2 conversions were enhanced upon the addition of Pt, from 54 % conversion when the AuPd catalyst was used, to 63 % when the 0.005Pt-AuPd catalyst was used. Optimal wt.% loadings of Pt in PtAuPd trimetallic catalysts were previously examined by Edwards et al, using CeO_2 as a support.[71] The authors observed that specific ratio of Pt:Au:Pd could result in strong synergistic effects and greatly promote H_2O_2 synthesis or degradation, but even small deviations away from these optimal ratios could diminish these promotional effects.[71] For example, a 2.45%Au-2.45%Pd-0.1%Pt/CeO_2 catalyst offered a productivity of 109 mol_{H2O2} kg_{cat}^{-1} hr^{-1}, but by increasing Pt to 0.2 %, productivity could be enhanced to 170 mol_{H2O2} kg_{cat}^{-1} hr^{-1}.[71] An analogous effect appears to have occurred in this work, using an Al_2O_3 support, given the decrease in H_2O_2 productivity when Pt is either increased or decreased from 0.01 %. It should be noted that in this work productivity values are likely significantly reduced, largely due to the higher operating temperatures used.

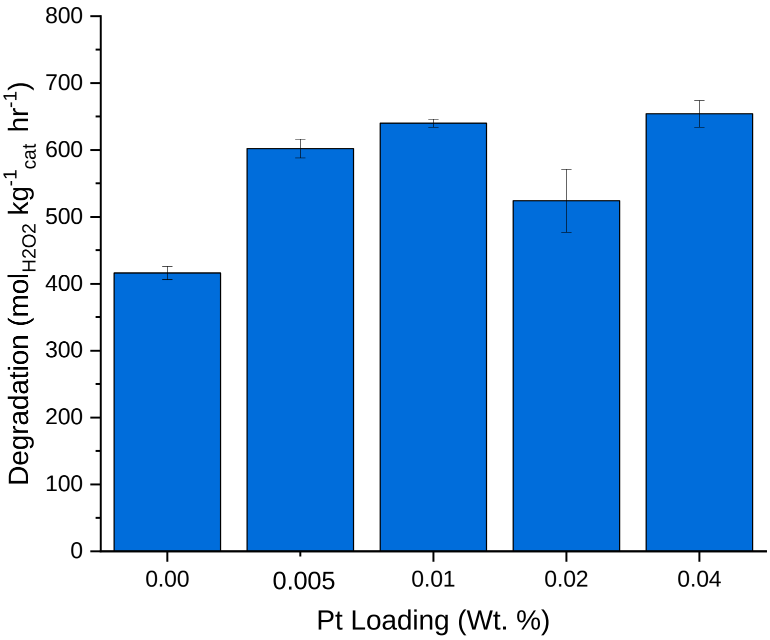

Figure 3.23. Effects of the addition of Pt into 0.5%Au-0.5%Pd/Al_2O_3 in the degradation of H_2O_2. Total metal loading fixed at 1 wt.% and ratio of Au:Pd set to 1:1 (wt/wt).
H_2O_2 degradation reaction conditions: Catalyst (0.01 g), H_2O_2 (50 wt.%, 0.69 g), H_2O (2.21 g), MeOH (5.6 g), 5% H_2/CO_2 (420 psi), 0.5 hr, 20 °C, 1200 rpm.

The ability of each catalyst to degrade H_2O_2 was also investigated and is shown in Table 3.16 and Figure 3.23. The incorporation of small quantities of Pt into AuPd catalysts was able to enhance levels of H_2O_2 degradation to higher levels than could be achieved with the AuPd catalyst alone. For example, the 0.01%Pt-AuPd catalyst offered an H_2O_2 degradation of 640, compared to the AuPd catalyst, which offered an H_2O_2 degradation of 416 mol_{H2O2} kg_{cat}^{-1} hr^{-1}. Similar levels of H_2O_2 degradation were obtained with other loadings of Pt, such as the 0.005Pt-AuPd and 0.04Pt-AuPd catalysts, which offered H_2O_2 degradation values of 602 and 654 mol_{H2O2} kg_{cat}^{-1} hr^{-1} respectively. In comparison, a monometallic 1%Pt catalyst offered a degradation value of 569 mol_{H2O2} kg_{cat}^{-1} hr^{-1}, demonstrating the strong ability of Pt to degrade H_2O_2, which has been observed previously in the literature.[226] The degradation value offered by the 0.02%Pt-AuPd catalyst of 524 mol_{H2O2} kg_{cat}^{-1} hr^{-1} is not contiguous with the rest of the data set, and is likely not representative of a real trend towards increasing H_2O_2 degradation arising from greater loadings of Pt.

Finally, the selective oxidation of benzyl alcohol via in-situ H_2O_2 synthesis was investigated using this series of trimetallic catalysts, the results of which are shown in Figure 3.24 and Table 3.17.

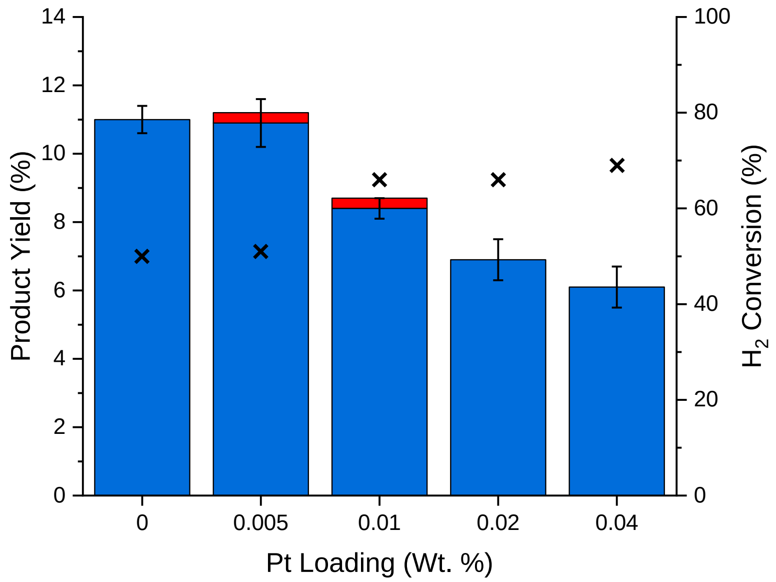

Figure 3.24. Effects of the addition of Pt into 0.5%Au-0.5%Pd/Al_2O_3 in the selective oxidation of benzyl alcohol via In-Situ H_2O_2 synthesis. Total metal loading set to 1 wt.%. Ratio of Au/Pd set to 1/1 (wt/wt). **Key;** benzaldehyde yield (*blue bars*), benzoic acid yield (*red bars*), hydrogen conversion (*crosses*). **Benzyl alcohol oxidation reaction conditions:** Catalyst (0.01 g), MeOH (7.13 g), benzyl alcohol (1.04 g, 9.62 mmol), mesitylene (0.42 g), 5% H_2/CO_2 (420 psi, 2.76 mmol), 25% O_2/CO_2 (160 psi, 5.24 mmol), 0.5 hr, 50 ^{O}C, 1200 rpm.

Table 3.17. Effects of the addition of Pt into 0.5%Au-0.5%Pd/Al_2O_3 catalyst towards the selective oxidation of benzyl alcohol via In-Situ H_2O_2 synthesis.

Catalyst	Pt Loading (wt.%)	Benzaldehyde Yield (%)	Benzoic Acid Yield (%)	Selectivity to Benzaldehyde (%)	Turnover Number (mol_{BA} mol_{metal}^{-1} hr^{-1})	H_2 Conversion (%)	H_2 Selectivity (%)	Residual H_2O_2 (mmol)
0.5Pt-0.5Pd	0.5	1.1	0	100	291	69	6	0.053
0.5Au-0.5Pd	0.0	11.0	0	100	2919	50	77	0.161
0.005Pt-AuPd	0.005	10.9	0.3	97	2896	51	74	0.128
0.01Pt-AuPd	0.01	8.4	0.3	97	2235	66	44	0.124
0.02Pt-AuPd	0.02	6.9	0	100	1841	66	36	0.129
0.04Pt-AuPd	0.04	6.1	0	100	1637	69	31	0.107

Benzyl alcohol oxidation reaction conditions: Catalyst (0.01 g), MeOH (7.13 g), benzyl alcohol (1.04 g, 9.62 mmol), mesitylene (0.42 g), 5% H_2/CO_2 (420 psi, 2.76 mmol), 25% O_2/CO_2 (160 psi, 5.24 mmol), 0.5 hr, 50 ^{O}C, 1200 rpm.

n.b. Total metal loading set to 1 wt.%. Ratio of Au:Pd set to 1:1 by mass.

The doping of 0.005 % Pt into an AuPd catalyst caused a small loss of selectivity to benzaldehyde, to 97.3 %, whilst H_2 conversion and benzaldehyde yield remained essentially unchanged when compared to the AuPd catalyst. Further increases in Pt content resulted in a loss of benzaldehyde yield, and a concurrent increase in H_2 conversion. For example, the 0.005Pt-AuPd catalyst exhibited an H_2 conversion of 51 % and a benzaldehyde yield of 10.9 %, whereas 69 % of H_2 was converted when the 0.04%Pt-AuPd catalyst was used, with a benzaldehyde yield of 6.1 %.

The increasing levels of H_2 conversion may be explained by the strong potential of Pt to catalyse hydrogenation reactions.[257-259] This may be causing enhanced levels of H_2O_2 degradation, generating H_2O before H_2O_2 or its reactive radical intermediates can be utilised in the oxidation of benzyl alcohol. Indeed, when this series of catalysts was tested for the degradation of H_2O_2, all Pt containing catalysts exhibited moderately or greatly enhanced levels of H_2O_2 degradation, except for the 0.005%Pt-AuPd catalyst, as shown in Table 3.16.

3.13 Conclusions

The catalytic activity of a series of supported bimetallic 0.5%X-0.5%Pd/Al_2O_3 catalysts were investigated towards the direct synthesis of H_2O_2 and towards the selective oxidation of benzyl alcohol via in-situ H_2O_2 synthesis. Whilst the 0.5%Au-0.5%Pd/Al_2O_3 catalyst did not offer the greatest levels H_2O_2 productivity, it achieved the greatest levels of benzyl alcohol conversion compared to AuPd catalysts using other support materials. Significant enhancements in benzyl alcohol conversion were demonstrated upon the incorporation of Au or Fe into Pd based catalysts, compared to an analogous Pd/Al_2O_3 monometallic catalyst.

Detailed comparisons were made for 1.0%Pd/Al_2O_3, 0.5%Au-0.5%Pd/Al_2O_3 and 0.5%Fe-0.5%Pd/Al_2O_3 using extended reaction times and sequential reactions, in addition to characterisation techniques such as STEM-HAADF, CO-DRIFTS and XPS. The activities of these catalysts in the selective oxidation of benzyl alcohol via in-situ H_2O_2 synthesis are shown in Table 3.18.

Overall, the greatest yield of benzaldehyde was offered by 0.5%Fe-0.5%Pd/Al_2O_3 when used in sequential reactions, which offered a benzyl alcohol conversion of 34.4 % at a selectivity to benzaldehyde of 97.1 % after 4 reactions. The greatest rate of reaction when standardised for total molar metal content was achieved by AuPd catalysts, due to the lower number of moles of Au compared to an equivalent mass of Fe.

Table 3.18. Comparison of key catalysts in the selective oxidation of benzyl alcohol via in-situ H_2O_2 synthesis.

Catalyst	Benzyl Alcohol Conversion (%)	Benzaldehyde Selectivity (%)	Turnover Number ($mol_{benzaldehyde}$ mol_{metal}^{-1} hr^{-1})	Selectivity based on H_2 (%)
1.0%Pd/Al_2O_3	1.3	100	266	50
0.5%Au-0.5%Pd/Al_2O_3	11.0	100	2919	77
0.5%Fe-0.5%Pd/Al_2O_3	10.3	97	1406	95

Benzyl alcohol oxidation reaction conditions: Catalyst (0.01 g), MeOH (7.13 g), benzyl alcohol (1.04 g, 9.62 mmol), mesitylene (0.42 g), 5% H_2/CO_2 (420 psi, 2.76 mmol), 25% O_2/CO_2 (160 psi, 5.24 mmol), 0.5 hr, 50 ^{O}C, 1200 rpm.

Optimisation of the metal ratios in the AuPd/Al_2O_3 catalyst allowed for a moderate increase in benzaldehyde yield and H_2 selectivity, when the relative concentration of Au in the catalyst was decreased and Pd increased. Conversely, the catalyst could be tuned towards enhanced H_2O_2 synthesis by increasing the concentration of Au and decreasing the concentration of Pd.

The use of a separate 1.0%Fe/Al_2O_3 co-catalyst in tandem with 0.5%Au-0.5%Pd/Al_2O_3 was able to further enhance yields of benzaldehyde by utilising residual H_2O_2 in solution, whilst the incorporation of Pt as a tertiary metal in an AuPd catalyst generally inhibited overall catalytic activity towards benzyl alcohol conversion.

3.14 References

1. Santonastaso, M., Freakley, S., et al, Oxidation of benzyl alcohol using in situ generated hydrogen peroxide. *Org. Process Res. Dev.* **2014,** *18*, 1455-1460.
2. Crombie, C., Lewis, R., et al., The Influence of Reaction Conditions on the Oxidation of Cyclohexane via the In-Situ Production of H2O2. *Catal. Lett.* **2021,** *151*, 164-171.
3. Martinez, J., Mazarío, J., et al., A tandem process for in situ H2O2 formation coupled with benzyl alcohol oxidation using Pd–Au bimetallic catalysts. *Dalton Trans.* **2022,** *51*, 17567-17578.
4. Santos, A., Lewis, R., et al., The oxidative degradation of phenol via in situ H2O2 synthesis using Pd supported Fe-modified ZSM-5 catalysts. *Catal. Sci. Technol.* **2022,** *12*, 2943-2953.
5. Richards, T., Harrhy, J., et al, A residue-free approach to water disinfection using catalytic in situ generation of reactive oxygen species. *Nat. Catal.* **2021,** *4*, 575-585.
6. Prieto, A., Palomino, M., et al, Propylene epoxidation with in situ generated H2O2 in supercritical conditions. *Catal. Today* **2014,** *227*, 87-95.
7. Russo, V., Tesser, R., et al., Chemical and technical aspects of propene oxide production via hydrogen peroxide (HPPO Process). *Ind. Eng. Chem. Red.* **2013,** *52*, 1168-1178.
8. Bradford Ryland, S. S., Practical Aerobic Oxidations of Alcohols and Amines with Homogeneous Copper/TEMPO and Related Catalyst Systems. *Angew. Chem.* **2014,** *53*, 8824-8838.
9. Crombie, C., Lewis, R., et al, Enhanced Selective Oxidation of Benzyl Alcohol via In Situ H2O2 Production over Supported Pd-Based Catalysts. *ACS Catal.* **2021,** *11*, 2701-2714.
10. Lewis, R., Hutchings, G., Recent Advances in the Direct Synthesis of H_2O_2. *Chem. Cat. Chem* **2019,** *11*, 298 - 308.
11. Yi, Y., Wang, L., et al., A review on research progress in the direct synthesis of hydrogen peroxide from hydrogen and oxygen: noble-metal catalytic method, fuel-cell method and plasma method. *Catal. Sci. Technol* **2016,** *6*, 1593.

12. Choudhary, V., Dhar, A., et al., A green process for chlorine-free benzaldehyde from the solvent-free oxidation of benzyl alcohol with molecular oxygen over a supported nano-size gold catalyst. *Green Chem.* **2005,** *7*, 768-770.
13. Lyu, J., Niu, J., et al., In Situ Hydrogen Peroxide Production for Selective Oxidation of Benzyl Alcohol over a Pd@Hierarchical Titanium Silicalite Catalyst. *ACS Omega* **2020,** *5*, 16865-16874.
14. Göksu, H., Burhan, H., et al, Oxidation of Benzyl Alcohol Compounds in the Presence of Carbon Hybrid Supported Platinum Nanoparticles (Pt@CHs) in Oxygen Atmosphere. *Sci. Rep.* **2020,** *10*, 5439.
15. Enache, D., Barker, D., et al, Solvent-free oxidation of benzyl alcohol using titania-supported gold–palladium catalysts: Effect of Au–Pd ratio on catalytic performance. *Catal. Today* **2007,** *122*, 407-411.
16. He, Q., Miedziak, P., et al, Switching-off toluene formation in the solvent-free oxidation of benzyl alcohol using supported trimetallic Au–Pd–Pt nanoparticles. *Faraday Discuss.* **2013,** *162*, 365-378.
17. Wu, P., Cao, Y., et al, Formation of PdO on Au–Pd bimetallic catalysts and the effect on benzyl alcohol oxidation. *J. Catal.* **2019,** *375*, 32-43.
18. Moreno, I., Dummer, M., et al., Selective oxidation of benzyl alcohol using in situ generated H_2O_2 over hierarchical Au-Pd titanium silicate catalysts. *Catal. Sci. Technol.* **2013,** *3*, 2425.
19. Lewis, R., Hutchings, G., Recent advances in the direct synthesis of H_2O_2. *ChemCatChem* **2019,** *11*, 298-308.
20. Chen, Z., Zou, P., et al., Nitrogen-Incorporated SBA-15 Mesoporous Molecular Sieve Supported Palladium for Solvent-Free Aerobic Oxidation of Benzyl Alcohol. *Catal. Letters* **2015,** *145*, 2029-2036.
21. Edwards, J., Solsona, B., Direct synthesis of hydrogen peroxide from H_2 and O_2 using Au-Pd/Fe_2O_3 catalysts. *J. Mater. Chem.* **2005,** *15*, 4595-4600.
22. Edwards, J., Pritchard, J., et al., The direct synthesis of hydrogen peroxide using platinum promoted gold–palladium catalysts. *Catal. Sci. Technol.* **2014,** *4*, 3244-3250.
23. Gong, X., Lewis, R., et al, Enhanced catalyst selectivity in the direct synthesis of H_2O_2 through Pt incorporation into TiO_2 supported AuPd catalysts. *Catal. Sci. Technol.* **2020,** *10*, 4635-4644.
24. Ntainjua, E., Edwards, J., et al, The role of the support in achieving high selectivity in the direct formation of hydrogen peroxide. *Green Chem.* **2008,** *10*, 1162-1169.
25. Richards, T., Lewis, R., et al, The Direct Synthesis of Hydrogen Peroxide Over Supported Pd-Based Catalysts: An Investigation into the Role of the Support and Secondary Metal Modifiers. *Catal. Lett.* **2022,** *153*, 32-40.
26. Duarte, F., Maldonado-Hódar, F., et al., Fenton-like degradation of azo-dye Orange II catalyzed by transition metals on carbon aerogels. *Appl. Catal. B: Environ.* **2009,** *85*, 139-147.
27. Chaliha, S., Bhattacharyya, K., Wet oxidative method for removal of 2,4,6-trichlorophenol in water using Fe(III), Co(II), Ni(II) supported MCM41 catalysts. *J. Hazard Mater.* **2008,** *150*, 728-736.
28. Salem, I., El-Maazawi, M., Kinetics and mechanism of color removal of methylene blue with hydrogen peroxide catalyzed by some supported alumina surfaces. *Chemosphere* **2000,** *41*, 1173-1180.
29. Bokare, A., Choi, W.,, Review of iron-free Fenton-like systems for activating H2O2 in advanced oxidation processes. *J. Hazard Mater.* **2014,** *275*, 121-135.
30. Santos, A., Lewis, R., et al., Direct synthesis of hydrogen peroxide over Au-Pd supported nanoparticles under ambient conditions. *Ind. Eng. Chem. Res.* **2019,** *58*, 12623-12631.
31. Barnes, A., Lewis, R., et al., Improving catalytic activity towards the direct synthesis of H_2O_2 through Cu incorporation into AuPd catalysts. *Catalysts* **2022,** *12*, 1396.
32. Brehm, J., Lewis, R., et al, The Direct Synthesis of Hydrogen Peroxide over AuPd Nanoparticles: An Investigation into Metal Loading. *Catal. Lett.* **2021,** *152*, 254-262.
33. Crole, D., Freakley, S., et al., Direct synthesis of hydrogen peroxide in water at ambient temperature. *Proc. R. Soc. A* **2016,** *472*, 20160156.

34. Sankar, M., Nowicka, E., et al, The benzaldehyde oxidation paradox explained by the interception of peroxy radical by benzyl alcohol. *Nat. Commun.* **2014,** *5*, 3332.
35. Crombie, C., Lewis, R., et al., The influence of reaction conditions on the oxidation of cyclohexane via the in-situ production of H_2O_2. *Catal. Letters* **2020,** *151*, 164-171.
36. Liu, Q., Bauer, J., et al., Direct synthesis of H_2O_2 from H_2 and O_2 over Pd–Pt/SiO_2 bimetallic catalysts in a H_2SO_4/ethanol system. *Appl. Catal. A-Gen.* **2008,** *339*, 130-136.
37. Ntainjua, E., Freakley, S., Hutchings, G., Direct synthesis of hydrogen peroxide using ruthenium catalysts. *Top. Catal.* **2012,** *55*, 718 - 722.
38. Edwards, J., Thomas, A., et al., Au-Pd supported nanocrystals as catalysts for the direct synthesis of hydrogen peroxide from H_2 and O_2. *Green Chem.* **2008,** *10*, 388-394.
39. Han, Y., Zhong, Z., et al, Au promotional effects on the synthesis of H_2O_2 directly from H_2 and O_2 on supported Pd-Au alloy catalysts. *J. Phys. Chem. C* **2007,** *111*, 8410 - 8413.
40. Li, J., Yoshizawa, K., Mechanistic aspects in the direct synthesis of hydrogen peroxide on PdAu catalyst from first principles. *Catal. Today* **2015,** *248*, 142-148.
41. Li, J., Ishihara, T., Yoshizawa, K., Theoretical revisit of the direct synthesis of H_2O_2 on Pd and Au@Pd surfaces: A comprehensive mechanistic study. *J. Phys. Chem. C* **2011,** *115*, 25359 - 25367.
42. Ham, H., Hwang, G., et al., On the role of Pd ensembles in selective H_2O_2 formation on PdAu alloys. *J. Phys. Chem. C* **2009,** *113*, 12943 - 12945.
43. Richards, T., Lewis, R., et al, The direct synthesis of hydrogen peroxide over supported Pd-based catalysts: An investigation into the role of the support and secondary metal modifiers. *Catal. Letters* **2022**.
44. Joshi, A., Delgass, N., Thomson, K., Investigation of Gold-Silver, Gold-Copper, and Gold-Palladium Dimers and Trimers for Hydrogen Peroxide Formation from H_2 and O_2. *J. Phys. Chem. C* **2007,** *111*, 7384-7395.
45. Barnes, A., Lewis, R., et al., Enhancing catalytic performance of AuPd catalysts towards the direct synthesis of H2O2 through incorporation of base metals. *Catal. Sci. Technol.* **2022,** *12*, 1986.
46. Ouyang, L., Da, G., et al, Insight into active sites of Pd–Au/TiO2 catalysts in hydrogen peroxide synthesis directly from H2 and O2. *J. Catal.* **2014,** *311*, 129-136.
47. Ouyang, L., Tian, P., et al, The origin of active sites for direct synthesis of H_2O_2 on Pd/TiO_2 catalysts: Interfaces of Pd and PdO domains. *J. Catal.* **2015,** *321*, 70-80.
48. Smirnova, N., Mashkovsky, I., et al, Local Structure of Pd_1 Single Sites on the Surface of PdIn Intermetallic Nanoparticles: A Combined DFT and CO-DRIFTS Study. *Catal.* **2021,** *11*, 1376.
49. Lentz, C., Jand, S., et al, DRIFTS study of CO adsorption on Pt nanoparticles supported by DFT calculations. *J. Mol. Catal. A Chem.* **2017,** *426*, 1-9.
50. Pawelec, B., Venezia, A., et al, AuPd alloy formation in Au-Pd/Al2O3 catalysts and its role on aromatics hydrogenation. *Appl. Surf. Sci.* **2005,** *242*, 380-391.
51. Zeinalipour-Yazdi, C., Willock, D., et al, CO adsorption over Pd nanoparticles: A general framework for IR simulations on nanoparticles. *Surf. Sci.* **2016,** *646*, 210-220.
52. Stakheev, A., Smirnova, N., et al, Single-atom Pd sites on the surface of Pd–In nanoparticles supported on g-Al2O3: a CO-DRIFTS study. *Mendeleev Commun.* **2017,** *27*, 515-517.
53. Sales, E., Jove, J., et al, Palladium, Palladium–Tin, and Palladium–Silver Catalysts in the Selective Hydrogenation of Hexadienes: TPR, M¨ossbauer, and Infrared Studies of Adsorbed CO. *J. Catal.* **2000,** *195*, 88-95.
54. Carter, J., Althahban, S., et al, Synergy and Anti-Synergy between Palladium and Gold in Nanoparticles Dispersed on a Reducible Support. *ACS Catal.* **2016,** *6*, 6623-6633.
55. Cattaneo, S., Freakley, S., et al, Cinnamaldehyde hydrogenation using Au–Pd catalysts prepared by sol immobilisation. *Catal. Sci. Technol.* **2018,** *8*, 1677-1685.
56. Sun, K., Wilson, A., et al, Catalytic Deoxygenation of Octanoic Acid over Supported Palladium: Effects of Particle Size and Alloying with Gold. *ACS Catal.* **2015,** *5*, 1939-1948.

57. Brehm, J., Lewis, R., et al, Enhancing the Chemo-Enzymatic One-Pot Oxidation of Cyclohexane via In Situ H_2O_2 Production over Supported Pd-Based Catalysts. *ACS Catal.* **2022,** *12*, 11776-11789.
58. Zhang, L., Zhang, B., et al., The Effect of Pretreatment on the Reactivity of Pd/Al2O3 in Room Temperature Formaldehyde Oxidation. *ChemCatChem* **2021,** *13*, 4133-4141.
59. Wilson, N., Priyadarshini, P., et al., Direct synthesis of H_2O_2 on Pd and Au_xPd_1 clusters: Understanding the effect of alloying Pd with Au. *J. Catal.* **2018,** *357*, 163 - 175.
60. Choudhary, V., Samanta, C., Role of chloride or bromide anions and protons for promoting the selctive oxidation of H_2 by O_2 to H_2O_2 over supported Pd catalysts in an aqueous medium. *J. Catal.* **2006,** *238*, 28-38.
61. Samanta, C., Choudhary, V., Direct synthesis of H_2O_2 from H_2 and O_2 over Pd/H-beta catalyst in an aqueous acidic medium: Influence of halide ions present in the catalyst or reaction medium on H_2O_2 formation. *Catal. Commun.* **2007,** *8*, 73-79.
62. Chinta, S., Lunsford, J., A mechanistic study of H_2O_2 and H_2O formation from H_2 and O_2 catalyzed by palladium in an aqueous medium. *J. Catal.* **2004,** *225*, 249-255.
63. Santos, A., Lewis, R., et al., The Oxidative Degradation of Phenol via in situ H_2O_2 Synthesis Using Pd Supported Fe-modified ZSM-5 Catalysts. *Catal. Sci. Technol.* **2022,** *12*, 2943.
64. Ye, Y., Chun, J., et al, A study of the palladium size effect on the direct synthesis of hydrogen peroxide from hydrogen and oxygen using highly uniform palladium nanoparticles supported on carbon. *Korean J. Chem. Eng.* **2012,** *29*, 1115-1118.
65. Tian, P., Ouyang, L., et al, The origin of palladium particle size effects in the direct synthesis of H_2O_2: Is smaller better? *J. Catal.* **2017,** *349*, 30-40.
66. Zhang, Q., Deng, W., Wang, Y., Effect of size of catalytically active phases in the dehydrogenation of alcohols and the challenging selective oxidation of hydrocarbons. *Chem. Commun.* **2011,** *47*, 9275-9292.
67. Edwards, J., Pritchard, J., et al, The Direct Synthesis of Hydrogen Peroxide Using Platinum-Promoted Gold–Palladium Catalysts. *Angew. Chem. Int. Ed.* **2014,** *53*, 2381-2384.
68. Richard Lewis, K. U., et. al., The direct synthesis of H_2O_2 using TS-1 supported catalysts. *ChemCatChem* **2019,** *11*, 1673-1680.
69. Li, H., Wang, L., et al., Synergetic interactions between neighbouring platinum monomers in CO_2 hydrogenation. *Nat. Nanotechnol.* **2018,** *13*, 411-417.
70. Lara, P., Philippot, K., The hydrogenation of nitroarenes mediated by platinum nanoparticles: an overview. *Catal. Sci. Technol.* **2014,** *4*, 2445-2465.
71. Lordi, V., Yao, N., Wei, J., Method for Supporting Platinum on Single-Walled Carbon Nanotubes for a Selective Hydrogenation Catalyst. *Chem. Mater.* **2001,** *13*, 733-737.

3.15 Appendix

Table A3.1. Comparison of catalysts in the literature for the selective oxidation of benzyl alcohol via *in-situ* H_2O_2 synthesis.

Catalyst	Mass of Catalyst (mg)	Ratio of H_2:O_2	Solvent	Temperature (°C)	Time (hr)	Benzyl Alcohol (mmol)	Benzyl Alcohol Conversion (%)	Selectivity to Benzaldehyde (%)	Turnover Number ($mol_{benzaldehyde}$ mol_{metal}^{-1} hr^{-1})	Reference
2.5%Au-2.5%Pd/TiO_2	10	1:1.9	MeOH	50	0.5	9.6	5.9	90	282	[27]
0.5%Fe-0.5%Pd/TiO_2	10	1:1.9	MeOH	50	0.5	9.6	5.8	96	783	[218]
0.5%Au-0.5%Pd/TiO_2	10	1:1.9	MeOH	50	0.5	9.6	2.8	100	743	[218]
0.1%Pd@HTS-1-OR	20	1:1.9	H_2O/MeOH	50	0.5	0.096	46.4	100	454	[131]
0.8%Pd-0.2%Au-H	5	1	H_2O	60	8	0.96	76.0	58	124	[130]
1.25%Au-1.25%Pd/TS-1	10	1:1.8	H_2O/MeOH	30	0.5	2.3	7.0	93	166	[114]

Table A3.2. Surface area of supports and supported 0.5%Au-0.5%Pd catalysts, as determined by BET.

Catalyst	**Surface Area ($m^2\ g^{-1}$)**
$AuPd/Al_2O_3$	80
Al_2O_3	83
$AuPd/CeO_2$	40
CeO_2	36
$AuPd/TiO_2$ (P25)	48
TiO_2 (P25)	53
$AuPd/Nb_2O_5$	3
Nb_2O_5	8
$AuPd/ZrO_2$	9
ZrO_2	21
AuPd/Carbon (G60)	777
Carbon (G60)	744

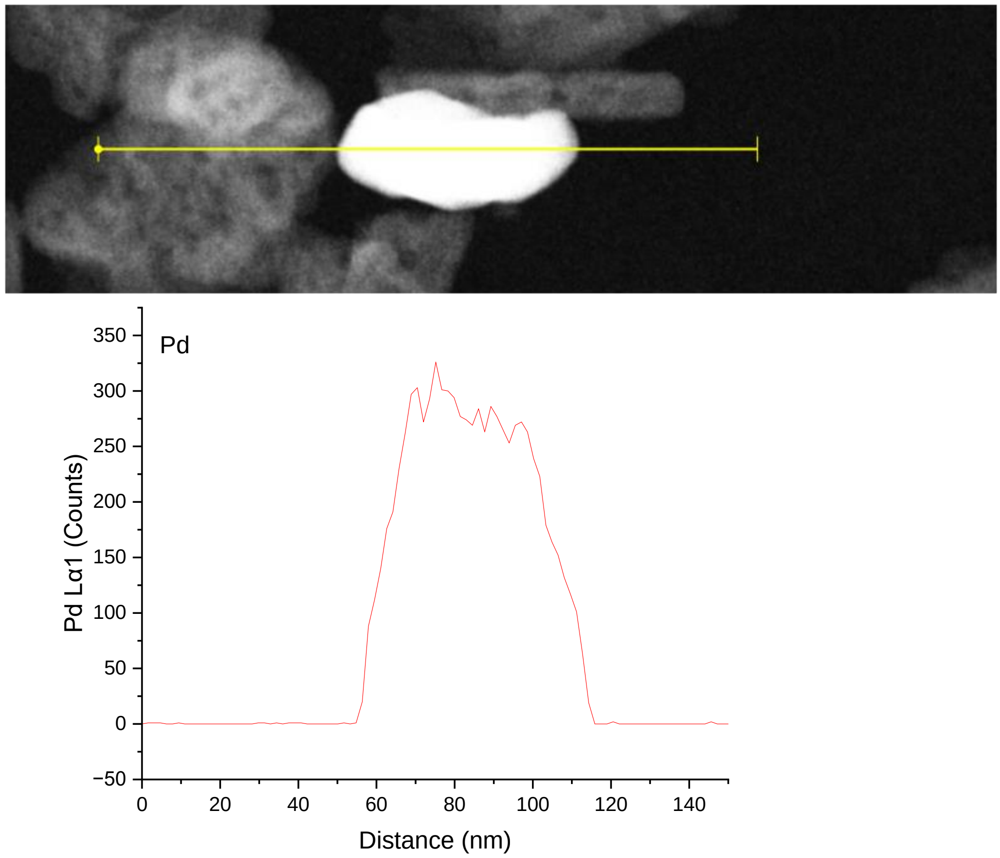

Figure A3.1. EDX linescan of Pd nanoparticle from the $1\%Pd/Al_2O_3$ catalyst.

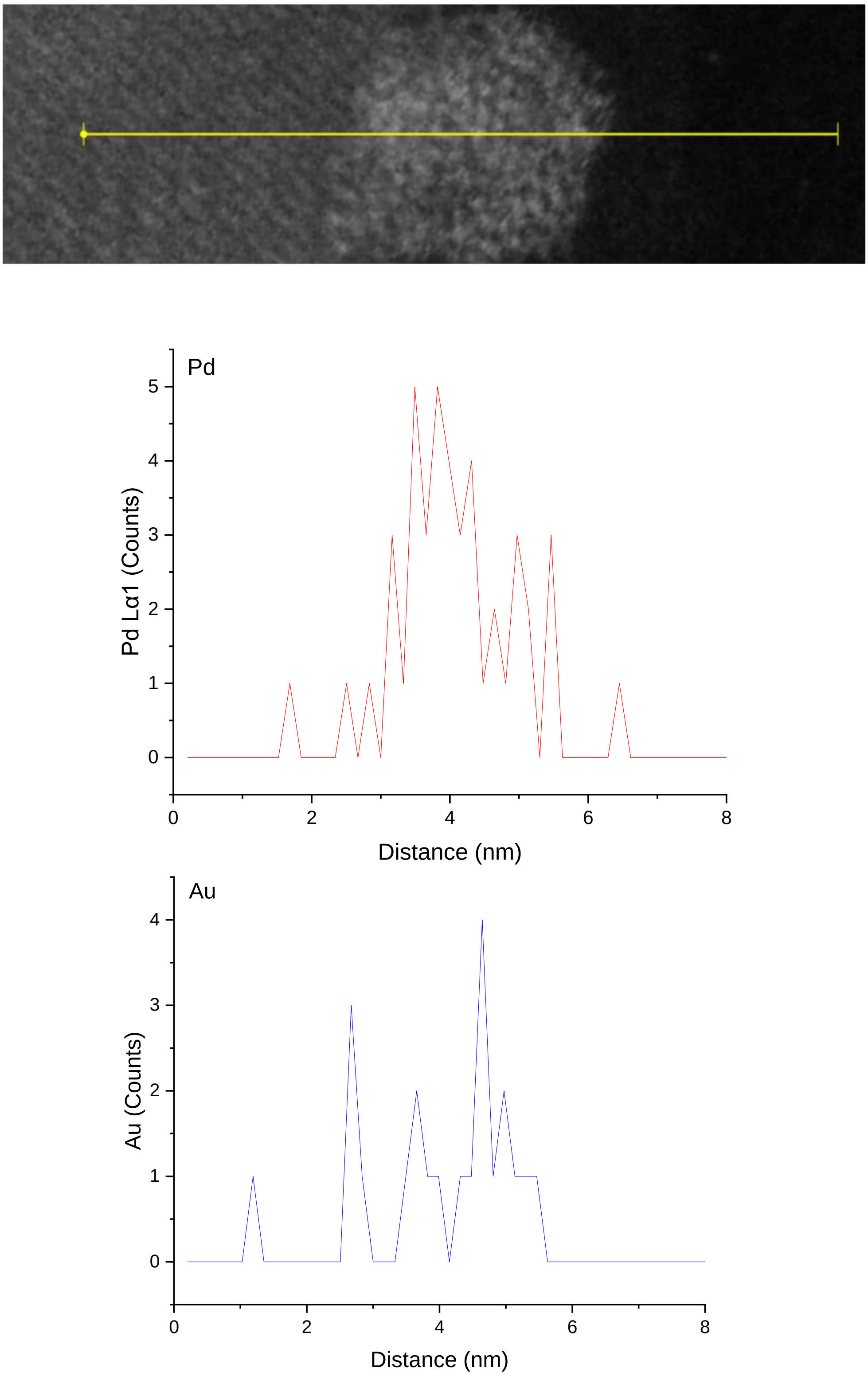

Figure A3.2. EDX linescan of AuPd nanoparticle from the 0.5%Au-0.5%Pd/Al_2O_3 catalyst. **Key;** Pd (*red*), Au (*blue*).

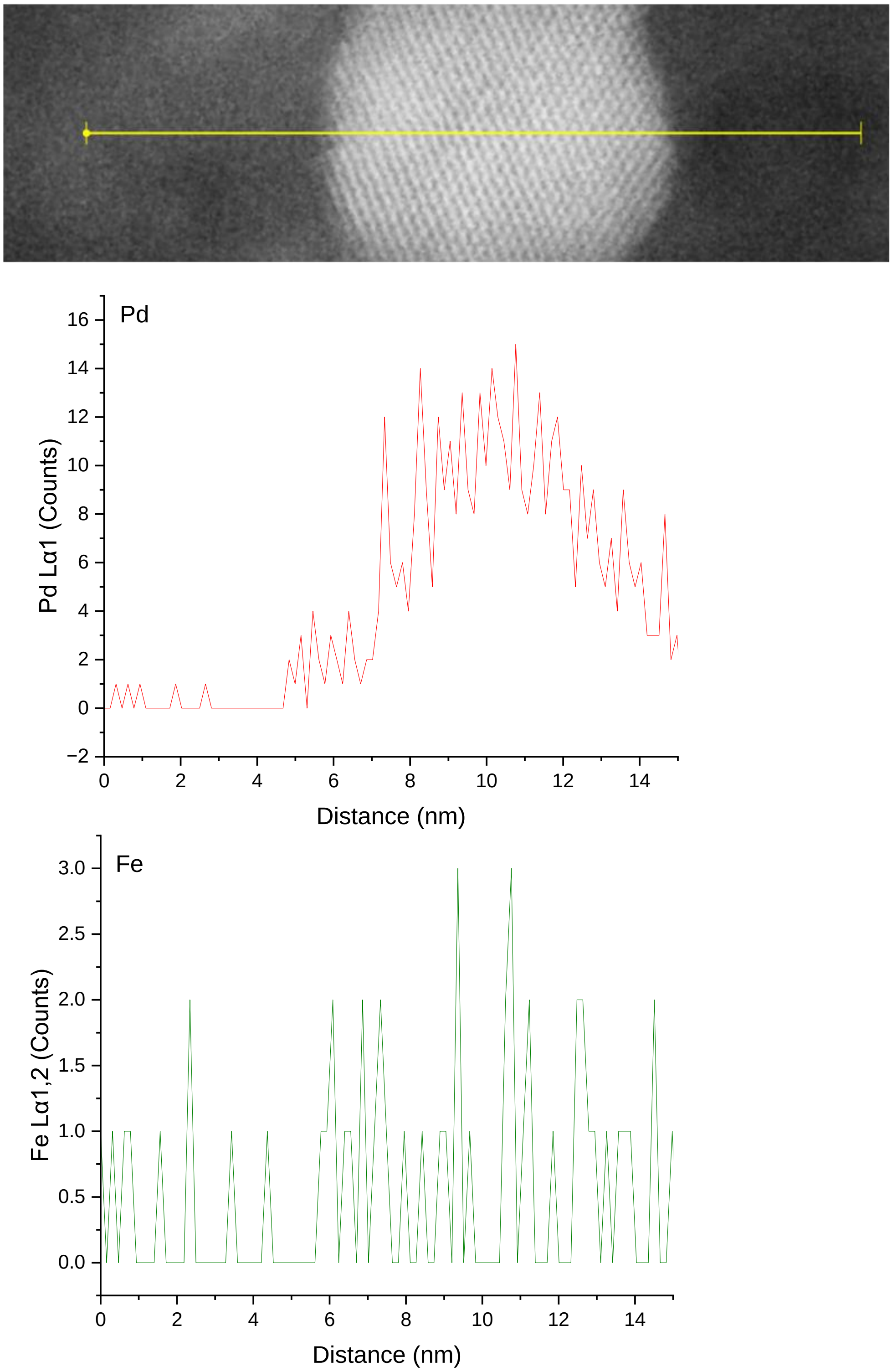

Figure A3.3. EDX linescan of an FePd nanoparticles from the 0.5%Fe-0.5%Pd/Al_2O_3 catalyst. **Key;** Pd (*red*), Fe (*green*).

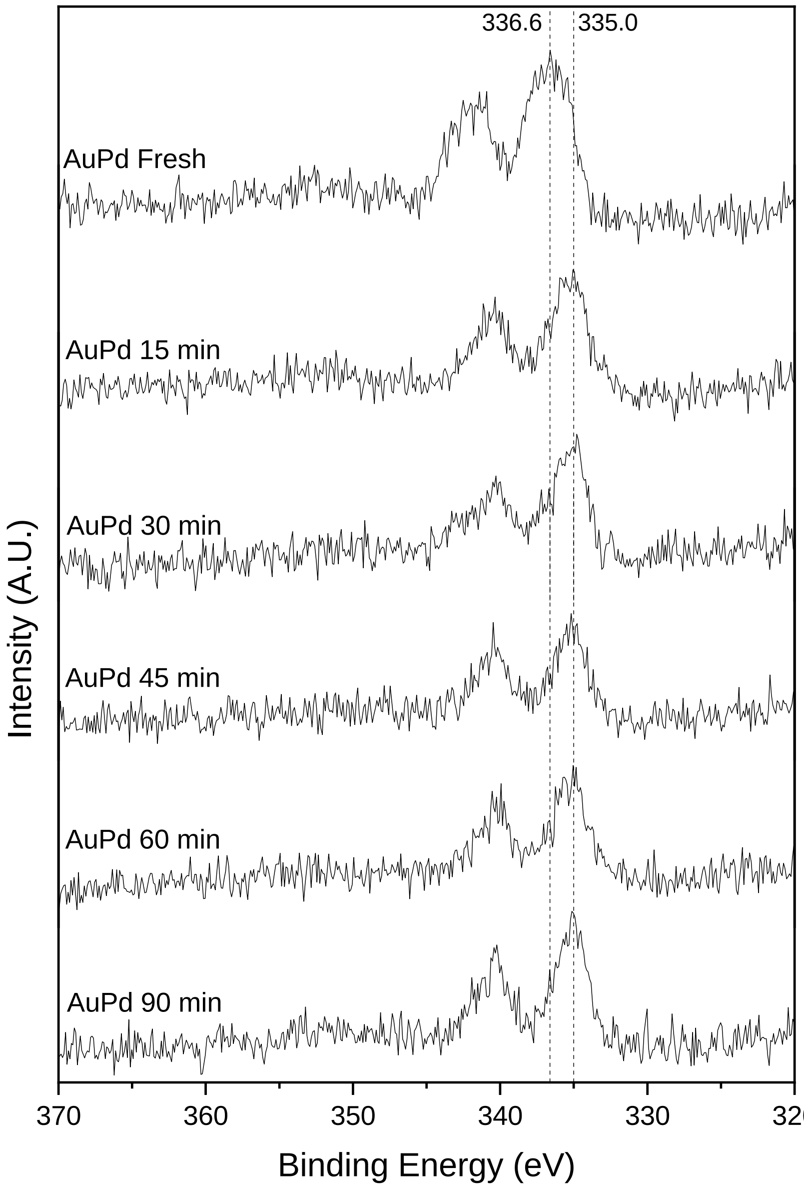

Figure A3.4. XPS Spectra of the 0.5%Au-0.5%Pd/Al_2O_3 catalyst, showing the change in binding energy of the 3d5/2 transition of Pd as a function of time over use in the oxidation of benzyl alcohol via in-situ H_2O_2 synthesis.

Benzyl alcohol oxidation reaction Conditions: Catalyst (0.01 g), MeOH (7.13 g), benzyl alcohol (1.04 g, 9.62 mmol), mesitylene (0.42 g), 5% H_2/CO_2 (420 psi, 2.76 mmol), 25% O_2/CO_2 (160 psi, 5.24 mmol), 0.5 hr, 50 ^{O}C, 1200 rpm.

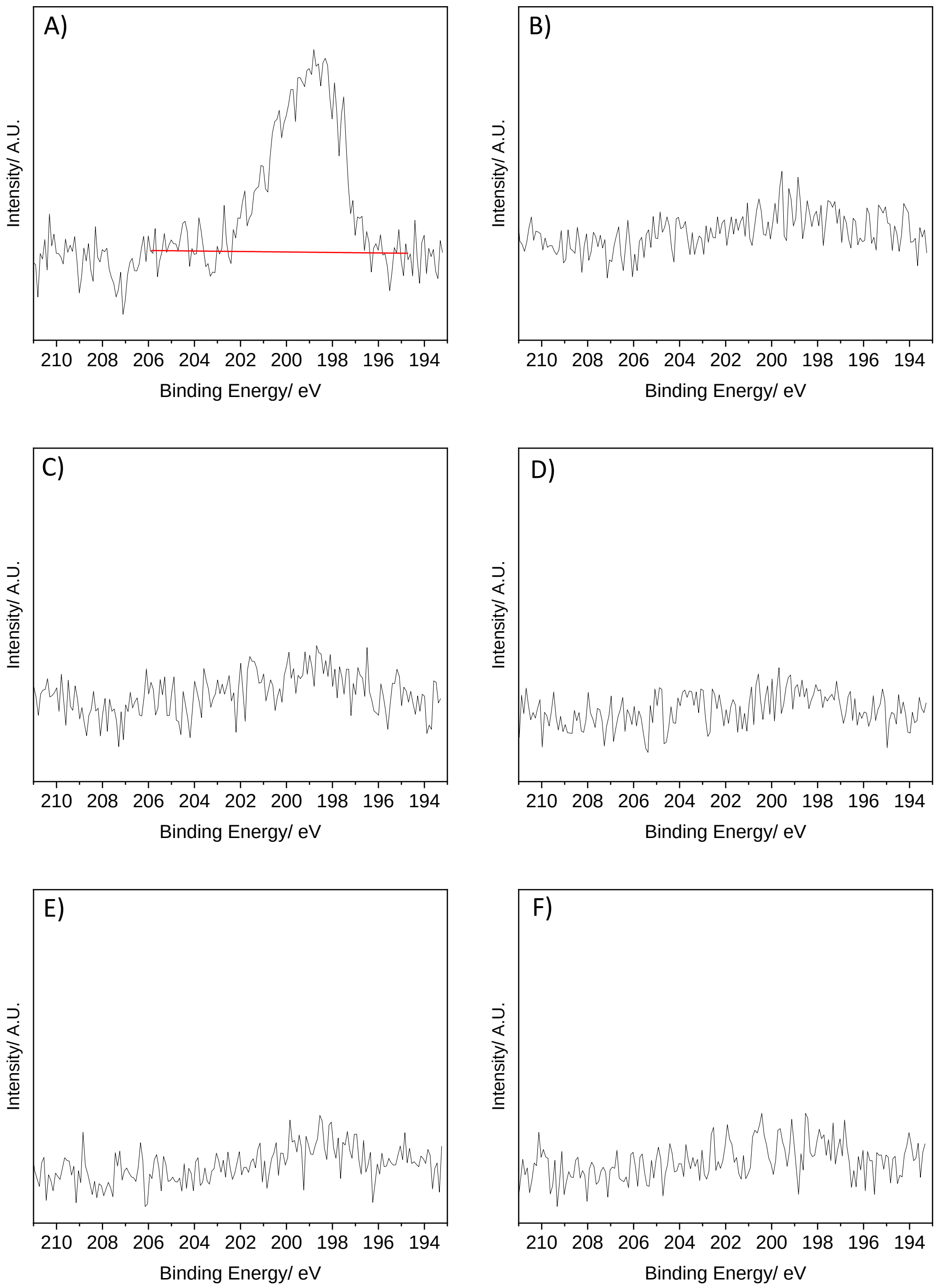

Figure A3.5. XPS spectra of 0.5%Au-0.5%Pd/Al_2O_3 showing change in Cl 2p region as a function of reaction time A) Fresh 0.5%Au-0.5%Pd/Al_2O_3, B) 15 min used 0.5%Au-0.5%Pd/Al_2O_3, C) 30 min used 0.5%Au-0.5%Pd/Al_2O_3, D) 45 min used 0.5%Au-0.5%Pd/Al_2O_3, E) 60min used 0.5%Au-0.5%Pd/Al_2O_3, F) 90 min used 0.5%Au-0.5%Pd/Al_2O_3.

Table A3.3. The in-situ oxidation of benzyl alcohol as a function of time using 0.5%Fe-0.5%Pd/Al_2O_3

Reaction Time (Min)	Benzaldehyde Yield (%)	Benzoic Acid Yield (%)	Selectivity to Benzaldehyde (%)	Turnover Number (mol_{BA} mol_{metal}^{-1} hr^{-1})	H_2 Conversion (%)	H_2 Selectivity (%)	Residual H_2O_2 (mmol)
0	0.0	0	-	-	0	0	0.000
15	6.1	0.00	100	1716	23	92	0.051
30	10.0	0.3	97	1406	38	95	0.075
45	11.9	0.4	97	1116	52	83	0.072
60	14.3	0.6	96	1006	61	85	0.070
90	16.4	0.7	96	769	72	83	0.068

Benzyl alcohol oxidation reaction conditions: Catalyst (0.01 g), MeOH (7.13 g), benzyl alcohol (1.04 g, 9.62 mmol), mesitylene (0.42 g), 5% H_2/CO_2 (420 psi, 2.76 mmol), 25% O_2/CO_2 (160 psi, 5.24 mmol), 0.5 hr, 50 ^{O}C, 1200 rpm.

Table A3.4. The in-situ oxidation of benzyl alcohol as a function of time using 0.5%Au-0.5%Pd/Al_2O_3.

Reaction Time (Min)	Benzaldehyde Yield (%)	Benzoic Acid Yield (%)	Selectivity to Benzaldehyde (%)	Turnover Number (mol_{BA} mol_{metal}^{-1} hr^{-1})	H_2 Conversion (%)	H_2 Selectivity (%)	Residual H_2O_2 (mmol)
0	0.0	0	-	-	0	0	0.000
15	5.8	0	100	3078	27	75	0.150
30	11.0	0	100	2919	50	77	0.161
45	12.0	0	100	2122	61	69	0.094
60	12.7	0	100	1685	68	65	0.083
90	13.8	0	100	1220	70	69	0.086

Benzyl alcohol oxidation reaction conditions: Catalyst (0.01 g), MeOH (7.13 g), benzyl alcohol (1.04 g, 9.62 mmol), mesitylene (0.42 g), 5% H_2/CO_2 (420 psi, 2.76 mmol), 25% O_2/CO_2 (160 psi, 5.24 mmol), 0.5 hr, 50 ^{O}C, 1200 rpm.

Table A3.5. The in-situ oxidation of benzyl alcohol as a function of time using 1.0% Pd/Al_2O_3.

Reaction Time (Min)	Benzaldehyde Yield (%)	Benzoic Acid Yield (%)	Selectivity to Benzaldehyde (%)	Turnover Number (mol_{BA} mol_{metal}^{-1} hr^{-1})	H_2 Conversion (%)	H_2 Selectivity (%)	Residual H_2O_2 (mmol)
0	0.0	0	-	-	0	0	0.000
15	0.9	0	100	368	6	52	0.050
30	1.3	0	100	266	9	50	0.057
45	1.5	0	100	204	13	40	0.074
60	1.9	0	100	194	20	33	0.069
90	2.5	0	100	170	34	34	0.072

Benzyl alcohol oxidation reaction conditions: Catalyst (0.01 g), MeOH (7.13 g), benzyl alcohol (1.04 g, 9.62 mmol), mesitylene (0.42 g), 5% H_2/CO_2 (420 psi, 2.76 mmol), 25% O_2/CO_2 (160 psi, 5.24 mmol), 0.5 hr, 50 ^{O}C, 1200 rpm.

Table A3.6. Sequential reactions of 0.5%Fe-0.5%Pd/Al_2O_3 in the selective oxidation of benzyl alcohol via In-Situ H_2O_2 synthesis

Reaction Number	Benzaldehyde Yield (%)	Additional Benzaldehyde Yield (%)	Benzoic Acid Yield (%)	Selectivity to Benzaldehyde (%)	Turnover Number (mol_{BA} mol_{metal}^{-1} hr^{-1})	H_2 Conversion (%)	H_2 Selectivity (%)	Residual H_2O_2 (mmol)
1	10.0	10.0	0.3	97	1406	38	95	0.075
2	19.7	9.7	0.7	97	1385	41	89	0.071
3	27.4	7.7	0.8	97	1285	33	83	0.090
4	33.4	6.0	1.0	97	1174	29	77	0.094

Benzyl alcohol oxidation reaction conditions: Catalyst (0.01 g), MeOH (7.13 g), benzyl alcohol (1.04 g, 9.62 mmol), mesitylene (0.42 g), 5% H_2/CO_2 (420 psi, 2.76 mmol), 25% O_2/CO_2 (160 psi, 5.24 mmol), 0.5 hr, 50 ^{O}C, 1200 rpm.

Table A3.7. Sequential reactions of 0.5%Au-0.5%Pd/Al_2O_3 in the selective oxidation of benzyl alcohol via In-Situ H_2O_2 synthesis

Reaction Number	Total Benzaldehyde Yield (%)	Additional Benzaldehyde Yield (%)	Benzoic Acid Yield (%)	Selectivity to Benzaldehyde (%)	Turnover Number (mol_{BA} mol_{metal}^{-1} hr^{-1})	H_2 Conversion (%)	H_2 Selectivity (%)	Residual H_2O_2 (mmol)
1	11.0	11.0	0	100	2919	50	77	0.161
2	20.7	9.7	0.5	98	2746	48	74	0.138
3	26.6	5.9	0.7	97	2352	40	48	0.130
4	32.3	5.7	0.9	97	2142	41	44	0.134

Benzyl alcohol oxidation reaction conditions: Catalyst (0.01 g), MeOH (7.13 g), benzyl alcohol (1.04 g, 9.62 mmol), mesitylene (0.42 g), 5% H_2/CO_2 (420 psi, 2.76 mmol), 25% O_2/CO_2 (160 psi, 5.24 mmol), 0.5 hr, 50 ^{O}C, 1200 rpm.

Table A3.8. Sequential reactions of 1.0%Pd/Al_2O_3 in the selective oxidation of benzyl alcohol via In-Situ H_2O_2 synthesis.

Reaction Number	Benzaldehyde Yield (%)	Additional Benzaldehyde Yield (%)	Benzoic Acid Yield (%)	Selectivity to Benzaldehyde (%)	Turnover Number (mol_{BA} mol_{metal}^{-1} hr^{-1})	H_2 Conversion (%)	H_2 Selectivity (%)	Residual H_2O_2 (mmol)
1	1.3	1.3	0	100	266	9	50	0.057
2	2.1	0.8	0	100	215	10	27	0.082
3	3.0	0.9	0	100	204	8	41	0.081
4	3.8	0.8	0	100	194	7	39	0.080

Benzyl alcohol oxidation reaction conditions: Catalyst (0.01 g), MeOH (7.13 g), benzyl alcohol (1.04 g, 9.62 mmol), mesitylene (0.42 g), 5% H_2/CO_2 (420 psi, 2.76 mmol), 25% O_2/CO_2 (160 psi, 5.24 mmol), 0.5 hr, 50 ^{O}C, 1200 rpm.

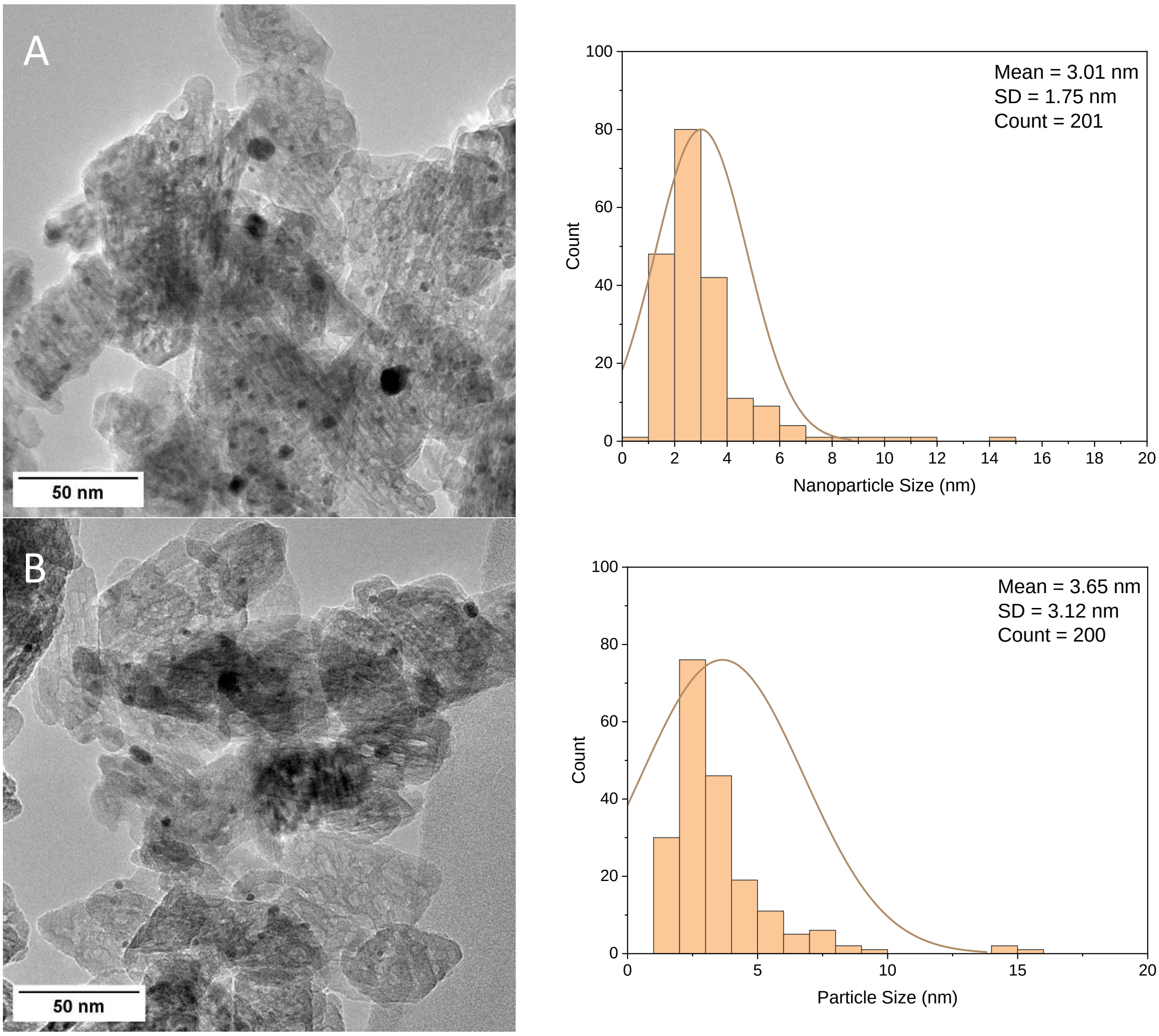

Figure A3.6. TEM images and particle size distributions of A) 0.5%Au-0.5%Pd/Al_2O_3 Fresh and B) 0.5%Au-0.5%Pd/Al_2O_3 Used.

4. The Effects of Preparation Methodology of Supported Pd Based Catalysts on the Selective Oxidation of Benzyl Alcohol via in-situ H_2O_2 Synthesis

4.1 Introduction

In Chapter 3, investigations were focussed largely on improving the activity of Pd-based catalysts towards the selective oxidation of benzyl alcohol via in-situ H_2O_2 synthesis, through optimising support materials, secondary or tertiary metals, and active metal ratios. However, the catalysts developed in this earlier body of work proved to be unstable under the conditions of the reaction. Therefore, further development will be needed in future work to improve the stability and reusability of this class of catalysts. In Chapter 3, catalysts were prepared exclusively using an excess chloride co-impregnation methodology in order to follow on from previous work on this type of reaction.[27, 218] As discussed in Chapter 3, Brehm *et al.* have previously studied a 0.5%Au-0.5%Pd/TiO_2 catalyst by an identical excess chloride co-impregnation methodology to that used in this work and observed a loss of activity in the H_2O_2 direct synthesis reaction upon re-use, which the authors attributed primarily to the loss of chloride surface species in-situ.[232] Indeed, similar observations were made in Chapter 3 of this study, with a deactivation of the 0.5%Au-0.5%Pd/Al_2O_3 catalyst towards the selective oxidation of benzyl alcohol via in-situ H_2O_2 synthesis, correlating with the loss of surface chloride, as identified by XPS.

Numerous other preparation methodologies have been utilised for catalysts that have subsequently been used in the direct synthesis of H_2O_2, with sol immobilisation and wet co-impregnation representing two ubiquitous and easily accessible methods.[46, 71, 226, 260, 261] AuPd catalysts prepared by sol immobilisation have been reported be highly active in the direct synthesis of H_2O_2, and to experience only a limited degree of deactivation upon re-use,[238] or even a subsequent enhancement to H_2O_2 productivity upon re-use.[58] Therefore, the possibility exists for a class of stable sol immobilisation catalysts to be developed for the benzyl alcohol oxidation via in-situ H_2O_2 synthesis, although the reusability of catalysts prepared by sol immobilisation was not investigated in this chapter. Alternatively, a wet co-impregnation methodology would provide an identical catalyst preparation procedure to the excess chloride method, but with lower quantities of additional Cl^-. Sankar *et al.* have previously demonstrated that a 0.5%Au-0.5%Pd/TiO_2 catalyst offered significantly enhanced levels of H_2O_2 productivity when prepared by an excess chloride co-impregnation method and reduced under flowing H_2, compared to a wet co-impregnation method which was subsequently oxidised in static air.[262] However, the authors did not create a reduced analogue of the wet co-impregnation catalyst and as previously discussed, the oxidation state of Pd is known to be highly significant in the direct synthesis of H_2O_2.[42] Therefore, the possibility remains for a highly active AuPd/Al_2O_3 catalyst to be synthesised using a wet co-impregnation methodology with a reductive heat treatment. Additionally, investigations into this class of catalyst could also help to elucidate the role of surface and solvated chloride in the selective oxidation of benzyl alcohol via in-situ H_2O_2 synthesis, which has thus far not been investigated in the literature.

Overall, the objective of the work presented in this chapter was to examine the effects of the preparation method and heat treatment of supported AuPd catalysts on their resultant catalytic activity towards the selective oxidation of benzyl alcohol via in-situ H_2O_2 synthesis. As previously discussed, factors such as Pd oxidation state, nanoparticle size and the presence of chloride during both catalyst preparation and during chemical reactions have been shown to be significant factors in the direct synthesis of H_2O_2 and it remains unclear to what extent these factors affect the oxidation of benzyl alcohol via in-situ H_2O_2 synthesis, these factors may be influenced by the method of catalyst preparation. Additionally, no publications have been released to date examining the effect of catalyst preparation method on the selective oxidation of benzyl alcohol via in-situ H_2O_2 synthesis, and beginning to explore this avenue of research is the primary motivation of this study.

4.2 The Effects of Preparation Method of a 0.5%Au-0.5%Pd/Al_2O_3 Catalyst on the Direct Synthesis of H_2O_2 and the Selective Oxidation of Benzyl Alcohol via in-situ H_2O_2 Synthesis

Firstly, the effects of both preparation method and oxidative versus reductive heat treatments were investigated using a 0.5%Au-0.5%Pd/Al_2O_3 catalyst. In terms of preparation methods, wet co-impregnation (C.Imp) and sol immobilisation (Sol) methodologies were compared to the previously used excess-chloride co-impregnation (EcI) method, previously studied in Chapter 3. These methods were selected for the reasons discussed in the introduction section, and for their simple preparation methodology, making them potentially highly desirable for industrial use. In addition to this, the effects of an oxidative (Ox) versus reductive (Red) heat treatment process were investigated because of the previously discussed strong link between Pd oxidation state and catalytic activity in the H_2O_2 synthesis reaction. A key outlining the abbreviations associated with each preparation method and heat treatment combination under investigation is shown in Table 4.1.

Table 4.1. Key describing preparation methods and heat treatments with their associated abbreviations.

Abbreviation	Preparation Method	Heat Treatment Atmosphere	Conditions
C.Imp Red	Wet Co-impregnation	Reduction, 5% H_2/Ar	500 °C, 4hr, 10 °C/min
C.Imp Ox	Wet Co-impregnation	Oxidation, Compressed Air	500 °C, 4hr, 10 °C/min
ECI Red	Excess Chloride Co-Impregnation	Reduction, 5% H_2/Ar	500 °C, 4hr, 10 °C/min
Sol Red	Sol Immobilisation	Reduction, 5% H_2/Ar	500 °C, 4hr, 10 °C/min
Sol Ox	Sol Immobilisation	Oxidation, Compressed Air	500 °C, 4hr, 10 °C/min

Firstly, 0.5%Au-0.5%Pd/Al_2O_3 catalysts were prepared through a C.Imp methodology previously reported in the literature,[132] and heat treated under either flowing 5% H_2/Ar (Red) or under flowing compressed air (Ox). Analogous AuPd/Al_2O_3 catalysts were also prepared using a previously reported sol-immobilisation methodology,[263] and heat treated under either of the reductive or oxidative conditions. These were then compared to the standard 0.5%Au-0.5%Pd/Al_2O_3 catalyst prepared through the EcI method from Chapter 3, which was heat treated under reductive conditions.

These catalysts were then utilised in the direct synthesis of H_2O_2, the results of which are shown in Figure 4.1 and Table 4.2.

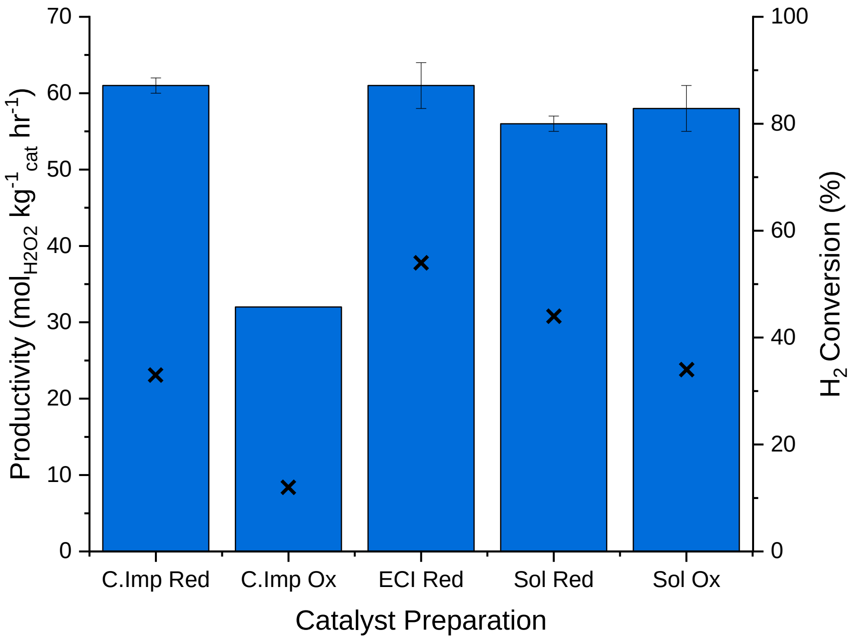

Figure 4.1. Comparison of the catalytic activities of supported 0.5%Au-0.5%Pd/Al_2O_3 in the direct synthesis of H_2O_2, using different preparation methods and heat treatments.

Key; productivity (blue bars), H_2 conversion (crosses)

H_2O_2 direct synthesis reaction conditions: Catalyst (0.01 g), H_2O (2.9 g), MeOH (5.6 g), 5% H_2/CO_2 (420 psi, 2.76 mmol), 25% O_2/CO_2 (160 psi, 5.24 mmol), 0.5 hr, 20 °C, 1200 rpm.

Table 4.2. Comparison of the catalytic activities of supported 0.5%Au-0.5%Pd/Al_2O_3 in the direct synthesis of H_2O_2 using different preparation methods and heat treatments.

Catalyst	Preparation Method	Productivity (mol_{H2O2} kg^{-1}_{cat} hr^{-1})	H_2 Conversion (%)	H_2O_2 Selectivity (%)	H_2O_2 Concentration (wt. %)
AuPd/Al_2O_3	Wet Co-impregnation/ Reduced	61	33	34	0.12
AuPd/Al_2O_3	wet Co-impregnation/ Oxidised	31	12	58	0.06
AuPd/Al_2O_3	Excess Chloride Co-Impregnation/ Reduced	61	54	19	0.12
AuPd/Al_2O_3	Sol Immobilisation/ Reduced	56	44	23	0.11
AuPd/Al_2O_3	Sol Immobilisation/ Oxidised	58	34	31	0.12

H_2O_2 direct synthesis reaction conditions: Catalyst (0.01 g), H_2O (2.9 g), MeOH (5.6 g), 5% H_2/CO_2 (420 psi, 2.76 mmol), 25% O_2/CO_2 (160 psi, 5.24 mmol), 0.5 hr, 20 °C, 1200 rpm.

In the direct synthesis of H_2O_2, no preparation method was able to offer an enhancement in H_2O_2 productivity compared to the AuPd/Al_2O_3 catalyst prepared by the EcI method. For example, an AuPd/Al_2O_3 catalyst, when prepared by C.imp Red, ECI Red and Sol Red offered productivity values of 61, 61 and 56 mol_{H2O2} kg^{-1}_{cat} hr^{-1} respectively. The Sol Ox catalyst offered a productivity of 58 mol_{H2O2} kg^{-1}_{cat} hr^{-1}, whereas the C.Imp Ox catalyst was significantly less active and offered a limited productivity of 31 mol_{H2O2} kg^{-1}_{cat} hr^{-1}. The low activity of the C.Imp Ox catalyst appears consistent with the work of Sankar *et al.* who observed similarly limited activity for the analogous 0.5%Au-0.5%Pd/TiO_2 catalyst when prepared by this methodology and oxidative heat treatment.[262]

Additionally, reduced catalysts appeared to convert greater levels of H_2 than their oxidised analogues. For example, the C.Imp Red catalyst offered an H_2 conversion of 33 %, compared to the 12 % offered by the C.Imp Ox catalyst, whilst the Sol Red catalyst consumed 44 % of the available H_2 compared to the 34 % consumed by the Sol Ox catalyst.

Comparisons of the H_2O_2 selectivity offered by each catalyst cannot be made from these data because iso-conversions of H_2 are required for a valid comparison of selectivity, and the majority of catalyst offered different levels of H_2 conversion over the 30-minute reaction time. To compare the H_2O_2 selectivity offered by each catalyst, future work should also compare different catalysts at iso-conversion of H_2. Additionally, conducting H_2O_2 degradation reactions for each catalyst would allow for a direct comparison of the ability of each catalyst to degrade H_2O_2. These metrics might provide additional information on any possible link between the direct synthesis of H_2O_2 and the selective oxidation of benzyl alcohol via in-situ H_2O_2 synthesis.

XPS analysis, conducted by Dr David Morgan (Cardiff Catalysis Institute) revealed the relative ratios of surface Pd^0 and Pd^{2+} for each catalyst before use, as shown in Table 4.3.

Table 4.3. Effects of preparation method and heat treatment on the oxidation state of surface Pd of 0.5%Au-0.5%Pd/Al_2O_3 as determined by XPS analysis.[a]

Catalyst	Preparation Method	Heat Treatment	Pd^0:Pd^{2+}
AuPd/Al_2O_3	wet co-impregnation	Reduced	0.36: 0.74
AuPd/Al_2O_3	wet co-impregnation	Oxidised	All Pd^{2+}
AuPd/Al_2O_3	Excess Chloride Co-Impregnation	Reduced	0.55: 0.45
AuPd/Al_2O_3	Sol Immobilisation	Reduced[b]	0.74: 0.26
AuPd/Al_2O_3	Sol Immobilisation	Oxidised	0.37: 0.63

[a]Catalysts were exposed to either reductive (5% H_2/Ar, 500 °C, 4 hr, 10°C min^{-1}) or oxidative heat treatments (compressed air, 500 °C, 4hr, 10°C min^{-1}) before XPS analysis.
[b]Catalyst oxidised (compressed air, 500 °C, 4hr, 10°C min^{-1}) prior to a reductive heat treatment (5% H_2/Ar, 500 °C, 4 hr, 10°C min^{-1}) before XPS analysis.

It should be noted that Pd speciation has been demonstrated to change in-situ as a result of the H_2 and O_2 atmosphere utilised in the direct synthesis of H_2O_2.[238]
From the data presented in Table 4.3, it was apparent that when the AuPd/Al_2O_3 catalyst was prepared by any methodology, the oxidation state of surface Pd was influenced by the subsequent heat treatment, but also the preparation method itself. For example, when prepared by the C.Imp method and calcined under flowing air, all Pd was present as Pd^{2+}, but when heat treated under flowing H_2/Ar, the ratio of Pd^0:Pd^{2+} was 0.36:0.64. Conversely the AuPd/Al_2O_3 catalyst prepared by the Sol Ox procedure featured a ratio of Pd^0:Pd^{2+} of 0.37:0.63, demonstrating that reduced Pd^0 was still present on the catalysts surface after calcination. This likely occurred because in this catalyst preparation method, $NaBH_4$ was used to reduce Pd during the catalyst preparation, and before the calcination process.
The greater levels of H_2 conversion offered by the reduced catalysts can be explained through a greater level of Pd^0 present at the catalyst surface, relative to Pd^{2+}. For example, the AuPd/Al_2O_3 catalyst prepared by the C.Imp Red method offered an H_2 conversion of 54 %, whereas the analogous AuPd/Al_2O_3 catalyst prepared by the C.Imp Ox method offered the significantly lower H_2 conversion of 12 %.
Pd^0 has been proposed to be a more active species in H_2O_2 degradation pathways than Pd^{2+} and consequently, heightened levels of Pd^0 can be associated with enhanced levels of degradation of H_2O_2 and the correspondingly greater conversion of H_2 necessary for this.[43, 48, 49, 264]

Ouyang *et al.* have suggested that mixed Pd^o and Pd^{2+} interfaces are highly active sites for the synthesis of H_2O_2, and thus proposed that a mixture of Pd oxidation states are required for efficient synthesis of H_2O_2.[42, 239] Additionally, Flaherty *et al.* also suggested a need for Pd nanoparticles to exist in mixed oxidation states, and the authors reported a significant induction period before H_2O_2 could be synthesised by PdO nanoparticles, whereas no induction period was observed for Pd^o nanoparticles.[51] Therefore, the absence of any surface Pd^0 species on the 0.5%Au-0.5%Pd/Al_2O_3 C.Imp Ox catalyst is a possible reason for its limited activity in the direct synthesis of H_2O_2. Although, it should be noted that under the reaction conditions utilised in the direct synthesis of H_2O_2, the in-situ reduction of Pd is a facile process and Pd based catalysts have been shown to undergo reduction over the course of the direct synthesis reacton, under conditions similar to those used in this work.[265, 266]

Following this, the series of catalysts were utilised in the selective oxidation of benzyl alcohol via in-situ H_2O_2 synthesis, the results of which are shown in Figure 4.2 and Table 4.4.

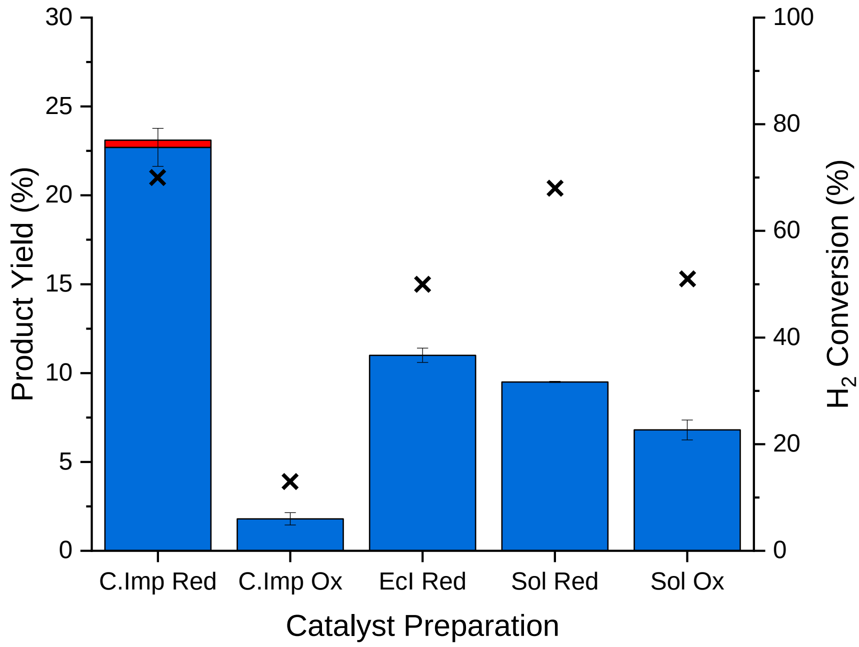

Figure 4.2. Comparison of the catalytic activities of supported 0.5%Au-0.5%Pd/Al_2O_3 on the oxidation of benzyl alcohol via in-situ H_2O_2 synthesis, using different preparation methods and heat treatments. **Key;** Benzaldehyde (blue bars), benzoic acid (red bars), H_2 conversion (crosses).

Benzyl alcohol oxidation reaction conditions: Catalyst (0.01 g), MeOH (7.13 g), benzyl alcohol (1.04 g, 9.62 mmol), mesitylene (0.42 g), 5% H_2/CO_2 (420 psi, 2.76 mmol), 25% O_2/CO_2 (160 psi, 5.24 mmol), 0.5 hr, 50 ^{O}C, 1200 rpm.

Table 4.4. Comparison of the catalytic activities of supported 0.5%Au-0.5%Pd/Al_2O_3 on the oxidation of benzyl alcohol using different preparation methods and heat treatments.

Preparation Method	Benzaldehyde Yield (%)	Benzoic Acid Yield (%)	Benzaldehyde Selectivity (%)	Turnover Number (mol_{BA} mol_{metal}^{-1} hr^{-1})	H_2 Conversion (%)	H_2 Selectivity (%)	Residual H_2O_2 (mmol)
Wet Co-impregnation/ Reduced	22.3	0.4	98	5916	70	113	0.112
Wet Co-impregnation/ Oxidised	1.8	0.0	100	478	13	48	0.029
Excess Chloride Co-Impregnation/ Reduced	11.0	0.0	100	2919	50	77	0.161
Sol Immobilisation/ Reduced	9.5	0.0	100	2520	69	49	0.089
Sol Immobilisation/ Oxidised	6.8	0.0	100	1804	51	46	0.113

Benzyl alcohol oxidation reaction conditions: Catalyst (0.01 g), MeOH (7.13 g), benzyl alcohol (1.04 g, 9.62 mmol), mesitylene (0.42 g), 5% H_2/CO_2 (420 psi, 2.76 mmol), 25% O_2/CO_2 (160 psi, 5.24 mmol), 0.5 hr, 50 ^{O}C, 1200 rpm.

When used in the selective oxidation of benzyl alcohol via in-situ H_2O_2 synthesis, a profound influence on catalytic activity was observed as a result of the preparation method and subsequent heat treatment.

For example, when prepared by the C.Imp Red methodology, AuPd/Al_2O_3 offered a benzaldehyde yield of 22.3 % and an H_2 conversion of 70 %. In stark contrast, the analogous C.Imp Ox catalyst could only achieve a benzaldehyde yield of 1.8 % and an H_2 conversion of 13 %. From this, it is likely that Pd oxidation state plays a significant role in the overall activity of the material. Indeed, a similar but less profound effect was also observed with the sol immobilisation catalysts, wherein the reduced catalyst offered a benzaldehyde yield of 9.5 %, and an H_2 conversion of 69 %, compared to the analogous oxidised catalyst, which offered a benzaldehyde yield of 6.8 %, with an H_2 conversion of 51 %. These observations represent a significant departure from the trends observed under the conditions for the direct synthesis of H_2O_2, wherein only small differences between the H_2O_2 productivity of each catalyst were observed, with the exception of the C.Imp Ox catalyst which also had a significantly lower H_2O_2 synthesis activity.

Overall, the catalysts that were heat treated under reductive conditions were more active for the oxidation of benzyl alcohol than the equivalent oxidised analogues and consumed more H_2.

To investigate further the origins of the different activities for each catalyst, nanoparticle size distributions that resulted from each catalyst preparation method were recorded using transmission electron microscopy (TEM) and are shown in Table 4.5.

Table 4.5. Particle size distributions as determined by TEM, of the 0.5%Au-0.5%Pd/Al_2O_3 catalyst when prepared by different preparation methods and heat treatments. Micrograph images and standard distribution histograms are shown in Figures A3.6, A4.2 and A4.6.

Catalyst Preparation Method	Mean Nanoparticle Size (nm)	Standard Deviation (nm)
C.Imp Red	3.5	2.2
C.Imp Ox	n.d.	n.d.
EcI Red	3.0	1.8
Sol Red	4.6	1.5
Sol Ox	4.5	1.2

When investigated by this technique, catalysts prepared by the sol immobilisation method resulted in nanoparticles with a mean size of 4.5 nm, whilst the C.Imp method resulted in a somewhat smaller mean particle size, with an average size of 3.5 nm. The smallest nanoparticles were formed by the EcI method, which generated nanoparticles with an average size of 3.0 nm. As previously discussed in Chapter 3, whilst no systematic studies investigating the size effects associated with supported AuPd nanoparticles utilised in the selective oxidation of benzyl alcohol via in-situ H_2O_2 synthesis have taken place, such investigations have taken place for both the direct synthesis of H_2O_2 and the aerobic oxidation of benzyl alcohol. For example, Youngjin *et al.* determined that carbon supported Pd nanoparticles with an average size of 3 nm offered the greatest yields of H_2O_2, compared to larger and less catalytically active nanoparticles.[254] Additionally, Tian *et al.* compared a series of Pd/hydroxyapatite catalysts with varying sizes and found that an average nanoparticle size of 1.5 nm offered the greatest selectivity towards H_2O_2 synthesis, and the greatest productivity towards H_2O_2 synthesis, with greater nanoparticle sizes again leading to a reduction in H_2O_2 selectivity and productivity.[53] In terms of the aerobic oxidation of benzyl alcohol, Zhang *et al.* reported that Pd/Al_2O_3 supported nanoparticles with a mean nanoparticle size of 3.6-4.3 nm exhibited an optimal turnover frequency of approximately 2.5 s^{-1} towards the oxidative dehydrogenation of benzyl alcohol.[255] Indeed, an optimal mean nanoparticle size for Pd/Al_2O_3 supported catalysts may also exist for its use in the selective oxidation of benzyl alcohol via in-situ H_2O_2 synthesis, although as stated, this has not yet been investigated in the literature. However, regardless of the preparation method used in this work, the resultant mean nanoparticle size was not hugely affected, with a difference in size of 1.6 nm between the catalysts produced by the Sol Red and EcI Red methodologies.

Additionally, it should be noted that resolution limitations associated with the instrument prevent accurate measurements for sub-nanometre particles and represents a limitation of this type of analysis.

XPS analysis conducted by Dr David Morgan (Cardiff Catalysis Institute) revealed the relative ratios of Pd^0 and Pd^{2+} present at the surface of the catalyst, as shown in Table 4.3. As previously noted, $AuPd/Al_2O_3$ when prepared by the C.Imp Red methodology featured a surface ratio of Pd^0:Pd^{2+} of 0.36:0.64, whereas the analogous C.Imp Ox catalyst featured only Pd^{2+} at the catalyst surface. However, the Sol Ox catalyst had a near identical ratio of surface Pd^0:Pd^{2+}, at 0.37:0.63, but offered a more limited conversion of benzyl alcohol of 6.8 %, compared to the C.Imp Red catalyst which offered a benzyl alcohol conversion of 22.3 %. Therefore, factors beyond the oxidation state of Pd likely also played a significant role in the benzyl alcohol oxidation reaction, such as nanoparticle size. Indeed, the AuPd catalyst synthesised via the Sol Ox method had a mean nanoparticle size of 4.45 nm, whereas for the C.Imp Red method, this was 3.47 nm. Whilst this difference of approximately 1 nm is only limited, it may be a contributing factor to the observed differences in catalytic activity.
In addition to nanoparticle size effects, it must also be considered that for the selective oxidation of benzyl alcohol via in-situ H_2O_2 synthesis, the oxidation state of surface Pd can change in-situ. This has been previously reported by Crombie *et al.* who observed a continual reduction of surface Pd sites as a function of time, from Pd^{2+} to Pd^0 under reaction conditions identical to those used herein.[218]
XPS analysis conducted by Dr David Morgan (Cardiff Catalysis Institute) which is shown in Figure A4.1, determined that whilst surface chloride is present on all catalysts prepared by either the C.Imp or EcI methodology, regardless of heat treatment protocol, neither sol catalysts appeared to have any surface chloride observable by XPS. This is likely a result of the preparation methodology associated with sol immobilisation, wherein a given catalyst is washed with deionised water (2 L) prior to the heat treatment step. Despite this lack of initial surface chloride, both the Sol Red and Sol Ox catalysts offer moderate yields of benzaldehyde, at 9.5 % and 6.8 % respectively, indicating that the presence of chloride in the reaction mixture is not necessary for either the synthesis of H_2O_2 or the oxidation of benzyl alcohol to take place. This observation further demonstrates the need for a systematic investigation into the effects of chloride incorporation in both the catalyst synthesis process and within the reaction mixture itself.

All catalysts proceeded with 100 % selectivity to benzaldehyde, except for the C.Imp Red catalyst, which had a product selectivity of 98.3 %, due to a small quantity of over-oxidation to benzoic acid. No other reaction products were observed, including toluene, benzene or benzyl benzoate. Surprisingly, the C.Imp Red catalyst offered an H_2 selectivity of 113 % towards benzyl alcohol conversion, assuming that the stoichiometry of H_2 consumption to product formation is a ratio of 1:1. This H_2 selectivity value includes the formation of both benzaldehyde and benzoic acid. This strongly suggests that a moderate contribution from O_2 may be occurring, or activation of benzyl alcohol by the catalyst. Generally, higher temperatures are used for the aerobic oxidation of benzyl alcohol, with temperatures in the range of 80-120^{o}C typical,[96, 102, 267-269] and a strong dependence on reaction temperature has been reported for benzyl alcohol conversion under aerobic conditions, with a significant loss in conversion associated with lower temperatures.[267-269] Additionally, Crombie *et al.* observed only minimal catalytic activity at 50 °C under aerobic conditions for an analogous 0.5%Au-0.5%Pd/TiO_2 catalyst, which offered less than 0.5 % conversion of benzyl alcohol, compared to 2.8 % conversion of benzyl alcohol when an H_2 and O_2 mixture was used.[218] Therefore, any significant extent of oxidation by O_2 would be an important observation, and this will be investigated in Section 4.4. Alternatively, some extent of activation of benzyl alcohol by the catalyst, via an initial hydrogen abstraction step could be taking place. This would alter the stoichiometry of the reaction with respect to H_2 and therefore also alter the H_2 selectivity. Indeed, formation of the benzyl alcohol radical by an AuPd/TiO_2 catalyst in the absence of H_2 and O_2 has been reported previously,[218] though it is unclear to what extent this may occur in the presence of the reactant gasses.

4.3 Comparison of Pd based Catalysts Prepared through Wet Co-impregnation and Excess Chloride Co-Impregnation Methodologies When Used in the Direct Synthesis of H_2O_2 and the Selective Oxidation of Benzyl Alcohol via in-situ H_2O_2 Synthesis

Due to the clear and profound enhancements associated with the C.Imp Red 0.5%Au-0.5%Pd/Al_2O_3 catalyst towards the selective oxidation of benzyl alcohol, compared to the previously used AuPd catalyst prepared by the EcI method, further study and development using catalysts prepared by the C.Imp Red method was undertaken. This C.Imp Red preparation method was then used to prepare the equivalent 1.0%Pd and 0.5%Pd monometallic catalysts, and an analogous 0.5%Fe-0.5%Pd/Al_2O_3 catalyst to that used in Chapter 3 that was also moderately active when prepared by the EcI methodology. These catalysts were then utilised in the direct synthesis of H_2O_2, the results of which are shown in Figure 4.3 and Table 4.6.

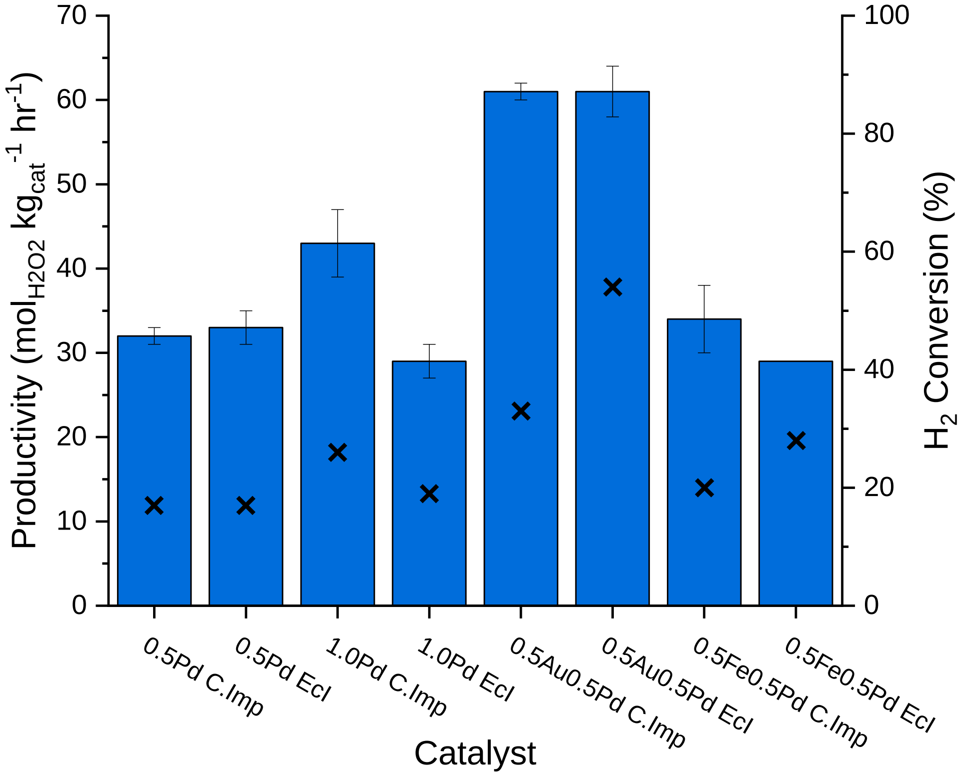

Figure 4.3. Comparison of the catalytic activities of supported Pd, AuPd and FePd/Al_2O_3 catalysts in the direct synthesis of H_2O_2, using the C.Imp Red and EcI catalyst preparation methods.
Key; Productivity (blue bars), H_2 conversion (crosses).
H_2O_2 direct synthesis reaction conditions: Catalyst (0.01 g), H_2O (2.9 g), MeOH (5.6 g), 5% H_2/CO_2 (420 psi, 2.76 mmol), 25% O_2/CO_2 (160 psi, 5.24 mmol), 0.5 hr, 20 °C, 1200 rpm.

Table 4.6. Comparison of the catalytic activities of supported Pd, AuPd and FePd/Al_2O_3 catalysts on the direct synthesis of H_2O_2 the C.Imp Red and EcI catalyst preparation methods.

Catalyst	Productivity (mol$_{H2O2}$ kg$^{-1}_{cat}$ hr^{-1})	Turnover Number (mol$_{H2O2}$ mol$_{metal}^{-1}$ hr^{-1})	H_2 Conversion (%)	H_2O_2 Selectivity (%)	H_2O_2 Concentration (wt. %)
0.5Pd C.Imp	32	683	17	33	0.07
0.5Pd EcI	33	702	17	33	0.07
1.0Pd C.Imp	43	459	26	30	0.09
1.0Pd EcI	29	309	19	28	0.06
0.5Au-0.5Pd C.Imp	61	849	33	34	0.12
0.5Au/0.5Pd EcI	61	837	54	19	0.12
0.5Fe-0.5Pd C.Imp	34	251	20	30	0.07
0.5Fe-0.5Pd EcI	29	214	19	28	0.06
0.5Au C.Imp	0	0	0	0	0.00
0.5Au EcI	0	0	0	0	0.00

H_2O_2 direct synthesis reaction conditions: Catalyst (0.01 g), H_2O (2.9 g), MeOH (5.6 g), 5% H_2/CO_2 (420 psi, 2.76 mmol), 25% O_2/CO_2 (160 psi, 5.24 mmol), 0.5 hr, 20 °C, 1200 rpm.

As previously demonstrated, a strong synergistic effect was observed when Au was incorporated with Pd on the support, compared to a Pd monometallic catalyst, such that both the productivity and H_2 conversion were enhanced for the 0.5%Au-0.5%Pd/Al_2O_3 catalyst compared to both the 1.0%Pd and 0.5%Pd catalysts. For example, the 0.5%Au-0.5%Pd/Al_2O_3 catalyst offered a productivity of 61, compared to a productivity of 43 offered by the 1.0%Pd/Al_2O_3 catalyst and 32 by the 0.5%Pd/Al_2O_3 catalyst.

As previously observed, the effects of the C.Imp Red preparation methodology compared to the EcI methodology on the direct synthesis of H_2O_2 are very limited. All catalysts when prepared by the C.Imp Red methodology offered approximately equivalent levels of H_2O_2 productivity compared to the analogous EcI catalysts. However, the effect on H_2 on conversion was more significant, with both the 0.5%Au-0.5%Pd/Al_2O_3 and 0.5%Fe-0.5%Pd/Al_2O_3 catalysts converting lower levels of H_2 when prepared by the C.Imp Red methodology. Indeed, the 0.5%Au-0.5%Pd/Al_2O_3 catalysts converted 54 % of H_2 when prepared by the EcI method, but only 33 % when prepared by the C.Imp Red method. However, this was not observed for all catalysts, and both the 1.0%Pd and 0.5%Pd C.Imp Red catalysts offered either equivalent or greater levels of H_2 conversion than their EcI analogues.

The effects of additional halide ions, such as Cl^- in the direct synthesis of H_2O_2 has been previously investigated in the literature, with their use often associated with enhanced yields of H_2O_2.[40, 88, 92, 251] One mechanism by which this has been suggested to occur is through the inhibition of H_2O_2 degradation pathways that result in H_2O formation. As previously discussed, it has been suggested that Cl^- may inhibit the scission of the O_2 bond, through either blocking highly active Pd sites, or through electronic modification of the catalyst.[88] Therefore, XPS analysis was conducted by Dr David Morgan to determine the relative surface abundance of chloride for each catalyst under investigation, as shown in Table 4.7.

Table 4.7. Relative abundance of surface chloride as a function of preparation methodology as determined by XPS analysis.

Catalyst[a]	**Preparation Methodology**	**Relative Abundance of Surface Chloride (%)**
1.0Pd	C.Imp Red	0.21
1.0Pd	EcI	0.19
0.5Pd	C.Imp Red	0.15
0.5Pd	EcI	0.16
0.5Au%-0.5Pd%	C.Imp Red	0.16
0.5Au%-0.5Pd%	EcI	0.18
0.5Fe%-0.5Pd%	C.Imp Red	0.25
0.5Fe%-0.5Pd%	EcI	0.27

[a]Catalysts were exposed to a reductive heat treatment (5% H_2/Ar, 500 °C, 4 hr, 10°C min^{-1}) prior to XPS analysis.

Interestingly, the preparation method had only a minimal effect on the level of surface chloride present on a given catalyst, with most catalysts having near identical levels of chloride, as observed via XPS to its corresponding analogue. For example, the 0.5%Au-0.5%Pd catalyst was observed to have a chloride surface abundance of either 0.16% or 0.18%, when prepared by either the C.Imp Red or EcI methodologies respectively.

This may be surprising given the greater levels of HCl utilised in the excess chloride co-impregnation methodology, compared to that utilised in the wet co-impregnation methodology. Specifically, the $PdCl_2$ precursor solution used in the catalyst preparation method by the excess chloride method holds a concentration of HCl of 0.58 M, whereas the $PdCl_2$ precursor solution used to prepare catalyst by the wet co-impregnation methodology only had an HCl concentration of 0.12 M.

This observation demonstrates that the lower levels of H_2 conversion exhibited by the 0.5%Au-0.5%Pd/Al_2O_3 and 0.5%Fe-0.5%Pd/Al_2O_3 catalysts when prepared by the C.Imp Red methodology may instead be a consequence of nanoparticle dispersion and Pd oxidation state arising from the effects of chloride during catalysts synthesis, and not an additive effect of chloride on the reaction itself.

Sankar *et al.* have previously investigated the relationship between the concentration of HCl during catalyst synthesis and the H_2O_2 productivity of the resultant AuPd/TiO_2 catalyst.[262] They determined that greater levels of HCl present in the metal deposition step of catalyst synthesis resulted in greater levels of H_2O_2 productivity, but that catalysts prepared in a medium containing higher concentrations of HCl were not stable to re-use.[262] To explain this enhanced activity, the authors suggested that the presence of greater concentrations of HCl may improve Pd dispersion by a mechanism of competitive binding to the support material.[262] Alternatively, the authors proposed that an excess of Cl^- might facilitate the formation of $[AuCl_4]^-$ and $[PdCl_4]^{2-}$ species, which they suggested could be optimal precursor species in the catalysts synthesis.[262]

The average nanoparticle size of the 0.5%Au-0.5%Pd/Al_2O_3 catalysts used in this work, when prepared by the C.Imp Red. Method, compared to the EcI method (Table 4.5) did not appear to change to any significant level because of the preparation method used, and only resulted in a decrease in average nanoparticle size of 0.46 nm.

Additionally, it must be considered that one reason for the observed similarities between the different catalyst preparation methods in terms of H_2O_2 productivity may be due to the ambient reaction temperatures utilised. H_2O_2 synthesis reactions in the literature are often carried out at 2 ^oC, but in this work they were conducted at 20 ^oC. As previously discussed, at elevated reaction temperatures, the H_2O_2 degradation reaction pathways are greatly enhanced, and any effect associated with the presence of chloride in catalysts synthesis, or in the reaction mixture might be dwarfed by the effects of increased reaction temperature.

These catalysts were then examined in the selective oxidation of benzyl alcohol via in-situ H_2O_2 synthesis and compared with their analogous catalysts prepared by the EcI method, which is shown in Figure 4.4 and Table 4.8.

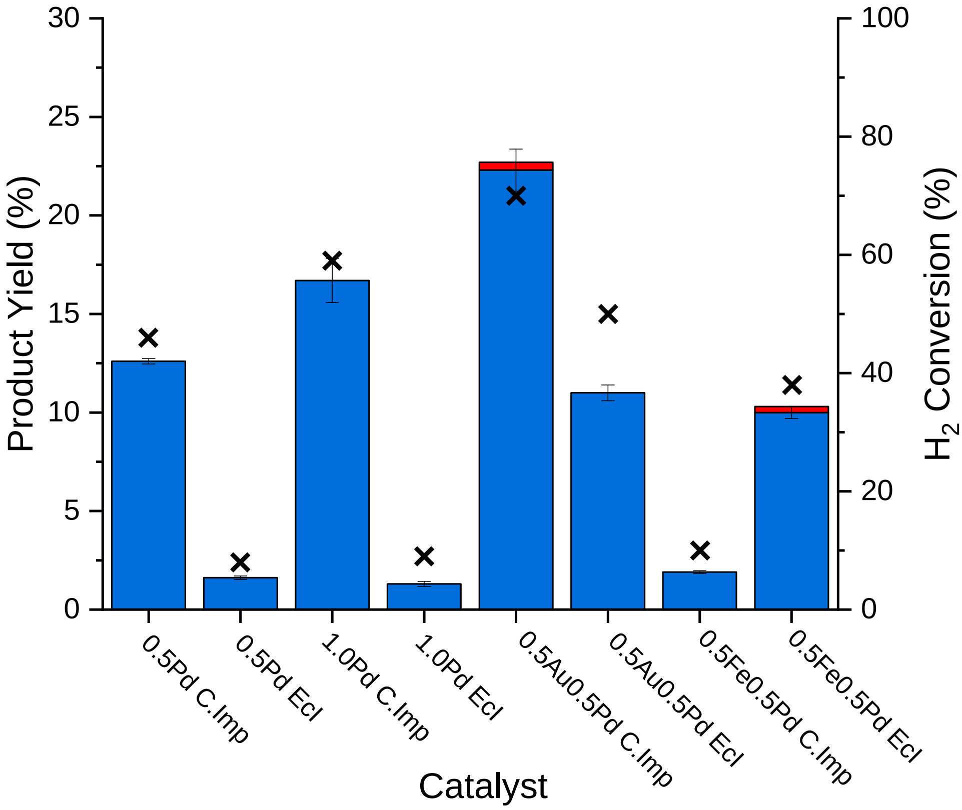

Figure 4.4. Comparison of the catalytic activities of supported Pd, AuPd and FePd/Al_2O_3 catalysts in the oxidation of benzyl alcohol using the C.Imp Red and EcI catalyst preparation methods.

Key; Benzaldehyde (blue bars), benzoic acid (red bars), H_2 conversion (crosses).

Benzyl alcohol oxidation reaction conditions: Catalyst (0.01 g), MeOH (7.13 g), benzyl alcohol (1.04 g, 9.62 mmol), mesitylene (0.42 g), 5% H_2/CO_2 (420 psi, 2.76 mmol), 25% O_2/CO_2 (160 psi, 5.24 mmol), 0.5 hr, 50 ^{O}C, 1200 rpm.

Table 4.8. Comparison of the catalytic activities of supported Pd, AuPd and FePd/Al_2O_3 catalysts on the oxidation of benzyl alcohol using the C.Imp Red and EcI catalyst preparation methods.

Catalyst	Preparation Method	Benzyl Alcohol Conversion (%)	Benzaldehyde Yield (%)	Benzoic Acid Yield (%)	Turnover Number ($mol_{benzaldehyde}$ mol_{metal}^{-1} hr^{-1})	H_2 Conversion (%)	H_2 Selectivity (%)	Residual H_2O_2 (mmol)
0.5Pd	C.Imp Red	12.6	12.6	0.0	5149	46	97	0.119
0.5Pd	EcI	1.6	1.6	0.0	654	8	70	0.063
1.0Pd	C.Imp Red	16.7	16.7	0.0	3412	59	99	0.117
1.0Pd	EcI	1.3	1.3	0.0	266	9	50	0.057
0.5Au/0.5Pd	C.Imp Red	22.7	22.3	0.4	5916	70	113	0.112
0.5Au/0.5Pd	EcI	11.0	11.0	0.0	2919	50	77	0.161
0.5Fe/0.5Pd	C.Imp Red	1.9	1.9	0.0	267	10	66	0.061
0.5Fe/0.5Pd	EcI	10.3	10.0	0.3	1406	38	95	0.075

Benzyl alcohol oxidation reaction conditions: Catalyst (0.01 g), MeOH (7.13 g), benzyl alcohol (1.04 g, 9.62 mmol), mesitylene (0.42 g), 5% H_2/CO_2 (420 psi, 2.76 mmol), 25% O_2/CO_2 (160 psi, 5.24 mmol), 0.5 hr, 50 ^{O}C, 1200 rpm.

In general, a remarkable enhancement in activity was observed when catalysts were prepared by the C.Imp Red methodology. Indeed, the 0.5%Au-0.5%Pd C.Imp catalyst, and both 0.5%Pd and 1%Pd C.Imp catalysts delivered high levels of benzaldehyde yield, far in excess of those attainable when catalysts were prepared by the EcI method. For example, a 1%Pd catalyst prepared through the EcI methodology gave a benzaldehyde yield of 1.3 %, compared to a 16.7 % yield when prepared through the C.Imp Red methodology. The 0.5%Pd C.Imp catalyst proved to also be an active catalyst, delivering a benzaldehyde yield of 12.6 %. Incorporating Au into this catalyst again delivered enhancements to the yields of benzaldehyde attainable when compared to the 1%Pd and 0.5%Pd monometallic catalysts, with the 0.5%Au-0.5%Pd C.Imp catalyst offering a benzaldehyde yield of 22.3 %.

This observation was unexpected, given the generally similar performances of each C.Imp Red catalyst with its EcI analogue in the direct synthesis of H_2O_2. As previously discussed, the only difference between either preparation technique is the concentration of HCl present during the metal deposition step of catalysts synthesis. Additionally, as shown in Table 4.7, the concentration of Cl^- present on the surface of the catalysts after heat treatment is generally close to identical for either preparation method. Therefore, the enhancement in catalytic activity cannot be associated with greater or lower levels of Cl^- introduced into the reaction mixture from the surface of the catalyst.

Analysis of the oxidation states of surface Pd via XPS, performed by Dr David Morgan (Cardiff Catalysis Institute) is shown in Table 4.9.

Table 4.9. Comparison of oxidation states of surface Pd in Pd, AuPd and FePd/Al_2O_3 supported catalysts, as determined by XPS analysis.[a]

Catalyst	Preparation Method	Heat Treatment	Pd^0: Pd^{2+}
0.5Pd	Wet Co-impregnation	Reduced	0.67: 0.33
0.5Pd	Excess Chloride Co-Impregnation	Reduced	0.49: 0.51
1.0Pd	Wet Co-impregnation	Reduced	0.63: 0.37
1.0Pd	Excess Chloride Co-Impregnation	Reduced	0.61: 0.39
0.5Au/0.5Pd	Wet Co-impregnation	Reduced	0.36: 0.64
0.5Au/0.5Pd	Excess Chloride Co-Impregnation	Reduced	0.55: 0.65
0.5Fe/0.5Pd	Wet Co-impregnation	Reduced	0.41: 0.59
0.5Fe/0.5Pd	Excess Chloride Co-Impregnation	Reduced	0.45: 0.55

[a]Catalysts were exposed to a reductive heat treatment (5% H_2/Ar, 500 °C, 4 hr, 10°C min^{-1}) prior to XPS analysis.

From this analysis no correlation can be made between the preparation methodology and the relative ratios of Pd^o and Pd^{2+}. Indeed, all catalysts featured surface Pd in a mixture of oxidation states with broadly similar ratios of Pd^0: Pd^{2+}. Consequently, the enhanced activity associated with the C.Imp Red class of catalysts cannot be assigned to a more optimal ratio of Pd^0: Pd^{2+}.

To further investigate the effects of each preparation method on the properties of the resultant catalysts, diffuse reflectance infrared Fourier transform spectroscopy was performed, using CO as a probe molecule (CO-DRIFTS), as shown in Figure 4.5.

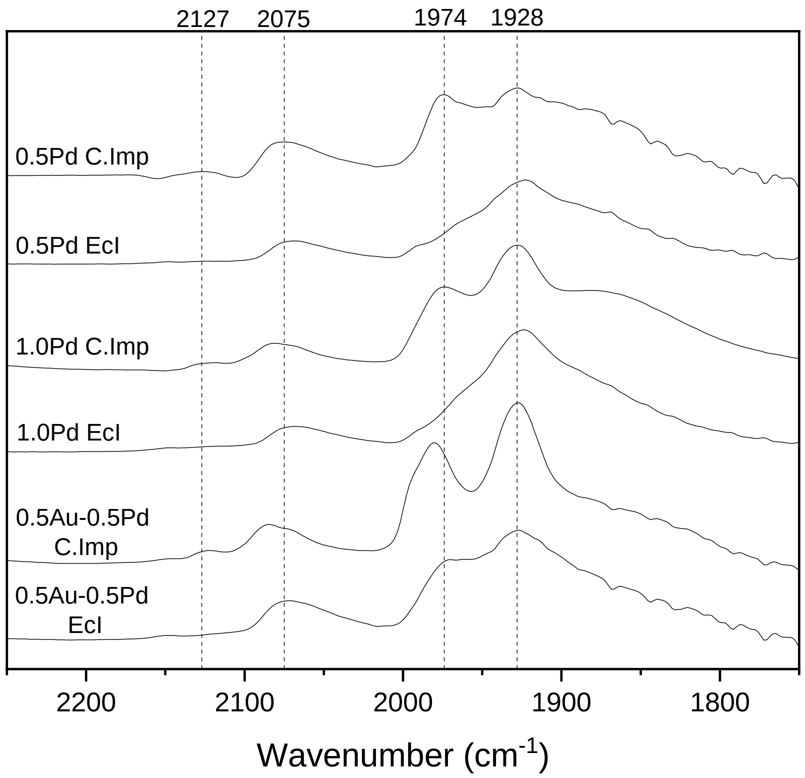

Figure 4.5. CO-DRIFTS spectra comparing analogous Pd and AuPd/Al_2O_3 supported catalysts when prepared by either the C.Imp or EcI catalyst preparation methodologies.

The signal centred on 2075 cm^{-1} can be assigned to the linear adsorption of CO at Pd sites, whilst the broad signals centred on 1974 and 1928 cm^{-1} are the respective result of two-fold bridging and threefold bridging of CO at Pd sites.[240-245] The occurrence of the low intensity absorbance signal at 2127 cm^{-1} has been reported in the literature to correspond to the interaction of CO with residual surface Pd^{2+} ions, stabilised by adjacent surface chloride ions.[242, 245] From the combined spectra, a number of key differences arise as a result of catalyst preparation method . Firstly, the signal centred on 1974 cm^{-1} and assigned to the two-fold bridging of CO is significantly enhanced for all catalysts when prepared by the C.Imp methodology. Indeed, for the 0.5%Pd EcI and 1.0%Pd EcI catalysts, three-fold bridging was strongly preferred, and the signal associated with two-fold bridging is significantly reduced or concealed within the larger envelope.

When considering both AuPd catalysts, whilst the signal assigned to two-fold CO bridging around 1974 cm^{-1} is present in both spectra, it appears with a much greater intensity for the C.Imp catalyst compared to the EcI catalyst, and the signal also appears at a greater wavenumber. This apparent shift in wavenumber cannot necessarily be attributed to any effect of the catalyst on CO binding without disambiguation of the two signals within the overall envelope, due to their overlapping nature. However, two-fold bridging of CO is again clearly promoted by the C.Imp preparation method.

As previously discussed, the position (wavenumber) and relative intensity of each signal may be a result of nanoparticle size[270] or due to electronic effects arising from Au sites adjacent to Pd.[62, 239, 246-248]
Both 0.5%Au-0.5%Pd catalysts exhibit nanoparticles with a very close mean size, suggesting that the overall shift in this signal may be a result of electronic effects.
In the case of the Pd catalysts, it was shown in Chapter 3 that the 1%Pd/Al_2O_3 catalyst prepared by the EcI method was primarily composed of large Pd nanoparticles, many tens of nm in in diameter. Conversely, the 1%Pd/Al_2O_3 prepared through the C.Imp method had an average nanoparticle size of 5.11 nm (Table 4.5).
Therefore, in the case of the 1%Pd C.Imp catalyst, the emergence of this two-fold bridging CO adsorption signal can be considered the result of a better dispersion on Pd nanoparticles, whilst an electron withdrawing effect of Au on adjacent Pd sites, or a superior extent of alloying between Au and Pd may also be contributing to the intensity of this signal observed for the 0.5%Au-0.5%Pd C.Imp catalyst.
The signal centred on 2075 cm^{-1} and associated with the linear adsorption of CO was also influenced by the catalyst preparation methodology. For example, for the 0.5%Pd C.Imp catalyst this signal appears at 2075 cm^{-1} but is red shifted to 2069 cm^{-1} for the 0.5%Pd EcI catalyst. Additionally, the spectrum of the 0.5%Au-0.5%Pd C.Imp catalyst appears to contain overlapping signals in the linear adsorption region, with two maxima observable at 2085 cm^{-1} and 2074 cm^{-1}, whilst a similar feature is also present in the spectrum of the 1%Pd C.imp catalyst. The occurrence of multiple overlapping signals in this region has previously been assigned to a heterogeneous nanoparticle dispersion, resulting in distinct and varied electronic environments dependent on the size of specific nanoparticles.[242]

To further investigate the distribution of nanoparticles in the catalysts prepared by the C.Imp Red methodology, scanning transmission electron microscopy (STEM) and energy-dispersive x-ray spectroscopy (EDX) was conducted by Junhong Liu (Shanghai Jiao Tong University) for the 1%Pd/Al_2O_3 and 0.5%Au-0.5%Pd/Al_2O_3 C.Imp Red catalysts, as shown in Figure 4.6 & 4.7.

A)

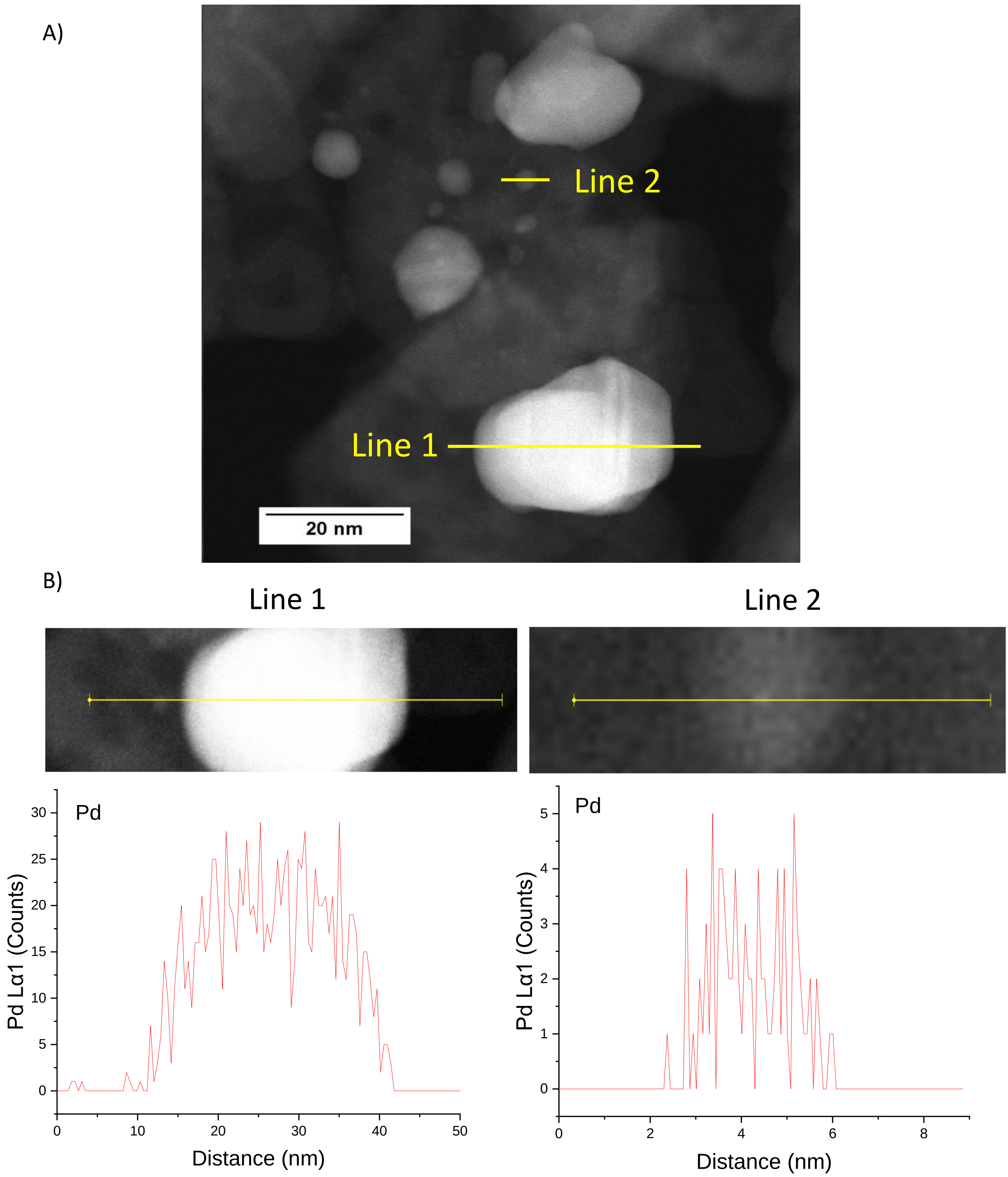

Figure 4.6. A) STEM micrograph of the 1%Pd/Al_2O_3 catalyst prepared by the C.Imp Red method. B) (EDX) linemapping of Pd in line 1 and line 2.

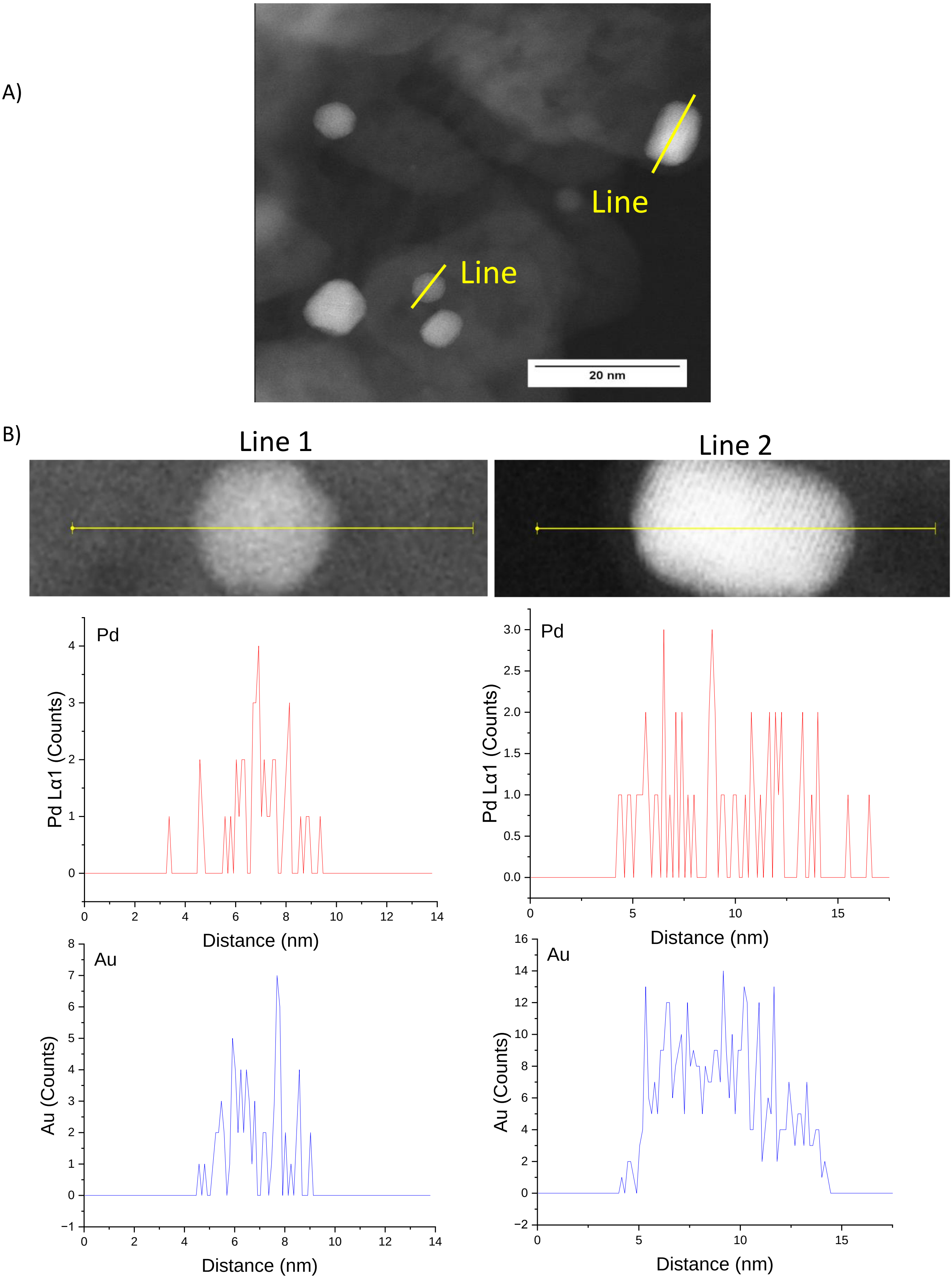

Figure 4.7. A) STEM micrograph of the 0.5%Au-0.5%Pd/Al_2O_3 catalyst prepared by the C.Imp Red method. B) Energy-dispersive x-ray (EDX) linemapping of Pd and Au in line 1 and line 2.
Key; Pd (*red*), Au (*blue*).

For the 1%Pd/Al_2O_3 catalyst, the presence of Pd nanoparticles was confirmed using EDX linescanning, as shown in Figure 4.6 B. From the STEM micrograph shown in Figure 4.6 A, it is clear that Pd is present in a range of particle sizes, ranging from tens of nm to several nm in diameter, with many larger and significantly smaller particles observable.
For the 0.5%Au-0.5%Pd/Al_2O_3 catalyst, the presence of AuPd alloyed nanoparticles was confirmed using EDX linescanning, as shown in Figure 4.7.
Particle size distributions were also determined for the 1%Pd/Al_2O_3 and 0.5%Au-0.5%Pd/Al_2O_3 catalysts, prepared by the C.Imp Red method, via transmission electron microscopy (TEM), and is shown in Table 4.10. Corresponding micrographs and histograms are shown in Section 4.12.

Table 4.10. Particle size distributions observed via TEM of Al_2O_3 supported Pd and AuPd catalysts, prepared by the C.Imp Red methodology.

Catalyst	Mean Nanoparticle Size (nm)	Standard Deviation (nm)
1%Pd/Al_2O_3	5.1	4.8
0.5%Au-0.5%Pd/Al_2O_3	3.5	2.2

For the 1%Pd/Al_2O_3 catalyst, the mean nanoparticle size was 5.1 nm, with a standard deviation of 4.8 nm, whilst the 0.5%Au-0.5%Pd/Al_2O_3 catalyst, had a mean nanoparticle size of 3.5 nm, with a standard deviation of 2.2 nm. This suggests that incorporating Au into the Pd based catalyst decreased both the mean nanoparticle size and reduced the size distribution compared to the 1%Pd/Al_2O_3 catalyst, which featured many larger nanoparticles.

4.4 The Oxidation of Benzyl Alcohol Under Aerobic and Reductive Conditions Using 0.5%Au-0.5%Pd and 1%Pd/Al_2O_3 Catalysts Prepared by the C.Imp Red Methodology

The oxidation of benzyl alcohol via in-situ H_2O_2 synthesis was shown by Crombie *et al.* to result in significantly enhanced yields of benzaldehyde compared to when aerobic oxidation conditions were used under otherwise identical reaction conditions.[218] However, the extent to which the in-situ H_2O_2 synthesis methodology may enhance yields of benzaldehyde over employing aerobic conditions or indeed preformed H_2O_2 was not yet determined for the 0.5%Au-0.5%Pd/Al_2O_3 and 1%Pd/Al_2O_3 catalysts. Therefore, a series of experiments were conducted in which O_2, H_2 and preformed commercial H_2O_2 were used separately and independently in the oxidation of benzyl alcohol, the results of which are shown in Figure 4.8 and Table 4.11.

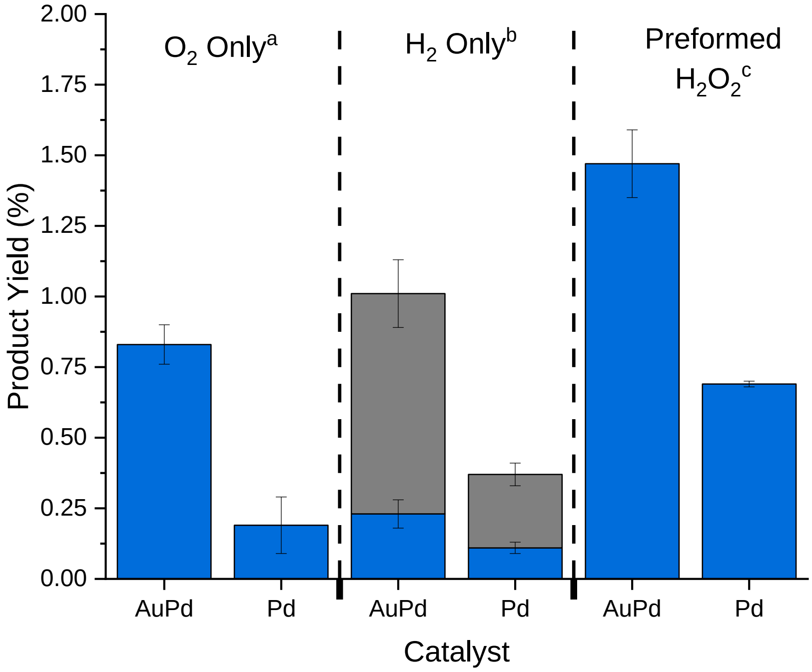

Figure 4.8. Catalytic activity of the 0.5%Au-0.5%Pd and 1.0%Pd/Al_2O_3 catalysts prepared by the C.Imp Red methodology, when using O_2, H_2 or H_2O_2 as reactants in the selective oxidation of benzyl alcohol. **Key;** benzaldehyde yield (*blue bars*), toluene yield (*grey bars)*.

Benzyl alcohol oxidation reaction conditions: [a]Catalyst (0.01 g), MeOH (7.13 g), benzyl alcohol (1.04 g, 9.62 mmol), mesitylene (0.42 g), CO_2 (420 psi), 25% O_2/CO_2 (160 psi, 5.24 mmol), 0.5 hr, 50 °C, 1200 rpm.

[b]Catalyst (0.01 g), MeOH (7.13 g), benzyl alcohol (1.04 g, 9.62 mmol), mesitylene (0.42 g), H_2/CO_2 (420 psi, 2.76 mmol), CO_2 (160 psi), 0.5 hr, 50 °C, 1200 rpm.

[c]Catalyst (0.01 g), MeOH (7.00 g), benzyl alcohol (1.04 g, 9.62 mmol), mesitylene (0.42 g), H_2O_2 (50 wt.%, 0.13 mL, 2.76 mmol), CO_2 (580 psi), 0.5 hr, 50 °C, 1200 rpm.

Table 4.11. Catalytic activity of the 0.5%Au-0.5%Pd and 1.0%Pd/Al_2O_3 catalysts prepared by the C.Imp Red methodology, when using O_2, H_2 or H_2O_2 as a reactant in the selective oxidation of benzyl.

Catalyst	Reaction Conditions	Benzyl Alcohol Conversion (%)	Benzaldehyde Yield (%)	Toluene Yield (%)	Benzaldehyde Selectivity (%)
AuPd	O_2 [a]	0.8	0.8	0.0	100
Pd	O_2 [a]	0.2	0.2	0.0	100
AuPd	H_2 [b]	1.0	0.2	0.8	20
Pd	H_2 [b]	0.4	0.1	0.3	25
AuPd	H_2O_2 [c]	1.5	1.5	0.0	100
Pd	H_2O_2 [c]	0.7	0.7	0.0	100
AuPd	in-situ H_2O_2[d]	22.7	0.4	0.0	98
Pd	in-situ H_2O_2[d]	16.7	0.0	0.0	100

Benzyl alcohol oxidation reaction conditions: [a]Catalyst (0.01 g), MeOH (7.13 g), benzyl alcohol (1.04 g, 9.62 mmol), mesitylene (0.42 g), CO_2 (420 psi), 25% O_2/CO_2 (160 psi, 5.24 mmol), 0.5 hr, 50 ^{o}C, 1200 rpm.

[b]Catalyst (0.01 g), MeOH (7.13 g), benzyl alcohol (1.04 g, 9.62 mmol), mesitylene (0.42 g), H_2/CO_2 (420 psi, 2.76 mmol), CO_2 (160 psi), 0.5 hr, 50 ^{o}C, 1200 rpm.

[c]Catalyst (0.01 g), MeOH (7.00 g), benzyl alcohol (1.04 g, 9.62 mmol), mesitylene (0.42 g), H_2O_2 (50 wt.%, 0.13 mL, 2.76 mmol), CO_2 (580 psi), 0.5 hr, 50 ^{o}C, 1200 rpm.

[d]Catalyst (0.01 g), MeOH (7.13 g), benzyl alcohol (1.04 g, 9.62 mmol), mesitylene (0.42 g), 5% H_2/CO_2 (420 psi, 2.76 mmol), 25% O_2/CO_2 (160 psi, 5.24 mmol), 0.5 hr, 50 ^{O}C, 1200 rpm.

Firstly, the oxidation of benzyl alcohol using O_2 was investigated for both catalysts, in which the 0.5%Au-0.5%Pd catalyst offered a benzaldehyde yield of 0.83 % and the 1%Pd catalyst offered a benzaldehyde yield of 0.19 %. Under the in-situ H_2O_2 synthesis conditions, each catalyst offered a benzaldehyde yield of 22.3 % and 16.7 % respectively, clearly demonstrating the significant enhancements that can be associated with incorporating both H_2 and O_2 into the reaction mixture. When the same experiment was conducted using H_2 as the only gaseous reagent, relatively high quantities of toluene were formed, in addition to only limited quantities of benzaldehyde. Indeed, the 0.5%Au-0.5%Pd catalyst converted 1.01 % of benzyl alcohol but only with a 22.8 % selectivity to benzaldehyde, whilst the 1%Pd catalyst converted only 0.37 % of benzyl alcohol at a similarly low 30% selectivity to benzaldehyde. The formation of toluene is likely the result of hydrogenation of benzyl alcohol, which has been shown to occur using Pd/Al_2O_3 supported catalysts.[271] However, the formation of toluene was not observed under the in-situ H_2O_2 synthesis conditions, demonstrating that this hydrogenation pathway was supressed when both H_2 and O_2 are used in tandem.

Finally, preformed commercial H_2O_2 was used in place of gaseous H_2 or O_2, in order to determine the efficacy of forming H_2O_2 in-situ. The number of moles of H_2O_2 was set to equal the number of moles of H_2 used in the in-situ H_2O_2 synthesis methodology and the total pressure was set to 580 psi with CO_2. When used under these conditions, the 0.5%Au-0.5%Pd/Al_2O_3 catalyst offered a benzaldehyde yield of 1.47 %, whilst the 1%Pd/Al_2O_3 offered a benzaldehyde yield of 0.69 %. Whilst both catalysts formed benzaldehyde with 100 % selectivity, the significantly greater yields offered under the in-situ H_2O_2 synthesis methodology demonstrate the high efficacy of the methodology at 50 ^{o}C compared to the aerobic oxidation route or when preformed H_2O_2 is employed.

It should be noted that directly comparing reactions using H_2 only, O_2 only and preformed H_2O_2 with those using H_2 and O_2 in confunction under the in-situ H_2O_2 synthesis procedure is not necessarily applicable. This is because it has been shown that the in-situ reduction of Pd based catalysts has been shown to occur under the in-situ H_2O_2 synthesis conditions,[218] and confirmed in this work, and results in the formation of increasing levels of Pd^0 as a function of time. Conversely, this clearly will not occur when only O_2 or preformed H_2O_2 are used in the absence of H_2, and therefore the real catalyst taking part in each reaction will feature different ratios of Pd^{2+} and Pd^0 when compared to its analogue in another reaction. This is to say that for example, the total oxidative contribution from O_2 on the oxidation of benzyl alcohol when both H_2 and O_2 are used in tandem under the in-situ H_2O_2 synthesis conditions, cannot be directly inferred from the data presented in Table 4.11.

To investigate this further, a reaction was conducted using the 0.5%Au-0.5%Pd/Al_2O_3 catalyst, wherein the oxidation of benzyl alcohol via in-situ H_2O_2 synthesis was conducted for 30 minutes using the standard H_2 and O_2 mixture. Following this, the gasses were purged and replaced with O_2 but not H_2. This was done to better understand the oxidative ability of O_2 in the presence of the actual reduced in-situ catalyst. Additionally, this was compared to a reference reaction in which both H_2 and O_2 were readded to the reactor. The results of this are shown in Table 4.12.

Table 4.12. Catalytic activity of the 0.5%Au-0.5%Pd/Al_2O_3 catalyst prepared by the C.Imp Red methodology, in oxidant dependent sequential reactions of the selective oxidation of benzyl alcohol via in-Situ H_2O_2 synthesis.

Reaction Number	Reaction Conditions	Total Benzyl Alcohol Conversion (%)	Total Benzaldehyde Yield (%)	Total Benzoic Acid Yield (%)	Benzaldehyde Selectivity (%)	Additional Benzyl Alcohol Conversion (%)	Residual H_2O_2 (mmol)
1[a]	H_2 + O_2[a]	22.7	22.3	0.4	98	22.3	0.112
2[b]	O_2[b]	26.4	26.0	0.4	99	3.7	0.079
2[a]	H_2 + O_2[a]	39.2	38.5	0.7	98	16.5	0.107

Benzyl alcohol oxidation reaction conditions: [a] Catalyst (0.01 g), MeOH (7.13 g), benzyl alcohol (1.04 g, 9.62 mmol), mesitylene (0.42 g), 5% H_2/CO_2 (420 psi, 2.76 mmol), 25% O_2/CO_2 (160 psi, 5.24 mmol), 0.5 hr, 50 ^{O}C, 1200 rpm.

[b]Catalyst (0.01 g), MeOH (7.13 g), benzyl alcohol (1.04 g, 9.62 mmol), mesitylene (0.42 g), CO_2 (420 psi), 25% O_2/CO_2 (160 psi, 5.24 mmol), 0.5 hr, 50 ^{o}C, 1200 rpm.

Whilst a benzaldehyde yield of 22.3 % was offered by the 0.5%Au-0.5%Pd/Al_2O_3 catalyst after a 30-minute reaction using both H_2 and O_2, when this reaction was recharged and repeated with only O_2, an additional benzaldehyde yield of 3.7 % was offered. Additionally, no benzoic acid was formed when O_2 was used in reaction 2, leading to a small increase in benzaldehyde selectivity from 98.3 % to 98.7 %. This additional yield of benzaldehyde was small relative to the yield of 16.5 % that can be achieved when H_2 and O_2 are used in tandem in sequential reactions. However, when O_2 was used as an oxidant without an initial reaction involving both H_2 and O_2 (Table 4.11), a benzaldehyde yield of only 0.83 % was observed.

This benzaldehyde yield of 3.7 % corresponds to 0.351 mmol of benzaldehyde and cannot be wholly attributed to oxidation by residual H_2O_2 because of the 0.112 mmol of residual H_2O_2 present at the start of reaction 2, only 0.033 mmol was degraded over the subsequent reaction and could only account for a maximum of 1/10 of the observed benzyl alcohol oxidation. Therefore, this enhanced activity may have been caused by in-situ changes to the catalyst as a result of the initial reaction using H_2 and O_2. For example, the in-situ reduction of Pd was observed (Figure 4.12) to take place in the presence of H_2 and O_2, and these higher levels of Pd^0 may be responsible for the observed promotion in aerobic oxidation. This is fully discussed in Section 4.7. It has been reported previously in the literature that an increasing proportion of PdO present in AuPd/silica supported catalysts resulted in a decreasing catalytic activity towards benzyl alcohol oxidation under aerobic conditions.[223]

Alternatively, some extent of nanoparticle agglomeration (Table 4.19) was shown to occur over the course of a reaction, and more optimal nanoparticle sizes than those present on the pre-use catalyst may also enhance aerobic oxidation.

Overall, this data demonstrates that whilst these unused AuPd/Al_2O_3 catalysts are not significantly active under aerobic conditions at 50 ^oC ,the actual in-situ catalyst may be more able to utilise O_2 as a primary oxidant, when present in a mixture of H_2 and O_2. This indeed may be a contributing factor to the high H_2 selectivity values reported herein for the selective oxidation of benzyl alcohol via in-situ H_2O_2 synthesis. However, to investigate this further, XPS analysis to confirm whether in-situ oxidation of Pd had occurred under the O_2 only reaction conditions should be conducted.

4.5 The Effects of Extended Reaction Times Using the 0.5%Au-0.5%Pd/Al_2O_3 and 1.0%Pd/Al_2O_3 Catalysts Prepared by the C.Imp Red Methodology on the Selective Oxidation of Benzyl Alcohol via in-situ H_2O_2 Synthesis

In order to determine the conversions of benzyl alcohol that can be attained by the 0.5%Au-0.5%Pd and 1%Pd/Al_2O_3 catalysts, when prepared via the C.Imp Red methodology, a series of benzyl alcohol oxidation reactions were conducted over extended reaction times of up to 90 minutes. This was done to provide a comparison of the catalytic activity of both catalysts when operating at equal conversions of H_2, and is shown in Figure 4.9 and Tables 4.13 and 4.14.

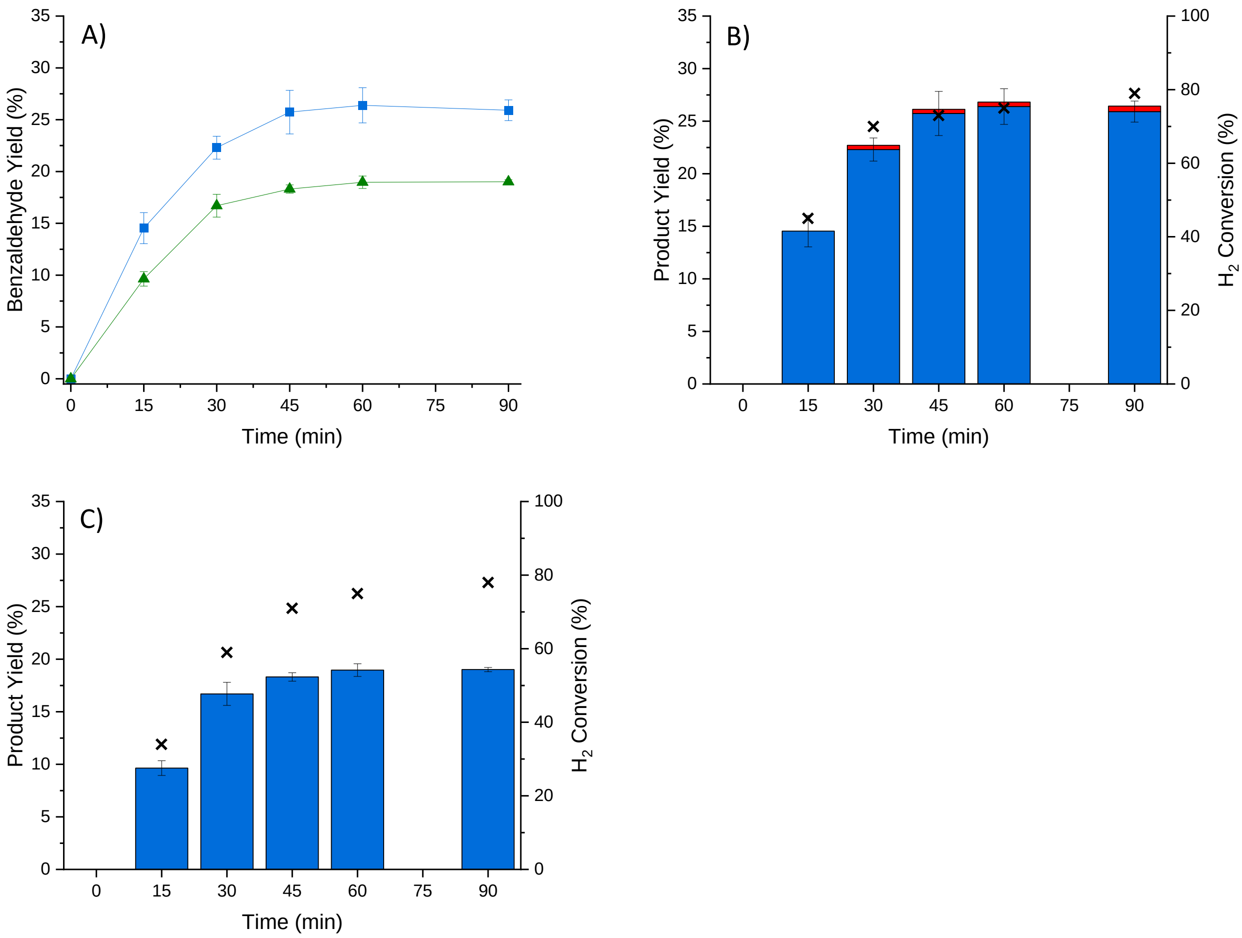

Figure 4.9. The effects of extended reaction times on the selective oxidation of benzyl alcohol via in-situ H_2O_2 synthesis, using; A) 0.5%Au-0.5%Pd/Al_2O_3 and 1%Pd/Al_2O_3. B) 0.5%Au-0.5%Pd/Al_2O_3, C) 1%Pd/Al_2O_3 catalysts prepared by the C.Imp Red methodology

Key; A) 0.5%Au-0.5%Pd/Al_2O_3 (blue *squares*) and 1%Pd/Al_2O_3 (*green triangles*), B-C) Benzaldehyde yield (*blue bars*), benzoic acid yield (*red bars*), H_2 conversion (*crosses*).

Benzyl alcohol oxidation reaction conditions: Catalyst (0.01 g), MeOH (7.13 g), benzyl alcohol (1.04 g, 9.62 mmol), mesitylene (0.42 g), 5% H_2/CO_2 (420 psi, 2.76 mmol), 25% O_2/CO_2 (160 psi, 5.24 mmol), 0.5 hr, 50 ^{O}C, 1200 rpm.

Table 4.13. The effects of extended reaction times on the selective oxidation of benzyl alcohol via in-situ H_2O_2 synthesis, using the 0.5%Au-0.5%Pd/Al_2O_3 catalyst prepared by the C.Imp Red methodology.

Reaction Time	Benzyl Alcohol Conversion (%)	Benzaldehyde Yield (%)	Benzoic Acid Yield (%)	Benzaldehyde Selectivity (%)	H_2 Conversion (%)	H_2 Selectivity (%)	Residual H_2O_2 (mmol)
15	14.5	14.5	0.0	100	45	112	0.100
30	22.7	22.3	0.4	98	70	113	0.112
45	26.1	25.7	0.4	98	73	124	0.070
60	26.8	26.4	0.4	98	75	126	0.054
90	26.4	25.9	0.5	98	79	127	0.041

Benzyl alcohol oxidation reaction conditions: Catalyst (0.01 g), MeOH (7.13 g), benzyl alcohol (1.04 g, 9.62 mmol), mesitylene (0.42 g), 5% H_2/CO_2 (420 psi, 2.76 mmol), 25% O_2/CO_2 (160 psi, 5.24 mmol), 0.5 hr, 50 ^{O}C, 1200 rpm.

Firstly, the 0.5%Au-0.5%Pd/Al_2O_3 catalyst was investigated in this manner, the results of which are shown in Table 4.13. A high level of benzyl alcohol conversion took place over the first 30 minutes of the reaction, wherein the catalyst offered a benzyl alcohol conversion of 22.7 %. However, at longer reaction times, a significant plateau in the rate of benzyl alcohol conversion occurred, and after a total reaction time of 90 minutes, a total of 26.4 % conversion of benzyl alcohol had occurred. The high rate of H_2 conversion of this catalyst is likely the cause of the significant decrease in benzyl alcohol conversion at reaction times longer than 30 minutes, with an H_2 conversion of 70 % observed after the first 30 minutes, but with only an additional 9 % H_2 converted over the subsequent 60 minutes. Interestingly, no benzoic acid was observed after the first 15 minutes of the reaction, but was observed at all subsequent reaction times, at a consistent product selectivity of approximately 2 %. Additionally, consistent with the previously examined ECI 0.5%Au-0.5%Pd/Al_2O_3 catalyst and with previous work,[218] the residual H_2O_2 present in the reaction mixture decreased significantly over the course of the reaction, from a maximum of 0.112 mmol, to 0.041 mmol after 90 minutes. This may be a result of the decreasing availability of H_2 to form H_2O_2, combined with its continued degradation and possible utilisation of existing H_2O_2 in the oxidation of benzyl alcohol.

The 1%Pd/Al_2O_3 catalyst was also investigated in this manner, the results of which are shown in Table 4.14.

Table 4.14. The effects of extended reaction times on the selective oxidation of benzyl alcohol via in-situ H_2O_2 synthesis, using the 1%Pd/Al_2O_3 catalyst prepared by the C.Imp Red methodology.

Reaction Time (min)	Benzyl Alcohol Conversion (%)	Benzaldehyde Yield (%)	Benzoic Acid Yield (%)	Benzaldehyde Selectivity (%)	H_2 Conversion (%)	H_2 Selectivity (%)	Residual H_2O_2 (mmol)
15	9.6	9.6	0.00	100	34	100	0.092
30	16.7	16.7	0.00	100	59	97	0.117
45	18.3	18.3	0.00	100	71	90	0.075
60	19.0	19.0	0.00	100	75	89	0.065
90	19.0	19.0	0.00	100	78	86	0.062

Benzyl alcohol oxidation reaction conditions: Catalyst (0.01 g), MeOH (7.13 g), benzyl alcohol (1.04 g, 9.62 mmol), mesitylene (0.42 g), 5% H_2/CO_2 (420 psi, 2.76 mmol), 25% O_2/CO_2 (160 psi, 5.24 mmol), 0.5 hr, 50 ^{O}C, 1200 rpm.

Similarly to the analogous 0.5%Au-0.5%Pd/Al_2O_3 catalyst, a plateau in catalytic activity was observed at reaction times greater than 30 minutes. For example, after 30 minutes a benzyl alcohol conversion of 16.7 % had been reached, but after 90 minutes to total conversion of benzyl alcohol had only increased to 19.0 %. This observation correlated well with the concurrent depletion of H_2 and again suggests that the diminishing availability of H_2 is the reason for a plateauing of catalytic activity as a function of time. However, the in-situ deactivation of either catalyst through mechanisms such as nanoparticle agglomeration, metal dissolution and changes to oxidation state are possibly still occurring, and their effects on catalytic activity will be examined in future sections. Interestingly, over the 90-minute reaction, no benzoic acid was formed, and 100 % selectivity towards benzaldehyde was observed. This may be a result of the relatively lower levels of benzyl alcohol conversion offered by the 1%Pd catalyst compared to the 0.5%Au-0.5%Pd analogue. However, the 1%Pd catalyst was able to offer a benzyl alcohol conversion of 19 % at 100 % selectivity to benzaldehyde after 90 minutes, whilst the 0.5%Au-0.5%Pd catalyst offered a 22.7 % conversion of benzyl alcohol after 30 minutes with a product selectivity of only 98.3 %.
This observation may suggest that the formation of benzoic acid was promoted by the inclusion of Au into the catalyst, or that benzoic acid formation is highly dependent on both the conversion of benzyl alcohol and the properties of the catalyst used.

4.6 The Effects of Sequential Reactions Using 0.5%Au-0.5%Pd/Al_2O_3 and 1%Pd/Al_2O_3 Catalysts Prepared by the C.Imp Red Methodology Towards the Selective Oxidation of Benzyl Alcohol via in-situ H_2O_2 Synthesis

To investigate the possibility of catalyst deactivation over the course of a reaction, a series of sequential reactions were carried out, using the 0.5%Au-0.5%Pd and 1%Pd/Al_2O_3 catalysts. To do this, the same reaction mixture and catalyst were retained across the series of sequential reactions, but reactant gasses were replaced every 30 minutes to restore the initial pressures of H_2 and O_2. The results of this study are shown in Figure 4.10 and Tables 4.15 and 4.16.

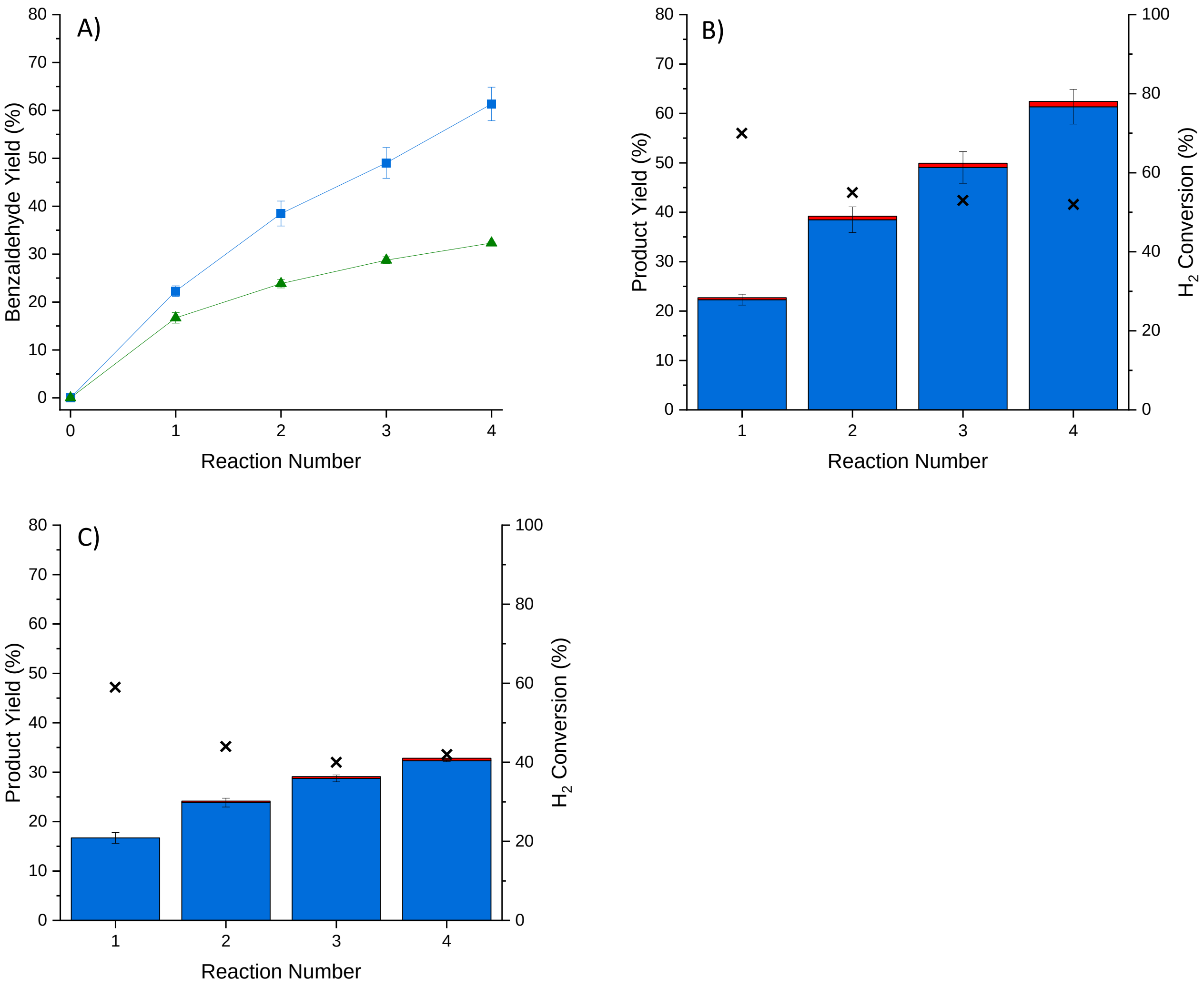

Figure 4.10. The effects of sequential reactions in the selective oxidation of benzyl alcohol via in-situ H_2O_2 synthesis, using; A) 0.5%Au-0.5%Pd/Al_2O_3 and 1%Pd/Al_2O_3. B) 0.5%Au-0.5%Pd/Al_2O_3, C) 1%Pd/Al_2O_3 prepared by the C.Imp Red methodology.
Key; A) 0.5%Au-0.5%Pd/Al_2O_3 (blue *squares*) and 1%Pd/Al_2O_3 (*green triangles*), B-C) Benzaldehyde yield (*blue bars*), benzoic acid yield (*red bars*), H_2 conversion (*crosses*).
Benzyl alcohol oxidation reaction conditions: Catalyst (0.01 g), MeOH (7.13 g), benzyl alcohol (1.04 g, 9.62 mmol), mesitylene (0.42 g), 5% H_2/CO_2 (420 psi, 2.76 mmol), 25% O_2/CO_2 (160 psi, 5.24 mmol), 0.5 hr, 50 ^{O}C, 1200 rpm.

Firstly, the 0.5%Au-0.5%Pd/Al_2O_3 catalyst was used in this manner, which is shown in Figure 4.10 B and Table 4.15.

Table 4.15. The effects of sequential reactions in the selective oxidation of benzyl alcohol via in-situ H_2O_2 synthesis, using the 0.5%Au-0.5%Pd/Al_2O_3 catalyst prepared by the C.Imp Red methodology.

Reaction Number	Benzyl Alcohol Conversion (%)	Benzaldehyde Yield (%)	Benzoic Acid Yield (%)	Benzaldehyde Selectivity (%)	Additional Benzyl Alcohol Conversion (%)	H_2 Conversion (%)	H_2 Selectivity (%)	Residual H_2O_2 (mmol)
1	22.7	22.3	0.4	98	22.3	70	113	0.112
2	39.2	38.5	0.7	98	16.5	55	100	0.107
3	49.9	49.1	0.9	98	10.7	53	70	0.095
4	62.4	61.4	1.1	98	12.5	52	99	0.094

Benzyl alcohol oxidation reaction conditions: Catalyst (0.01 g), MeOH (7.13 g), benzyl alcohol (1.04 g, 9.62 mmol), mesitylene (0.42 g), 5% H_2/CO_2 (420 psi, 2.76 mmol), 25% O_2/CO_2 (160 psi, 5.24 mmol), 0.5 hr, 50 ^{O}C, 1200 rpm.

Over the course of each sequential reaction, product selectivity towards benzaldehyde remained at approximately 98 %, with benzoic acid formation accounting for the remaining conversion of benzyl alcohol. Consistent with previous observations, conversions of benzyl alcohol were significantly enhanced when reactant gasses were replaced compared to when longer reaction times were used (Figure 4.9 B, Table 4.13). For example, after a 60-minute reaction, a benzyl alcohol conversion of 26.8 % had been offered by the 0.5%Au-0.5%Pd/Al_2O_3 catalyst, compared to the 39.2 % conversion that was observed using the same catalyst, and when the reactant gasses were replaced after 30 minutes. This further supports the hypothesis that the high levels of H_2 conversion result in the inhibition of benzyl alcohol conversion when the remaining pressure of H_2 is sufficiently lowered. In terms of catalyst deactivation, a modest but clear decrease in H_2 conversion was observed after the first reaction, decreasing from 70 % to 55 %, which was also accompanied by a large decrease in additional benzyl alcohol conversion. Indeed, 22.7 % of the initially available benzyl alcohol was converted after reaction 1, but only a further 15.8 % was converted after reaction 2, with levels of benzyl alcohol conversion decreasing further in subsequent reactions. This decrease in conversion may be a result of both a deactivation of the catalyst itself, and the decreasing availability of benzyl alcohol, although both factors will be explored in a future section. However, it should be noted that after reaction 1, 77.3 % of the initial benzyl alcohol was still present in the reaction mixture.

Finally, the residual H_2O_2 present in the reaction mixture decreases from 0.112 mmol after reaction 1, to 0.094 mmol after reaction number 4, suggesting that the catalyst does not lose any significant capability to generate H_2O_2 in-situ under the reaction conditions utilised.

Following this, the 1%Pd/Al_2O_3 catalyst was investigated in the same manner, as shown in Figure 4.10 C and Table 4.16.

Table 4.16. The effects of sequential reactions in the selective oxidation of benzyl alcohol via in-situ H_2O_2 synthesis, using the 1%Pd/Al_2O_3 catalyst prepared by the C.Imp Red methodology.

Reaction Number	Benzyl Alcohol Conversion (%)	Benzaldehyde Yield (%)	Benzoic Acid Yield (%)	Benzaldehyde Selectivity (%)	Additional Benzyl Alcohol Conversion (%)	H_2 Conversion (%)	H_2 Selectivity (%)	Residual H_2O_2 (mmol)
1	16.7	16.7	0.0	100	16.7	59	99	0.117
2	24.2	23.9	0.3	99	7.5	44	60	0.106
3	29.1	28.8	0.4	99	4.9	40	44	0.105
4	32.8	32.3	0.5	99	3.7	42	21	0.105

Benzyl alcohol oxidation reaction conditions: Catalyst (0.01 g), MeOH (7.13 g), benzyl alcohol (1.04 g, 9.62 mmol), mesitylene (0.42 g), 5% H_2/CO_2 (420 psi, 2.76 mmol), 25% O_2/CO_2 (160 psi, 5.24 mmol), 0.5 hr, 50 ^{O}C, 1200 rpm.

Despite offering a product selectivity of 100 % towards benzaldehyde after 1 reaction, small quantities of benzoic acid were formed over subsequent reaction to offer a final selectivity towards benzaldehyde of 98.5 % after 4 reactions. Again, benzyl alcohol conversions were enhanced across a 60-minute reaction when reactant gasses were replaced after 30 minutes, which offered a benzyl alcohol conversion of 24.2 %. This is compared to a 60-minute reaction (Figure 4.9 C, Table 4.14) utilising the same reactant gasses with no replenishment of H_2, which offered a benzyl alcohol conversion of 19.0 %. However, a more profound decrease in the additional benzyl alcohol conversion was observed over subsequent reactions when using the 1%Pd/Al_2O_3 catalyst, compared to the analogous 0.5%Au-0.5%Pd/Al_2O_3 catalyst. For example, whilst using the 1%Pd/Al_2O_3 catalyst, 16.7 % of benzyl alcohol was converted after reaction 1, but only an additional 3.7 % of benzyl alcohol was converted after reaction 4. This is compared to the catalytic activity of the 0.5%Au-0.5%Pd/Al_2O_3 catalyst, which offered a benzyl alcohol conversion of 22.7 % after reaction 1, but still an additional 12.5 % after reaction 4.

4.7 Evaluation of the Re-Usability of the 0.5%Au-0.5%Pd/Al_2O_3 and 1%Pd/Al_2O_3 Catalysts Prepared by the C.Imp Red Methodology Towards the Selective Oxidation of Benzyl Alcohol via in-situ H_2O_2 Synthesis

A moderate extent of catalytic deactivation may have been occurring over the course of sequential reactions for both 1%Pd and 0.5%Au-0.5%Pd catalysts. Whilst the decreasing availability of reactants may have contributed to the decreasing conversions of benzyl alcohol observed over sequential reactions (Figure 4.10), the decrease in H_2 conversion over subsequent reactions indicates that some deactivation of the catalyst may be occurring.

To examine this further, re-use reactions were conducted using both catalysts, wherein a given catalyst was recovered after an initial benzyl alcohol oxidation reaction, washed with HPLC grade H_2O and dried under a vacuum at room temperature, and used again in a second reaction. The results of this are shown in Figure 4.11 and Table 4.17.

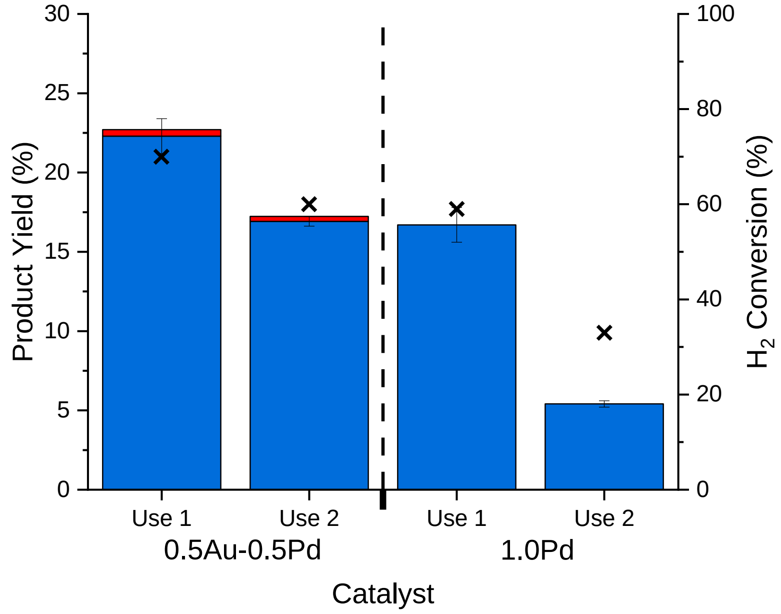

Figure 4.11. Effects of re-using the 0.5%Au-0.5%Pd and 1.0%Pd/Al_2O_3 catalysts prepared by the C.Imp Red methodology towards the selective oxidation of benzyl alcohol via in-situ H_2O_2 synthesis.
Key; benzaldehyde yield (*blue bars*), benzoic acid yield (*red bars)*, H_2 conversion (*crosses*).
Reaction conditions: Catalyst (0.01 g), MeOH (7.13 g), benzyl alcohol (1.04 g, 9.62 mmol), mesitylene (0.42 g), 5% H_2/CO_2 (420 psi, 2.76 mmol), 25% O_2/CO_2 (160 psi, 5.24 mmol), 0.5 hr, 50 ^{O}C, 1200 rpm.

Table 4.17. Effects of re-using the 0.5%Au-0.5%Pd and 1.0%Pd/Al_2O_3 catalysts prepared by the C.Imp Red methodology towards the selective oxidation of benzyl alcohol via in-Situ H_2O_2 synthesis.

Catalyst	Reaction Number	Benzyl Alcohol Conversion (%)	Benzaldehyde Yield (%)	Benzoic Acid Yield (%)	Benzaldehyde Selectivity (%)	H_2 Conversion (%)	H_2 Selectivity (%)	Residual H_2O_2 (mmol)
AuPd	Use 1	22.7	22.3	0.4	98	70	113	0.112
AuPd	Use 2	17.2	16.9	0.3	98	60	100	0.109
Pd	Use 1	16.7	16.7	0.0	100	59	99	0.117
Pd	Use 2	5.4	5.4	0.0	100	33	58	0.113

Benzyl alcohol oxidation reaction conditions: Catalyst (0.01 g), MeOH (7.13 g), benzyl alcohol (1.04 g, 9.62 mmol), mesitylene (0.42 g), 5% H_2/CO_2 (420 psi, 2.76 mmol), 25% O_2/CO_2 (160 psi, 5.24 mmol), 0.5 hr, 50 ^{O}C, 1200 rpm.

When the 0.5%Au-0.5%Pd/Al_2O_3 catalyst was investigated in this manner, a clear loss in catalytic activity was observed when the catalyst was re-used. For example, benzyl alcohol conversion decreased from 22.7 % after use 1 to 17.2 % after use 2. Additionally, H_2 conversion decreased from 70 % to 60 %. A more severe loss in catalytic activity was observed for the 1%Pd/Al_2O_3 catalyst, which offered a loss in benzyl alcohol conversion from 16.7 % to 5.4 %, with an H_2 conversion decreasing from 59 % to 33 %. Interestingly, the residual H_2O_2 observed in the final reaction mixtures did not decrease by a significant amount as a result of re-using the catalyst, suggesting that any decrease in benzyl alcohol conversion cannot be assigned to a decreased availability of H_2O_2. Therefore, to further investigate the origins of this loss of catalytic activity, ICP-MS was used to determine the loss of catalytic metal from the surface of the catalyst. This is shown in Table 4.18.

Table 4.18. Metal dissolution of the 0.5%Au-0.5%Pd and 1%Pd/Al_2O_3 catalysts prepared by the C.Imp Red methodology, over the course of the selective oxidation of benzyl alcohol via in-Situ H_2O_2 synthesis, using ICP-MS

Catalyst	Concentration of Pd in Reaction Solution (µg/L)	Total Loss of Pd (%)	Concentration of Au in Reaction Solution (µg/L)	Total loss of Au (%)
0.5%Au-0.5%Pd	4.25	0.09	1.27	0.03
1%Pd	9.26	0.09	0.00	0.00

Reaction conditions: Catalyst (0.01 g), MeOH (7.13 g), benzyl alcohol (1.04 g, 9.62 mmol), mesitylene (0.42 g), 5% H_2/CO_2 (420 psi, 2.76 mmol), 25% O_2/CO_2 (160 psi, 5.24 mmol), 0.5 hr, 50 ^{O}C, 1200 rpm.

After the 0.5%Au-0.5%Pd/Al_2O_3 catalyst was used in the benzyl alcohol oxidation reaction, 4.25 µg/L of Pd and 1.27 µg/L of Au was observed in the reaction mixture, which correspond to a total loss of 0.085 % of Pd and 0.025 % of Au from the surface of the catalyst. Similar levels of metal dissolution were observed using the 1%Pd/Al_2O_3 catalyst, the use of which resulted in 9.26 µg/L of Pd present in the reaction solution, which corresponded to a loss of Pd of 0.093 % of the total mass of Pd present on the catalyst. These data suggests that a loss of catalytic metal is not likely a factor in the observed loss of catalytic activity upon re-use, due to only very low levels of metal dissolution. Following this, TEM was used to investigate the possible agglomeration of nanoparticles over the course of the oxidation of benzyl alcohol. The results of this are shown in Table 4.19.

Table 4.19. Particle size distributions observed via TEM, of the 0.5%Au-0.5%Pd and 1%Pd/Al_2O_3 catalysts prepared by the C.Imp Red methodology, before and after use in the selective oxidation of benzyl alcohol via in-situ H_2O_2 synthesis.

Catalyst	Use	Mean Nanoparticle Size (nm)	Standard Deviation (nm)
AuPd	Fresh	3.5	2.2
AuPd	Used[a]	4.7	3.3
Pd	Fresh	5.1	4.8
Pd	Used[a]	7.5	5.6

Benzyl alcohol oxidation reaction conditions: [a]Catalyst (0.05 g), MeOH (7.13 g), benzyl alcohol (1.04 g), mesitylene (0.42 g), 5% H_2/CO_2 (420 psi), 25% O_2/CO_2 (160 psi), 0.5 hr, 50 °C, 1200 rpm.

Both catalysts analysed in this way appeared to undergo some extent of nanoparticle agglomeration as a result of their use in the benzyl alcohol reaction. For example, the 0.5%Au-0.5%Pd/Al_2O_3 catalyst had a mean nanoparticle size of 3.47 nm before use, at a standard deviation of 2.2 nm. This increased to a mean nanoparticle size of 4.72 nm with a standard deviation of 3.3 nm. For the 1%Pd/Al_2O_3 catalyst, the increase in mean nanoparticle size was more pronounced, and increased from 5.11 nm to 7.50 nm, with standard deviations increasing from 4.8nm to 5.6 nm.

Ultimately, it is possible that the increase in mean nanoparticle size associated with the use of the catalyst played some role in the observed loss of catalytic activity.

As previously noted, Crombie *et al.* reported that when using the analogous 0.5%Au-0.5%Pd/TiO_2 and 1%Pd/TiO_2 catalysts, prepared by an identical EcI methodology to that used herein, the total reduction of Pd occurred under identical benzyl alcohol oxidation reaction conditions to those used herein.[218] To begin to investigate the role of changing Pd oxidation state, XPS analysis of fresh and used 0.5%Au-0.5%Pd/Al_2O_3 and 1%Pd/Al_2O_3 catalysts was conducted by Dr David Morgan (Cardiff Catalysis Institute) and is presented in Figure 4.12.

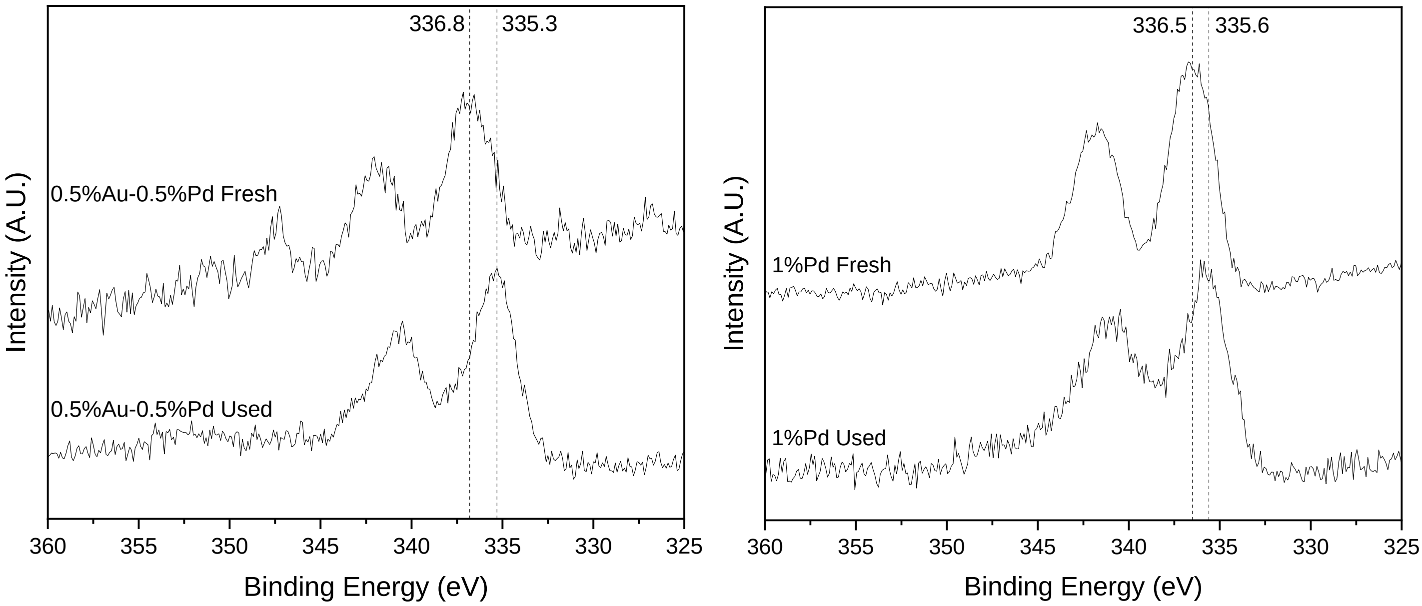

Figure 4.12. XPS spectra of the Pd3d regions of fresh and used 0.5%Au-0.5%Pd/Al_2O_3 and 1%Pd/Al_2O_3 catalysts, prepared by the C.Imp Red methodology.
Benzyl alcohol oxidation reaction Conditions: Catalyst (0.01 g), MeOH (7.13 g), benzyl alcohol (1.04 g, 9.62 mmol), mesitylene (0.42 g), 5% H_2/CO_2 (420 psi, 2.76 mmol), 25% O_2/CO_2 (160 psi, 5.24 mmol), 0.5 hr, 50 ^{O}C, 1200 rpm.

The fresh 0.5%Au-0.5%Pd/Al_2O_3 catalyst was previously shown to contain a mixture of Pd^0 and Pd^{2+} states in a ratio of Pd^0:Pd^{2+} of 0.36:0.64 (Table 4.9) prior to use in the benzyl alcohol oxidation reaction via in-situ H_2O_2 synthesis. Indeed, this was shown by a signal associated with the Pd3d$_{5/2}$ region which corresponded to a binding energy of 336.5 eV. When this catalyst was used in the standard 30-minute reaction and an XPS spectra of the subsequent catalyst collected, a shift in binding energy of the same signal was observed, from 336.8 eV to 335.3 eV. This shift in binding energy demonstrated that in-situ reduction of surface Pd had occurred over the course of the reaction,[53] leading to an increasing prevalence of surface Pd^0 sites which is in agreement with the work of Crombie *et al.*[218] Indeed, the authors also proposed that the shift from a mixture of Pd^{2+} and Pd^0 sites, to solely Pd^0 sites may be the cause of an observed decrease in catalytic activity, which is in agreement with the observations presented herein. When the same analysis was conducted using the 1%Pd/Al_2O_3 catalyst, a shift in the binding energy of the signal associated with the $Pd3d_{5/2}$ region was again observed. In this instance, a shift from 336.5 eV for the fresh catalyst, to 335.6 eV for the used catalyst took place. Again, this demonstrates an in-situ reduction of Pd in the H_2/O_2 environment of the reaction occurred and is likely a contributing factor in the overall loss of catalytic activity that took place upon re-use of the catalyst.

4.8 The Effects of the Choice of Support Material for Supported 0.5%Au-0.5%Pd Catalysts in the Direct Synthesis of H_2O_2 and the Selective Oxidation of Benzyl Alcohol via in-situ H_2O_2 Synthesis

It was determined that the 0.5%Au-0.5%Pd/Al_2O_3 catalyst, when prepared through the C.Imp Red methodology, represented the most active catalyst for the oxidation of benzyl alcohol via in-situ H_2O_2 synthesis presented in this work. To develop this catalyst further, a range of metal oxides and a few-layer-graphene support material was investigated for use with these AuPd nanoparticles, when prepared by the C.Imp Red method. The metal oxides investigated were selected based on previously reported use in the direct synthesis of H_2O_2.[46, 227] The surface area for each catalyst tested and the corresponding support was determined using 5-point BET and is shown in Table A4.2.

The series of catalysts was first examined in the direct synthesis of H_2O_2, the results of which are shown in Figure 4.13 and Table 4.20.

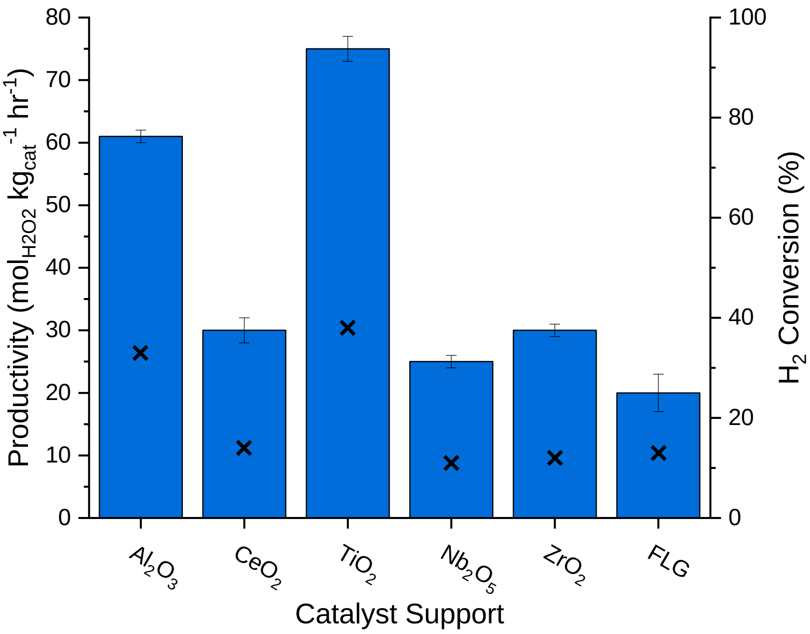

Figure 4.13. Comparison of the catalytic activity of supported 0.5%Au-0.5%Pd catalysts prepared by the C.Imp Red methodology, towards the direct synthesis of H_2O_2 using different support materials. **Key;** Productivity (blue bars), H_2 conversion (crosses).
H_2O_2 direct synthesis reaction conditions: Catalyst (0.01 g), H_2O (2.9 g), MeOH (5.6 g), 5% H_2/CO_2 (420 psi, 2.76 mmol), 25% O_2/CO_2 (160 psi, 5.24 mmol), 0.5 hr, 20 °C, 1200 rpm.

Table 4.20. Comparison of the catalytic activities of supported 0.5%Au-0.5%Pd prepared by the C.Imp Red methodology, towards the direct synthesis of H_2O_2 using different support materials.

Catalyst Support	Productivity (mol_{H2O2} kg^{-1}_{cat} hr^{-1})	H_2 Conversion (%)	H_2O_2 Selectivity (%)	H_2O_2 Concentration (wt. %)
Al_2O_3	61	33	34	0.12
CeO_2	30	14	40	0.06
TiO_2	75	38	36	0.15
Nb_2O_5	25	11	43	0.05
ZrO_2	30	12	47	0.06
FLG	20	13	28	0.04

H_2O_2 direct synthesis reaction conditions: Catalyst (0.01 g), H_2O (2.9 g), MeOH (5.6 g), 5% H_2/CO_2 (420 psi, 2.76 mmol), 25% O_2/CO_2 (160 psi, 5.24 mmol), 0.5 hr, 20 °C, 1200 rpm.

In good agreement with the work presented in Chapter 3, and with previous literature,[227] the AuPd/TiO_2 catalyst facilitated the greatest activity towards H_2O_2 synthesis, which offered an H_2O_2 productivity of 75 mol_{H2O2} kg^{-1}_{cat} hr^{-1}, followed by the AuPd/Al_2O_3 catalyst, which offered an H_2O_2 productivity of 61 mol_{H2O2} kg^{-1}_{cat} hr^{-1}. The other metal oxide and carbon supported catalysts offered much more limited levels of H_2O_2 productivity, such as the AuPd/FLG catalyst, which offered an H_2O_2 productivity of 20 mol_{H2O2} kg^{-1}_{cat} hr^{-1}.

When compared to the equivalent catalysts prepared through the EcI methodology (Chapter 3), H_2O_2 productivity values are broadly equivalent between the two preparation methods, though H_2 conversion is generally lower for catalysts prepared through the C.Imp Red methodology.

Following this, the series of catalysts were used in the selective oxidation of benzyl alcohol via in-situ H_2O_2 synthesis, the results of which are shown in Figure 4.14 and Table 4.21.

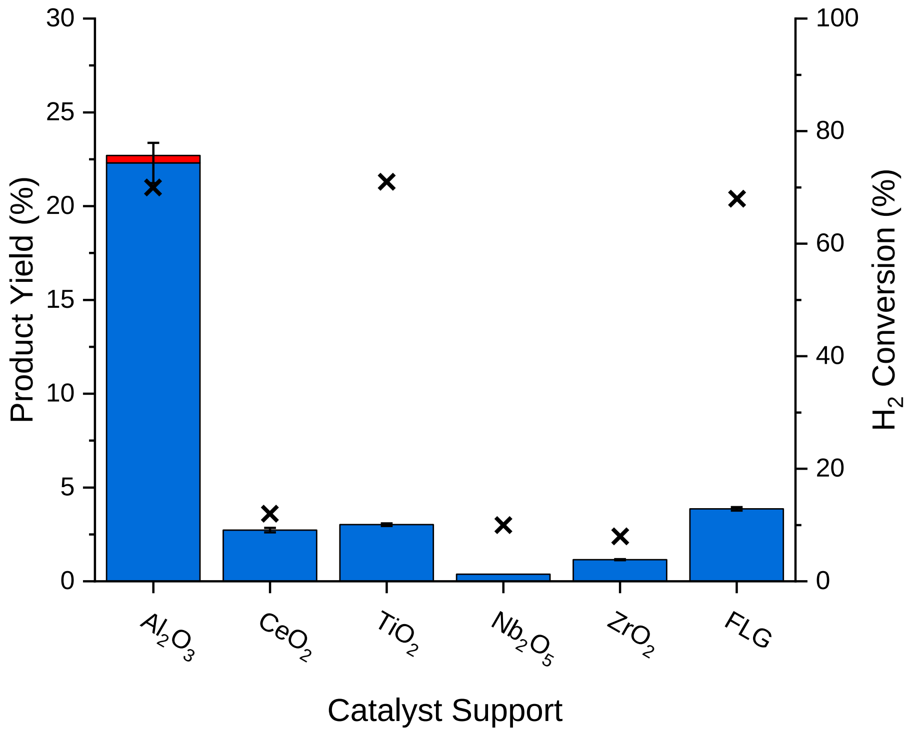

Figure 4.14. Comparison of the catalytic activities of supported 0.5%Au-0.5%Pd catalysts prepared by the C.Imp Red methodology, towards the oxidation of benzyl alcohol using different support materials. **Key;** Benzaldehyde (blue bars), benzoic acid (red bars), H_2 conversion (crosses).
Benzyl alcohol oxidation reaction conditions: Catalyst (0.01 g), MeOH (7.13 g), benzyl alcohol (1.04 g, 9.62 mmol), mesitylene (0.42 g), 5% H_2/CO_2 (420 psi, 2.76 mmol), 25% O_2/CO_2 (160 psi, 5.24 mmol), 0.5 hr, 50 ^{O}C, 1200 rpm.

Table 4.21. Comparison of the catalytic activities of supported 0.5%Au-0.5%Pd catalysts prepared by the C.Imp Red methodology, towards the selective oxidation of benzyl alcohol using different support materials.

Catalyst Support	Benzaldehyde Yield (%)	Benzoic Acid Yield (%)	Benzaldehyde Selectivity (%)	H_2 Conversion (%)	H_2 Selectivity (%)	Residual H_2O_2 (mmol)
Al_2O_3	22.3	0.4	98	70	113	0.112
CeO_2	2.7	0.0	100	12	79	0.073
TiO_2	3.0	0.0	100	71	15	0.112
Nb_2O_5	0.4	0.0	100	10	13	0.100
ZrO_2	1.2	0.0	100	8	50	0.070
FLG	3.9	0.0	100	68	20	0.040

Benzyl alcohol oxidation reaction conditions: Catalyst (0.01 g), MeOH (7.13 g), benzyl alcohol (1.04 g, 9.62 mmol), mesitylene (0.42 g), 5% H_2/CO_2 (420 psi, 2.76 mmol), 25% O_2/CO_2 (160 psi, 5.24 mmol), 0.5 hr, 50 ^{O}C, 1200 rpm.

From this investigation, it appeared that the Al_2O_3 supported catalyst exhibited a profoundly high activity toward the oxidation of benzyl alcohol, relative to the other metal oxide and carbon supports tested. For example, whist the 0.5%Au-0.5%Pd/Al_2O_3 catalyst offered a benzaldehyde yield of 22.3 %, the 0.5%Au-0.5%Pd/FLG catalyst only resulted in a benzaldehyde yield of 3.9 %, with the 0.5%Au-0.5%Pd/TiO_2 catalyst offering a benzaldehyde yield of only 3 %. The relatively low activity of these alternative supports shows that the significant enhancements observed when preparing supported 0.5%Au-0.5%Pd/Al_2O_3 nanoparticle catalysts by the C.Imp Red methodology does not universally deliver catalytic improvements when applied to other support materials. Additionally, the high levels of H_2 conversion exhibited by TiO_2 (71 %) and FLG (68 %) supported catalysts, despite their relatively low levels of benzaldehyde yield, indicates that reactant H_2 and O_2 gases were consumed extensively in either the non-selective formation of H_2O, or converted into H_2O_2 and subsequently degraded into H_2O before many of the proposed reactive intermediate species could be utilised in the oxidation of benzyl alcohol.

One possible factor to explain the profound enhancements in catalytic activity when Al_2O_3 is used as a catalyst support, compared to any of the other metal oxide or carbon materials, may lie within the isoelectric point of the supports themselves. For example, Al_2O_3 materials generally have weakly to moderately basic characteristics, whilst the other metal oxides studied, from CeO_2 to ZrO_2, generally exhibit varying levels of acidic character.[227] This is significant because basic supports have been suggested to potentially facilitate H-abstraction processes,[96] which could likely be an initial step in the overall benzyl alcohol oxidation mechanism. Indeed, as previously discussed, the occurrence of a benzyl alcohol radical under both aerobic oxidation conditions, and under an H_2/O_2 environment has been reported in the literature.[100, 218] Additionally, Crombie *et al.* demonstrated that TiO_2 supported Pd based catalysts could generate benzyl alcohol radicals via H-abstraction, in an anaerobic environment, in the absence of any reactant gasses, signalling that the catalyst itself has some ability to carry out this reaction step.[218]

As has previously been observed, there appears to be no correlation between the H_2O_2 productivity of a given catalyst, and its yield of benzaldehyde. Additionally, no link can be drawn between benzaldehyde yield or the residual concentration of H_2O_2 left in a reaction mixture following a benzyl alcohol oxidation reaction.

4.9 The Effects of AuPd Metal Ratio on the Catalytic activity of a AuPd/Al_2O_3 Catalyst Prepared by the C.Imp Red Methodology, Towards the Direct Synthesis of H_2O_2 and Selective Oxidation of Benzyl Alcohol via in-situ H_2O_2 Synthesis

From Chapter 3, it was observed that the ratio of Au:Pd present in an AuPd/Al_2O_3 supported catalyst was highly influential on both the catalysts' ability to synthesise H_2O_2 and to oxidise benzyl alcohol via in-situ H_2O_2 synthesis. Therefore, the effects of Au:Pd ratio were explored again using an AuPd/Al_2O_3 catalyst, prepared through the C.Imp Red methodology. These catalysts were utilised in the direct synthesis of H_2O_2, the results of which are shown in Figure 4.15 and Table 4.22.

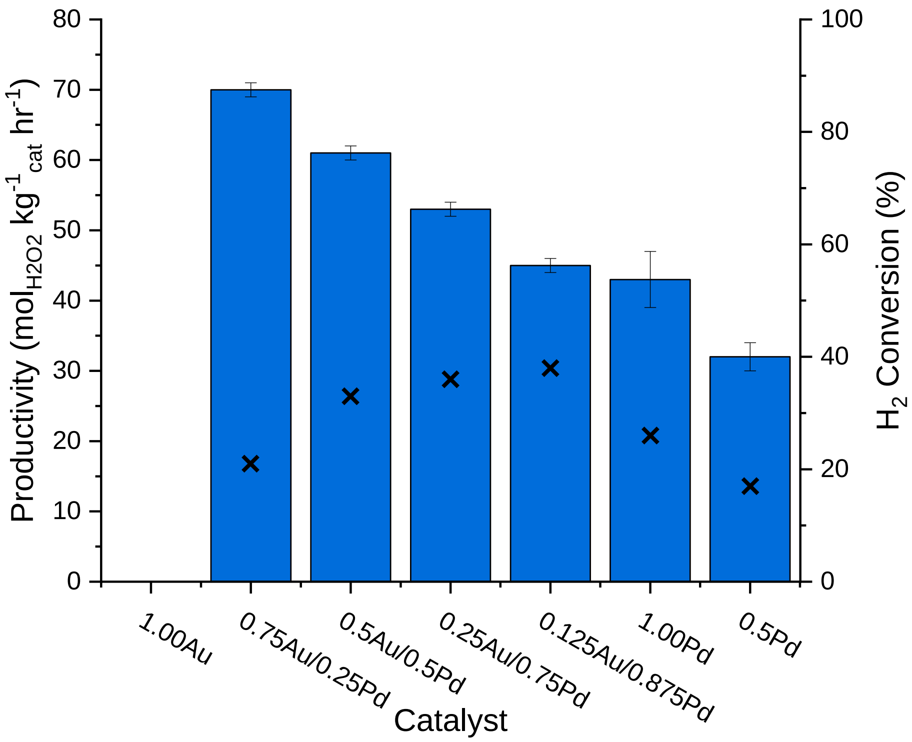

Figure 4.15. Comparison of the catalytic activities of supported Pd/Al_2O_3 and AuPd/Al_2O_3 catalysts prepared by the C.Imp Red methodology towards the direct synthesis of H_2O_2 using different Au:Pd metal ratios. Total metal loading of AuPd fixed at 1 wt.%.

Key; Productivity (blue bars), H_2 conversion (crosses).

H_2O_2 direct synthesis reaction conditions: Catalyst (0.01 g), H_2O (2.9 g), MeOH (5.6 g), 5% H_2/CO_2 (420 psi, 2.76 mmol), 25% O_2/CO_2 (160 psi, 5.24 mmol), 0.5 hr, 20 °C, 1200 rpm.

Table 4.22. Comparison of the catalytic activities of supported Pd/Al_2O_3 and $AuPd/Al_2O_3$ catalysts prepared by the C.Imp Red methodology towards the direct synthesis of H_2O_2 using different Au:Pd metal ratios. Total metal loading of AuPd fixed at 1 wt.%.

Catalyst	Productivity ($mol_{H2O2}\ kg_{cat}^{-1}\ hr^{-1}$)	Turnover Number ($mol_{H2O2}\ kg^{-1}_{cat}\ hr^{-1}$)	H_2 Conversion (%)	H_2O_2 Selectivity (%)	H_2O_2 Concentration (wt. %)
1.0Au	0	0	0	0	0.00
0.75Au-0.25Pd	70	1122	21	59	0.14
0.5Au-0.5Pd	61	849	33	34	0.12
0.25Au-0.75Pd	53	633	36	26	0.11
0.125Au-0.875Pd	45	609	38	25	0.10
1.0Pd	43	456	26	30	0.09
0.5Pd	32	683	17	34	0.07

H_2O_2 direct synthesis reaction conditions: Catalyst (0.01 g), H_2O (2.9 g), MeOH (5.6 g), 5% H_2/CO_2 (420 psi, 2.76 mmol), 25% O_2/CO_2 (160 psi, 5.24 mmol), 0.5 hr, 20 °C, 1200 rpm.

From these data, it was determined that 1%Au/Al_2O_3 catalyst was unable to synthesise H_2O_2 and consumed no H_2. Both monometallic Pd catalysts offered moderate H_2O_2 productivity values, with limited levels of H_2 conversion. For example, the 0.5%Pd catalyst offered a productivity of 32 $mol_{H2O2}\ kg^{-1}_{cat}\ hr^{-1}$, with 17 % of the available H_2 converted, compared to the 1%Pd catalyst, which offered a productivity of 43 $mol_{H2O2}\ kg^{-1}_{cat}\ hr^{-1}$ and an H_2 conversion of 26 %. Again, in agreement with the work presented in Chapter 3, strong synergistic effects were associated with the incorporation of Au in the Pd based catalyst and resulted in enhanced levels of H_2 conversion and H_2O_2 productivity.

Additionally, both the H_2 conversion and H_2O_2 productivity were further influenced by the relative ratios of Au and Pd present in the surface of the catalyst, wherein catalysts with greater ratios of Au:Pd resulted in higher values of H_2O_2 productivity. For example, whilst the 0125%Au-0.875%Pd catalyst offered an H_2O_2 productivity of 45 $mol_{H2O2}\ kg^{-1}_{cat}\ hr^{-1}$ and an H_2 conversion of 38 %, the 0.75%Au-0.25%Pd offered an H_2O_2 productivity of 70 $mol_{H2O2}\ kg^{-1}_{cat}\ hr^{-1}$, with an H_2 conversion of 21 %.

These observations are in agreement with the work presented in Chapter 3, using the analogous series of $AuPd/Al_2O_3$ catalysts prepared by the EcI methodology and reductive heat treatment, and also with the work of Santos *et al.* who also observed an increase in H_2O_2 productivity accompanying $AuPd/TiO_2$ catalysts with greater ratios of Au:Pd, when prepared by an almost identical EcI methodology.[231] One possible origin of this enhancement has been suggested to be as a result of a greater increase in the activation enthalpy of H_2O formation relative to that of H_2O_2 formation, upon increasing Au content of an AuPd catalyst,[40] resulting in increasing H_2O_2 selectivity. Alternatively, DFT calculations have suggested that the incorporation of Au sites into a Pd surface inhibits the dissociation of the O_2 bond, which ultimately leads to H_2O formation, whilst also promoting the dissociation of H_2O_2.[63, 64]

Whilst it is clear that catalysts with higher levels of Au and lower levels of Pd offered the highest levels of productivity and lower H_2 conversions, comparisons of H_2O_2 selectivity cannot be made unless iso-conversion of H_2 is reached for each catalyst.
To further investigate this, each catalyst in this series should be tested at iso-conversion of H_2 to generate a valid dataset in terms of H_2O_2 selectivity.

This series of catalysts was then utilised in the selective oxidation of benzyl alcohol via in-situ H_2O_2 synthesis, the results of which are shown in Figure 4.16 and Table 4.23.

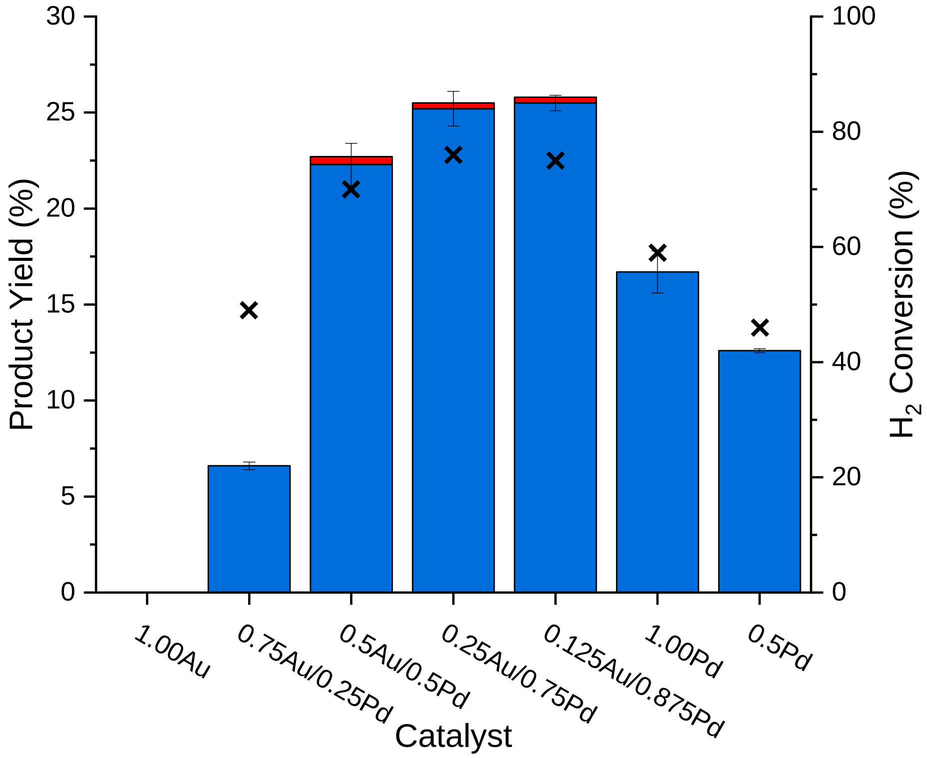

Figure 4.16. Comparison of the catalytic activities of supported Pd and $AuPd/Al_2O_3$ catalysts prepared by the C.Imp Red methodology towards the oxidation of benzyl alcohol using different Au:Pd metal ratios. Total metal loading of AuPd fixed at 1 wt.%.
Key; Benzaldehyde (blue bars), benzoic acid (red bars), H_2 conversion (crosses).
Benzyl alcohol oxidation reaction conditions: Catalyst (0.01 g), MeOH (7.13 g), benzyl alcohol (1.04 g, 9.62 mmol), mesitylene (0.42 g), 5% H_2/CO_2 (420 psi, 2.76 mmol), 25% O_2/CO_2 (160 psi, 5.24 mmol), 0.5 hr, 50 ^{O}C, 1200 rpm.

Table 4.23. Comparison of the catalytic activities of supported Pd and AuPd/Al_2O_3 catalysts prepared by the C.Imp Red methodology towards the oxidation of benzyl alcohol using different Au:Pd metal ratios. Total metal loading of AuPd fixed at 1 wt.%.

Catalyst Support	Benzaldehyde Yield (%)	Benzoic Acid Yield (%)	Benzaldehyde Selectivity (%)	Turnover Number ($mol_{benzaldehyde}$ mol_{metal}^{-1} hr^{-1})	H_2 Conversion (%)	H_2 Selectivity (%)	Residual H_2O_2 (mmol)
1.0Au	0	0.0	0	0	0	-	0.000
0.75Au-0.25Pd	6.6	0.0	100	2058	49	47	0.168
0.5Au-0.5Pd	22.3	0.4	98	5916	70	113	0.112
0.25Au-0.75Pd	25.2	0.3	99	5818	76	119	0.087
0.125Au0-875Pd	25.5	0.3	100	5528	75	115	0.080
1.0Pd	16.7	0.0	100	3412	59	99	0.117
0.5Pd	12.6	0.0	100	5149	46	97	0.119

Benzyl alcohol oxidation reaction conditions: Catalyst (0.01 g), MeOH (7.13 g), benzyl alcohol (1.04 g, 9.62 mmol), mesitylene (0.42 g), 5% H_2/CO_2 (420 psi, 2.76 mmol), 25% O_2/CO_2 (160 psi, 5.24 mmol), 0.5 hr, 50 ^{O}C, 1200 rpm.

The 1%Au/Al_2O_3 catalyst was inactive for both the direct synthesis of H_2O_2 and for the oxidation of benzyl alcohol. Conversely, both monometallic 0.5%Pd and 1%Pd catalysts were highly active toward the oxidation of benzyl alcohol, offering benzaldehyde yields of 12.6 % and 16.7 % respectively.

When a bimetallic AuPd catalyst was used, the yield of benzaldehyde was dependent on the relative ratios of Au and Pd. Indeed, increasing the Pd content above a 0.5%Au-0.5%Pd ratio caused a modest promotional effect on the oxidation of benzyl alcohol, resulting in enhanced yields of benzaldehyde.

For example, the 0.25%Au-0.75%Pd catalyst achieved a benzaldehyde yield of 25.2 %, compared to the 0.75%Au-0.25%Pd catalyst, which could only deliver a benzaldehyde yield of 6.6 %. Conversely, in good agreement with the results of the corresponding H_2O_2 synthesis reactions in this Section, the concentration of residual H_2O_2 present in a given reaction mixture was greatly increased when the total Au content of a given catalyst was increased, whilst the corresponding Pd content was proportionally decreased. Indeed, 0.087 mmol of H_2O_2 were present in the post reaction solution when the 0.25%Au-0.75%Pd catalyst was used, whereas 0.168 mmol of H_2O_2 were present when the 0.75%Au-0.25%Pd catalyst was used.

A comparison between the benzyl alcohol conversion and H_2O_2 synthesis offered by each catalyst in this series is shown in Figure 4.17.

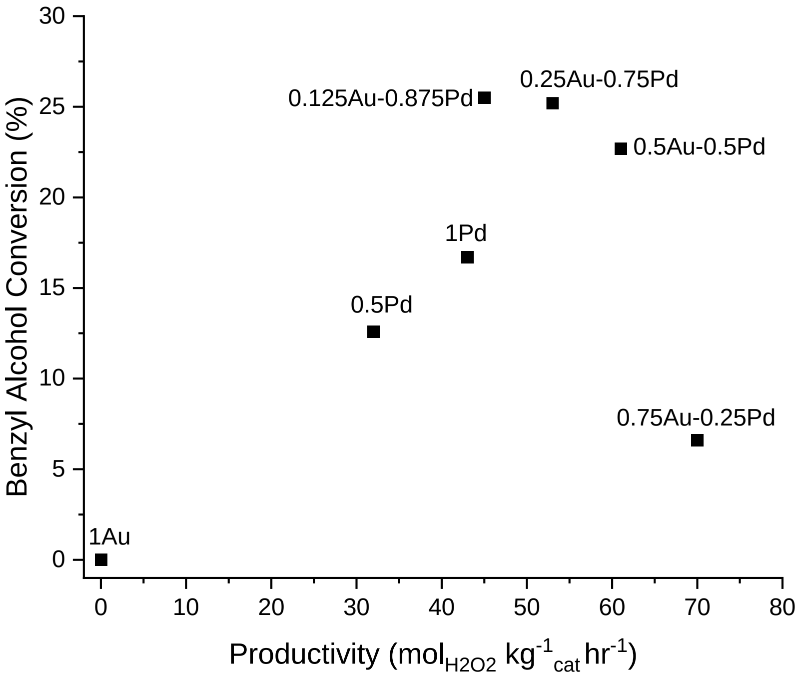

Figure 4.17. Comparison of the reported benzyl alcohol conversions and H_2O_2 productivity values offered by Pd and $AuPd/Al_2O_3$ catalysts with different Au:Pd ratios.
Benzyl alcohol oxidation reaction Conditions: Catalyst (0.01 g), MeOH (7.13 g), benzyl alcohol (1.04 g, 9.62 mmol), mesitylene (0.42 g), 5% H_2/CO_2 (420 psi, 2.76 mmol), 25% O_2/CO_2 (160 psi, 5.24 mmol), 0.5 hr, 50 ^{O}C, 1200 rpm.
H_2O_2 direct synthesis reaction conditions: Catalyst (0.01 g), H_2O (2.9 g), MeOH (5.6 g), 5% H_2/CO_2 (420 psi, 2.76 mmol), 25% O_2/CO_2 (160 psi, 5.24 mmol), 0.5 hr, 20 °C, 1200 rpm.

From the comparison of both the oxidation of benzyl alcohol and direct synthesis of H_2O_2 offered by each catalyst, it was determined that catalysts with greater proportions of Pd than Au favoured benzyl alcohol oxidation, whilst increasing the proportion of Au promoted the direct synthesis of H_2O_2 and inhibited the extent of benzyl alcohol oxidation. For example, the 0.125Au-0.875Pd catalyst offered a benzyl alcohol conversion of 25.5 % and a productivity of 45 mol_{H2O2} kg^{-1}_{cat} hr^{-1}, whilst the 0.75Au-0.25Pd catalyst offered a benzyl alcohol conversion of 6.6 % but a productivity of 70 mol_{H2O2} kg^{-1}_{cat} hr^{-1}.

This inverse relationship between benzyl alcohol oxidation and the direct synthesis of H_2O_2 was also observed with the analogous $AuPd/Al_2O_3$ catalysts prepared through the EcI methodology in Chapter 3. Indeed, this may represent a generically applicable feature of these supported AuPd catalysts, wherein enhancements in the catalytic selectivity towards H_2O_2 synthesis correspondingly inhibit the oxidation of benzyl alcohol and vice versa.

To further investigate the origins of this observation, diffuse reflectance infrared Fourier transform spectroscopy was performed for this series of catalysts, using CO as a probe molecule, and is shown in Figure 4.18.

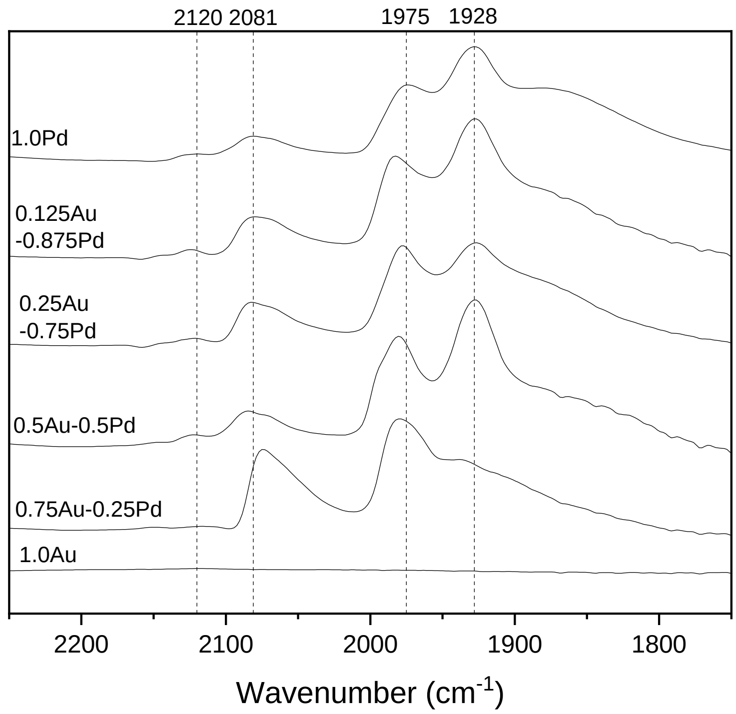

Figure 4.18. CO-DRIFTS spectra comparing a range of Au:Pd ratios of AuPd/Al_2O_3 catalysts, the prepared by the C.Imp Red methodology.

As previously discussed, the adsorption signal centred on 2081 cm^{-1} are a result of CO linearly adsorbed at Pd sites, whilst the broad signal centred on 1975 and 1928 cm^{-1} are a result of bridging and threefold bridging of CO at Pd sites.[240-245] The occurrence of the low intensity absorbance signal at 2120 cm^{-1} has been reported in the literature to correspond to the interaction of CO with residual surface Pd^{2+} ions, stabilised by adjacent surface chloride ions.[242, 245]

Interestingly, all AuPd bimetallic catalysts exhibit a well-defined signal at 1928 cm^{-1}, corresponding to a three-fold bridging configuration, with the exception of the 0.75%Au-0.25%Pd catalyst. Instead, the two-fold bridging signal at 1975 cm^{-1} dominates, whilst the relative intensity of the linear adsorption signal is also significantly enhanced and centred on 2072 cm^{-1}. This may indicate that as total Au content in the catalyst increases, the increasing presence of Au disrupts large ensembles of Pd that facilitate threefold bridging, in favour of twofold or linear CO adsorption. It should be noted that the 0.75%Au-0.25%Pd catalyst did not offer an increased reactivity towards the oxidation of benzyl alcohol compared to the 1%Pd catalyst, and also was the only catalyst to exhibit the above features, in addition to featuring no signal at 2120 cm^{-1}, possibly due to the lower levels of surface Pd. As such, it is possible that some or all of these observed differences may represent catalytically significant physical characteristics for an AuPd catalyst. For example, in terms of linear adsorption on the 0.75%Au-0.25%Pd catalyst, the signal at 2120 cm^{-1} is absent and the signal at 2081 cm^{-1} is shifted to a lower frequency, implying a greater degree of electron donation to CO compared to the other AuPd catalyst, which correspondingly may feature more electron deficient Pd sites for CO adsorption. Additionally, as stated, the signal associated with threefold bridging is suppressed relative to the twofold bridging signal, whereas the other catalysts with equal or greater levels of Pd to Au, threefold bridging is well facilitated.

Alternatively, this disruption of large Pd ensembles may be a result of smaller mean nanoparticle sizes arising as a result of the lower Pd content of the catalyst.

To consider any particle size effects associated with these adsorption modes and the overall catalytic activity, a TEM particle size analysis was conducted, the results of which are shown in Table 4.24.

Table 4.24. Particle size distributions observed via TEM of Pd/Al_2O_3 and $AuPd/Al_2O_3$ catalysts prepared by the C.Imp Red methodology, with varying metal loadings and metal loading ratios.

Catalyst	Mean Nanoparticle Size (nm)	Standard Deviation (nm)
0.5%Pd	3.0	1.7
1%Pd	5.1	4.8
0.125%Au-0.875%Pd	3.5	2.1
0.25%Au-0.75%Pd	3.1	1.8
0.5%Au-0.5%Pd	3.5	2.2
0.75%Au-0.25%Pd	2.4	1.4

Whilst similar benzaldehyde yields were produced by both the 0.5%Pd and 1%Pd catalysts, at 12.6 % and 16.7 % respectively, a moderate difference in nanoparticle size was observed. Indeed, whilst the 0.5%Pd catalyst has a mean nanoparticle size of 2.97 nm, the 1%Pd catalyst had larger nanoparticles with a mean size of 5.1 nm. All AuPd catalysts featured nanoparticles with an average size that fell within this range, with the exception of the 0.75%Au-0.25%Pd catalyst, which had the smallest mean nanoparticle size of 2.4 nm. Consequently, it is possible that the reduction in three-fold bridging of CO associated with this catalyst was a result of the small particle size, combined with high Au content disrupting any larger Pd ensembles that facilitate this adsorption mode. Otherwise, no systematic study has been conducted into the effects of the size of AuPd nanoparticles on the oxidation of benzyl alcohol via in-situ H_2O_2 synthesis, and no clear correlation can be made from this data set to link nanoparticle size to catalytic activity.

4.10 Conclusions

In summary, the efficacy of an in-situ H_2O_2 synthesis approach for the selective oxidation of benzyl alcohol has been further demonstrated when utilising appropriate catalysts, wherein significantly greater yields of benzaldehyde could be produced compared to if O_2 or preformed commercial H_2O_2 were used as oxidants at 50 ^oC. Additionally, all catalysts tested via this in-situ H_2O_2 synthesis method offered a high product selectivity towards benzaldehyde (>97 %) and formed only small quantities of benzoic acid in some instances.

Profound enhancements in catalytic activity were observed towards the selective oxidation of benzyl alcohol, when $AuPd/Al_2O_3$ and Pd/Al_2O_3 supported catalysts were prepared through a wet co-impregnation methodology with a reductive heat treatment, compared to both an excess chloride co-impregnation and sol immobilisation methodology, as shown in Table 4.25.

Table 4.25. Comparison of the catalytic activity of $AuPd/Al_2O_3$ and Pd/Al_2O_3 catalysts prepared by the C.Imp Red methodology when used in the selective oxidation of benzyl alcohol via in-situ H_2O_2 synthesis.

Catalyst	Preparation Methodology	Benzyl Alcohol Conversion (%)	Benzaldehyde Yield (%)	Benzoic Acid Yield (%)	Benzaldehyde Selectivity (%)
0.5%Au-0.5%Pd	C.Imp Red.	22.7	22.3	0.4	98
1%Pd	C.Imp Red.	16.7	16.7	0.0	100
0.5%Au-0.5%Pd	EcI	11.0	11.0	0.0	100
1%Pd	EcI	1.3	1.3	0.0	100
0.5%Au-0.5%Pd	Sol Red.	9.5	9.5	0.0	100

Benzyl alcohol oxidation reaction conditions: Catalyst (0.01 g), MeOH (7.13 g), benzyl alcohol (1.04 g, 9.62 mmol), mesitylene (0.42 g), 5% H_2/CO_2 (420 psi, 2.76 mmol), 25% O_2/CO_2 (160 psi, 5.24 mmol), 0.5 hr, 50 ^{O}C, 1200 rpm.

Additional studies were conducted using the 0.5%Au-0.5%Pd/Al_2O_3 and 1%Pd/Al_2O_3 catalysts prepared through the C.Imp Red. method, which revealed the extent of catalytic deactivation for each catalyst in addition to probing several mechanisms by which this could be taking place. This was done through extended reaction times (Figure 4.9), sequential reactions (Figure 4.10) and re-use experiments (Figure 4.11). Indeed, metal dissolution (Table 4.18) was shown to be low for any given metal (<0.1 %) after a 30-minute reaction, whilst some agglomeration of catalytic metal was also observed. Additionally, the in-situ reduction of Pd was reported.

A comparison of the catalytic activity towards benzyl alcohol oxidation via in-situ H_2O_2 synthesis of the most active catalysts presented in the literature and of several catalysts utilised in this Chapter and Chapter 3 are shown in Table A4.1, demonstrating the high activity of Al_2O_3 supported catalysts towards this reaction, compared to previously reported catalysts.

4.11 References

1. Crombie, C., Lewis, R., et al, Enhanced Selective Oxidation of Benzyl Alcohol via In Situ H2O2 Production over Supported Pd-Based Catalysts. *ACS Catal.* **2021,** *11*, 2701-2714.
2. Santonastaso, M., Freakley, S., et al, Oxidation of benzyl alcohol using in situ generated hydrogen peroxide. *Org. Process Res. Dev.* **2014,** *18*, 1455-1460.
3. Brehm, J., Lewis, R., et al, The Direct Synthesis of Hydrogen Peroxide over AuPd Nanoparticles: An Investigation into Metal Loading. *Catal. Lett.* **2021,** *152*, 254-262.
4. Lewis, R., Ueura, K., et al, Highly efficient catalytic production of oximes from ketones using in situ–generated H_2O_2. *Science* **2022,** *376*, 615-620.
5. Lewis, R., Ueura, K., et al, Cyclohexanone ammoximation via in situ H_2O_2 production using TS-1 supported catalysts. *Green Chem.* **2022,** *24*, 9496.
6. Ntainjua, E., Edwards, J., et al, The role of the support in achieving high selectivity in the direct formation of hydrogen peroxide. *Green Chem.* **2008,** *10*, 1162-1169.
7. Gong, X., Lewis, R., et al, Enhanced catalyst selectivity in the direct synthesis of H_2O_2 through Pt incorporation into TiO_2 supported AuPd catalysts. *Catal. Sci. Technol.* **2020,** *10*, 4635-4644.

8. Edwards, J., Pritchard, J., et al, The Direct Synthesis of Hydrogen Peroxide Using Platinum-Promoted Gold–Palladium Catalysts. *Angew. Chem. Int. Ed.* **2014,** *53*, 2381-2384.
9. Barnes, A., Lewis, R., et al, Enhancing catalytic performance of AuPd catalysts towards the direct synthesis of H2O2 through incorporation of base metals. *Catal. Sci. Technol.* **2022,** *12*, 1986.
10. Gong, X., Lewis, R., et al, Enhanced catalyst selectivity in the direct synthesis of H_2O_2 through Pt incorporation into TiO_2 supported AuPd catalysts. *Catal. Sci. Technol.* **2020,** *10*, 4635.
11. M. Sankar, H. Q., et al., Synthesis of Stable Ligand-free Gold-Palladium Nanoparticles Using a Simple Excess Anion Method. *ACS Nano* **2012,** *6*, 6600-6613.
12. Ouyang, L., Tian, P., et al, The origin of active sites for direct synthesis of H_2O_2 on Pd/TiO_2 catalysts: Interfaces of Pd and PdO domains. *J. Catal.* **2015,** *321*, 70-80.
13. Richards, T., Harrhy, J., et al, A residue-free approach to water disinfection using catalytic in situ generation of reactive oxygen species. *Nat. Catal.* **2021,** *4*, 575-585.
14. Lopez-Sanchez, J., Dimitratos, N., et al, Au–Pd supported nanocrystals prepared by a sol immobilisation technique as catalysts for selective chemical synthesis. *Phys. Chem. Chem. Phys.* **2008,** *10*, 1921-1930.
15. Gaikwad, A., Sansare S., Choudhary, V., Direct oxidation of hydrogen to hydrogen peroxide over Pd-containing fluorinated or sulfated Al_2O_3, ZrO_2, CeO_2, ThO_2, Y_2O_3 and Ga_2O_3 catalysts in stirred slurry reactor at ambient conditions. *J. Mol. Catal. A Chem.* **2002,** *181*, 143-149.
16. Choudhary, C., Gaikwad, A., Sansare, S., Activation of supported Pd metal catalysts for selective oxidation of hydrogen to hydrogen peroxide. *Catal. Letters* **2002,** *83*, 235-239.
17. Blanco-Brieva, G., Cano-Serrano, E., et al, Direct synthesis of hydrogen peroxide solution with palladium-loaded sulfonic acid polystyrene resins. *Chem. Commun.* **2004,** *0*, 1184-1185.
18. Wang, F., Xia, C., et al, How does the oxidation state of palladium surface affect the reactivity and selectivity of direct synthesis of hydrogen peroxide from hydrogen and oxygen gases? A density functional study. *J. Am. Chem. Soc.* **2019,** *141*, 901-910.
19. Ouyang, L., Da, G., et al, Insight into active sites of Pd–Au/TiO2 catalysts in hydrogen peroxide synthesis directly from H2 and O2. *J. Catal.* **2014,** *311*, 129-136.
20. Flaherty, D., Direct synthesis of H_2O_2 from H_2 and O_2 on Pd catalysts: Current understanding, outstanding questions and research needs. *ACS Catal.* **2018,** *8*, 1520-1527.
21. Lunsford, J., The direct formation of H2O2 from H2 and O2 over palladium catalysts. *J. Catal.* **2003,** *216*, 455-460.
22. Melada, S., Rioda, R., et al, Direct synthesis of hydrogen peroxide on zirconia-supported catalysts under mild conditions. *J. Catal.* **2006,** *239*, 422-430.
23. Ye, Y., Chun, J., et al, A study of the palladium size effect on the direct synthesis of hydrogen peroxide from hydrogen and oxygen using highly uniform palladium nanoparticles supported on carbon. *Korean J. Chem. Eng.* **2012,** *29*, 1115-1118.
24. Tian, P., Ouyang, L., et al, The origin of palladium particle size effects in the direct synthesis of H_2O_2: Is smaller better? *J. Catal.* **2017,** *349*, 30-40.
25. Zhang, Q., Deng, W., Wang, Y., Effect of size of catalytically active phases in the dehydrogenation of alcohols and the challenging selective oxidation of hydrocarbons. *Chem. Commun.* **2011,** *47*, 9275-9292.
26. Chan-Thaw, C., Sacara, A., Villa, A., Selective benzyl alcohol oxidation over Pd catalysts. *Catalysts* **2018,** *8*, 431.
27. Savara, A., Chan-Thaw, C., et al, Benzyl Alcohol Oxidation on Carbon-Supported Pd Nanoparticles: Elucidating the Reaction Mechanism. *ChemCatChem* **2014,** *6*, 3464-3473.
28. Yang, Z., Zhao, X., et al, Catalytic properties of palygorskite supported Ru and Pd for efficient oxidation of alcohols. *Catal. Commun.* **2015,** *65*, 34-40.
29. Wu, H., Zhang, Q., Wang, Ye., Solvent-Free Aerobic Oxidation of Alcohols Catalyzed by an Efficient and Recyclable Palladium Heterogeneous Catalyst. *Adv. Synth. Catal.* **2005,** *347*, 1356-1360.
30. Cao, E., Sankar, M., et al, Reaction and Raman spectroscopic studies of alcohol oxidation on gold–palladium catalysts in microstructured reactors. *Chem. Eng. J.* **2011,** *167*, 734-743.

31. Qingsheng Liu, J. L., The roles of chloride ions in the direct formation of H_2O_2 from H_2 and O_2 over Pd/SiO_2 catalyst in a H_2SO_4/ethanol system. *J. Catal.* **2006,** *239*, 237-243.
32. Wilson, N., Flaherty, D., Mechanism for the direct synthesis of H_2O_2 on Pd clusters: heterolytic reaction pathways at the liquid-solid interface. *J. Am. Chem. Soc.* **2016,** *138*, 574 - 586.
33. Choudhary, V., Samanta, C., Role of chloride or bromide anions and protons for promoting the selctive oxidation of H_2 by O_2 to H_2O_2 over supported Pd catalysts in an aqueous medium. *J. Catal.* **2006,** *238*, 28-38.
34. Samanta, C., Choudhary, V., Direct synthesis of H_2O_2 from H_2 and O_2 over Pd/H-beta catalyst in an aqueous acidic medium: Influence of halide ions present in the catalyst or reaction medium on H_2O_2 formation. *Catal. Commun.* **2007,** *8*, 73-79.
35. Sales, E., Jove, J., et al, Palladium, Palladium–Tin, and Palladium–Silver Catalysts in the Selective Hydrogenation of Hexadienes: TPR, M¨ossbauer, and Infrared Studies of Adsorbed CO. *J. Catal.* **2000,** *195*, 88-95.
36. Stakheev, A., Smirnova, N., et al, Single-atom Pd sites on the surface of Pd–In nanoparticles supported on g-Al2O3: a CO-DRIFTS study. *Mendeleev Commun.* **2017,** *27*, 515-517.
37. Zeinalipour-Yazdi, C., Willock, D., et al, CO adsorption over Pd nanoparticles: A general framework for IR simulations on nanoparticles. *Surf. Sci.* **2016,** *646*, 210-220.
38. Pawelec, B., Venezia, A., et al, AuPd alloy formation in Au-Pd/Al2O3 catalysts and its role on aromatics hydrogenation. *Appl. Surf. Sci.* **2005,** *242*, 380-391.
39. Lentz, C., Jand, S., et al, DRIFTS study of CO adsorption on Pt nanoparticles supported by DFT calculations. *J. Mol. Catal. A Chem.* **2017,** *426*, 1-9.
40. Smirnova, N., Mashkovsky, I., et al, Local Structure of Pd_1 Single Sites on the Surface of PdIn Intermetallic Nanoparticles: A Combined DFT and CO-DRIFTS Study. *Catal.* **2021,** *11*, 1376.
41. Zhang, L., Zhang, B., et al, The Effect of Pretreatment on the Reactivity of Pd/Al2O3 in Room Temperature Formaldehyde Oxidation. *Chem. Cat. Chem.* **2021,** *13*, 4133-4141.
42. Han, Y., Zhong, Z., et al, Au promotional effects on the synthesis of H_2O_2 directly from H_2 and O_2 on supported Pd-Au alloy catalysts. *J. Phys. Chem. C* **2007,** *111*, 8410 - 8413.
43. Carter, J., Althahban, S., et al, Synergy and Anti-Synergy between Palladium and Gold in Nanoparticles Dispersed on a Reducible Support. *ACS Catal.* **2016,** *6*, 6623-6633.
44. Cattaneo, S., Freakley, S., et al, Cinnamaldehyde hydrogenation using Au–Pd catalysts prepared by sol immobilisation. *Catal. Sci. Technol.* **2018,** *8*, 1677-1685.
45. Sun, K., Wilson, A., et al, Catalytic Deoxygenation of Octanoic Acid over Supported Palladium: Effects of Particle Size and Alloying with Gold. *ACS Catal.* **2015,** *5*, 1939-1948.
46. Perret, N., Cárdenas-Lizana, F., Keane, M., Selective hydrogenation of benzaldehyde to benzyl alcohol over Au/Al_2O_3. *Catal. Commun.* **2011,** *16*, 159-164.
47. Wu, P., Cao, Y., et al, Formation of PdO on Au–Pd bimetallic catalysts and the effect on benzyl alcohol oxidation. *J. Catal.* **2019,** *375*, 32-43.
48. Richards, T., Lewis, R., et al, The Direct Synthesis of Hydrogen Peroxide Over Supported Pd-Based Catalysts: An Investigation into the Role of the Support and Secondary Metal Modifiers. *Catal. Lett.* **2022,** *153*, 32-40.
49. Sankar, M., Nowicka, E., et al, The benzaldehyde oxidation paradox explained by the interception of peroxy radical by benzyl alcohol. *Nat. Commun.* **2014,** *5*, 3332.
50. Santos, A., Lewis, R., et al, Direct synthesis of hydrogen peroxide over Au-Pd supported nanoparticles under ambient conditions. *Ind. Eng. Chem. Res.* **2019,** *58*, 12623-12631.
51. Li, J., Ishihara, T., Yoshizawa, K., Theoretical revisit of the direct synthesis of H_2O_2 on Pd and Au@Pd surfaces: A comprehensive mechanistic study. *J. Phys. Chem. C* **2011,** *115*, 25359 - 25367.
52. Ham, H., Hwang, G., et al., On the role of Pd ensembles in selective H_2O_2 formation on PdAu alloys. *J. Phys. Chem. C* **2009,** *113*, 12943 - 12945.
53. Lyu, J., Niu, J., et al., In Situ Hydrogen Peroxide Production for Selective Oxidation of Benzyl Alcohol over a Pd@Hierarchical Titanium Silicalite Catalyst. *ACS Omega* **2020,** *5*, 16865-16874.

54. Martinez, J., Mazarío, J., et al., A tandem process for in situ H2O2 formation coupled with benzyl alcohol oxidation using Pd–Au bimetallic catalysts. *Dalton Trans.* **2022,** *51*, 17567-17578.
55. Moreno, I., Dummer, M., et al., Selective oxidation of benzyl alcohol using in situ generated H_2O_2 over hierarchical Au-Pd titanium silicate catalysts. *Catal. Sci. Technol.* **2013,** *3*, 2425.

4.12 Appendix

Table A4.1. Comparison of catalysts in the literature for the selective oxidation of benzyl alcohol via *in-situ* H_2O_2 synthesis.

Catalyst	Mass of Catalyst (mg)	Ratio of H_2:O_2	Solvent	Temperature (°C)	Time (hr)	Benzyl Alcohol (mmol)	Benzyl Alcohol Conversion (%)	Benzaldehyde Selectivity (%)	Turnover Number ($mol_{benzaldehyde}$ mol_{metal}^{-1} hr^{-1})	Reference
2.5%Au-2.5%Pd/TiO_2	10	1:1.9	MeOH	50	0.5	9.6	5.9	90	282	[27]
0.5%Fe-0.5%Pd/TiO_2	10	1:1.9	MeOH	50	0.5	9.6	5.8	96	783	[218]
0.5%Au-0.5%Pd/TiO_2	10	1:1.9	MeOH	50	0.5	9.6	2.8	100	743	[218]
0.1%Pd@HTS-1-OR	20	1:1.9	H_2O/MeOH	50	0.5	0.096	46.4	100	454	[131]
0.8%Pd-0.2%Au-H	5	1	H_2O	60	8	0.96	76.0	58	124	[130]
1.25%Au-1.25%Pd/TS-1	10	1:1.8	H_2O/MeOH	30	0.5	2.3	7.0	93	166	[114]
0.5%Au-0.5%Pd/Al_2O_3 (EcI)	10	1:1.9	MeOH	50	0.5	9.6	11.0	100	2919	This Work (Chapter 3)
0.5%Fe-0.5%Pd/Al_2O_3 (EcI)	10	1:1.9	MeOH	50	0.5	9.6	10.0	97	1406	This Work (Chapter 3)
0.5%Au-0.5%Pd/Al_2O_3 (C.Imp Red)	10	1:1.9	MeOH	50	0.5	9.6	22.7	98	5916	This Work (Chapter 4)
1% Pd/Al_2O_3 (C.Imp Red)	10	1:1.9	MeOH	50	0.5	9.6	16.7	100	3412	This Work (Chapter 4)

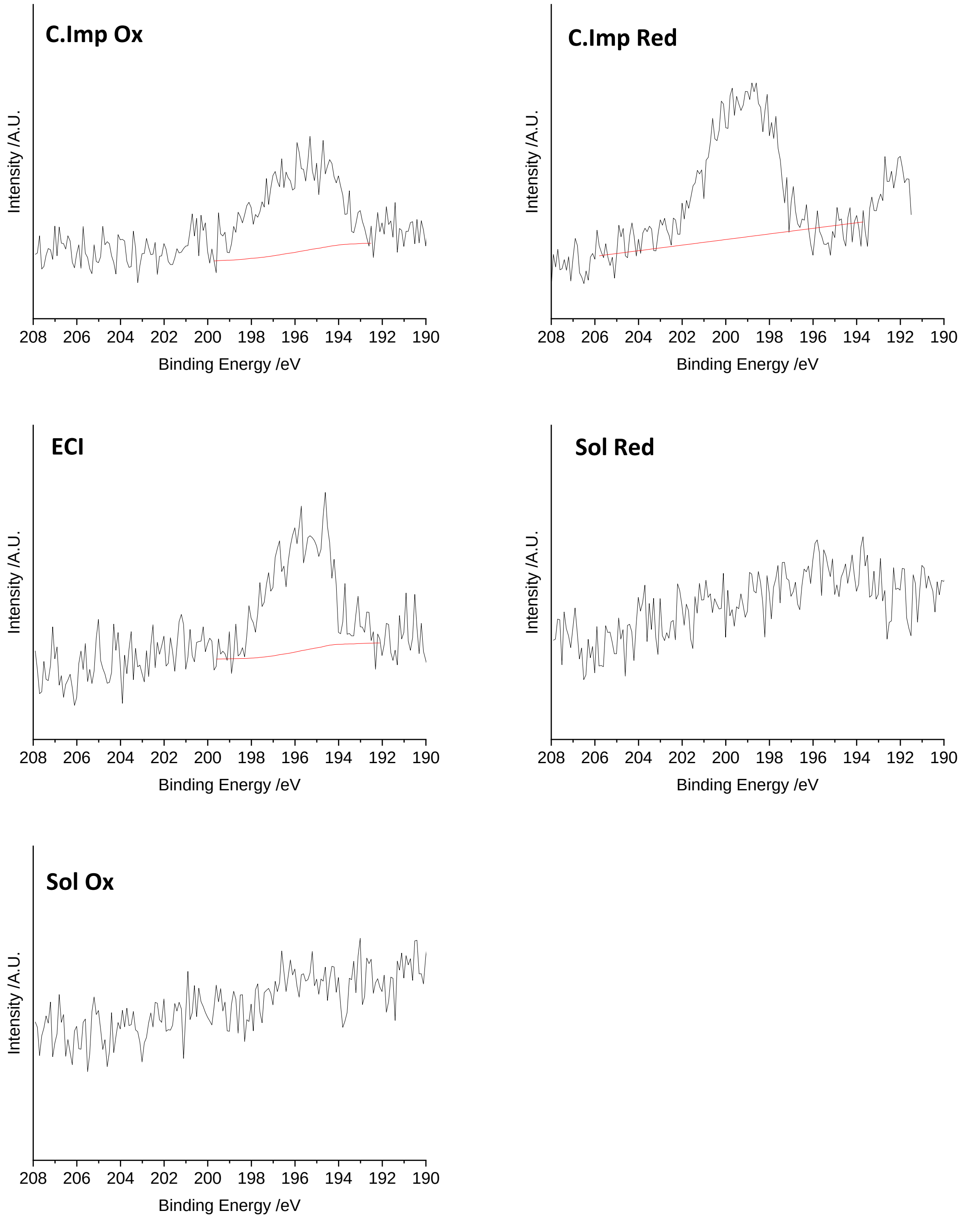

Figure A4.1. XPS Spectra of Cl 2p regions of 0.5%Au-0.5%Pd/Al_2O_3 when prepared by different methodologies and heat treatments

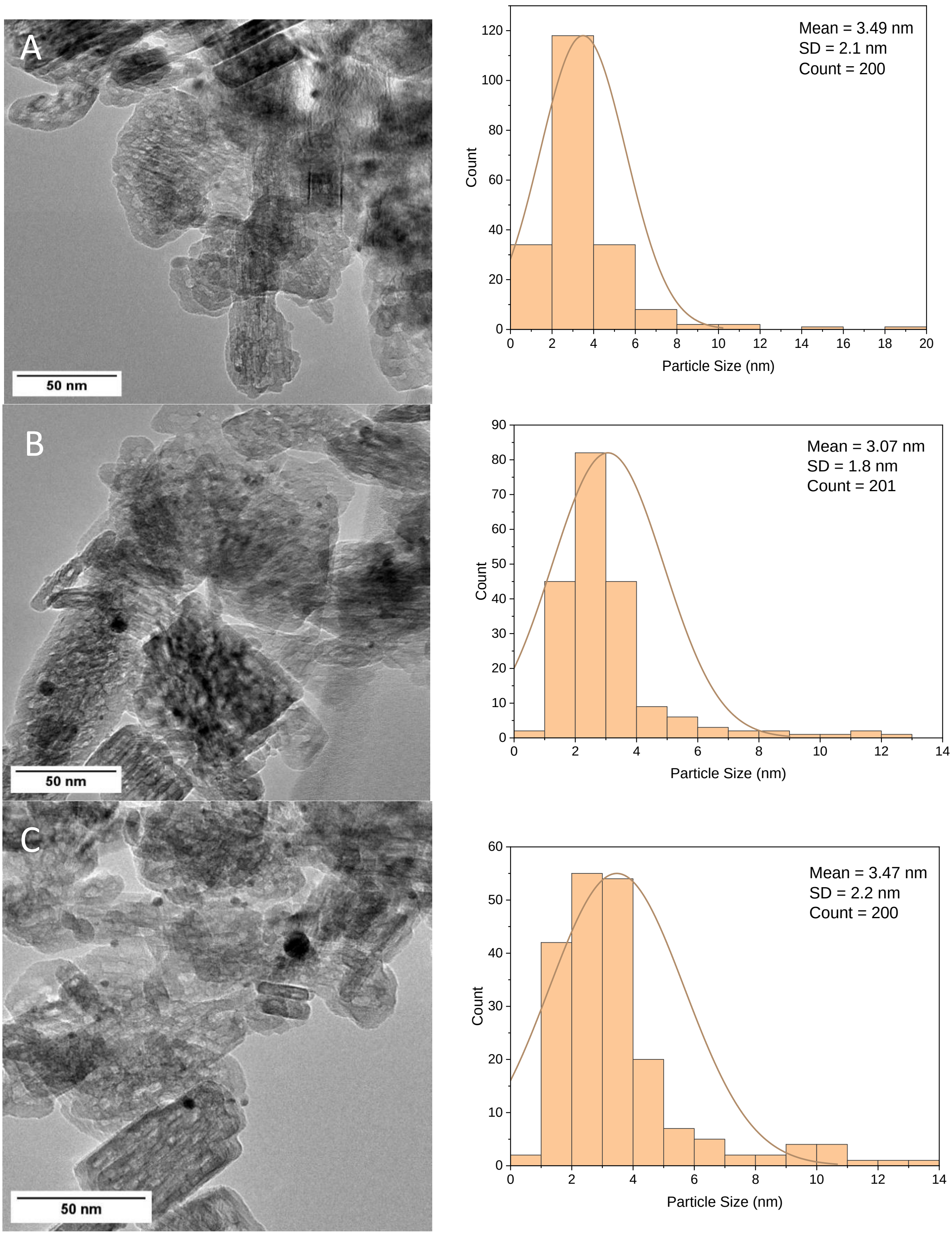
A
50 nm
Mean = 3.49 nm
SD = 2.1 nm
Count = 200
Count
Particle Size (nm)
B
50 nm
Mean = 3.07 nm
SD = 1.8 nm
Count = 201
Count
Particle Size (nm)
C
50 nm
Mean = 3.47 nm
SD = 2.2 nm
Count = 200
Count
Particle Size (nm)

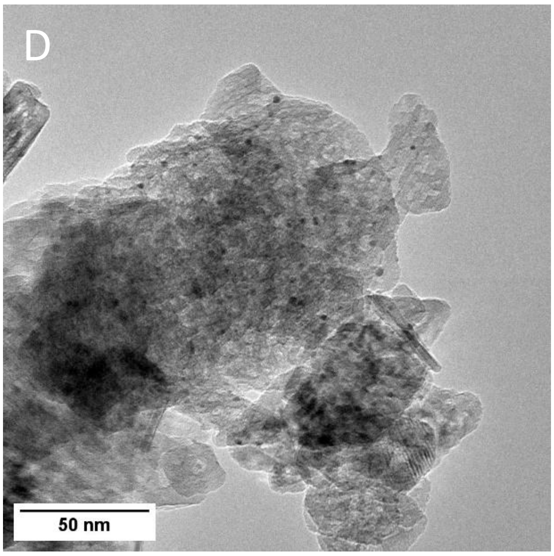

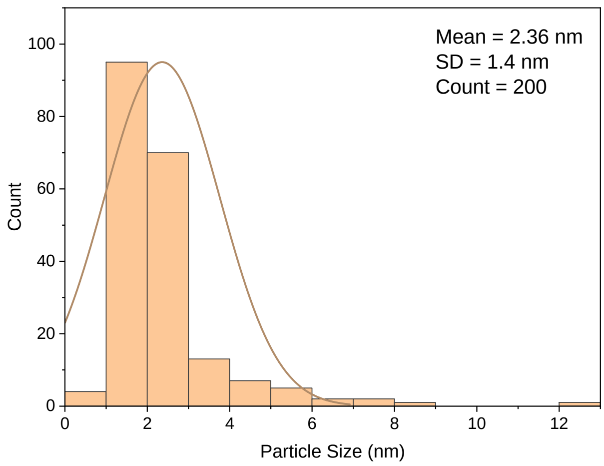

Figure A4.2. TEM images and particle size distributions of A) 0.125%Au-0.875%Pd/Al_2O_3, B) 0.25%Au-0.75%Pd/Al_2O_3, C) 0.5%Au-0.5%Pd/Al_2O_3 and D) 0.75%Au-0.25%Pd/Al_2O_3, prepared via a C.Imp Red methodology.

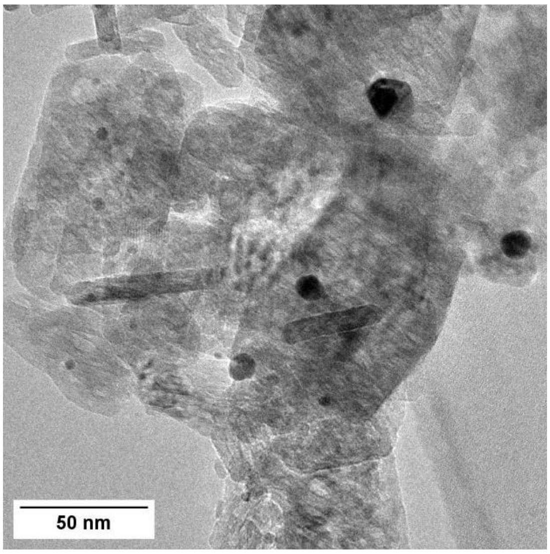

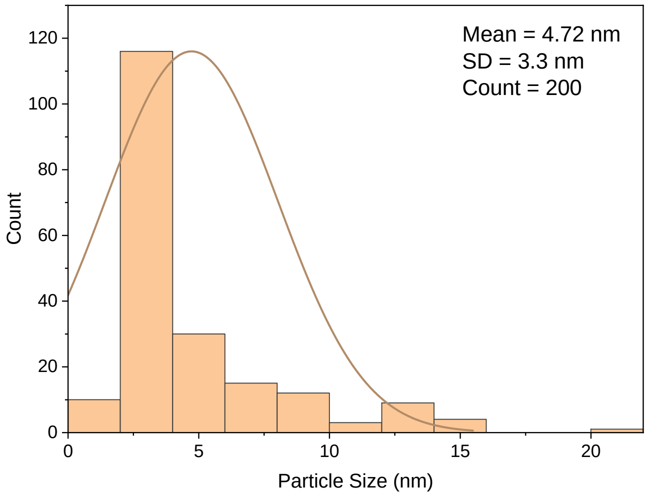

Figure A4.3. TEM image and particle size distribution for 0.5%Au-0.5%Pd/Al_2O_3 post reaction, prepared via a C.Imp Red methodology.

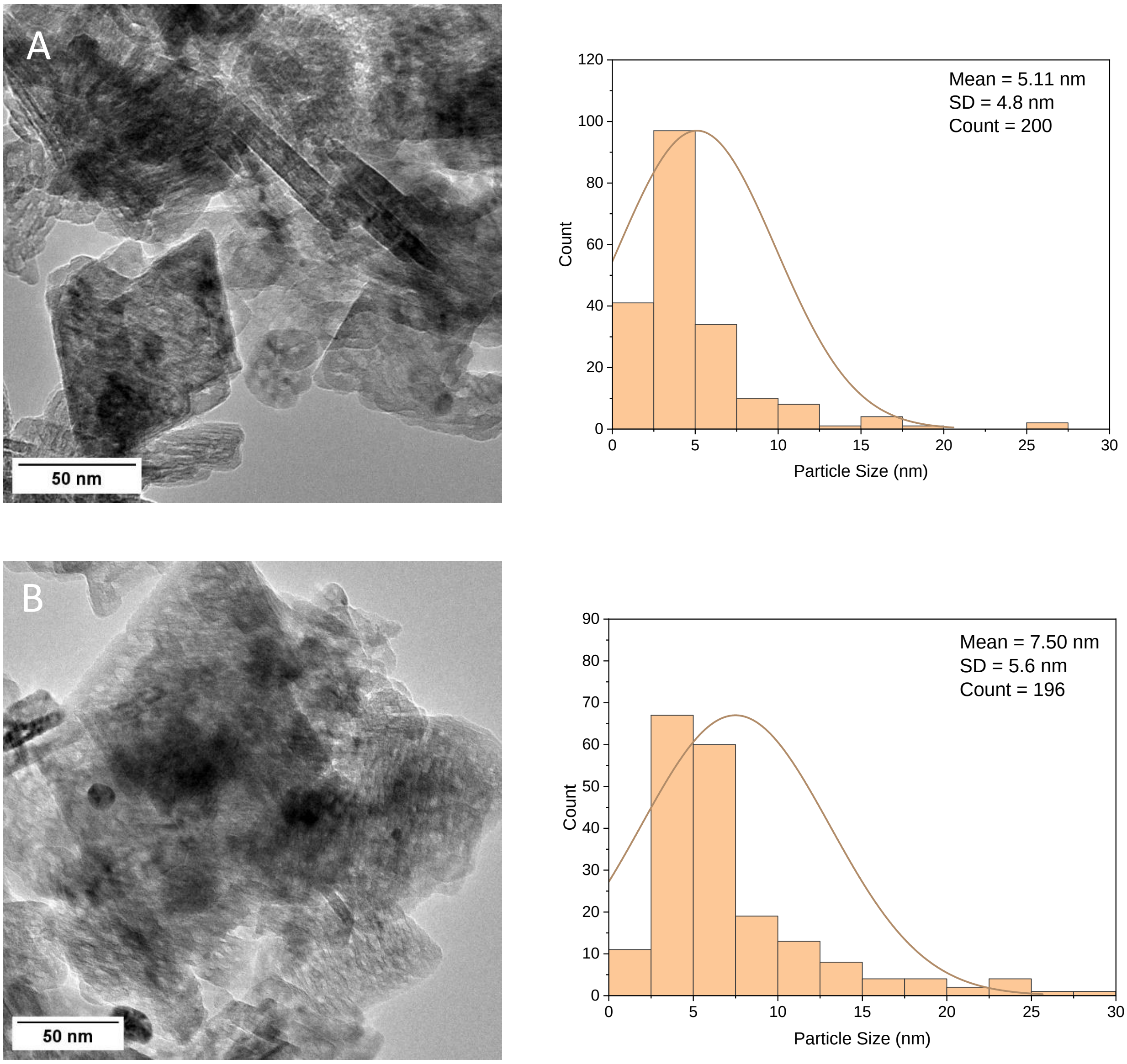

Figure A4.4. TEM images and particle size distributions of A) 1%Pd/Al_2O_3 pre-reaction and B) 1%Pd/Al_2O_3 post reaction, prepared via a C.Imp Red methodology.

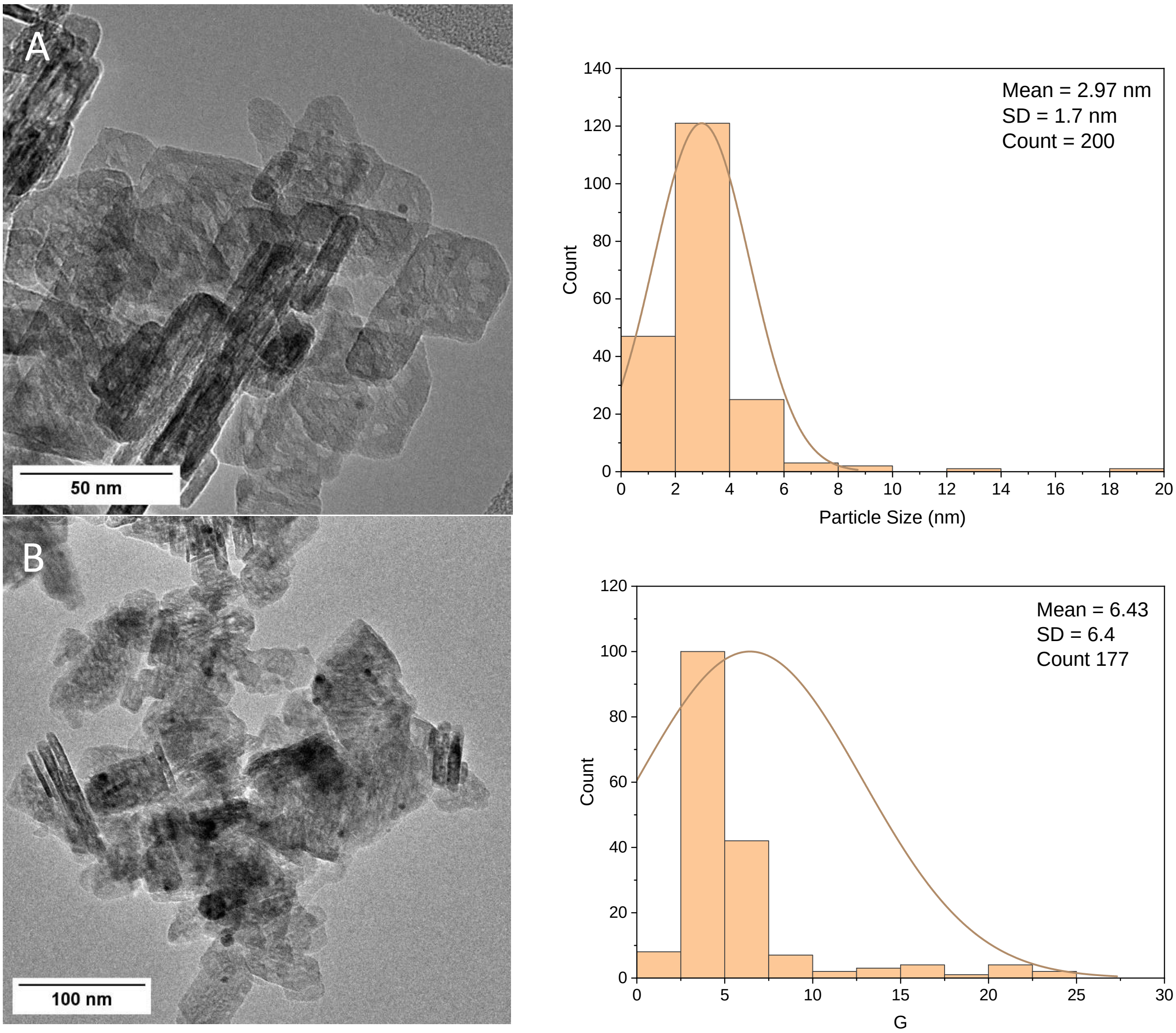

Figure A4.5. TEM images and particle size distributions of A) 0.5%Pd/Al_2O_3 and B) 0.5%Pd/Al_2O_3 post reaction, prepared via a C.Imp Red methodology.

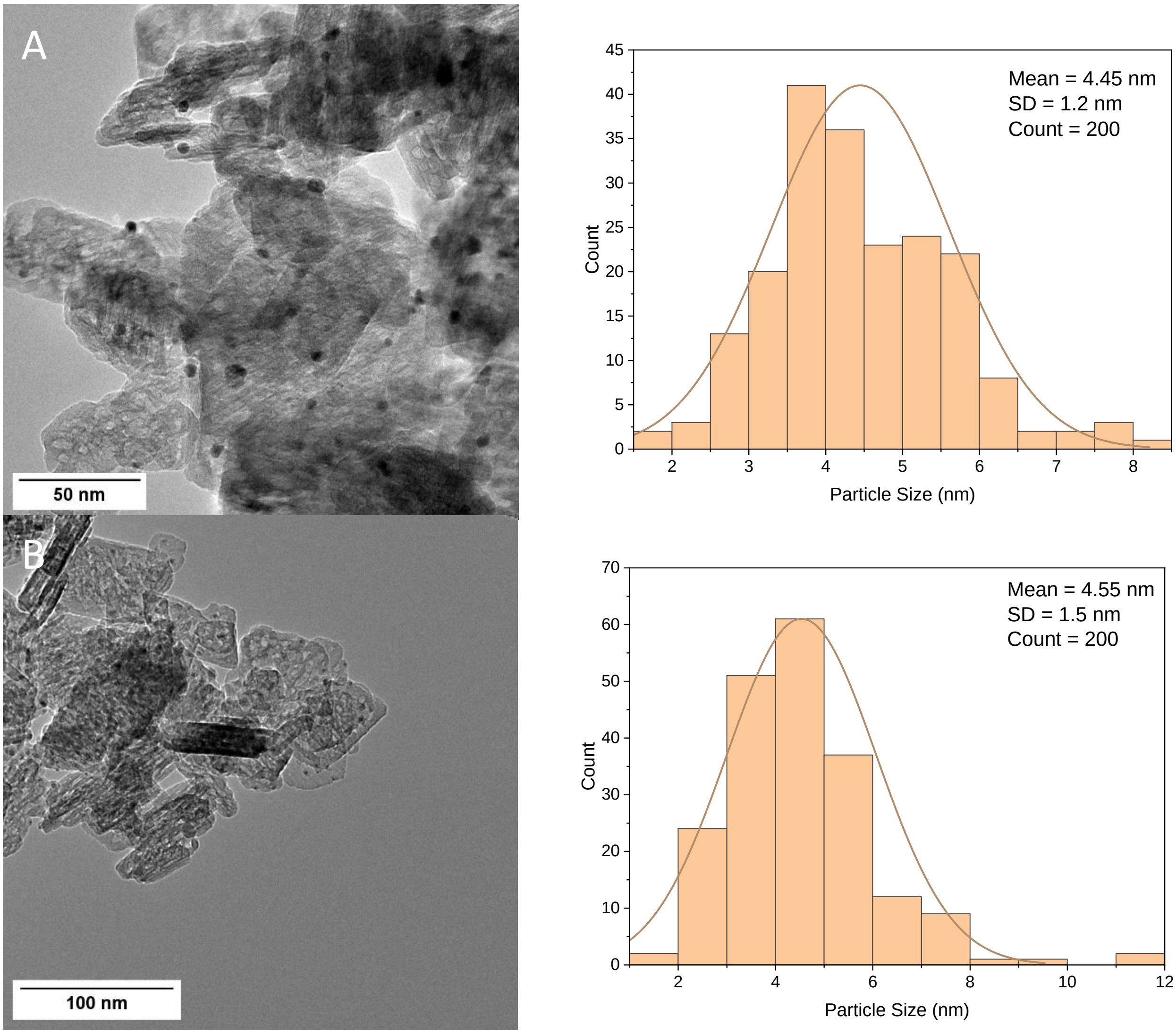

Figure A4.6. TEM images and particle size distributions of A) 0.5%Au-0.5%Pd/Al_2O_3 Sol Ox, and B) 0.5%Au-0.5%Pd/Al_2O_3 Sol Red.

Table A4.2. Surface area of supports and supported 0.5%Au-0.5%Pd catalysts when prepared by the C.Imp Red. method, as determined by BET.

Catalyst	Surface Area (M^2 g^{-1})
AuPd/Al_2O_3	74
Al_2O_3	83
AuPd/CeO_2	43
CeO_2	36
AuPd/TiO_2 (P25)	42
TiO_2 (P25)	53
AuPd/Nb_2O_5	8
Nb_2O_5	8
AuPd/ZrO_2	9
ZrO_2	21
AuPd/FLG	793
FLG	742

Table A4.3. Effects of Au:Pd ratio on the oxidation state of surface Pd, using AuPd/Al_2O_3 catalysts prepared using a wet co-impregnation methodology.[a]

Catalyst	Pd^0:Pd^{2+}
0.5Pd/Al_2O_3	0.67 : 0.33
1.0Pd/Al_2O_3	0.63 : 0.37
0.125Au-0.875Pd/Al_2O_3	0.35 : 0.65
0.25Au-0.75Pd/Al_2O_3	0.39 : 0.61
0.5Au-0.5Pd/Al_2O_3	0.36 : 0.64
0.75Au-0.25Pd/Al_2O_3	0.60 : 0.40

[a]Catalysts were exposed to a reductive heat treatment (5% H_2/Ar, 500 °C, 4 hr, 10°C min^{-1}) before XPS analysis.

5 Ascorbic Acid Promoted Catalytic Wet Peroxide Oxidation of Phenol, Using γ-Al_2O_3 Supported Catalysts

5.1 Introduction

Fenton's reagent was first utilised in 1896 by Henry Fenton, when he demonstrated the degradation of tartaric acid using a mixture of Fe^{2+} and H_2O_2.[272] This system operates as shown in Equations 5.1 and 5.2, wherein Fe^{2+} can react catalytically with H_2O_2 to form Fe^{3+} and a hydroxyl radical, whilst Fe^{3+} may react with H_2O_2 to be reduced to Fe^{2+} whilst generating a hydroperoxyl radical.[273]

Eq. 5.1 $$Fe^{2+} + H_2O_2 \rightarrow Fe^{3+} + {}^{\bullet}OH + {}^{-}OH \qquad k = 63\ M^{-1}\ s^{-1}$$

Eq. 5.2 $$Fe^{3+} + H_2O_2 \rightarrow Fe^{2+} + {}^{\bullet}OOH + H^{+} \qquad k = 0.002\text{-}0.01\ M^{-1}\ s^{-1}$$

As previously discussed, these oxygen-based radicals are highly active oxidants with the potential to oxidise a wide variety of organic compounds.[274] For example, in recent years, significant research has been conducted using similar Fe/H_2O_2 systems for the treatment of industrial wastewater, the degradation of specific organic pollutants, the degradation of dyes and the removal of antibiotics from waste streams.[275-279]

However, limitations are associated with the use of these homogeneous Fenton's systems. For example, Fenton's reagent operates most efficiently at pH of approximately 3.5,[274, 280] often necessitating the acidification of reaction media, whilst the subsequent removal of homogeneous Fe from product streams adds additional cost and complexity to any process involving their use. At higher pH values, the predominant $[Fe(H_2O)_6]^{3+}$ complex is insoluble (pH >5) and undergoes precipitation reactions that results in the conversion of catalytically active Fe^{2+} to inactive and insoluble precipitates, such as $Fe_2O_3{\cdot}nH_2O$. [280, 281]

To overcome these limitations, heterogeneous catalysts have been investigated in the literature, such as supported metal nanoparticle catalysts,[164, 178, 181, 282-284] although additional challenges are presented when heterogenous catalysts are used, such as limiting the extent of metal leaching and preventing catalyst deactivation.

An alternate approach taken to overcome the limitations associated with Fe based catalysts has been to utilise other metals as catalysts. Indeed, Cu-based catalysts have been studied extensively for this class of reaction and have been reported to function in an analogous manner to Fe based catalysts, as shown in Equations 5.3 and 5.4.[280, 285, 286]

Eq. 5.3 $$Cu^{+} + H_2O_2 \rightarrow Cu^{2+} + {}^{\bullet}OH + {}^{-}OH \qquad k = 1.0 \times 10^{4}\ M^{-1}\ s^{-1}$$

Eq. 5.4 $$Cu^{2+} + H_2O_2 \rightarrow Cu^{+} + {}^{\bullet}OOH + H^{+} \qquad k = 1.2 \times 10^{-6}\ M^{-1}\ s^{-1}$$

Unlike the $[Fe(H_2O)_6]^{3+}$ complex, which is insoluble at a neutral pH, the $[Cu(H_2O)_6]^{2+}$ complex remains soluble, and therefore may function over a greater pH range.[280]

In addition to optimisation of the catalyst, further enhancements to the oxidative efficacy of a Fenton type system can be achieved through the incorporation of ascorbic acid into the reaction medium.[287] For example, Bolobajev *et al.* reported that the iron sulfate catalysed degradation of alachlor by an Fe^{3+}/H_2O_2/ascorbic acid system was moderately enhanced

compared to using an Fe^{2+}/H_2O_2 system and that the degradation of alachor was significantly enhanced compared to when an Fe^{3+}/H_2O_2 system was used.[194] The authors attributed this enhancement in activity to the continual in-situ reduction of Fe^{3+} to Fe^{2+}, leading to greater levels of $^{\bullet}OH$ generation.[194] A similar observation was also made by Xiao *et al.* who utilised CuO nanosheets in tandem with H_2O_2 and ascorbic acid in the catalytic degradation of rhodamine B.[285] The authors observed that enhanced levels of rhodamine B degradation could be achieved through the addition of ascorbic acid to the reaction, which they attributed to in-situ reduction of Cu^{2+} to Cu^{+}, and an associated enhancement in $^{\bullet}OH$ generation.[285]
Whilst the exact mechanism is still debated, it should be noted that ascorbic acid may be converted to an ascorbate radical by a one-electron reduction process in the presence of a catalytic metal such as Fe or Cu.[192, 288] However, it has been reported that the ascorbate radical is relatively unreactive compared to hydroxyl and hydroperoxyl radicals,[288] and it is unclear to what extent this ascorbate radical may take part directly in the oxidation of a target molecule.

The topic of investigation in this study was the ascorbic acid promoted catalytic wet peroxide oxidation reaction, focusing on the oxidation of phenol as a model reaction system. This reaction was chosen because the oxidation of phenol via a catalytic wet peroxide oxidation system has been well studied in the literature.[164, 277, 282, 289, 290] A general reaction scheme for the oxidation of phenol is shown in Figure 5.1, however, it should be noted that many differing specific reaction pathways have been proposed in the literature.[291, 292]

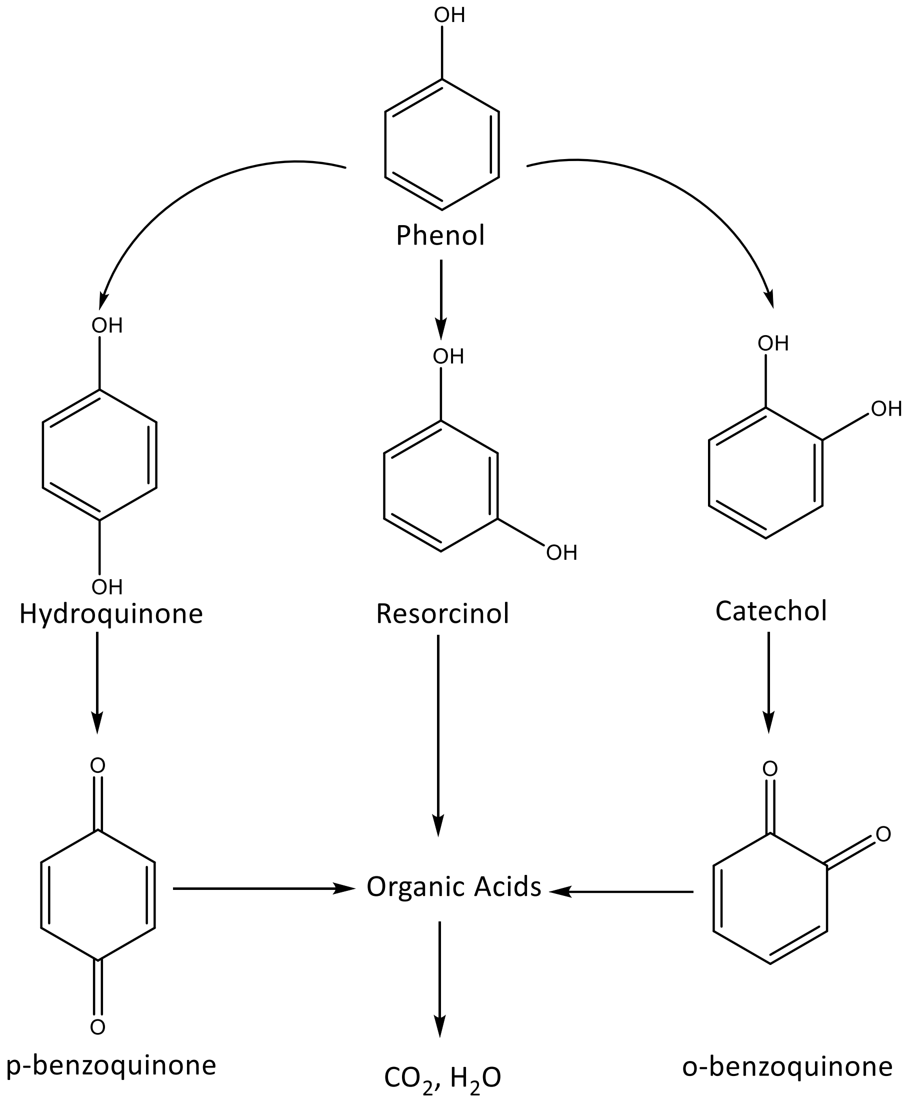

Figure 5.1. General reaction pathway for the oxidation of phenol with hydroxyl radicals under acidic conditions. [156, 291]

The objective of this work was to investigate the efficacy of utilising both ascorbic acid and H_2O_2 with a supported metal catalyst using the phenol oxidation reaction as a model system. Key areas of investigation included the choice of catalytic metal, the concentrations of reactants used, the effects of any additional additives and the choice of H_2O_2 source.

Note on methodology: This Chapter of work was conducted in collaboration with a sponsor company (Selden Research Ltd.), who aimed to develop a system incorporating the use of a heterogeneous catalyst with H_2O_2 and ascorbic acid to disinfect surfaces. As a result, the specific methodology of catalyst testing used throughout this Chapter was employed in order to be consistent with work done by other researchers towards this application, such as the use of a catalyst bed separating the catalyst and reaction solution, and the use of ambient temperature and pressure.

5.2 The Choice Metal for Al_2O_3 Supported Catalysts for the Catalytic Wet Peroxide Oxidation of Phenol

Whilst Fe has historically been the most commonly used metal for catalytic wet peroxide oxidation reactions, such as in Fenton's reagent, numerous other metals have also been shown to function by an analogous mechanism.[280] For example, Cu, Mn and Co have all been reported to be capable of generating hydroxyl radicals from H_2O_2.[280] Indeed, Cu based catalysts represent a particularly well studied analogue to Fe containing systems, with numerous homogeneous and heterogeneous examples reported in the literature, including $CuSO_4$, CuO, Cu/Al_2O_3, Cu/SBA-15 and Cu slag.[293-297] Moreover, Fe and Cu based catalysts have already been utilised alongside ascorbic acid and H_2O_2 in the oxidation of alachlor and rhodamine B respectively, wherein enhancements to the oxidation of the target molecule correlated with the addition of ascorbic acid.[285, 287] Therefore, a range of catalytic metals may be applicable for use in a catalytic wet peroxide oxidation, enhanced by ascorbic acid.

In order to select a suitable active metal for use in the investigation, a series of Al_2O_3 supported catalysts (2 wt.%) with previously reported activity in catalytic wet peroxide oxidation reactions were synthesised by a conventional impregnation methodology and heat treated under static air.[280] These are shown in Table 5.1. The metals selected were based on previously reported uses in the literature alongside H_2O_2 in catalytic wet peroxide oxidation reactions. For example, in addition to the Cu and Fe based catalysts discussed above, Mn has been utilised in the oxidation of phenol, norfloxacin and methylene blue,[298-300] whilst Co has been used to oxidise a wide range of organic compounds in the presence of H_2O_2.[293, 301]

Note on heat treatment conditions: The conditions used for the Cu/Al_2O_3 catalyst were selected to be consistent with the work done by Selden Research Ltd.
Heat treatments for the Fe, Mn and Co/Al_2O_3 catalysts were based on protocols reported previously in the literature.

Table 5.1. Al_2O_3 supported catalysts synthesised for use in the catalytic wet peroxide oxidation of phenol. Metal loadings set to 2 wt.%

Catalyst	Precursor	Heat Treatment Conditions
Cu/Al_2O_3	$Cu(NO_3)_2 \cdot 2.5H_2O$	750 ^oC, 3 hours, 10 ^oC/min, compressed air
Fe/Al_2O_3	$FeCl_3$	500 ^oC, 3 hours, 10 ^oC/min, compressed air[302]
Mn/Al_2O_3	$MnCl_2$	400 ^oC, 3 hours, 10 ^oC/min, compressed air[303, 304]
Co/Al_2O_3	$Co(NO_3)_2 \cdot 6H_2O$	500 ^oC, 3 hours, 10 ^oC/min, compressed air[305]

An initial set of reaction conditions were used, in which an aqueous solution containing ascorbic acid (0.4 wt.%) and sodium percarbonate (0.3 wt.%) as the source of H_2O_2 was passed through the loaded catalyst bed before being added to the phenolic solution (1000 ppm). The configuration of the catalyst bed and reactor is shown in Figure 5.2. It should be noted that the supported catalyst was present in the catalyst bed as a powder and did not come into contact with the phenolic solution.

n.b. The term 'oxidant mixture' is used to describe the mixture of H_2O with ascorbic acid and/or sodium percarbonate prior to its addition to the phenol solution. The combination of the phenol solution and the oxidant mixture is referred to as the reaction mixture. Additionally, because both the oxidant mixture and the phenolic solution were mixed, the initial concentration of phenol at the beginning of a given reaction was 500 ppm.

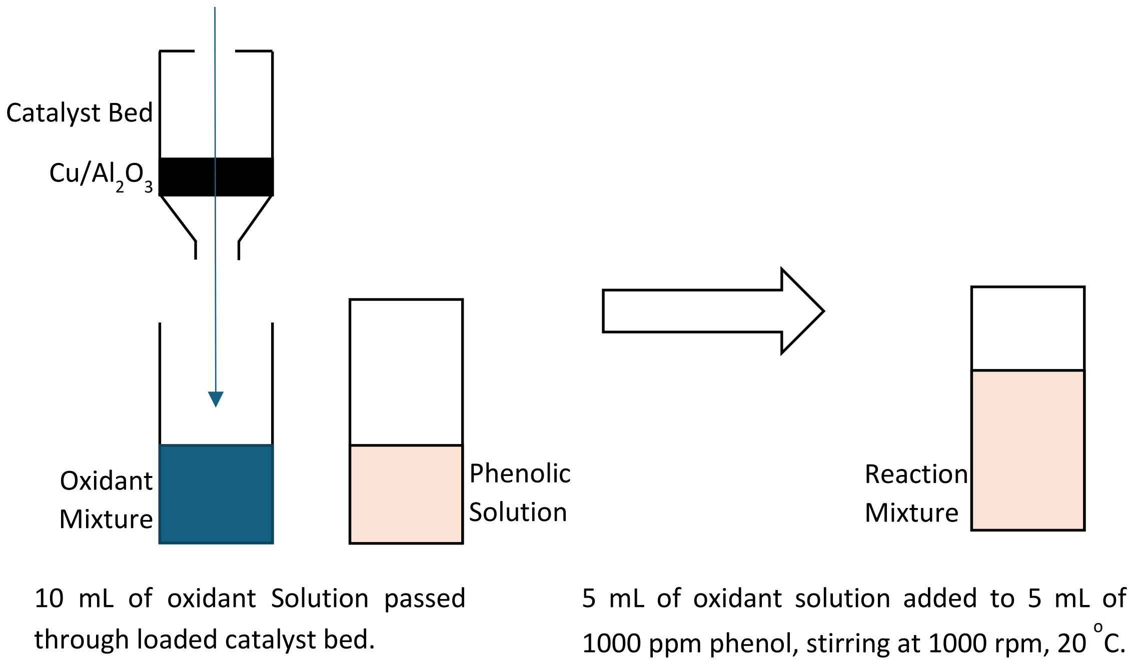

Figure 5.2. Schematic diagram showing the configuration of the catalyst bed and reactor.

The concentrations of ascorbic acid and sodium percarbonate initially utilised in this study were based on preceding work within the research group, whilst ambient reaction conditions were used in accordance with the intended application of the overall reaction system as a disinfectant.

Each Al_2O_3 supported catalyst was then evaluated for catalytic activity in the catalytic wet peroxide oxidation of phenol, the results of which are shown in Figure 5.3 and Table 5.2.

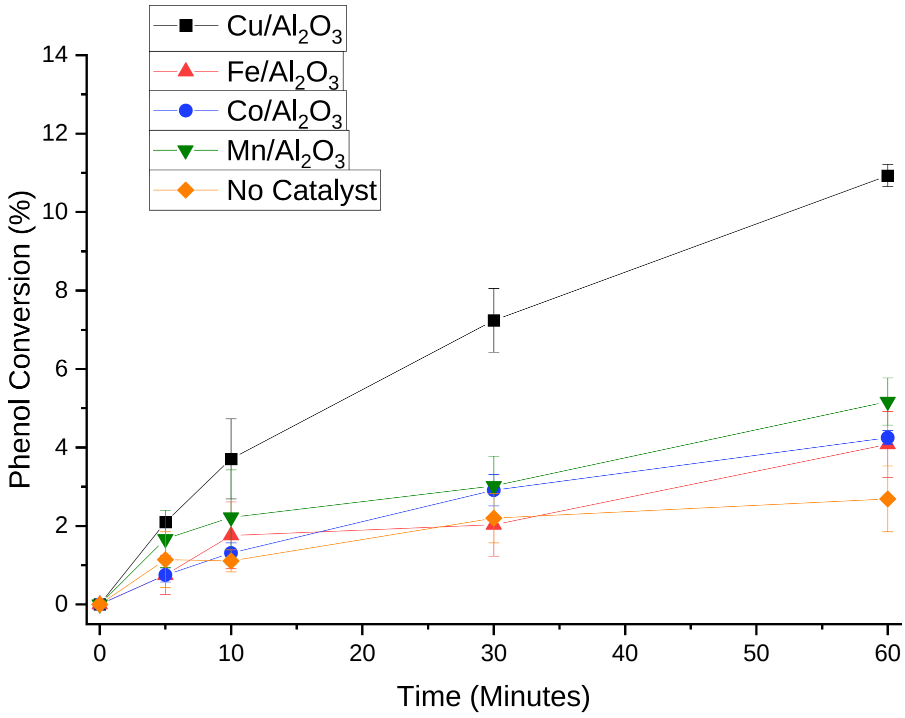

Figure 5.3. The catalytic wet peroxide oxidation of phenol, using a range of Al_2O_3 supported catalysts. **Phenol oxidation reaction conditions:** Catalyst (100 mg), H_2O (10 mL), phenol (500 ppm, 0.053 mmol), ascorbic acid (0.114 mmol), sodium percarbonate (0.096 mmol), 1.0 hr, 20 ^{0}C, 1000 rpm.

Table 5.2. The catalytic wet peroxide oxidation of phenol, using a range of Al_2O_3 supported catalysts.

Catalyst	Phenol Conversion (%)	Catechol Yield (%)	Hydroquinone Yield (%)	Organic Acid Yield (%)
Cu/Al_2O_3	10.9	4.2	4.1	2.9
Fe/Al_2O_3	4.1	1.9	2.1	0.0
Mn/Al_2O_3	5.2	2.5	2.7	0.0
Co/Al_2O_3	4.3	2.0	2.2	0.0
No catalyst	2.7	1.3	1.4	0.0

Phenol oxidation reaction conditions: Catalyst (100 mg), H_2O (10 mL), phenol (500 ppm, 0.053 mmol), ascorbic acid (0.114 mmol), sodium percarbonate (0.096 mmol), 1.0 hr, 20 ^{0}C, 1000 rpm.

When used in the catalytic wet peroxide oxidation of phenol, all catalysts offered an enhanced level of phenol conversion above that which was observed in the absence of a catalyst. Interestingly, when no catalyst was used, 2.7 % of phenol was converted, demonstrating some limited capability for the sodium percarbonate and ascorbic acid mixture to oxidise phenol. The greatest extent of phenol oxidation was achieved using the Cu/Al_2O_3 catalyst, which offered a phenol conversion of 10.9 %, whilst more moderate levels of phenol conversion were achieved by the Fe, Mn, and Co based catalysts. For example, the Fe/Al_2O_3 catalyst offered a limited phenol conversion of 4.1 %, whilst the Mn/Al_2O_3 and Co/Al_2O_3 catalysts offered phenol conversions of 5.2 % and 4.3 % respectively. The primary products of the oxidation reaction were hydroquinone and catechol, which formed in approximately equal ratios for all catalysts used, whilst no resorcinol was observable. Additionally, when the Cu/Al_2O_3 catalyst was used, the formation of organic acids was also observed. Many possible organic acid products exist, including muconic acid, maleic acid, oxalic acid, formic acid, acetic acid and oxalic acid.[282] However, separating and calibrating each acid via the HPLC methodology used was not achievable due to the similar retention times of the many acid products and ascorbic acid, and consequently, individual yields of organic acids were not determined. Additionally, the extent of possible mineralization to CO_2 and H_2O was not determined, because the reaction was done in aqueous solution, in an unsealed reactor vessel.

The absence of any observable benzoquinone derivatives was unexpected, because benzoquinones have been reported to exist in equilibrium with their corresponding dihydroxybenzoquinones, as shown in Figure 5.1.[291] Additionally, the presence of p-benzoquinone has been reported during the phenol oxidation reaction by analogous Fe/H_2O_2 systems.[291, 292] The absence of p-benzoquinone as a reaction product in this work may be a result of the reactivity of ascorbic acid, which is a reducing agent, [306, 307] and may be regenerating the dihydroxybenzoquinone form over the benzoquinone,[308] although no investigation was done towards this hypothesis.

The lack of resorcinol formation, in favour of catechol and hydroquinone synthesis can be attributed to the activation of the *ortho* and *para* sites of the phenyl ring, relative to the *meta* site, by the hydroxyl group of phenol through the relative balance of electron withdrawing (inductive) effects and resonance (mesomeric) effects.[309]

Additionally, the initial or final concentrations of H_2O_2 in-situ could not be determined for this reaction methodology. This was because the commonly used redox titration method involving cerium sulfate and a ferroin indicator[238] was unsuitable due to a false positive result occurring as a result of the presence of ascorbic acid. Methods using UV-Vis spectroscopy[249] also could not be used due to a strong colouration of the reaction mixture that arose due to the formation of catechol and the degradation of ascorbic acid, which obscured any peak associated with H_2O_2.

To investigate the physical properties of the Cu present in the Cu/Al_2O_3 catalyst, XPS was conducted by Dr David Morgan at Cardiff University, the results of which are shown in Figure 5.4.

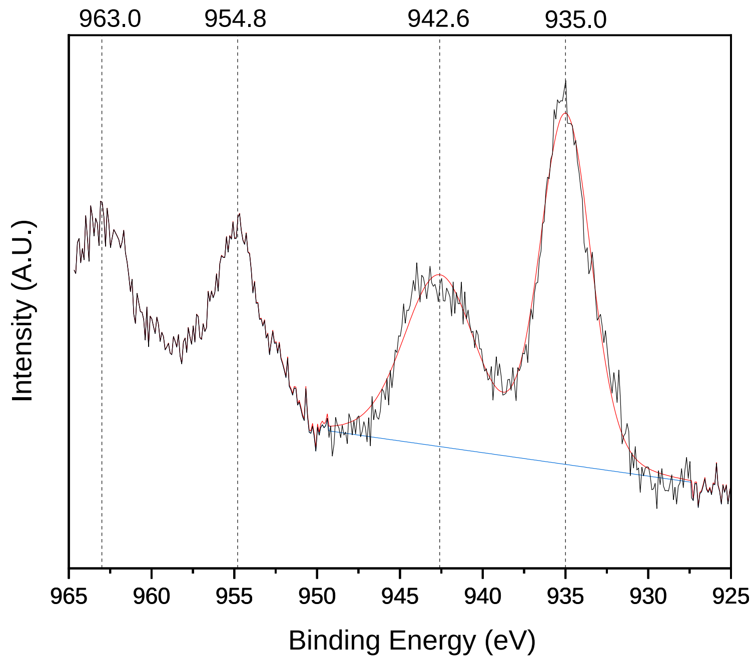

Figure 5.4. XPS Spectrum of Cu 2p transitions for $2\%Cu/Al_2O_3$.

From the spectrum shown in Figure 5.4, the $Cu2p_{3/2}$ and $Cu2p_{1/2}$ transitions appear at 935 eV and 954.8 eV respectively, whilst the features appearing at 942.6 eV and 963.0 eV are satellite peaks. The occurrence of these satellite peaks has been reported to occur in the presence of Cu in the d^9 electronic state, and arising as a result of an electron transfer process from a ligand electronic orbital to the 3d orbital of Cu.[310-313]

Previously in the literature, a binding energy of 935 eV for the $Cu2p_{3/2}$ has been attributed to the presence of $CuAl_2O_4$ spinel structures,[313, 314] suggesting that surface Cu in the Cu/Al_2O_3 catalyst used herein is present in a spinel structure. The formation of Cu spinel structures has been reported in the literature to require high temperature calcination processes.[315, 316] For example, Salvati-Niasari *et al.* prepared $CuAl_2O_4$ by a sol-gel method and observed that calcination of the precursor at 400 °C resulted in the formation of CuO nanocrystals, whereas calcination of the precursor at 800 °C yielded $CuAl_2O_4$ nanocrystals.[316] Therefore, it is possible that the high calcination temperature (750 °C) used in this work to synthesise the Cu/Al_2O_3 catalyst resulted in the formation of Cu^{2+} spinel structures.

The surface area of each Al_2O_3 supported metal catalyst was then determined using 5-point BET, the results of which are shown in Table 5.3.

Table 5.3. Surface area of Al_2O_3 supported metal catalysts investigated, determined by 5-point BET.

Catalyst	**Surface Area ($m^2\ g^{-1}$)**
Al_2O_3	79
Cu/Al_2O_3	67
Fe/Al_2O_3	65
Mn/Al_2O_3	68
Co/Al_2O_3	76

From this analysis, it was observed that the Al_2O_3 support had a surface area of 79 $m^2\ g^{-1}$, whilst any supported metal catalyst experienced some decrease in surface area as a result of the catalyst synthesis process. For example, the Fe/Al_2O_3 and Cu/Al_2O_3 catalysts had surface areas of 65 and 67 $m^2\ g^{-1}$ respectively whilst the Co/Al_2O_3 catalyst had the greatest surface area of 76 $m^2\ g^{-1}$.

X-ray diffraction data was collected for both the 2%Cu/Al_2O_3 catalyst and Al_2O_3 support and is shown in Figure 5.5. Due to the low metal loadings of Cu utilised in this project, no reflection associated with Cu could be observed, though they may have been obscured by the intense reflections associated with the Al_2O_3 support . The diffractogram of Al_2O_3 showed peaks at 2-theta values of approximately 67, 61, 46, 40, 37 and 33 which corresponds to γ-Al_2O_3 (Reference Code 00 010 0425)[317] and confirms this to be the morphology of the Al_2O_3 support.

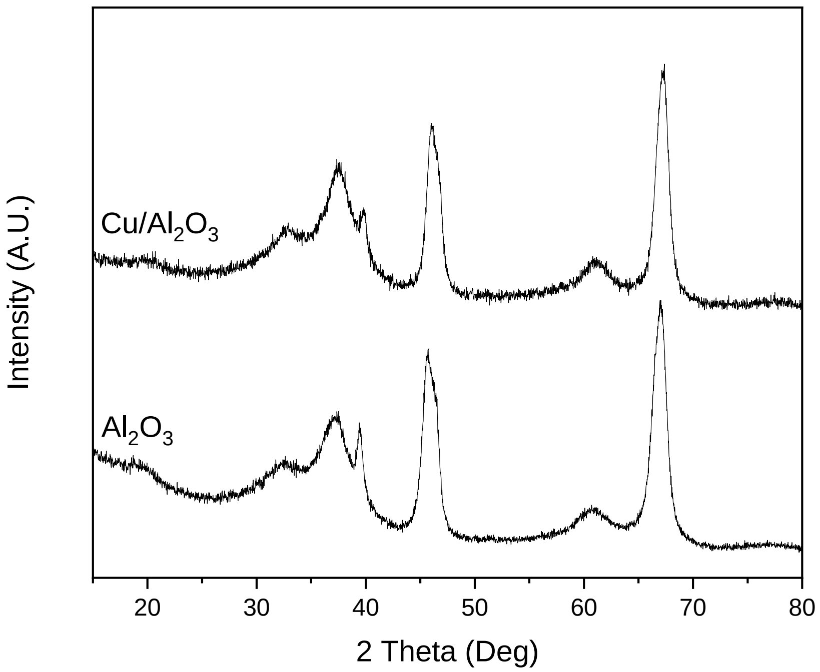

Figure 5.5. X-Ray Diffractogram of the Al_2O_3 support and 2%Cu/Al_2O_3 catalyst.
n.b. γ-Al_2O_3 (Reference Code 00 010 0425)[317]

5.3 The Effects of Reaction Mixture Composition Towards the Catalytic Wet Peroxide Oxidation of Phenol

When used in the catalytic wet peroxide oxidation of phenol, the Cu/Al_2O_3 catalyst offered the greatest phenol conversion of the supported metals tested and was selected for use in proceeding studies.

As discussed, several publications have previously reported the enhanced oxidative activity of Fe or Cu/H_2O_2 systems when in the presence of ascorbic acid.[194, 285] Therefore, in order to confirm whether this promoting effect may be occurring in this reaction system, a series of 'blank reactions' were conducted, where the ability of each component in the reaction mixture was investigated for its ability to oxidise phenol. The results of this are shown in Figure 5.6 and Table 5.4.

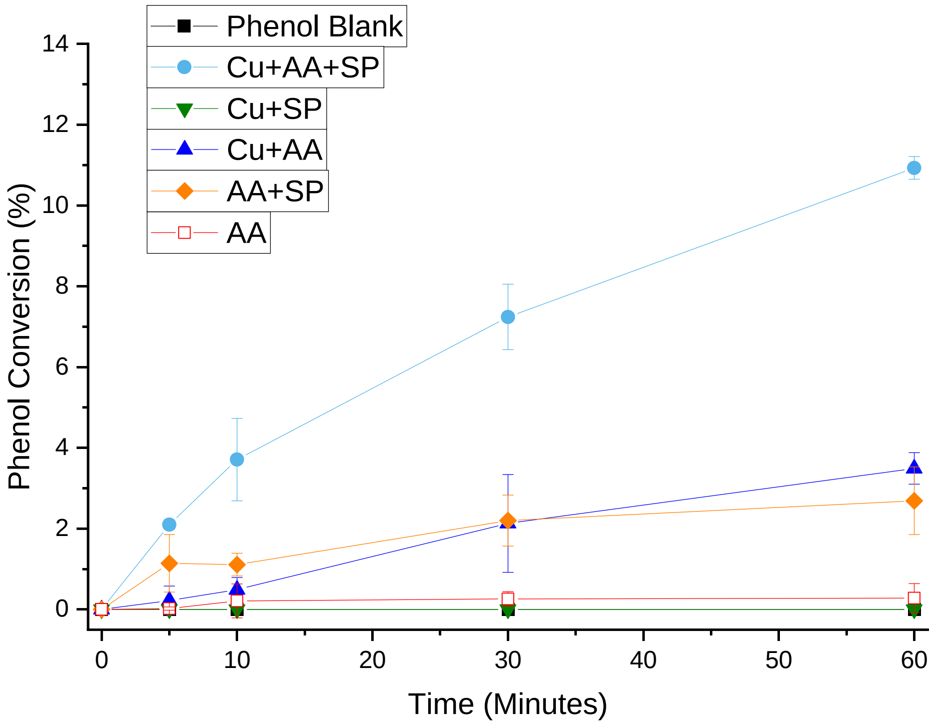

Figure 5.6. The catalytic wet peroxide oxidation of phenol, using a range of reaction components.
Key; Cu (Cu/Al_2O_3), AA (ascorbic acid) and SP (sodium percarbonate).
Phenol oxidation reaction conditions: Catalyst (100 mg), H_2O (10 mL), phenol (500 ppm, 0.053 mmol), ascorbic acid (0.114 mmol), sodium percarbonate (0.096 mmol), 1.0 hr, 20 ^{0}C, 1000 rpm. (Where applicable)

Table 5.4. The catalytic wet peroxide oxidation of phenol, using a range of reaction components.

Catalyst	Reactants	Phenol Conversion (%)	Catechol Yield (%)	Hydroquinone Yield (%)	Organic Acid Yield (%)
Al_2O_3	None	0.0	0.0	0.0	0.0
Cu/Al_2O_3	Ascorbic acid, sodium percarbonate	10.9	4.2	4.1	2.9
Cu/Al_2O_3	Sodium percarbonate	0.0	0.0	0.0	0.0
Cu/Al_2O_3	Ascorbic acid	3.5	1.6	1.7	0.0
Al_2O_3	Ascorbic acid, sodium percarbonate	2.7	1.2	1.5	0.0
Al_2O_3	Ascorbic acid	0.3	0.2	0.1	0.0

Phenol oxidation reaction conditions: Catalyst (100 mg), H_2O (10 mL), phenol (500 ppm, 0.053 mmol), ascorbic acid (0.114 mmol), sodium percarbonate (0.096 mmol), 1.0 hr, 20 ^{0}C, 1000 rpm. (Where applicable)

Firstly, a 'phenol blank' was tested, wherein only H_2O was passed through the catalyst bed, which contained only the Al_2O_3 support. Following this, the H_2O was added to the phenol solution. Under the mild reaction conditions, and in the absence of any other reactant, no oxidation of phenol was observed, confirming that no auto oxidation was taking place, or loss of phenol due to evaporation.

Interestingly, when a solution of sodium percarbonate was used in this way with the Cu/Al_2O_3 catalyst, no phenol oxidation occurred over the course of the subsequent reaction. This was an unexpected result which demonstrated that ascorbic acid not only promoted phenol conversion when used in tandem with sodium percarbonate but is required for any oxidation to occur at all. One possible reason for the lack of oxidation when sodium percarbonate was used with the Cu/Al_2O_3 catalyst likely originates from the physical setup of the reaction. For example, the catalyst was immobilised in a catalyst bed separate from the reaction mixture. Consequently, any radical species that may have been generated at the surface of the catalyst from the degradation of H_2O_2 could not immediately be consumed in the oxidation of phenol, and given the extremely short lifetime of $^{\bullet}OH$ radicals,[318] it is likely that termination reactions depleted any radical oxidant species that may have been generated.

Conversely, in the absence of both a catalyst and sodium percarbonate, ascorbic acid was able to offer a phenol conversion of 0.3 %, but this value was enhanced to 3.5 % when ascorbic acid was activated by the Cu/Al_2O_3 catalyst prior its addition to the phenol solution.

Zhou *et al.* have previously investigated the oxidation of ascorbic acid by O_2 in the presence of $CuSO_4$.[319] The authors reported that aerobic oxidation of ascorbic acid took place in the presence of a Cu catalyst, forming dehydroascorbic acid and significant quantities of H_2O_2 as reaction products, whilst $^{\bullet}OH$ radicals were also generated in-situ.[319] Equation 5.5 outlines this process, wherein ascorbic acid (AH_2) is oxidised to dehydroascorbic acid (DA), by O_2 and

Cu^{2+}.[308] Subsequently generated H_2O_2 may then react with Cu^+ to form hydroxyl radicals as shown previously in Equation 5.3.

Eq. 5.5 $$AH_2 + O_2 + Cu^{2+} \rightarrow DA + H_2O_2 + Cu^+$$

Whilst in the work of Zhou *et al.* the reactor was continually supplied with O_2, dissolved atmospheric O_2 was present in this work. However, the in-situ formation of H_2O_2 and the subsequent generation of $^\bullet OH$ radicals by the Cu catalysed oxidation of ascorbic acid may have been responsible for the conversion of phenol observed under these conditions.

Finally, as previously reported, when ascorbic acid and sodium percarbonate was used in tandem with the Cu/Al_2O_3 catalyst, a phenol conversion of 10.9 % was offered, clearly demonstrating the moderate enhancement to oxidation when both components are utilised in the presence of the Cu catalyst.

To better understand the role of Cu in the reaction mixture, microwave plasma atomic emission spectroscopy (MP-AES) was used to measure the extent of Cu dissolution taking place when the $2\%Cu/Al_2O_3$ catalyst was used alongside each reaction formulation. The results of this are shown in Table 5.5.

Table 5.5. The Cu dissolution of the $2\%Cu/Al_2O_3$ catalyst by ascorbic acid and sodium percarbonate when used in the catalytic wet peroxide oxidation of phenol.

Oxidant Mixture Composition	Cu Present in Reaction Mixture (ppm)	Total Dissolution of Cu (%)	Initial pH of Oxidant Mixture
H_2O	0	0	7.02
H_2O, ascorbic acid, sodium percarbonate	2.8	0.69	9.05
H_2O, ascorbic acid	11.2	2.80	3.02
H_2O, sodium percarbonate	0.1	-	n.d.

Phenol oxidation reaction conditions: Catalyst (100 mg), H_2O (10 mL), phenol (500 ppm, 0.053 mmol), ascorbic acid (0.114 mmol), sodium percarbonate (0.096 mmol), 1.0 hr, 20 ^{0}C, 1000 rpm. (Where applicable)

When the oxidant mixture containing H_2O and ascorbic acid was used, the greatest extent of leaching was observed, wherein 11.2 ppm of Cu was detected within the reaction mixture, which corresponded to a total loss of 2.8 % of Cu from the catalyst. Conversely, when the H_2O and sodium percarbonate mixture was used, in the absence of ascorbic acid, only 0.1 ppm Cu was detected, which falls below the rated detection limit for the instrument, and consequently could not be determined accurately by AES.

However, when the H_2O/ascorbic acid/sodium percarbonate oxidant mixture was used, only 2.8 ppm of Cu was detectable in the reaction mixture, which corresponded to a total loss of Cu of 0.69 % from the catalyst. From this observation, it was concluded that the incorporation of sodium percarbonate protected the Cu catalyst from much of the significant metal leaching that occurred when ascorbic acid was used in isolation, whilst also notably enhancing phenol conversion.

This observation can be rationalised in terms of the pH of each respective oxidant mixture. For example, the H_2O/ascorbic acid mixture has an initial pH of 3.02, whilst the H_2O/ascorbic acid/sodium percarbonate mixture had an initial pH of 9.05. The link between metal leaching and pH has previously been reported in the literature, where strongly basic, or moderately or strongly acidic media often facilitate significantly enhanced levels of metal leaching relative to more neutral conditions.[158, 320, 321] Therefore, it is likely that the moderately acidic conditions associated with ascorbic acid promoted the leaching of Cu, whilst the basic percarbonate modulated the solution pH with the effect of limiting Cu dissolution.
The role of leached Cu metal on the oxidation of phenol will be investigated in Section 5.6, however, it should be noted that both homogeneous leached metal and immobilised heterogeneous metal may contribute to overall catalytic activity.[322, 323]

Ascorbic acid is known to degrade aerobically in aqueous solution,[324] in the presence of transition metals such as Cu and Fe,[308] and also in the presence of H_2O_2,[325] subsequently forming products including dehydroascorbic acid, xylosone, 3-hydroxy-2-pyrone, 2-furoic acid and 2,3-diketogluonic acid. [308, 325, 326] A general schematic for the aerobic degradation of ascorbic acid is shown in Figure 5.7, in which a number of previously identified products are displayed.[308]

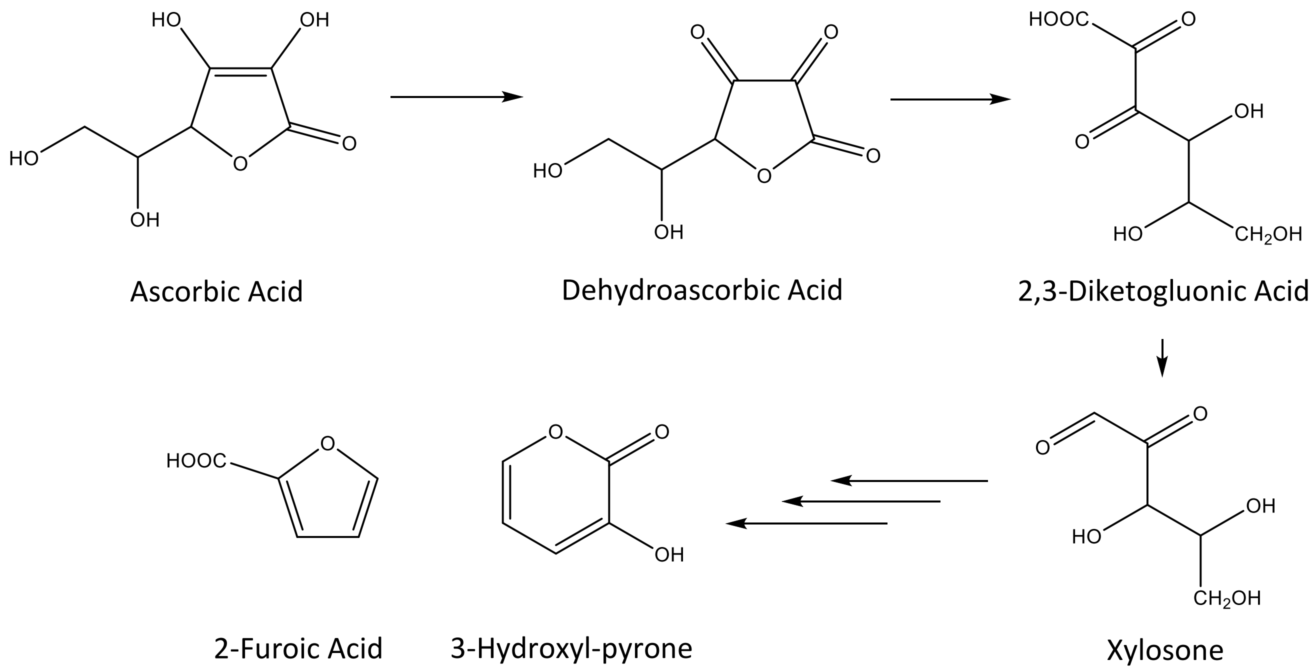

Figure 5.7. General reaction scheme for the aerobic degradation of ascorbic acid. [308]

To further investigate the oxidant mixture and determine whether any possible reactions between the ascorbic acid and H_2O_2 components prior to their addition to the reaction mixture might be limiting the conversion of phenol, oxidant mixtures were aged up to 60 minutes before use. Aging of oxidant mixtures was done both before and after exposure to the Cu/Al_2O_3 catalyst, the results of which are shown in Figure 5.8 and Table 5.6.

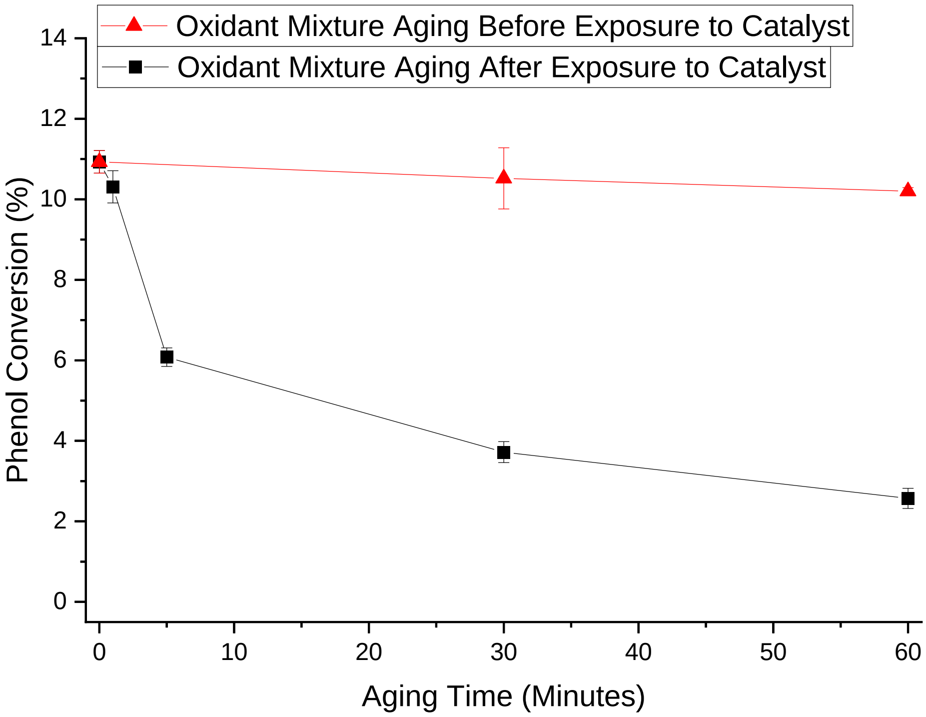

Figure 5.8. The effects of oxidant mixture aging towards the catalytic wet air oxidation of phenol, before and after exposure to a catalyst, using a 2%Cu/Al_2O_3 catalyst.
Phenol oxidation reaction conditions: Catalyst (100 mg), H_2O (10 mL), phenol (500 ppm, 0.053 mmol), ascorbic acid (0.114 mmol), sodium percarbonate (0.096 mmol), 1.0 hr, 20 ^{0}C, 1000 rpm.

Table 5.6. The effects of oxidant mixture aging towards the catalytic wet air oxidation of phenol, before and after exposure to a catalyst, using a 2%Cu/Al_2O_3 catalyst

Time Aged Before Use (min)	Exposure To Catalyst	Phenol Conversion After 60 Minute Reaction (%)
0	Before Aging	10.9
1	Before Aging	10.3
5	Before Aging	6.1
30	Before Aging	3.7
60	Before Aging	2.6
0	After Aging	10.9
30	After Aging	10.5
60	After Aging	10.2

Phenol oxidation reaction conditions: Catalyst (100 mg), H_2O (10 mL), phenol (500 ppm, 0.053 mmol), ascorbic acid (0.114 mmol), sodium percarbonate (0.096 mmol), 1.0 hr, 20 ^{0}C, 1000 rpm.

From these data, it was determined that aging of the oxidant mixture without exposing it to the Cu/Al_2O_3 catalyst did not significantly limit the extent of phenol oxidation that could be achieved. For example, a fresh oxidant mixture offered a phenol conversion of 10.9 %, whilst one that had been aged for 60 minutes offered a phenol conversion of 10.2 %. Conversely, if the oxidant mixture was exposed to the Cu/Al_2O_3 catalyst prior to use, a significant loss in phenol conversion could be observed, depending on length of time prior to use. Under this regime, after 60 minutes of aging, a phenol conversion of 2.6 % was observed. The most severe loss in activity occurred within the first 5 minutes of aging, wherein the conversion of phenol offered decreased from 10.9 % to 6.1 %.

Cu has been demonstrated in the literature to be capable of the oxidative degradation of ascorbic acid through redox reactions directly with the ascorbic acid, resulting in a continual decrease in the concentration of the acid.[285, 319, 327] Additionally, as previously discussed, Fenton-type reactions between Cu and H_2O_2 are well known to degrade H_2O_2 via the formation of radical oxygen species.[280] Therefore, in the absence of a catalyst, any possible degradation of ascorbic acid and H_2O_2 only had a very limited effect on the extent of the subsequent catalytic wet peroxide oxidation of phenol. However, the exposure of the oxidant mixture to the Cu catalyst resulted in a severe loss of phenol conversion, likely due to Cu catalysed degradation of ascorbic acid and H_2O_2.

5.4 Optimisation of Reaction Conditions Towards the Catalytic Wet Peroxide Oxidation of Phenol

Whilst the combined oxidative activity of ascorbic acid and sodium percarbonate was shown in this study to be greater than the sum of each component when used individually, ascorbic acid and carbonate have been reported in the literature to be efficient radical scavenging agents.[288, 328-332] Therefore, it is be possible that excessive concentrations of either ascorbic acid or sodium percarbonate may inhibit the overall oxidation of phenol through a mechanism of radical scavenging.

To investigate this possibility, a study was conducted on the effects of the specific concentrations of both ascorbic acid and sodium percarbonate on the extent of phenol oxidation that could be attained. Firstly, the effects of the concentration of sodium percarbonate were investigated, the results of which are shown in Figure 5.9 and Table 5.7.

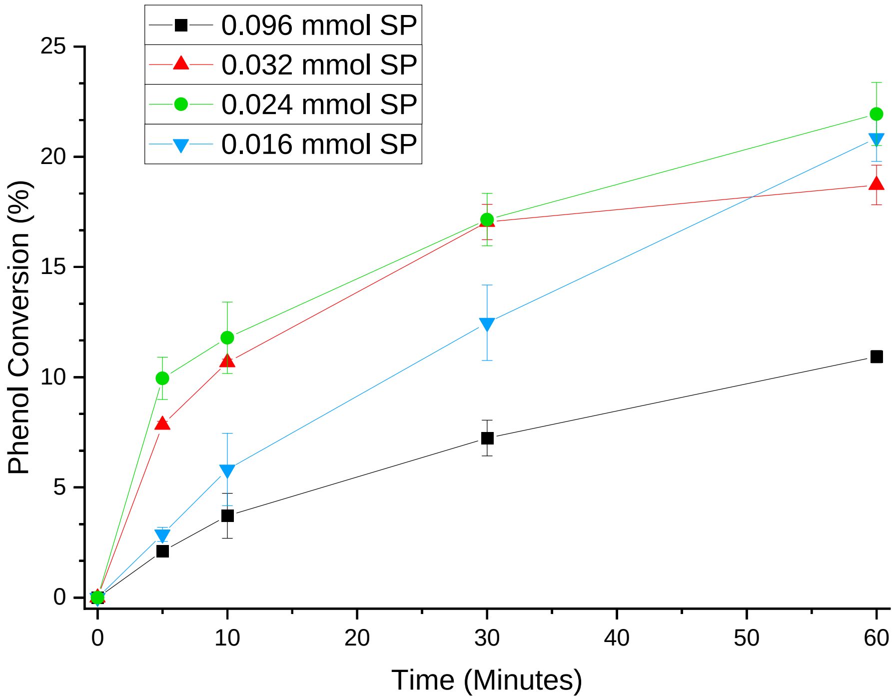

Figure 5.9. The effects of sodium percarbonate (SP) concentration on the catalytic wet peroxide oxidation of phenol, using a 2%Cu/Al_2O_3 catalyst.

Phenol oxidation reaction conditions: Catalyst (100 mg), H_2O (10 mL), phenol (500 ppm, 0.053 mmol), ascorbic acid (0.114 mmol), sodium percarbonate (0.016 - 0.096 mmol), 1.0 hr, 20 ^{0}C, 1000 rpm.

Table 5.7. The effects of sodium percarbonate concentration on the catalytic wet peroxide oxidation of phenol, using a 2%Cu/Al_2O_3 catalyst.

Moles of Sodium Percarbonate (mmol)	Total Phenol Conversion (%)	Catechol Yield (%)	Hydroquinone Yield (%)	Organic Acid Yield (%)
0.096	10.9	4.2	4.1	2.9
0.032	18.7	7.6	7.6	3.4
0.024	21.9	9.8	9.2	3.0
0.016	20.9	9.5	8.7	2.7

Phenol oxidation reaction conditions: Catalyst (100 mg), H_2O (10 mL), phenol (500 ppm, 0.053 mmol), ascorbic acid (0.114 mmol), sodium percarbonate (0.016 - 0.096 mmol), 1.0 hr, 20 ^{0}C, 1000 rpm.

Four different amounts of sodium percarbonate were tested, from 0.096 mmol, which corresponded to initial concentration of sodium percarbonate used in earlier Sections of this Chapter, decreasing to 0.016 mmol. Interestingly, profound enhancements towards phenol conversion were observed when the amount of sodium percarbonate used in the reaction mixture was decreased below the initial value of 0.096 mmol. For example, whilst a phenol conversion of 10.9 % was offered when 0.096 mmol of sodium percarbonate was used, phenol conversions of 18.7 % and 21.9 % respectively were offered when 0.032 mmol and 0.024 mmol of sodium percarbonate were instead used. When 0.016 mmol of sodium percarbonate was used, which represents six times decrease in the number of moles of sodium percarbonate, a phenol conversion value of 20.9 % was attained. Additionally, both catechol and hydroquinone were the only phenolic products observed, which formed in approximately equal ratios under all conditions investigated. Otherwise, smaller quantities of organic acids were also formed under all reaction conditions tested.

It was evident that despite having significantly lower quantities of both H_2O_2 and sodium percarbonate present in the reaction mixture, a greater extent of total phenol conversion was achieved under otherwise identical reaction conditions. As previously discussed, in the literature carbonate has been demonstrated to act as a radical scavenger[328-331] and excessive quantities may be capable of limiting the extent of phenol oxidation by quenching the highly reactive $^{\bullet}OH$ radical (E^o= 2.85 V)[333] in favour of the less reactive $CO_3^{\bullet -}$ radical (E^o = 1.50 V).[331] To confirm if the presence of carbonate may be limiting the efficiency of the overall reaction, an analogous reaction using preformed H_2O_2 in place of sodium percarbonate will be investigated later in this chapter (Section 5.5).

To further investigate the effects of this varying quantity of sodium percarbonate on the reaction mixture, MP-AES was used to determine the extent of Cu dissolution from the 2%Cu/Al_2O_3 catalyst. Additionally, in-situ pH measurements were taken throughout the course of the reaction for the reaction mixtures containing 0.096 mmol and 0.032 mmol of sodium percarbonate. The results of these investigations are shown in Tables 5.8 & 5.9.

Table 5.8. The effects of sodium percarbonate concentration on pH during the catalytic wet peroxide oxidation of phenol, using a 2%Cu/Al_2O_3 catalyst.

Time (minutes)	pH of Reaction Mixture Using 0.096 mmol Sodium Percarbonate[a]	pH of Reaction Mixture Using 0.032 mmol Sodium Percarbonate[b]
0	7.21	4.95
10	6.97	5.64
30	6.89	6.44
60	6.79	6.21

Phenol oxidation reaction conditions: [a]Catalyst (100 mg), H_2O (10 mL), phenol (500 ppm, 0.053 mmol), ascorbic acid (0.114 mmol), sodium percarbonate (0.096 mmol), 1.0 hr, 20 ^{0}C, 1000 rpm.
[b]Catalyst (100 mg), H_2O (10 mL), phenol (500 ppm, 0.053 mmol), ascorbic acid (0.114 mmol), sodium percarbonate (0.032 mmol), 1.0 hr, 20 ^{0}C, 1000 rpm.

Table 5.9. The effects of sodium percarbonate concentration on Cu dissolution during the catalytic wet peroxide oxidation of phenol, using a 2%Cu/Al_2O_3 catalyst.

Moles of Sodium Percarbonate (mmol)	Cu Present in Reaction Mixture (ppm)	Total Dissolution of Cu (%)
0.096 [a]	2.8	0.69
0.032 [b]	10.8	2.71

Phenol oxidation reaction conditions: [a]Catalyst (100 mg), H_2O (10 mL), phenol (500 ppm, 0.053 mmol), ascorbic acid (0.114 mmol), sodium percarbonate (0.096 mmol), 1.0 hr, 20 ^{0}C, 1000 rpm.
[b]Catalyst (100 mg), H_2O (10 mL), phenol (500 ppm, 0.053 mmol), ascorbic acid (0.114 mmol), sodium percarbonate (0.032 mmol), 1.0 hr, 20 ^{0}C, 1000 rpm.

As previously discussed in this chapter, when 0.096 mmol of sodium percarbonate was incorporated into the reaction mixture, an initial pH of 7.21 was observed. Conversely, when 0.032 mmol of sodium percarbonate were instead used, an initial pH of 4.95 was observed, representing the moderately acidic medium that resulted from the lower concentrations of carbonate present in the solution. Consequently, Cu leaching was more extensive under the low sodium percarbonate conditions, wherein 10.8 ppm of Cu was observed in solution, and corresponding to a total loss of Cu of 2.71 % from the 2%Cu/Al_2O_3 catalyst.
From this analysis, significantly higher levels of homogeneous Cu were present in the reaction solution when low concentrations of sodium percarbonate were used compared to higher concentrations. Indeed, both heterogeneous metal and homogeneous metal may play a catalytic role in the reaction, and greater levels of leached homogeneous Cu may be a contributing factor towards the enhanced levels of phenol conversion observed.[322, 323] The catalytic contribution of leached Cu will be considered in Section 5.6.

Having determined that the concentration of sodium percarbonate had a profound influence on the conversion of phenol, the effects of the concentration of ascorbic acid was next investigated in the same manner. To do this, a series of reaction mixtures containing 0.000 – 0.143 mmol of ascorbic acid and 0.096 mmol of sodium percarbonate were utilised with the 2%Cu/Al_2O_3 catalyst, for the catalytic wet peroxide oxidation of phenol. The results of this are shown in Figure 5.10 and Table 5.10.

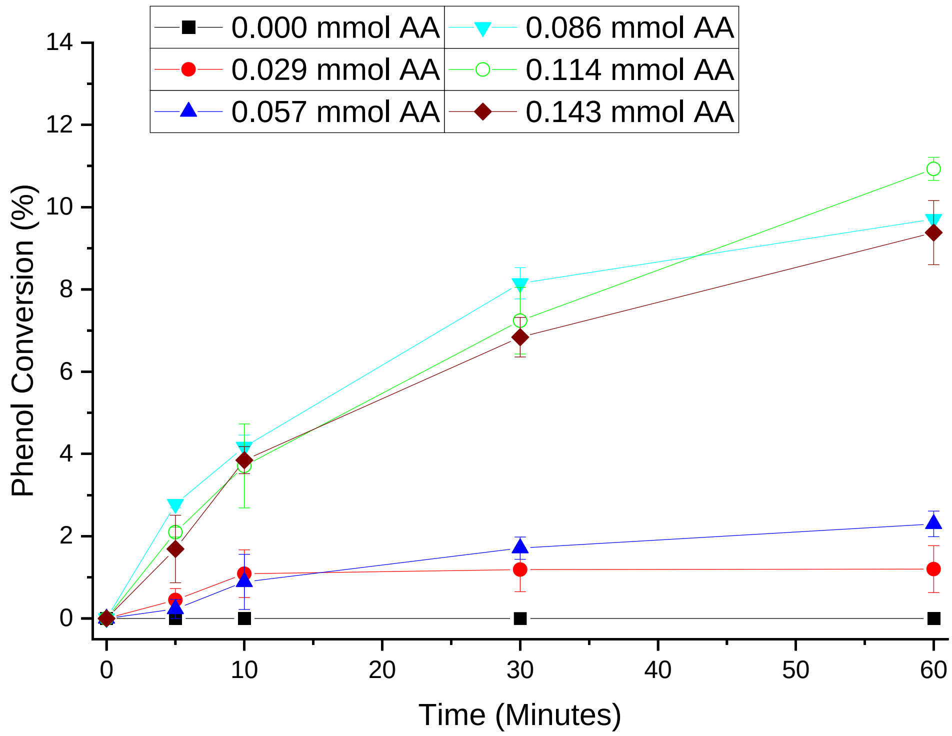

Figure 5.10. The effects of ascorbic acid (AA) concentration on the catalytic wet peroxide oxidation of phenol, using a 2%Cu/Al_2O_3 catalyst.

Phenol oxidation reaction conditions: Catalyst (100 mg), H_2O (10 mL), phenol (500 ppm, 0.053 mmol), ascorbic acid (0.000 - 0.143 mmol), sodium percarbonate (0.096 mmol), 1.0 hr, 20 ^{0}C, 1000 rpm.

Table 5.10. The effects of ascorbic acid (AA) concentration on the catalytic wet peroxide oxidation of phenol, using a 2%Cu/Al_2O_3 catalyst.

Moles of Ascorbic acid (mmol)	Total Phenol Conversion (%)	Catechol Yield (%)	Hydroquinone Yield (%)	Organic Acid Yield (%)
0.000	0.0	0.0	0.0	0.0
0.029	1.2	0.5	0.6	0.0
0.057	2.3	1.3	1.1	0.0
0.086	9.7	4.0	3.8	1.9
0.114	10.9	4.2	4.1	2.9
0.143	9.4	4.4	4.3	0.8

Phenol oxidation reaction conditions: Catalyst (100 mg), H_2O (10 mL), phenol (500 ppm, 0.053 mmol), ascorbic acid (0.000 - 0.143 mmol), sodium percarbonate (0.096 mmol), 1.0 hr, 20 ^{0}C, 1000 rpm.

As demonstrated previously (Table 5.4), no phenol was oxidised in the absence of ascorbic acid. Additionally, when low concentrations of ascorbic acid were used, only very limited phenol conversions were offered. For example, in the presence of 0.029 and 0.057 mmol of ascorbic acid, phenol conversions of 1.2 and 2.3 % were observed respectively. However, a profound enhancement in phenol conversion occurred when levels of ascorbic acid were increased above 0.056 mmol. Indeed, using 0.086 mmol of ascorbic acid facilitated a phenol conversion of 9.7 %, whilst a solution containing 0.114 mmol offered a phenol conversion of 10.9 %. From these data, it was determined that the lowest concentrations of ascorbic acid investigated were insufficient to facilitate even modest levels of phenol conversion. However, increasingly greater levels of ascorbic acid beyond 0.114 mmol also failed to offer any enhancement towards the oxidative activity.

As discussed, the presence of ascorbic acid in a catalytic wet peroxide oxidation reaction has been suggested to facilitate the redox cycling of the catalytic metal.[194, 285] The redox cycling of Cu with H_2O_2 is shown in Equations 5.3 and 5.4. [280, 285, 286]

Eq. 5.3 $\quad Cu^+ + H_2O_2 \rightarrow Cu^{2+} + {}^{\bullet}OH + {}^{-}OH \quad k = 1.0 \times 10^4\ M^{-1}\ s^{-1}$

Eq. 5.4 $\quad Cu^{2+} + H_2O_2 \rightarrow Cu^+ + {}^{\bullet}OOH + H^+ \quad k = 1.2 \times 10^{-6}\ M^{-1}\ s^{-1}$

The formation of hydroxyl radicals requires the oxidation of Cu^+ by H_2O_2, whilst the reduction of Cu^{2+} by H_2O_2 generates the less reactive hydroperoxyl radical. Additionally, the reaction of Cu^{2+} with H_2O_2 has been shown to be significantly slower ($k = 1.2 \times 10^{-6}\ M^{-1}\ s^{-1}$) than the reaction of Cu^+ with H_2O_2 ($k = 1.0 \times 10^4\ M^{-1}\ s^{-1}$), and represents a rate limiting step in the catalytic process.[285] Therefore, the origin of the increased activity associated with the use of ascorbic acid has been suggested to be a result of the in-situ reduction of Cu^{2+} by ascorbic acid, which accelerates the generation of Cu^+ species and enhances the overall rate of formation of hydroxyl radicals.[194, 285]

The low phenol conversions observed in this work when low concentrations of ascorbic acid were used may then be related to the efficiency of the reduction of Cu^{2+}, wherein insufficient ascorbic acid is present to reduce significant quantities of Cu^{2+}.

Alternatively, this effect may be a result of catalytic contributions of homogeneous leached Cu metal. It was reported in Table 5.5 that both ascorbic acid and sodium percarbonate had a significant effect on the extent of metal dissolution, wherein 2.8 ppm of Cu was observed when ascorbic acid and sodium percarbonate were present in the oxidant mixture, whilst 0.1 ppm of leached Cu was observed when only sodium percarbonate was used. Therefore, it is possible that reducing the concentration of ascorbic acid may have limited the extent of Cu leaching due to the more basic pH of the mixture, leading to a lower overall level of phenol conversion. The catalytic contributions of homogeneous Cu metal will be investigated in Section 5.6.

5.5 Effects of the Source of H_2O_2 Towards the Catalytic Wet Peroxide Oxidation of Phenol

As observed previously, the extent of phenol oxidation offered during the catalytic wet peroxide oxidation reaction was enhanced when ascorbic acid and sodium percarbonate were used in tandem with the Cu/Al_2O_3 catalyst. Sodium percarbonate was initially selected as the source of H_2O_2 because of its ease of use and storage as a solid, compared to preformed aqueous H_2O_2 which requires storage at low temperatures and at higher concentrations is highly corrosive. Previously, the use of percarbonate was shown to influence the pH of the reaction medium (Table 5.8), wherein weakly acidic (pH 4.95) or neutral (pH 7.21) reaction mixtures could be created. The role of pH in catalytic wet peroxide oxidation reactions varies depending on the metal used, and whether the catalyst is homogeneous or heterogeneous.[280] For example, in the case of homogeneous Fe, an optimal pH of approximately 3.5 has been reported in the literature, whilst heterogeneous Fe may operate over a significantly wider pH range.[280, 285, 334] Conversely, both homogeneous and heterogeneous Cu have been shown to operate under conditions with either acidic or neutral pH values.

Additionally, as previously discussed, carbonate has been demonstrated in the literature to be an efficient scavenger of $^{\bullet}OH$ radicals, which given the reported radical based oxidation mechanism, may be inhibiting the extent of phenol oxidation that could be achieved.[328-331] Indeed, in several publications relating to photocatalytic systems, the resulting carbonate radical ($CO_3^{\bullet -}/CO_3^{2-}$, $E^o = 1.50$ V)[331] has been shown to be less reactive than the hydroxyl radical ($HO^{\bullet}/HO^-$, $E^o = 2.85$ V).[333]

To investigate any possible influences of both the pH of the reaction mixture, and the possibility of radical scavenging limiting the extent of phenol oxidation, sodium percarbonate was replaced with a corresponding number of moles of preformed commercial H_2O_2 to deliver an equal initial concentration of H_2O_2 under both sets of conditions. Additionally, tert-butyl hydroperoxide (t-BHP) was also examined in this manner, due to its previously reported oxidative ability alongside Cu and Fe catalysts.[335-337] The results of this investigation are shown in Figure 5.11 and Table 5.11.

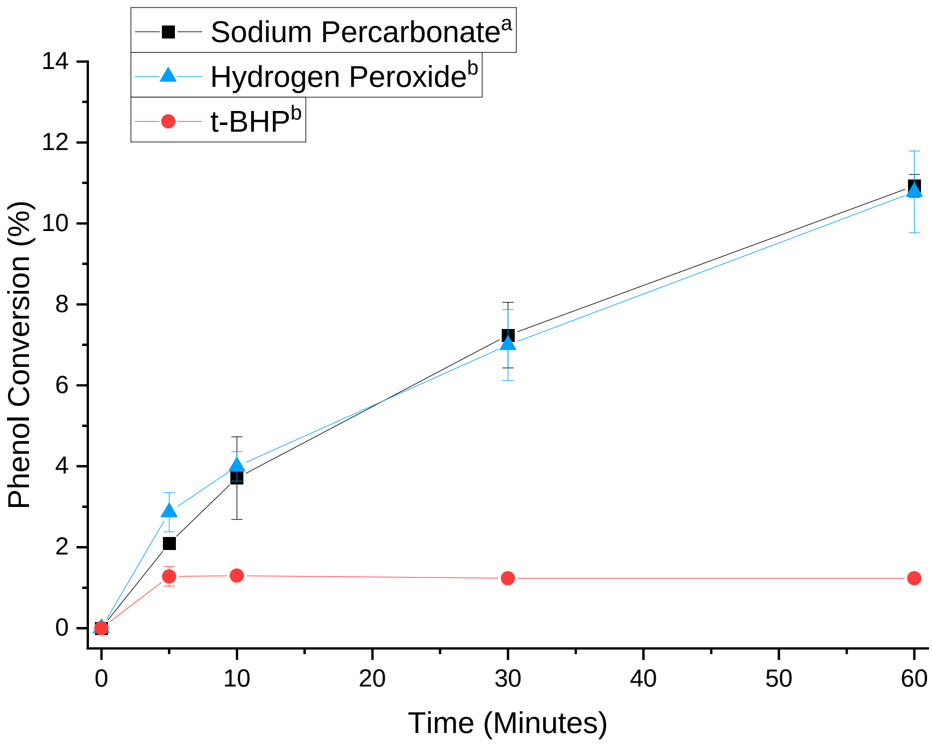

Figure 5.11. The effects of H_2O_2 source on the catalytic wet peroxide oxidation of phenol. Using a 2%Cu/Al_2O_3 catalyst.

Phenol oxidation reaction conditions: [a]Catalyst (100 mg), H_2O (10 mL), phenol (500 ppm, 0.053 mmol), ascorbic acid (0.114 mmol), sodium percarbonate (0.096 mmol), 1.0 hr, 20 ^{0}C, 1000 rpm.
[b]Catalyst (100 mg), H_2O (10 mL), phenol (500 ppm, 0.053 mmol), ascorbic acid (0.114 mmol), H_2O_2 source (0.144 mmol), 1.0 hr, 20 ^{0}C, 1000 rpm.

Table 5.11. The effects of H_2O_2 source on the catalytic wet peroxide oxidation of phenol, using a 2%Cu/Al_2O_3 catalyst.

Oxidant	Phenol Conversion (%)	Catechol Yield (%)	Hydroquinone Yield (%)	Organic Acid Yield/ Mineralization (%)
Sodium Percarbonate[a]	10.9	4.2	4.1	2.9
Preformed H_2O_2[b]	10.8	5.4	2.2	3.2
t-BHP[b]	1.2	0.6	0.6	0.0

Phenol oxidation reaction conditions: [a]Catalyst (100 mg), H_2O (10 mL), phenol (500 ppm, 0.053 mmol), ascorbic acid (0.114 mmol), sodium percarbonate (0.096 mmol), 1.0 hr, 20 ^{0}C, 1000 rpm.
[b]Catalyst (100 mg), H_2O (10 mL), phenol (500 ppm, 0.053 mmol), ascorbic acid (0.114 mmol), H_2O_2 source (0.144 mmol), 1.0 hr, 20 ^{0}C, 1000 rpm.

When t-BHP was used in this way, only 1.2 % of phenol was converted. When compared to the phenol conversion of 3.5 % offered when ascorbic acid was used with the Cu/Al_2O_3 catalyst (Table 5.4) in the absence of and H_2O_2, it suggests that the incorporation of t-BHP was detrimental to the overall oxidation reaction and limited conversion. Additionally, the use of either sodium percarbonate or preformed H_2O_2 offered equivalent levels of phenol conversion, at 10.9 % and 10.8 % respectively. However, differences were observed in the product distribution that arose from the use of each oxidant source. For example, whilst the use of sodium percarbonate resulted in the formation of catechol and hydroquinone in equal quantities, the use of preformed H_2O_2 instead promoted catechol formation over hydroquinone. Indeed, a catechol yield of 5.4 % was offered under these conditions, compared to a hydroquinone yield of 2.2 % and a further 3.2 % of phenol conversion attributed to the formation of organic acids or CO_2 and H_2O.

To investigate this observation further, the in-situ pH of each reaction was studied as a function of time, as is shown in Table 5.12. Additionally, the resulting dissolution of Cu from the Cu/Al_2O_3 catalyst is shown in Table 5.13.

Table 5.12. The effect of H_2O_2 source on the pH of the resulting reaction mixture.

Time (minutes)	pH of Reaction Mixture Using Sodium Percarbonate[a]	pH of Reaction Mixture Using Preformed H_2O_2[b]
0	7.21	3.31
10	6.97	3.22
30	6.89	3.18
60	6.79	3.12

Phenol oxidation reaction conditions: [a]Catalyst (100 mg), H_2O (10 mL), phenol (500 ppm, 0.053 mmol), ascorbic acid (0.114 mmol), sodium percarbonate (0.096 mmol), 1.0 hr, 20 ^{0}C, 1000 rpm.
[b]Catalyst (100 mg), H_2O (10 mL), phenol (500 ppm, 0.053 mmol), ascorbic acid (0.114 mmol), H_2O_2 (0.144 mmol), 1.0 hr, 20 ^{0}C, 1000 rpm.

As previously discussed, an identical phenol conversion was offered when using either sodium percarbonate or preformed H_2O_2 as the source of reactive oxygen species, whilst use of the latter favoured catechol formation over hydroquinone. When the pH of each reaction mixture was examined, a strong effect arising from the presence of carbonate was observed on the acidity of the reaction medium. For example, an aqueous solution of ascorbic acid and sodium percarbonate had an initial pH of 9.05 (Table 5.5). Upon addition to the phenolic solution, the pH was decreased to 7.21 due to dilution in the reaction medium, and gradually decreased to 6.79 over the proceeding 60-minute reaction, likely because of the formation of organic acids. Conversely, when preformed H_2O_2 was used, the pH of the reaction mixture decreased from 3.31 to 3.12 over 60 minutes, confirming the strong basic contribution from carbonate, and the appreciably more acidic conditions that arose when preformed H_2O_2 was used, due to the acidic contributions from ascorbic acid and possibly some contribution from acidic stabilising agents that are often present in commercial preformed H_2O_2 samples.

Additionally, in agreement with previous observations in this study, the pH was a key factor in determining the extent of Cu leaching from the catalyst. For example, when sodium percarbonate was used, only 2.8 ppm of Cu was observable in solution, corresponding to a 0.69 % loss of Cu from the catalyst. When preformed H_2O_2 was used, 10.7 ppm of Cu was observable in solution, which corresponded to a loss of Cu of 2.67 % from the catalyst. This value is almost identical to the 2.80 % loss of Cu that was observed when ascorbic acid alone was used with the Cu catalyst (Table 5.5) and confirms that the reduced metal leaching is a result of the more basic pH arising from the presence of carbonate.

Table 5.13. The effect of H_2O_2 source on the dissolution of Cu from a 2%Cu/Al_2O_3 catalyst during the catalytic wet peroxide oxidation of phenol. Determined by MP-AES.

Oxidant	Cu Present in Solution (ppm)	Total Cu Dissolution (%)
Sodium Percarbonate[a]	2.8	0.69
Preformed H_2O_2[b]	10.7	2.67

Phenol oxidation reaction conditions: [a]Catalyst (100 mg), H_2O (10 mL), phenol (500 ppm, 0.053 mmol), ascorbic acid (0.114 mmol), sodium percarbonate (0.096 mmol), 1.0 hr, 20 ^{0}C, 1000 rpm. [b]Catalyst (100 mg), H_2O (10 mL), phenol (500 ppm, 0.053 mmol), ascorbic acid (0.114 mmol), H_2O_2 (0.144 mmol), 1.0 hr, 20 ^{0}C, 1000 rpm.

5.6 Determination of the Catalytic Contributions from Homogeneous Leached Cu Towards the Catalytic Wet Peroxide Oxidation of Phenol

The presence of homogeneous Cu as a result of metal leaching had been confirmed via MP-AES and was shown to have a dependence on the pH of the oxidant mixture. However, the relative catalytic contributions of the heterogeneous Cu/Al_2O_3 catalyst seated in the catalyst bed, and the leached homogeneous Cu present in the reaction mixture had not yet been established. As previously discussed, both heterogeneous and homogeneous metal may have catalytic contributions[322, 323] and Cu^{2+} complexes, such as $Cu(NO_3)_2$ and $CuSO_4$, in addition to other ligated Cu complexes have been demonstrated to be active catalysts in analogous reaction systems.[280, 293, 338]
To investigate the catalytic contributions of homogeneous leached Cu, the Cu/Al_2O_3 catalyst was omitted from the experimental procedure, and instead equivalent concentrations of $CuCl_2$ were added to reaction mixtures corresponding to the observed leached Cu concentrations of 10.8 and 2.8 ppm, as reported in Table 5.9. A Cu^{2+} salt was selected to correspond with the heterogeneous Cu/Al_2O_3 catalyst, which featured Cu present as Cu^{2+} in a spinel structure, as shown in Figure 5.4.

This was done for the two sets of reaction conditions, containing either the higher 0.096 mmol of sodium percarbonate, or the lower 0.032 mmol. The results of this are shown in Figure 5.12 and Table 5.14.

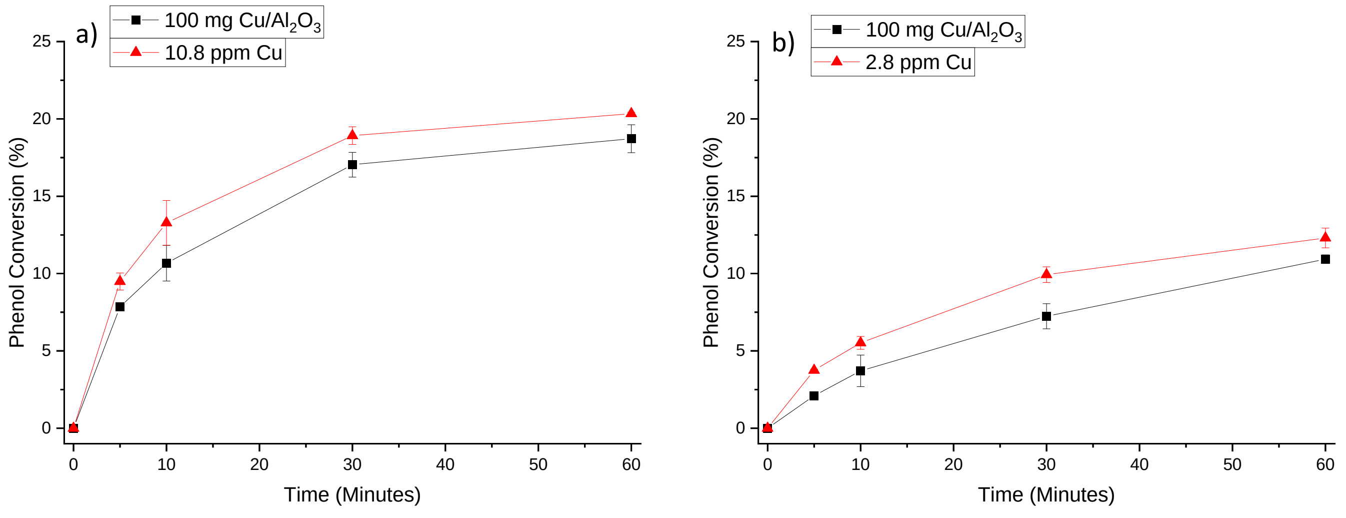

Figure 5.12. Comparison of the catalytic activity of $CuCl_2$ and Cu/Al_2O_3 towards the catalytic wet peroxide oxidation of phenol.

Phenol oxidation reaction conditions: [a]Catalyst (100 mg) or Cu Cu^{2+} (10.8 ppm) , H_2O (10 mL), phenol (500 ppm, 0.053 mmol), ascorbic acid (0.114 mmol), sodium percarbonate (0.032 mmol), 1.0 hr, 20 ^{0}C, 1000 rpm.

[b]Catalyst (100 mg) or Cu^{2+} (2.8 ppm) , H_2O (10 mL), phenol (500 ppm, 0.053 mmol), ascorbic acid (0.114 mmol), sodium percarbonate (0.096 mmol), 1.0 hr, 20 ^{0}C, 1000 rpm.

Table 5.14. Comparison of the catalytic activity of $CuCl_2$ and Cu/Al_2O_3 towards the catalytic wet peroxide oxidation of phenol.

Reaction Conditions	Catalyst	Phenol Conversion (%)	Catechol Conversion (%)	Hydroquinone Conversion (%)	Organic Acid Yield/ Mineralization (%)
a	Cu/Al_2O_3	18.7	7.6	7.6	3.4
a	$CuCl_2$	20.3	10.1	7.3	2.9
b	Cu/Al_2O_3	10.9	4.2	4.1	2.9
b	$CuCl_2$	12.3	5.4	5.7	1.2

Phenol oxidation reaction conditions: [a]2%Cu/Al_2O_3 (100 mg) or Cu^{2+} (10.8 ppm) from $CuCl_2$, H_2O (10 mL), phenol (500 ppm, 0.053 mmol), ascorbic acid (0.114 mmol), sodium percarbonate (0.032 mmol), 1.0 hr, 20 ^{0}C, 1000 rpm.

[b]2%Cu/Al_2O_3 (100 mg) or Cu^{2+} (2.8 ppm) from $CuCl_2$, H_2O (10 mL), phenol (500 ppm, 0.053 mmol), ascorbic acid (0.114 mmol), sodium percarbonate (0.096 mmol), 1.0 hr, 20 ^{0}C, 1000 rpm.

Under reaction conditions 'a' (Table 5.14), wherein 0.032 mmol of sodium percarbonate was used, the Cu/Al_2O_3 catalyst offered a total phenol conversion of 18.7 %. It should be noted that both heterogeneous Cu/Al_2O_3 situated in the catalyst bed, and 2.8 ppm of homogeneous leached Cu were present in this reaction. However, when the only Cu present was 2.8 ppm of Cu^{2+} from homogeneous $CuCl_2$, a total phenol conversion of 20.3 % was offered. Similar trends were also observed under reaction conditions ‘b’ (Table 5.14), in which the higher 0.096 mmol of sodium percarbonate, alongside the Cu/Al_2O_3 catalyst offered a phenol conversion of 10.9 %, compared to the 12.3 % offered by the $CuCl_2$ catalyst at a concentration of 10.8 ppm.

Whilst $CuCl_2$ cannot be considered a perfect analogue to leached Cu species from the Cu/Al_2O_3 catalyst, due to the additional presence of Cl^- ions as either ligands or dissolved in solution, bulk CuO, which represents the closes analogue, is insoluble in water and thus was not suitable for use in this analysis.

However, it should be noted that from these data, it was apparent that slightly higher conversions of phenol could be achieved by dosing the reaction mixture with an equivalent concentration of Cu^{2+} to match the observed leaching of Cu from the Cu/Al_2O_3 catalyst. This observation may suggest that all or most of the catalytic activity resulting from the use of the Cu/Al_2O_3 catalyst originated from homogeneous leached Cu, and not from the heterogeneous Cu stored in the catalyst bed, which may have only served the role of supplying the reaction mixture with catalytically active leached Cu.

This result was unexpected, given the previously reported activity of heterogeneous Cu catalysts in catalytic wet peroxide oxidation type reactions[280]. However, this lack of heterogeneous catalytic contributions from the Cu/Al_2O_3 catalyst was likely a result of the specific testing methodology required for the project. Specifically, the Cu/Al_2O_3 catalyst was required to be immobilised in a separate catalyst bed, with the ascorbic acid and sodium percarbonate solution passed over it before addition to the reaction mixture. Consequently, there was only a short duration of contact between the heterogeneous Cu and any reactants, whilst leached Cu is present in the reaction mixture for the entire duration of the reaction.

From Section 5.4, and presented again in Table 5.14, a correlation was observed in which the concentration of sodium percarbonate used appeared to have a direct effect on the observed conversion of phenol and the extent of Cu leaching. For example, when 0.032 mmol of sodium percarbonate was used, a phenol conversion of 18.7 % was observed, accompanied by 10.8 ppm of leached Cu. Additionally, when 0.096 mmol of sodium percarbonate was used, a phenol conversion of 10.9 % was offered, accompanied by 2.8 ppm of leached Cu.

Given that the catalytic contributions of leached Cu had now been confirmed, it could be determined whether the additional Cu leaching associated with using lower concentrations of sodium percarbonate was a contributing factor in the greater levels of phenol oxidation offered under those conditions. To establish this, homogeneous $CuCl_2$ was added to the standard reaction mixtures so that 10.8 and 2.8 ppm solutions of Cu were achieved, without the use of the Cu/Al_2O_3 catalyst. The results of this are shown in Figure 5.13 and Table 5.15.

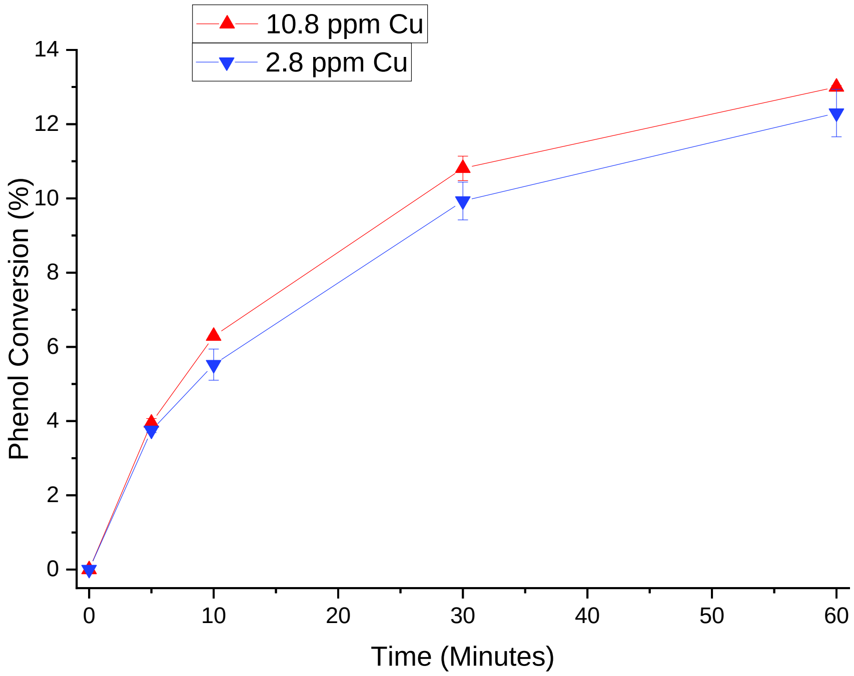

Figure 5.13. Comparison of the catalytic activity of 10.8 and 2.8 ppm of Cu from $CuCl_2$ towards the catalytic wet peroxide oxidation of phenol.
Phenol oxidation reaction conditions: $CuCl_2$ (2.8 or 10.8 ppm Cu^{2+}) , H_2O (10 mL), phenol (500 ppm, 0.053 mmol), ascorbic acid (0.114 mmol), sodium percarbonate (0.096 mmol), 1.0 hr, 20 ^{0}C, 1000 rpm.

Table 5.15. Comparison of the catalytic activity of 10.8 and 2.8 ppm of Cu^{2+} from $CuCl_2$ towards the catalytic wet peroxide oxidation of phenol.

Concentration of Cu (ppm)	Phenol Conversion (%)	Catechol Conversion (%)	Hydroquinone Conversion (%)	Organic Acid Yield/ Mineralization (%)
10.8	13.0	5.0	5.9	2.1
2.8	12.3	5.4	5.7	1.2

Phenol oxidation reaction conditions: $CuCl_2$ (2.8 or 10.8 ppm Cu^{2+}) , H_2O (10 mL), phenol (500 ppm, 0.053 mmol), ascorbic acid (0.114 mmol), sodium percarbonate (0.096 mmol), 1.0 hr, 20 ^{0}C, 1000 rpm.

When 10.8 ppm of Cu^{2+} was added to the reaction mixture, a total phenol conversion of 13 % was offered, compared to the 12.3 % offered when 2.8 ppm of Cu^{2+} was present. This demonstrates that the concentration of Cu leachate was not likely a contributing factor to the enhanced phenol conversions associated with lower concentrations of sodium percarbonate.

5.7 The Effects of Formulation Additives to the Reaction Mixture Towards the Catalytic Wet Peroxide Oxidation of Phenol

In a series of parallel investigations conducted by other researchers at Cardiff University, an identical Cu/Al_2O_3 catalyst, ascorbic acid and H_2O_2 system was used to degrade Acid Red 14. The structure of Acid Red 14 is shown in Figure A5.1. These researchers determined that greater conversions of acid red 14 could be attained when additional components, such as polyethylene glycol 400 (PEG 400) or n-butanol were incorporated into the reaction mixture. PEG has been demonstrated in the literature to form free radicals which have been exploited in radical oxidation reactions, often as an initiator of free radicals.[339-342] Therefore, to examine the enhanced conversions of Acid Red 14 observed in parallel investigations, a series of additives were selected for use in the catalytic wet peroxide oxidation of phenol.

PEG 400 and n-butanol were selected due to the previously discussed enhancements towards the oxidation of Acid Red 14. PEG 200, ethanol, and t-butanol were also investigated due to their structural and chemical similarities with either PEG 400 or n-butanol respectively. The chemical structures of each additive used is shown in Figure A5.2.

The results of this study are shown in Figure 5.14 and Table 5.16.

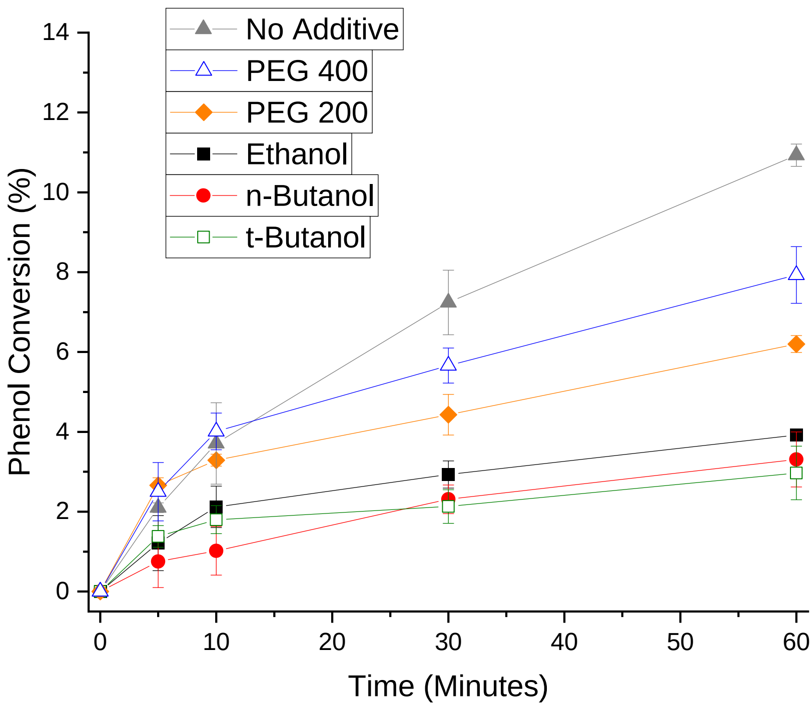

Figure 5.14. The effects of additive components towards the catalytic wet air peroxide oxidation of phenol, using a 2%Cu/Al_2O_3 catalyst.

Phenol oxidation reaction conditions: Catalyst (100 mg), H_2O (10 mL), phenol (500 ppm, 0.053 mmol), ascorbic acid (0.114 mmol), sodium percarbonate (0.096 mmol), additive (1 wt.%), 1.0 hr, 20 ^{0}C, 1000 rpm.

Table 5.16. The effects of additive components towards the catalytic wet air peroxide oxidation of phenol, using a 2%Cu/Al_2O_3 catalyst.

Additive Component	Phenol Conversion (%)	Catechol Yield (%)	Hydroquinone Yield (%)	Organic Acid Yield (%)
None	10.9	4.2	4.1	2.9
PEG 400	7.9	3.6	3.4	0.9
PEG 200	6.2	2.4	2.4	0.4
Ethanol	3.9	2.0	1.9	0.0
n-Butanol	3.3	1.6	1.6	0.0
t-Butanol	3.0	1.4	1.5	0.0

Phenol oxidation reaction conditions: Catalyst (100 mg), H_2O (10 mL), phenol (500 ppm, 0.053 mmol), ascorbic acid (0.114 mmol), sodium percarbonate (0.096 mmol), additive (1 wt.%), 1.0 hr, 20 ^{0}C, 1000 rpm.

As a result of incorporating any additive components into the reaction mixture, conversions of phenol were decreased. For example, whilst a phenol conversion of 10.9 % was achieved in the absence of any additive, the use of both PEG 400 and PEG 200 resulted in more limited phenol conversions of 7.9 % and 6.2 % respectively. Additionally, the incorporation of any of the alcohols caused a greater limiting effect on the conversion of phenol, such as ethanol, which offered a phenol conversion of only 3.9 %.

Alcohols such as methanol, ethanol, n-butanol and t-butanol have been reported to be effective scavengers of hydroxyl radicals.[343-346] Therefore, it is likely that the additives selected, in the quantities employed in this study were able to effectively scavenge radicals and thus, reduce the overall extent of phenol oxidation.

5.8 The Effects of the Choice of Reducing Agent Towards the Catalytic Wet Peroxide Oxidation of Phenol

As previously discussed, ascorbic acid has been reported to enhance the oxidative activity of several Cu/H_2O_2 systems towards target organic compounds.[194, 285] However, other reducing agents have been also been demonstrated to act in an identical manner. For example, hydroxylamine has been reported to reduce catalytic Fe^{3+} in-situ during analogous oxidation reactions.[347-349] Due to safety concerns and the intended applications of this project, hydroxylamine was not suitable for use in this reaction system, however, in principle other reducing agents may be capable of similar enhancements towards catalytic activity. Indeed, in the literature glucose has been shown to be capable of the reduction of Cu and may represent another mild and non-toxic alternative.[350, 351]

To investigate this, ascorbic acid was replaced with equivalent moles of either glucose or gluconic acid, and the resultant mixture tested for activity towards the catalytic wet peroxide oxidation of phenol. The results of this are shown in Figure 5.15 and Table 5.17.

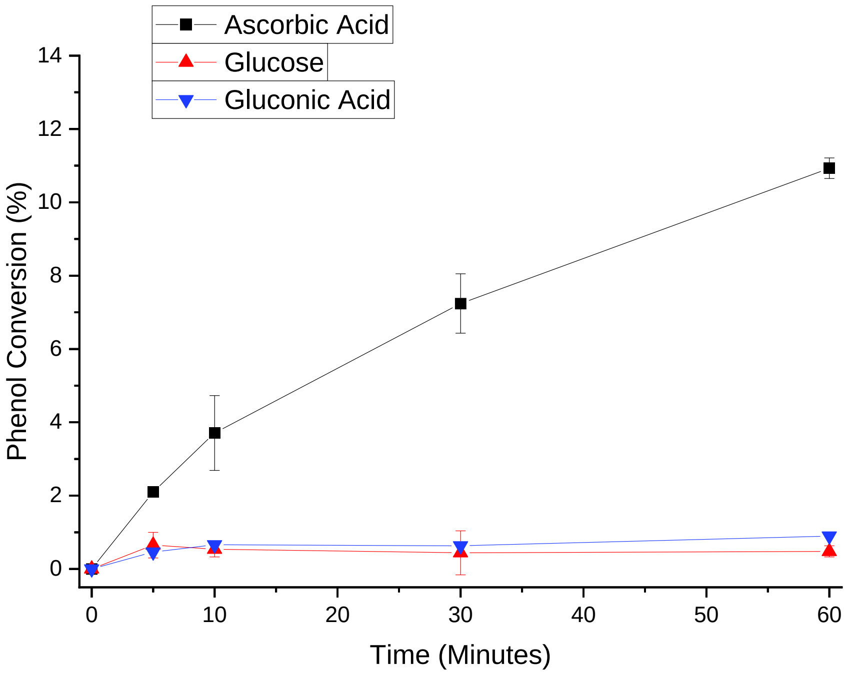

Figure 5.15. Effects of the choice of reducing agent on the catalytic wet peroxide oxidation of phenol, using a 2%Cu/Al_2O_3 catalyst.
Phenol oxidation reaction conditions: Catalyst (100 mg), H_2O (10 mL), phenol (500 ppm, 0.053 mmol), reducing agent (0.114 mmol), sodium percarbonate (0.096 mmol), 1.0 hr, 20 ^{0}C, 1000 rpm.

Table 5.17. Effects of the choice of reducing agent on the catalytic wet peroxide oxidation of phenol, using a 2%Cu/Al_2O_3 catalyst.

Reducing Agent	Phenol Conversion (%)	Catechol Conversion (%)	Hydroquinone Conversion (%)	Organic Acid Yield (%)
Ascorbic Acid	10.9	4.2	4.1	2.9
Glucose	0.5	0.2	0.2	0.0
Gluconic Acid	0.9	0.4	0.5	0.0

Phenol oxidation reaction conditions: Catalyst (100 mg), H_2O (10 mL), phenol (500 ppm, 0.053 mmol), reducing agent (0.114 mmol), sodium percarbonate (0.096 mmol), additive (1 wt.%), 1.0 hr, 20 ^{0}C, 1000 rpm.

As previously reported in this work, the reaction mixture containing ascorbic acid offered a phenol conversion of 10.9 %, whilst reactions utilising glucose or gluconic acid offered significantly reduced phenol conversions of 0.5 % and 0.9 % respectively. The low conversion of phenol offered by solutions containing glucose may be rationalised by the relative acidity of glucose when compared to that of ascorbic acid. For example, the pK_a of ascorbic acid (for the first deprotonation) is 4.17,[352] whilst glucose has been reported to have a pK_a of 12.16.[353] Whilst it was not measured in this project, given the relative pk_a values of the two compounds, it could be expected that the reaction mixture containing glucose might be notably less acidic than the ascorbic acid containing mixture, and given the strong basic contributions from sodium percarbonate, would likely overall have an basic pH. This may result in only very low levels of Cu leaching, ultimately causing the low levels of phenol conversion observed due to limited concentrations of homogeneous Cu, as was observed when only sodium percarbonate was used as a reactant (Tables 5.4 & 5.5).

Conversely, whilst gluconic acid has a significantly lower pk_a value (3.7),[354] and thus higher levels of acidity, it lacks any reported capability as a reducing agent, and likely only causes leaching of Cu, without the occurrence of the proposed in-situ reduction of Cu^{2+} that has been reported to be the origin of the enhanced catalytic activity associated with ascorbic acid.[194, 285]

5.9 Re-evaluation of the Catalytic Activity of Al_2O_3 Supported Metal Catalysts Using Optimised Reaction Conditions Towards the Catalytic Wet Peroxide Oxidation of Phenol

In Section 5.4, it was reported that the conversion of phenol could be greatly enhanced when relatively lower concentrations of sodium percarbonate were used in the catalytic wet peroxide oxidation of phenol. For example, when using the Cu/Al_2O_3 catalyst with a reaction mixture containing 0.096 mmol of sodium percarbonate, a phenol conversion of 10.9 % was offered, whereas when the same catalyst was used with a reaction mixture containing 0.032 mmol of sodium percarbonate, the conversion of phenol was enhanced to 18.7 %.

Additionally, the pH of the reaction mixture and resultant leaching of catalytic metal was also strongly influenced by the concentration of sodium percarbonate. Indeed, when 0.096 mmol of sodium percarbonate was used in the reaction mixture, an initial pH of 7.21 was observed, whereas an initial pH of 4.95 was observed when 0.032 mmol was used. (Table 5.9)

It has been reported previously in the literature that in Fenton-type reaction homogeneous Fe catalysts require acidic conditions (pH 3.5) to function optimally, and that at a neutral pH, the resultant $[Fe(H_2O)_6]^{3+}$ species that forms under these neutral conditions is insoluble and leads to a loss of catalytic Fe due to precipitation reactions.[280, 281] In Section 5.2, it was observed that the Fe/Al_2O_3 catalyst offered only a limited phenol conversion (4.1 %) when compared to the phenol conversion observed in the absence of a catalyst (2.7 %). However, the pH of this reaction mixture was 7.21, which given the insolubility of $[Fe(H_2O)_6]^{3+}$ under these conditions, likely resulted in the precipitation of any leached homogeneous Fe species that might be present, greatly inhibiting the conversion of phenol. Therefore, in order to determine the activity of the Fe/Al_2O_3 catalyst towards the catalytic wet peroxide oxidation of phenol under more optimal reaction conditions, the low concentration of sodium percarbonate (0.032 mmol) which results in a more acidic reaction mixture (pH 4.95) was utilised alongside the previously tested Al_2O_3 supported metal catalysts (Section 5.2). The results of this are shown in Figure 5.16 and Table 5.18.

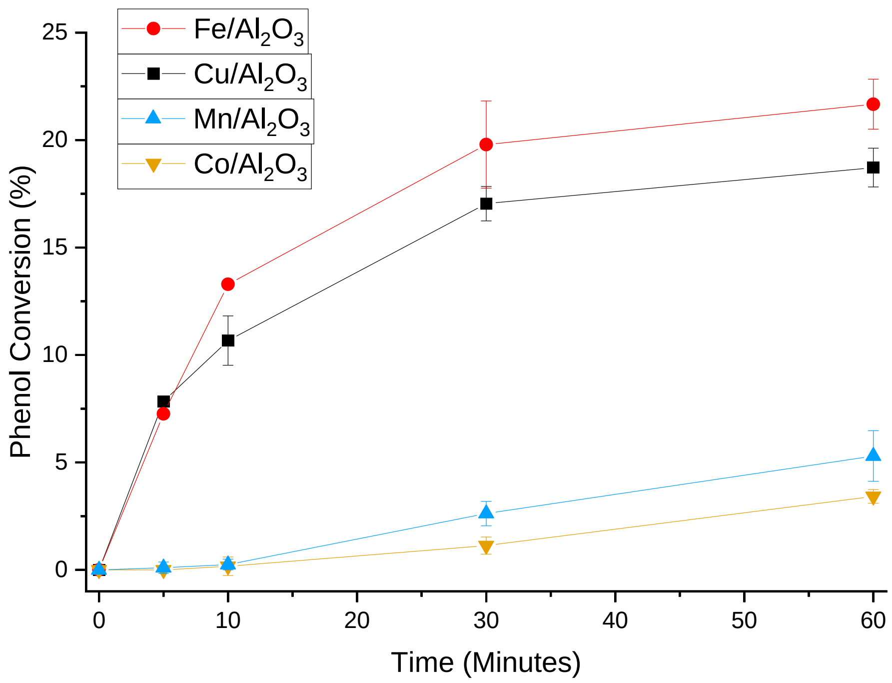

Figure 5.16. The catalytic wet peroxide oxidation of phenol, using a range of Al_2O_3 supported catalysts. **Phenol oxidation reaction conditions:** Catalyst (100 mg), H_2O (10 mL), phenol (500 ppm, 0.053 mmol), ascorbic acid (0.114 mmol), sodium percarbonate (0.032 mmol), 1.0 hr, 20 ^{0}C, 1000 rpm.

Table 5.18. The catalytic wet peroxide oxidation of phenol, using a range of Al_2O_3 supported catalysts.

Catalyst	Phenol Conversion (%)	Catechol Yield (%)	Hydroquinone yield (%)	Organic Acid Yield (%)
Cu/Al_2O_3	18.7	7.6	7.6	3.4
Fe/Al_2O_3	21.7	8.0	9.4	4.2
Mn/Al_2O_3	5.3	3.0	2.3	0.0
Co/Al_2O_3	3.4	2.0	1.3	0.0

Phenol oxidation reaction conditions: Catalyst (100 mg), H_2O (10 mL), phenol (500 ppm, 0.053 mmol), ascorbic acid (0.114 mmol), sodium percarbonate (0.032 mmol), 1.0 hr, 20 ^{0}C, 1000 rpm.

In addition to the previously reported enhancements to catalytic activity offered by the Cu/Al_2O_3 catalyst under these reaction conditions, the Fe/Al_2O_3 catalyst also offered significantly enhanced levels of phenol conversion. For example, the conversion of phenol increased from 4.1 % to 21.7 %, whilst the yield of organic acids/mineralisation increased from 0 % to 4.2 %. This may suggest that the correspondingly lower pH of the reaction mixture resulted in either greater Fe leaching from the heterogeneous Fe/Al_2O_3, or lower levels of Fe precipitation, resulting in higher concentrations of homogeneous catalytic Fe. Additionally, both Mn/Al_2O_3 and Co/Al_2O_3 catalysts facilitated very limited conversions of phenol, offering 5.3 % and 3.4 % respectively. These are almost identical levels of catalytic activity compared to when higher concentrations of sodium percarbonate (0.096 mmol) were used, which offered 5.2 and 4.3 % respectively for the Mn/Al_2O_3 and Co/Al_2O_3 catalysts, and thus no enhancement towards phenol conversion was achieved by either catalyst. These data demonstrate that both Cu and Fe are suitable catalysts for use in this reaction, given appropriate reaction conditions.

5.10 Conclusions

In summary, this Chapter has investigated the effects of ascorbic acid on the catalytic wet peroxide oxidation of phenol using a range of Al_2O_3 supported metal catalysts. Using Cu/Al_2O_3 and Fe/Al_2O_3 catalysts, the greatest levels of phenol conversion were offered in the presence of both ascorbic acid and sodium percarbonate. However, Fe based catalysts required acidic reaction conditions for high levels of catalytic activity to occur.
Whilst in the literature, the role of ascorbic acid is often associated with the in-situ reduction of catalytic metal,[194, 285] in this project, ascorbic acid was shown to be crucial for the occurrence of catalyst leaching, which delivered homogeneous catalytic metal to the reaction mixture.

The main products of the oxidation of phenol were catechol and hydroquinone, with no observed formation of resorcinol or benzoquinone derivatives. Smaller quantities of organic acids were also observed as reaction products.
Optimisation of the concentration of sodium percarbonate was undertaken, as shown in Table 5.19, and promoted the extent of phenol oxidation whilst also increasing the levels of metal dissolution from the catalyst due to the increased acidity of the reaction mixture.

Table 5.19. Comparison of the 2%Cu/Al_2O_3 and 2%Fe/Al_2O_3 catalysts towards the catalytic wet peroxide oxidation of phenol.

Catalyst	Moles of Sodium Percarbonate (mmol)	Phenol Conversion (%)	Catechol Yield (%)	Hydroquinone Yield (%)	Organic Acid Yield (%)
Cu/Al_2O_3	0.096	10.9	4.2	4.1	2.9
Cu/Al_2O_3	0.032	18.7	7.6	7.6	3.4
Fe/Al_2O_3	0.096	4.1	1.9	2.1	0.0
Fe/Al_2O_3	0.032	21.7	8.0	9.4	4.2

Phenol oxidation reaction conditions: Catalyst (100 mg), H_2O (10 mL), phenol (500 ppm, 0.053 mmol), ascorbic acid (0.114 mmol), sodium percarbonate (0.032 – 0.096 mmol), 1.0 hr, 20 ^{0}C, 1000 rpm.

Homogeneous metal species were determined to be the origin of catalytic activity, through a series of analogous reactions using $CuCl_2$ as a source of Cu^{2+}. Additionally, the incorporation of radical scavengers such as PEG and ethanol limited the efficacy of the phenol oxidation reaction.

5.11 References

1. Fenton, H., The constitution of a new dibasic acid, resulting from the oxidation of tartaric acid. *J. Chem. Soc., Trans.* **1896,** *69*.
2. Pignatello, J., Oliveros, E., MacKay, A., Advanced Oxidation Processes for Organic Contaminant Destruction Based on the Fenton Reaction and Related Chemistry. *Crit. Rev. Environ. Sci. Technol.* **2006,** *36*, 1-84.
3. Pouran, S., Raman, A., Daud, W., Review on the application of modified iron oxides as heterogeneous catalysts in Fenton reactions. *J. Clean. Prod.* **2014,** *64*, 24-35.
4. Jain, B., Singh, A., et al, Treatment of organic pollutants by homogeneous and heterogeneous Fenton reaction processes. *Environ. Chem. Lett.* **2018,** *16*, 947-967.
5. Mandal, T., Maity, S., et al, Advanced oxidation process and biotreatment: Their roles in combined industrial wastewater treatment. *Desalination* **2010,** *250*, 87-94.
6. Yalfani, M., Contreras, S., et al, Phenol degradation by Fenton's process using catalytic in situ generated hydrogen peroxide. *Appl. Catal. B: Environ.* **2009,** *89*, 519-526.
7. Acisli, O., Khataee, A., et al, Combination of ultrasonic and Fenton processes in the presence of magnetite nanostructures prepared by high energy planetary ball mill. *Ultrason. Sonochem.* **2017,** *34*, 754-762.
8. Ay, F., Kargi, F., Advanced oxidation of amoxicillin by Fenton's reagent treatment. *J. Hazard. Mater.* **2010,** *179*, 622-627.
9. Bokare, A., Choi, W., Review of iron-free fenton-like systems for activating H_2O_2 in advanced oxidation process. *J. Hazard. Mater.* **2014,** *275*, 121 - 135.
10. Zhang, Y., Zhou, M., A critical review of the application of chelating agents to enable Fenton and Fenton-like reactions at high pH values. *J. Hazard. Mater.* **2019,** *362*, 436-450.
11. Santos, A., Lewis, R., et al, The oxidative degradation of phenol via in situ H_2O_2 synthesis using Pd supported Fe-modified ZSM-5 catalysts. *Catal. Sci. Technol.* **2022,** *22*, 2943-2953.
12. Diao, Z., Xu, X., et al, Enhanced catalytic degradation of ciprofloxacin with FeS2/SiO2 microspheres as heterogeneous Fenton catalyst: Kinetics, reaction pathways and mechanism. *J. Hazard. Mater.* **2017,** *327*, 108-115.
13. Liou, R., Chen, S., CuO impregnated activated carbon for catalytic wet peroxide oxidation of phenol. *J. Hazard. Mater.* **2009,** *172*, 498-506.
14. Wu, Y., Zhang, H., Yan, Y., High efficiency of phenol oxidation in a structured fixed bed over Cu-ZSM-5/PSSF prepared by ion-exchanged method. *Chem. Eng. J.* **2020,** *380*, 122466.
15. Bautista, P., Mohedano, A., et al, Highly stable Fe/γ-Al2O3 catalyst for catalytic wet peroxide oxidation. *J. Chem. Technol. Biotechnol.* **2010,** *86*, 497.
16. Sun, Q., Liu, M., et al, Synthesis of Fe/M (M = Mn, Co, Ni) bimetallic metal organic frameworks and their catalytic activity for phenol degradation under mild conditions. *Inorg. Chem. Front.* **2017,** *4*, 144-153.
17. Xiao, B., Wu, M., et al, Facile Synthesis of CuO Nanosheets and Efficient Degradation of Rhodamine B in a Copper Oxide/Ascorbic Acid/Hydrogen Peroxide System: Kinetics, Fate of Ascorbic Acid, and Mechanism. *ChemistrySelect* **2020,** *5*, 6075-6082.
18. Sun, B., Li, H., et al, Degradation of Organic Dyes over Fenton-Like Cu2O–Cu/C Catalysts. *Ind. Eng. Chem. Res.* **2018,** *57*, 14011-14021.
19. Sun, H., Xie, G., et al, Ascorbic acid promoted magnetite Fenton degradation of alachlor: Mechanistic insights and kinetic modeling. *Appl. Catal. B: Environ.* **2020,** *267*, 118383.
20. Bolobajev, J., Trapido, M., Goi, A., Improvement in iron activation ability of alachlor Fenton-like oxidation by ascorbic acid. *Chem. Eng. J.* **2015,** *281*, 566-574.
21. Tu, Y., Njus, D., Schlegel, H., A theoretical study of ascorbic acid oxidation and $HOO^{\cdot}/O2^{\cdot-}$ radical scavenging. *Org. Biomol. Chem.* **2017,** *15*, 4417-4431.
22. Boatright, W., Oxygen dependency of one-electron reactions generating ascorbate radicals and hydrogen peroxide from ascorbic acid. *Food Chem.* **2016,** *196*, 1361-1367.

23. Babuponnusami, A., Muthukumar, K., Advanced oxidation of phenol: A comparison between Fenton, electro-Fenton, sono-electro-Fenton and photo-electro-Fenton processes. *Chem. Eng. J.* **2012,** *183*, 1-9.
24. Luo, M., Bowden, D., Brimblecombe, P., Catalytic property of Fe-Al pillared clay for Fenton oxidation of phenol by H2O2. *Appl. Catal. B: Environ.* **2009,** *85*, 201-206.
25. Zazo, J., Casas, J., et al, Chemical Pathway and Kinetics of Phenol Oxidation by Fenton's Reagent. *Environ. Sci. Technol.* **2005,** *39*, 9295-9302.
26. Santos, A., Yustos, P., et al, Route of the catalytic oxidation of phenol in aqueous phase. *Appl. Catal. B: Environ.* **2002,** *39*, 97-113.
27. Mijangos, F., Varona, F., Villota, N., Changes in Solution Color During Phenol Oxidation by Fenton Reagent. *Environ. Sci. Technol.* **2006,** *40*, 5538-5543.
28. Garbriel, J., Baldrian, P., et al, Degradation of BTEX and PAHs by Co(II) and Cu(II)-based radical-generating systems. *Appl. Catal. B: Environ.* **2004,** *51*, 159-164.
29. Fink, L., Dror, I., Berkowitz, B., Enrofloxacin oxidative degradation facilitated by metal oxide nanoparticles. *Chemosphere* **2012,** *86*, 144-149.
30. Kim, J., Metcalfe, I., Investigation of the generation of hydroxyl radicals and their oxidative role in the presence of heterogeneous copper catalysts. *Chemosphere* **2007,** *69*, 689-696.
31. Melero, J., Calleja, G., et al, Nanocomposite of crystalline Fe2O3 and CuO particles and mesostructured SBA-15 silica as an active catalyst for wet peroxide oxidation processes. *Catal. Commun.* **2006,** *7*, 478-483.
32. Huanosta-Gutiérrez, T., Dantas, R., et al, Evaluation of copper slag to catalyze advanced oxidation processes for the removal of phenol in water. *J. Hazard. Mater.* **2012,** *213-214*, 325-330.
33. L. Kong, W. W., et al, Active coordinatively unsaturated manganese monoxide-containing mesoporous carbon catalyst in wet peroxide oxidation. *ACS Catal.* **2012,** *2*, 2577-2586.
34. Sui, M., She, L., et al, Ordered mesoporous manganese oxide as catalyst for hydrogen peroxide oxidation of norfloxacin in water. *Chin. J. Catal.* **2013,** *34*, 536-541.
35. Sriskandakumar, T., Opembe, N., et al, Green decomposition of organic dyes using octahedral molecular sieve manganese oxide catalysts. *J. phys. Chem. A* **2009,** *113*, 1523-1530.
36. Verma, P., Baldrian, P., Nerud, F., Decolorization of structurally different synthetic dyes using cobalt(II)/ascorbic acid/hydrogen peroxide system. *Chemosphere* **2003,** *50*, 975-979.
37. Hernandez-Onono, J., Infantes-Molina, A., et al, A novel heterogeneous photo-Fenton Fe/Al2O3 catalyst for dye degradation. *J. Photocem. Photobiol., A.* **2021,** *421*, 113529.
38. Ryu, H., Song, M., et al, Removal of toluene using ozone at room temperature over mesoporous Mn/Al2O3 catalysts. *Environ. Res.* **2019,** *172*, 649-657.
39. Rekha, M., Manjunath, H., Nagaraju, N., Mn/Al2O3 and Mn/ZrO2 as selective catalysts for the synthesis of bis(indolyl)methanes: The role of surface acidity and particle morphology. *J. Ind. Eng. Chem.* **2013,** *19*, 337-346.
40. Zhang, R., Li, P., et al, CO catalytic combustion over Co/Al2O3: Influence of diverse textural properties of alumina supports on the related oxidation activities. *Catal. Today* **2013,** *216*, 169-177.
41. Creutz, C., Complexities of ascorbate as a reducing agent. *Inorg. Chem.* **1981,** *20*, 4449-4452.
42. Palomba, M., Carotenuto, G., Longo, A.,, A Brief Review: The Use of L-Ascorbic Acid as a Green Reducing Agent of Graphene Oxide. *Materials* **2022,** *15*, 6456.
43. Bradshaw, M., Barril, C., et al, Ascorbic Acid: A Review of its Chemistry and Reactivity in Relation to a Wine Environment. *Crit. Rev. Food Sci. Nutr.* **2011,** *51*, 479 - 498.
44. Enache, T., Oliveira-Brett, A., Phenol and para-substituted phenols electrochemical oxidation pathways. *J. Electroanal. Chem.* **2011,** *655*, 9-16.
45. Barnes, A., Lewis, R., et al, Enhancing catalytic performance of AuPd catalysts towards the direct synthesis of H2O2 through incorporation of base metals. *Catal. Sci. Technol.* **2022,** *12*, 1986.
46. Brehm, J., Lewis, R., et al, Enhancing the Chemo-Enzymatic One-Pot Oxidation of Cyclohexane via In Situ H_2O_2 Production over Supported Pd-Based Catalysts. *ACS Catal.* **2022,** *12*, 11776-11789.

47. Ghodselahi, T., Vesahgi, M., et al, XPS study of the Cu@Cu2O core-shell nanoparticles. *Appl. Surf. Sci.* **2008,** *255*, 2730-2734.
48. Li, B., Luo, X., et al, Immobilization of Cu(II) in KIT-6 supported Co3O4 and catalytic performance for epoxidation of styrene. *Appl. Surf. Sci.* **2015,** *359*, 609-620.
49. Conradie, J., Erasmus, E., XPS photoelectron lines, satellite structures and Wagner plot of Cu(II) β-diketonato complexes explained in terms of its electronic environment. *J. Electron. Spectros. Relat. Phenomena* **2022,** *259*, 147241.
50. Porta, P., Campa, M., et al, CuO-ZnO-Al,O, Mixed Oxides: Preparation, Bulk and Surface Characterization. *J. Mater. Chem.* **1993,** *3*, 505-511.
51. Velu, S., Suzuki, K., et al, XPS, XANES and EXAFS investigations of CuO/ZnO/Al2O3/ZrO2 mixed oxidecatalysts. *Phys. Chem. Chem. Phys.* **2002,** *4*, 1990-1999.
52. Tan, R., Hwang, S., et al, Solution synthesis and activation of spinel CuAl2O4 film for solar water-splitting. *J. Catal.* **2021,** *400*, 218-227.
53. Salvati-Niasari, M., Davar, F., Farhadi, M., Synthesis and characterization of spinel-type CuAl2O4 nanocrystalline by modified sol–gel method. *J. Solgel Sci. Technol.* **2009,** *51*, 48-52.
54. Chauruka, S., Hassanpour, A., et al, Effect of mill type on the size reduction and phase transformation of gamma alumina. *Chem. Eng. Sci.* **2015,** *134*, 774-783.
55. Suzuki, H., Araki, S., Yamamoto, H., Evaluation of Advanced Oxidation Processes (AOP) Using O_3, UV and TiO_2 for the Degradation of Phenol in Water. *J. Water. Process. Eng.* **2015,** *7*, 54 - 60.
56. Zhou, P., Zhang, J., et al, Generation of hydrogen peroxide and hydroxyl radical resulting from oxygen-dependent oxidation of l-ascorbic acid via copper redox-catalyzed reactions. *RSC Adv.* **2016,** *6*, 38541-38547.
57. Márquez, J., Levchuk, I., Sillanpää, M., Application of Catalytic Wet Peroxide Oxidation for Industrial and Urban Wastewater Treatment: A Review. *Catalysts* **2018,** *8*, 673.
58. Dijkstra, J., Meeussen, J., Rob Comans, Leaching of Heavy Metals from Contaminated Soils: An Experimental and Modeling Study. *Environ. Sci. Technol.* **2004,** *38*, 4390-4395.
59. Komonweeraket, K., Cetin, B., et al, Effects of pH on the leaching mechanisms of elements from fly ash mixed soils. *Fuel* **2015,** *140*, 788-802.
60. He, J., Yang, X., et al, Interfacial mechanisms of heterogeneous Fenton reactions catalyzed by iron-based materials: A review. *J. Environ. Sci.* **2016,** *39*, 97-109.
61. Thomas, N., Dionysiou, D., Pillai, S., Heterogeneous Fenton catalysts: A review of recent advances. *J. Hazard. Mater.* **2021,** *404*, 124082.
62. Yuan, J., Chen, F., Degradation of Ascorbic Acid in Aqueous Solution. *J. Agric. Food Chem.* **1998,** *46*, 5078-5082.
63. Deutsch, J., Ascorbic Acid Oxidation by Hydrogen Peroxide. *Anal. Biochem.* **1998,** *255*, 1-7.
64. Nemet, I., Monnier, V., Vitamic C Degradation Products and Pathways in the Human Lens. *J. Biol. Chem.* **2011,** *286*, 37128 - 37136.
65. B. Beker, I. S., et al, Protection of ascorbic acid from copper(II)-catalyzed oxidative degradation in the presence of flavonoids: quercetin, catechin and morin. *Int. J. Food Sci. Nutr.* **2011,** *62*, 504-512.
66. Gultekin, I., Ince, N., Degradation of Reactive Azo Dyes by UV/H_2O_2: Impact of Radical Scavengers. *J. Environ. Sci. Health - Toxic/Hazard* **2004,** *39*, 1069-1081.
67. Augusto, O., Bonini, M., et al, Nitrogen dioxide and carbonate radical anion: two emerging radicals in biology. *Free Radic. Biol. Med.* **2002,** *32*, 841-859.
68. Mehrvar, M., Anderson, W., Moo-Young, M., Photocatalytic degradation of aqueous organic solvents in the presence of hydroxyl radical scavengers. *Int. J. Photoenergy* **2001,** *3*.
69. Schneider, J., Firak, D., et al, Use of scavenger agents in heterogeneous photocatalysis: truths, half-truths, and misinterpretations. *Phys. Chem. Chem. Phys.* **2020,** *22*, 15723-15733.
70. Niki, E., Action of ascorbic acid as a scavenger of active and stable oxygen radicals. *Am. J. Clin. Nutr.* **1991,** *54*, 1119S-1124S.

71. Suzuki, H., Araki, S., Yamamoto, H.,, Evaluation of advanced oxidation precesses (AOP) using O3, UV, and TiO_2 for the degradation of phenol in water. *J. Water Process. Eng.* **2015,** *7*, 54-60.
72. Zhu, Y., Zhu, R., et al, Strategies for enhancing the heterogeneous Fenton catalytic reactivity: A review. *Appl. Catal. B: Environ.* **2019,** *255*, 117739.
73. Ratnikov, M., Doyle, M., Mechanistic Investigation of Oxidative Mannich Reaction with tert-Butyl Hydroperoxide. The Role of Transition Metal Salt. *J. Am. Chem. Soc.* **2013,** *135*, 1549-1557.
74. Rothenberg, G., Feldberg, L., et al, Copper-catalyzed homolytic and heterolytic benzylic and allylic oxidation using tert-butyl hydroperoxide. *J. Chem. Soc., Perkins Trans. 2* **1998,** (11), 2429-2434.
75. Nakanishi, M., Bolm, C., Iron-Catalyzed Benzylic Oxidation with Aqueous tert-Butyl Hydroperoxide. *Adv. Synth. Catal.* **2007,** *349*, 861-864.
76. Caudo, S., Centi, G., et al, Homogeneous versus heterogeneous catalytic reactions to eliminate organics from waste water using H_2O_2. *Top. Catal.* **2006,** *40*, 207-219.
77. Hecht, E., Yeh, G., Zhang, K., Evidence of free radical generation from the interaction of polyethylene glycol with PVC medical tubing. *J. Pharm. Biomed. Anal.* **2021,** *197*, 113955.
78. Wang, J., He, L., et al, The Free-Radical Chemistry of Polyethylene Glycol: Organic Reactions in Compressed Carbon Dioxide. *ChemSusChem* **2009,** *2*, 755-760.
79. Wang, J., He, L., Polyethylene glycol radical-initiated benzylic C–H bond oxygenation in compressed carbon dioxide. *New J. Chem.* **2009,** *33*, 1637-1640.
80. Wang, J., He, L., Miao, C.,, Polyethylene glycol radical-initiated oxidation of benzylic alcohols in compressed carbon dioxide. *Green Chem.* **2009,** *11*, 1013-1017.
81. Berndt, T., Richters, S., et al, Hydroxyl radical-induced formation of highly oxidized organic compounds. *Nat. Commun.* **2016,** *7*, 13677.
82. Schneider, J., Firak, D., et al, Use of scavenger agents in heterogenous photocatalysis: truths, half-truths, and misinterpretations. *Phys. Chem. Chem. Phys* **2020,** *22*, 15723.
83. Parker, K., Mitch, W., Halogen radicals contribute to photooxidation in coastal and estuarine waters. *Earth Planet Sci.* **2016,** *113*, 5868-5873.
84. Wang, L., Li, B., et al, Overlooked Formation of H2O2 during the Hydroxyl Radical-Scavenging Process When Using Alcohols as Scavengers. *Environ. Sci. Technol.* **2022,** *56*, 3386-3396.
85. Meng, S., Zhou, P., Reducing agents enhanced Fenton-like oxidation (Fe(III)/Peroxydisulfate): Substrate specific reactivity of reactive oxygen species. *Water Res.* **2022,** *218*, 118412.
86. L. Chen, J. M., et al, Strong Enhancement on Fenton Oxidation by Addition of Hydroxylamine to Accelerate the Ferric and Ferrous Iron Cycles. *Environ. Sci. Technol.* **2011,** *45*, 3925-3930.
87. Wang, C., Yu, G., et al, Degradation of norfloxacin by hydroxylamine enhanced fenton system: Kinetics, mechanism and degradation pathway. *Chemosphere* **2021,** *270*, 129408.
88. Bollenbach, M., Wagner, P., et al, d-Glucose: An Efficient Reducing Agent for a Copper(II)-Mediated Arylation of Primary Amines in Water. *ChemSusChem* **2016,** *9*, 3244-3249.
89. M. Jin, G. H., et al, Shape-Controlled Synthesis of Copper Nanocrystals in an Aqueous Solution with Glucose as a Reducing Agent and Hexadecylamine as a Capping Agent. *Angew. Chem. Int. Ed.* **2011,** *50*, 10560-10564.
90. Hurd, C., The acidities of ascorbic and sialic acids. *J. Chem. Educ.* **1970,** *47*, 481-482.
91. Bosch, L., Fyles, T., James, T., Binary and ternary phenylboronic acid complexes with saccharides and Lewis bases. *Tetrahedron* **2004,** *60*, 11175-11190.
92. Ramachandran, S., Fontanille, P., et al, Gluconic Acid: Properties, Applications and Microbial Production. *Food Technol. Biotechnol.* **2006,** *44*, 185-195.

5.12 Appendix

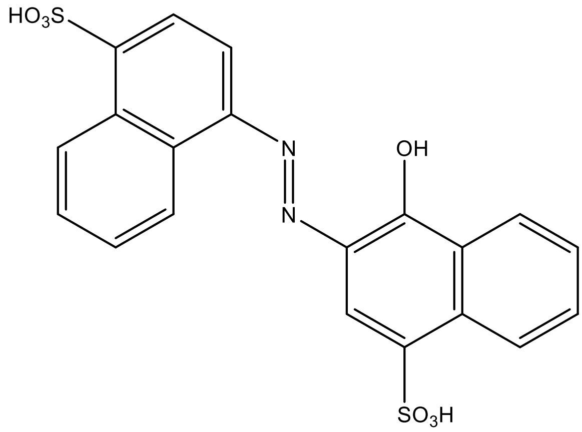

Figure A5.1. Chemical structure of Acid Red 14

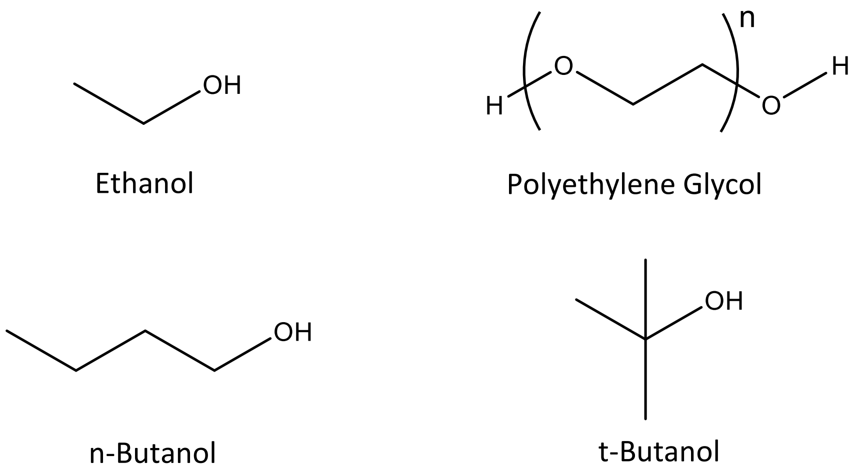

Figure A5.2. Chemical structures of ethanol, polyethylene glycol, n-butanol and t-butanol.

6 Conclusions and Future Work

6.1 The Selective Oxidation of Benzyl Alcohol via the in-situ Production of H_2O_2 Using Supported Pd Based Catalysts

Previous studies in the literature[27, 114, 130, 131, 218] have utilised Pd-based heterogeneous catalysts for the selective oxidation of benzyl alcohol via in-situ H_2O_2 synthesis, such an approach offers clear improvements in benzyl alcohol conversion at 50 ^oC, compared to that achieved using an aerobic oxidation methodology, which typically requires temperatures in the range of 80-120 ^oC.[219-221] It has been proposed by Santonastaso *et al.*[27] that a radical reaction mechanism was likely responsible for the oxidation of benzyl alcohol via in-situ H_2O_2 synthesis, and Crombie *et al.*[218] later reported the generation of either hydroxyl or hydroperoxyl radicals in-situ, in addition to methoxyl radicals generated from the methanol solvent. Additionally, greater levels of benzyl alcohol conversion offered by a given catalyst has previously been linked to greater levels of radical generation in-situ.[218]

In Chapter 3 of this Thesis, several parameters of catalyst design were investigated with the objective of improving catalytic performance towards the selective oxidation of benzyl alcohol beyond that which has been reported previously.[27, 114, 130, 131, 218] Firstly, the role of catalyst support material was investigated, focussing on a range of metal oxides and it was observed that catalysts supported on γ-Al_2O_3 offered significantly enhanced catalytic performance. Following this, an investigation into the effects of a secondary metal in an γ-Al_2O_3 supported Pd-based catalyst was conducted. It was determined that from a range of secondary metals (Au, Pt, Ru, Cu, Fe, Mn, Co, Zn), the combination of either Au or Fe with Pd offered the highest conversions of benzyl alcohol at 11.0 % and 10.3 % conversion for the 0.5%Au-0.5%Pd/Al_2O_3 and 0.5%Fe-0.5%Pd/Al_2O_3 catalysts respectively.

A summary of the catalytic activity of the Pd/Al_2O_3, AuPd/Al_2O_3 and FePd/Al_2O_3 catalysts compared to analogous catalysts supported on TiO_2 as reported in the literature, and prepared through an identical procedure are shown in Table 6.1. A key observation from this Chapter was the enhanced catalytic activity towards benzyl alcohol oxidation upon the alloying of Au or Fe with Pd in an Al_2O_3 supported catalyst, compared to catalysts employed previously in the literature.

Table 6.1. Comparison of γ-Al_2O_3 and TiO_2 supported AuPd and FePd catalysts towards the oxidation of benzyl alcohol, from this work and the work of Crombie *et al*.[218]

Catalyst	Benzyl Alcohol Conversion (%)	Benzaldehyde Selectivity (%)	Turnover Number (mol_{BA} mol_{metal}^{-1} hr^{-1})	Reference
Pd/Al_2O_3	1.3	100	266	This work
AuPd/Al_2O_3	11.0	100	2919	This work
FePd/Al_2O_3	10.3	97	1406	This work
Pd/TiO_2	1.8	100	367	[218]
AuPd/TiO_2	2.8	100	743	[218]
FePd/TiO_2	5.8	96	783	[218]

Benzyl alcohol oxidation reaction conditions: Catalyst (0.01 g), MeOH (7.13 g), benzyl alcohol (1.04 g, 9.62 mmol), mesitylene (0.42 g), 5% H_2/CO_2 (420 psi, 2.76 mmol), 25% O_2/CO_2 (160 psi, 5.24 mmol), 0.5 hr, 50 ^oC, 1200 rpm.

Following this, detailed comparisons of the $AuPd/Al_2O_3$ and $FePd/Al_2O_3$ catalysts were made with the Pd/Al_2O_3 catalyst, focussing on benzyl alcohol conversions at extended reaction times, over sequential reactions and across re-use reactions.
When used over extended reaction times, the results of which are summarised in Table 6.2, the $FePd/Al_2O_3$ catalyst offered the greatest conversion of benzyl alcohol (16.4 % over 90 minutes), compared to the $AuPd/Al_2O_3$ catalyst, which offered a benzyl alcohol conversion of 13.8 %. When compared to the Pd/Al_2O_3 catalyst, which offered a benzyl alcohol conversion of 2.5 %, the profound enhancements towards catalytic activity are apparent from the incorporation of an appropriate secondary metal with Pd.

Table 6.2. Comparison of Pd-based catalysts towards the oxidation of benzyl alcohol over 90-minutes.

Catalyst	Benzyl Alcohol Conversion (%)	Benzaldehyde Selectivity (%)	Turnover Number (mol_{BA} mol_{metal}^{-1} hr^{-1})
$AuPd/Al_2O_3$	13.8	100	1220
$FePd/Al_2O_3$	16.4	96	769
Pd/Al_2O_3	2.5	100	170

Benzyl alcohol oxidation reaction conditions: Catalyst (0.01 g), MeOH (7.13 g), benzyl alcohol (1.04 g, 9.62 mmol), mesitylene (0.42 g), 5% H_2/CO_2 (420 psi, 2.76 mmol), 25% O_2/CO_2 (160 psi, 5.24 mmol), 1.5 hr, 50 ^{O}C, 1200 rpm.

Investigations over sequential reaction are summarised in Table 6.3, which revealed a maximum benzyl alcohol conversion of 33.4 % and 32.3 % offered by the $FePd/Al_2O_3$ and $AuPd/Al_2O_3$ catalysts respectively. The Pd/Al_2O_3 offered a very limited conversion of 3.8 %, again demonstrating the necessity of a secondary metal to facilitate high conversions of benzyl alcohol.

Table 6.3. Comparison of catalytic activity of Pd-based catalysts towards the oxidation of benzyl alcohol after four sequential reactions.

Catalyst	Benzyl Alcohol Conversion (%)	Benzaldehyde Selectivity (%)	Turnover Number (mol_{BA} mol_{metal}^{-1} hr^{-1})
$AuPd/Al_2O_3$	32.3	97	2142
$FePd/Al_2O_3$	33.4	97	1174
Pd/Al_2O_3	3.8	100	194

Benzyl alcohol oxidation reaction conditions: Catalyst (0.01 g), MeOH (7.13 g), benzyl alcohol (1.04 g, 9.62 mmol), mesitylene (0.42 g), 5% H_2/CO_2 (420 psi, 2.76 mmol), 25% O_2/CO_2 (160 psi, 5.24 mmol), 2.0 hr, 50 ^{O}C, 1200 rpm.

Re-use reactions suggested that a degree of catalyst deactivation took place over one re-use for the $AuPd/Al_2O_3$, $FePd/Al_2O_3$ and Pd/Al_2O_3 catalysts, the results of which are summarised in Table 6.4. Proposals for the origins of this loss in catalytic activity upon re-use included the in-situ reduction of Pd, the restructuring of nanoparticles and a loss of surface chloride species from the catalyst. This was in agreement with the work of Brehm *et al.*[232] who correlated a decrease in catalytic activity towards the direct synthesis of H_2O_2 with a loss of surface chloride species upon re-use of an $AuPd/TiO_2$ catalyst.

A similar loss of catalytic activity occurred for both the $AuPd/Al_2O_3$ and $FePd/Al_2O_3$ catalysts, which after one re-use offered benzyl alcohol conversion rates of 4.6 % and 4.3 % respectively.

Table 6.4. Summary of catalytic activity of Pd-based catalysts towards the oxidation of benzyl alcohol when re-used.

Catalyst	Reaction Number	Benzyl Alcohol Conversion (%)	Benzaldehyde Selectivity (%)	Turnover Number (mol_{BA} mol_{metal}^{-1} hr^{-1})
$AuPd/Al_2O_3$	Use 1	11.0	100	2919
$AuPd/Al_2O_3$	Use 2[a]	4.6	100	1220
$FePd/Al_2O_3$	Use 1	10.3	96	1406
$FePd/Al_2O_3$	Use 2[a]	4.3	100	604
Pd/Al_2O_3	Use 1	1.3	100	266
Pd/Al_2O_3	Use 2[a]	0.5	100	117

Benzyl alcohol oxidation reaction conditions: Catalyst (0.01 g), MeOH (7.13 g), benzyl alcohol (1.04 g, 9.62 mmol), mesitylene (0.42 g), 5% H_2/CO_2 (420 psi, 2.76 mmol), 25% O_2/CO_2 (160 psi, 5.24 mmol), 0.5 hr, 50 ^{O}C, 1200 rpm.

[a] After use 1, catalyst was filtered, washed three times with HPLC grade H_2O (3 x 5 mL) and dried under vacuum at room temperature for 18 hr.

Finally, the use of an Fe/Al_2O_3 co-catalyst in tandem with the $AuPd/Al_2O_3$ catalyst as a physical mixture offered enhanced levels of benzyl alcohol conversion relative to the use of only the $AuPd/Al_2O_3$ catalyst, demonstrating the feasibility of incorporating a Fenton-type catalyst to utilise residual H_2O_2 that is present in the reaction mixture.

6.1.1 Future Work

In Chapter 3, it was determined that from the metal oxides investigated, the γ-Al_2O_3 supported AuPd catalyst offered the highest levels of benzyl alcohol conversion. However, a thorough investigation into the origin of the high catalytic activity associated with catalysts supported on γ-Al_2O_3 was not conducted. Numerous factors associated with the support material may have an effect on the catalytic activity of the resultant catalyst, including the pore volume, surface functionalisation, metal-support interactions, nanoparticle dispersion and support acidity.[46, 73, 355] Therefore, future work should establish the factors responsible for the high catalytic activity of γ-Al_2O_3 supported catalysts relative to other support materials.

It was also observed that using a 1%Fe/Al_2O_3 co-catalyst in tandem with a 0.5%Au-0.5%Pd/Al_2O_3 catalyst resulted in greater conversion of benzyl alcohol whilst still retaining a high selectivity towards benzaldehyde (97 %) (Section 3.11). No investigation was carried out to optimise this Fe based co-catalyst and factors such as metal loading, preparation method, heat treatment conditions, the choice of support material and the choice of metal may all be significant. For example, the Fe/Al_2O_3 catalyst was proposed to operate via Fenton-type chemistry, wherein hydroxyl and hydroperoxyl radicals are generated from H_2O_2, although numerous other metals have been demonstrated to function in an analogous manner, such as Cu and Co.[8] Therefore, alternative Fenton active metals should be investigated as a means to increase yields of benzaldehyde by utilising residual H_2O_2 present in the reaction mixture.

From the results of the extended reaction time experiments (Section 3.7), sequential reactions (Section 3.8), and catalyst re-use experiments (Section 3.10), it was proposed that a degree of catalyst deactivation may be occurring. However, to gain a deeper understanding of the extent of catalyst deactivation occurring in-situ, future investigations could utilise a flow system. By keeping the concentration of reactants constant in a flow system, the effects of the diminishing availability of benzyl alcohol and H_2 on the rate of reaction could be removed, elucidating the extent of catalyst deactivation in-situ. This may also allow for further investigations into the origins of the loss of activity, with factors including the reduction of Pd, the agglomeration of nanoparticles and the loss of chloride from the reaction likely contributing to this to varying extent.

The oxidative contribution from O_2 under the 'oxidation of benzyl alcohol via in-situ H_2O_2' reaction conditions is also unclear but may be significant (Section 3.4). It was proposed in Chapter 3 that whilst very low conversion of benzyl alcohol were offered using γ-Al_2O_3 supported catalysts under aerobic conditions, the in-situ reduction of Pd under an H_2 containing environment may have led to enhancements in oxidation from O_2 due to greater levels of Pd^0. Analysis of the oxidation state of Pd under aerobic conditions via XPS may support this claim, if oxidation of Pd does indeed occur, resulting in greater levels of Pd^{2+} which has been demonstrated in the literature to decrease levels of benzyl alcohol conversion relative to Pd^0 under aerobic conditions.[223]

6.2 The Effects of Preparation Methodology of Supported Pd Based Catalysts on the Selective Oxidation of Benzyl Alcohol via in-situ H_2O_2 Synthesis

Whilst significant enhancements in catalytic activity were achieved towards the selective oxidation of benzyl alcohol via in-situ H_2O_2 synthesis compared to catalysts previously reported in the literature, the catalysts developed in this study appeared to undergo a degree deactivation over the course of the reaction. This limits the usefulness of the class of catalysts developed in Chapter 3 and required further investigations to synthesise a new class of catalysts that were more resistant to deactivation.

Firstly, the method of catalyst preparation was investigated, wherein the resultant catalytic activity towards the oxidation of benzyl alcohol via in-situ H_2O_2 synthesis of an AuPd/Al_2O_3 catalyst was determined, when prepared by either an excess chloride co-impregnation, wet co-impregnation, or sol immobilisation methodology. Additionally, the effects of the use of a reductive or oxidative heat treatment towards catalytic activity were also investigated. The results of this are summarised in Table 6.5. A key observation in this Chapter was the profound effect of the catalyst preparation method towards the catalytic oxidation of benzyl alcohol when using an Al_2O_3 supported AuPd catalyst.

Table 6.5. Effects of catalyst preparation method and heat treatment on the selective oxidation of benzyl alcohol via in-situ H_2O_2 synthesis, using a 0.5%Au-0.5%Pd/Al_2O_3 catalyst.

Preparation Method/ Heat Treatment [a]	Benzyl Alcohol Conversion (%)	Benzaldehyde Selectivity (%)	Turnover Number (mol_{BA} mol_{metal}^{-1} hr^{-1})	Initial Ratio of Pd^0: Pd^{2+}
Wet co-impregnation/ reduced	22.7	98	5916	0.36: 0.74
Wet co-impregnation/ oxidised	1.8	100	478	All Pd^{2+}
Excess chloride co-impregnation/ reduced	11.0	100	2919	0.55: 0.45
Sol Immobilisation/ reduced	9.5	100	2520	0.74: 0.26
Sol Immobilisation/ oxidised	6.8	100	1804	0.37: 0.63

Benzyl alcohol oxidation reaction conditions: Catalyst (0.01 g), MeOH (7.13 g), benzyl alcohol (1.04 g, 9.62 mmol), mesitylene (0.42 g), 5% H_2/CO_2 (420 psi, 2.76 mmol), 25% O_2/CO_2 (160 psi, 5.24 mmol), 0.5 hr, 50 ^oC, 1200 rpm.

[a] Catalysts were exposed to either reductive (5% H_2/Ar, 500 °C, 4 hr, 10°C min^{-1}) or oxidative heat treatments (compressed air, 500 °C, 4hr, 10°C min^{-1}).

Significantly enhanced levels of benzyl alcohol conversion were offered by the AuPd/Al_2O_3 catalyst prepared by a wet co-impregnation method, and heat treated under reductive conditions (22.7 % conversion), when compared to any other preparation methodology. Comparisons between these catalysts were made using techniques including CO-DRIFTS, EM and XPS.

Investigations using Pd/Al_2O_3 and AuPd/Al_2O_3 catalysts prepared via wet co-impregnation and exposed to a reductive heat treatment were conducted. Particular focus was paid to comparing the benzyl alcohol conversion offered by the AuPd/Al_2O_3 catalyst under aerobic-only conditions and when both H_2 and O_2 were used in tandem. It was demonstrated that catalytic activity was limited under aerobic-only conditions, and the use of H_2 and O_2 in tandem had a significant promotional effect on the conversion of benzyl alcohol. However, it was also proposed that the in-situ reduction of Pd^{2+} to Pd^0 by H_2 may also have promoted the occurrence an aerobic oxidation pathway operating in tandem to the in-situ H_2 + O_2 pathway.

Detailed comparisons of the Pd/Al_2O_3 and AuPd/Al_2O_3 catalysts were then made across extended reaction times, sequential reactions, and re-use reactions in the selective oxidation of benzyl alcohol via in-situ H_2O_2 synthesis. When used over extended reaction times, the results of which are summarised in Table 6.6, the AuPd/Al_2O_3 catalyst offered the highest conversion of benzyl alcohol of 26.4 %, whilst the Pd/Al_2O_3 catalyst offered a conversion of 19.0 %.

Table 6.6. Comparison of Pd-based catalysts towards the oxidation of benzyl alcohol over 90-minutes. Prepared by the wet co-impregnation method and heat treated under reductive conditions.

Catalyst	Benzyl Alcohol Conversion (%)	Benzaldehyde Selectivity (%)	Turnover Number (mol_{BA} mol_{metal}^{-1} hr^{-1})
Pd/Al_2O_3	19.0	100	1294
$AuPd/Al_2O_3$	26.4	98	2290

Benzyl alcohol oxidation reaction conditions: Catalyst (0.01 g), MeOH (7.13 g), benzyl alcohol (1.04 g, 9.62 mmol), mesitylene (0.42 g), 5% H_2/CO_2 (420 psi, 2.76 mmol), 25% O_2/CO_2 (160 psi, 5.24 mmol), 1.5 hr, 50 ^{O}C, 1200 rpm.

Investigations over sequential reactions, are summarised in Table 6.7, which revealed the greatest extent of benzyl alcohol of 62.4 %, which was offered by the $AuPd/Al_2O_3$ catalyst, whilst the Pd/Al_2O_3 catalyst offered a benzyl alcohol conversion of 32.8 %. The high conversion offered by these catalysts over sequential reactions demonstrated the efficacy of Pd-based catalysts when prepared through the wet impregnation methodology, followed by heat treatment under reductive conditions.

Table 6.7. Comparison of catalytic activity of Pd-based catalysts towards the oxidation of benzyl alcohol after four sequential reactions. Prepared by the wet impregnation method and heat treated under reductive conditions.

Catalyst	Benzyl Alcohol Conversion (%)	Benzaldehyde Selectivity (%)	Turnover Number (mol_{BA} mol_{metal}^{-1} hr^{-1})
Pd/Al_2O_3	32.8	99	1644
$AuPd/Al_2O_3$	62.4	98	4072

Benzyl alcohol oxidation reaction conditions: Catalyst (0.01 g), MeOH (7.13 g), benzyl alcohol (1.04 g, 9.62 mmol), mesitylene (0.42 g), 5% H_2/CO_2 (420 psi, 2.76 mmol), 25% O_2/CO_2 (160 psi, 5.24 mmol), 2.0 hr, 50 ^{O}C, 1200 rpm.

Re-use reactions suggested that similarly to the analogous Pd-based catalysts prepared through the excess chloride co-impregnation method, deactivation of the catalyst was occurring upon re-use of the catalyst. However, this was observed to the least significant for the $AuPd/Al_2O_3$ catalyst, wherein the conversion of benzyl alcohol decreased from 22.7 % upon first use to 17.2 % upon re-use. Mechanisms such as the in-situ reduction of Pd, the agglomeration of nanoparticles and the dissolution of catalytic metal were investigated as possible mechanisms for this observed deactivation.

Finally, other metal oxides were investigated as support materials for AuPd nanoparticle catalysts when prepared via the wet co-impregnation method, and it was determined that only catalysts supported on γ-Al_2O_3 were able to offer enhanced levels of benzyl alcohol conversion compared to those offered by analogous catalysts prepared via the excess chloride co-impregnation method. The results of this are outlined in Table 6.8.

Table 6.8. Comparison of the catalytic activities of supported 0.5%Au-0.5%Pd catalysts prepared by the C.Imp Red methodology, towards the selective oxidation of benzyl alcohol using different support materials.

Catalyst Support	Benzyl Alcohol Conversion (%)	Benzaldehyde Selectivity (%)	Turnover Number (mol_{BA} mol_{metal}^{-1} hr^{-1})
Al_2O_3	22.7	98	5916
CeO_2	2.7	100	716
TiO_2	3.0	100	796
Nb_2O_5	0.4	100	106
ZrO_2	1.2	100	318
FLG	3.9	100	1035

Benzyl alcohol oxidation reaction conditions: Catalyst (0.01 g), MeOH (7.13 g), benzyl alcohol (1.04 g, 9.62 mmol), mesitylene (0.42 g), 5% H_2/CO_2 (420 psi, 2.76 mmol), 25% O_2/CO_2 (160 psi, 5.24 mmol), 0.5 hr, 50 ^{O}C, 1200 rpm.

6.2.1 Future Work

Whilst the high efficacy of the $AuPd/Al_2O_3$ catalysts relative to other support materials has been demonstrated, numerous questions related to the origin of this high catalytic activity remain. Firstly, the concentration of HCl incorporated into the catalyst preparation methodology was demonstrated to be a significant factor in the resultant activity of the catalyst towards benzyl alcohol oxidation. Indeed, significant enhancements in catalytic activity were observed when a low concentration of HCl was incorporated into the catalyst preparation, whereas a higher concentration of HCl corresponded to a lower catalytic activity. Therefore, the possibility exists for the tuning of the concentration of HCl during catalyst preparation to enhance catalytic activity. The relationship between HCl concentration and the physical properties of the catalyst can then be investigated, and a possible structure-activity relationship elucidated. Sankar *et al.*[262]have previously reported that an excess of chloride ions during the preparation of the catalyst aided in the dispersion of AuPd nanoparticles, which the authors correlated to an observed enhancement towards the direct synthesis of H_2O_2. Additionally, a possible size dependency relationship may exist, given previously reported size dependencies for both the direct synthesis of H_2O_2 and the aerobic oxidation of benzyl alcohol.[53, 254] Therefore, a systematic study into the effects of size of Pd and AuPd nanoparticles may establish this relationship if one exists and inform future catalyst design methodologies.

In Chapter 4 and in Chapter 3, it was demonstrated that using an γ-Al_2O_3 support could significantly enhance the catalytic activity of AuPd nanoparticles towards the oxidation of benzyl alcohol via in-situ H_2O_2 synthesis, compared to several other metal oxide support materials. Whilst the iso-electric point of the support was cited as a possible reason for this, due to the reported significance of the iso-electric point towards the direct synthesis of H_2O_2,[46] and for basic support materials to potentially facilitate the H-abstraction of alcohols,[96] no further investigation was done. However, numerous other factors associated with the support may contribute to catalytic activity, such as the surface area of the support, surface functionalisation and metal-support interactions. Therefore, the properties of the support material itself may be tuneable in a way that enhances catalytic activity. For example, the surface area of the support may have an effect on Pd distribution, whilst surface functionalisation may improve bonding between Pd and the support and reduce metal dissolution or have an electronic effect on some Pd sites.

Each catalyst that was utilised for the oxidation of benzyl alcohol via in-situ H_2O_2 synthesis was also tested for activity towards the direct synthesis of H_2O_2. However, clear correlations were not apparent between the two reactions. Further studies that investigate the relationship between these two reactions should also investigate the ability of each catalyst to degrade H_2O_2, which may indicate how selectively they can utilise H_2O_2 for the oxidation of benzyl alcohol. For this purpose, reactions using dilute preformed commercial H_2O_2 for the selective oxidation of benzyl alcohol may also provide insight.

Finally, using extended reaction times and conducting sequential reactions of the oxidation of benzyl alcohol via in-situ H_2O_2 synthesis revealed the need for consistent high partial pressures of H_2 and O_2 for oxidation to take place. To overcome the limitations of the batch system that was utilised in this study, a flow system could be used to continually feed an optimal ratio of H_2 and O_2 to maximise benzyl alcohol oxidation whilst avoiding the kinetic limitations of a continually diminishing partial pressure of H_2 or availability of benzyl alcohol.

6.3 Ascorbic Acid Promotion of the Catalytic Wet Peroxide Oxidation of Phenol, Using γ-Al_2O_3 Supported Catalysts

It has been previously reported in the literature that the addition of ascorbic acid to Fenton-type reaction systems involving H_2O_2 and either Cu or Fe can enhance the oxidative degradation of target molecules such as alachlor and Rhodamine B.[194, 285] In Chapter 5 of this thesis, in association with Selden Research Ltd., investigations were focussed towards enhancing the oxidative activity associated with the incorporation of ascorbic acid with sodium percarbonate (a source of H_2O_2), using a heterogeneous γ-Al_2O_3 supported catalyst. The oxidation of phenol was used as a model reaction.

Initial work investigated a series of 2 wt.% metal catalysts (Fe, Cu, Mn and Co) with previously reported use in Fenton-type reactions[280] and determined that a Cu/Al_2O_3 catalyst offered the greatest conversion of phenol. Following this, the effect of each component of the oxidant mixture towards the oxidation of phenol was determined independently and is summarised in Table 6.9.

Table 6.9. The catalytic wet peroxide oxidation of phenol, using a range of reaction components.

Catalyst	Reactants	Phenol Conversion (%)	Cu Present in Reaction Mixture (ppm)	Initial pH of Oxidant Mixture
Al_2O_3	None	0.0	n.d.	7.02
Cu/Al_2O_3	Ascorbic acid, sodium percarbonate	10.9	2.8	9.05
Cu/Al_2O_3	Sodium percarbonate	0.0	0.1	n.d.
Cu/Al_2O_3	Ascorbic acid	3.5	11.2	3.02
Al_2O_3	Ascorbic acid, sodium percarbonate	2.7	n.d.	9.05
Al_2O_3	Ascorbic acid	0.3	n.d.	3.02

Phenol oxidation reaction Conditions: Catalyst (100 mg), H_2O (10 mL), phenol (500 ppm, 0.053 mmol), ascorbic acid (0.114 mmol), sodium percarbonate (0.096 mmol), 1.0 hr, 20 ^{0}C, 1000 rpm. (Where applicable)

Further investigations into the optimisation of the components of the reaction mixture revealed that the extent of phenol conversion could be further enhanced by utilising lower concentrations of sodium percarbonate compared to that used in Table 6.9. Additionally, as is shown in Table 6.10, when the Fe/Al_2O_3 catalyst was tested using the optimised concentration of sodium percarbonate, significantly enhanced levels of phenol conversion were offered, compared to when higher concentrations of sodium percarbonate were used. This effect was attributed to the lower pH of the reaction mixture when lower concentrations of sodium percarbonate were used.

Table 6.10. Comparison of the 2%Cu/Al_2O_3 and 2%Fe/Al_2O_3 catalysts towards the catalytic wet peroxide oxidation of phenol, using different concentrations of sodium percarbonate

Catalyst	Moles of Sodium Percarbonate (mmol)	Phenol Conversion (%)	Initial pH of Reaction Mixture
Cu/Al_2O_3	0.096	10.9	7.21
Cu/Al_2O_3	0.032	18.7	4.95
Fe/Al_2O_3	0.096	4.1	7.21
Fe/Al_2O_3	0.032	21.7	4.95

Phenol oxidation reaction conditions: Catalyst (100 mg), H_2O (10 mL), phenol (500 ppm, 0.053 mmol), ascorbic acid (0.114 mmol), sodium percarbonate (0.032 – 0.096 mmol), 1.0 hr, 20 ^{0}C, 1000 rpm.

By comparing the catalytic activity of the Cu/Al_2O_2 catalyst and an equivalent number of moles of Cu^{2+} from $CuCl_2$ as a homogeneous Cu source, it was determined that all catalytic activity was likely attributable to homogeneous Cu leachate from the Cu/Al_2O_3 catalyst, and not from the heterogeneous Cu immobilised on the support material.

6.3.1 Future Work

Whilst the use of ascorbic acid was linked to the leaching of catalytic metal, no investigation towards the in-situ reduction of Cu^{2+} by ascorbic acid was conducted. Consequently, from the work presented in Chapter 5, it cannot be claimed that the ascorbic acid had any effect on the reaction beyond the dissolution of catalytic metal. To investigate this further, homogeneous Cu or Fe salts should be used as the catalytic metal source in future investigations, to remove any influence of catalyst leaching on observed activity.
Additionally, no work was conducted towards optimising the concentration of catalytic metal used for the reaction system. Given the apparent independence of leached Cu concentration (Table 5.13) on total phenol oxidation, it may be determined that lower concentrations of Cu can still offer equivalent conversion of phenol. Indeed, utilising lower catalyst concentrations may elucidate any mass transport limitations that may exist, such as the diffusion of atmospheric O_2 into the reaction mixture.

Furthermore, no Cu leaching data was collected during the optimisation of the concentration of ascorbic acid (Table 5.10), and an explicit understanding of the relationship between ascorbic acid concentration and metal dissolution may assist in the optimisation of reaction conditions for future projects, in terms of selecting appropriate catalyst masses and metal loadings.

The original objective of this study was to maximise the oxidative efficacy of the metal/ascorbic acid/H_2O_2 system to disinfect surfaces, using phenol oxidation as a model system. Future investigations should be focussed on translating the factors that maximise phenol oxidation, such as the optimisation of H_2O_2 concentration and pH, into an anti-microbial context.

6.4 References

1. Moreno, I., Dummer, M., et al., Selective oxidation of benzyl alcohol using in situ generated H_2O_2 over hierarchical Au-Pd titanium silicate catalysts. *Catal. Sci. Technol.* **2013,** *3*, 2425.
2. Santonastaso, M., Freakley, S., et al, Oxidation of benzyl alcohol using in situ generated hydrogen peroxide. *Org. Process Res. Dev.* **2014,** *18*, 1455-1460.
3. Crombie, C., Lewis, R., et al, Enhanced Selective Oxidation of Benzyl Alcohol via In Situ H_2O_2 Production over Supported Pd-Based Catalysts. *ACS Catal.* **2021,** *11*, 2701-2714.
4. Lyu, J., Niu, J., et al., In Situ Hydrogen Peroxide Production for Selective Oxidation of Benzyl Alcohol over a Pd@Hierarchical Titanium Silicalite Catalyst. *ACS Omega* **2020,** *5*, 16865-16874.
5. Martinez, J., Mazarío, J., et al., A tandem process for in situ H_2O_2 formation coupled with benzyl alcohol oxidation using Pd–Au bimetallic catalysts. *Dalton Trans.* **2022,** *51*, 17567-17578.
6. Choudhary, V., Dhar, A., et al., A green process for chlorine-free benzaldehyde from the solvent-free oxidation of benzyl alcohol with molecular oxygen over a supported nano-size gold catalyst. *Green Chem.* **2005,** *7*, 768-770.
7. Göksu, H., Burhan, H., et al, Oxidation of Benzyl Alcohol Compounds in the Presence of Carbon Hybrid Supported Platinum Nanoparticles (Pt@CHs) in Oxygen Atmosphere. *Sci. Rep.* **2020,** *10*, 5439.
8. Enache, D., Barker, D., et al, Solvent-free oxidation of benzyl alcohol using titania-supported gold–palladium catalysts: Effect of Au–Pd ratio on catalytic performance. *Catal. Today* **2007,** *122*, 407-411.

9. Brehm, J., Lewis, R., et al, The Direct Synthesis of Hydrogen Peroxide over AuPd Nanoparticles: An Investigation into Metal Loading. *Catal. Lett.* **2021,** *152*, 254-262.
10. Yook, S., Kwon, H., et al., Significant Roles of Carbon Pore and Surface Structure in AuPd/C Catalyst for Achieving High Chemoselectivity in Direct Hydrogen Peroxide Synthesis. *ACS Sustainable Chem. Eng.* **2017,** *5*, 1208-1216.
11. Ntainjua, E., Edwards, J., et al, The role of the support in achieving high selectivity in the direct formation of hydrogen peroxide. *Green Chem.* **2008,** *10*, 1162-1169.
12. Liu, S., Deng, Y., et al., Understanding the Role of Boron on the Interface Modulation of the Pd/TiO2 Catalyst for Direct Synthesis of H_2O_2. *ACS Sustainable Chem. Eng.* **2022,** *10*, 3264-3275.
13. Bokare, A., Choi, W.,, Review of iron-free Fenton-like systems for activating H2O2 in advanced oxidation processes. *J. Hazard Mater.* **2014,** *275*, 121-135.
14. Wu, P., Cao, Y., et al, Formation of PdO on Au–Pd bimetallic catalysts and the effect on benzyl alcohol oxidation. *J. Catal.* **2019,** *375*, 32-43.
15. Sankar, M., Qian, H., et al., Synthesis of Stable Ligand-free Gold-Palladium Nanoparticles Using a Simple Excess Anion Method. *ACS Nano* **2012,** *6*, 6600-6613.
16. Ye, Y., Chun, J., et al, A study of the palladium size effect on the direct synthesis of hydrogen peroxide from hydrogen and oxygen using highly uniform palladium nanoparticles supported on carbon. *Korean J. Chem. Eng.* **2012,** *29*, 1115-1118.
17. Tian, P., Ouyang, L., et al, The origin of palladium particle size effects in the direct synthesis of H_2O_2: Is smaller better? *J. Catal.* **2017,** *349*, 30-40.
18. Chan-Thaw, C., Savara, A., Villa, A., Selective benzyl alcohol oxidation over Pd catalysts. *Catalysts* **2018,** *8*, 431.
19. Bolobajev, J., Trapido, M., Goi, A., Improvement in iron activation ability of alachlor Fenton-like oxidation by ascorbic acid. *Chem. Eng. J.* **2015,** *281*, 566-574.
20. Xiao, B., Wu, M., et al, Facile Synthesis of CuO Nanosheets and Efficient Degradation of Rhodamine B in a Copper Oxide/Ascorbic Acid/Hydrogen Peroxide System: Kinetics, Fate of Ascorbic Acid, and Mechanism. *ChemistrySelect* **2020,** *5*, 6075-6082.
21. Bokare, A., Choi, W., Review of iron-free fenton-like systems for activating H_2O_2 in advanced oxidation process. *J. Hazard. Mater.* **2014,** *275*, 121 - 135.